Salmon farms move to land for a cleaner future p. 530

Earlier dates for fish and their ecosystems pp. 567 & 572

Browse the buffet of Gordon Research Conferences p. 592

Science

$15
10 FEBRUARY 2023
science.org
AAAS

CHANGING COLOR

Regulation of carotenoid pigment variation pp. 534 & 576

"One of the advantages of being a scientist is that you can choose who you work with."

Shruti Naik, PhD
Assistant Professor at New York University's Grossman School of Medicine

Hear Shruti Naik, PhD and others explore how human connections drive science forward.

Find the podcasts here
abcam.me/together

Science AAAS | progress happens together abcam

CONTENTS

10 FEBRUARY 2023 • VOLUME 379
ISSUE 6632

Growing Atlantic salmon entirely on land could help meet rising demand while lowering environmental impact.

PHOTO: NARAYAN MAHON

NEWS

IN BRIEF

520 News at a glance

IN DEPTH

522 Should an also-ran in human evolution get more respect?
Oldest Oldowan tools—seen as a hallmark of our own genus—found with bones of an unexpected hominin *By A. Gibbons*
RESEARCH ARTICLE p. 561

523 Autism researchers face off over language
Terminology dispute underscores divide about what direction the field should take
By R. Zamzow

524 Repurposed drug battles 'brain-eating' amoeba
A drug for urinary tract infections may also treat *Balamuthia mandrillaris*
By K. Kornei

526 Could a popular antiviral supercharge the pandemic?
Molnupiravir appears to be speeding SARS-CoV-2 evolution *By R. F. Service*

527 Neotropical bird scientists call for an end to bias
Two manifestos offer recommendations for shifting field's flawed "northern lens"
By E. Rodríguez Mega

528 Global alarm system watches for methane
Artificial intelligence–powered scans of satellite data detect leaks of the greenhouse gas *By P. Voosen*

FEATURES

530 Oceans away
Is raising salmon on land the next big thing in farming fish? *By E. Stokstad*

INSIGHTS

PERSPECTIVES

534 Unusual suspects in flower color evolution
The expression of phased small interfering RNAs caused monkeyflower color evolution
By M. Monniaux
RESEARCH ARTICLE p. 576

536 Probing matter with nonlinear spectroscopy
Ultrafast nonlinear spectroscopy can unravel the dynamics of highly excited electronic states *By S. R. Leone and D. M. Neumark*

538 Exaggerated responses to a virus long gone
Multisystem inflammatory syndrome in children is caused by abnormal cell activation
By P. Brodin
RESEARCH ARTICLE p. 554

539 A window into prebiotic worlds?
Zircons reveal the geochemistry of Earth's earliest hydrothermal systems
By L. E. Rodriguez
RESEARCH ARTICLE p. 582

POLICY FORUM

541 Public views on polygenic screening of embryos
Understanding moral acceptability and willingness to use is crucial for informing policy *By M. N. Meyer* et al.

BOOKS ET AL.

544 Lost and found in El Salvador
Separated by civil war, families turn to genetic testing to locate missing children
By V. Penchaszadeh

545 Hacking and the social contract
Although technical fixes can help, solutions must focus on broader societal factors at play
By V. Mayer-Schönberger

LETTERS

547 Soil microplastics pollution in agriculture
By L. He et al.

548 Understanding the limits of AI coding
By J. Hendler

548 Effective implementation of new biodiversity pact
By R. Buckley

Abbott

ONE TEST. THREE ANSWERS.

A new tool for differential diagnosis of COVID-19 and flu

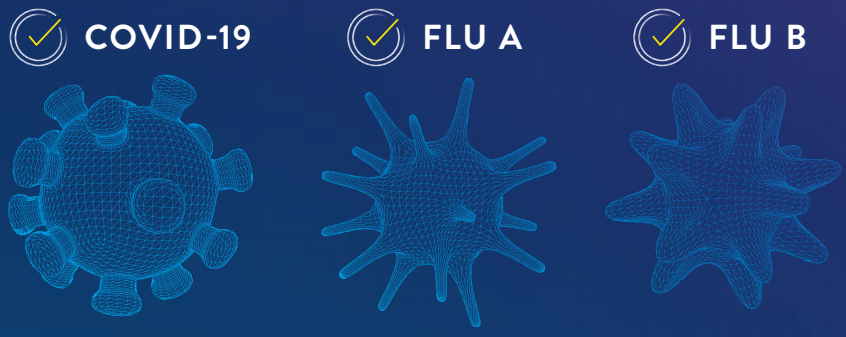

COVID-19 and flu have similar symptoms, which is why the ease and efficiency of testing with the Panbio™ COVID-19/Flu A&B Rapid Panel is a great choice for differential diagnosis.

One test provides three results in just 15 minutes — speeding your ability to diagnose and make treatment decisions at the point of care.

One test means less demand on physicians, staff and lab workers. One swab means less discomfort for patients. One set of answers for COVID-19 and flu empowers timely decision-making to effectively treat patients, help prevent further transmission and avoid unnecessary antibiotic use.

LEARN MORE AT **GLOBALPOINTOFCARE.ABBOTT**

© 2023 Abbott. All rights reserved. All trademarks referenced are trademarks of either the Abbott group of companies or their respective owners. Any photos displayed are for illustrative purposes only. COL-17861-01 01/23

RESEARCH

IN BRIEF

549 From *Science* and other journals

REVIEW

552 Epigenetics
Epigenetics as a mediator of plasticity in cancer *A. P. Feinberg and A. Levchenko*
REVIEW SUMMARY; FOR FULL TEXT: DOI.ORG/10.1126/SCIENCE.AAW3835

RESEARCH ARTICLES

553 Development
Mitochondria metabolism sets the species-specific tempo of neuronal development *R. Iwata* et al.
RESEARCH ARTICLE SUMMARY; FOR FULL TEXT: DOI.ORG/10.1126/SCIENCE.ABN4705

554 Coronavirus
Inborn errors of OAS–RNase L in SARS-CoV-2–related multisystem inflammatory syndrome in children *D. Lee* et al.
RESEARCH ARTICLE SUMMARY; FOR FULL TEXT: DOI.ORG/10.1126/SCIENCE.ABO3627
PERSPECTIVE p. 538

Nanophotonics
555 Negative refraction in hyperbolic hetero-bicrystals *A. J. Sternbach* et al.
558 Gate-tunable negative refraction of mid-infrared polaritons *H. Hu* et al.

Negative and positive refraction is observed at the interface of two crystals, on the left and right, respectively.

ILLUSTRATIONS: (LEFT TO RIGHT) ELLA MARU STUDIO; DINGHUA YANG

An artist's reconstruction of the Guiyang Biota, which evolved 1.5 million years after the Permian-Triassic mass extinction and is one of the earliest known modern-type marine ecosystems.

561 Hominin evolution
Expanded geographic distribution and dietary strategies of the earliest Oldowan hominins and *Paranthropus* *T. W. Plummer* et al.
NEWS STORY p. 522

567 Paleontology
A Mesozoic fossil lagerstätte from 250.8 million years ago shows a modern-type marine ecosystem *X. Dai* et al.

572 Fish evolution
Genome structures resolve the early diversification of teleost fishes *E. Parey* et al.

576 Plant science
Taxon-specific, phased siRNAs underlie a speciation locus in monkeyflowers *M. Liang* et al.
PERSPECTIVE p. 534

582 Geochemistry
Relatively oxidized fluids fed Earth's earliest hydrothermal systems *D. Trail and T. M. McCollom*
PERSPECTIVE p. 539; PODCAST

586 Virology
Inhibition of cellular RNA methyltransferase abrogates influenza virus capping and replication *Y. Tsukamoto* et al.

DEPARTMENTS

519 Editorial
Students and postdocs deserve more
By S. M. Malcom and S. Parikh

614 Working Life
What no one told me
By H. Mastro

ON THE COVER

A flower color locus that underlies pollinator-mediated speciation in monkeyflowers (*Mimulus*) produces regulatory small RNAs that suppress the accumulation of yellow carotenoid pigments. Variation in the level of these small RNAs through either natural mutations or transgenic manipulation contributes to a great diversity of flower color in *Mimulus*, as shown in this image. See pages 534 and 576. *Image: Photo: Peter Morenus/University of Connecticut*

Gordon Research Conferences.....592
Science Careers.....611

SCIENCE (ISSN 0036-8075) is published weekly on Friday, except last week in December, by the American Association for the Advancement of Science, 1200 New York Avenue, NW, Washington, DC 20005. Periodicals mail postage (publication No. 484460) paid at Washington, DC, and additional mailing offices. Copyright © 2023 by the American Association for the Advancement of Science. The title SCIENCE is a registered trademark of the AAAS. Domestic individual membership, including subscription (12 months): $165 ($74 allocated to subscription). Domestic institutional subscription (51 issues): $2411; Foreign postage extra: Air assist delivery: $107. First class, airmail, student, and emeritus rates on request. Canadian rates with GST available upon request, GST #125488122. Publications Mail Agreement Number 1069624. **Printed in the U.S.A.**
Change of address: Allow 4 weeks, giving old and new addresses and 8-digit account number. **Postmaster:** Send change of address to AAAS, P.O. Box 96178, Washington, DC 20090–6178. **Single-copy sales:** $15 each plus shipping and handling available from backissues.science.org; bulk rate on request. **Authorization to reproduce** material for internal or personal use under circumstances not falling within the fair use provisions of the Copyright Act can be obtained through the Copyright Clearance Center (CCC), www.copyright.com. The identification code for *Science* is 0036-8075. *Science* is indexed in the *Reader's Guide to Periodical Literature* and in several specialized indexes.

RUTGERS CONGRATULATES OUR NEWEST AAAS FELLOWS

Paul Copeland
Professor of Biochemistry and Molecular Biology, Robert Wood Johnson Medical School
Advancements in understanding the molecular mechanism of mRNA translation and trace element metabolism

Robert Kopp
Professor of Earth and Planetary Sciences, School of Arts and Sciences; Co-Director, University Office of Climate Action
Innovations in climate science, particularly using statistical process modeling to estimate sea level change

Shuchismita Dutta
Associate Research Professor, Institute for Quantitative Biomedicine
Innovations in molecular visualization education for teachers, undergraduates, and the public

Malin Pinsky
Associate Professor of Ecology, Evolution, and Natural Resources, School of Environmental and Biological Sciences
Advancements in marine biology, particularly for predictions about the impacts of climate change and population dynamics

Bonnie Firestein
Professor of Cell Biology and Neuroscience, School of Arts and Sciences
Contributions to molecular and cellular neuroscience, particularly the development of, and strategies to repair, damaged neural circuits

Jaideep Vaidya
Distinguished Professor and Vice Chair of Management Science and Information Systems, Rutgers Business School
Contributions to privacy protection in data analytics, information sharing, and access control management

William Hallman
Professor and Chair of Human Ecology, School of Environmental and Biological Sciences
Advancements in risk analysis, assessment, and communication, and educating the public on important scientific issues

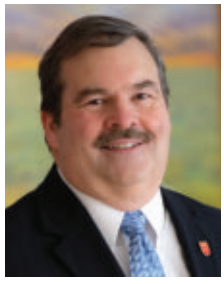

Rachael Winfree
Professor of Ecology, Evolution, and Natural Resources, School of Environmental and Biological Sciences
Advancements in ecosystem services, particularly contributions to pollination ecology and conservation

Saurabh Jha
Professor of Physics and Astronomy, School of Arts and Sciences
Contributions to the study of Type Ia supernovae, including insights on their intrinsic properties and their use as cosmological probes

EXCELLENCE IS EARNED

RUTGERS

EDITORIAL

Students and postdocs deserve more

A slow-motion crisis is underway among graduate students and postdocs in the United States who comprise today's indispensable research and teaching workforce and tomorrow's scientific leaders. Low pay, lack of benefits, and sometimes toxic research environments have persisted for years. Frustrated graduate students, postdocs, and nontenured faculty are protesting and pursuing unionization to address worsening conditions. A few senior leaders are starting to recognize that today's research environment is much more challenging than that of their sepia-tinted memories. In response, some universities have offered salary and benefits relief. Unionization and overdue adjustments are incomplete and temporary responses to deeply embedded problems—with long-term implications that everyone may regret. So where do solutions lie?

For the past 70 years, universities in the United States have supported fundamental research, operating under the premise that research and education should be integrated. How that integration is carried out must be reformed because over the course of seven decades, the research ecosystem has been optimized to flawed incentives.

In the current system, a student or scholar will "apprentice" to a more senior scientist, with training exchanged for low wages. But how low is too low? The model works when there are mentoring, a supportive research environment, and growth opportunities that lead to rewarding, independent careers. Unfortunately, each provision of this contract is strained. Training times are longer than necessary. Mentoring is not rewarded. Tenure track positions are limited, and other career options are not spotlighted. Senior scientists and administrators who want to do the right thing are constrained by the incentives of the system itself. Sadly, when some senior scientists take advantage of the huge differences in power, there may be exploitation, harassment, or worse. Not enough safeguards are in place to prevent these abuses of power that are built into the system itself.

It is understandable that every actor in this training system seeks to advance their own position. Unfortunately, the disadvantages inevitably flow to the graduate students and postdocs. Getting the maximum research for the dollar too often devolves to more students and postdocs receiving less than they need and less than the value they bring to the enterprise. As it is, the federal government does not pay the full cost of research. University presidents and provosts are rewarded for securing shiny new buildings and research centers while squeezing the most work possible out of trainees and contingent faculty. It is hard to expect money to come from inside this broken system to supplement low salaries and stipends.

Compounding the financial obstacles, graduate students and postdocs need more skills and knowledge than ever, often leading to longer preparation times before they are viewed as "independent" and capable of striking out on their own. Their careers are in the hands of one or two senior scientists whose incentives generally are to produce the most possible research rather than the best experience and prospects for their students.

> "...many must leave academia for a salary sufficient to support their own families."

To survive this prolonged apprenticeship, many students must take out loans for living expenses, disproportionately discouraging students of color and those from low-income households. Without a safety net, many must leave academia for a salary sufficient to support their own families. Careers outside academia are valuable and rewarding, but society also needs a diverse and talented academy.

Solutions will not come without changing the incentives that led to such deeply engrained problems. Only federal funding agencies, including the National Institutes of Health, National Science Foundation, and Department of Energy, have the influence to align incentives for administrators, researchers, and others toward a healthier environment. Determining the metrics of a healthy research environment, and supporting and rewarding scientists and institutions that optimize these metrics, would be a start. Many may not like the consequences, such as fewer but bigger grants or smaller labs, but doing nothing is unsustainable. American writer James Baldwin famously said, "Not everything that is faced can be changed, but nothing can be changed until it is faced." It is past time for those who lead the scientific enterprise to face up to the fact that the student and postdoctoral experience is not how it might be remembered. Otherwise, everyone will bear witness to a system that is crumbling under its own weight.

–Shirley M. Malcom and Sudip Parikh

Shirley M. Malcom is a senior advisor and director of the STEM Equity Achievement (SEA) Change program at the American Association for the Advancement of Science (AAAS, the publisher of *Science*), Washington, DC, USA. smalcom@aaas.org

Sudip Parikh is the chief executive officer of AAAS and executive publisher of the *Science* journals. sparikh@aaas.org

10.1126/science.adh0336

NEWS

IN BRIEF

Edited by
Jeffrey Brainard

CLIMATE CHANGE

Melting glaciers threaten millions downstream

Peru's 70-meter-deep Lake Palcacocha, fed by melting glaciers, threatens the nearby city of Huaraz, population 100,000.

About 15 million people in 30 countries face injury or death from unstable glacial lakes, a study says. As Earth's climate has warmed, glaciers have rapidly melted in high mountain ranges across the globe, and the resulting water accumulates in unstable gouges cut by the glaciers as they retreat. The lakes' banks can burst, flooding nearby communities; such outbursts have killed at least 12,000 people worldwide. The first global assessment of the threat, published this week in *Nature Communications*, estimates that half of the 15 million people threatened live at high elevations in Asia. More than 1 million are at risk in one glacier basin, the Khyber Pakhtunkhwa in Pakistan. Other high-risk areas identified in the report are in Peru and China.

Sabatini to get lab, second chance

#METOO | Two donors have agreed to fund a new laboratory for David Sabatini, the prominent biologist who was fired by the Howard Hughes Medical Institute and resigned from the Whitehead Institute for Biomedical Research in 2021. A probe there had found he sexually harassed a junior scientist, fostered a sexualized lab environment, threatened retaliation against lab members if they questioned his conduct, and obstructed the investigation, which was conducted by an outside law firm. Sabatini has disputed the findings and sued Whitehead and the junior scientist, Kristin Knouse, for defamation and emotional distress. (She countersued.) Billionaire hedge fund manager Bill Ackman said last week that his Pershing Square Foundation—for which Sabatini has reviewed grant applications—and an anonymous partner will, in equal parts, fund a new Sabatini lab for $5 million per year for 5 years. Its location, structure, and size haven't been determined. "I called him and said, 'We think it's important that you get back to work,'" Ackman told *Science*. Other Sabatini supporters say the probe of the biologist was unfair and his punishment disproportionate. Sabatini's critics say the funding is a humiliating brush off of women and others in science who are harassed by senior scientists on whom their careers depend.

EU eyes ban on 'forever' chemicals

REGULATION | In one of the most sweeping proposals of its kind, the European Chemicals Agency (ECHA) is considering asking the European Union to ban per- and polyfluoroalkyl substances (PFAS), called forever chemicals because they accumulate and persist in the environment. On 7 February, ECHA published a proposal that would ban the entire PFAS category, which includes more than 10,000 substances. Used in thousands of consumer products such as stain-resistant fabrics and nonstick cookware, PFAS have been linked to health problems. ECHA will begin a 6-month scientific evaluation of the health and socioeconomic impacts of a ban. Those results will be forwarded to the European Commission, which together with member states will decide whether to restrict the substances. Other governments have taken more limited steps to restrict the chemicals, and industry groups have generally opposed restricting the entire class of compounds, arguing they have many essential uses.

Science boosted in U.K. shuffle

POLICY | Under a reorganization announced this week, the United Kingdom will get a standalone ministry

PHOTO: LUKA GONZALES/AFP/GETTY IMAGES

for science, innovation, and technology and its head will have a seat in the prime minister's Cabinet. The ministry will be led by Michelle Donelan, previously the higher education minister. The shuffle—the latest of many under Conservative leadership since 2010—also creates separate ministries for energy and trade, which were previously combined with science. Commentators said the new structure could bring greater influence and funding to science, but cautioned that the separated ministries may now work less cohesively and compete for resources.

Indonesia head draws heat

LEADERSHIP | The science committee of Indonesia's Parliament is calling on the nation's president to fire the head of its embattled research agency. The demand follows controversy over the government's efforts to consolidate 38 research agencies under the National Research and Innovation Agency (BRIN). After Laksana Tri Handoko became the agency's head in 2021, BRIN laid off hundreds of research assistants and downsized and renamed the prestigious Eijkman Institute for Molecular Biology. Also fueling the complaints was a recent audit that found more than 65% of BRIN's $400 million budget this year is not allocated to research project grants. Handoko has said the agency should prioritize spending on research equipment. His critics include members of a coalition of opposition parties that aims to win the presidency in next year's elections.

Big bridge, lower carbon

CLIMATE SCIENCE | Techniques to capture and store carbon dioxide (CO_2) emitted in manufacturing steel and concrete can reduce global warming, but are expensive. Relative to the total construction costs of a long bridge, however, they can be cost effective, a case study has found. Its authors considered Louisiana's 38-kilometer-long Lake Pontchartrain Causeway, which opened in 1956. CO_2 removal technologies available today could have captured 51% of the gas emitted by factories that made the bridge's steel and concrete while increasing its cost by only 1%, according to a 2 February paper in *Environmental Science and Technology*. The authors say the findings could inform similar cost-benefit analyses for other construction projects. The world's cement and steel industries together account for approximately 15% of global CO_2 emissions.

Progress by degrees

The percentage of U.S. science, technology, engineering, and math (STEM) degree recipients who identify as an underrepresented racial or ethnic minority (URM) increased from 2011 to 2020, but remains below URM's share of the population ages 18 to 34 for all degrees except associate.

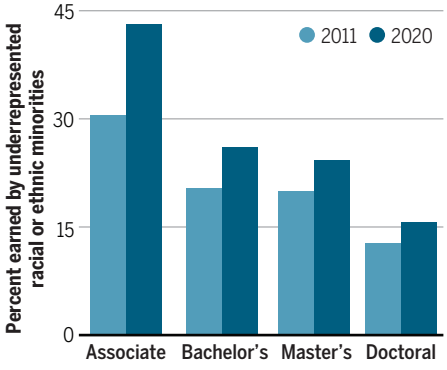

Diversity gains in U.S. STEM

HIGHER EDUCATION | More people from underrepresented racial and ethnic minority groups are earning science, technology, engineering, and math (STEM) degrees at U.S. institutions than ever before, a report indicates. But the many efforts to increase diversity have far to go. Only 16% of STEM Ph.D.s, 24% of master's degrees, and 26% of bachelor's degrees were awarded to Black, Hispanic, American Indian, or Alaska Native students in 2020, according to the report released last week by the National Science Foundation. That is still significantly lower than these groups' total share of the population ages 18 to 34. In a sign that those numbers for graduate degrees may be poised to increase, the agency noted a 56% increase from 2017 to 2021 in the number of Hispanic students pursuing them.

Inhaling soot is a bad chess move

ENVIRONMENT | Chess players who breathe relatively high levels of fine soot particles may be more likely to make mistakes, researchers say. Previous studies have linked fine particulate matter with brain diseases and decreased cognitive function; the new investigation used a controlled method to focus on the pollutants' effects on high-pressure, rapid-fire decision-making. The authors examined 609 chess matches across three different tournaments between 2017 and 2019. They adjusted for the skill level of each player's opponent and used artificial intelligence to assess the quality of each side's moves. (It defined as errors moves that put the player in position to lose.) The research team also used sensors in the competition halls to measure levels of PM2.5 particles—fine particulate matter measuring 2.5 microns or less. The group found that an increase in PM2.5 particles of 10 micrograms per cubic meter raised the probability that players made a mistake by 26%. The scientists found no effect on performance from increased levels of carbon dioxide or temperature. The range of PM2.5 levels measured was similar to those found in U.S. cities. The findings highlight the need for installing air filters that can eliminate the small particles, the authors say. Their study was published last week in *Management Science*.

CREDITS: (GRAPHIC) K. FRANKLIN/*SCIENCE*; (DATA) *DIVERSITY AND STEM: WOMEN, MINORITIES, AND PERSONS WITH DISABILITIES*, NATIONAL CENTER FOR SCIENCE AND ENGINEERING STATISTICS/NATIONAL SCIENCE FOUNDATION 2023; (PHOTO) JUST LIFE/SHUTTERSTOCK

PALEOANTHROPOLOGY

Should an also-ran in human evolution get more respect?

Oldest Oldowan tools—seen as a hallmark of our own genus—found with bones of an unexpected hominin

By **Ann Gibbons**

As thunder boomed and dark rain clouds gathered on the last day of the field season in Kenya in 2017, paleoanthropologist Emma Finestone was rushing to record the location of fossils while excavators were hoisting an ancient hippo skeleton out of the ground. "I was worried she would get struck by lightning because she was on top of a hill," says Tom Plummer, a paleoanthropologist at Queens College who led the excavation at Nyayanga, near Lake Victoria.

Finestone received a shock of a different kind as the hippo was removed. Beneath it, Blasto Onyango, head preparator of the National Museums of Kenya, found a huge hominin molar. It lay intermingled with hammerstones and sharp flakes that Finestone recognized as early Oldowan tools, an ancient technological breakthrough long thought to be a defining hallmark of our genus, *Homo*. But the molar was from a very different human relative: *Paranthropus*, known for its huge teeth and crested ape-size skull, not toolmaking skills. "When we found the *Paranthropus* molar, it got really, really exciting," says Finestone, of the Cleveland Museum of Natural History.

The tools, dated to about 2.8 million years ago, are the oldest known examples of the Oldowan toolkit. They also hint that *Paranthropus*, often seen as an also-ran in the story of human evolution, might have made or at least used tools. "I have been skeptical of *Paranthropus* using stone tools. … But maybe we do have multiple hominins using the Oldowan," Finestone says. "We know very little about the beginnings of stone tools and the emergence of early *Homo*," says paleoanthropologist Sileshi Semaw of Spain's National Research Center for Human Evolution (CENIEH), who is not part of this study. This is "why the Nyayanga discovery is important."

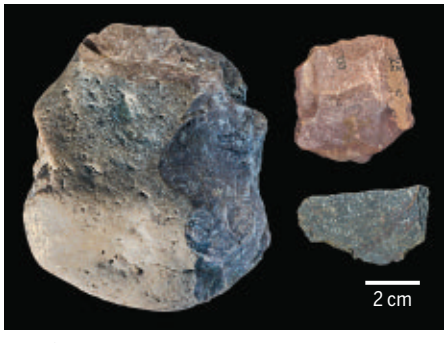

An Oldowan core and flakes were among the tools found near a *Paranthropus* molar.

It's not the first time stone tools have been found with fossils of *Paranthropus*, a genus with several species that lived from about 2.8 million to 1.2 million years ago across Africa. In 1955, Louis and Mary Leakey discovered the Nutcracker Man, a skull with a robust jaw and teeth now classified as *Paranthropus boisei*, in the same 1.8-million-year-old layer of sediments as Oldowan tools. But Mary Leakey soon found a skull of *Homo habilis* (Latin for "handyman") in the same layer and thought that species, in our own genus, was a better fit as the principal toolmaker. *Paranthropus*, with its powerful jaws and teeth, was seen as not needing tools to process tough food. "*Homo* was always given credit for the tools," says paleoanthropologist Bernard Wood of George Washington University.

As more Oldowan tools were discovered across Africa and beyond, most researchers concluded that their appearance coincided with the earliest fossils of *Homo*, dating to 2.8 million years ago in Ethiopia. Many saw the Oldowan as a key technological revolution that helped early *Homo* expand its diet, adapt to different habitats, and rapidly extend its range in Africa and beyond to Asia, where some of the oldest *Homo* fossils are found with Oldowan tools, also known as Mode 1 tools. All of this, the theory goes, helped fuel *Homo*'s expanding brain.

But the 2011 discovery of crude stone tools

IMAGES: (TOP TO BOTTOM) ROMAN UCHYTEL/PREHISTORIC FAUNA STUDIO; T.W. PLUMMER/HOMA PENINSULA PALEOANTHROPOLOGY PROJECT

With its powerful jaws and teeth, *Paranthropus* (shown in a composite photo illustration) was thought to have no need for stone tools to process food.

dating to 3.3 million years ago at Lomekwi in northern Kenya threw a wrench in that neat view. The tools predated *Homo* and showed that an earlier hominin, perhaps *Australopithecus afarensis*, already knew how to make flakes, albeit less sophisticated than those of the Oldowan. Ever since, researchers have been eager to find fossils and tools dating to the roughly 500,000-year gap in the fossil record between 3.3 million years and 2.8 million years ago, says archaeologist Sonia Harmand of Stony Brook University, who reported the Lomekwi tools.

The new tools and molars from Nyayanga fall right in that gap. The ancient butchers left two hippo carcasses, many large-animal bones bearing cutmarks from tools, and 330 artifacts, including blades used to cut meat and plants. Plummer's team used multiple methods to date the site to about 2.8 million years ago, with a range of 2.58 million to 3.03 million years. "They've made a solid case with the evidence they have," says geologist Craig Feibel of Rutgers University, Piscataway.

By that time, toolmakers were already skilled at knapping. "They are not newbies—they have bashed rocks together before," says Peter Ditchfield, a geologist at the University of Oxford who was part of the dating team. "This hints at an earlier stem to the Oldowan."

The site of the discovery, more than 1300 kilometers from the next oldest Oldowan tools in Ethiopia, also shows the technology spread faster and farther than was thought, says Mohamed Sahnouni, an archaeologist at CENIEH who has dated other Oldowan tools to 2.4 million years ago at a site in Algeria. The real "whodunnit" now, says co-author Rick Potts of the Smithsonian Institution's National Museum of Natural History, is: Who was the toolmaker? "We're not claiming that *Paranthropus* made the tools, but I think it could have used them," he says.

But there are other contenders as well. As many as a half-dozen species of *Homo*, *Australopithecus*, and *Paranthropus* lived in eastern Africa at that time. "We're starting to see … lots of different species around that could have been able to make stone tools," Harmand says. "I like the idea that they might have learned directly from each other."

The team will return to Nyayanga this summer to look for answers. "This time period keeps getting more and more interesting," Plummer says. "We have Oldowan tool use extended back, *Paranthropus* extended back, and early *Homo* extended back. It's a time when there's a lot of different lineages at critical points in their evolution." ■

SCIENTIFIC COMMUNITY

Autism researchers face off over language

Terminology dispute underscores divide about what direction the field should take

By **Rachel Zamzow**

A long-smoldering debate among scientists studying autism has erupted. At issue is language—for example, whether researchers should describe autism as a "disorder," "disability," or "difference," and whether its associated features should be called "symptoms" or simply "traits." In scientific papers and commentaries published in recent months, some have decried ableist language among their colleagues whereas others have defended traditional terminology—with both sides saying they have the best interests of autistic people in mind. The vitriol is harming the field and silencing researchers, some fear, but others see it as a long-overdue reckoning.

Since autism's earliest descriptions in the academic literature as a condition affecting social interaction and communication, researchers and clinicians have framed it as a medical disorder, with a set of symptoms to be treated. Historically, autistic children have been institutionalized and subjected to treatments involving physical punishment, food restriction, and electric shocks. Even today, the most widely used autism therapy—applied behavior analysis—is seen by some as a harmful tool of normalization. Many autistic people and their families have instead embraced the view that their difficulties lie not with their autism, but with a society that isn't built to support them.

> **"Specificity is always going to be more rigorous and accurate than generalization."**
> **Monique Botha**, University of Stirling

But according to some autism researchers, the field still too often defaults to terms with negative connotations. For example, in addition to "symptom" and "disorder," many scientists use the term "comorbid" rather than the more neutral "co-occurring" to describe conditions that tend to accompany autism. Similarly, some argue the oft-used phrase "people with autism," as opposed to "autistic person," can imply that autism is necessarily an unwanted harmful condition.

In a recent survey of 195 autism researchers, 60% of responses included views about autistic people the study authors deemed dehumanizing, objectifying, or stigmatizing. Some responses described autistic people as "shut down from the outside world" or "completely inexpressive and apparently without emotions," according to the November 2022 *Frontiers in Psychology* study. "What is worse than I thought was how blatant a lot of the content was, which shows that, for [a] large proportion of participants, they did not consider the things they were saying to be problematic at all," says lead author Monique Botha, a psychologist at the University of Stirling.

Ableist language and the mindset that underlies it also trickles down to study design, says Botha, who is autistic. In studies testing autism interventions, for example, researchers rarely track adverse reactions such as physical harm or psychological distress, found a 2021 study led by Kristen Bottema-Beutel, who studies special education at Boston College. This oversight suggests many researchers see autistic people as less than human, Botha says. "It's one of the most pervasive practices that genuinely keeps me up at night."

At the same time, others argue that making certain terms off-limits stifles the scientific process. "If you can't use words like 'challenging behaviors' or 'severe disorder' or 'symptoms' or 'comorbid disorder,' then how are you supposed to study those things?" asks Alison Singer, president of the Autism Science Foundation, who laid out these concerns in a December 2022 commentary in *Autism Research*. Singer and others, including her three co-authors, fear that using neutral terminology—such as "traits" or "features" in place of "symptoms"—downplays the experiences of autistic people who, like Singer's daughter, have significant difficulty communicating, intellectual disabilities, or critical health concerns. It "trivializes the severity of autism," says Singer, who is nonautistic. Botha, Bottema-Beutel, and 61 other re-

searchers, clinicians, and advocates have submitted a letter to the editor rebutting Singer's commentary.

Singer and others also worry that moving toward neutral language could lead major funding agencies to shift support from research exploring autism's underlying biological causes and potential treatments to other sectors, such as services and supports for autistic people—though whether this would be a positive or negative change is also a subject of debate. For now, the bulk of funding for the field falls squarely on the side of biological research in the United States, as well as in the United Kingdom and Australia.

Amid the ongoing language dispute, researchers on all sides report coming under attack, in the form of vitriolic Twitter exchanges, remarks at conferences, and being shouted down during talks. This increasingly hostile environment threatens to drive some scientists out of the field altogether—something Botha says they have seen firsthand among autistic researchers.

Dehumanizing language is common among autism researchers, psychologist Monique Botha found in a recent study.

"People are getting reluctant to give public presentations or to be too vocal about what they're finding," says David Amaral, a neuroscientist at the University of California, Davis, who is nonautistic. "Science is supposed to be about communication." He wrote a December 2022 editorial in *Autism Research*, for which he is editor-in-chief, calling for civility across the board.

But, Botha says, "Civility is only possible when there is an equal playing field," which can't exist, they say, as long as the field marginalizes autistic people. Zeroing in on the heated nature of the debate is to "entirely overlook what autistic people are saying or protesting."

Some hold more moderate positions, such as Zack Williams, an M.D.-Ph.D. candidate in neuroscience at Vanderbilt University. "If we have the appropriate language to say something in a neutral and nonoffensive way, we should do it by default," says Williams, who is autistic and a co-author of the letter to the editor responding to Singer's commentary. But, "If someone goes and says 'autism spectrum disorder,' they shouldn't be canceled," he says; the focus should be on whether and how the research is helping autistic people.

Others say the field is too fractured to even try to resolve the divide. "I think that we don't have a unified field anymore, and I think the sooner we recognize that the less pain will be there," says Helen Tager-Flusberg, a psychologist at Boston University. Tager-Flusberg, who is nonautistic, and others say one source of the friction is the use of a single set of terms for an extremely heterogeneous condition. She argues for splitting the field and adopting separate terminology. But the autistic community largely thinks dividing them into groups such as "high-" or "low-functioning" is harmful and unnecessarily segregating, according to a December study exploring the language preferences of 654 English-speaking autistic adults across 30 countries.

"I don't get why we can't have common ground," says Bottema-Beutel, who is nonautistic. "I don't think that anyone who is saying we should avoid dehumanizing language is saying we should avoid accurately describing people and what they need."

"Why not just be specific?" Botha asks. For example, if a study's sample includes autistic people who are nonspeaking, have intellectual disability, and require supported living, just say that. Phrasing like this doesn't minimize the very real challenges some autistic people experience—but it also doesn't dehumanize them, Botha says. "Specificity is always going to be more rigorous and accurate than generalization." ■

Rachel Zamzow is a freelance journalist in Waco, Texas.

BIOMEDICINE

Repurposed drug battles 'brain-eating' amoeba

A drug for urinary tract infections may also treat *Balamuthia mandrillaris*

By **Katherine Kornei**

In the summer of 2021, a 54-year-old man was brought to a hospital in Northern California after an unexplained seizure. When an MRI revealed a mysterious mass in the left side of his brain, he was transferred to the University of California, San Francisco (UCSF) Medical Center. A brain biopsy and other tests revealed not a tumor, but an incredibly rare infection of the central nervous system caused by the amoeba *Balamuthia mandrillaris*. One of several "brain-eating" amoebae that occasionally spark headlines, the pathogen kills more than 90% of people who contract it.

But despite initial setbacks, the patient survived and has largely recovered after experimental treatment with a decades-old drug. As his UCSF medical team recounted in *Emerging Infectious Diseases* last month, a desperate hunt for a cure led them to a study published several years ago. In it, researchers showed a drug originally developed in Europe to quell urinary tract infections was effective against Balamuthia in the laboratory. That discovery sent the medical team rushing to obtain the drug, nitroxoline, from abroad so it could be given for the first time to a Balamuthia patient.

Researchers not involved with the case call the man's recovery a breakthrough in treating a brain infection that's long been presumed to be a death sentence. "It's the best that I ever remember seeing with Balamuthia," says Dennis Kyle, a cell biologist at the University of Georgia, Athens, who studies amoebic diseases. The drug, which is not approved for regular use in the United States, has also been effective against other pathogenic amoebae in laboratory tests, according to the UCSF team.

Balamuthia mandrillaris was first identified in 1986—not in a hospital but at the

PHOTO: MONIQUE BOTHA

San Diego Wild Animal Park, where staff were eagerly anticipating the birth of a mandrill, the largest species of monkey. But one day, Nyani, the mother-to-be, began dragging her right arm on the ground. Within 48 hours she became lethargic, and she eventually stopped moving and died. A postmortem evaluation of Nyani's brain tissue revealed hemorrhaging and centimeter-scale lesions. The culprits were plainly visible: Amoebae were eating Nyani's brain.

Researchers later determined the organism represented a new species of amoeba, constituting its own genus. Balamuthia lives in soil, dust, and water, and it's believed to enter the body via the lungs or via skin cuts. (Its full name is a nod to both Nyani's species and the late William Balamuth, a zoologist at UC Berkeley who studied amoebae.)

In the past few decades, only about 100 human cases of Balamuthia have been confirmed in the United States. "The vast majority of doctors, even infectious disease doctors, have never seen a case," says UCSF infectious disease physician-scientist Natasha Spottiswoode.

That was true for her as well until the California man came under her care 2 years ago. Even after his initial MRI results came back, the UCSF medical team, led by Spottiswoode, had no reason to contemplate a Balamuthia infection because brain masses can be caused by a slew of more common ailments such as cancer, bacterial abscesses, and tuberculosis. But after a biopsy of the brain mass revealed what appeared to be amoebae, the team sent a piece of the man's infected tissue to the University of Washington, Seattle, for a polymerase chain reaction (PCR) test that could confirm an amoebic infection and even identify the kind. The results came back positive for Balamuthia.

Spottiswoode and her colleagues started the patient on an aggressive suite of antiparasitic, antibacterial, and antifungal drugs delivered via 47 daily pills and an intravenous drip. But the drug cocktail was somewhat ad hoc, Spottiswoode admits. "It's what's recommended because it was what happened to be used in patients who survived," she says.

It can also be highly toxic: The man's blood sugar levels and white blood cell count both dipped dangerously low, and he suffered from kidney failure. All the while, the man's lesions kept growing. Desperate to save her patient, Spottiswoode began poring over research about Balamuthia.

Balamuthia mandrillaris

One day, she found a 2018 study in the journal *mBio* in which a team led by Joseph DeRisi, a biochemist also at UCSF and president of the Chan Zuckerberg Biohub, had painstakingly screened more than 2100 drugs in the laboratory to identify compounds effective against Balamuthia. The effort, DeRisi recalls, "was inspired by our frustration" of watching an ultimately fatal progression of Balamuthia in a 74-year-old woman being cared for at UCSF.

One compound stood out in their screening: nitroxoline. But DeRisi and his collaborators haven't, until now, had a chance to see it tested in an infected person. Balamuthia cases are so rare, DeRisi says, and "by the time you contact the treating clinical team, the patients are dead."

When Spottiswoode reached out to DeRisi, he urged her on. But nitroxoline is not approved by the Food and Drug Administration, which meant the medical team had to file an Emergency Investigational New Drug application for permission to use it—and then find a source for the drug. Asieris Pharmaceuticals, a company developing nitroxoline to treat bladder cancer, ultimately provided several hundred pills from its R&D facility in Shanghai and has continued to send resupply shipments, all pro bono.

After just 1 week of treatment with nitroxoline, the patient's lesions shrank. Follow-up MRIs have revealed continued improvement, and the patient is now living at home. "I think he's very much on his way to being one of the survivors of this disease," Spottiswoode told a group of her colleagues in October 2022.

The UCSF team has been in touch with the Centers for Disease Control and Prevention about keeping nitroxoline on hand for future use. It should be available as an "emergency standby medication for 24-hour delivery anywhere in the United States," DeRisi says. But to save patients, doctors also have to rapidly diagnose a Balamuthia infection. Currently, a clinician must suspect an amoebic infection in the first place and then order a specific PCR test.

"If you don't think of what's there, then you'll never find it," says Michael Wilson, a neurologist at UCSF and a member of the research team.

He notes that a technique called metagenomic next-generation sequencing, pioneered by DeRisi, could speed diagnosis. The approach involves sequencing genetic material from a patient sample and comparing it with enormous libraries of genetic code from millions of known pathogens. "You let the database match tell you what organisms are in there," Wilson says. "You're not going in with a preconceived notion."

Spottiswoode and her colleagues are now working with other doctors overseeing Balamuthia cases. Just recently, a second patient was started on the drug, and the initial results are already encouraging, she says. Spottiswoode is hoping her frantic search will have a lasting payoff for other Balamuthia patients. "For every patient who exists with this disease, there's a team of doctors where I was, which is basically desperate to find something that will help." ■

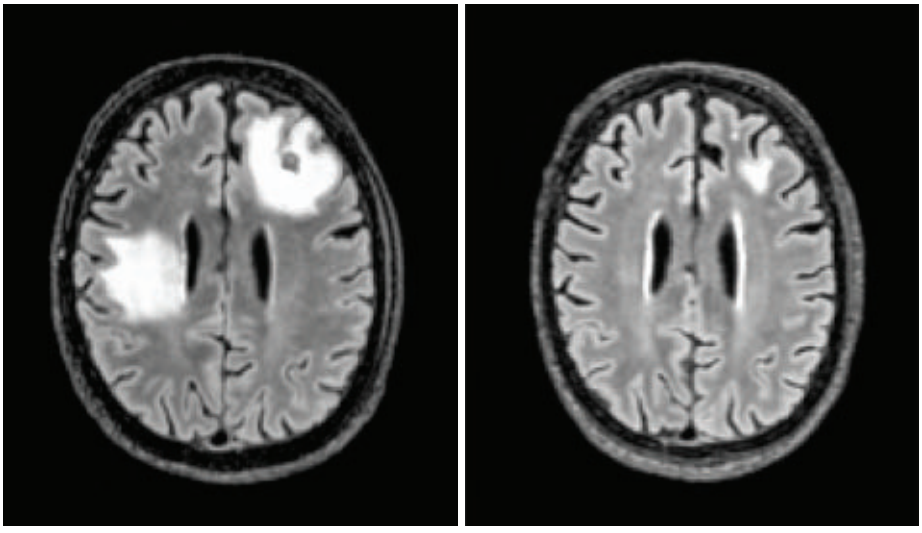

MRI scans of a man whose brain was infected with the amoeba *Balamuthia mandrillaris* show a dramatic difference in inflammation (white) before and after (right) treatment with an experimental drug.

PHOTOS: (TOP TO BOTTOM) K. YAMANOUCHI, H. ARIMA, Y. SAKAMOTO *ET AL.*/WIKIMEDIA COMMONS; N. SPOTTISWOODE *ET AL. EMERG. INFECT. DIS.* (1) 197-201 (2023)

Katherine Kornei is a journalist based in Portland, Oregon.

COVID-19

Could a popular antiviral supercharge the pandemic?

Molnupiravir appears to be speeding SARS-CoV-2 evolution

By **Robert F. Service**

A widely used COVID-19 drug may be driving the appearance of new SARS-CoV-2 variants, sparking concerns it could prolong the pandemic. The drug, molnupiravir, produced by Merck & Co., is designed to kill the virus by inducing mutations in its genome. A survey of viral genomes reported in a new preprint, however, suggests some people treated with the drug generate novel viruses that not only remain viable, but spread.

"It's very clear that viable mutant viruses can survive [molnupiravir treatment] and compete [with existing variants]," says virologist William Haseltine, chair of ACCESS Health International. "I think we are courting disaster." But a Merck spokesperson disputes that the drug has led to the emergence of widely circulating variants, and some researchers downplayed the significance of molnupiravir-caused mutations. "Right now, it's much ado about nothing," says Raymond Schinazi, a medicinal chemist at the Emory University School of Medicine, noting that the virus is already mutating rapidly.

Molnupiravir was authorized in the United Kingdom and the United States in late 2021, and dozens of other countries have followed. In 2022, Merck estimated global sales at more than $5 billion. Though that is well below the $18.9 billion in 2022 sales for Paxlovid, another oral SARS-CoV-2 antiviral, molnupiravir remains popular in certain countries.

From the start, however, Haseltine and others worried about the drug's mechanism, which involves introducing so many mutations into the viral genome that it can no longer reproduce. One fear was that mutated virus would survive and propagate—and perhaps turn out to be more transmissible or virulent than before. Before the U.S. Food and Drug Administration authorized the drug, a Merck spokesperson called the worry "an interesting hypothetical concern."

Nevertheless, researchers and citizen scientists from around the globe began to scan SARS-CoV-2 genome sequences deposited in the international GISAID database, looking for the kinds of mutations expected to be caused by molnupiravir. Rather than inducing random changes in the virus' RNA genome, the drug is more likely to cause specific nucleic acid substitutions, with guanine switching to adenine and cytosine to uracil.

One virus hunter, Ryan Hisner, a middle school science and math teacher in Monroe, Indiana, identified dozens of sequences that showed clusters of those hallmark substitutions. Hisner raised his concerns on Twitter and ultimately teamed up with Thomas Peacock, a virologist from Imperial College London. With other colleagues, the pair systematically reviewed more than 13 million SARS-CoV-2 sequences in GISAID and analyzed those with clusters of more than 20 mutations. In a preprint posted on 27 January, they report that a large subset showed the hallmark substitutions; all dated from 2022, after molnupiravir began to be widely used.

These signature clusters were up to 100 times more common in countries where molnupiravir was widely used than in those where it was not (see graphic, above). Tracking the dates and locations of the sequences showed some of the mutated strains were spreading in the community. "Clearly something is happening here," Peacock says.

Whether the changes will lead to variants that are more pathogenic or transmissible is unclear, the researchers say. "We are not coming to a conclusion about risk," says team member Theo Sanderson, a geneticist at the Francis Crick Institute. Haseltine, however, likens the danger to keeping a pet lion. "Just because it didn't bite you yesterday doesn't mean it won't bite you today," he says.

The Merck spokesperson says the link between the mutations and the drug is unproved. "The authors … rely on circumstantial associations between viral sequence origin and time frame of sequence collection," she says. But the new result comes on the heels of two others that could change the risk-benefit calculus for the drug.

In one, researchers in Australia found evidence that molnupiravir treatment may be leading to new variants in immunocompromised patients. Because these patients' immune systems have trouble clearing the virus, viral variants can accrue large numbers of mutations, possibly causing big leaps in viral behavior. Repeatedly sequencing SARS-CoV-2 genomes from nine patients, five of whom received the drug and four who did not, the researchers found that treated individuals harbored an average of 30 new variants each within 10 days of the initial dose, far more than the untreated patients. "Our study demonstrates that this commonly used antiviral can 'supercharge' viral evolution in immunocompromised patients, potentially generating new variants and prolonging the pandemic," the authors wrote in a 22 December 2022 preprint.

A second report, on 28 January in *The Lancet*, suggests that, at least among people vaccinated against COVID-19, molnupiravir offers limited benefits. The study tracked 26,411 vaccinated participants in the United Kingdom's PANORAMIC clinical trial, roughly half of whom were given the drug. It did reduce symptom severity and improve recovery times, but it did not lower the frequency of COVID-19–associated hospitalizations or deaths among high-risk adults.

The new studies don't prove molnupiravir is causing the emergence of dangerous new SARS-CoV-2 variants, says Ravindra Gupta, a clinical microbiologist at the University of Cambridge. But he argues the drug's limited benefit suggests it's no longer worth the risk. "These results do call into question whether molnupiravir should be used." ■

A drug's fingerprint?

An analysis of SARS-CoV-2 genomes submitted to a global database shows guanine-to-adenine mutations, often induced by molnupiravir, are more common in countries where the drug is widely used, such as Australia, the United Kingdom, and the United States, than in countries where molnupiravir use is low, such as Canada and France.

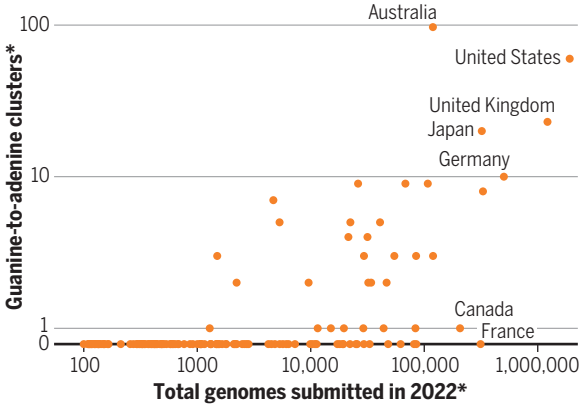

*Logarithmic scales were used for the axes. Countries with fewer than 100 total genomes submitted in 2022 were excluded.

CREDITS: (GRAPHIC) K. FRANKLIN/*SCIENCE*; (DATA) T. SANDERSON *ET AL.*, MEDRXIV, HTTPS://DOI.ORG/10.1101/2023.01.26.23284998 (2023)

Ornithologist Francisca Helena Aguiar-Silva (right) tracks raptors in Brazil. She and others aim to improve work on neotropical birds such as the black-fronted piping guan (left).

PHOTOS: (LEFT TO RIGHT) DANIELA ZAFFIGNANI; OLIVIER JAUDOIN

ORNITHOLOGY

Neotropical bird scientists call for an end to bias

Two manifestos offer recommendations for shifting field's flawed "northern lens"

By **Emiliano Rodríguez Mega**

Two years ago, some ornithologists were outraged by the publication of a paper that highlighted how much scientists still don't know about birds from Latin America and the Caribbean. Many criticized the authors—based at universities in the United States and the United Kingdom—for citing few studies by scientists from the region and from journals that don't publish in English. Others said the paper, published in *Ornithological Advances*, perpetuated an elitist, exclusionary, "northern" approach that overlooked, for instance, the knowledge of Indigenous people.

"It made me angry," recalls bird ecologist Ernesto Ruelas Inzunza of the University of Veracruz in Xalapa, Mexico. "Deliberately or not," he says, the article ignored "that today's neotropical ornithology is nurtured by Latin American and Caribbean scientists." He and others vowed to change that, by smashing barriers they say have disadvantaged ornithologists from neotropical nations and deprived the field of their contributions. This week, their resolve bore fruit in two papers published in *Ornithological Applications*.

In one, 124 authors from the region examine numerous factors—including a shortage of funding, few Latin American ornithologists in leadership roles, and a bias against citing papers in Spanish and Portuguese—they say have often marginalized the region's researchers. In the other, a smaller group offers 14 recommendations for how the field's major journals can revise their policies and practices to improve the flow of science from the region's bird scientists.

Both papers identify "language hegemony," the use of English by major journals, as a problem. Few people in neotropical nations are native English speakers, the authors note, so journals often ask researchers from the region to have their manuscripts edited by a professional. But that can cost up to $600—more than many Latin American scientists make in a month. To lower the language barrier, the authors recommend journals accept manuscripts in Spanish and Portuguese for review, then translate them into English if accepted for publication—and also consider publishing a version in a second language.

Language hegemony also hinders clear communication about bird names and imposes a "northern lens" on the field, the authors say. Journals and meetings often require the use of English names, they note, "rather than the scientific (Latin) names that are supposed to be a global standard." Such rules not only require Latin American researchers to learn the English names, which were often imposed by Europeans studying museum specimens, but also discourage the use of names developed by Indigenous people, which can carry valuable information about how a bird sings or where it lives.

"We continue to legitimize the idea that what's important is European knowledge," says Kristina Cockle, a Canadian ornithologist at the Institute of Subtropical Biology in Argentina, where she has lived for nearly 20 years. She and her co-authors urge funders and others to encourage collaboration with local communities, including by allowing nonacademics to help develop research questions, co-lead projects, and author papers.

Funders and others also need to do more to encourage studies of the basic biology of neotropical birds, the authors say. Descriptive information, such as a bird's diet or behavior, is often foundational to broader insights into ecology and evolution, they note, and much of it comes from fieldwork in the neotropics. But such work is often ineligible for funding and can be hard to publish in key journals, which favor studies of ecology, biogeography, or conservation.

The papers offer examples of how a lack of data from the neotropics has allowed flawed ideas to linger. In the 1990s, North American researchers published an influential study indicating neotropical birds thought to be monogamous cheated on their partners less often than monogamous species in temperate regions. But Valentina Ferretti, an evolutionary ecologist at the Institute of Ecology, Genetics, and Evolution in Argentina, noted the study's sample included few neotropical species. In 2019, after adding data that she and other researchers had gathered on additional species, she found there was no clear geographic pattern. "It's a mistake to come up with theories that are based on only a minority of bird diversity," Ferretti says.

The papers "will undoubtedly sensitize" ornithologists from the north about the challenges their colleagues face in the south, says ornithologist Joseph Wunderle of the U.S. Forest Service, who is based in Puerto Rico.

The lead author of the 2020 study that ignited the discussion, ornithologist Alexander Lees of Manchester Metropolitan University, says he hopes the new papers catalyze change. Initially, he felt stung by the criticism, particularly because he has collaborated for decades with local researchers in the Brazilian Amazon. Now, he thinks his paper could produce "a bit of a funny legacy. … [I]f it means that the field grows and becomes more inclusive, then, you know, I'll take that." ■

Emiliano Rodríguez Mega is a journalist in Mexico City.

ATMOSPHERIC SCIENCE

Global alarm system watches for methane

Artificial intelligence–powered scans of satellite data detect leaks of the greenhouse gas

By **Paul Voosen**

Methane is a stealthy greenhouse gas, erupting unpredictably from sources such as pipelines and gas fields. Scientists have wanted to catch these emitters in the act. In the past, watchdogs had to monitor likely sites from the ground or by airplane. Now, massive, short-lived leaks can be detected automatically, from space, anywhere in the world—a first step toward plugging them and slowing climate change.

The new technique, which uses artificial intelligence (AI) to scan through the 12 million daily observations collected by a European satellite, could aid future efforts to spot plumes in data collected by satellites, such as the International Methane Emissions Observatory announced in 2021 by the United Nations. Although so far the technique only captures the largest blowouts, there's no better place to begin, says Ilse Aben, an atmospheric scientist at the Netherlands Institute for Space Research (SRON) and co-author of the new work. "That's the low-hanging fruit," she says. "If you're putting in the effort to stop leaks of methane, better to start with the big ones."

The SRON team behind the work, which appeared last month as a preprint in the journal *Atmospheric Chemistry and Physics*, has now begun posting its weekly results on its website. Last month alone, they detected 192 methane plumes—some persistent, some intermittent—with an emissions rate greater than 10 tons per hour, concentrated in Asia but popping up on every continent except Antarctica.

Although methane in the atmosphere lasts for little more than a decade before decomposing, it is far more effective at trapping heat than carbon dioxide (CO_2). Since 2006, atmospheric methane levels have grown some 7%, and the gas is responsible for roughly one-third of the 1.2°C of warming since preindustrial times. As the world approaches 1.5°C, the presumed threshold of "dangerous" warming, action to reduce methane releases has been seen as a way to buy a bit more breathing room to achieve longer term CO_2 cuts.

In the past, researchers had to target locations already known to have methane releases to find new ones, says Riley Duren, a remote-sensing scientist at the University of Arizona and CEO of Carbon Mapper, a $100 million project that later this year will launch a pair of satellites designed to spot plumes of methane and CO_2. The new technique, he says, "helps lay the foundation for future operational monitoring with the expanding global ecosystem of methane satellites."

Pinpointing a source

A plume of methane over southern New Mexico was detected from orbit. A new technique automates the search for leaks of the potent greenhouse gas.

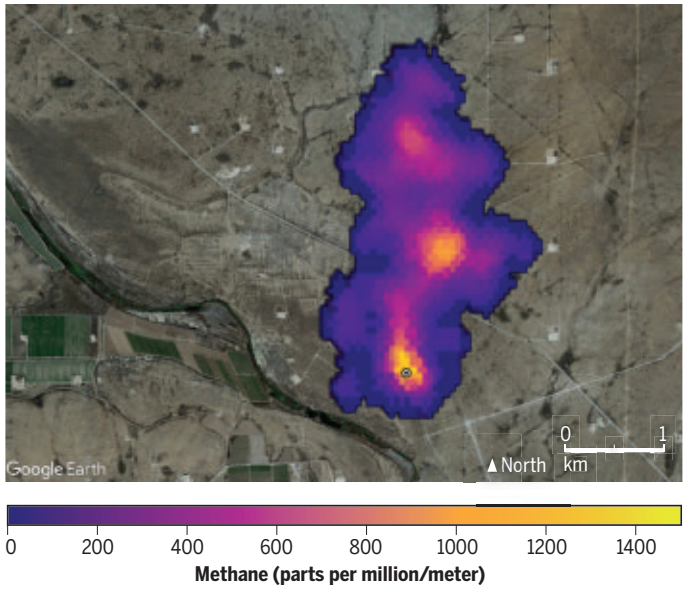

SRON's automatic methane spotter relies on the Tropospheric Monitoring Instrument (TROPOMI) aboard the Sentinel-5 Precursor satellite, launched in 2017 as part of Europe's Copernicus program of Earth observation. Designed to monitor atmospheric pollution, TROPOMI's spectrometer has also proved capable of detecting the infrared glow of methane. Investigators began to use the spectrometer to monitor regions already known to be large methane sources. But Aben says they realized the satellite's frequent global coverage should enable it to sound the alarm about any large methane releases.

The problem was the sheer volume of data, which made it hard to spot the plumes. Berend Schuit, a doctoral student at SRON, turned to AI for help. First he went through years of TROPOMI data, ending in 2020, identifying some 800 scenes of confirmed plumes, along with 2000 scenes without them. Armed with these scenes, Schuit and his colleagues trained their AI algorithm to recognize the plumes. But it spat out too many false positives, often caused by artifacts such as the stray edge of a cloud. Eventually, they were able to produce a reliable filter by training a second AI to spot signs that a result might be spurious, such as an increase in reflectivity from clouds or an inconsistency between the wind direction and the path of a "plume."

The team then tested the algorithms on TROPOMI's measurements from 2021, finding 2974 unique methane plumes that they could confidently identify from just one satellite pass. More than 40% were associated with oil and gas development, another one-third with landfills, and 20% with coal mines.

TROPOMI's roughly 5-kilometer resolution is not fine enough to spot the precise facility responsible for each plume. But data from future satellites should sharpen the pictures. This constellation will grow rapidly in the next few years, including with the launch of the Environmental Defense Fund's MethaneSAT later this year, followed by Carbon Mapper and other satellites with even higher resolution.

Methane measurements from space have weaknesses, including difficulty distinguishing fresh plumes from gas already in the air, says Xin Lan, a carbon cycle scientist at the Earth System Research Laboratories of the National Oceanic and Atmospheric Administration. And much of the recent methane rise has come not from individual large emitters, but from more distributed sources, including tropical wetlands, which could be emitting more methane in response to warming. But this warning system is still welcome, Lan says. "The ability to detect emissions," she says, "is the first step for action to reduce them." ■

GRAPHIC: NASA/JPL-CALTECH. ADAPTED BY C. BICKEL/*SCIENCE*

eppendorf & Science

PRIZE FOR NEURO BIOLOGY

2022 Winner
Ann Kennedy, Ph.D.
Northwestern University Feinberg School of Medicine, Chicago, USA
For research on brain activity underlying aggression

Tell the World About Your Work!

Application Deadline
June 15, 2023

Eppendorf & Science Prize for Neurobiology
The annual Eppendorf & Science Prize for Neurobiology is an international prize which honors young scientists for their outstanding contributions to neurobiological research based on methods of molecular and cell biology. The winner and finalists are selected by a committee of independent scientists, chaired by *Science*'s Senior Editor, Dr. Peter Stern. If you are 35 years of age or younger and doing great research, now is the time to apply for this prize.

As the Grand Prize Winner, you could be next to receive
> Prize money of US$25,000
> Publication of your work in *Science*
> Full support to attend the Prize Ceremony held in conjunction with the Annual Meeting of the Society for Neuroscience in the USA
> 10-year AAAS membership and online subscription to *Science*
> Complimentary products worth US$1,000 from Eppendorf
> An invitation to visit Eppendorf in Hamburg, Germany

It's easy to apply! Write a 1,000-word essay and tell the world about your work. Learn more at:

eppendorf.com/prize

eppendorf Science AAAS

AAAS® and Science® are registered trademarks of the American Association for the Advancement of Science, USA. Eppendorf® and the Eppendorf Brand Design are registered trademarks of Eppendorf SE, Germany. All rights reserved, including graphics and images. Copyright © 2023 by Eppendorf SE. Photography: Saverio Truglia.

OCEANS AWAY

Is raising salmon on land the next big thing in farming fish?

By **Erik Stokstad**, *in Northfield, Wisconsin*

When drivers on Highway 94 pass this tiny town, some are struck by a mysterious nocturnal glow. Pink light emanates from the world's largest aquaponic greenhouse, which can produce up to 2 million kilograms of salad greens each year. Less obvious, but also unique at this scale, is the source of the nutrients used to fertilize the crops: wastewater flowing from huge nearby tanks teeming with Atlantic salmon. The silvery fish grow indoors, far from the ocean where wild salmon normally spend the bulk of their lives.

On a recent winter day, the surrounding farmland blanketed in snow, Steve Summerfelt opened the door to the fish house. Hundreds of meter-long fish swam vigorously in each house-size tank, while an overhead crane delivered a 1-ton sack of feed into an automated dispenser. Rumbling pumps and tanks filled with sand, separated from the fish tanks by a soundproof wall, treated wastewater that had been stripped of fish poop. Nitrogen and phosphorus were diverted to the vast greenhouse while cleansed water recirculated to the salmon. "Sometimes the water is so clean it looks like the fish are swimming in air," says Summerfelt, an engineer who is head of R&D at the company, called Superior Fresh.

The sprawling facility is just one of dozens of indoor salmon farms that have sprung up around the world in recent years, as investors have pumped money into what many see as the next big thing in farmed fish. Over the past decade, global sales of pink-fleshed farmed salmon have nearly doubled to $12 billion, and demand is expected to keep growing. Traditionally, that bounty has been raised in large floating cages, called net pens, located in coastal waters. But environmental concerns and limited room for expansion have prompted companies to explore moving operations ashore.

"Industry is realizing that this is a way to expand," says Chris Good, head of research at the Conservation Fund's Freshwater Institute, a nonprofit research institute that supports sustainable aquaculture. Firms are fine-tuning technologies they hope will ultimately enable them to raise huge numbers of salmon in land-based facilities. These cold-water fish can already be found in some improbable places, including semitropical Florida and the arid Gobi Desert.

For salmon farming to flourish on land—and compete with existing sources—firms will have to overcome some formidable challenges, including dealing with the fish waste and developing salmon variants that thrive in tanks. Growing salmon, says Karl Øystein Øyehaug, chief operating officer of Atlantic Sapphire, another land-based farming firm, "is much, much more complicated" than farming other seafood species. The challenges are driving vigorous research efforts at universities and government laboratories.

Here in rural Wisconsin, Summerfelt—who spent 26 years conducting aquaculture research at the Freshwater Institute—has helped launch a salmon ranch that is putting innovative solutions into practice. These fish, unlike those at most salmon farms, never touch a drop of saltwater. The filters that purify the water use cheap sand instead of the costlier materials often found elsewhere. And instead of simply dumping its waste, Superior Fresh recycles it as fertilizer for the crops in that huge glowing greenhouse.

Summerfelt believes such approaches are key to making land-based salmon farms both economically viable and environmentally sound. They've also made him something of a maverick in the industry. Still, Summerfelt "has had a huge influence," says Bendik Fyhn Terjesen, a fish physiologist with the Cermaq Group in Norway, a leading producer of farmed salmon. "All people in industry know him and his work."

ALTHOUGH SALMON is considered seafood, wild salmon are no strangers to land. The hatchlings begin their lives in coastal streams, where females lay thousands of eggs each. The new generation heads downstream to the ocean as hand-size smolts. Adult fish typically wander the high seas for several years before returning to their home streams to spawn.

PHOTO: NARAYAN MAHON

Life in a tank can help salmon grow faster, and with a lower risk of disease, by providing optimal conditions.

In the 1730s, a German naturalist began taking salmon eggs from streams and trying to hatch them. Less than a century later, Europeans were building hatcheries to mass raise fish to supplement declining wild stocks. These efforts didn't have much success, but in the 1960s they fueled the emergence of the salmon farming industry. Norwegian farmers began to use cages floating in fjords to raise Atlantic salmon, fattened on special feed. The cold, clean water was just what the fish were used to, and they were protected from predators. Today, fish raised in net pens, particularly off Norway and Chile, account for 70% of the 3.7 million tons of salmon eaten worldwide each year.

Even as the industry has boomed—and consumer demand shows no signs of slackening—it has begun to face constraints. Prime nearshore areas are often already filled with pens, and some coastal communities have resisted new farms, concerned about their impact on views, recreational boating, and commercial fishing. Researchers, regulators, and environmental groups have raised alarms about the pollution produced by tightly packed fish, as well as the parasitic lice and diseases that can spread from farmed to wild salmon. They also note that escapees can breed with wild fish, potentially weakening the genetic makeup of native stocks. Such concerns have led some areas, including British Columbia and Washington state, to consider barring or restricting new coastal fish farms.

These developments have catalyzed efforts to grow salmon entirely on land in using what is known as a recirculating aquaculture system. The approach offers several advantages, researchers say. Land-based facilities can help managers control environmental conditions and reduce disease risks, and they don't face the same space limits as ocean farms. Production can also be moved closer to markets, and in principle growing salmon on land could contain the risks of pollution.

AquaBounty, a firm with corporate headquarters in Maynard, Massachusetts, has long anticipated growing salmon in tanks. In 1991, the company began to commercialize a strain of Atlantic salmon genetically engineered for faster and more efficient growth. When U.S. and Canadian regulators finally approved the fish for sale years later, they required that the salmon be raised entirely on land to prevent interbreeding with wild fish. The company is now raising up to 1450 tons at two farms, in Indiana and on Prince Edward Island, and building a third in Ohio.

Over the past decade, investors have poured billions of dollars into new land-based salmon farms. Atlantic Sapphire has some of the largest ambitions, aiming to grow 220,000 tons a year by 2031. The company's Norwegian founders wanted to raise and sell salmon near North American markets to avoid the need for expensive and carbon-intensive air freight from Norway. "We refer to it as the insanity of the salmon market," Øyehaug says.

The company decided to set up shop in Florida, near the Everglades. It might seem like an unlikely location, but executives say the site has some hidden advantages: They can pump freshwater for newborn salmon from one aquifer, pump saltwater from a different aquifer for the smolts that normally move to the ocean, and then inject the wastewater into a separate cavern. "What we're doing involves micromanaging a huge number of different water quality parameters that all need to be perfect," Øyehaug says. Getting it right can be tricky. In 2021, about 500,000 salmon died at the Florida facility after a clogged drain increased turbidity that may have generated deadly gases. The company's output that year was just 2400 tons, far short of its long-range target. (Superior Fresh sells about 680 tons of salmon per year.)

Other companies have faced protests over plans to build salmon farms in Maine and California. Some communities fear the farms will deplete precious groundwater, or pollute aquifers or surface waters with their waste. In Maryland, one firm canceled plans to build a farm after scientists said its wastewater could harm endangered sturgeon.

NOW 59, Summerfelt eats salmon at least 4 days a week. When he had his blood tested, his levels of omega-3 fatty acids, healthful compounds found in oily fish, were "off the chart," he says. He has spent decades thinking about how to farm fish in a more sustainable way. In the late 1980s, after studying chemical engineering, he was looking for a doctoral project. His father, a fish biologist, suggested looking at the feasibility of converting abandoned wastewater treatment plants into aquaculture farms. "That sounds fun," he remembers thinking. After wrapping up the project, his first job was at the Freshwater Institute.

Summerfelt eventually became director of aquaculture research at the institute and helped develop a demonstration unit, the largest at that time, for growing Atlantic salmon commercially. In 2013, he was contacted by Brandon Gottsacker, a recent graduate of the University of Wisconsin, Stevens Point, who was interested in setting up a fish farm. Gottsacker spent a year studying at the Freshwater Institute, and then he and Summerfelt drew up the plans for Superior Fresh, which is backed by Karen Wanek and her husband Todd Wanek, owner and CEO of Ashley Furniture, the world's largest furniture manufacturer.

Steve Summerfelt (left), now at Superior Fresh (right), has helped enable farming of Atlantic salmon entirely on land.

The firm began to raise salmon in a pilot-scale plant in 2016. Two years later, Summerfelt left the Freshwater Institute to join Superior Fresh full time. "I finally said, 'I want to jump in,' because I couldn't see anyone else in the industry doing it right." The plant has since expanded 10-fold; now, a dozen tanks each hold up to 50,000 kilograms of fish at harvest.

Designing Superior Fresh gave Summerfelt a chance to realize some of his unorthodox ideas. One involved dealing with waste, a

PHOTOS: (LEFT TO RIGHT) NARAYAN MAHON; SUPERIOR FRESH

Salmon and salad

New land-based salmon farms have environmental advantages over marine production. But they face the challenge of dealing with the waste from the many salmon in tanks. One company, Superior Fresh, recycles the water and converts fish waste into fertilizer for an adjacent greenhouse. The rest is added to fields.

1 Indoor facility
Tight biosecurity lowers the risk of disease introduction. Isolation from wild salmon means farmed fish can't spread parasites or viruses.

2 Fish tanks
Optimal growing conditions mean high growth rates and year-round production. Welfare is easier to monitor.

3 Water treatment filters
Microbes convert toxic ammonia to nutrients for plants. Managers can adjust conditions for fish health, for example, by adding oxygen.

4 Aquaponic greenhouse
Salad greens grow in pallets that float in water from the fish tanks. Plants take up nutrients and provide extra revenue.

5 Local efficiency
Land farms use more power than sea pens, but can be closer to markets. Shipping fish by truck rather than air boosts overall energy efficiency.

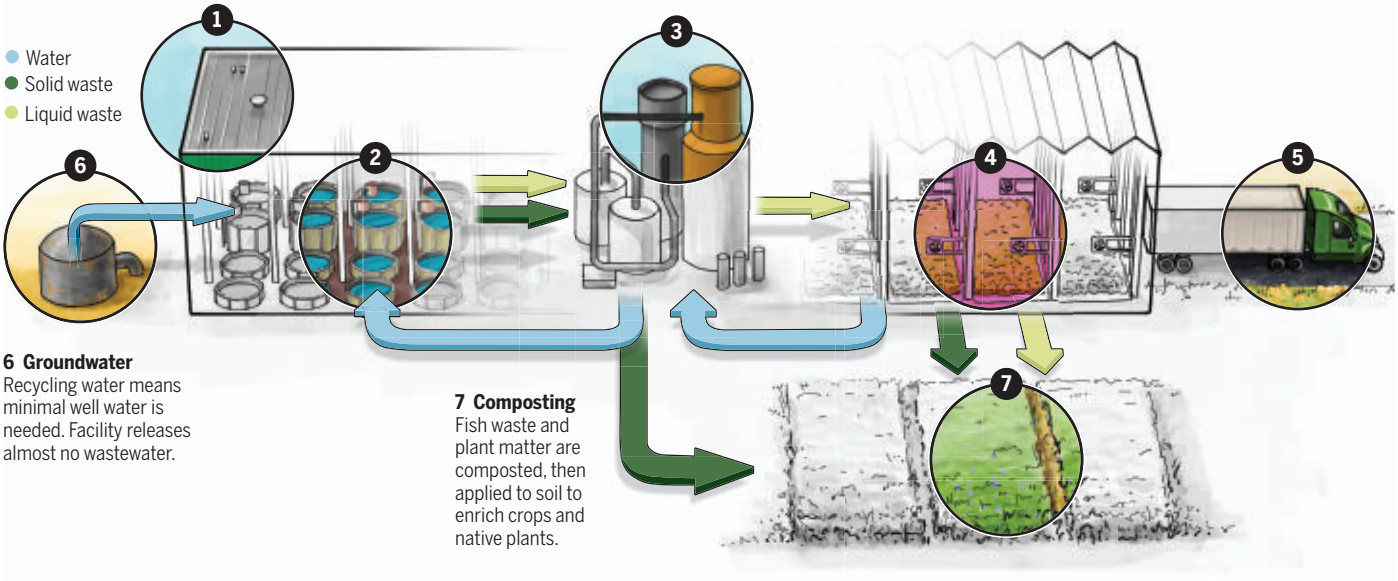

6 Groundwater
Recycling water means minimal well water is needed. Facility releases almost no wastewater.

7 Composting
Fish waste and plant matter are composted, then applied to soil to enrich crops and native plants.

problem facing all factory farms with confined animals. In net-pen aquaculture, up to 80% of the phosphorus and 60% of nitrogen in the feed is wasted as some drifts away uneaten and the fish excrete unused nutrients. The leftover nutrients can fuel harmful algal blooms and acidification of coastal water.

On land, salmon farmers have other options. Atlantic Sapphire, for example, landfills solid waste and pumps liquid waste underground. Other companies convert their wastes to biogas, which is burned for energy. To extract as much value as possible from the nutrients, Superior Fresh uses them to grow greenhouse crops sold in about 2000 supermarkets and convenience stores. They also restore soil nutrients in nearby fields.

Microbes in the indoor tanks can transform the toxic ammonia in wastewater into nitrate, a form of nitrogen that can be used by plants. Most land-based salmon farms rely on a technology called a moving bed bioreactor to purify the water. It uses countless small plastic chips that swirl in bubbling water, providing a substrate for the microbial communities. Summerfelt, however, had long studied a different approach: using biofilters containing sand grains, which provide a much greater surface area for microbes to colonize. Sand is also cheap and readily available.

Inside Superior Fresh's fish house, Summerfelt's 6-meter-tall sand biofilters tower over a sump the size of a swimming pool. Large pumps constantly push water up through the grains. "The whole technology is based on injecting the water underneath it to lift it continuously, so the sand bed doesn't ever collapse," Summerfelt says. Superior Fresh keeps other aspects of the filtration system confidential and prohibits photographs.

Unlike at most other farms, the salmon at Superior Fresh spend their entire lives in freshwater. Everything is simpler without salt, Summerfelt says. Freshwater means less corrosion of metal pumps and pipes, and less risk in using ozone to purify the water; in saltwater, ozone can cause the buildup of toxic bromine. The absence of salt also makes dealing with waste easier, because biosolids can be composted and liquids diverted to nearby farm fields—a nonstarter if they were contaminated with salt.

Other firms don't share Summerfelt's enthusiasm for either approach. They suggest that although freshwater might be simpler, it's not necessarily optimal for the fish. Young salmon get a growth spurt when they first encounter salinity, and brackish water is optimal for salmon's regulation of water and ions. In freshwater, they must expend more energy keeping the right balance, potentially slowing their growth. Brackish water can also inhibit bacterial diseases. And some producers feel saltwater improves the taste.

Using sand as a filter can be problematic as well, researchers say. "When operating properly, it's great," says animal health specialist Deborah Bouchard, who directs the Aquaculture Research Institute at the University of Maine, Orono. But if a disease outbreak strikes, sand can be much more difficult to disinfect. Terjesen adds another concern: "If sand gets out of your biofilter then you are in big, big trouble with your pumps, which will break down immediately."

TANKS FULL OF SALMON in another unlikely location—a basement in downtown Baltimore—are a testing ground for other approaches to raising healthy fish efficiently on land. There, fish reproductive physiologist Yonathan Zohar of the University of Maryland's Institute of Marine and Environmental Technology (IMET) recently tossed a handful of brown pellets into a 4-meter-wide tank. "Be careful, the fish—they splash," he said as several hundred large salmon lunged for the food. The scene is part of a $10 million consortium, funded by the U.S. Department of Agriculture in September 2021. Led by Zohar, who specializes in aquaculture, the partners are working on a range of biological and engineering challenges.

One is water quality. The tank was surrounded by a humming, bubbling, and frothing tangle of filtration pipes and equipment. Zohar and his colleagues are

GRAPHIC: V. ALTOUNIAN/*SCIENCE*

Pink lights help Superior Fresh's leafy greens grow through the night in the world's largest aquaponic greenhouse.

PHOTO: SUPERIOR FRESH

studying the microbes that live inside these filters, ultimately hoping to develop bacterial communities that are tailored to the specific fish strains, feed, and conditions used in land-based farms, which could make it easier to maintain water quality. "With optimal microbes the process becomes faster and more efficient," says Keiko Saito, a microbiologist at IMET. "It's balanced like an ecosystem in nature."

Nearby, Ph.D. student Matthew Stromberg, an avid angler and tinkerer, fiddled with the controls of a purification chamber, a shoulder-height blue metal tank. He is testing a system that relies on ultraviolet (UV) light and a titanium catalyst to break down the water-borne chemicals that can give land-reared salmon a muddy flavor. Bacteria that grow in biofilms produce these metabolites, geosmin and 2-methylisoborneol, and they can be eliminated by purging salmon in separate tanks with clean, untreated water. But this step adds time and cost. Summerfelt is also testing the UV system at Superior Fresh. Last year, he and others reported in *Aquacultural Engineering* that the system, manufactured by Exciton Clean, efficiently reduces the unwanted molecules.

In a separate room, Zohar and his colleagues are working to optimize salmon for spending their entire lives in captivity. Here, trays containing thousands of translucent orange salmon eggs, each the size of a pea, sit in refrigerated chambers. The eggs come from adult salmon in nearby tanks, which were bred by research partners in Maine. As part of ongoing trials, Zohar and his IMET colleague Ten-Tsao Wong will immerse some of the unfertilized eggs in a bath containing antisense RNA, to disrupt the development of the gonads.

The goal is to prevent a salmon's sexual maturation, so that the fish instead continue to invest their energy in muscle growth, ensuring large fillets. The researchers note that sexually immature fish are also less sensitive to stress, which can make their flesh less appealing. Ultimately, antisense might be used in commercial operations to prevent maturation without genetically modifying the fish.

FOR OCEANGOING FISH confined to tanks, stress is a constant risk, especially when they are handled. "When the fish don't want to be moved, they can really hurt themselves," says Åsa Maria Espmark, an aquaculture researcher with Nofima, the Norwegian food research institute.

Summerfelt and his colleagues are keenly interested in keeping their fish calm. The biggest challenge comes when the growing fish must be moved to the largest tanks, which requires a large centrifugal pump. The somersaulting journey can leave some fish bruised and unwilling to eat for days.

When it is time to harvest Superior Fresh's salmon, workers in waterproof clothing use a long-handled net to carefully lift the fish onto a portable sluiceway. Within seconds, they land in a machine that stuns them. Within a day, the cleaned fish are being trucked to market, where they can fetch well over $10 per kilogram.

That's about twice the price of the cheapest pen-raised salmon. And analysts say it will likely be difficult for land-based farms to compete on cost. But Superior Fresh and other firms have found buyers by offering a locally produced and sometimes higher quality fish. Superior Fresh, for example, claims the feed it uses—which contains more fish oil—gives the company's salmon twice as much of the healthful omega-3 fatty acids as other farmed salmon. The firm is also betting that, by integrating its salmon farm with its greenhouses, it can become a model for a profitable and environmentally sensitive business.

Superior Fresh already has plans to expand, with new farms on the East and West coasts. And Summerfelt is once again thinking about how to improve aquaculture practices. He envisions using even bigger tanks, for example, with each holding 3 million liters of water—and some 67,500 shimmering salmon. "It is about economy of scale," he says. And there is plenty of room for fish on land. ■

PLANT BIOLOGY

Unusual suspects in flower color evolution

The expression of phased small interfering RNAs caused monkeyflower color evolution

By **Marie Monniaux**

Pigmentation in flower petals mainly relies on anthocyanins and carotenoids, two classes of pigments whose biosynthetic and regulatory pathways are well characterized (*1*) and constitute theoretically ideal targets for evolution to create new color patterns. However, evolution of flower color sometimes works in mysterious ways. On page 576 of this issue, Liang *et al.* (*2*) show that a major speciation locus in *Mimulus* (monkeyflowers) that causes change in flower color contains a noncoding inverted repeat region. This repeat produces a long noncoding RNA that is cleaved into small interfering RNAs (siRNAs) in a regularly spaced ("phased") pattern, and some of these siRNAs regulate the translation of a carotenoid biosynthesis regulator. The finding that flower color change was caused by an inverted repeat that produces phased siRNAs constitutes an unexpected molecular mechanism for flower morphological evolution.

Flowers display a stunning diversity of shapes, sizes, and colors, which makes them amenable to studying the mechanisms that underlie morphological evolution. Flower color is a deceivingly simple trait that has been extremely labile during evolution: Sister species from several genera can show substantially different pigmentation patterns, and repeated shifts in flower color are observed within a single genus. In most cases, changes in flower color during evolution are simply caused by regulatory or coding mutations in the genes that control pigment biosynthesis. For example, the evolution of red floral color in *Petunia* involved changes in multiple players of the anthocyanin biosynthesis pathway (*3*).

However, this is not always the case, according to the findings of Liang *et al.*, who looked for the molecular determinant for carotenoid deposition in petals of monkeyflowers. Out of the many different coloration phenotypes found in this genus (see the photo), Liang *et al.* focused their study on two of them: flowers with pale pink petals (low levels of anthocyanins and no carotenoids) and yellow nectar guides (high local amounts of carotenoids) and flowers with bright red petals (a combination of high levels of both anthocyanins and carotenoids).

A single locus called *YELLOW UPPER* (*YUP*) was found to govern carotenoid deposition in monkeyflowers but was never finely mapped (*4*). *YUP* is a classical example of a speciation locus because exchanging *YUP* alleles between species is sufficient to directly influence pollinator visits and cause reproductive isolation of emerging species (*5*). By crossing two monkeyflower species that had not been used in previous studies, Liang *et al.* narrowed down *YUP* to an interval containing eight protein-coding genes. However, they found that reducing the expression of these

Laboratoire de Reproduction et Développement des Plantes, ENS de Lyon, CNRS, INRAE, UCBL, Lyon, France.
Email: marie.monniaux@ens-lyon.fr

PHOTO: PETER MORENUS/UNIVERSITY OF CONNECTICUT

The petal pigmentation of *Mimulus* (monkeyflowers) involves a long noncoding RNA that generates small interfering RNAs.

ight genes did not affect carotenoid deposition. The authors instead identified a long inverted repeat that was being actively transcribed in this region; this repeat produced abundant secondary siRNAs in a phased pattern, called phasiRNAs (*6*). PhasiRNAs can originate from a long noncoding RNA that is cleaved into secondary siRNAs. Cleavage sites in the RNA that contains phasiRNAs are regularly spaced, which generates a phased accumulation of siRNAs. But of the pool of phasiRNAs that accumulates, one siRNA is more abundant, and, in the case of *YUP*, the major siRNA matched the sequence of *REDUCED CAROTENOID PIGMENTATION 2* (*RCP2*), which encodes a major activator of carotenoid biosynthesis (*7*).

Liang *et al.* found that a functional *YUP* locus would produce abundant siRNAs that target *RCP2* and thereby reduce carotenoid accumulation in the petals of the pale pink flowers. The authors demonstrated that the siRNA targets *RCP2* mainly by reducing its translation. Moreover, they provided a satisfactory explanation for why carotenoids accumulate in the yellow nectar guides, which serve as guiding signals for bumble bee visitation: They found that another activator of carotenoid biosynthesis, RCP1, is present in nectar guides and that RCP1 represses *YUP* transcription so that the phasiRNAs are not produced. In species with bright red–colored petals, mutations in the *YUP* sequence have disrupted the phased pattern of phasiRNA production, and, as a result, the major siRNA that targets *RCP2* is not produced and carotenoid accumulation is not repressed.

Liang *et al.* also found that the sequence of *YUP* strongly matches that of a *CYTOCHROME P450* (*CYP450*) gene found a small distance away, suggesting that *YUP* originated from the duplication and inversion of part of this gene. CYP450 enzymes take part in a large range of biosynthetic reactions during plant development (for example, they participate in the production of membrane sterols, plant hormones, or defense compounds) but were unlikely to be specific players in flower color evolution, and they share no phylogenetic relationship with *RCP2*. Pinpointing the unexpected origin and mode of action of the *YUP* locus would have been impossible without a well-established model genus such as *Mimulus*, which comes with genomic information and efficient transgenesis protocols.

Liang *et al.* also found *YUP* to be physically linked to two regulators of anthocyanin production in petals—*PETAL LOBE ANTHOCYANIN* (*PELAN*) (*8*) and *SISTER OF LIGHT AREAS1* (*SOLAR*) (*2*)—in a small region that they propose acts as a superlocus that controls petal pigmentation. A superlocus (or supergene) is a group of genes that participate in a related function and are physically close on a chromosome; these genes are therefore inherited as a single locus. This allows a favorable combination of alleles to be maintained through generations, which is particularly important to avoid the dissolution of pollination syndromes (the suite of traits jointly recognized by pollinators) over generations. A superlocus in *Petunia* contains genes that control petal visible color, ultraviolet absorption, floral scent production, pistil length, and stamen length (*9*). In monkeyflowers, the *YUP-PELAN-SOLAR* superlocus controls most of the carotenoid and anthocyanin accumulation in the petals, which could maintain the two distinct petal pigmentation phenotypes that are recognized by different pollinators.

That noncoding regions of the genome, such as the *YUP* locus, underlie morphological evolution is not conceptually new, but evidence for such mechanisms is rare (*10*). Intriguingly, recent studies have identified other unusual molecular mechanisms that are involved in floral evolution. For example, similar to *YUP*, the recent appearance of a yellow pigmentation pattern in the petals of *Antirrhinum* (snapdragon) is caused by the *SULF* locus, an inverted duplication that generates siRNAs that target a pigment biosynthesis gene (*11*). In monkeyflowers, a reduction in anthocyanin accumulation in pale pink petals was found to be caused by an alternative start codon in the 5′ untranslated region of *PELAN*, which causes reduced translation (*12*). This was unforeseen because most of the cis-regulatory changes that have been found to shape phenotypic variation affect transcription (*10*). In *Capsella*, the reduction of petal size has recently evolved through mutations in the *CYP724A1* gene, a member of the *CYP450* gene family that is involved in the synthesis of brassinosteroids, a plant hormone that controls cell proliferation (*13*). The mutations were found in the exons of *CYP724A1* and increased splicing efficiency and transcription (*13*). Excessive levels of brassinosteroids limit cell proliferation, which results in smaller petals. That exonic mutations affect splicing efficiency is rarely reported because they are more likely to affect protein function, and this effect could have been completely overlooked.

Therefore, it appears that each step of the regulation of gene expression, in all its complexity (including recruitment of transcription factors, initiation of transcription, splicing, mRNA stability, and translation efficiency), might be a possible target for morphological evolution. In particular, mutations that affect protein translation or stability have been largely overlooked (*14*), but researchers of evolution now have to address these types of challenges for the field to move forward.

Is there something special about flower evolution that explains why it involves uncommon molecular mechanisms more frequently than the evolution of other traits in plants? It is probably more likely to be the case that flowers are visually attractive [and scientists are as sensitive to this as insects can be (*15*)] and their morphology is extremely diverse and directly affects reproductive isolation and speciation; therefore, they constitute an excellent system to explore the molecular determinants of morphological evolution. This has revealed the unforeseen but likely widespread ways that diversity can be generated through evolution. ■

REFERENCES AND NOTES

1. E. Grotewold, *Annu. Rev. Plant Biol.* **57**, 761 (2006).
2. M. Liang *et al.*, *Science* **379**, 576 (2023).
3. A. E. Berardi *et al.*, *Plant Cell* **33**, 2273 (2021).
4. H. D. Bradshaw Jr. *et al.*, *Nature* **376**, 762 (1995).
5. H. D. Bradshaw Jr., D. W. Schemske, *Nature* **426**, 176 (2003).
6. Y. Liu *et al.*, *Plant Cell* **32**, 3059 (2020).
7. L. E. Stanley *et al.*, *Plant Cell* **32**, 1536 (2020).
8. Y.-W. Yuan *et al.*, *New Phytol.* **204**, 1013 (2014).
9. K. Hermann *et al.*, *Curr. Biol.* **23**, 873 (2013).
10. A. Martin, V. Orgogozo, *Evolution* **67**, 1235 (2013).
11. D. Bradley *et al.*, *Science* **358**, 925 (2017).
12. M. Liang, C. E. Foster, Y.-W. Yuan, *Sci. Adv.* **8**, eabo1113 (2022).
13. U. Fujikura *et al.*, *Dev. Cell* **44**, 192 (2018).
14. A. E. Berardi, *Sci. Adv.* **8**, eade2347 (2022).
15. M. Adamo *et al.*, *Nat. Plants* **7**, 574 (2021).

10.1126/science.adg2774

CHEMICAL PHYSICS

Probing matter with nonlinear spectroscopy

Ultrafast nonlinear spectroscopy can unravel the dynamics of highly excited electronic states

By **Stephen R. Leone**[1,2,3] *and* **Daniel M. Neumark**[1,2]

In the Bohr model of the atom, the nominal orbiting period for a 1*s* electron in the hydrogen atom is 150 as (1 as = 10^{-18} s). Attosecond light pulses are thus in principle short enough to follow electron dynamics in real time (*1*). Moreover, with such pulses, the time-resolved measurements can be extended to subfemtosecond lifetimes, probe electronic and vibrational coherences in atoms and molecules, and by means of attosecond photochemistry, follow the earliest dynamics of photoexcited molecules as they dissociate or isomerize. Attosecond light pulses have recently been incorporated into four-wave mixing (FWM) experiments in gases and solids, by combining one attosecond pulse with two visible optical pulses or multiple attosecond pulses themselves. This now allows more accurate determination of quantum pathways in transient electronic states.

Attosecond pulses generally lie in the extreme ultraviolet (XUV; from 15 to 100 eV) and soft x-ray (SXR; from 100 to 2000 eV) regions of the electromagnetic spectrum. XUV light below 30 eV generally excites valence electrons in atoms and molecules into unoccupied orbitals, whereas higher-energy photons typically excite core electrons into unoccupied valence orbitals. Because core electrons are localized on specific atoms, the energies of core-to-valence transitions are highly element specific and thus allow monitoring of the evolving electronic environment on specific atoms in photoexcited molecules. As an example, one can use attosecond XUV pulses to monitor core-to-valence transitions around 47 eV on the iodine atom in photoexcited iodomethane (CH_3I). This experiment captures the instant of passage through a conical intersection (CI), a multidimensional crossing between electronic states in a polyatomic molecule in which the outcome of a photodissociation event is determined (*2*). More generally, CIs mitigate photodamage of molecules and regulate many processes in living systems.

To understand the technical challenges involved in generating attosecond light pulses, it must be understood that light with a wavelength λ represents an electromagnetic field with period λ/c, where c is the speed of light, and that the minimum duration of a light pulse is approximately one optical period. For near-infrared (NIR) light at 800 nm, which is the center wavelength of the titanium-sapphire lasers that are most commonly used in ultrafast applications, the optical period is 2.6 fs. This value represents an approximate lower bound to the shortest achievable pulse at 800 nm. Therefore, higher photon energies are needed for which the period is correspondingly shorter; for example, at 100 eV (12.5 nm) the optical period is 41 as. Hence, in many of the attosecond experiments performed to date, the attosecond pulses are formed through the process of high harmonic generation (HHG) by using a tabletop laser system; HHG provides a relatively straightforward means of upconverting infrared and visible electromagnetic radiation into XUV and SXR wavelengths.

In HHG (*3*), an intense femtosecond laser pulse interacts with a nonlinear medium—typically, inert gases at low pressure. The rare gas atoms undergo tunnel or field ionization driven by the oscillating electric field of the laser. As the sign of the oscillating electric field reverses, the electron is driven back toward the ion and recombines, converting the gained kinetic energy into an attosecond burst of XUV or SXR light upon recollision. Methods have been developed that select a single burst from this process, a so-called isolated attosecond pulse. It is now possible to obtain 50 isolated pulses whose photon energies extend well into the SXR region (*4*). This allows the investigation of core-to-valence transitions in an expanding number of elements because

Nonlinear spectroscopy with extreme-ultraviolet attosecond laser pulses

Attosecond four-wave mixing experiment
Extreme ultraviolet (XUV) pulses and two near-infrared (NIR) beams pass through a sample. The off-axis emission is spatially separated from the incident XUV beam and dispersed by a grating onto a charge-coupled device (CCD) camera.

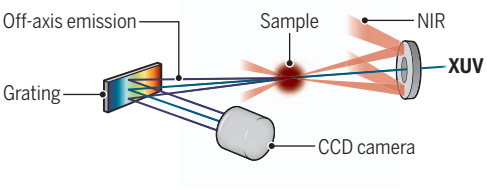

Quantum pathway
This reveals a possible quantum pathway involving one XUV ($+k_{XUV}$) and two NIR photons ($-k_{NIR}$ and $+k_{NIR}$) that leads to off-axis emission (k_{EMIT}).

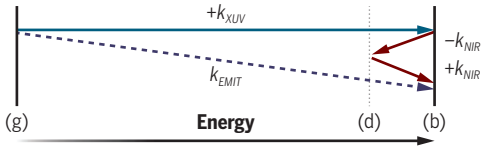

Rydberg series
XUV excitation of the 3s Rydberg state of O_2 at 22 eV decays by autoionization or dissociation.

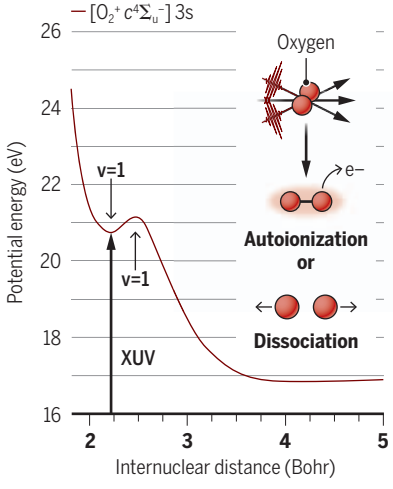

Core-exciton wave function
XUV excitation of a core-exciton in solid NaCl at 20 to 45 eV excites a 2p core electron on the Na ion to a vacant 3s

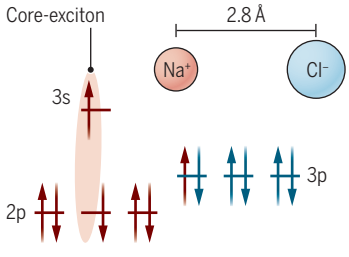

Na^+ core-exciton wave function

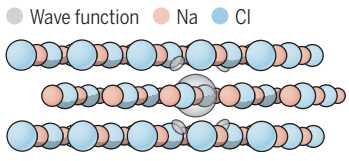

GRAPHIC: A. MASTIN/*SCIENCE*

the energies of these transitions generally increase with atomic number (*5*). Isolated attosecond pulses can also be generated with free-electron lasers (FELs) (*6*). These accelerator-based light sources are much more expensive and complex than tabletop systems, but the reported attosecond pulse intensities and photon energies are considerably higher.

One of the most powerful experimental methods in attosecond science is attosecond transient absorption (ATAS) (*7*). This approach explores ultrafast dynamics in both gas-phase and solid targets. In its most straightforward implementation, a NIR, visible, or UV pulse photoexcites the sample, and the resulting dynamics are probed with a time-delayed, broadband attosecond pulse that passes through the sample and is then spectrally dispersed by a grating onto an x-ray camera. An appealing feature of this method is that even though the attosecond pulse has a large range of possible energies (10 to 40 eV), the spectral resolution is determined by the grating-camera combination and is typically 0.02 to 0.2 eV.

A distinctive example of ATAS is its application to the electronic nonadiabatic (state-switching) dynamics that occur upon ionization of ethylene (C_2H_4) (*8*). Gas-phase C_2H_4 is ionized through its interaction with a 10-fs pulse at a wavelength of 1.6 μm. The dynamics of the resulting $C_2H_4^+$ cation are followed by transient absorption of a broadband attosecond pulse spanning 250 to 450 eV (28 to 50 nm). The probe pulse covers the region of carbon core-to-valence transitions around 280 to 290 eV in which a C(1*s*) electron is excited to an unoccupied valence orbital. The energies of these transitions depend sensitively on the electronic state of the cation. In this work (*8*), the cation is formed initially in its first excited state (the D_1 state) but then undergoes a nonadiabatic transition to its ground state (the D_0 state) in 6.8 fs. The high time resolution in this experiment thus shows that electronic state switching—of which passage through a CI—occurs almost immediately after photoexcitation.

These experiments can also be carried out in the reverse order, in which the attosecond pulse interacts with the sample first, creating a coherent superposition of highly excited electronic and vibrational states. In this case, transmission of the attosecond pulse is affected by the subsequent NIR pulse, provided that the second pulse arrives before the highly excited states decay (*9*). In this way, lifetimes can be obtained for the excited states created by the attosecond pulse with respect to, for example, processes such as autoionization, dissociation, and Auger-Meitner decay (in which one electron fills a vacancy and a different electron is ejected).

However, because multiple quantum pathways contribute to transient absorption in this configuration, the resulting signals can be challenging to interpret. To address this challenge, nonlinear spectroscopic techniques are being developed, one of which is attosecond FWM (see the figure). These experiments are based on ideas developed in infrared and visible FWM experiments, in which a third-order polarization created by three light fields interacting with a sample yields an emission signal at a new angle that is determined by phase matching considerations dictated by momentum conservation of the light field (*10*).

In tabletop experiments, an attosecond XUV or SXR beam is incident on a target and crossed by two NIR beams at a slight angle. The two NIR pulses can be independently delayed. However, the experiments are often run in either a "bright-state" mode, in which the two NIR pulses are coincident and their time delay relative to the XUV pulse is varied, or a "dark-state" mode, in which the XUV and one NIR pulse are coincident and the delay between those two pulses and the second NIR pulse is varied. In a bright-state scan, the FWM persists only over the lifetime of the bright state, yielding the lifetime of this state. Similarly, a dark-state scan probes states that are accessible only by a two-photon (XUV+NIR) transition. The noncollinear geometry of the beams provides angular phase-matching separation to distinguish the various photon interaction pathways.

Attosecond FWM has been used to probe the decay dynamics of very short-lived electronic states in both gas-phase and solid samples. As an example, attosecond FWM was applied to the 3*s* Rydberg state of oxygen (O_2) that lies at 21 eV (*11*). This state is a member of a Rydberg series that converges to the $c^4S^-_u$ state of O_2^+. It comprises a very shallow well that supports two vibrational levels. These vibrational states can decay through predissociation to form two O atoms, or through autoionization to $O_2^+ + e^-$. Bright-state scans were carried out on the valence (v) = 0 and v = 1 levels supported by the potential energy curve, yielding lifetimes of 5.8 and 4.5 fs, respectively. Analysis of these results shows that autoionization is the dominant decay channel for both vibrational states. Moreover, although the v = 1 level predissociates more rapidly than the v = 0 level, its autoionization rate is higher too, and both channels need to be accounted for to interpret the results. This experiment (*11*) provides an exquisite probe of the competition between these two channels, which is of fundamental interest in understanding the decay dynamics of highly excited molecular electronic states.

Attosecond FWM can also be applied to solid samples, such as the dynamics of core excitons in solid sodium chloride (NaCl) (*12*). NaCl exhibits strong absorption bands around 33.5 eV that are attributed to excitation of Na(2p) core electrons into localized electronic states of unoccupied Na(3s) orbitals, essentially creating a localized hydrogenic-like Rydberg state within the solid. A combination of bright- and dark-state scans shows evidence for at least five distinct states underlying this absorption band, all of which exhibit decoherence lifetimes of less than 10 fs. These short lifetimes are attributed mainly to electronic effects, including configuration interactions from electron-electron correlation that couple the multiple electronic states that compose the excitonic bands in this energy range.

These attosecond FWM experiments pave the way for more ambitious nonlinear attosecond and x-ray spectroscopy experiments, some of which are already being carried out at FELs (*13*). Moreover, such experiments provide the foundation for nonlinear spectroscopy experiments with multiple attosecond XUV and/or SXR light pulses (*14*). Current tabletop laser systems do not provide sufficient flux at high photon energies to conduct such multiple-attosecond-pulse experiments, but it will be possible to perform them at FELs in the future. For example, one proposed experiment that combines x-ray diffraction and stimulated x-ray Raman spectroscopy has the capability to directly probe the changes in electron density associated with passage through a CI (*15*). ■

[1]Department of Chemistry, University of California, Berkeley, CA, USA. [2]Chemical Sciences Division, Lawrence Berkeley National Laboratory, Berkeley, CA, USA. [3]Department of Physics, University of California, Berkeley, CA, USA. Email: dneumark@berkeley.edu; srl@berkeley.edu

REFERENCES AND NOTES

1. M. Drescher *et al.*, *Science* **291**, 1923 (2001).
2. K. F. Chang *et al.*, *J. Chem. Phys.* **154**, 234301 (2021).
3. P. B. Corkum, *Phys. Rev. Lett.* **71**, 1994 (1993).
4. J. Li *et al.*, *Nat. Commun.* **8**, 186 (2017).
5. T. Popmintchev *et al.*, *Science* **336**, 1287 (2012).
6. J. Duris *et al.*, *Nat. Photonics* **14**, 30 (2020).
7. E. Goulielmakis *et al.*, *Nature* **466**, 739 (2010).
8. K. S. Zinchenko *et al.*, *Science* **371**, 489 (2021).
9. H. Wang *et al.*, *Phys. Rev. Lett.* **105**, 143002 (2010).
10. P. Hamm, M. Zanni, *Concepts and Methods of 2D Infrared Spectroscopy* (Cambridge Univ. Press, 2011).
11. Y.-C. Lin *et al.*, *Faraday Discuss.* **228**, 537 (2021).
12. J. D. Gaynor *et al.*, *Phys. Rev. B* **103**, 245140 (2021).
13. F. Bencivenga *et al.*, *Nature* **520**, 205 (2015).
14. M. Kowaleski *et al.*, *Chem. Rev.* **117**, 12165 (2017).
15. Y. Nam *et al.*, *J. Phys. Chem. Lett.* **12**, 12300 (2021).

ACKNOWLEDGMENTS

The authors are primarily supported by the director, Office of Basic Energy Science, Chemical Sciences Division of the US Department of Energy, under contract DE-AC02-05CH11231. Additional support was provided by the Air Force Office of Scientific Research under grant FA9550-20-1-0334 (to S.R.L.).

10.1126/science.add4509

CORONAVIRUS

Exaggerated responses to a virus long gone

Multisystem inflammatory syndrome in children is caused by abnormal cell activation

By **Petter Brodin**[1,2]

The clearest determinant of COVID-19 severity is age, with the majority of children experiencing mild or asymptomatic infections (*1*). But one disease presentation observed during the peak of the pandemic shows an opposite pattern. The rare but sometimes life-threatening multisystem inflammatory syndrome in children (MIS-C) has been a major cause of pediatric morbidity and mortality during the pandemic. Symptoms of MIS-C overlap partially with Kawasaki disease, a postinfectious vasculitis, and with toxic shock syndrome, a bacterial toxin–mediated disease caused by nonspecific activation of T lymphocytes by so-called superantigens. On page 554 of this issue, Lee *et al.* (*2*) report that variants in genes encoding the 2′-5′-oligoadenylate synthetase (OAS)–ribonuclease L (RNase L) viral RNA sensing pathway lead to exuberant inflammatory responses in myeloid cells in individuals with MIS-C. But why does MIS-C develop 1 month after the initial infection?

The strength and early activation of the type I interferon (IFN-I) pathway at the site of initial severe acute respiratory syndrome coronavirus 2 (SARS-CoV-2) infection—the airways and mouth—is the most important determinant of disease severity; individuals who fail to mount such responses are at higher risk of severe COVID-19 and death (*3*). Children on average seem to have a primed and more efficient IFN-I system in the airway mucosa and consequently respond efficiently, leading to mostly mild and even asymptomatic disease (*4*). Such efficient IFN-I responses also likely occur in children who subsequently develop MIS-C because most such children report mild and sometimes unnoticeable COVID-19, and often the infection is apparent only through a symptomatic parent or sibling. The finding by Lee *et al.* that variants causing exuberant antiviral inflammatory responses are overrepresented in 558 children with MIS-C elucidates a previously unknown aspect of disease pathogenesis but also presents a paradox. It is unclear why children carrying these variants do not present exuberant inflammatory responses upon initial infection.

Another important observation, reported by multiple groups investigating children with MIS-C (*5*), presents a similar paradox. Given overlapping clinical presentations among children with MIS-C and patients with toxic shock syndrome—a disease caused by bacterial toxins that nonspecifically activate T lymphocytes through the expression of superantigens—a search for superantigens in SARS-CoV-2 infections was initiated. Superantigens are bacterial or viral proteins that bind T cell receptors (TCRs) in nonspecific ways, in contrast to the peptide complexed with a major histocompatibility complex (MHC) molecule that only triggers a subset of T cells that recognize such complexes through their TCR. Structural modeling revealed one potential superantigen motif within the Spike protein (*6*). A disproportionate increase in T cells carrying the variable-β21.3 (Vβ21.3) chain of the TCR paired with various Vα chains in children with MIS-C has been reported (*5*), which indirectly suggests SARS-CoV-2 superantigen–mediated T cell activation. Additionally, Lee *et al.* show that some of the MIS-C patients with OAS–RNAse L pathway mutations have disproportionate expansion of T cells expressing the Vβ21.3 chain, suggesting combined or even synergistic effects of these phenomena underlying MIS-C (see the figure).

Analyses of plasma cytokines indicate broad T cell activation in children with MIS-C and autoantibody repertoires, suggesting that such T cells can also lead to widespread B cell activation and loss of tolerance (*7*–*12*). This could explain additional aspects of the disease presentation and responses to immunomodulatory therapies, such as intravenous immunoglobulins. Similar to exuberant myeloid cell responses in patients with deficiencies in the OAS–RNase L pathway, why would a superantigen-mediated disease present 1 to 2 months after the initial infection? These questions remain to be answered and present intriguing possibilities for future research.

SARS-CoV-2 vaccination or prior infection reduce the risk of developing MIS-C, although there are some reports of rare vaccine-triggered MIS (MIS-V) (*13*). However, it is difficult to be sure of a causal role for SARS-CoV-2 vaccination in triggering MIS-V in populations with extensive SARS-CoV-2 circulation and possible simultaneous exposure to virus and vaccine. It would be interesting to investigate the genetic variants reported by Lee *et al.* in the context of suspected MIS-V because mRNA encoding the Spike protein from vaccines would also be expected to trigger exuberant responses in individuals with OAS–RNase L deficiencies. Interestingly, with increasing population immunity and/or changing properties of SARS-CoV-2 variants, decreasing rates of MIS-C have been seen during 2022. Long Covid, another postinfectious disorder that is triggered by SARS-CoV-2 infection, also has multisystem involvement that partially overlaps with the clinical features of MIS-C, including vasculopathy, coagulopathy, and immune cell activation. Variants in the OAS–RNase L pathway

Exuberant inflammatory responses in MIS-C

Persistence of SARS-CoV-2 in the intestine of children with MIS-C could drive a self-propagating hyperactivation loop of tissue-resident myeloid cells and T cells. Variants in the OAS–RNase L viral RNA sensing pathway could drive inflammatory responses while a SARS-CoV-2–derived superantigen nonspecifically activates T cells expressing the Vβ21.3 chain of the TCR.

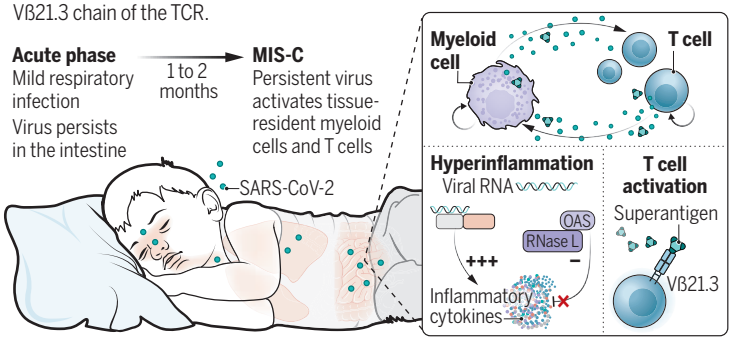

MIS-C, multisystem inflammatory syndrome in children; OAS, 2′-5′-oligoadenylate synthetase; RNase L, ribonuclease L; SARS-CoV-2, severe acute respiratory syndrome coronavirus 2; TCR, T cell receptor; Vβ21.3, variable-β21.3.

GRAPHIC: N. CARY/*SCIENCE*

[1]Department of Women's and Children's Health, Karolinska Institutet, Solna, Sweden. [2]Department of Immunology and Inflammation, Imperial College London, London, UK.
Email: petter.brodin@ki.se

would also be of interest in children who develop Long Covid (*14*).

Overall, the findings of Lee *et al.* together with reports of superantigen-mediated T cell activation, the rapid response to immunomodulatory therapies, and the rare reoccurrence of inflammation after a few days of treatment suggest that MIS-C is driven by a dysregulated and possibly self-propagating loop of activated myeloid cells and T cells. The main question to be resolved relates to the delayed presentation after acute infection and the role of SARS-CoV-2 in specifically driving MIS-C disease. Most children with MIS-C have negative SARS-CoV-2 polymerase chain reaction (PCR) tests in the respiratory tract, but the virus may persist elsewhere and drive MIS-C. SARS-CoV-2 can persist for a longer period in the intestines, particularly in children, and most children with MIS-C present with intestinal symptoms, including pain, vomiting, or loose stools (*15*).

One possible explanation for the delayed presentation is viral persistence in the intestine and the need for repeated stimulation to pathogenically activate myeloid and T cells. A potential explanation for the delayed presentation in MIS-C is viral persistence and repeated stimulation of intestinal myeloid cells and T cells. It is also possible that the reason for MIS-C not occurring during acute infection in the airways but only during the postinfectious phase is a result of distinct aspects of tissue-resident cells in the intestine. The dependency on repeated stimulation of tissue-resident cells could explain the delayed presentation of disease, despite the systemic expression of predisposing OAS–RNase L variants. Support for this idea comes from the observation that SARS-CoV-2 persists in the stool of MIS-C patients, and increased intestinal permeability and inflammation lead to detectable Spike protein in circulation (*15*). Thus, the rarity of MIS-C could be explained by the frequencies of predisposing variants, such as those reported by Lee *et al.*, and possible variants associated with superantigen-mediated T cell activation (*12*). ■

REFERENCES AND NOTES

1. C. Smith *et al.*, *Nat. Med.* **28**, 185 (2022).
2. D. Lee *et al.*, *Science* **379**, eabo3627 (2023).
3. Q. Zhang *et al.*, *Nature* **603**, 587 (2022).
4. P. Brodin, *Immunity* **55**, 201 (2022).
5. M. N. Rivas *et al.*, *Front. Immunol.* **13**, 941009 (2022).
6. M. H. Cheng *et al.*, *Proc. Natl. Acad. Sci. U.S.A.* **117**, 25254 (2020).
7. C. R. Consiglio *et al.*, *Cell* **183**, 968 (2020).
8. C. N. Gruber *et al.*, *Cell* **183**, 982 (2020).
9. K. Sacco *et al.*, *Nat. Med.* **28**, 1050 (2022).
10. A. Ramaswamy *et al.*, *Immunity* **54**, 1083 (2021).
11. M. Moreews *et al.*, *Sci. Immunol.* **6**, eabh1516 (2021).
12. R. A. Porritt *et al.*, *J. Clin. Invest.* **131**, e151520 (2021).
13. N. Ouldali *et al.*, *Lancet Reg. Health Eur.* **17**, 100393 (2022).
14. P. Brodin *et al.*, *Nat. Med.* **28**, 879 (2022).
15. L. M. Yonker *et al.*, *J. Clin. Invest.* **131**, e149633 (2021).

10.1126/science.adg2776

GEOCHEMISTRY

A window into prebiotic worlds?

Zircons reveal the geochemistry of Earth's earliest hydrothermal systems

By **Laura E. Rodriguez**

To search for life on other worlds, understanding the prebiotic chemistry of those worlds is necessary (*1*). However, to know which organic compounds form in the absence of life, and the conditions conducive for life's emergence, requires an understanding of the geochemical environment (e.g., fluid salinity, metal availability, etc.) in which those compounds existed. As Earth is the only example for life, origins-of-life studies simulating early Earth conditions can inform this endeavor. Unfortunately, the geological record of early Earth is sparse, and the constituents of ancient rock specimens have been heavily altered over time. Consequently, the fluid geochemistry of prebiotic environments on early Earth remains uncertain. On page 582 of this issue, Trail and McCollom (*2*) report that zircons—natural silicate minerals in Earth's crust—can constrain the fluid geochemistry of ancient hydrothermal systems. This provides a potential path to unraveling the fluid composition of early Earth and discerning life's origins.

"...contrary to popular opinion, relatively oxidizing systems...can create exceptionally favorable conditions for prebiotic synthesis."

The origins of life on Earth are generally thought to have occurred sometime between 4.5 and 3.5 billion years (Ga) ago. This range is partially constrained by the oldest accepted evidence for life—3.48-Ga-old fossilized stromatolites. These are carbonate structures produced by photosynthetic microorganisms that were discovered in the Dresser Formation, Australia, an area containing some of Earth's oldest rocks (*3*). Additionally, formation of the Moon constrained how early life could have arisen. It is generally thought that the Moon formed during a collision between Earth and another small planet. This impact event likely would have wiped out any life predating 4.5 Ga ago (*4*). Despite there being scarce geologic evidence of this period, a broad understanding of the early Earth has been informed by 3.3- to 4.4-Ga-old zircon ($ZrSiO_4$) specimens from Jack Hills, Australia.

Zircons are extremely resilient minerals and can survive beyond the weathering away of their host rock. Upon crystallization, zircons record the isotopic and elemental signature of their surroundings. Hence, studies of zircons formed in ancient mantle melts have revealed much of what is known about early Earth, including that liquid water was present by ~4.3 Ga ago (*5*). They also indicate that ~4.4 Ga ago, Earth's mantle was near its current redox state (the balance of oxidants and reductants) (*6*).

The redox state of the early Earth has been at the center of origins-of-life discussions since the field took off, with many suggesting that a reducing atmosphere—that is, one dominated by gases that donate electrons (H_2, NH_3, CH_4, and H_2S)—was required for life to arise (*7*). Earth's early atmosphere was composed of mantle gases expelled during volcanism. The speciation of mantle gases was controlled by the mantle redox state, measured by the amount of oxygen present (oxygen fugacity, fO_2). Within the mantle, the fO_2 is buffered by the surrounding mineral assemblage. For present-day Earth, the mineral buffer is fayalite, magnetite, and quartz (FMQ), which favors outgassing of neutral and weakly oxidized gases (N_2, H_2O, CO_2, and SO_2) (*8*). Given that Earth's mantle ~4.4 to 3.8 Ga ago had an estimated FMQ value similar to that of the present day, the prebiotic atmosphere was likely redox-neutral (*6*).

Zircons (>650°C, ~5 to 10 kbar) have been used to deduce the redox state of the mantle and, in turn, inform the atmospheric composition of the early Earth. What is less known is the redox state and geochemistry of near-surface aqueous environments where prebiotic organic chemistry relevant to the origins of life would have been most prevalent. Notably, zircons formed in mantle melts can be transported upward in the

Lunar and Planetary Institute, Universities Space Research Association (USRA), 3600 Bay Area Boulevard, Houston, TX 77058, USA. Email: lrodriguez@lpi.usra.edu

crust where they are exposed and altered by hydrothermal (>100°C) fluids (*9*). Upon recrystallization, the zircons capture the geochemistry of these fluids (see the figure).

Leveraging synthetic zircons, Trail and McCollom devised an approach to determine the geochemistry of the hydrothermal fluids (~580°C) from which eight of the Jack Hills zircons had recrystallized ~3.9 Ga ago (*10*). The synthetic zircons were crystallized in hydrothermal fluids (1200° to 900°C, 10 kbar) of varying redox states to formulate an equation that calculated fO_2 from redox-sensitive cerium (Ce^{3+}, Ce^{4+}) and redox-insensitive elements lanthanum (La) and praseodymium (Pr). The partition coefficient—a ratio of total Ce in the fluid versus in zircon—was determined and normalized to the partition coefficients of La and Pr. Notably, Ce^{4+} is more readily captured in crystallizing zircons than Ce^{3+}. Thus, normalizing to La and Pr reveals if there is excess Ce in zircon, which would indicate that the zircon formed in oxidized fluids enriched in Ce^{4+}. Using this calibration, Trail and McCollom determined that the redox state of the hydrothermal fluids from which the eight Jack Hills zircons formed was slightly more oxidized than the upper mantle from that time period (*11*).

Once equipped with the fO_2, temperature (*10*), and salinity (*10*) of the hydrothermal fluids, Trail and McCollom simulated the geochemical evolution of the fluids as they progressed upward through Earth's crust. Although the fluids were relatively more oxidized than the modern mantle, the lithospheric fluids at equilibrium (580°C, 5 kbar) were predicted to have been enriched in H_2S (versus SO_4) and transition metals (Cu, Mn, and Zn) that together could have driven abiotic carbon fixation—the conversion of inorganic carbon into organic compounds (*12*). The models suggested that by the time the fluids breached the surface, they would have been enriched in ions with known catalytic potential (Fe^{2+}, Fe^{3+}, Ni^{2+}, Mn^{2+}, and Ca^{2+}) and reduced gases (CH_4 and H_2S). A pool sourced from these ancient hydrothermal fluids would have thus been ripe for prebiotic organic synthesis. In sum, Trail and McCollom have shown that, contrary to popular opinion, relatively oxidizing systems—which are thought to not be conducive for origins-of-life chemistry (*7*)—can create exceptionally favorable conditions for prebiotic synthesis.

The calibration and approach developed by Trail and McCollom could be applied to characterize the geochemistry of other hydrothermal systems captured within ancient zircons, including those found on other worlds. Mars is predicted to have a preponderance of zircons (*13*) from rocks that had been altered by ancient fluids. Indeed, zircons that recrystallized within hydrothermal fluids have been identified in martian meteorites (*14*). The NASA–European Space Agency's Mars Sample Return campaign will return samples collected from within the Jezero crater which, having been subjected to impact-induced hydrothermal alteration ~3.8 Ga ago (*15*), could host recrystallized zircons that captured the geochemistry of potentially prebiotic fluids. Applying the approach from Trail and McCollom to these samples may not only inform the habitability of Mars but could also provide geochemical constraints for prebiotic studies. Such constraints, in turn, could elucidate the origins of martian organics detected within these samples and the probability of their having an abiotic or biotic origin. ■

Zircons capture the geochemistry of ancient Earth

The habitability of aqueous environments on early Earth can be discerned from chemical information captured in zircons, resilient silicate minerals found in the mantle and crust. Fluid geochemistry deduced from zircons can serve as input for models and simulations to explore the synthesis of organic compounds in ancient fluids.

Zircon exposure to hydrothermal fluids

Natural zircons from igneous rocks are present in mantle melts. These zircons can transport upward into the crust where they can be exposed to—and altered by—hydrothermal fluids. Fluid sources include rainfall or seawater that circulate fluids into and out of the crust.

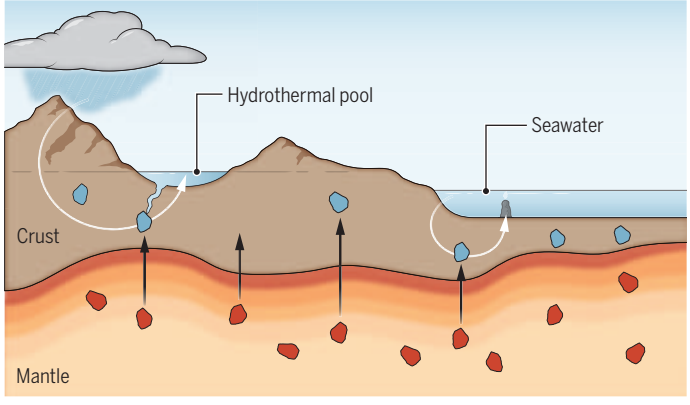

Zircon crystallization

A zircon crystal present in the crust can dissolve into its elemental constituents in a hydrothermal fluid. Consequently, its age, as determined by uranium (U) decay into lead (Pb), is lost. However, zircons can recrystallize, trapping certain constituents of the environment. This process "records" the geochemistry of the fluid and resets its age.

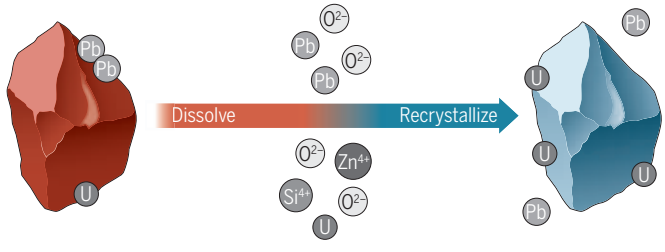

A snapshot of ancient hydrothermal fluids

As zircon recrystallizes, certain ions (Ce^{3+}, Ce^{4+}, Cl^-, Ti^{4+}) are incorporated, depending on the redox state, salinity, and temperature of the fluid environment. For example, in a high-salinity fluid, the crystal traps more Cl^-; at higher temperatures, it traps more Ti^{4+}.

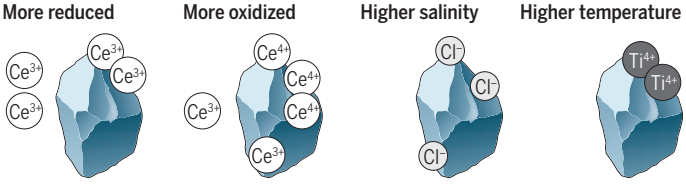

GRAPHIC: A. FISHER/*SCIENCE*

REFERENCES AND NOTES

1. L. M. Barge, L. E. Rodriguez, J. M. Weber, B. P. Theiling, *Astrobiology* **22**, 481 (2022).
2. D. Trail, T. M. McCollom, *Science* **379**, 582 (2023).
3. R. J. Baumgartner *et al.*, *Geology* **47**, 1039 (2019).
4. G. R. Osinski *et al.*, *Astrobiology* **20**, 1121 (2020).
5. S. J. Mojzsis, T. M. Harrison, R. T. Pidgeon, *Nature* **409**, 178 (2001).
6. D. J. Smythe, J. M. Brenan, *Earth Planet. Sci. Lett.* **453**, 260 (2016).
7. G. Schlesinger, S. L. Miller, *J. Mol. Evol.* **19**, 383 (1983).
8. J. F. Kasting, *Science* **259**, 920 (1993).
9. M. J. Bojanowski, B. Bagiński, E. Clarkson, R. Macdonald, L. Marynowski, *Contrib. Mineral. Petrol.* **164**, 245 (2012).
10. H. Tang, D. Trail, E. A. Bell, T. M. Harrison, *Geochem. Perspect. Lett.* **9**, 49 (2019).
11. L. Gao *et al.*, *Nat. Commun.* **13**, 3283 (2022).
12. G. D. Cody *et al.*, *Geochim. Cosmochim. Acta* **68**, 2185 (2004).
13. M. M. Costa *et al.*, *Proc. Natl. Acad. Sci. U.S.A.* **117**, 30973 (2020).
14. M. Guitreau, J. Flahaut, *Nat. Commun.* **10**, 2457 (2019).
15. K. A. Farley *et al.*, *Science* **377**, 1512 (2022).

ACKNOWLEDGMENTS

This article is Lunar and Planetary Institute (LPI) contribution no. 2874. LPI is operated by Universities Space Research Association under a cooperative agreement with the Science Mission Directorate of NASA.

10.1126/science.adg2630

POLICY FORUM

HUMAN GENETICS

Public views on polygenic screening of embryos

Understanding moral acceptability and willingness to use is crucial for informing policy

By **Michelle N. Meyer[1,2], Tammy Tan[3], Daniel J. Benjamin[3,4,5], David Laibson[3,6], Patrick Turley[3,7,8]**

For decades, people have used genetic information to exercise control over the kinds of children they will have. These technologies have largely targeted chromosomal and monogenic disorders and traits; but most human phenotypes are highly polygenic (and influenced by the environment). One technology that targets the entire genome—preimplantation genetic testing for polygenic risk (PGT-P)—uses polygenic indexes (PGIs) to predict the expected value of the phenotype(s) that would arise for each embryo if successfully transferred; parents can use these predictions to select an embryo for in vitro fertilization (IVF). Seeing gaps in evidence and analysis relevant for potential policy discussions around PGT-P, we conducted a survey of public attitudes. Our data suggest that it would be unwise to assume that use of PGT-P—even for controversial traits—will be limited to idiosyncratic individuals, or that it has little potential to cause or contribute to society-wide changes and inequities.

Historically, technologies to enable control over offspring have included carrier screening, ultrasound, preimplantation genetic diagnosis, amniocentesis, chorionic villus sampling, noninvasive prenatal screening, and selective abortion. Using them, people have selected against diseases such as Huntington's, Down syndrome and other trisomies, and alleles [such as pathogenic breast cancer gene (*BRCA*) variants] that increase an individual's lifetime risk of certain diseases. They have also selected for biological sex and conditions such as deafness. In contrast to those, a PGI—also called a polygenic risk score—is based on the estimated associations (calculated from a large-scale genetic study) between common genetic variants and a particular phenotype. This gene-based index can then be used to make phenotypic predictions—not only to avoid serious disease but also to try to select for phenotypes such as greater cognitive ability or educational attainment.

Another technology that targets the entire genome and could, in principle, vastly expand our ability to select for or against any heritable phenotype is germline genome editing (hereafter "gene editing")—for instance, with clustered regularly interspaced short palindromic repeats (CRISPR). This might someday be used to try to influence offspring characteristics by making thousands of DNA edits (or more) to a gamete or embryo.

> **"...public views should influence policy-making but alone do not determine appropriate policy."**

However—with the notable exception of three Chinese children whose C-C chemokine receptor type 5 (*CCR5*) genes were illicitly edited while they were embryos in a misguided attempt to provide them with AIDS resistance (*1, 2*)—gene editing has not been used. Indeed, it is not permitted in some 70 countries (*1*), and experts have called for a global moratorium (*2*).

PGT-P, by contrast, is already offered by at least one US company whose embryo screening business operates in several countries and US states (*3*). Yet it has received far less academic, policy, and regulatory analysis than gene editing, leading to calls for urgent research about public attitudes towards PGT-P (*4*). Recent surveys have measured acceptance of gene editing (*5*, *6*), intentions to use gene editing (*7*), and views about whether certain forms of embryo selection should be legally permitted (*8*). Someone's view about whether the law should prohibit a technology may be distinct from their view of whether the technology is morally acceptable, and both may be distinct from whether they themselves would use the technology. To our knowledge, this paper is the first to measure PGT-P use intentions—and the effects of social norming on these intentions.

ACCEPTABILITY AND WILLINGNESS

In January 2022, we conducted a preregistered, nationally representative US survey-based experiment on the attitudes of 6823 people towards three services: PGT-P, gene editing, and—as a nongenetic benchmark for attitudes toward interventions targeted at college admissions—courses to prepare for the SAT test (effective *N* after applying weights, 3805; see table S1 for sample characteristics). We randomized participants to answer two questions, in randomized order, about one of these three services. One question asked whether the respondent views the service as morally acceptable, morally wrong, or not a moral issue; participants could also indicate whether they were unsure. For this question, both PGT-P and gene editing were described as being potentially used for "medical and nonmedical traits."

The other question measured willingness to use each service by asking participants how likely it was—on a scale from 0 to 100%—that they would use the service to increase the odds that their offspring will attend a top-100 college by selecting for genetic variants, or enrolling their child in courses, associated with higher educational attainment. We asked participants to assume that each service was free. We also asked them to assume a realistic effect size: We told them that about 3% of high school seniors attend a top-100 ranked college, and that each service would raise their likelihood of having such a child by two percentage points (from 3 to 5%). In the cases of gene editing and PGT-P, we asked them to assume that they were already using IVF and that the add-on service was safe. Finally, we further randomized participants within each "service condition" to be told that it was used on average by either "1 out of every 10" or "9 out of every 10" similarly situated people (for the PGT-P and gene editing arms, "people currently having babies"; for the SAT prep arm, "people who currently have high-school–age children").

[1]Department of Bioethics and Decision Sciences, Geisinger Health System, Danville, PA 17822, USA. [2]Geisinger Commonwealth School of Medicine, Scranton, PA 18510, USA. [3]National Bureau of Economic Research, Cambridge, MA 02138, USA. [4]Anderson School of Management, University of California Los Angeles, Los Angeles, CA 90095, USA. [5]David Geffen School of Medicine, University of California Los Angeles, Los Angeles, CA 90095, USA. [6]Department of Economics, Harvard University, Cambridge, MA 02138, USA. [7]Center for Economic and Social Research, University of Southern California, Los Angeles, CA 90089, USA. [8]Department of Economics, University of Southern California, Los Angeles, CA 90089, USA.
Email: michellenmeyer@gmail.com

SOCIAL NORM, AGE, AND EDUCATION

A minority of participants (41%) said they had no moral objection to gene editing for "certain medical and nonmedical traits" (i.e., they reported it was morally acceptable or not a moral issue), and a majority of participants reported no moral objection to PGT-P (58%) or SAT prep (76%) (fig. S1 and table S2). On average, participants said they were 34% likely to use gene editing, 43% likely to use PGT-P, and 69% likely to use SAT prep to increase the odds of their child attending a top-100 college (see the figure and table S2). Furthermore, a material fraction of participants reported a >50% likelihood of using each service (28% gene editing, 38% PGT-P, 68% SAT prep; table S2). As predicted, those who were told that 90% of relevant people use each service were more likely to say that they, too, would use it, compared to those who were told that 10% of people were using it. The mean willingness to use gene editing, PGT-P, and SAT prep was 4 (P = 0.020), 5 (P = 0.007), and 4 (P = 0.022) percentage points higher, respectively, for those in the 90% condition (table S3). These effect sizes are typical of those reported for behavioral intentions from other social norm manipulations.

A recent study of 2233 UK residents between the ages of 16 and 75 found that those under 35 were more likely than older participants to "support" (rather than "oppose") both sex selection by IVF patients and embryo gene editing for "preferred characteristics" such as "eye color, height, hair color, etc." (*5*). In the first of two exploratory analyses that we conducted, although the moral attitudes of those under 35 years of age toward all three services were statistically indistinguishable when compared to the full sample (all P values > 0.59; fig. S1 and table S4), those under 35 reported a higher willingness than the full sample to use gene editing (41% versus 34%, $P = 4.0 \times 10^{-4}$), PGT-P (48% versus 43%, P = 0.013), and SAT prep (72% versus 69%, P = 0.039) for educational attainment (see the figure and table S4). (All of these estimates account for sample overlap between the two groups; the statistically equivalent tests comparing those under 35 and those 35 and older are in table S4.) Approximately equal moral acceptance among age groups but differential willingness to use these services might reflect younger people being the natural use population for reproductive technologies and (as recent students rather than parents) SAT prep.

In the second exploratory analysis, compared to those with less educational attainment, those who had at least a bachelor's degree were more likely to say that gene editing (46% versus 39%, P = 0.012), PGT-P (65% versus 54%, $P = 1.7 \times 10^{-4}$), and SAT prep (86% versus 71%, $P = 3.9 \times 10^{-10}$) are morally acceptable or not a moral issue (see the figure and table S5). They also reported a greater likelihood that they themselves would use gene editing (38% versus 32%, P = 0.008), PGT-P (48% versus 40%, $P = 1.6 \times 10^{-4}$), and SAT prep (78% versus 67%, $P = 4.7 \times 10^{-17}$) to increase the odds that their child attends a top-100 college (see the figure and table S5). These results might reflect parents' tendency to try to mirror their own educational outcomes in the outcomes of their offspring, which would have implications for other phenotypes.

DISCUSSION

In the US, there appears to be both greater moral acceptance of, and greater willingness under certain circumstances to use, PGT-P versus gene editing—and the more people use PGT-P, the more likely others say they would, too. Those circumstances, of course, matter. We asked participants to assume that each service is safe; because CRISPR currently carries considerable risks to offspring (*2*), our results may overestimate acceptability of and willingness to use CRISPR. Additionally, we (accurately) portrayed PGT-P as available but gene editing as a future technology; people's views of gene editing might become more positive if it becomes available. To isolate participants' attitudes about shaping offspring characteristics, in assessing willingness to use, we also asked them to assume that each service was free—and, for PGT-P and gene editing, that they were already using IVF. Our data thus do not measure willingness to use PGT-P or gene editing among those who would not otherwise already be using IVF. However, the number of babies born through assisted reproductive technologies has more than tripled between 1996 and 2017 (*9*). Moreover, developments in stem cell research are expected to make IVF much less financially and physically costly (*10*).

Other aspects of the scenario we presented suggest that our results may represent an underestimate of acceptability and potential uptake. For one, in measuring potential uptake, we asked about an especially controversial use of these technologies: not to avoid serious disease, but to increase the odds that the resulting child will be admitted to a top-100 college. Prior surveys measured attitudes toward gene editing and PGT-P without quantifying how effective the technology would be,

Moral acceptability and willingness to use, by age and education

Left: Mean likelihood of using gene editing, preimplantation genetic testing for polygenic risk (PGT-P), and courses to prepare for the SAT college admissions test, to increase participants' chances of having a child who attends a top-100 college by 2 percentage points (from 3% to 5%). Error bars are 95% confidence intervals. Low educational attainment reflects associate degree or below, high reflects bachelor's degree or above. See supplementary materials for P values and standard errors. Right: Degree of moral acceptability of each service. Some bars do not sum to 100% owing to rounding.

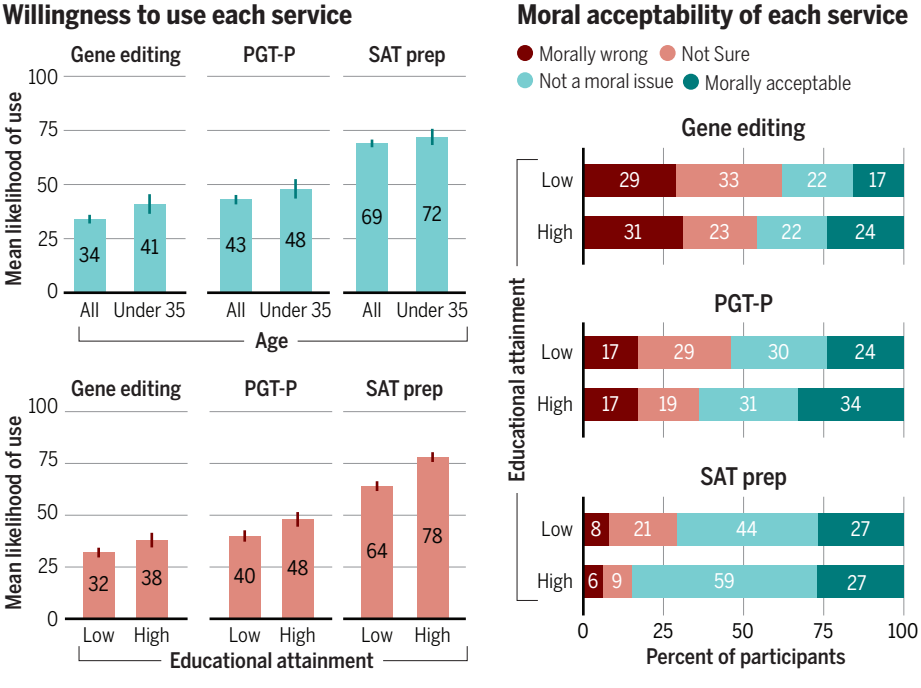

GRAPHIC: K. FRANKLIN/*SCIENCE*

whereas we stipulated a realistic effect size (see supplementary materials). In prior research, we expressed concern that an unrealistic lay view of what PGT-P can deliver might drive appetite for the service. We recommended (inter alia) that advertised effect sizes focus on absolute gains rather than relative (proportional) gains, which seem large in part because they are calculated from a small base (*11*). Others have similarly warned that PGT-P is of "limited utility" for phenotypes such as height and cognitive ability (*12*). Yet, although we cannot know whether the realistic effect size that we stipulated, appropriately communicated in absolute terms, was perceived by participants as large or small, it still resulted in a substantial share of people expressing interest in using PGT-P.

As important as how many people are interested in PGT-P is which people are interested. That potential uptake is higher among younger generations compared to the full sample is notable, because younger generations are the ones who are in a position to use PGT-P. Some critics of PGT-P argue that the technology's effectiveness in selecting for offspring phenotype is trivial. But PGT-P has been estimated by multiple independent researchers to have some impact, even if the expected gains are not what some consumers might imagine and some companies might suggest (*11*–*13*). That those who themselves have higher educational attainment are more interested in using PGT-P for this phenotype raises the risk that PGT-P will exacerbate existing inequalities. Over several generations, the gains from PGT-P could build on one another, resulting in familial transfers of socially-favored phenotypes that mirror and—given the costs of IVF—amplify unequal familial transfers of wealth.

CONCLUSION

Media reports of early adopters of PGT-P might suggest that it is a fringe issue unworthy of policy attention (*14*). But the sharp turn in public opinion about IVF itself shows that innovations that are initially met with limited uptake and even active resistance can quickly become normalized and widely adopted. A 1969 Harris poll found that most Americans objected to IVF, and the American Medical Association called for a moratorium on IVF research. In 1978, 1 month after the well-publicized birth of the first IVF baby, the same poll found that over 60% supported IVF and would consider using it themselves (*15*). In our survey, 78% said they view IVF as morally acceptable or not a moral issue; only 6% said it was morally wrong (table S6). A 2016 survey of 185 countries, including the US, found that only 18% "agreed with the use of" gene editing for intelligence, and a 2017 survey of 11 countries, again including the US, found very little intention to use gene editing to "enhance" offspring "memory and learning capacities" and little variation across countries (*7*). In light of our recent findings of much higher gene editing acceptance (41%) and substantial gene editing and PGT-P use intentions in the US to increase educational attainment, it is plausible that considerable gene editing and PGT-P use intention now also characterizes attitudes in other countries.

Public views of technology should influence policy-making in a democratic society. Experts who are critical of a technology should not assume that the public shares their knowledge or viewpoint. Understanding which members of the public are most likely to use a technology can inform predictions about societal impact—for example, the extent to which it is likely to enlarge existing or create new disparities. Much more should be learned about the public's reflexive as well as considered judgments. For instance, which other traits do people want to select for or against? How does relaxing the assumptions of free access and safety affect the rates, and distribution across groups, of moral acceptability and willingness to use? We should learn the extent to which people who would not otherwise use IVF would do so to use PGT-P. More subtly, legal frameworks for reproductive technologies vary widely (*1*); the current US path is one of continuing to treat offspring-influencing technologies as a matter of individual, private choice, despite their potential societal impact. People might have preferences against societal inequality that coexist with the preference to improve outcomes for their own family members. Specifically, someone might prefer that inequality be reduced at the aggregate level, but still choose an inequality-amplifying technology for themselves. Our study does not explore these issues, and future work should.

But despite their relevance, public attitudes alone do not determine appropriate policy. Additional research and diverse expert input should inform several policy questions: Given our limited knowledge of the unintended effects of selecting for and against particular phenotypes, does widespread use of PGT-P pose acceptable population risks? How can the complexities of PGT-P—e.g., pleiotropy, relative risk reduction—be conveyed to achieve appropriate consumer literacy? Given the costs of PGT-P and those of IVF and that PGIs developed with participants of European genetic ancestries are less predictive for those of other genetic ancestries, we must consider the extent to which a free market for PGT-P might exacerbate or create new health or social inequities, and ask whether society should tolerate that result. How can we ensure that those with traits that others select against remain fully welcomed members of our society? Should PGT-P be limited to certain traits, and if so, who would draw that line, and how? Finally, in the wake of the 2022 decision by the US Supreme Court in *Dobbs v. Jackson Women's Health Organization*, the US is experiencing uncertainty about the legal status not only of abortion but also of other reproductive decisions that are unprecedented in the past half century. Could choices about PGT-P be regulated without further threatening other reproductive choices?

Aside from urging the Federal Trade Commission to ensure proper communication of PGT-P and its expected gains (*10*), we do not prejudge what additional regulation, if any, is warranted. But we call on any policy choice—including not to further intervene—to be made deliberately, after input by experts and the public. ■

REFERENCES AND NOTES

1. F. Baylis, M. Darnovsky, K. Hasson, T. M. Krahn, *CRISPR J.* **3**, 365 (2020).
2. E. S. Lander *et al.*, *Nature* **567**, 165 (2019).
3. LifeView, https://www.lifeview.com/tests_pgtp.html.
4. G. Lázaro-Muñoz, S. Pereira, S. Carmi, T. Lencz, *Genet. Med.* **23**, 432 (2021).
5. Progress Educational Trust, "Fertility, Genomics and Embryo Research: Public Attitudes and Understanding," June 2022; https://www.progress.org.uk/wp-content/uploads/2022/06/pet_fertilitygenomicsembryoresearch.pdf.
6. T. McCaughey *et al.*, *Cell Stem Cell* **18**, 569 (2016).
7. G. Gaskell *et al.*, *Nat. Biotechnol.* **35**, 1021 (2017).
8. S. Zhang, R. A. Johnson, J. Novembre, E. Freeland, D. Conley, *Soc. Sci. Med.* **274**, 113796 (2021).
9. S. Sunderam *et al.*, *MMWR Surveill. Summ.* **69**, 1 (2020).
10. H. T. Greely, *The End of Sex and the Future of Human Reproduction* (Harvard Univ. Press, 2018).
11. P. Turley *et al.*, *N. Engl. J. Med.* **385**, 78 (2021).
12. E. Karavani *et al.*, *Cell* **179**, 1424 (2019).
13. T. Lencz *et al.*, *eLife* **10**, e64716 (2021).
14. C. Goldberg, "The Pandora's box of embryo testing is officially open," *Bloomberg*, 26 May 2022; https://www.bloomberg.com/news/features/2022-05-26/dna-testing-for-embryos-promises-to-predict-genetic-diseases#xj4y7vzkg.
15. A. V. Bell, in *Misconception: Social Class and Infertility in America* (Rutgers Univ. Press, 2014), p. 6.

ACKNOWLEDGMENTS

The authors are supported by Open Philanthropy grant 010623-00001 (M.N.M., P.T., D.J.B.); National Institute on Aging grant R24-AG065184 (T.T., D.J.B.); National Institute on Aging grant R01-AG042568 (T.T., D.J.B.) and R00-AG062787-04 (P.T.); and Pershing Square Fund for Research on the Foundations of Human Behavior (D.L.). Survey materials and code are available at https://osf.io/krj8t/. All Understanding America Study (UAS) data are available at https://uasdata.usc.edu.

SUPPLEMENTARY MATERIALS

science.org/doi/10.1126/science.ade1083

10.1126/science.ade1083

BOOKS *et al.*

Children gather in the Mesa Grande refugee camp in Honduras, 40 km from the Salvadoran border.

PHOTO: PHILIPPE BOURGOIS

ANTHROPOLOGY

Lost and found in El Salvador

Separated by civil war, families turn to genetic testing to locate missing children

By **Victor Penchaszadeh**

Between 1979 and 1992, the people of El Salvador were subjected to a civil war that claimed the lives of at least 75,000, left thousands disabled, and resulted in more than 1 million displaced and innumerable disappeared persons. The disappearance of children, specifically, numbered in the thousands and occurred under a variety of circumstances. Some were separated from their families as they fled attacks or were abducted by the military for various reasons; others were forcibly placed in orphanages or smuggled from the country and illegally adopted abroad.

In 1994, in the absence of any governmental support, Jon Cortina, a Spanish Jesuit priest who lived and preached in El Salvador, founded the nongovernmental organization Pro-Búsqueda ("For the Search"), which was dedicated to finding the missing children. DNA testing of youth suspected of having been disappeared became a crucial tool used by the group, as the organization worked to find matches in a database of relatives searching for missing family members built with the support of a group of forensic geneticists from the United States.

In 2005, more than a decade after the end of the war, Elizabeth Barnert, a Cuban American of Jewish descent, who was then a young medical student in California, volunteered to go to El Salvador to research and write about the psychosocial and human rights issues surrounding the disappeared children. Her new book, *Reunion*, documents her experience over the next 17 years, as she completed her medical and public health studies at the University of California, conducted research in El Salvador, and worked with Pro-Búsqueda to document the reunification of long-separated families.

Reunion opens with a foreword by Philippe Bourgois, an American anthropologist who worked with indigent communities in El Salvador during the war and who provides a very useful historical account of the country. This section emphasizes the prevailing social injustice, authoritarianism, and political repression during the decades that preceded the civil war.

The book itself is a collection of moving narratives that document a number of encounters and interviews conducted by the author over many years with relatives of disappeared children as well as with "jóvenes encontrados" (found youth) themselves. Working with Pro-Búsqueda, the author followed up on dozens of very sensitive cases of forced separation and documented the efforts of parents and family members to find their missing loved ones. Some of the found youth Barnert meets were discovered still living in orphanages, whereas many others had been adopted illegally by American or European families during the war. Most of the latter were aware that they had been adopted from El Salvador and were very keen to learn more about their biological families.

Barnert's ability to describe the diverse feelings of the book's protagonists—be they searching relatives or found youth—is admirable, and many of the stories she recounts, particularly those described by mothers of disappeared children, are truly harrowing. One mother describes having lost a child during the crossing of a river in the middle of a battle, for example, while another recounts being forced to give up her newborn for adoption because she could not care for her. Among the found youth interviewed, Barnert documents psychological troubles attributable to identity ambivalence as well as pervasive feelings of abandonment that have led some to join armed gangs.

The most emotional intensity takes place during family reunions after identification. Although each "case" is distinctive, a common denominator among searching relatives and found youth is psychological pain and suffering. Barnert's compassionate approach to her interviews helps bring to the surface many complex feelings for her subjects and, hopefully, contributes to their healing.

Reunion
Elizabeth Barnert
University of California Press, 2023. 370 pp.

This book, beautifully written from the heart, is an essential tool for anyone interested in recent Latin America history, which has been plagued by authoritarian regimes and military dictatorships that have violated fundamental human rights. Among an endless list of atrocities, the book rightly focuses on the right to identity as a fundamental human right and a basis for dignity, freedom, and truth. ■

The reviewer is at the Department of Genetics and Human Rights, Universidad Nacional de Tres de Febrero, Buenos Aires, Argentina. Email: victorpenchas@gmail.com

10.1126/science.adg2895

Hacking and the social contract

Although technical fixes can help, solutions must focus on broader societal factors at play

A Hacker's Mind: How the Powerful Bend Society's Rules, and How to Bend Them Back
Bruce Schneier
Norton, 2023. 304 pp.

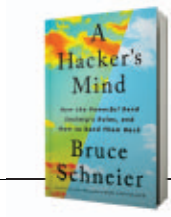

By **Viktor Mayer-Schönberger**

The concept of "hacking" is not an invention of the digital age. Nor is it a purely technical process, although today it often requires some technical expertise. Humans have always tried to find loopholes in the systems of rules we find ourselves beholden to. When we reach a wall, we try to find a way around it.

Bruce Schneier's *A Hacker's Mind* is a collection of fairly short, often insightful commentaries about hacking. Schneier is one of the nation's most well-known cybersecurity experts, and his prose is clear, jargon-free, and a pleasure to read. A reader might pick up this book for the numerous instructive cases and vignettes it offers, but conceptually, *A Hacker's Mind* advances an important point; and it is hugely revealing that Schneier—a computer scientist—is making it.

People have long sought to hack society's conventions and legal norms—from taking advantage of tax loopholes to creatively evading military drafts—and they do so most often by bending social rules. Hence, Schneier sees hacking as a social rather than a technical phenomenon.

This might sound like a simple reframing, but it has huge consequences. It effectively dispenses with the naïve hope that hacking can be "solved" through technical fixes, although technology can, of course, be a part of the solution. Effective responses, argues Schneier, need to be socially anchored as well.

When we talk about hacks, we often think of their negative consequences, or what economists call "externalities": taxes go unpaid, cars designed to cheat emissions inspections pollute the environment. But some hackers repurpose a social system for their own ends. For instance, a group of kids hacked the prohibition of free-form text communication in Disney's online kids game Club Penguin by using their avatars' body positions to communicate letters. Seen from this perspective, hackers can be social innovators—probing, reinterpreting, circumventing, and even breaking established norms.

Schneier is at his best when he details the balancing act in society between our social systems that ensure rules are followed and the importance of keeping an open mind toward norm innovation–causing hacking. We ought to conceive of hacking as a human behavior that is neither intrinsically dangerous nor inherently laudable, he argues. To judge its value, we need to evaluate a hack along multiple dimensions and in context. The result often highlights complicated trade-offs. We can be impressed, for example, by a hack's effectiveness but loathe its unethical nature, as with the "Double Irish with a Dutch Sandwich," an intricate tax hack that reduced US corporations' tax liability by billions, or find it disruptive, but eventually come to accept it as the new normal, as we did with dunking in basketball, a practice that leagues initially tried to ban but was eventually accepted, as fans liked it.

By giving hacking a social meaning, we link it to the human desire to influence the decisions and behaviors of others and we shift focus to social systems that provide boundaries but are themselves mutable. *A Hacker's Mind* is highly recommended reading, precisely because of the broader context it provides on this point, without which remedies remain elusive.

Perhaps the only limitation of the book is that Schneier does not go far enough in his analysis. For instance, he repeatedly embarks on examinations of the social and technical interplay of a particular case—how Boeing got away with the problematic Maneuvering Characteristics Augmentation System (MCAS) hack in its 737 aircraft, or how banks successfully hacked the Dodd-Frank Act that aimed to regulate derivatives—only to reduce the problem to simple questions of power and wealth. The rich and powerful hack unconstrained, he argues, while the rest of us are forced to follow the rules. As social science research has shown time and again, that is too meek an explanation (*1*).

In other instances, Schneier offers thoughtful descriptions of the social elements of a hack but then advocates a technical fix. He makes clear that such fixes are only one part of a comprehensive solution, but one cannot help but see the computer scientist attempting to fix bugs at such moments. As Schneier seems to have discovered himself, understanding social systems is hard and reverting to trotted paths enticing.

That Schneier has pushed himself beyond his own comfort zone, confronting hacking as something bigger and more multifaceted than simply sand in the machinery of digital systems, is what makes *A Hacker's Mind* unique and valuable. If his message is received, our social systems will soon begin to evolve to interact with hacking with greater agility, nuance, and even—in some instances—appreciation. ■

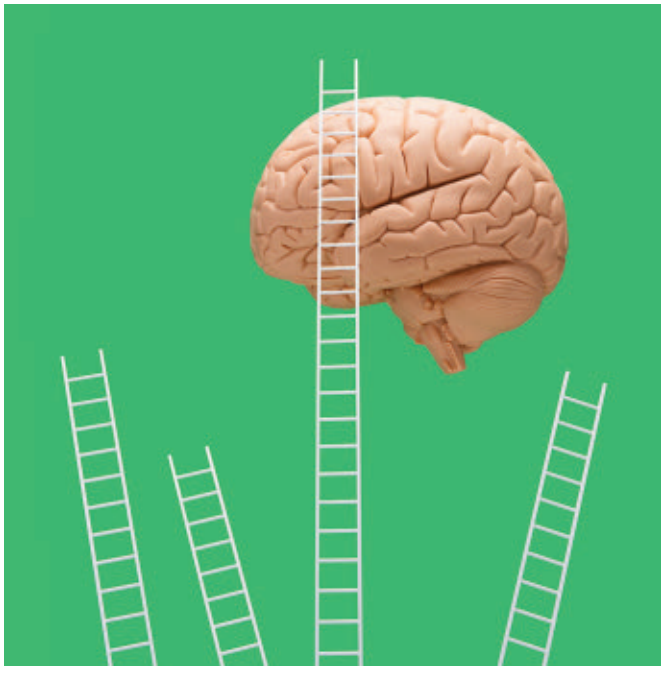

ILLUSTRATION: PM IMAGES/GETTY IMAGES

The reviewer is at the Oxford Internet Institute, University of Oxford, Oxford OX1 3JS, UK. Email: viktor.ms@oii.ox.ac.uk

REFERENCES AND NOTES

1. For example, Lawrence Lessig argues in *Republic, Lost* (Twelve, 2011) that even lobbying Congress is not only about money but also about information.

10.1126/science.adg3002

The Vetlesen Prize 2023

Achievement in the Earth Sciences

The Lamont-Doherty Earth Observatory and The G. Unger Vetlesen Foundation are pleased to congratulate the 2023 Vetlesen Prize Laureate

David Kohlstedt for his pioneering work showing how processes occurring at inaccessible depths of the Earth drive what happens on our planet's surface.

Columbia University will present David Kohlstedt with the 2023 Vetlesen Prize at a formal dinner in April 2023.

lamont.columbia.edu/about/vetlesen-prize

The Vetlesen Prize honors scientific achievement that results in a clearer understanding of the Earth, its history, or its relation to the universe.

Columbia Climate School
Lamont-Doherty Earth Observatory

NEWS FROM Science | AAAS

Subscribe to **News from Science** for unlimited access to authoritative, up-to-the-minute news on research and science policy.

bit.ly/NewsFromScience

LETTERS

Plastics used in agriculture can lead to soil contamination.

PHOTO: DENG HEPING/VCG VIA GETTY IMAGES

Edited by **Jennifer Sills**

Soil microplastics pollution in agriculture

Soil microplastics contaminate the soil when macroplastics used in farming decompose, threatening both agriculture and human health (*1*). Demand for agricultural plastics to regulate field climate is estimated to increase by 50% by 2030 (*2*). Emergency action is required to mitigate soil microplastics pollution and to help guide sustainable agricultural production.

Frequent extreme weather and growing food demand have exacerbated reliance on plastics to increase grain yield (*3*). Plastics used in agriculture include greenhouses and plastic films for temperature control, irrigation pipes, and seed plastic coating to prevent pests and diseases. When these plastics are left to decompose in the fields, microplastics enter the soil (*4*), decreasing the number, diversity, movement, and reproduction rate of soil biota (*5*). Microplastics can also change the physiochemical properties of soil, such as its structure, water-holding capacity, and density (*6*), which could restrict root growth, nutrient uptake, and yield of future crops (*7*).

Soil microplastics can be transferred to humans through the food chain or water cycle (*8*). Microplastic particles have been found in human intestines, lungs, blood, brain, and breast milk (*9*). These foreign substances can cause tissue rejection and inflammation, similar to the impact of particulate matter of less than 2.5 μm on the human respiratory system (*10*). Moreover, most compounds added to plastics, such as plasticizers, stabilizers, and pigments, are harmful to the human endocrine system (*11*).

Mitigating the damages of soil microplastics in farmland will require comprehensive action, including research, production, administration, and legislation. The global soil microplastics content in farmland caused by agricultural plastics must be quantified by combining long-term field monitoring, satellite remote sensing, and theoretical modeling. The potential damages of soil microplastics to land productivity, soil and field biodiversity, and human health must be determined. The site-specific maximum threshold for agricultural plastics use must be determined, especially in key agricultural regions with high microplastics content. Coordinated action plans such as consistent monitoring and assessment, global and cross-sectoral cooperation, and open data sharing are urgently required. Governments should encourage the transition to affordable biodegradable plastics through policy incentives, technological innovation, agricultural subsidies, public outreach, and collaboration with other stakeholders such as nongovernmental organizations, scientists, and industry. Farmers should receive incentives to explore nature-based farm equipment, phase out single-use plastic film, and prioritize reusable plastic products. Scientists should work to create affordable biodegradable agricultural plastic options and technology that can remove microplastics from the soil. Finally, legislation must be passed to regulate the use of agricultural plastics and the level of microplastics pollution in soil.

Liuyue He[1], Zhongbin Li[1], Qian Jia[2], Zhenci Xu[3]*
[1]School of Remote Sensing and Information Engineering, Wuhan University, Wuhan 430079, China. [2]College of Environmental Science and Engineering, Tongji University, Shanghai 200092, China. [3]Department of Geography, The University of Hong Kong, Hong Kong 999077, China.
*Corresponding author. Email: xuzhenci@hku.hk

REFERENCES AND NOTES

1. United Nations Environment Programme, "Plastics in agriculture–an environmental challenge" (2022); https://www.unep.org/resources/emerging-issues/plastics-agriculture-environmental-challenge.
2. Food and Agriculture Organization, "Assessment of agricultural plastics and their sustainability: A call for action" (2021); https://www.fao.org/documents/card/en/c/cb7856en.
3. J. Yates *et al.*, *Nat. Food* **2**, 80 (2021).
4. C. M. Rochman, *Science* **360**, 28 (2018).
5. F. Zhu *et al.*, *Bull. Environ. Contam. Toxicol.* **102**, 741 (2019).
6. M. C. Rillig, A. Lehmann, *Science* **368**, 1430 (2020).
7. M. C. Rillig *et al.*, *New Phytol.* **223**, 1066 (2019).
8. Y. S. Jung *et al.*, *Environ. Pollut.* **315**, 120442 (2022).
9. A. D. Vethaak, J. Legler, *Science* **371**, 672 (2021).
10. X. Z. Lim, *Nature* **593**, 22 (2021).
11. M. Sendra *et al.*, *J. Hazard. Mater.* **409**, 124975 (2021).

10.1126/science.adf6098

Understanding the limits of AI coding

In the 9 December 2022 issue, the Research Article "Competition-level code generation with AlphaCode" (Y. Li *et al.*, p. 1092) and the accompanying Perspective, "AlphaCode and 'data-driven' programming" (J. Z. Kolter, p. 1056) describe an artificial intelligence (AI)–based system for generating code. The authors explain that the system can be used for small coding problems, such as tests for computing students, and that they are far from being useful in computing applications that include millions of lines of code, such as word processing. As we enter an era of AI where tools like AlphaCode and chatGPT will change how tasks are performed, it is important to understand the boundaries of what they can and cannot do.

To make sure that code can be maintained and managed by other programmers, human developers use mnemonic variable names and embed explanatory comments. Understanding, debugging, and extending code written by other humans remains a formidable challenge—perhaps even more difficult than producing the code in the first place. In addition, many techniques are used for validation and verification, and code used in mission-critical applications, such as airline flight systems, goes through substantial quality assurance testing. AI models have yet to address the challenges of maintaining code, ensuring that users can decipher it, and subjecting programs to safety protocols.

Understanding and evaluating the limits of these techniques is crucial before they are put into real-world use. Some testing of capabilities has been applied to language generation tools (*1*, *2*), but AI coding remains a nascent field. The Technology Policy Committee of the Association for Computing Machinery recommends more investment in transparency and accountability for AI algorithms (*3*). The promise of systems like AlphaCode must be carefully balanced against the risks of their use. The interaction between AI code-generation systems and human programmers must be resolved before such systems can become an integral part of the future of computing.

James Hendler
Future of Computing Institute, Rensselaer Polytechnic Institute, Troy, NY, USA and Technology Policy Council, Association for Computing Machinery, New York, NY, USA.
Email: hendler@cs.rpi.edu

REFERENCES AND NOTES

1. J. Wei et al., *arXiv* 10.48550/arXiv.2206.07682 (2022).
2. K. Valmeekam, A. Olmo, S. Sreedharan, S. Kambhampati, *arXiv* 10.48550/arXiv.2206.10498 (2022).
3. ACM Technology Policy Council, "Statement on principles for responsible algorithmic systems" (2022); https://www.acm.org/binaries/content/assets/public-policy/final-joint-ai-statement-update.pdf.

10.1126/science.adg4246

Effective implementation of new biodiversity pact

In his *Science* Insider piece "New biodiversity pact sets ambitious goals, but will nations deliver?" (22 December 2022, https://scim.ag/1jG). E. Stokstad explains that the Kunming-Montréal Global Biodiversity Framework (GBF) of the Convention on Biological Diversity (CBD) is scientifically strong but legally weak. The GBF lacks hallmarks of effective international agreements, such as reciprocal responsibilities, dispute resolution systems, uncompromisable goals, and noncompliance penalties. For the GBF to be effective, these shortfalls must be addressed.

As Stokstad reports, the GBF aims to protect 30% of all lands and oceans, but the goal is global rather than national, which makes accountability difficult. Countries such as Brazil, Indonesia, and the Democratic Republic of Congo, which have more than 30% rainforest cover, are likely to continue current rapid deforestation (*1*). Moreover, because conservation goals pertain to all ecosystems and do not prioritize biodiverse areas, a country could declare rangelands as protected areas while continuing to allow logging in rainforests. Countries could also allow areas to be logged or cleared before declaring them as national parks, as has happened in Australia (*2*). The wording of the GBF (*3*) would allow countries to count the national park toward the target for protected land and then restore the area and count it again, this time toward GBF's separate target for restoration.

The GBF multilateral fund of US$30 billion per year (*4*) is more than 10 times the aggregate budgets of all developing-country parks agencies worldwide (*5*), and it could enable them to fund new land purchases, protection, and anti-poaching measures. However, these funds represent a transfer of just 0.1% of international trade (*6*) and just 0.03% of global gross national product (*7*) from taxpayers in developed nations to governments in developing nations. Meanwhile, multinational corporations that primarily serve wealthy countries continue to exploit developing countries' natural resources.

The framework provides for an additional US$170 billion per year for biodiversity funding within each country's own borders (*4*), including mechanisms such as ecosystem services payments and the purchase and protection of unprotected land of high conservation value to compensate for biodiversity loss elsewhere. However, such purchases, known as biodiversity offsets, are subject to political manipulation and largely unsuccessful (*8*). Offsets have even been claimed within an existing national park (*9*), already fully protected by law.

The US$30 billion per year the GBF international fund will be distributed through the Global Environment Facility (*4*). This new GBF sum is more than 80 times Global Environment Facility's 2022 to 2026 biodiversity allocation (*10*). Most Global Environment Facility funds go to newly industrialized rather than developing nations, and there is a risk that the organization will disseminate GBF funds similarly.

To strengthen the GBF, all financial transfers during its implementation need auditable accounting. Every new protected area needs internationally transparent boundaries, budgets, standards, and monitoring; the World Heritage model (*11*, *12*) could serve as an example. Penalties are needed for noncompliance. For example, countries that declare reserves but don't protect them could be charged a levy on exports, used to fund new reserves elsewhere. CBD could require these as conditions of GBF funds, with additional monitoring by nongovernmental organizations and research scientists.

Ralf Buckley
Griffith University, Gold Coast, QLD 4222, Australia. Email: r.buckley@griffith.edu.au

REFERENCES AND NOTES

1. D. M. Lapola *et al.*, *Science* **379**, eabp8622 (2023).
2. J. Ward, "The relative net economic benefits of logging and tourism in native Australian forests," PhD Thesis, Griffith University, Gold Coast (1999).
3. UN Environment Programme (UNEP), *Kunming-Montreal Global Biodiversity Framework: CBD/COP/15/L.25* (2022).
4. UNEP, *Financial Mechanism: CBD/COP/15/L.33* (2022).
5. R. Buckley *et al.*, *PLOS ONE* **7**, e44134 (2012).
6. "Global trade set to hit record $32 trillion in 2022, but outlook increasingly gloomy for 2023," UNCTAD (2022).
7. International Monetary Fund, World Datasets (2022); https://www.imf.org/external/datamapper/profile/WEOWORLD.
8. S. zu Ermgassen *et al.*, *Conserv. Lett.* **12**, e12664 (2019).
9. L. Cox, "NSW government seeks to use national park management to offset Warragamba Dam wall project," *The Guardian* (2022).
10. Global Environment Facility, "Initial GEF-8 star country allocations: GEF/C.63/Inf.05" (2022).
11. UN Educational, Scientific, and Cultural Organization (UNESCO), State of Conservation Information System (2023); https://whc.unesco.org/en/soc/.
12. UNESCO, World Heritage Convention: Periodic Reporting (2023); https://whc.unesco.org/en/periodicreporting/.

10.1126/science.adg5018

RESEARCH

IN *SCIENCE* JOURNALS

Edited by **Michael Funk**

PHOTO: DAI *ET AL.*

New fossils from a site in China, including the ammonoid shell pictured here, reveal a surprisingly diverse ecosystem in the early Triassic.

PALEONTOLOGY

Mass extinction rebellion

The Triassic recovery of life from the devastating end-Permian mass extinction was an amazing period of evolution. Whether biodiversity had to rebuild from near annihilation or from refugia is a matter of conjecture, but recovery heralded the development of recognizably modern ecosystems. Dai *et al*. present examples of diverse fishes, ammonoids, bivalves, protists, and malacostracan arthropods from a fossil site dated approximately 1 million years after the crisis. These fossil assemblages, particularly the presence of vertebrate predators, reveal a surprisingly early diversity of animals after the end-Permian mass extinction. —CA and SNV

Science, adf1622, this issue p. 567

NANOPHOTONICS

Nanoscale negative refraction

Refraction is a familiar effect in which a light beam alters direction as it propagates from one medium to another. Negative refraction is a nonintuitive but well-established effect in which the light beam is bent in the "wrong" direction. Two groups now independently demonstrate negative refraction at the interface of two-dimensional van der Waal materials. Hu *et al*. used molybdenum trioxide with a graphene overlayer to show that in-plane negative refraction of mid-infrared (mid-IR) polaritons occurs at the interface and is gate tunable. Sternbach *et al*. used molybdenum trioxide/hexagonal boron nitride bicrystals to show that negative refraction of mid-IR polaritons occurs for propagation normal to the interface. Polaritonic negative refraction in the mid-IR provides opportunities for optical and thermal applications such as IR super-resolution imaging, nanoscale thermal manipulation, and chemical sensing devices with enhanced sensitivity. —ISO

Science, adf1251, adf1065, this issue pp. 558 and 555

VIROLOGY

Catching out cap snatching

Soome virus families hijack part of their hosts' RNA to enable their own replication in a process called cap snatching. Before they can enact a snatch, influenza viruses specifically require host cap maturation by a host methyltransferase called MTr1. Tsukamoto *et al*. screened a compound library and found that trifluoromethyl-tubercidin (TFMT) inhibits host Mtr1 and suppresses virus replication. TFMT inhibits host cap RNA maturation and impedes binding of host cap RNAs with the viral polymerase, thus disabling viral replication. TFMT was not only effective in inhibiting viral replication in human lung cells, but was also effective in mice, displayed little toxicity, and acted in synergy with approved anti-influenza drugs. —CA

Science, add0875, this issue p. 586

COMPLEMENT

Lung protection by local complement

Complement proteins are innate immune defense molecules that protect the host against pathogenic microorganisms. The activities of the C3 component of complement are mostly attributed to circulating C3 primarily synthesized by hepatocytes. Sahu *et al*. used mouse models of conditional gene deletion to investigate the contribution of local C3 protein production in the lung to protecting the pulmonary mucosal surface from cell damage caused by *Pseudomonas aeruginosa* infection. Mice lacking C3 only in lung epithelial cells exhibited more pronounced acute lung injury

than control mice even when circulating C3 levels were maintained at near-normal levels by maintenance of liver C3 production. These findings point to lung epithelial cell–intrinsic protective functions provided by C3 as being an essential contributor to the first-line defense against bacterial pneumonia. —IRW

Sci. Immunol. **8**, eabp9547 (2023).

HOMININ EVOLUTION

Earlier Oldowan

Oldowan tools, consisting of stones with one to a few flakes removed, are the oldest widespread and temporally persistent hominin tools. The oldest of these were previously known from around 2.6 million years ago in Ethiopia, and by 2 million years ago, they were found to be quite widespread. Plummer *et al*. report on an older fossil site from around 3 to 2.6 million years ago in Kenya, where Oldowan tools were not only present, but were also being used to process a variety of foods, including hippopotamus. Thus, it appears that these tools were widespread much earlier than previous estimates and were widely used for food processing. Which hominins were using these tools remains uncertain, but *Paranthropus* fossils occur at the site. —SNV

Science, abo7452, this issue p. 561

FISH EVOLUTION

Debate resolved?

Teleost (or "ray-finned") fishes make up half of all vertebrates, but there has been long-standing debate about their early evolution. Using new genomes from fishes in the basal group that includes tarpons and eels, as well as approaches that integrate patterns of genome structure not just sequence, Parey *et al*. show that this group forms a monophyletic lineage within another group that includes the arapaima and elephant nose fishes. This single lineage is resolved as sister to all the other teleosts, settling a debate about patterns of early fish evolution. —SNV

Science, abq4257, this issue p. 572

MALARIA

A different antibody angle

Natural killer (NK) cells have been shown to mediate immune responses against the malaria parasite *Plasmodium falciparum* using multiple effector functions. Odera *et al*. now show that *P. falciparum* merozoites marked by antibodies can induce NK cell degranulation and interferon-γ production. This response was not strain specific and reduced invasion of merozoites into uninfected red blood cells. Using a controlled human malaria infection study in adults, the authors observed that antibody-dependent NK (ab-NK) cell activity correlated directly with the control of parasitemia. In addition, in a cohort of children living in an endemic malaria setting, ab-NK cell frequency increased with age, was boosted during *P. falciparum* infection, and was linked to a reduced risk of clinical malaria. These findings highlight a key role for antibody-mediated NK cell responses during malaria. —CNF

Sci. Transl. Med. **15**, eabn5993 (2023).

Analysis of fish genomes reveals the evolutionary relationships between teleost fishes, a diverse group that includes eels (such as the giant moray eel, pictured here), zebrafish, and the giant arapaima.

IN OTHER JOURNALS

Edited by **Caroline Ash** *and* **Jesse Smith**

ICE SHEETS

In winter like in summer

Water from melting of the surface of the Greenland ice sheet can flow through channels in the ice to the base of the ice sheet, where it may reduce the friction between the ice sheet and the underlying bed and thereby accelerate the flow of the overlying ice. This process normally occurs in the summer, but Maier *et al*. show that meltwater-induced ice flow also can occur during the winter. These wintertime events, which are caused by the cascading release of water stored in supraglacial lakes, are likely to have a larger impact on ice dynamics than previously realized. —HJS *Geophys. Res. Lett.* 10.1029/2022GL102251 (2023).

Summertime melting of surface ice can be stored in supraglacial lakes and released to the bottom of the ice sheet during winter.

PHOTOS: (LEFT TO RIGHT) CINOBY /ISTOCKPHOTO; WANDERLUSTER/ISTOCKPHOTO

QUANTUM SIMULATION

Spotting quantum avalanches

Disorder can prevent interacting quantum systems from thermalizing, a phenomenon known as many-body localization. If, however, a section of the system is free of disorder, then that subsystem has been predicted to thermalize and grow in an avalanche-like process. To test this prediction, Léonard *et al.* used a chain of 12 interacting cold atoms, the right half of which were subjected to a disorder potential. After a quench, the clean left half of the chain quickly thermalized. The disordered right half initially resisted thermalization, but at longer times, characteristic anticorrelations appeared that were strongest near the interface between the two halves. The dynamics of the anticorrelation spread were consistent with a quantum avalanche. —JS

Nat. Phys. 10.1038/s41567-022-01887-3 (2023).

PHOTONICS

Optically addressing 3D laser arrays

Coping with the insatiable need for the transfer and processing of vast amounts of data is expected to see a shift from mainly electronics-based platforms to either hybrid opto-electronic or solely optical platforms. Such a shift to an integrated photonics technology requires the ability to use and address arrays of optical sources. Song *et al.* demonstrate the ability to fabricate three-dimensional (3D) arrays of photonic crystal nanolasers by printing them along the length of an optic fiber. They then show that each nanolaser can be addressed individually through an interference effect by simply adjusting the pulse width and polarization of the input light into the optic fiber. The ability to program such a 3D array offers possibilities for developing high-density optical circuits and may have applications in sensing. —ISO

Optica **9**, 1424 (2022).

IMMUNOTHERAPY

Off-the-shelf T cell therapy

Multiple myeloma is characterized by the accumulation of malignant plasma cells in the bone marrow. Various B cell maturation antigen (BCMA)–targeted drugs are approved for the treatment of relapsed/refractory multiple myeloma, including an engineered chimeric antigen receptor (CAR) T cell therapy. However, extracting T cells from individual patients to produce autologous CAR T cells presents numerous challenges. ALLO-715 is an allogeneic, "off-the-shelf" BCMA-targeted CAR T cell therapy. Mailankody *et al*. report interim results from the ongoing first-in-human phase 1 trial of ALLO-715 in 43 patients with relapsed/refractory multiple myeloma. CAR T cell regimens are associated with adverse events that are treatable if managed early. ALLO-715 treatment resulted in grade 3 or higher adverse events in 88% of patients, but 70.8% of patients had a partial response or better with a median duration of 8.3 months. Therefore, ALLO-715 treatment appears to be feasible and could be beneficial for treating multiple myeloma. —GKA

Nat. Med. 10.1038/s41591-022-02182-7 (2023).

PHYSIOLOGY

Searching muscle and fat regulators

Extracellular fluid contains proteins that are difficult to detect or are absent in serum. Such proteins include secreted regulatory factors that control tissue physiology. Mittenbühler *et al.* adapted a technique in which low-speed centrifugation allowed the rapid isolation of proteins from the extracellular fluid of muscle or fat from mice. The authors then applied mass spectrometry to identify proteins whose abundance changed in response to cold exposure or exercise. Some unexpected myokines and adipokines emerged, which could potentially mediate signaling involved in some of the well-known beneficial physiological effects of exercise. —LBR

Cell Metab. 10.1016/j.cmet.2022.12.014 (2023).

MICROBIOTA

Honeybee self-medication

Plants generate a range of toxic metabolites, many of which are intended to deter insect pests. Pollinators are also exposed to these so-called xenobiotic compounds in nectar and pollen. Some of these chemicals can confer benefits to pollinators against pathogens, but it is a question of getting the dose right. Compared with other insects, bees lack the genetic capacity to fully metabolize xenobiotics, so Motta *et al.* investigated whether the bee microbiome could supply the missing functions. Honeybees feeding on almond blossom ingest the cyanogenic glycoside amygdalin when foraging. The authors found that microbiota-depleted bees metabolized amygdalin to the more toxic prunasin, which accumulated in the insect's gut. Bees with a full complement of gut microbiota, including one called *Bifidobacterium* wkB204, can fully degrade amygdalin by means of a glycoside hydrolase 3. Host and microbiota thus join forces to maintain levels of a potential toxin at tolerable levels to ward off parasites. —CA

eLife **11**, e82595 (2022).

PLANT SCIENCE

Nematodes hijack root development

Cyst nematode parasites cause substantial damage to crop plants. These parasites invade plant roots, destroying internal root tissue structure and inducing root branching to provide additional feeding sites. Guarneri *et al.* found that cyst nematode infection triggers the accumulation of the plant hormone jasmonic acid and up-regulates a key transcription factor for root induction. These events lead to increased local biosynthesis of auxin that initiates de novo root formation in a similar manner to wound-associated root induction. Although infected plants maintained their overall root system size, increased secondary root growth was balanced by reduced primary root lengths. Therefore, pathogens can manipulate the dynamic responses of root systems for their own benefit. —MRS *New Phytol.* **237**, 807 (2023).

Cyst nematodes (*Heterodera rostochiensis* is shown) are important crop plant pests because of the damage they cause by stimulating secondary root growth.

PHOTO: NIGEL CATTLIN/SCIENCE SOURCE

ALSO IN *SCIENCE* JOURNALS

Edited by **Michael Funk**

CHEMICAL PHYSICS

Unraveling excited electronic states

For more than 100 years, linear spectroscopy has served as the primary means of exploring and validating quantum mechanical energy levels of atoms and molecules. With strong light fields, nonlinear spectroscopic methods using multiple pulses yield sensitive molecular information and provide powerful tools, such as magnetic resonance imaging. A recent revolution uses multiple x-ray pulses and newly developed nonlinear x-ray spectroscopy methods to derive time-resolved atomic, molecular, and solid-state dynamics. In a Perspective, Leone and Neumark discuss nonlinear attosecond four-wave mixing in which an x-ray pulse is merged with two optical pulses in molecules and materials to unveil ultrashort processes such as quantum pathways in transient electronic states. —GKA

Science, add4509, this issue p. 536

EPIGENETICS

Plasticity of cancer cell phenotypes

During differentiation, cells adopt phenotypic states of progressive specificity. Cancer cells violate this property, instead adopting increased plasticity of structure and function. Epigenetic change has been considered a developmental landscape that can channel specific differentiation events and define and constrain distinct phenotypic and gene expression states. In a Review, Feinberg and Levchenko discuss how cancer epigenetic landscapes can be defined quantitatively, borrowing from theory used in physical sciences to define potential energy and its relationship to physical or chemical states. This strategy has yielded new insights whereby stochastic changes in the epigenetic landscape of cancer cells drive oncogenic phenotypes. Such analyses can also reveal pathogenic signaling and therapeutic targets. —GKA

Science, aaw3835, this issue p. 552

DEVELOPMENT

Metabolism sets neuronal development pace

The pace of neuronal development varies between species, and the relatively slow development of the human brain may help allow its exceptional complexity. Iwata *et al*. propose that the pace of neuronal development depends on the rate of metabolic activity in mitochondria. Human and mouse neurons exhibited distinct paces of development in culture correlated with the tricarboxylic acid (TCA) cycle and oxidative activity in mitochondria. Manipulations to increase oxygen consumption rates and TCA cycle activity in human cells increased the rate of neuronal development. Slowing metabolic rates in mouse neurons slowed neuronal maturation. Thus, metabolic rates in mitochondria appear to somehow help set the speed of neuronal development. —LBR

Science, abn4705, this issue p. 553

CORONAVIRUS

OAS–RNase L pathway the "MIS-C"ing link?

Multisystem inflammatory syndrome in children (MIS-C) is a severe complication of severe acute respiratory syndrome coronavirus 2 (SARS-CoV-2) that affects one in 10,000 infected children, is reminiscent of Kawasaki disease, and its etiology remains unknown. Lee *et al*. performed whole-exome and whole-genome sequencing on a cohort of MIS-C patients and uncovered autosomal-recessive deficiencies of OAS1, OAS2, or RNase L in around 1% of the cohort (see the Perspective by Brodin). These genes are components of a signaling pathway that suppresses inflammation in double-stranded RNA-stimulated mononuclear phagocytes. Thus, single-gene recessive inborn errors of the OAS–RNase L pathway can result in uncontrolled inflammatory cytokine production by mononuclear phagocytes after SARS-CoV-2 infection, potentially explaining the origins of MIS-C in some children. —STS

Science, abo3627, this issue p. 554; see also adg2776, p. 538

GEOCHEMISTRY

Testing Earth's water

The chemistry of aqueous systems early in Earth's history is important for the eventual development of life on the planet. However, the relative lack of rocks from billions of years ago presents a great challenge for solving this puzzle. Trail and McCollom used the chemistry of four-billion-year-old zircons to estimate the fluid chemistry and temperature for mineral formation (see the Perspective by Rodriguez). They found more oxidizing fluids feeding hydrothermal pools than previously expected, which has implications for how minerals and organics may have formed in the time just after Earth's accretion. —BG

Science, adc8751, this issue p. 582; see also adg2630, p. 539

PLANT SCIENCE

Noncoding gene drives floral speciation

In monkeyflowers (*Mimulus* spp.), variation in the *YELLOW UPPER* (*YUP*) genetic locus causes changes in flower color patterns that in turn drive speciation with shifts in whether the flower is pollinated by bees or by hummingbirds. Liang *et al*. now show that the locus does not encode a protein (see the Perspective by Monniaux). Instead, *YUP* produces phased small interfering RNAs (siRNAs) that regulate floral carotenoid pigmentation. Revealing the opportunistic nature of evolution, the locus evolved from a fragment of a gene encoding a cytochrome protein not involved in floral pigment production. —PJH

Science, adf1323, this issue p. 576; see also adg2774, p. 534

CALCIUM SIGNALING

Restoring a quiescent state for STIM1

Gain-of-function mutations in the endoplasmic reticulum Ca^{2+} sensor STIM1 result in constitutive activity of the plasma membrane Ca^{2+} channel Orai1 and underlie a disease called Stormorken syndrome. Gamage *et al.* found that deletion of a glutamate residue in STIM1 reversed the effects of a common Stormorken syndrome–associated mutation. Mice expressing STIM1 with both modifications were phenotypically similar to wild-type mice. The combined modifications restored the protein domain interactions that prevent STIM1 from associating with and activating Orai1 in the absence of stimuli. —WW

Sci. Signal. **16**, eadd0509 (2023).

AAAS.ORG/COMMUNITY

AAAS' Member Community is a one-stop destination for scientists and STEM enthusiasts alike. It's "Where Science Gets Social": a community where facts matter, ideas are big and there's always a reason to come hang out, share, discuss and explore.

Member COMMUNITY
AAAS

AMERICAN ASSOCIATION FOR THE ADVANCEMENT OF SCIENCE

REVIEW SUMMARY

EPIGENETICS

Epigenetics as a mediator of plasticity in cancer

Andrew P. Feinberg* and Andre Levchenko*

BACKGROUND: During differentiation, living cells within complex organisms adopt phenotypic states of progressive specificity. Cancerous cells and tissues violate this property, adopting increased plasticity of cell states, tissue structure, and function during their progression. The information about the repertoire of normal differentiation outcomes is genetically encoded, but the information about the particular realization of this potential and cell regulation in response to the environment is encoded epigenetically in DNA methylation and biochemical modification of chromatin. Dating back to Conrad Waddington's prescient work, epigenetic change has been viewed schematically as a developmental landscape that can channel specific differentiation events and define and constrain distinct phenotypic and gene expression states. More recently, cancer onset and progression have been viewed as a reversal or deformation of this landscape. In the physical sciences, potential energy landscapes and their relationships to the probability distribution of physical or chemical states have been developed and refined for decades, but they have only recently been applied to more quantitatively realize Waddington's classical landscape idea. Such approaches are particularly appealing in describing the cancer epigenetic landscape given that the plasticity of cell states realized on such a landscape lies at the functional core of the disease.

ADVANCES: Recent developments in experimental technologies, including single cell–resolution analysis of mRNA and protein expression as well as molecular assays of epigenetic modifications of DNA and histones, have enriched our understanding of the diversity of phenotypic states defined by genomic information and epigenetic control. In this work, we expand on the emerging view that there is considerable variability in the expression of biological molecules even within presumably isogenic cells in normal homeostatic tissues or in well-defined cell lines in cell culture. This revelation suggests that the biological processes may be essentially stochastic and that biological variability on the cellular level can be indicative of—or even drive—important aspects of biological function. This analysis has also enabled assessment of the probability distributions of different cellular states, or quasipotential energy, and the use of these to determine the associated entropy, a measure of informational uncertainty. These measures, which we define in detail, enable a precise and quantitative definition of the underlying epigenetic landscapes, coordinately reflected by gene expression landscapes. Cancer-related genetic and epigenetic alterations can increase the entropy of the landscape as a whole and result in higher variability and occupancy of otherwise cryptic attractors. An increase in entropy and thus heterogeneity of the responses—rather than alteration of the average response—is emerging as a key and often overlooked feature of the landscape deformation in cancer pathogenesis. Changes in entropy can also accompany cell differentiation and aging in ways that further inform cancer etiology. They also permit distinguishing phenotypic plasticity from phenotypic heterogeneity. Using recent observations and landscape conceptualization, we outline several scenarios that can occur during precancerous and cancerous progression. We also discuss the molecular mechanisms enabling these scenarios, relating them to specific landscape transformations. We suggest how the relationship between the epigenetic landscape alterations and corresponding phenotypic changes can be quantitatively assessed and used to further understand the information transfer in signaling pathways and to develop new therapeutic interventions. This approach can also incorporate recently introduced ideas of the archetypical states of cells within normal and cancerous tissues.

OUTLOOK: New integrated theoretical and experimental methods in quantitative analyses of the cancer epigenetic landscape provide the tools to understand the connections between genetic and environmental drivers of cancer evolution and the relationships between epigenetic regulatory networks that mediate the landscape. Continued advances in single-cell measurements, including assessment of DNA methylation, genomic sequencing, and chromatin analysis, will allow further understanding of the dynamics of the landscapes having progressively increasing complexity and accounting for tumor evolution, progression to invasive and metastatic spread, and associated alterations in anatomical organization and structure. Moreover, a greater understanding of biological stochasticity, defined mathematically as epigenetic and gene expression entropy, can uncover the cellular actors and mechanisms by which cancer plasticity enables escape from natural defenses and therapeutic interventions. ■

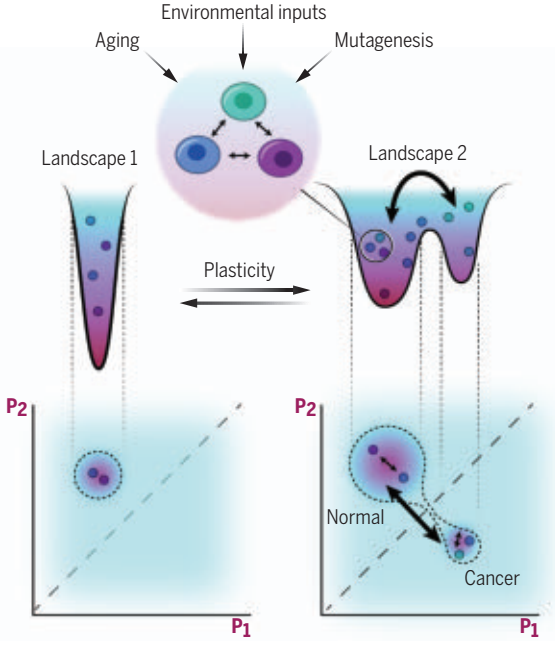

Epigenetic landscapes and phenotypic plasticity in cancer. Regulatory networks can define the number and probabilities of stable cellular states adopted by a cell population, representing attractors in the epigenetic landscape. Diverse inputs can promote transitions (and corresponding phenotypic plasticity) between cellular states within landscapes corresponding to the normal tissue (fewer attractors) and cancerous tumors (emergence of new attractors), as defined by parameters P1 and P2 that correspond to effective concentrations of landscape-defining molecules.

The list of author affiliations is available in the full article online.
*Corresponding author. Email: afeinberg@jhu.edu (A.P.F.); andre.levchenko@yale.edu (A.L.)
Cite this article as A. P. Feinberg and A. Levchenko, *Science* 379, eaaw3835 (2023). DOI: 10.1126/science.aaw3835

READ THE FULL ARTICLE AT
https://doi.org/10.1126/science.aaw3835

REVIEW

EPIGENETICS

Epigenetics as a mediator of plasticity in cancer

Andrew P. Feinberg[1]* and Andre Levchenko[2]*

The concept of an epigenetic landscape describing potential cellular fates arising from pluripotent cells, first advanced by Conrad Waddington, has evolved in light of experiments showing nondeterministic outcomes of regulatory processes and mathematical methods for quantifying stochasticity. In this Review, we discuss modern approaches to epigenetic and gene regulation landscapes and the associated ideas of entropy and attractor states, illustrating how their definitions are both more precise and relevant to understanding cancer etiology and the plasticity of cancerous states. We address the interplay between different types of regulatory landscapes and how their changes underlie cancer progression. We also consider the roles of cellular aging and intrinsic and extrinsic stimuli in modulating cellular states and how landscape alterations can be quantitatively mapped onto phenotypic outcomes and thereby used in therapy development.

Tumor cell heterogeneity and phenotypic plasticity have long been known to be principal drivers of invasion and metastasis (*1*). Complex and diverse behaviors displayed by cancer cells frequently involve coordinated expression of multiple genes, constituting programs that may be very distinct from those defining the phenotypes of the tissue of origin. Because oncogenic transformations are frequently accompanied by extensive mutagenesis, analysis of phenotypic heterogeneity displayed by cancer cell populations has typically been ascribed to the emergence of multiple genetically distinct clonal cell subpopulations within the same tumor (*2*). This genetic heterogeneity should be distinguished from phenotypic heterogeneity (i.e., the emergence of stable phenotypic states in an isogenic population) and phenotypic plasticity (i.e., the ability of cells to adopt different phenotypic states transiently). Phenotypic plasticity is thought to underlie complex phenotypic changes, such as epithelial-mesenchymal transition (EMT), drug resistance, and increased cell proliferation (*3*–*6*). Therefore, although genetic mutations may increase the probability of new phenotypic states, they may not completely define them and may not be strictly necessary for their emergence.

Elucidation of the interplay between epigenetic states and regulation of gene expression is crucial for our understanding of phenotypic plasticity. Multiple questions remain regarding coupling of these regulatory mechanisms. For example, because many regulators of gene expression may also have epigenetic modification capabilities—e.g., by recruiting DNA methylases and histone acetyltransferases—it is not clear whether epigenetic control might be viewed as a constituent part of transcriptional regulation or whether it has independent and essential roles not fully predictable by the analysis of gene networks alone.

In this Review, we argue that epigenetic mechanisms can have several key functions that are frequently not evident from traditional quantitative approaches involving the analysis of transcriptional regulation or RNA and protein stability. In particular, epigenetic regulation may have a critical role in regulating variability of gene expression, accounting for variance in current cellular states and the emergence of new ones. Recent methodological advances allow us to explicitly define and measure epigenetic landscapes that, along with gene regulation landscapes, can be used to much more precisely understand the etiology of cancer and to better understand the mechanisms underlying phenotypic plasticity and heterogeneity.

Theoretical approaches to describe genetic and epigenetic landscapes

Regulatory networks impose complex interdependencies on gene expression, which are commonly modeled using ordinary differential equations (ODEs) (Box 1, Eq. 1). A related concept of landscape introduced by Waddington and further elaborated mathematically (*3*, *7*–*9*) has been instructive for simpler and well-characterized systems but has faced important challenges. In particular, molecular interactions constituting regulatory networks are frequently unknown and may be restricted by epigenetic mechanisms, such as DNA methylation. Furthermore, these interactions and networks are subject to biomolecular noise or variability of molecular concentrations or alterations of molecular states (*10*–*12*), which are crucial for nondeterministic, many-fate behaviors of the system. Although the Waddington landscape is frequently interpreted as the epigenetic landscape, these concepts may no longer be fully synonymous. Whereas the term epigenetic previously referred to any mechanism outside traditional gene expression control, today it more commonly refers to a specific set of regulatory processes affecting in particular DNA methylation and chromatin modifications.

The probabilistic nature of biochemical processes has been historically addressed in several ways. Most simply, added noise might be described by extending the ODE description using the Langevin approach (Box 1, Eq. 1). However, this approach can break down if the number of molecules becomes very small, making the functions defining the ODE system behavior discontinuous. This consideration drove a conceptual quantum leap, akin to the transition from classical to quantum mechanics in physics. In this view, instead of describing the biological variables, such as molecular concentrations, one operates with the probabilities that system-defining variables take on certain values. This probabilistic dynamics is captured by the master equation, based on the Markovian assumption about the system dynamics (Box 1, Eq. 2). However, although appearing superficially simple, such equations require advanced computational resources to solve or estimate, though some success has been achieved for simpler cases (*13*–*15*). A fundamental challenge facing both the Langevin and master equation approaches is the lack of complete knowledge of the mechanisms that govern interactions between system variables. To date, relatively few biological networks have been fully characterized, and frequently this mechanistic characterization is only semiquantitative. It is therefore difficult to theoretically or computationally predict the probability distributions of different molecular and cellular states. However, one can now directly experimentally estimate these probabilities (*16*–*18*) and thus attempt to solve an inverse problem of reconstructing the mechanisms underlying gene expression regulation and the corresponding genetic and epigenetic landscapes from experimental data.

The inferences based on experimentally obtained probability distributions can be put on a solid theoretical foundation that provides specific meanings to the notions of epigenetic and genetic landscapes, distinct from those implied by Waddington. Critical to this approach is the fundamental connection of potential energy and probability distributions provided by the Gibbs-Boltzmann approach (Box 1, Eqs. 3 and 4), which are particularly useful for definition and analysis of landscape attractors corresponding to specific coherent molecular, cellular, and phenotypic states. Specifically, this approach associates the probability of

[1]Center for Epigenetics, Johns Hopkins University Schools of Medicine, Biomedical Engineering, and Public Health, Baltimore, MD 21205, USA. [2]Yale Systems Biology Institute and Department of Biomedical Engineering, Yale University, West Haven, CT 06516, USA.
*Corresponding author. Email: afeinberg@jhu.edu (A.P.F.); andre.levchenko@yale.edu (A.L.)

Box 1. Mathematical analysis of stochastic biological systems.

Biological systems are governed by underlying interactions that could be described mathematically. These interactions can be stochastic because of the variability of the participating elements (molecular modifications, molecular and cellular numbers, etc.). The mathematical approach frequently used to capture stochastic interactions is the Langevin approximation based on the ODEs describing temporal dynamics of variables x_i, using the function $f(\boldsymbol{x})$ of the vector $\boldsymbol{x}$ of all variables x_j, with the added noise terms $\eta(x_i)$

$$\frac{dx_i}{dt} = f_i(\boldsymbol{x}) + \eta_i(x_i) \quad (1)$$

An alternative but equivalent description that is particularly useful for systems with very small values of x_i that are expressed as whole numbers is to consider the dynamics of probabilities of x_i rather than the dynamics of x_i themselves. This is done using the so-called master equation based on the assumption that the underlying processes are Markovian (memoryless)

$$\frac{dP(x_i)}{dt} = \sum\nolimits_j k_{ij} P(x_j) \quad (2)$$

Unfortunately, other than for a few relatively simple systems, the mechanistic information that would define the functions $f(\boldsymbol{x})$ and k_{ij} is largely incomplete for most biological systems. Therefore, it is frequently hard to use these models for real biological systems to characterize their dynamic behavior and thus landscapes. Instead, it has proven easier to experimentally measure the distributions $P(x_i)$. Therefore, the problem can be inverted—i.e., reconstructing the underlying regulatory landscape from the knowledge of $P(x_i)$. The recipe for doing so is provided by statistical mechanics (Boltzmann-Gibbs distribution) and in particular the relationship between the energy $U(x_i)$ associated with a specific x_i and the probability of this value of the variable (the energy here is quasipotential, corresponding to measuring the energy in units of k_BT—i.e., the product of the Boltzmann constant k_B and temperature T)

$$U(x_i) = -\ln P(x_i) - \ln\left[\sum\nolimits_j e^{-U(x_i)}\right] \quad (3)$$

If the distribution of different values that can be taken by variables x_i is constant (i.e., the landscape does not change), then the second term in Eq. 3 is constant and, because the energy $U(x_i)$ is only determined up to a constant, it can be omitted for the analysis of a constant landscape

$$U(x_i) \simeq -\ln P(x_i) \quad (4)$$

The relationship (Eq. 3) can be used to directly define the energy (quasipotential) landscape corresponding to the gene expression and epigenetic landscapes and to relate it to the entropy of the system, again up to a constant

$$H(x) = -\sum\nolimits_i P(x_i)\log P(x_i) \simeq -\sum\nolimits_i P(x_i)\ln P(x_i) \simeq \langle U(x_i)\rangle \quad (5)$$

This relationship, linking the entropy and average energy $\langle U\rangle$ for a system, emphasizes the global nature of the entropy measure, involving summation over multiple states. Thus, as illustrated in Fig. 1, different landscapes may have the same entropy and thus cannot be uniquely distinguished using this function of the state. Conversely, the distributions captured by $P(x_i)$ and $U(x_i)$, can be more informative.

Finally, the mutual information is defined as the change of entropy (and thus the underlying landscape) of a state $\Delta H(x)$ given a regulatory event or a signal. If the entropy decreases, the mutual information is positive, which provides a measure of comparison between two distributions. Another important measure of dissimilarity between two distributions $P(x_i)$ and $Q(x_i)$ is the frequently used Kullback-Leibler (KL) divergence

$$D_{KL}(P\|Q) = \sum\nolimits_i P(x_i)\log\left[\frac{P(x_i)}{Q(x_i)}\right] \quad (6)$$

Mutual information is thus the KL divergence between the joint distribution of the variable values before and after the event (or signal) and the product of their marginal distributions. A symmetrized version of the KL divergence of particular value in comparing epigenetic landscapes is the Jensen-Shannon distance, defined as

$$\mathrm{JSD}(P\|Q) = \frac{1}{2}D_{KL}(P\|M) + \frac{1}{2}D_{KL}(Q\|M) \text{ where } M = \frac{1}{2}(P+Q) \quad (7)$$

any outcome—e.g., gene expression or DNA methylation pattern and the corresponding phenotypic outcome—with a generically defined quasipotential energy, a term adapted from physics to describe the origin of probability distributions of the possible cellular states (states with lower energy are occupied with higher probability; see Fig. 1A and the definition in Box 1, Eq. 3). This association allows one to define the corresponding genetic (gene expression) or epigenetic (e.g., DNA methylation markers) landscapes as the quasipotential energy distributions. This landscape definition is consistent with the one implied by the Waddingtonian ODE approach, affording easy interpretation and visualization. The attractors within this landscape representation would be seen as the values of biological variables for which the local and global energy minima would be reached, thus constituting states with high relative probability values (Fig. 1A). The stability of the attractor is further defined by such landscape characteristics as the depth and width of the corresponding energy wells and the proximity, and thus accessibility, of other attractors (*19*). Increased variability or noise makes energy wells effectively more shallow, thereby widening the distribution of biological variables (*20*). This allows cellular networks to explore multiple states across different attractors. The local energy (landscape) minima may be realized in different cells within a population or could only be accessible in specific developmental, physiological, or pathological situations. Below, we illustrate and discuss these and other important ideas, such as the entropy associated with the whole landscape and specific attractor states and the information associated with changes of this entropy (Box 1), particularly in the context of emergence and progression of cancer.

Landscape models of cancer

Gene regulatory landscapes can be evaluated from experimentally determined gene expression probability distributions, particularly those yielded by single-cell RNA sequencing (scRNA-seq) data or from the analysis of multiple tissue samples (e.g., cancerous tissues from multiple patients) (Fig. 1A). The landscape attractors in these distributions correspond to groups of coordinately expressed genes and gene products, whose abundance and activity may be regulated by self-sustaining feedback interactions, endowing cells with specific phenotypic properties. Cancerous states may represent the genetic landscape attractors that are inaccessible in untransformed tissues but can be unmasked by oncogenic mutations (*19*, *21*). This is exemplified by the emergence of the mesenchymal state in EMT (*3*). The Langevin ODE approach has been used to analyze a tristable regulatory circuit assumed to control

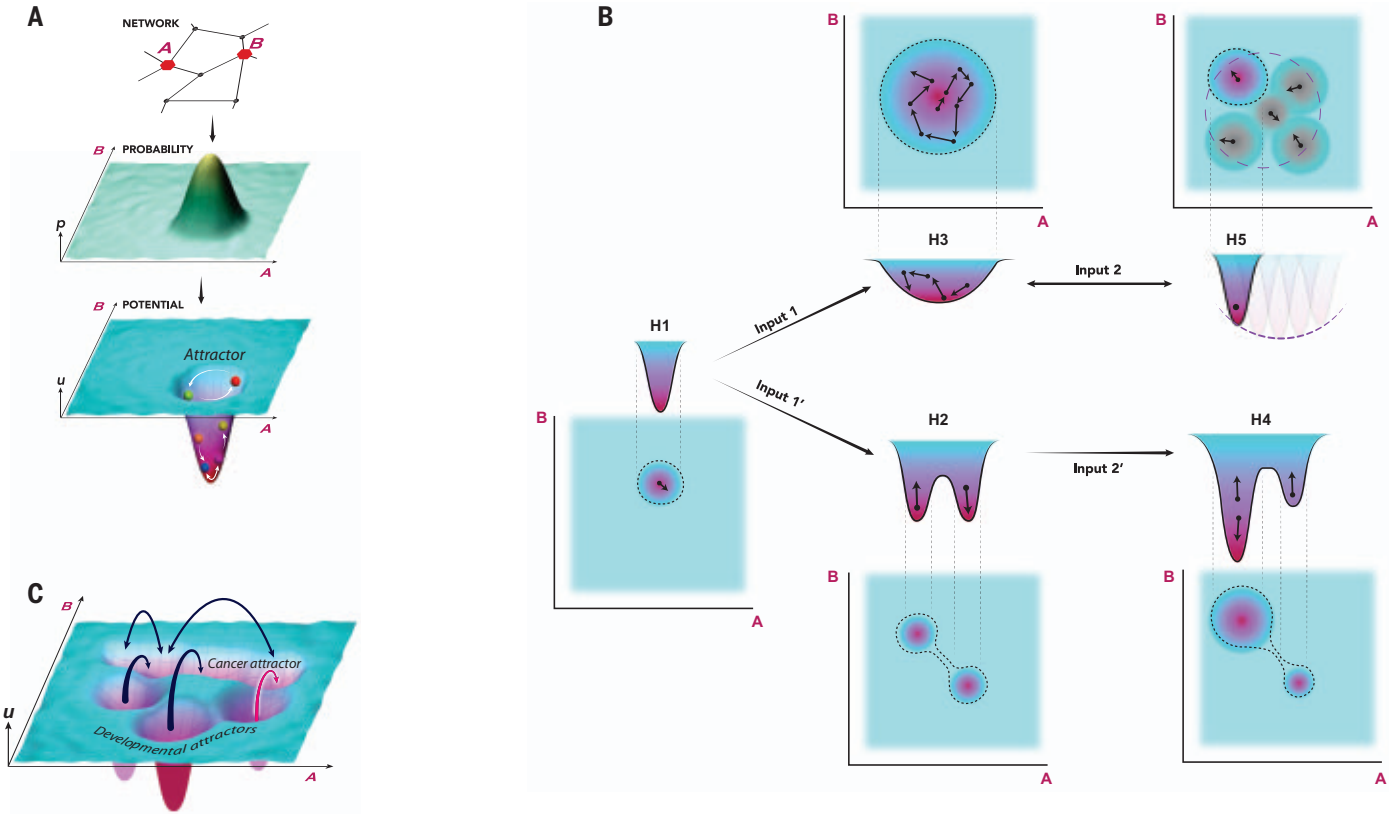

Fig. 1. Gene expression and epigenetic landscapes control normal and cancer cell functions. (**A**) Gene regulatory networks and availability of genes for expression can define the probabilistic distributions of proteins expressed within a cell population. In this example, the network of interacting proteins that includes the molecules A and B (top) and the underlying epigenetic control determining the availability of the corresponding genes for expression define the distribution of the expression of molecules A and B (middle). This probability distribution can be experimentally measured and converted into a gene expression landscape by calculating the corresponding quasipotential distribution (bottom) (see Box 1). The epigenetic landscape can be similarly determined by experimentally measuring the probabilistic distributions of epialleles, measuring DNA methylation marks at specific loci, or by performing other measurements of epigenetic regulation across populations of cells and tissues and then also converting these probability distributions into corresponding underlying quasipotential landscapes. The landscape analysis allows conceptual accounting for abundance and dynamics of molecular species, shown here as a trajectory of a particle inside a quasipotential well, with the particle position defined by the current concentrations of A and B that can change probabilistically in time, with the quasipotential wells interpreted as the landscape attractors. (**B**) Various scenarios of landscape alterations and the corresponding changes in the molecular distributions, shown as joint distributions of the molecules A and B and the corresponding entropies H1 to H5. Implementation of these scenarios in the context of carcinogens is extensively illustrated and discussed in the text. Oncogenic mutations of epigenetic modifiers and modulators or environmental inputs can lead to the formation of new stable attractors with the overall entropy H2 greater than the original entropy H1 (H2 > H1), generating phenotypic heterogeneity (input 1′) or, alternatively, enlarging the existing attractor with the new entropy H3 > H1, generating a more plastic state (phenotypic plasticity), with cells capable of stochastically and dynamically exploring this attractor and thus transiently adopting different phenotypes. In both cases, entropy increases versus H1 and it is possible that H2 = H3, thus making entropy less discriminating than the full landscape picture in the analysis of cell states. These new landscapes can be further altered by oncogenic and environmental inputs, so that one of the attractors becomes dominant (input 2′), associated with a lower entropy value (H4 < H2) or, alternatively, with the narrowing of the wider (and more plastic) attractor (input 2; H5 < H3). Again, it is possible that H4 = H5, requiring the landscape analysis rather than entropy analysis alone for full characterization. The narrowing of the wide attractor because of either environmental or intrinsic inputs (input 2) is frequently reversible and context dependent, further elaborating the more plastic overall state (transient nature of input 2 described by a bidirectional arrow). The transiently occupied attractors can be simultaneously occupied by distinct cells in the population. Small arrows correspond to stochastic fluctuations of molecular concentrations within individual attractors. (**C**) Gene regulation and epigenetic landscapes of cancer cells can be complex and have multiple attractors, corresponding to distinct and stable cell states and phenotypes, which may be reshaped by oncogenic mutations, cell aging, environmental inputs, and other perturbations, leading to mutual accessibility of the attractors, more plastic cell states, and an increase in the phenotypic plasticity.

epithelial-mesenchymal plasticity (*22*). Additionally, four attractor states have been proposed to control EMT, including metastatic, antimetastatic, and two intermediate states (*23*). These studies have illustrated putative feedback-based mechanisms of emergence of well-defined attractors in cancer-associated gene regulation landscapes. However, they were based primarily on theoretical modeling constructs that require experimental validation, as we discuss below. Alternatively, the properties of experimentally measured regulatory landscapes can be inferred without imposing hypothetical mechanisms.

A key consequence of both the emergence of new attractors and elevated variability within the same attractors is the increase in the entropy of the underlying regulatory landscapes (inputs 1 and 1′ in Fig. 1B; see Box 1). Indeed, it is consistently observed that the entropy of gene expression increases in cancer versus the

corresponding noncancerous tissue of origin, as revealed, for example, by examining gene expression data alone (*24*) or by integrating these data with protein interaction networks (to account for molecular interactions stabilizing the attractors) (*25*). A similar approach using protein-interaction networks and RNA-seq for multiple tissue samples rather than single cells within the same sample has suggested that tumor progression is associated with increasing entropy (*26*). This approach was further used to link the entropy of gene expression to the pluripotency of the underlying cell population (*27*) and to demonstrate that specific cell differentiation, in contrast to cancer emergence, could be represented by emergent attractors associated with progressively lower variability and entropy. Consistent with this analysis, it was shown that cancer stemness may be inferred from increased entropy of the attractor defining a specific cell subpopulation (*27*). Notably, this analysis revealed that decreased entropy was associated not only with cell fate–specifying molecular circuits, but also with specific cancer-related phenotypic states, such as increased cell proliferation (*21*), implying correlated gene expression and molecular interaction of the components of the cell cycle, representing another example of a well-defined attractor in the gene expression landscape. However, this high proliferation attractor may not be fully stable, with recent studies suggesting that cells may stochastically transition into and out of a cell proliferation state (*6*, *28*). Other studies have pointed to a transient rather than stable nature of other key cancer-associated phenotypes—e.g., drug resistance and EMT—which indicates that they may be a consequence of phenotypic plasticity within a broader attractor state, potentially allowing these phenotypes to be transiently achieved (*29*–*32*). This broader attractor may be associated with a higher entropy stemness state, whereas each of the transiently visited phenotypic states may have much lower associated entropy—i.e., they can be considered subattractors that can be occupied by the cells either stochastically or in response to environmental inputs (*33*) (inputs 1 and 2 in Fig. 1B).

These studies reveal that reasons for higher entropy in gene expression networks in cancer cells can be complex, because the same increase in entropy could be due to the emergence of new stable attractors in the cell population (phenotypic diversity; input 1′ in Fig. 1B) or increased noisiness of the individual attractors that may already be present in the normal, precancerous tissue or emerge as a result of cell dedifferentiation (phenotypic plasticity; input 1 in Fig. 1B). Furthermore, phenotypic plasticity can enable the emergence of transiently stable, stochastically visited attractors that can nevertheless have important functional phenotypic characteristics, such as EMT, cell proliferation, and drug resistance (input 2 in Fig. 1B). These phenotypes may be related to those occurring separately in normal development and tissue homeostasis but might become mutually accessible in the context of a larger underlying attractor in the phenotypically plastic cancerous states (Fig. 1C). Thus, a more detailed landscape analysis is required to understand the mechanisms underlying the emergence and dynamics of cancerous cell populations. Furthermore, these studies leave the following questions open: What controls the availability of various transcriptional programs that enable diverse landscape attractors and what mechanisms regulate the transitions between different attractor states and thus the degree of plasticity of various phenotypes?

In contrast to gene regulation landscapes, in which variables, such as molecular concentrations, can be viewed as continuously adopting multiple values, epigenetic landscapes are essentially binary or digital in nature—e.g., the methylation patterns of specific CpG sites or the presence or absence of specific histone modifications. Nevertheless, the landscape analysis framework can also be used for these types of experimental data. For instance, epigenetic variation in the patterns of sets of four consecutive CpG sites display increasing stochasticity in aging fibroblasts and in cancer cells within particular regions of the genome (*34*). The patterns of consecutive CpG sites, also known as epialleles, can thus be treated probabilistically, with their distributions within the same tumor estimated using a Bayesian model (*35*). The probability analysis lends itself to examination of entropy and information metrics (defined in Box 1), which was applied to several brain tumor and normal samples, revealing an increased methylation entropy of Alu repeat sequences (*36*). The epigenetic patterns of epialleles may display certain correlations, interpreted as specific attractor states in the underlying landscapes. Mechanistically, these correlated patterns may arise because DNA methylation at heritable (i.e., CpG) dinucleotides is affected by the state of the cell or location in the genome as well as the nearest CpG neighbors, because DNA methyltransferase I, the enzyme that copies CpG from the parent to the daughter strand during DNA replication, resides at the replication fork, conferring a nonrandom methylation pattern to nearby CpG dinucleotides.

The underlying landscapes may be more formally defined recognizing the binary nature of the experimental data by exploiting the Ising model, introduced in the 1930s for one-dimensional magnetic dipoles with binary states that are also influenced by external forces and the nearest dipole neighbors (*37*). It also allowed a highly accurate computation of the Shannon normalized methylation entropy (NME) for DNA methylation. Furthermore, the Ising model enabled a more sophisticated analysis, such as the calculation of the Jensen-Shannon distance to evaluate the mutual information between two epigenomes and thus to rank genomic features by their relative contribution to epigenetic landscape change (*38*). This more-rigorous treatment revealed substantial entropy increases in the epigenetic landscapes of a variety of cancer types compared with matched normal tissues of origin (*37*). Notably, it was found that an increase in disordered methylation patterns predicts poor clinical outcomes in chronic lymphocytic leukemia (*39*) and acute myelogenous leukemia (AML) (*40*). This recent progress has been conspicuous because cancer epigenetics was thought to be computationally intractable owing to being derived from hundreds of landscapes of normal tissue (*41*).

The increase in epigenetic landscape entropy observed in various cancers is accompanied by a greater variability in gene expression (*42*), thus linking epigenetic and gene regulation landscapes. A possible explanation for this linkage is that genetic programs accounting for new phenotypic properties can become accessible because of increased epigenetic variability, leading to the emergence of new gene regulation attractors. This hypothesis is supported by the observation that the increased variation in gene methylation and expression is often enriched in genomic regions that are larger than a single gene (*42*, *43*)—e.g., regions associated with EMT (*42*) or smaller domains observed in pancreatic cancer (*44*), perhaps related to hypomethylated regions inferred for hematopoietic stem cells (*45*). Thus, epigenetic control of multiple genes needed to enable a specific phenotype could loosen, and the corresponding genetic attractor may emerge and enable variable onset of a new phenotypic state in a cell population. It has in fact been found that the transition to the mesenchymal state depends on altered chromatin accessibility of the DNA regions incorporating EMT-related genes (*46*). Furthermore, large heterochromatic domains related to developmentally regulated EMT (*47*) are topologically altered in colon cancer (*48*). These data suggest that a key cancer-related phenotype is enabled by changes in both gene expression landscape (actualization of a cryptic attractor state) and epigenetic landscape (changes in DNA and histone markers that enable accessibility to the genetic information encoding components of this newly accessible genetic landscape attractor).

Together, these results suggest that a key condition for the emergence of a new attractor in the genetic landscape is the epigenetic reorganization of the corresponding genetic material, leading to increasing stochastic variability within the current attractor and increased probability of transition to a new state (*20*) (input 1 in Fig. 1B). It is therefore of interest to explore the

triggers of epigenetic and gene regulation landscape reorganization that occur during carcinogenesis, a task that is complicated by interdependencies of epigenetic and gene regulation mechanisms. Indeed, epigenetic modification, for example, DNA methylation of gene regulatory sequences, can directly influence gene expression, and many transcription factors can recruit epigenetic regulators, which suggests substantial epigenetic and genetic landscape interdependence (Fig. 2). To provide more detailed insight into oncogenic processes that shape and are shaped by epigenetic and gene regulation landscapes, it will be instructive to examine the genetic and environmental inputs that can lead to precancerous and cancerous states.

Interplay between epigenetic and genetic landscapes

How can the large number of recurrent somatic mutations that drive carcinogenesis be connected to the pathways and genes responsible for cancer phenotypes (*49*)? Traditionally, this question has been addressed by analyzing the effects of various mutations on the magnitude of phenotypic changes, such as increased proliferation, in response to overexpression of diverse mitogenic regulators. What is currently less understood is how the increased variability (and thus entropy) of epigenetic and gene expression regulation is linked to cancer progression. Such analyses are now progressively enabled by the rank ordering of oncogenic mutations using metrics such as the Jensen-Shannon distance (Box 1, Eq. 7), which establish the effect size and its importance in epigenetic control of cancer etiology (*38*).

The roles of mutations affecting molecules that directly (so-called epigenetic modifiers) and indirectly (epigenetic modulators) control epigenetic landscapes through their enzymatic functions (*50*) can be elucidated in cancerous states (Fig. 2). For example, in AML, driver mutations can affect both epigenetic modulator molecules [such as transcription factors and signaling pathways that can recruit epigenetic modifiers to specific gene targets (*51*)] and modifier molecules [such as the DNA demethylation-related gene *TET2*, which is directly mutated in a subset of AML patients (*52*)]. Analysis of epiallele distribution across AML patients with different driver mutations has indicated an increase in the entropy of epiallele distribution, consistent with other cancers. Notably, this analysis revealed a more fine-grained epigenetic landscape structure underlying entropy increase. In particular, epialleles commonly showed specific patterns for a subset of modulator mutations, whereas the distribution was much broader for modifier mutations. This study further indicated that tighter and more specific epiallele distributions were correlated with better clinical outcomes, whereas broader distributions were generally associated with poor clinical prognoses. Furthermore, higher epiallele diversity was associated with gene expression hypervariability and, thus, likely higher phenotypic and developmental plasticity. This result was consistent with an independent analysis of AML involving genetic rearrangement of the the histone methyltransferase gene *KMT2A* (also known as *MLL*), which, when compared with untransformed controls, also demonstrated a greatly increased epigenetic entropy (more specifically, NME) and high expression variability of genes implicated in AML etiology (*53*). Notably, animal models of AML revealed that epigenetic variability was a precursor of transformation to AML, pointing to the causal rather than correlative nature of the greater entropy states (*52*). Overall, these data suggest that mutations affecting particular regulatory pathways may result in adoption of specific genetic and epigenetic states (narrow and stable landscape attractors). Conversely, dysregulation of epigenetic modifiers can lead to a much broader epiallele distribution, which may result in broader, more noisy attractors; phenotypic plasticity; and poorer prognosis (input 1 in Fig. 1B and Fig. 2). A greater phenotypic plasticity enabled by a more global epigenetic dysregulation may enhance the escape of cancer cells from various treatments and other pressures, including immune surveillance.

Whereas mutational alterations of some modulators can lead to the emergence of specific attractor states, mutations of other modulator proteins may exert their effect indirectly by regulating the broad specificity epigenetic modifiers, thereby also leading to extensive epigenetic alterations and broader, more plastic attractor states. For example, inhibition of DNA methylation was highly effective in AML patients harboring *TP53* mutations (encoding the tumor suppressor p53) but had much lower effects in tumors with wild-type (WT) *TP53* (*54*). These results were supported by lung cancer xenograft studies and in vitro experiments (*55*), which together suggest that p53 is an epigenetic modulator that is critically important

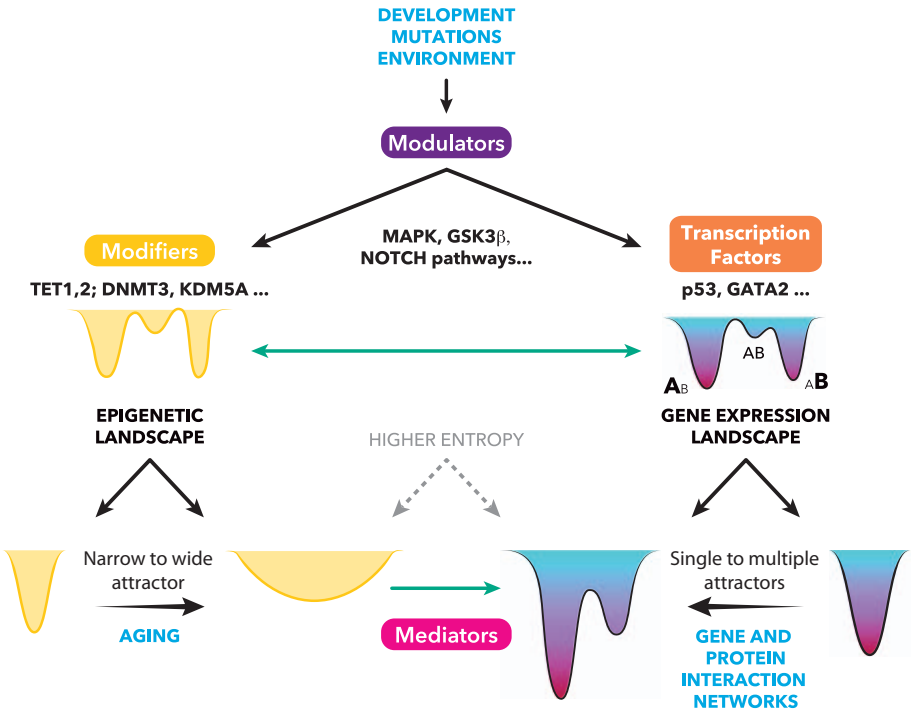

Fig. 2. Interplay between epigenetic and gene expression landscapes. Developmental and environmental factors and genetic mutations can affect diverse modulators of epigenetic control and gene expression, such as signaling and cell communication networks, frequently leading to diversification of cell states. These modulators may directly affect mediators of epigenetic states, such as DNA demethylases, and gene expression, such as transcription factors, which also can directly interact with each other. Examples of these molecular regulators discussed in the text are shown here. The result is alterations of the epigenetic and gene regulation landscapes that are tightly coupled, for example through the action of mediators of epigenetic control, influencing accessibility of genes for regulation, and the magnitude and variability of gene expression. Certain additional inputs may be more specific to each of the landscapes, such as the epigenetic drift with cell aging primarily leading to a widening of the landscape attractors, higher plasticity and higher entropy of the state, or protein-protein interaction and gene regulatory networks, stabilizing various attractors and serving to decrease the plasticity and entropy.

for epigenetic stability. In embryonic stem cells (ESCs), p53 restricts the expression of modifiers *DNMT3A* and *DNMT3B*, thus inhibiting methylation, and regulates *TET1* and *TET2*, making the loss of *TRP53* a major driver of epigenetic heterogeneity (*55*, *56*). Other genes commonly mutated in AML, including *WT1*, *IDH1*, and *IDH2*, can also have more global effects on epigenetic landscapes through inducing loss of TET2 function (*57*). These results suggest that although epigenetic modifiers may not be mutated in specific tumors, in many cases, the effect of modulator mutations can lead to changes in the methylation status of a large number of genes, similar to the effects of modifier mutations. The more specific, targeting effects of modifiers can be revealed through comparative gene expression analysis, for example by searching for enrichment of binding sites for specific transcription factors in the control regions of epigenetically variable genes. Enrichment of specific binding sites would suggest that a particular transcription factor can both recruit an epigenetic modifier to a particular gene and more directly control the expression of this gene once it is epigenetically modified. This type of analysis yielded a number of putative modulator proteins, including GATA2, coupled to epiallele variation in many AML subtypes driven by distinct mutation events (*52*). Similar studies have further suggested specific roles of NFKB1 and MYBL1 as modulator proteins controlling the drug resistance phenotype in chronic lymphocytic leukemia (*58*).

Overall, these studies suggest the following refinement of our understanding of the interplay between genetic and epigenetic landscapes in the emergence of genetically driven cancers (Fig. 2). The effect of mutations in mediator and a subset of modulator genes may be broad, encompassing multiple genes across the genome and generating a high degree of epiallelic and genetic heterogeneity, which correlates with poor clinical outcome. The effect of mutations in another subset of modulators may be more specific, leading to the emergence of less variable epiallele distributions and coordinated gene expression patterns, corresponding to a limited number of coupled attractors in genetic and epigenetic landscapes. In both cases, the entropy of epigenetic and genetic landscapes goes up but for different reasons: In the former case, a more plastic state implies a noisy and relatively unstable attractor state, whereas in the latter case, increased entropy may correspond to the emergence and coexistence of new stable attractors in the genetic and epigenetic spaces (Fig. 1B). This view implies that there may be different landscape paths to cancer, but the emergence of a more plastic, less defined attractor state may be particularly interesting to consider, because it may be related to both more pluripotent stem cell–like states and increased plasticity of cancer cells.

Stabilization of attractor states by endogenous and exogenous inputs

Exogenous inputs

Enhanced variability of both gene expression and epiallele abundance indicative of broad genetic and epigenetic attractors may permit cells to transiently achieve multiple alternative states that could be potentially further stabilized by additional inputs. For example, genetic perturbations of *DNMT3A* and *DNMT3B* markedly increase genetic and epigenetic entropy in ESCs, whereas the effects on mean methylation are much more modest (*59*). Furthermore, several genes that are differentially controlled by this perturbation can promote cellular differentiation. Notably, genetic perturbations of *DNMT* and *TET* genes revealed that the differentiated state is a separate attractor in the genetic landscape and that this attractor exists dynamically, with cells reaching and leaving it according to the relative activities of DNMT and TET enzymes (*60*). These results are consistent with the current understanding of the importance of epigenetic regulation of induced pluripotency by the Yamanaka factors, particularly the increased expression of TET enzymes to stabilize this state (*61*). Critically, this differentiation attractor can also be regulated by modulators in the form of signaling pathways, particularly dual inhibition of mitogen-activated protein kinase (MAPK) signaling and glycogen synthase kinase-3β (GSK3β) (*62*–*64*), which suggests that external signaling inputs can stabilize the differentiation state.

The insights from epigenetic regulation of stemness can elucidate how conditional attractors can emerge and be stabilized, for example by exogenous signaling inputs in cancer (input 2 in Fig. 1B). As an example of signaling attractor stabilization, it was found in two independent studies that paracrine signaling involving insulin-like growth factor 1 (IGF-1) receptor activation or NOTCH pathway signaling can lead to an altered chromatin structure that is mediated by the histone demethylases KDM5 and KDM6, respectively, which in turn control the drug resistance phenotype (*5*, *65*). The acquisition of this phenotype was, in both cases, transient and stochastic, suggesting continuous transitions between distinct states associated with two or more attractors in the underlying landscape. The dynamic acquisition can be analyzed in substantial detail in vivo, as was the case for AML in a genetically engineered mouse model (*66*).

Metaplasia

The landscape-based analysis implies that a loss of stabilizing inputs, exogenous or endogenous, may make transitions to other available attractors more likely, maintaining a plastic state and metaplastic tissue composition. A particularly interesting example of this is found in kidney differentiation. WT1, a tissue-specifying transcription factor that is critical for embryonic kidney development, can be seen as a molecule stabilizing the corresponding differentiation program attractor. Loss-of-function mutation of *WT1* leading to a loss of DNA binding in the germline causes Denys-Drash syndrome with renal dysplasia (*67*). The resultant absence of *WT1* in somatic cells leads to metaplastic transdifferentiation of early pronephric cells into other mesodermal elements, such as skeletal muscle, fat, and cartilage, and generation of preneoplastic intralobar nephrogenic rests relatively early in the developmental axis, increasing the risk of Wilms tumor development (*68*). WT1 also controls EMT, likely through interaction with the YAP transcriptional coregulator in controlling E-cadherin expression (*69*), which may modulate the tissue organization and further influence the metaplastic state. Timed experimental activation of stem cell reprogramming factors in the developing mouse kidney can induce Wilms tumor in the absence of other perturbations, including absence of any *WT1* mutations (*70*). This same effect arises from loss of imprinting (LOI) of *IGF2* in Beckwith-Wiedemann syndrome, or sporadically in the general population, with hyperproliferation of developing nephrons also creating predisposition for Wilms tumor development. These results are consistent with losses of stabilizing control leading to a broad, variable, and plastic landscape attractor, which can also decrease the probability of occupying the attractor corresponding to a stably differentiated nephron state (Fig. 1B and Fig. 3).

Metaplastic states do not need to involve processes that occur early in development or depend on reprogramming cues. Rather they may arise from stabilization of one of the mutually accessible attractors even in the mature adult tissue (input 2′ in Fig. 1B). Acinar-ductal metaplasia (ADM) (i.e., the process in which acinar cells in the pancreas differentiate into ductal cells) can occur in the untransformed adult pancreas as a part of the tissue repair process (*71*) but may also lead to preneoplastic lesions and, ultimately, progression to pancreatic ductal adenocarcinoma (PDAC) (*72*). In addition to ADM, which may occur as a normal adaptive process, destabilization of the attractor corresponding to the acinar cell type can lead to the emergence of pancreatic intraepithelial neoplasms (PanINs). Furthermore, other cell types may also emerge in this process, for example tuft cells. This attractor destabilization may involve mutations of modulators *KRAS* and *DPC4* (also known as *SMAD4*) and up-regulation of *KLF4* during inflammation or injury (*73*, *74*) as well as changes in the epigenetic control of key regulators,

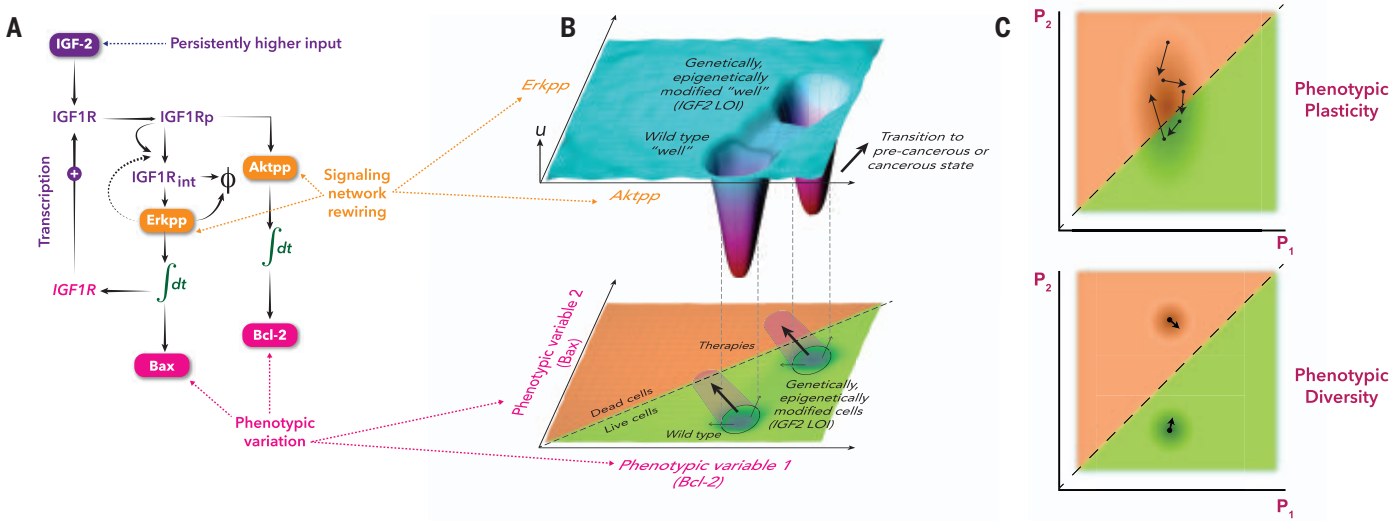

Fig. 3. Connection between an epigenetic landscape and variable phenotypic outcomes. (**A**) An epigenetic alteration—LOI of the *IGF2* gene, implicated in Wilms tumor, doubling the signaling input—can lead to rewiring of the signaling network activated by the IGF2 receptor IGF1R (depicted as IGF1Rp) through altered receptor trafficking (IGF1Rint), degradation (ϕ), and altered balance of activation of the downstream signaling pathways activating Erk (Erkpp) and Akt (Aktpp) kinases. Rebalancing of Erk and Akt activities translates into transcriptional up-regulation of IGF1R and a higher proliferation rate but also rebalancing of pro- and antiapoptotic protein abundances (BAX versus Bcl-2, respectively), leading to an increased propensity for cell death (*108*). The integral signs represent integration over time of signaling activities. (**B**) The landscape alterations that correspond to a change in phenotype (top) are the altered expression and activity of signaling pathway molecules (and thus gene regulatory landscapes in the bottom panel) in response to alteration of epigenetic landscapes (IGF2 LOI). This leads to emergence of a new attractor in addition to the WT attractor, resulting in a mosaic WT-LOI cell distribution in the tissue. This landscape alteration can be mapped onto, for example, the apoptosis phenotype-defining network by a quantitative analysis of the dependence of the BCL family protein distributions on the signaling inputs, thus enabling a direct translation of the landscape alterations into phenotype distributions. In this example, the mapping can be visualized as WT and LOI cell distributions mapped with respect to the areas of cell survival and death on the (BAX, Bcl-2) phenotypic plane, which suggests how treatments targeting LOI cells may be developed to spare the WT cells. Arrows in the lower panel represent the effect of drugs, such as IGF1R inhibitors, shifting the landscape and phenotypic distribution toward the boundary separating survival and death, with the red areas depicting the effect on the WT and LOI cell populations. (**C**) A more general view of landscape mapping onto the apoptosis phenotypic plane. By analogy with Fig. 1B, one can contrast mapping of a large attractor versus two more limited attractors, representing the difference between a plastic and stochastic state (phenotypic plasticity) versus a state with two alternative stable attractors (phenotypic diversity). The more plastic state can allow cells to escape from the death area to the survival area even in the presence of a treatment [such as in (B)], by stochastically exploring the available attractor, whereas a combination of more stable attractors (with the same overall entropy as the more plastic state) can allow for selective targeting of one but not the other attractor. Therefore, the treatment strategy suggested in (B) may benefit from the initial intervention, stabilizing smaller attractors within a larger one and thus decreasing the plasticity of the state, particularly through epigenetic perturbations.

such as AATK, as revealed by studies of a mouse model of ADM and pancreatic cancer (*75*).

Another example of an environmentally induced metaplastic process occurs in Barrett's esophagus. In this case, the environmental stimulus (modulator) is acid reflux and inflammatory cytokine enrichment, which promote transdifferentiation of normal squamous epithelium of the esophagus into intestine-like columnar epithelium (*76*). Animal and human data suggest that in this setting, the attractor corresponding to the esophageal cell type is compromised as a result of induction of intestinal-specific factors CDX1 and CDX2, which might be induced by inflammatory inputs and can self-stabilize through autoregulation (*77*). This process is associated with a bimodality in the DNA methylation distribution reflective of coexistence of esophageal and intestinal attractors, characteristic of this type of metaplasia (*78*). Transdifferentiation in this setting is again a major risk factor of ensuing development of esophageal adenocarcinoma.

Together, these observations suggest that metaplasia or alternative differentiation can be an important characteristic of premalignant tissue states. Consequently, the new states explored by the cells may not be random but frequently belong to closely related lineages (*79*), in agreement with the expectation that cells explore adjacent attractors along the underlying epigenetic and genetic landscapes because of an increased stochasticity and thus entropy of the regulatory networks (Fig. 1C). Notably, up-regulation of epigenetic modifiers, such as ARID1A, is commonly observed both in the metaplastic states and multiple cancers (*80*–*82*). Tissue disorganization related to metaplasia as well as the common dysregulation of the EMT-MET program can further perturb local cell-cell interactions, leading to hyperplasia and the onset of neoplastic growth (*83*–*85*).

Therefore, if these genetic or environmental inputs occur in tissues with a high potential for metaplasticity, the occupancy of the attractors may change. The occupancy of the previously dominant attractors may become less likely, whereas preexisting alternative attractors can be occupied with higher probabilities, leading to further metaplasia and potentially cancerous states (Fig. 1B). In another scenario, if epigenetic modulators are directly affected by genetic mutations or environmental inputs, even tissues with low initial plasticity can become more plastic and permit occupancy of previously inaccessible, cryptic attractors (input 1′ in Fig. 1B). These attractors can become stable as a result of either internal feedback or additional stabilizing mutations, or they can remain transient and stochastically visited depending on the presence of an external cue. The higher degree of epigenetic plasticity and conditional, rather than stable, attractors can increase the corresponding phenotypic plasticity, which can result in poor prognosis because of increased metastatic propensity, drug resistance, or immune escape. In this sense, stabilization of particular attractors, by reducing the plasticity of cell regulation, can make

cancer progression more predictable and potentially increase the probability of success of personalized therapeutic interventions.

Attractor stability and aging

Stabilization of conditional attractors by an environmental cue enabled by dysregulated epigenetic control can occur through a variety of mechanisms but particularly through the activation of intracellular signaling networks. Indeed, new attractors, such as the mesenchymal cell state emerging in EMT, can be triggered by biochemical and biomechanical inputs from the microenvironment, and increased cell proliferation can be controlled by a progressive accumulation of growth factors and other ligands in the cellular milieu (*69*). Attractor stabilization may result in a decrease in entropy of gene expression and epiallele occurrence, which can be precisely quantified experimentally and used to evaluate the information carried by the signaling input (*86*) (see Box 1; information is defined as the decrease in entropy after an input). The entropy decrease is frequently modest, with only 1 bit of information about the signal amplitude commonly transferred in such events on a cell-by-cell basis (*12*, *86*–*92*). Coordination of signaling between multiple cells can allow for an increase in this information transfer and thus further entropy decrease; however, because cellular communication is noisy, the effect may also not be very substantial (*93*). A further entropy decrease can occur if cells are engaged in response to the same input but are not necessarily communicating (*92*).

One bit of information is sufficient to define a binary phenotypic outcome, such as cell death/survival, differentiation/self-renewal, or proliferation/migration. This binary outcome frequently reflects occupancy of alternative attractor states modulated by the signaling input (inputs 2 and 2′ in Fig. 1B). In the context of cancer progression, multiple external cues can trigger signaling events, leading to diversification of cell responses through conditional occupancy of different attractors as a function of the combinations of different cues (and their persistence) in a specific tumor location or the cues received by cancer cells during metastatic spread. Similar quantitative analysis can be used to gauge the effects of different mutations and drug treatments that can perturb the entropy of different attractors more specifically or the entropy associated with the overall epigenetic or genetic state more generally (*12*).

In contrast to the entropy decrease because of signaling inputs, entropy of a particular attractor and thus the associated phenotypic plasticity can also naturally increase because of epigenetic drift (input 1 in Fig. 1B). Epigenetic drift occurs both in tissue culture and in vivo with increasing age of cells and organisms (*94*–*97*). In the context of hyperproliferation associated with cancer, epigenetic drift is because of epimutations accumulating with the increasing number of cell divisions, which can happen at a high frequency (*98*). This increasing entropy of the epigenetic landscape is distinct from the recurrent changes in DNA methylation serving as a basis for the epigenetic clocks (*99*). Unlike the age-related DNA hyper- or hypomethylation signatures at specific CpG sites, epigenetic drift is a reflection of increased DNA methylation variability, which frequently occurs at loci related to malignancy and can be predictive of cancer emergence (*100*). One example of this site specificity is methylation at the locus encoding polycomb repressive complex-2 (PRC2) (itself responsible for trimethylation of H3K27) (*98*). The entropy increase associated with epigenetic drift may also explain the emergence of a rare 5% subpopulation of bipotent-like breast cancer progenitor cells (*101*). Intratumor epigenetic drift may be dependent on the replication history of the individual clones, leading to a continually expanding spectrum of EMT identities in colorectal tumors (*102*). Overall, the landscape entropy is not static and can decrease and increase in a quantifiable fashion, even without genetic alterations, creating a more complex context for normal tissue function and progression to cancer.

Mapping regulatory landscapes onto phenotypic responses

Can quantitatively assessed changes in epigenetic and genetic landscapes inform the selection of appropriate treatments? Because treatments are driven by disease-specific phenotypes and alterations of landscapes occur at the level of DNA modifications and molecular networks, it is important to consider in more detail how the specific phenotypes are controlled. In many cases, a phenotypic state is defined by a specific biomolecular circuit. For instance, cell migration phenotypes are controlled by cytoskeleton reorganization, which in turn is frequently controlled by a subset of Rho-family small guanosine triphosphatases (GTPases) (*103*, *104*). Similarly, cell proliferation is phenotypically driven by the circuit involving regulation of cyclin-dependent kinases (*105*). It is therefore important to understand how the function of these specific, phenotype-defining circuits may be influenced by the more global changes in cellular regulatory networks, as discussed below for the case of apoptosis.

Although the molecular circuits controlling apoptosis are complex, one can use the relative abundances of pro- and antiapoptotic members of the BCL protein family controlling the phenotypic outcomes of either regulated cell death (relatively higher abundance of proapoptotic proteins, such as Bax) or cytoprotection (relatively higher abundance of antiapoptotic proteins, such as Bcl-2) (*106*, *107*) (Fig. 3A). The equally matched abundance of pro- and antiapoptotic proteins defines the boundary between these states within a phenotypic space (life versus death) onto which the epigenetic and genetic landscapes can be mapped (Fig. 3B). This mapping is based on biochemical input-output relatonships between the phenotype-defining molecules and the upstream genetic and epigenetic mediators, and it is a natural dimensionality reduction mechanism that allows the evaluation of effects of the underlying molecular network variability and regulation. In many circumstances—e.g., in the turnover of multiple epithelial tissues—the entropy associated with the underlying landscape and thus variability in the expression of apoptosis proteins can result in a subset of cells undergoing cell death even under homeostatic conditions. The distribution of cells across the epigenetic landscape can therefore define the fractions of cells displaying different phenotypes.

The mapping of signaling network activity onto this apoptosis-regulating circuit (Fig. 3B) can be established experimentally and visualized in two dimensions as the joint single-cell distributions of Bcl-2–Bax pairs. The regulatory landscapes upstream of the phenotype-defining molecular circuit control the relative abundances of the proteins in these pairs, which can alter in response to an epigenetic change, such as LOI of *IGF2* (*108*). The misregulation of the signaling inputs resulting from epigenetic alteration [particularly the rebalancing of signaling through growth factor–responsive extracellular signal–regulated kinase (ERK)–MAPK and AKT pathways] is the key aspect of the newly emerging attractor state that translates into a new Bcl-2–Bax distribution, resulting in a higher propensity for cell death (Fig. 3C). Therefore, an epigenetic landscape change, in addition to promoting higher cell proliferation and tissue hyperplasia, creates a vulnerability (an increased propensity to undergo apoptosis) that can be exploited to selectively eliminate the cell population undergoing *IGF2* LOI. These landscape perturbations cause the LOI cells but not the WT cells to cross the death boundary (Fig. 3C), thus predicting the therapeutic window relevant to this precancerous state for specific drugs, such as receptor tyrosine kinase inhibitors (*108*). This analysis highlights the direct translation of landscape concepts to the development of more-targeted therapeutic approaches, particularly if an epigenetic alteration is considered an important therapeutic target (*109*).

This phenotypic mapping analysis can be further extended within the recently introduced framework of cellular archetypes in tissues (*31*, *32*). Archetypes are defined as extreme phenotypic states spanning the available optimized phenotypic space and thus reflecting the available degrees of freedom of

the phenotypic plasticity. The analysis of Wilms tumor patient samples revealed three archetypal phenotypic states, suggesting a more complex landscape distribution in vivo. More-advanced stages of the disease, accompanied by emergence of *IGF2* LOI, lead to a shift of cell population from a relatively uniform distribution across three archtypes—an epithelial and two mesenchymal states (one of which is also characterized by higher cell proliferation)—toward a greater abundance of mesenchymal states versus the epithelial one (*30*). This result suggested a specific landscape change, potentially resulting from an increased expression of *IGF2* promoting more aggressive cell behaviors related to cell proliferation and EMT. Despite this more complex landscape structure, we suggest that phenotypic mapping analysis can still be used to target specific cell states.

In general, measuring and mapping genetic and epigenetic landscapes onto phenotypic spaces can be an effective strategy to both infer the corresponding phenotypic diversity and target specific subpopulations defined by landscape attractors. Notably, it can also elucidate the effects of phenotypic plasticity and guide corresponding treatment strategies. If mutations, epigenetic changes, or environmental inputs leading to the emergence of precancerous and cancerous states also increase the plasticity within emerging attractors, cell populations may be substantially less targetable owing to a larger overlap with WT attractors and faster escape from a vulnerable area of the attractor (Fig. 3C). This consideration both provides further interpretation for poor prognostic correlates of the more plastic tumor attractors and suggests that cancer treatment should reduce plasticity. More specifically, the clinical intervention would be aimed at reshaping the underlying landscape to first stabilize the cancer-specific attractors by perturbing the attractor-defining pathways and molecular circuits and to then eliminate cells occupying these attractors while minimizing the effect on untransformed cells.

Conclusions and future directions

The studies reviewed here support the utility of the genetic and epigenetic landscape approaches in our understanding of cancer etiology, ultimately allowing us to arrive at a more general and conceptual understanding of carcinogenesis. Notably, this approach presents a detailed view of the system, which may focus on a specific attractor but may also focus on a combination of multiple attractors and dynamic transitions between them. Conversely, entropy is frequently a less-resolved and more global metric of the overall diversity of cell states. Both approaches are useful and frequently complementary. For example, the landscape view may be better at capturing the difference between an increase in phenotypic plasticity—i.e., the ability of cells (and their molecular networks) to dynamically explore diverse states and corresponding phenotypes—and phenotypic diversity—i.e., stable occupancy of different attractors by different cells in the population (Fig. 3C). In both cases, the entropy of the tumor tissue may be higher compared with the parental WT tissue state, but the landscapes would be distinct, which can be a crucial level of resolution to determine prognosis and possible interventions. Nevertheless, entropy can still be a convenient metric, particularly in assessing the effects of signaling inputs, mutational and epigenetic perturbations, or medical interventions. In particular, changes in entropy [assessed for example through different information theory–based measures (Box 1)] can quantitatively characterize the effects of these diverse inputs or evaluate how long-term processes, such as cellular aging, may affect cellular landscapes.

New experimental approaches may also allow further analysis of causality versus correlation in the relationship between landscape alterations and the emergence of cancer states. For instance, new CRISPR methods can allow recruitment of specific epigenetic modifiers to a targeted locus within the genome and direct control of epigenetic and gene expression variability and attractor properties (*29*). Studies such as this combined with further analysis of precancerous states in patients and animal models involving specific perturbations of genetic and epigenetic mechanisms can provide further data to refine our understanding of cancer-specific lanscapes.

Within oncology applications, key advantages of the landscape and entropy concepts lie in an improvement of our understanding of cancer etiology and development of approaches for targeted and personalized cancer treatments. More plastic attractors can allow cells to potentially rapidly adjust to both pharmacological and immune therapeutic interventions as well as enable cells to dynamically switch between diverse phenotypic states required, for example, for metastatic spread. Therefore, arguably, further approaches may focus on a combination of treatments that would not only attempt to eliminate specific cell subpopulations but also reduce the phenotypic plasticity of tumor cells. In developing these approaches, characterization of the underlying landscapes will be of particular importance. In these efforts, it will be important to refine our understanding of how the landscapes determined on the epigenetic and gene regulation levels can be quantitatively translated into the corresponding descriptions of the activity of the molecular circuits controlling specific phenotypes. Such phenotypic mapping can direct more-specific drug development efforts and quantitatively establish the therapeutic windows of specific compounds.

In this Review, we primarily focused on DNA methylation as a key epigenetic mechanism for which landscape and entropic analysis has already been performed in diverse biological systems. However, epigenetic control can occur on other levels, including through histone modifications. As rich data accounting for further levels of epigenetic control are gathered, an important challenge will be to understand whether extensive, landscape-based description of all levels of epigenetic and gene regulatory controls is necessary or whether this complexity and data dimensionality can be reduced to a simpler measurement set. In these efforts, a key role may be played by various machine learning techniques to reveal mutual interdependencies of various molecular control mechanisms and their influences on phenotypic plasticity.

REFERENCES AND NOTES

1. I. J. Fidler, Tumor heterogeneity and the biology of cancer invasion and metastasis. *Cancer Res.* **38**, 2651–2660 (1978). pmid: 354778
2. P. C. Nowell, The clonal evolution of tumor cell populations. *Science* **194**, 23–28 (1976). doi: 10.1126/science.959840; pmid: 959840
3. D. Jia, M. K. Jolly, P. Kulkarni, H. Levine, Phenotypic Plasticity and Cell Fate Decisions in Cancer: Insights from Dynamical Systems Theory. *Cancers* **9**, 70 (2017). doi: 10.3390/cancers9070070; pmid: 28640191
4. A. Sacchetti *et al*., Phenotypic plasticity underlies local invasion and distant metastasis in colon cancer. *eLife* **10**, e61461 (2021). doi: 10.7554/eLife.61461; pmid: 34036938
5. S. V. Sharma *et al*., A chromatin-mediated reversible drug-tolerant state in cancer cell subpopulations. *Cell* **141**, 69–80 (2010). doi: 10.1016/j.cell.2010.02.027; pmid: 20371346
6. C. A. Chang *et al*., Ontogeny and Vulnerabilities of Drug-Tolerant Persisters in HER2^{+} Breast Cancer. *Cancer Discov.* **12**, 1022–1045 (2022). doi: 10.1158/2159-8290.CD-20-1265; pmid: 34911733
7. J. X. Zhou, M. D. Aliyu, E. Aurell, S. Huang, Quasi-potential landscape in complex multi-stable systems. *J. R. Soc. Interface* **9**, 3539–3553 (2012). doi: 10.1098/rsif.2012.0434; pmid: 22933187
8. J. Wang, K. Zhang, L. Xu, E. Wang, Quantifying the Waddington landscape and biological paths for development and differentiation. *Proc. Natl. Acad. Sci. U.S.A.* **108**, 8257–8262 (2011). doi: 10.1073/pnas.1017017108; pmid: 21536909
9. C. Li, J. Wang, Landscape and flux reveal a new global view and physical quantification of mammalian cell cycle. *Proc. Natl. Acad. Sci. U.S.A.* **111**, 14130–14135 (2014). doi: 10.1073/pnas.1408628111; pmid: 25228772
10. G. Balázsi, A. van Oudenaarden, J. J. Collins, Cellular decision making and biological noise: From microbes to mammals. *Cell* **144**, 910–925 (2011). doi: 10.1016/j.cell.2011.01.030; pmid: 21414483
11. N. Eling, M. D. Morgan, J. C. Marioni, Challenges in measuring and understanding biological noise. *Nat. Rev. Genet.* **20**, 536–548 (2019). doi: 10.1038/s41576-019-0130-6; pmid: 31114032
12. A. Levchenko, I. Nemenman, Cellular noise and information transmission. *Curr. Opin. Biotechnol.* **28**, 156–164 (2014). doi: 10.1016/j.copbio.2014.05.002; pmid: 24922112
13. A. Golightly, C. S. Gillespie, in *In Silico Systems Biology*, M. V. Schneider, Ed. (Springer, 2013), pp. 169–187.
14. D. T. Gillespie, A. Hellander, L. R. Petzold, Perspective: Stochastic algorithms for chemical kinetics. *J. Chem. Phys.* **138**, 170901 (2013). doi: 10.1063/1.4801941
15. M. Ullah, O. Wolkenhauer, Stochastic approaches in systems biology. *Wiley Interdiscip. Rev. Syst. Biol. Med.* **2**, 385–397 (2010). doi: 10.1002/wsbm.78; pmid: 20836037
16. D. Grün, A. van Oudenaarden, Design and analysis of single-cell sequencing experiments. *Cell* **163**, 799–810 (2015). doi: 10.1016/j.cell.2015.10.039; pmid: 26544934
17. G. Kelsey, O. Stegle, W. Reik, Single-cell epigenomics: Recording the past and predicting the future. *Science* **358**, 69–75 (2017). doi: 10.1126/science.aan6826; pmid: 28983045

18. E. Shema, B. E. Bernstein, J. D. Buenrostro, Single-cell and single-molecule epigenomics to uncover genome regulation at unprecedented resolution. *Nat. Genet.* **51**, 19–25 (2019). doi: 10.1038/s41588-018-0290-x; pmid: 30559489
19. Q. Li *et al*., Dynamics inside the cancer cell attractor reveal cell heterogeneity, limits of stability, and escape. *Proc. Natl. Acad. Sci. U.S.A.* **113**, 2672–2677 (2016). doi: 10.1073/pnas.1519210113; pmid: 26929366
20. E. Pujadas, A. P. Feinberg, Regulated noise in the epigenetic landscape of development and disease. *Cell* **148**, 1123–1131 (2012). doi: 10.1016/j.cell.2012.02.045; pmid: 22424224
21. A. Taherian Fard, M. A. Ragan, Modeling the Attractor Landscape of Disease Progression: A Network-Based Approach. *Front. Genet.* **8**, 48 (2017). doi: 10.3389/fgene.2017.00048; pmid: 28458684
22. S. Tripathi, P. Chakraborty, H. Levine, M. K. Jolly, A mechanism for epithelial-mesenchymal heterogeneity in a population of cancer cells. *PLOS Comput. Biol.* **16**, e1007619 (2020). doi: 10.1371/journal.pcbi.1007619; pmid: 32040502
23. Y. Cheng *et al*., Role of metastasis-associated lung adenocarcinoma transcript-1 (MALAT-1) in pancreatic cancer. *PLOS ONE* **13**, e0192264 (2018). doi: 10.1371/journal.pone.0192264; pmid: 29389953
24. W. N. van Wieringen, A. W. van der Vaart, Statistical analysis of the cancer cell's molecular entropy using high-throughput data. *Bioinformatics* **27**, 556–563 (2011). doi: 10.1093/bioinformatics/btq704; pmid: 21172912
25. J. West, G. Bianconi, S. Severini, A. E. Teschendorff, Differential network entropy reveals cancer system hallmarks. *Sci. Rep.* **2**, 802 (2012). doi: 10.1038/srep00802; pmid: 23150773
26. F. Cheng, C. Liu, B. Shen, Z. Zhao, Investigating cellular network heterogeneity and modularity in cancer: A network entropy and unbalanced motif approach. *BMC Syst. Biol.* **10**, 65 (2016). doi: 10.1186/s12918-016-0309-9; pmid: 27585651
27. A. E. Teschendorff, T. Enver, Single-cell entropy for accurate estimation of differentiation potency from a cell's transcriptome. *Nat. Commun.* **8**, 15599 (2017). doi: 10.1038/ncomms15599; pmid: 28569836
28. R. Chaligne *et al*., Epigenetic encoding, heritability and plasticity of glioma transcriptional cell states. *Nat. Genet.* **53**, 1469–1479 (2021). doi: 10.1038/s41588-021-00927-7; pmid: 34594037
29. A. Lu *et al*., Reprogrammable CRISPR/dCas9-based recruitment of DNMT1 for site-specific DNA demethylation and gene regulation. *Cell Discov.* **5**, 22 (2019). doi: 10.1038/s41421-019-0090-1; pmid: 31016028
30. A. Trink *et al*., Geometry of Gene Expression Space of Wilms' Tumors From Human Patients. *Neoplasia* **20**, 871–881 (2018). doi: 10.1016/j.neo.2018.06.006; pmid: 30029183
31. J. Hausser, U. Alon, Tumour heterogeneity and the evolutionary trade-offs of cancer. *Nat. Rev. Cancer* **20**, 247–257 (2020). doi: 10.1038/s41568-020-0241-6; pmid: 32094544
32. J. Hausser *et al*., Tumor diversity and the trade-off between universal cancer tasks. *Nat. Commun.* **10**, 5423 (2019). doi: 10.1038/s41467-019-13195-1; pmid: 31780652
33. P. B. Gupta *et al*., Stochastic state transitions give rise to phenotypic equilibrium in populations of cancer cells. *Cell* **146**, 633–644 (2011). doi: 10.1016/j.cell.2011.07.026; pmid: 21854987
34. G. Landan *et al*., Epigenetic polymorphism and the stochastic formation of differentially methylated regions in normal and cancerous tissues. *Nat. Genet.* **44**, 1207–1214 (2012). doi: 10.1038/ng.2442; pmid: 23064413
35. J. E. Barrett *et al*., Quantification of tumour evolution and heterogeneity via Bayesian epiallele detection. *BMC Bioinformatics* **18**, 354 (2017). doi: 10.1186/s12859-017-1753-2; pmid: 28743252
36. H. Xie *et al*., Genome-wide quantitative assessment of variation in DNA methylation patterns. *Nucleic Acids Res.* **39**, 4099–4108 (2011). doi: 10.1093/nar/gkr017; pmid: 21278160
37. G. Jenkinson, E. Pujadas, J. Goutsias, A. P. Feinberg, Potential energy landscapes identify the information-theoretic nature of the epigenome. *Nat. Genet.* **49**, 719–729 (2017). doi: 10.1038/ng.3811; pmid: 28346445
38. G. Jenkinson, J. Abante, M. A. Koldobskiy, A. P. Feinberg, J. Goutsias, Ranking genomic features using an information-theoretic measure of epigenetic discordance. *BMC Bioinformatics* **20**, 175 (2019). doi: 10.1186/s12859-019-2777-6; pmid: 30961526
39. D. A. Landau *et al*., Locally disordered methylation forms the basis of intratumor methylome variation in chronic lymphocytic leukemia. *Cancer Cell* **26**, 813–825 (2014). doi: 10.1016/j.ccell.2014.10.012; pmid: 25490447
40. S. Li *et al*., Distinct evolution and dynamics of epigenetic and genetic heterogeneity in acute myeloid leukemia. *Nat. Med.* **22**, 792–799 (2016). doi: 10.1038/nm.4125; pmid: 27322744
41. The American Association for Cancer Research Human Epigenome Task Force, European Union, Network of Excellence, Scientific Advisory Board, Moving AHEAD with an international human epigenome project. *Nature* **454**, 711–715 (2008). doi: 10.1038/454711a; pmid: 18685699
42. K. D. Hansen *et al*., Increased methylation variation in epigenetic domains across cancer types. *Nat. Genet.* **43**, 768–775 (2011). doi: 10.1038/ng.865; pmid: 21706001
43. B. P. Berman *et al*., Regions of focal DNA hypermethylation and long-range hypomethylation in colorectal cancer coincide with nuclear lamina–associated domains. *Nat. Genet.* **44**, 40–46 (2012). doi: 10.1038/ng.969; pmid: 22120008
44. O. G. McDonald *et al*., Epigenomic reprogramming during pancreatic cancer progression links anabolic glucose metabolism to distant metastasis. *Nat. Genet.* **49**, 367–376 (2017). doi: 10.1038/ng.3753; pmid: 28092686
45. M. Jeong *et al*., Large conserved domains of low DNA methylation maintained by Dnmt3a. *Nat. Genet.* **46**, 17–23 (2014). doi: 10.1038/ng.2836; pmid: 24270360
46. K. S. Johnson *et al*., Gene expression and chromatin accessibility during progressive EMT and MET linked to dynamic CTCF engagement. *bioRxiv*2020.05.11.089110 [Preprint] (2020); doi: 10.1101/2020.05.11.089110
47. O. G. McDonald, H. Wu, W. Timp, A. Doi, A. P. Feinberg, Genome-scale epigenetic reprogramming during epithelial-to-mesenchymal transition. *Nat. Struct. Mol. Biol.* **18**, 867–874 (2011). doi: 10.1038/nsmb.2084; pmid: 21725293
48. S. E. Johnstone *et al*., Large-Scale Topological Changes Restrain Malignant Progression in Colorectal Cancer. *Cell* **182**, 1474–1489.e23 (2020). doi: 10.1016/j.cell.2020.07.030; pmid: 32841603
49. L. A. Garraway, E. S. Lander, Lessons from the cancer genome. *Cell* **153**, 17–37 (2013). doi: 10.1016/j.cell.2013.03.002; pmid: 23540688
50. A. P. Feinberg, M. A. Koldobskiy, A. Göndör, Epigenetic modulators, modifiers and mediators in cancer aetiology and progression. *Nat. Rev. Genet.* **17**, 284–299 (2016). doi: 10.1038/nrg.2016.13; pmid: 26972587
51. T. Zhen *et al*., RUNX1 and CBFβ-SMMHC transactivate target genes together in abnormal myeloid progenitors for leukemia development. *Blood* **136**, 2373–2385 (2020). doi: 10.1182/blood.2020007747; pmid: 32929473
52. S. Li *et al*., Somatic Mutations Drive Specific, but Reversible, Epigenetic Heterogeneity States in AML. *Cancer Discov.* **10**, 1934–1949 (2020). doi: 10.1158/2159-8290.CD-19-0897; pmid: 32938585
53. M. A. Koldobskiy *et al*., A Dysregulated DNA Methylation Landscape Linked to Gene Expression in MLL-Rearranged AML. *Epigenetics* **15**, 841–858 (2020). doi: 10.1080/15592294.2020.1734149; pmid: 32114880
54. A. J. Levine, The p53 protein plays a central role in the mechanism of action of epigentic drugs that alter the methylation of cytosine residues in DNA. *Oncotarget* **8**, 7228–7230 (2017). doi: 10.18632/oncotarget.14805; pmid: 28129641
55. P. T. Filipczak *et al*., p53-Suppressed Oncogene TET1 Prevents Cellular Aging in Lung Cancer. *Cancer Res.* **79**, 1758–1768 (2019). doi: 10.1158/0008-5472.CAN-18-1234; pmid: 30622117
56. A. Tovy *et al*., p53 is essential for DNA methylation homeostasis in naïve embryonic stem cells, and its loss promotes clonal heterogeneity. *Genes Dev.* **31**, 959–972 (2017). doi: 10.1101/gad.299198.117; pmid: 28607180
57. R. Rampal *et al*., DNA hydroxymethylation profiling reveals that *WT1* mutations result in loss of TET2 function in acute myeloid leukemia. *Cell Rep.* **9**, 1841–1855 (2014). doi: 10.1016/j.celrep.2014.11.004; pmid: 25482556
58. A. Marusyk, M. Janiszewska, K. Polyak, Intratumor heterogeneity: The rosetta stone of therapy resistance. *Cancer Cell* **37**, 471–484 (2020). doi: 10.1016/j.ccell.2020.03.007; pmid: 32289271
59. A. M. Tsankov *et al*., Loss of DNA methyltransferase activity in primed human ES cells triggers increased cell-cell variability and transcriptional repression. *Development* **146**, dev174722 (2019). doi: 10.1242/dev.174722; pmid: 31515224
60. Z. S. Singer *et al*., Dynamic heterogeneity and DNA methylation in embryonic stem cells. *Mol. Cell* **55**, 319–331 (2014). doi: 10.1016/j.molcel.2014.06.029; pmid: 25038413
61. Y. Costa *et al*., NANOG-dependent function of TET1 and TET2 in establishment of pluripotency. *Nature* **495**, 370–374 (2013). doi: 10.1038/nature11925; pmid: 23395962
62. C. A. Doege *et al*., Early-stage epigenetic modification during somatic cell reprogramming by Parp1 and Tet2. *Nature* **488**, 652–655 (2012). doi: 10.1038/nature11333; pmid: 22902501
63. Y. Gao *et al*., Replacement of Oct4 by Tet1 during iPSC induction reveals an important role of DNA methylation and hydroxymethylation in reprogramming. *Cell Stem Cell* **12**, 453–469 (2013). doi: 10.1016/j.stem.2013.02.005; pmid: 23499384
64. J. Silva *et al*., Nanog is the gateway to the pluripotent ground state. *Cell* **138**, 722–737 (2009). doi: 10.1016/j.cell.2009.07.039; pmid: 19703398
65. B. B. Liau *et al*., Adaptive Chromatin Remodeling Drives Glioblastoma Stem Cell Plasticity and Drug Tolerance. *Cell Stem Cell* **20**, 233–246.e7 (2017). doi: 10.1016/j.stem.2016.11.003; pmid: 27989769
66. R. C. Rockne *et al*., State-Transition Analysis of Time-Sequential Gene Expression Identifies Critical Points That Predict Development of Acute Myeloid Leukemia. *Cancer Res.* **80**, 3157–3169 (2020). doi: 10.1158/0008-5472.CAN-20-0354; pmid: 32414754
67. J. Pelletier *et al*., Germline mutations in the Wilms' tumor suppressor gene are associated with abnormal urogenital development in Denys-Drash syndrome. *Cell* **67**, 437–447 (1991). doi: 10.1016/0092-8674(91)90194-4; pmid: 1655284
68. A. Schedl, N. Hastie, Multiple roles for the Wilms' tumour suppressor gene, WT1 in genitourinary development. *Mol. Cell. Endocrinol.* **140**, 65–69 (1998). doi: 10.1016/S0303-7207(98)00031-8; pmid: 9722170
69. J. Park *et al*., Switch-like enhancement of epithelial-mesenchymal transition by YAP through feedback regulation of WT1 and Rho-family GTPases. *Nat. Commun.* **10**, 2797 (2019). doi: 10.1038/s41467-019-10729-5; pmid: 31243273
70. K. Ohnishi *et al*., Premature termination of reprogramming in vivo leads to cancer development through altered epigenetic regulation. *Cell* **156**, 663–677 (2014). doi: 10.1016/j.cell.2014.01.005; pmid: 24529372
71. M. Reichert, A. K. Rustgi, Pancreatic ductal cells in development, regeneration, and neoplasia. *J. Clin. Invest.* **121**, 4572–4578 (2011). doi: 10.1172/JCI57131; pmid: 22133881
72. P. Storz, Acinar cell plasticity and development of pancreatic ductal adenocarcinoma. *Nat. Rev. Gastroenterol. Hepatol.* **14**, 296–304 (2017). doi: 10.1038/nrgastro.2017.12; pmid: 28270694
73. D. Wei *et al*., KLF4 is essential for induction of cellular identity change and acinar-to-ductal reprogramming during early pancreatic carcinogenesis. *Cancer Cell* **29**, 324–338 (2016). doi: 10.1016/j.ccell.2016.02.005; pmid: 26977883
74. V. Giroux, A. K. Rustgi, Metaplasia: Tissue injury adaptation and a precursor to the dysplasia-cancer sequence. *Nat. Rev. Cancer* **17**, 594–604 (2017). doi: 10.1038/nrc.2017.68; pmid: 28860646
75. L. Y. Ding *et al*., Epigenetic silencing of *AATK* in acinar to ductal metaplasia in murine model of pancreatic cancer. *Clin. Epigenetics* **12**, 87 (2020). doi: 10.1186/s13148-020-00878-6; pmid: 32552862
76. S. J. Spechler, R. F. Souza, Barrett's esophagus. *N. Engl. J. Med.* **371**, 836–845 (2014). doi: 10.1056/NEJMra1314704; pmid: 25162890
77. R. Barros *et al*., CDX2 autoregulation in human intestinal metaplasia of the stomach: Impact on the stability of the phenotype. *Gut* **60**, 290–298 (2011). doi: 10.1136/gut.2010.222323; pmid: 21148572
78. E. G. Luebeck *et al*., Identification of a key role of widespread epigenetic drift in Barrett's esophagus and esophageal adenocarcinoma. *Clin. Epigenetics* **9**, 113 (2017). doi: 10.1186/s13148-017-0409-4; pmid: 29046735
79. J. Wu *et al*., A single-cell survey of cellular hierarchy in acute myeloid leukemia. *J. Hematol. Oncol.* **13**, 128 (2020). doi: 10.1186/s13045-020-00941-y; pmid: 32977829
80. M. M. Streppel *et al*., Next-generation sequencing of endoscopic biopsies identifies *ARID1A* as a tumor-suppressor gene in Barrett's esophagus. *Oncogene* **33**, 347–357 (2014). doi: 10.1038/onc.2012.586; pmid: 23318448
81. G. Livshits *et al*., Arid1a restrains Kras-dependent changes in acinar cell identity. *eLife* **7**, e35216 (2018). doi: 10.7554/eLife.35216; pmid: 30014851
82. T. D. Treger, T. Chowdhury, K. Pritchard-Jones, S. Behjati, The genetic changes of Wilms tumour. *Nat. Rev. Nephrol.* **15**, 240–251 (2019). doi: 10.1038/s41581-019-0112-0; pmid: 30705419
83. V. Conteduca *et al*., Barrett's esophagus and esophageal cancer: An overview. *Int. J. Oncol.* **41**, 414–424 (2012). doi: 10.3892/ijo.2012.1481; pmid: 22615011

84. J. H. Taube *et al*., Core epithelial-to-mesenchymal transition interactome gene-expression signature is associated with claudin-low and metaplastic breast cancer subtypes. *Proc. Natl. Acad. Sci. U.S.A.* **107**, 15449–15454 (2010). doi: 10.1073/pnas.1004900107; pmid: 20713713
85. A. D. Rhim *et al*., EMT and dissemination precede pancreatic tumor formation. *Cell* **148**, 349–361 (2012). doi: 10.1016/j.cell.2011.11.025; pmid: 22265420
86. R. Cheong, A. Rhee, C. J. Wang, I. Nemenman, A. Levchenko, Information transduction capacity of noisy biochemical signaling networks. *Science* **334**, 354–358 (2011). doi: 10.1126/science.1204553; pmid: 21921160
87. A. Rhee, R. Cheong, A. Levchenko, The application of information theory to biochemical signaling systems. *Phys. Biol.* **9**, 045011 (2012). doi: 10.1088/1478-3975/9/4/045011; pmid: 22872091
88. M. D. Brennan, R. Cheong, A. Levchenko, How information theory handles cell signaling and uncertainty. *Science* **338**, 334–335 (2012). doi: 10.1126/science.1227946; pmid: 23087235
89. S. Uda *et al*., Robustness and compensation of information transmission of signaling pathways. *Science* **341**, 558–561 (2013). doi: 10.1126/science.1234511; pmid: 23908238
90. J. Selimkhanov *et al*., Accurate information transmission through dynamic biochemical signaling networks. *Science* **346**, 1370–1373 (2014). doi: 10.1126/science.1254933; pmid: 25504722
91. A. S. Hansen, E. K. O'Shea, Limits on information transduction through amplitude and frequency regulation of transcription factor activity. *eLife* **4**, e06559 (2015). doi: 10.7554/eLife.06559; pmid: 25985085
92. R. Suderman, J. A. Bachman, A. Smith, P. K. Sorger, E. J. Deeds, Fundamental trade-offs between information flow in single cells and cellular populations. *Proc. Natl. Acad. Sci. U.S.A.* **114**, 5755–5760 (2017). doi: 10.1073/pnas.1615660114; pmid: 28500273
93. D. Ellison *et al*., Cell-cell communication enhances the capacity of cell ensembles to sense shallow gradients during morphogenesis. *Proc. Natl. Acad. Sci. U.S.A.* **113**, E679–E688 (2016). doi: 10.1073/pnas.1516503113; pmid: 26792522
94. A. R. Mendelsohn, J. W. Larrick, Epigenetic drift is a determinant of mammalian lifespan. *Rejuvenation Res.* **20**, 430–436 (2017). doi: 10.1089/rej.2017.2024; pmid: 28942711
95. S. Maegawa *et al*., Widespread and tissue specific age-related DNA methylation changes in mice. *Genome Res.* **20**, 332–340 (2010). doi: 10.1101/gr.096826.109; pmid: 20107151
96. A. E. Teschendorff, J. West, S. Beck, Age-associated epigenetic drift: Implications, and a case of epigenetic thrift? *Hum. Mol. Genet.* **22**, R7–R15 (2013). doi: 10.1093/hmg/ddt375; pmid: 23918660
97. H. Takeshima, T. Ushijima, Accumulation of genetic and epigenetic alterations in normal cells and cancer risk. *NPJ Precis. Oncol.* **3**, 7 (2019). doi: 10.1038/s41698-019-0079-0; pmid: 30854468
98. S. C. Zheng, M. Widschwendter, A. E. Teschendorff, Epigenetic drift, epigenetic clocks and cancer risk. *Epigenomics* **8**, 705–719 (2016). doi: 10.2217/epi-2015-0017; pmid: 27104983
99. S. Horvath, DNA methylation age of human tissues and cell types. *Genome Biol.* **14**, 3156 (2013). doi: 10.1186/gb-2013-14-10-r115; pmid: 24138928
100. A. E. Teschendorff, A. Jones, M. Widschwendter, Stochastic epigenetic outliers can define field defects in cancer. *BMC Bioinformatics* **17**, 178 (2016). doi: 10.1186/s12859-016-1056-z; pmid: 27103033
101. W. Chen *et al*., Single-cell landscape in mammary epithelium reveals bipotent-like cells associated with breast cancer risk and outcome. *Commun. Biol.* **2**, 306 (2019). doi: 10.1038/s42003-019-0554-8; pmid: 31428694
102. Z. Meir, Z. Mukamel, E. Chomsky, A. Lifshitz, A. Tanay, Single-cell analysis of clonal maintenance of transcriptional and epigenetic states in cancer cells. *Nat. Genet.* **52**, 709–718 (2020). doi: 10.1038/s41588-020-0645-y; pmid: 32601473
103. C. D. Lawson, A. J. Ridley, Rho GTPase signaling complexes in cell migration and invasion. *J. Cell Biol.* **217**, 447–457 (2018). doi: 10.1083/jcb.201612069; pmid: 29233866
104. W. R. Holmes, J. Park, A. Levchenko, L. Edelstein-Keshet, A mathematical model coupling polarity signaling to cell adhesion explains diverse cell migration patterns. *PLOS Comput. Biol.* **13**, e1005524 (2017). doi: 10.1371/journal.pcbi.1005524; pmid: 28472054
105. O. Kapuy *et al*., System-level feedbacks control cell cycle progression. *FEBS Lett.* **583**, 3992–3998 (2009). doi: 10.1016/j.febslet.2009.08.023; pmid: 19703449
106. L. D. Walensky, BCL-2 in the crosshairs: Tipping the balance of life and death. *Cell Death Differ.* **13**, 1339–1350 (2006). doi: 10.1038/sj.cdd.4401992; pmid: 16763614
107. R. J. Youle, A. Strasser, The BCL-2 protein family: Opposing activities that mediate cell death. *Nat. Rev. Mol. Cell Biol.* **9**, 47–59 (2008). doi: 10.1038/nrm2308; pmid: 18097445
108. K. G. Vanaja, W. Timp, A. P. Feinberg, A. Levchenko, A loss of epigenetic control can promote cell death through reversing the balance of pathways in a signaling network. *Mol. Cell* **72**, 60–70.e3 (2018). doi: 10.1016/j.molcel.2018.08.025; pmid: 30244832
109. H. Zhong *et al*., Overproduction of IGF-2 drives a subset of colorectal cancer cells, which specifically respond to an anti-IGF therapeutic antibody and combination therapies. *Oncogene* **36**, 797–806 (2017). doi: 10.1038/onc.2016.248; pmid: 27399333

ACKNOWLEDGMENTS

We thank O. Kilic and J. Fairman for illustration preparation. **Funding:** This study was supported by NIH grants R01CA54358 to A.P.F. and U54CA209992 to A.L. **Competing interests:** A.P.F. is an inventor on a pending US patent related to this work ("Detecting cancer through generalized loss of stability of epigenetic domains," US20210071262A1, EP2707506B1). The authors declare no other competing interests. **License information:** Copyright © 2023 the authors, some rights reserved; exclusive licensee American Association for the Advancement of Science. No claim to original US government works. https://www.science.org/about/science-licenses-journal-article-reuse

Submitted 24 December 2020; accepted 22 December 2022
10.1126/science.aaw3835

1848 SOCIETY
AAAS

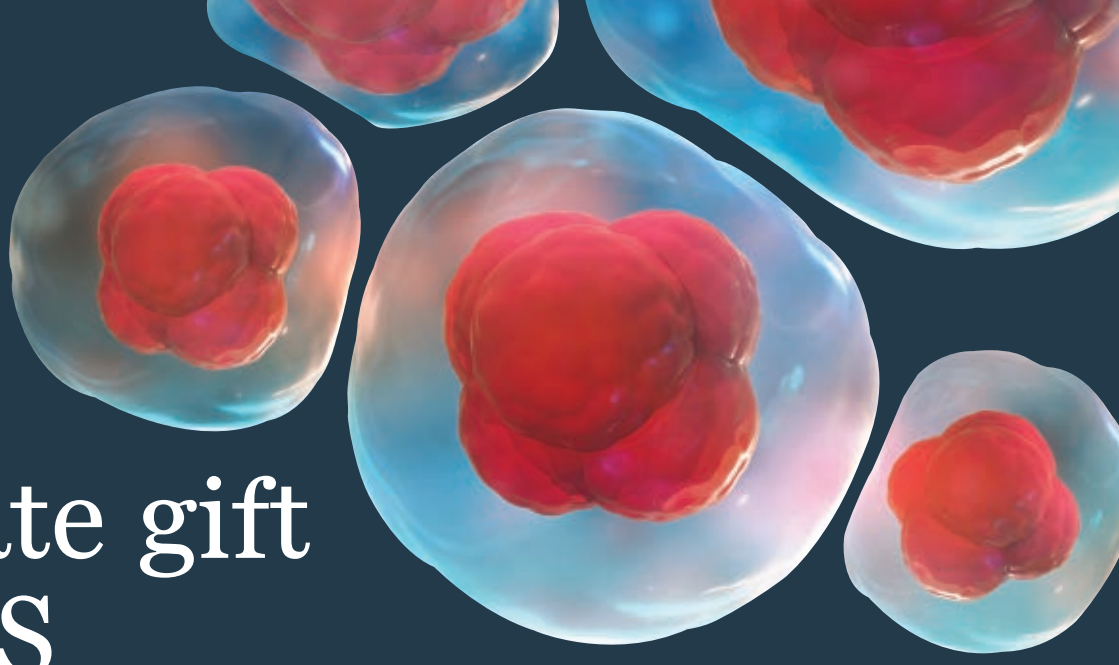

An estate gift to AAAS

Going all the way back to 1848, our founding year, the American Association for the Advancement of Science (AAAS) has been deeply committed to advancing science, engineering and innovation around the world for the benefit of all people.

Today, we are dedicated to advocating for science and scientific evidence to be fully and positively integrated into public policy and for the community to speak with one voice to advance science and engineering in the United States and around the world.

By making AAAS a beneficiary of your will, trust, retirement plan or life insurance policy, you will become a member of our 1848 Society and will help fuel our work on behalf of science and society – including publishing the world's most promising, innovative research in the *Science* family of journals and engaging in the issues that matter locally, nationally and around the world.

"As a teacher and instructor, I bear responsibility for the younger generations. If you have extra resources, concentrate them on organizations, like AAAS, that are doing work for all."

—Prof. Elisabeth Ervin-Blankenheim, 1848 Society member

If you intend to include AAAS in your estate plans, provide this information to your lawyer or financial adviser:

Legal Name: American Association for the Advancement of Science
Federal Tax ID Number: 53-0196568
Address: 1200 New York Avenue, NW, Washington, DC 20005

If you would like more information on making an estate gift to AAAS, cut out and return the form below or send an email to philanthropy@aaas.org. Additional details are also available online at **www.aaas.org/1848Society**.

AMERICAN ASSOCIATION FOR THE ADVANCEMENT OF SCIENCE

cut here

Yes, I would like more information about joining the AAAS 1848 Society.

1848 SOCIETY
AAAS

PLEASE CONTACT ME AT:

Name: _____

Address: _____

City: _____ State: _____ Zip code: _____ Country: _____

Email: _____ Phone: _____

RETURN THIS FORM TO:
AAAS Office of Philanthropy and Strategic Partnerships • 1200 New York Avenue, NW • Washington, DC 20005 USA

RESEARCH ARTICLE SUMMARY

DEVELOPMENT

Mitochondria metabolism sets the species-specific tempo of neuronal development

Ryohei Iwata†, Pierre Casimir†, Emir Erkol, Leïla Boubakar, Mélanie Planque, Isabel M. Gallego López, Martyna Ditkowska, Vaiva Gaspariunaite, Sofie Beckers, Daan Remans, Katlijn Vints, Anke Vandekeere, Suresh Poovathingal, Matthew Bird, Ine Vlaeminck, Eline Creemers, Keimpe Wierda, Nikky Corthout, Pieter Vermeersch, Sébastien Carpentier, Kristofer Davie, Massimiliano Mazzone, Natalia V. Gounko, Stein Aerts, Bart Ghesquière, Sarah-Maria Fendt, Pierre Vanderhaeghen*

INTRODUCTION: During embryonic development, the temporal sequence of events is usually conserved throughout evolution, but it can occur at very different time scales depending on the species or cell type considered. The human cerebral cortex is characterized by a considerably prolonged timing of neuronal development compared with other species, taking months to years to reach maturity compared with only a few weeks in the mouse. The resulting neoteny is thought to be a key mechanism enabling enhanced function and plasticity of the human brain. Human and nonhuman cortical neurons cultured in vitro or xenotransplanted into the mouse brain develop along their species-specific timeline. This suggests that species-specific developmental timing is controlled by cell-intrinsic mechanisms, but these remain essentially unknown.

RATIONALE: Metabolism and mitochondria are key drivers of cell fate transitions in many systems, including the developing brain. Here, we tested whether they could be involved in the species-specific tempo of cortical neuron development and human brain neoteny.

We developed a system of genetic birth-dating to label newly born neurons with high temporal and cellular resolution, and directly compared the development of human and mouse cortical neurons over time. We thus profiled, across time and species, mitochondria morphology, gene expression, oxygen consumption, and glucose metabolism. Next, we used pharmacological or genetic manipulation of human or mouse neurons to enhance or decrease their mitochondria function, and determined the consequences on the speed of neuronal development.

RESULTS: We found that mitochondria are initially low in size and quantity in newborn neurons, and then grow gradually as neurons undergo maturation following a species-specific timeline. Whereas in mouse neurons, mitochondria reach mature patterns in 3 to 4 weeks, they only do so after several months in human neurons.

We next measured mitochondria oxidative activity and glucose metabolism in human and mouse developing cortical neurons. This revealed a species-specific timeline of functional maturation of mitochondria, with mouse neurons displaying a much faster increase in mitochondria-dependent oxidative activity than human neurons. We also found that human cortical neurons displayed lower levels of mitochondria-driven glucose metabolism than did mouse neurons at the same age.

Finally, we tested whether mitochondria function affects neuronal developmental timing. We performed pharmacological or genetic manipulation of human developing cortical neurons to enhance mitochondria oxidative metabolism. This led to accelerated neuronal maturation, with neurons exhibiting more mature features weeks ahead of time, including complex morphology, increased electrical excitability, and functional synapse formation. Similar treatments on mouse neurons also led to faster maturation, whereas inhibition of mitochondria metabolism in mouse neurons led to a decrease in developmental rates.

CONCLUSION: Our work identifies a species-specific temporal pattern of mitochondria and metabolic development that sets the tempo of neuronal maturation. Accelerated human neuronal maturation using metabolic manipulation might benefit pluripotent stem cell–based modeling of neural diseases, which remains greatly hindered by protracted neuron development. Tools to accelerate or decelerate neuronal development could allow testing of the impact of neuronal neoteny on brain function, plasticity, and disease. ■

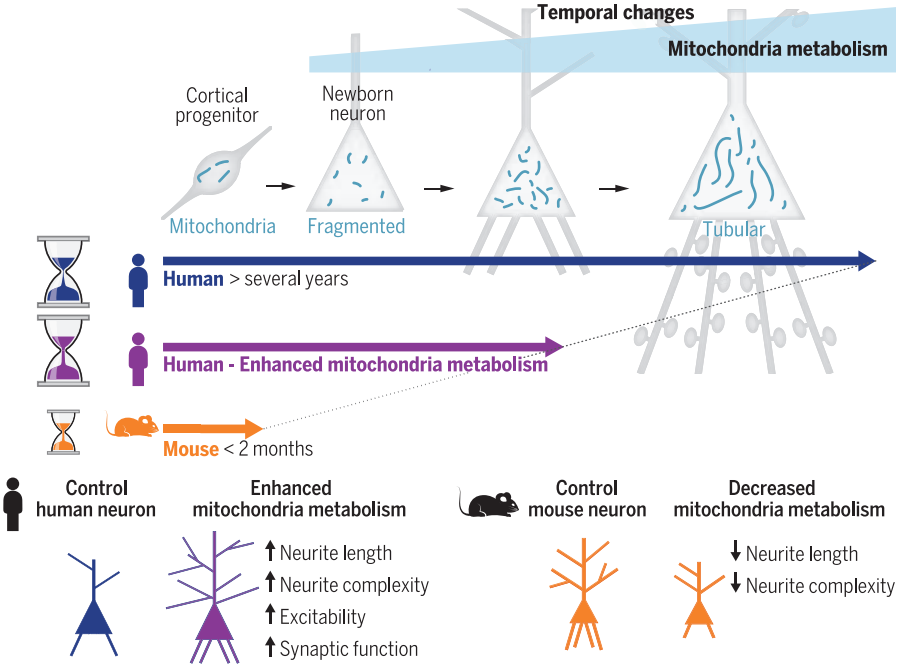

Mitochondria metabolism sets the tempo of neuronal development. Mitochondria dynamics and metabolism display species-specific timelines during cortical neuron development. In newborn neurons, mitochondria are small in number and metabolic activity, and then increase gradually during neuronal maturation. Enhanced mitochondria metabolism in human neurons leads to accelerated maturation, including increased neurite complexity, excitability, and synaptic function. Decreased mitochondria metabolism in mouse neurons leads to decelerated neuronal maturation.

The list of author affiliations is available in the full article online.
*Corresponding author. Email: pierre.vanderhaeghen@kuleuven.be
†These authors contributed equally to this work.
Cite this article as R. Iwata *et al.*, *Science* **379**, eabn4705 (2023). DOI: 10.1126/science.abn4705

READ THE FULL ARTICLE AT
https://doi.org/10.1126/science.abn4705

RESEARCH ARTICLE

DEVELOPMENT

Mitochondria metabolism sets the species-specific tempo of neuronal development

Ryohei Iwata[1,2,3]†, Pierre Casimir[1,2,3]†, Emir Erkol[1,2], Leïla Boubakar[1,2,3], Mélanie Planque[4,5], Isabel M. Gallego López[1,2], Martyna Ditkowska[1,2], Vaiva Gaspariunaite[1,2], Sofie Beckers[1,2], Daan Remans[1,2], Katlijn Vints[2,6], Anke Vandekeere[4,5], Suresh Poovathingal[1], Matthew Bird[7], Ine Vlaeminck[1,8], Eline Creemers[1,8], Keimpe Wierda[1,8], Nikky Corthout[1,9], Pieter Vermeersch[10], Sébastien Carpentier[11], Kristofer Davie[1], Massimiliano Mazzone[12,13], Natalia V. Gounko[2,6], Stein Aerts[1,2], Bart Ghesquière[14], Sarah-Maria Fendt[4,5], Pierre Vanderhaeghen[1,2,3]*

Neuronal development in the human cerebral cortex is considerably prolonged compared with that of other mammals. We explored whether mitochondria influence the species-specific timing of cortical neuron maturation. By comparing human and mouse cortical neuronal maturation at high temporal and cell resolution, we found a slower mitochondria development in human cortical neurons compared with that in the mouse, together with lower mitochondria metabolic activity, particularly that of oxidative phosphorylation. Stimulation of mitochondria metabolism in human neurons resulted in accelerated development in vitro and in vivo, leading to maturation of cells weeks ahead of time, whereas its inhibition in mouse neurons led to decreased rates of maturation. Mitochondria are thus important regulators of the pace of neuronal development underlying human-specific brain neoteny.

Developmental processes display species-specific differences in timeline, or heterochrony, which can lead to divergence in size, cell composition, or organ function (*1*–*3*). Human brain development is characterized by a prolonged timing of maturation of cortical neurons compared with that of other species (*4*). Such neoteny may underlie the enhanced performance of the human brain (*5*). Human and nonhuman primate cortical neurons derived from pluripotent stem cells (PSCs) and xenotransplanted into the mouse brain develop along their species-specific timeline (*6*–*8*), pointing to cell-intrinsic developmental timing mechanisms. Metabolism and mitochondria are drivers of cell fate transitions (*9*–*12*) and maturation (*13*–*15*) in many systems, including the brain (*16*–*21*). Species differences in metabolism at the organism level are linked to developmental growth (*22*, *23*), but whether metabolism influences species-specific developmental tempo remains unclear.

[1]VIB-KU Leuven Center for Brain & Disease Research, 3000 Leuven, Belgium. [2]KU Leuven, Department of Neurosciences & Leuven Brain Institute, 3000 Leuven, Belgium. [3]Université Libre de Bruxelles (ULB), Institut de Recherches en Biologie Humaine et Moléculaire (IRIBHM), and ULB Neuroscience Institute (UNI), 1070 Brussels, Belgium. [4]Laboratory of Cellular Metabolism and Metabolic Regulation, VIB-KU Leuven Center for Cancer Biology, VIB, 3000 Leuven, Belgium. [5]Laboratory of Cellular Metabolism and Metabolic Regulation, Department of Oncology, KU Leuven and Leuven Cancer Institute (LKI), 3000 Leuven, Belgium. [6]VIB-KU Leuven Center for Brain & Disease Research, Electron Microscopy Platform & VIB-Bioimaging Core, 3000 Leuven, Belgium. [7]Clinical Department of Laboratory Medicine, University Hospitals Leuven, 3000 Leuven, Belgium. [8]Electrophysiology Unit, VIB-KU Leuven Center for Brain & Disease Research, 3000 Leuven, Belgium. [9]VIB Bio Imaging Core, 3000 Leuven, Belgium. [10]Department of Cardiovascular Sciences, KU Leuven, Leuven, Belgium, and Department of Laboratory Medicine, University Hospitals Leuven, 3000 Leuven, Belgium. [11]SYBIOMA, KU Leuven Center for SYstems BIOlogy based MAss spectrometry, 3000 Leuven, Belgium. [12]Laboratory of Tumor Inflammation and Angiogenesis, Center for Cancer Biology, VIB, 3000 Leuven, Belgium. [13]Laboratory of Tumor Inflammation and Angiogenesis, Center for Cancer Biology, Department of Oncology, KU Leuven, 3000 Leuven, Belgium. [14]Metabolomics Expertise Center, Center for Cancer Biology, VIB, KU Leuven, 3000 Leuven, Belgium.
*Corresponding author. Email: pierre.vanderhaeghen@kuleuven.be
†These authors contributed equally to this work.

Mitochondria development during cortical neuronal maturation follows a species-specific timeline

To test whether metabolism influences the species-specific timing of neuronal development, we used in vitro cultures of cortical pyramidal neurons derived from PSCs (human and mouse) or from embryonic brain (mouse), which recapitulate species-specific timelines of corticogenesis (*6*, *24*) (fig. S1A). Given that neurogenesis is not synchronous, it is challenging to study neuronal maturation because populations of neurons born at different time points coexist at the same stage of brain development. To study neuronal development with optimal temporal resolution, we developed a neuronal birth-dating system called neuroD1-dependent newborn neuron (NNN) labeling. NNN combines the expression of tamoxifen-inducible $CreER^{T2}$ (Cre recombinase fused to a mutant estrogen receptor ligand-binding domain) under the control of the promoter of *Neuronal Differentiation 1* (*NeuroD1*), together with the Cre-dependent reporters enhanced green fluorescent protein (eGFP) and truncated CD8, enabling the identification or purification of the labeled cells (Fig. 1A and fig. S1B). Because the *NeuroD1* promoter is turned on transiently at the time of neuron generation, a pulse of 4-hydroxy-tamoxifen (4-OHT) allowed the selective labeling of a cohort of neurons born at precise time points, as assessed by 5-ethynyl-2′-deoxyuridine nuclear labeling (fig. S1, C to E), which revealed a timely progression in growth and complexity (Fig. 1B). To maximize the number of neuronal cells born at similar time points, the cultures were treated simultaneously with the gamma-secretase inhibitor *N*-[*N*-(3,5-difluorophenacetyl)-L-alanyl]-*S*-phenylglycine t-butyl ester (DAPT), which inhibits Notch signaling and thereby increases cortical neurogenesis, and cells were purified by $CD8^+$ magnetic-activated cell sorting (MACS) purification. The purified NNN-labeled neurons thus displayed homogeneous maturation patterns and identity (Fig. 1C and fig. S1, F and G).

To examine mitochondrial dynamics during cortical neuron development, we combined NNN labeling with mitochondria tagging with emerald-green fluorescent protein fused to mitochondrial targeting sequence of cytochrome c oxidase subunit 8A (COX8A) (Fig. 1, D to F). We observed that mitochondria were initially small and sparse in newly born mouse neurons (*20*) and gradually grew in size and quantity over 3 weeks during neuronal maturation, and the same was observed in mouse PSC–derived cortical neurons (Fig. 1, D and F, and fig. S2). However a similar examination of PSC-derived human cortical neurons revealed a more prolonged timeline of mitochondria development, spanning several months (Fig. 1, E and F). We monitored mitochondria dynamics in developing cortical neurons in vivo. We labeled mouse cortical neurons with eGFP by in utero electroporation at embryonic day 14.5 (E14.5), followed by a time course of correlative light and electron microscopy (CLEM) analysis (Fig. 1G and fig. S3A). This confirmed that mitochondria gradually reach maximal levels of growth and size in 3 weeks in mouse cortical neurons in vivo (Fig. 1F). We also xenotransplanted DAPT-treated PSC-derived human cortical neurons transduced with eGFP. In this system, xenotransplanted neurons display a months-long protracted pattern of maturation (*7*). CLEM performed on such neurons revealed slower mitochondria growth than in their mouse counterparts, taking months to reach similar mitochondrial development (Fig. 1H and fig. S3B). We used transmission electron microscopy to visualize mitochondria ultrastructure in greater detail. In newborn neurons, mitochondria were mostly devoid of cristae, whereas there were more, better defined cristae as neurons matured, following a species-specific timeline that was more protracted in human neurons (fig. S3, C and D). Thus, mitochondria morphological development

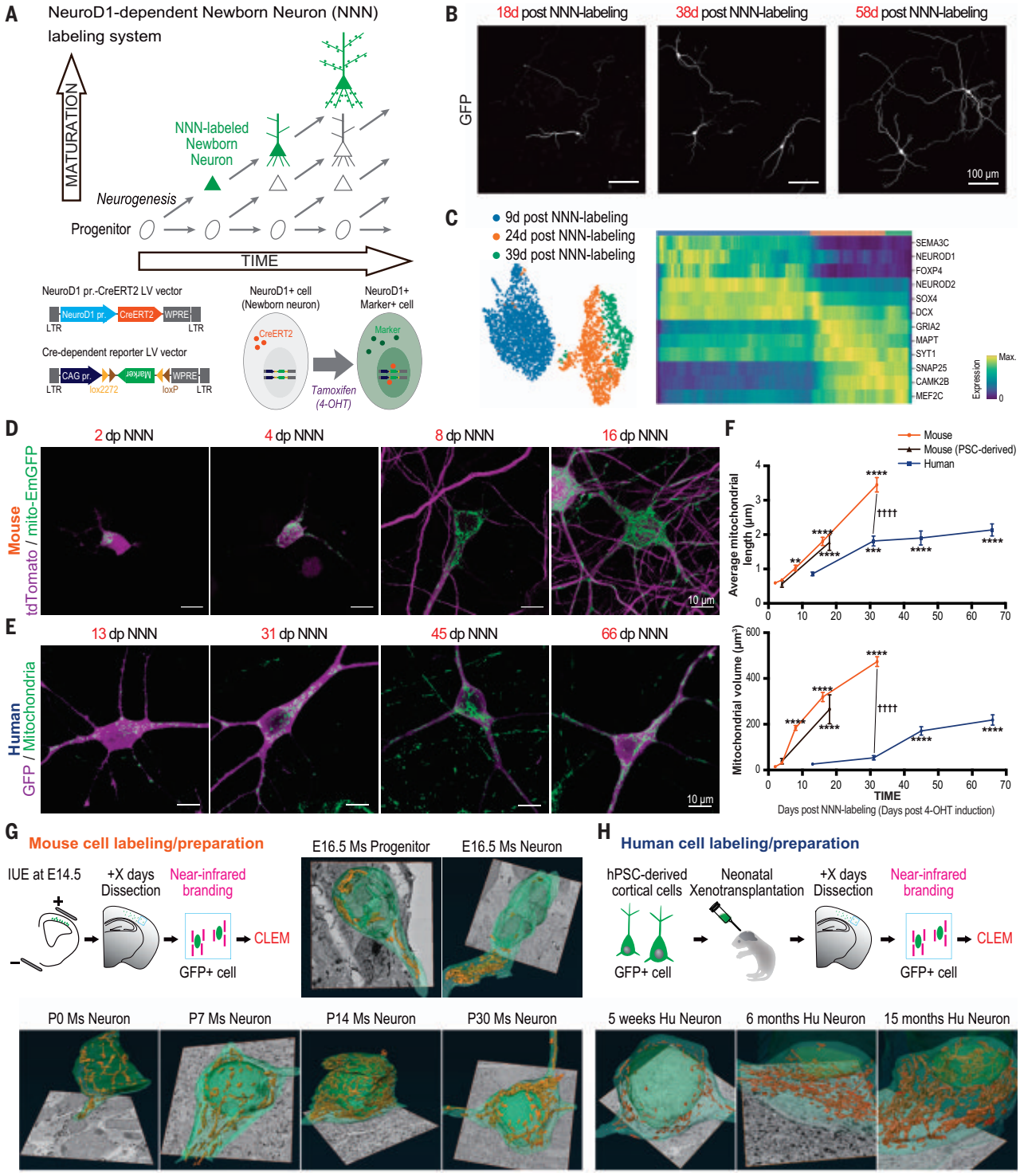

Fig. 1. Interspecies differences in mitochondria biogenesis and dynamics during neuronal development. (**A**) Schematic of the NNN-labeling system. (**B**) Representative images after NNN labeling in human PSC-derived cortical neurons. (**C**) Left: Uniform manifold approximation and projection (UMAP) of MACS-purified NNN-labeled cells. Right: Heatmap of gene expression after pseudotime analysis. (**D** and **E**) Representative images of mitochondrial morphology in NNN-labeled mouse (D) and human (E) neurons. (**F**) Quantification of mitochondrial length (top) and mitochondria volume (bottom) per cell. Mouse: 2, 4, 8, 16, and 32 days post (dp) NNN labeling: length: n = 10, 11, 10, 10, and 5 cells, respectively; volume: n = 6, 8, 10, 9, and 5, respectively. PSC-derived mouse: 4 and 18 dp NNN labeling: length: n = 9 and 9, respectively; volume: n = 9 and 9, respectively. Human: 13, 31, 45, and 66 dp NNN labeling: length: n = 20, 15, 17, and 18, respectively; volume: n = 9, 11, 22, and 20, respectively. (**G** and **H**) Schematic of mouse (Ms) or human (Hu) cortical neuron birth-dating followed by CLEM, and representative images. E, embryonic day; P, postnatal day. Yellow indicates mitochondria. Bottom images are 20 × 20 µm. (F) Data are shown as mean ± SEM. Dunnett's multiple-comparisons test or unpaired t test were used to compare with first time point. Unpaired t test or Mann-Whitney test was used to compare mouse and human. $^{**}P < 0.01$, $^{***}P < 0.001$, $^{****}P < 0.0001$, and ††††$P < 0.0001$.

follows a species-specific timeline that is highly correlated with neuronal maturation.

Mitochondria metabolic activity is lower in human than in mouse developing neurons

We examined the functional properties of mitochondria during neuronal development, focusing on mitochondrial oxidative phosphorylation (OXPHOS) and electron transport chain (ETC) capacity (Fig. 2, A to C). We measured the mitochondrial oxygen consumption rate (OCR) using oxygraphy (*25*) on highly enriched preparations (>95% neurons) of mouse and human cortical neurons at similar time points after birth (fig. S4, A and B). From early stages, mitochondrial OCR was higher in mouse than in human neurons, and also increased more rapidly, which is consistent with their morphological development (Fig. 2, A to C, and fig. S4, C to E). As a result, stimulated OCR was >10 times higher in mouse than in human counterparts after 2 weeks of differentiation (Fig. 2, B and C, and fig. S4). The increased mitochondria ETC activity during mouse neuronal development was confirmed by mitochondria membrane potential measurement using tetramethylrhodamine methyl ester (fig. S5).

We next examined glucose metabolism using mass spectrometry–based ^{13}C tracer analysis (*26*) of enriched preparations of human and mouse developing cortical neurons at similar ages (19 days after neuronal birth) (Fig. 2, D to F, and fig. S6A). Although this led to similar labeling of glycolytic metabolites in the two species, it revealed a higher enrichment of lactate from $^{13}C_6$-glucose and a higher secretion of lactate in human than in mouse neurons (Fig. 2, D to F, and figs. S6 and S7).

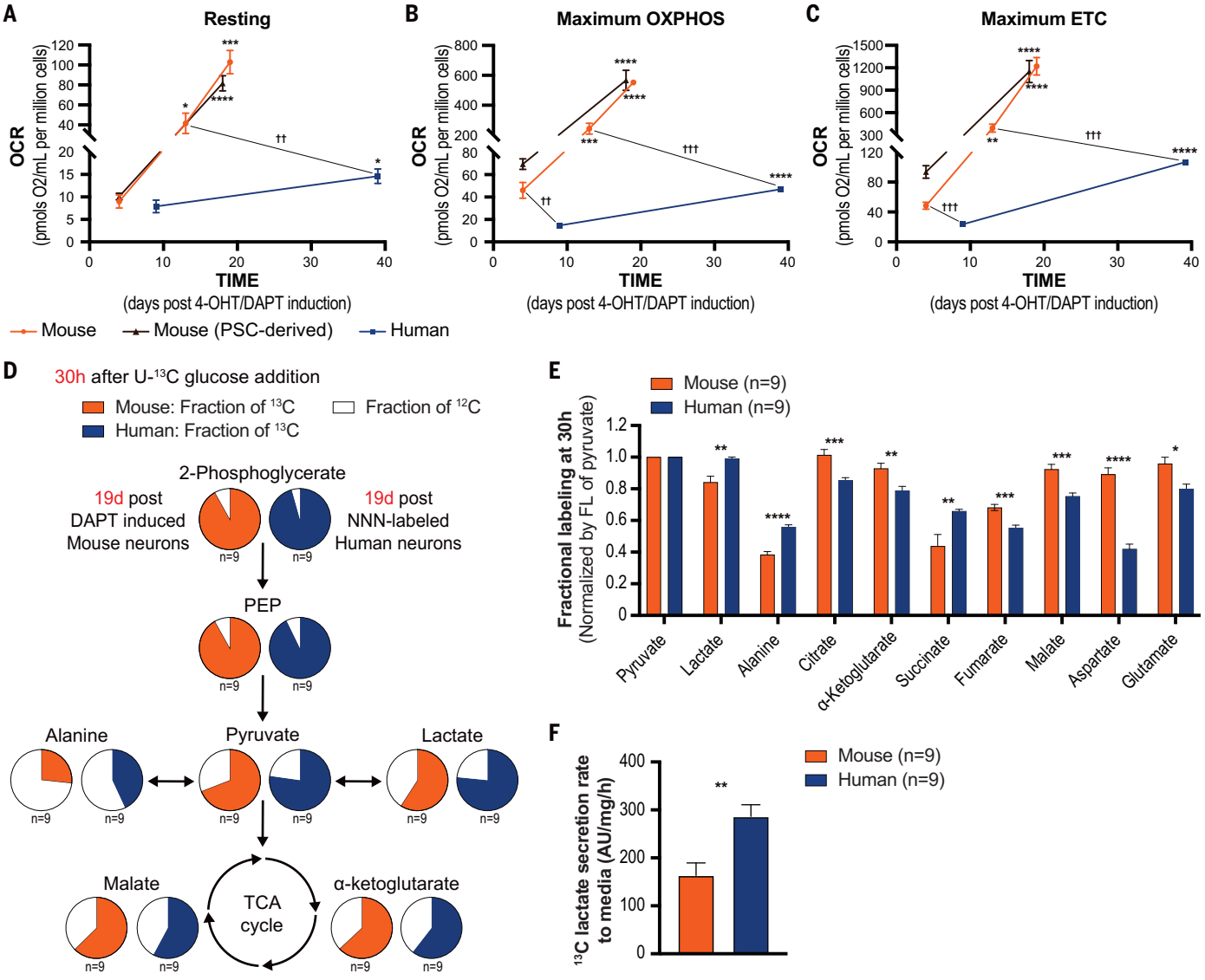

Fig. 2. Interspecies differences in mitochondria metabolism during neuronal development. (**A** to **C**) Quantification of OCR during neuronal development from at least two biological replicates. (A) Resting OCR. (B) Maximum OXPHOS capacity under coupled condition. (C) Maximum ETC capacity under uncoupled condition. Mouse: 4, 13, and 19 dp DAPT induction: n = 6, 8, and 4, respectively. PSC-derived mouse: 4 and 18 dp DAPT induction: n = 14 and 16, respectively. Human: 9 and 37 to 41 dp NNN labeling, n = 6 and 7, respectively. (**D**) ^{13}C enrichment patterns of the metabolites in mouse (orange) and human (blue). PEP, phosphoenolpyruvate. (**E**) Fractional labeling of metabolites normalized by the labeled fraction of pyruvate at 30 hours after tracer addition. (**F**) ^{13}C-labeled lactate secretion rate. AU, arbitrary units. All data are shown as mean ± SEM. For (A) to (C), Dunnett's or Dunn's multiple-comparisons test (mouse) and unpaired t test or Mann-Whitney test (PSC mouse and human) were used to compare with first time point. For (E) and (F), unpaired t test or Mann-Whitney test was used to compare mouse and human. *P < 0.05, **P < 0.01 or ††P < 0.01, ***P < 0.001 or †††P < 0.001, and ****P < 0.0001.

Conversely, the labeling of tricarboxylic acid (TCA) cycle metabolites was comparatively lower in human than in mouse neurons, indicating lower mitochondria metabolic activity (Fig. 2E). Whole-cell oxidized nicotinamide adenine dinucleotide (NAD^+) and reduced NAD (NADH) measurements revealed that the amounts of NAD^+ and NADH were both higher in human neurons, whereas the NAD^+/NADH ratio was similar in both species (fig. S6H). This may suggest a difference in NAD recovery and synthesis between the two species. We also found a higher ratio of reduced glutathione to oxidized glutathione in human neurons (fig. S6D), indicating a lower oxidative stress in human cells consistent with a lower activity of the mitochondrial ETC (Fig. 2C). Adenosine triphosphate (ATP) and adenosine diphosphate (ADP) levels and ATP/ADP ratios were higher in human than in mouse neurons, whereas their fractional labeling from glucose was lower (fig. S6, E and F), suggesting more de novo biosynthesis in mouse neurons.

These data indicate that human developing cortical neurons have lower mitochondria-driven TCA cycle and oxidative activity than do their mouse counterparts at a similar age.

Oxygraphy data point to temporal differences in mitochondrial metabolism during neuronal maturation. To gain insights into what might cause such differences and their in vivo relevance, we examined our single-cell RNA-sequencing data from in vitro birth-dated human neurons with those from human and mouse fetal cortex in vivo (*27*, *28*) (Fig. 3 and figs. S8 to S11). The in vitro and in vivo patterns of expression of mitochondrial or metabolic genes were similar and correlated (Fig. 3, E and F), providing in vivo validation of our in vitro observations. Human and mouse cells had similar temporal patterning of mitochondrial and metabolic genes, with an overall increase in genes related to oxidative phosphorylation and a decrease in genes related to glycolysis, which occurred earlier in mouse than in human neurons (Fig. 3, F and J, and data S2).

Increasing mitochondria activity in human neurons leads to accelerated neuronal maturation

We tested whether the species differences observed in mitochondria metabolic functions could set the speed of neuronal maturation. Glucose tracer experiments revealed an interspecies difference in the conversion of pyruvate to lactate (Fig. 2, D to F), which is catalyzed by lactate dehydrogenase (LDH). LDH is composed of A and B subunits, both of which were expressed in both mouse and human cortical neurons, with higher amounts in human than in mouse (fig. S12).

LDHA favors the conversion of pyruvate to lactate, and LDHB favors the conversion of lactate to pyruvate (*29*) (Fig. 4A). To enhance mitochondria activity in developing neurons, we therefore targeted LDHA. Treatment with a chemical inhibitor of LDHA, GSK-2837808A (hereafter referred to as GSK) (*30*), resulted in increased mitochondria OCR in human neurons (Fig. 4B and fig. S13), consistent with earlier reports (*31*). Similarly, exposure of cells to free fatty acids (AlbuMAX), a fuel in addition to glucose for mitochondrial TCA cycle activity, led to increased OCR, as did its combination with GSK (referred to as AlbuMAX-GSK) (Fig. 4B and fig. S13). These treatments, alone or in combination, led to increased OCR, but not to the level found in mouse neurons (compare Fig. 2, A to C, with Fig. 4B), even with higher concentrations of GSK (fig. S14).

We examined the impact of AlbuMAX-GSK treatment on mitochondria morphology and protein composition. Morphology analyses did not reveal significant effects on mitochondria length and volume (fig. S16, F to H). Western blot analyses did not reveal changes in most tested mitochondria proteins, but some key components were increased in abundance after the treatment, specifically COXII, a component of complex IV (fig. S17). The effects of AlbuMAX-GSK treatments on OCR could still be detected at similar levels of magnitude 1 to 5 days after stopping the treatment (fig. S15). Thus, there appears to be selective molecular and metabolic effects of LDH inhibition leading to increased OXPHOS, rather than global effects on mitochondria biogenesis or dynamics. This could contribute to the observed limits of the effects obtained after manipulations of mitochondria function in human neurons, which never reached the levels found in mouse neurons. None of the treatments enhancing mitochondria appeared to cause changes in neuronal identity or survival, because the amounts of apoptosis remained low and identity marker expression was unchanged after AlbuMAX-GSK treatments (figs. S13G and S16, A to E).

We tested the impact of these treatments on neuronal developmental rates. To determine the speed of maturation, we assessed neuronal excitability by measuring the response of neurons to membrane depolarization induced by the addition of KCl using as a readout the expression of the activity-dependent immediate-early gene *Neuronal PAS Domain Protein 4* (*NPAS4*) (*32*). Few NNN-labeled human cortical neurons responded to KCl shortly after their birth (9 to 24 days), but most of them became responsive weeks later (39 days) (Fig. 4C and fig. S13E). We then examined the impact of LDHA inhibitors on human cortical neuron maturation by treating the cells from day 9 to 23, when the neurons were still poorly responsive to KCl (Fig. 4D and fig. S13F). LDHA inhibitor treatment was stopped for 1 to 5 days before assessing maturation to distinguish the effects on neuronal development from an acute impact on mitochondria function (Fig. 4, D and E, and fig. S15). Few untreated neurons responded to KCl treatment, but inhibition of LDHA increased the proportion of neurons displaying NPAS4 responses (Fig. 4D), indicating acceleration of neuronal maturation in response to increased mitochondrial respiration (Fig. 4B). Increased neuronal maturation was also observed with other treatments that enhance mitochondrial metabolism, including AlbuMAX and PS10, a pyruvate dehydrogenase (PDH) kinase (PDK1-4) inhibitor (*33*) that increases the conversion of pyruvate into acetyl-CoA. The effects of AlbuMAX and GSK were additive (Fig. 4, D and E), further linking mitochondrial metabolic activity to the speed of neuronal maturation. These experiments were performed on human cortical neurons cultured on mouse astrocytes, but a similar acceleration was observed after the same treatment on pure neuronal populations (figs. S13, H to J, S14, C to E, and S15, C to E).

Increased mitochondrial activity appears to lead to accelerated neuronal differentiation. We tested this further by performing patch-clamp recordings of human cortical neurons after AlbuMAX-GSK treatment. This resulted in an increased frequency and amplitude of synaptic currents (Fig. 4, H and I), together with a decrease of membrane potential (fig. S18), consistent with a global increase in the functional maturation of the treated neurons. We also found an increased number of puncta containing the presynaptic marker synapsin I on dendrites of treated neurons (Fig. 4, F and G). The density of synapsin I puncta in 24-day-old treated human neurons was still lower than that in 13-day-old mouse neurons (fig. S16, J and K).

We examined the consequences of AlbuMAX-GSK treatment on neuronal morphogenesis, a crucial parameter of neuronal maturation. AlbuMAX-GSK–treated human cortical neurons had larger neuronal size and increased dendritic length and complexity (Fig. 5, A and B). The morphology of 24-day-old AlbuMAX-GSK–treated neurons reached the same maturation level as for 58-day-old control neurons (Figs. 1B and 5A), indicating that enhanced mitochondrial metabolism could accelerate neuronal morphological development several weeks ahead of time.

To explore the relevance of these observations across species, we tested the influence of mitochondria activity on rates of mouse neuron maturation. Treatment of mouse neurons with AlbuMAX-GSK resulted in increased dendritic growth, although to a lesser extent than in human neurons (Fig. 5, C and D). Reduction of mitochondria activity using either 2-cyano-3-(1-phenyl-1H-indol-e-yl)-2-peopenoic acid (UK-5099) as a mitochondrial pyruvate carrier inhibitor or rotenone as an ETC complex I

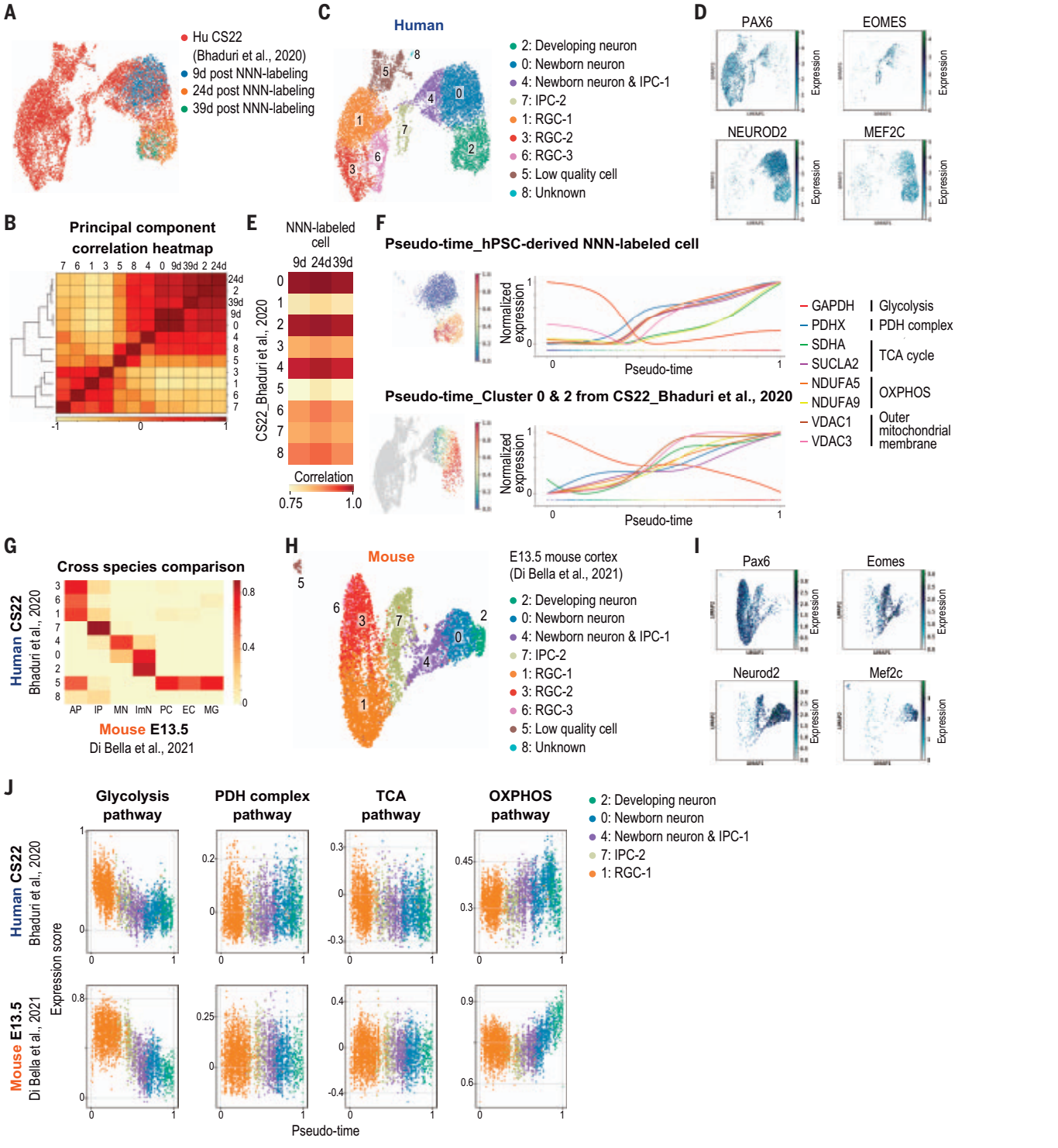

Fig. 3. Temporal pattern of expression of metabolic genes during neuronal development. (**A** to **C**) UMAP of NNN-labeled human cortical neurons and human cortical cells from Carnegie stage (CS) 22 (*27*). (B) Principal component correlation heatmap. (C) Unsupervised Leiden clustering and classification of cells after integration with Harmony algorithm. (**D**) Normalized expressions of PAX6, EOMES, NEUROD2, and MEF2C are shown as radial glial cells (RGCs), intermediate progenitor cells (IPCs), excitatory neurons, and developing neuron markers, respectively. (**E**) Heatmap of Pearson correlation coefficients per time point of the mean scores of metabolic pathways (glycolysis, PDH complex, TCA, and OXPHOS; table S1). (**F**) Expression trends of representative metabolic pathway genes plotted along the pseudotime axis for NNN-labeled neurons (top) and CS22 neurons (bottom) from cluster 0 and 2. (**G**) Heatmap of cell type alignment scores representing the cross-species comparison of E13.5 mouse and CS22 human using SAMap. (**H**) UMAP of mouse cortical cells showing transferred annotations from merged human cells to the mouse dataset. (**I**) Normalized expressions of Pax6, Eomes, Neurod2, and Mef2c. (**J**) Temporal pattern of metabolic pathway score in CS22 human (top) and E13.5 mouse (bottom).

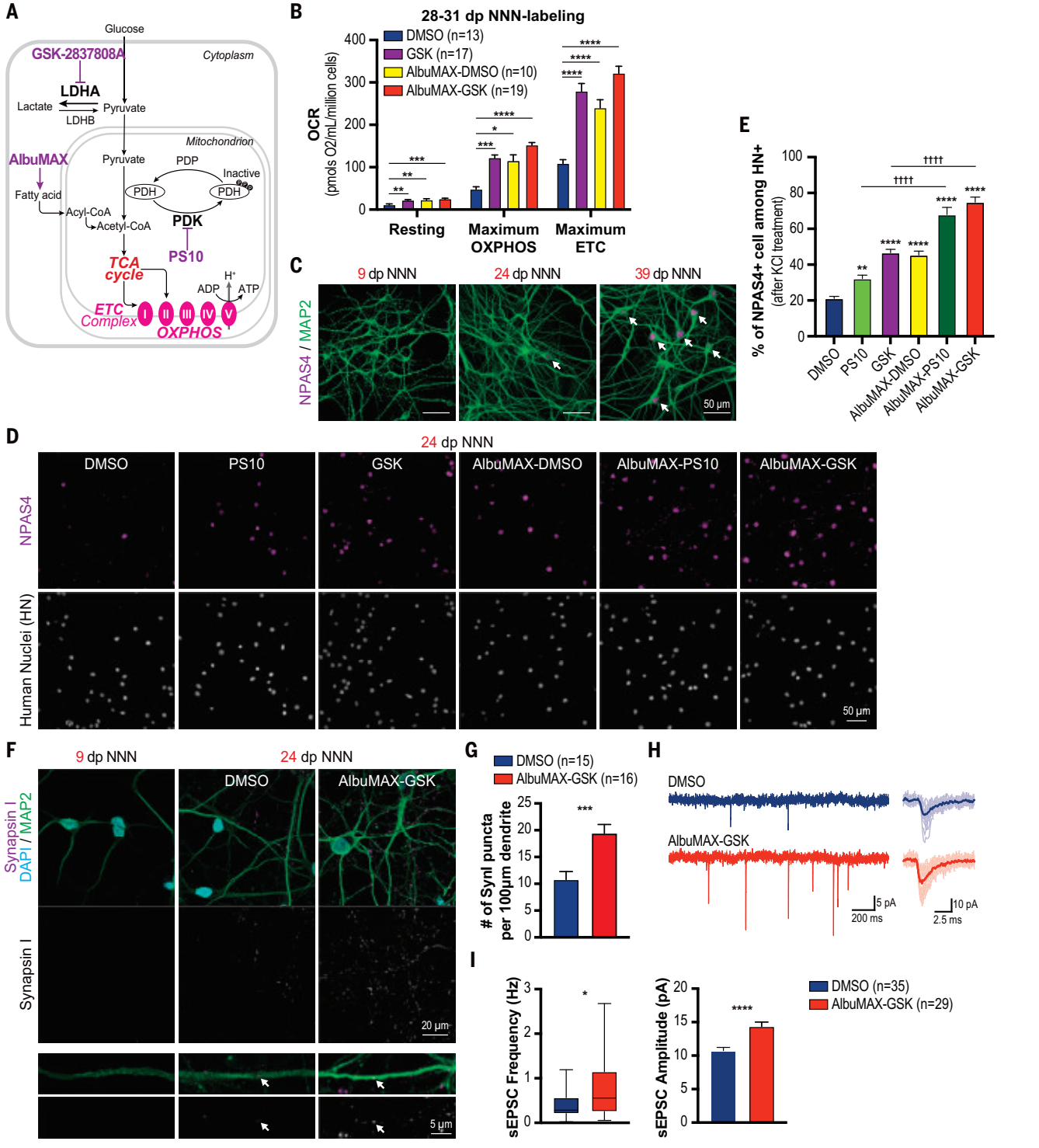

Fig. 4. Increasing mitochondria metabolism accelerates human neuronal maturation. (**A**) Schematic of metabolic pathways targeted by indicated chemical compounds. PDK/*P*, pyruvate dehydrogenase kinase/phosphatase. (**B**) Quantified OCR from 28 to 31 dp NNN-labeled human neurons after treatment with the indicated chemical compounds. (**C**) Representative images of KCl-induced NPAS4 expression in NNN-labeled human neurons over time. Arrow indicates NPAS4+ neurons. (**D** and **E**) Representative images (D) and quantification (E) of NPAS4+ neurons induced by KCl after treatment with the indicated chemical compounds from three independent biological replicates. Dimethylsulfoxide (DMSO): $n = 20$ regions of interest, PS10: $n = 20$, GSK: $n = 15$, AlbuMAX-DMSO: $n = 15$, AlbuMAX-PS10: $n = 10$, and AlbuMAX-GSK: $n = 20$. (**F** and **G**) Representative images (F) and quantification (G) of synapsin I puncta on dendrites from three independent biological replicates. (**H**) Trace of spontaneous excitatory postsynaptic current (sEPSC). (**I**) Quantification of sEPSC frequency (left) and amplitude (right). All data are shown as mean ± SEM as determined by Dunnett's or Dunn's multiple-comparisons test (B); Tukey's multiple-comparisons test (E); unpaired *t* test (G); or unpaired *t* test or Mann-Whitney test (I). $^{*}P < 0.05$, $^{**}P < 0.01$, $^{***}P < 0.001$, $^{****}P < 0.0001$, and ††††$P < 0.0001$.

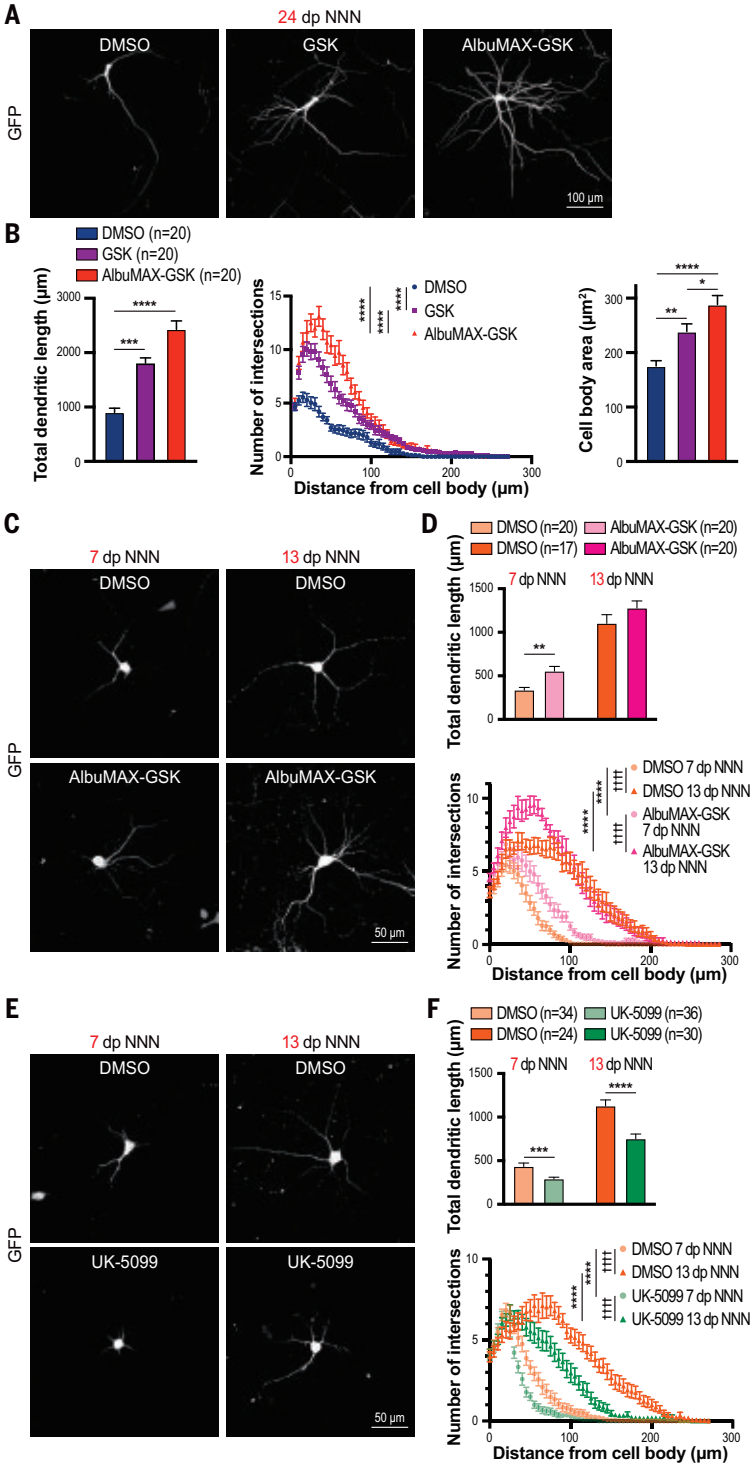

Fig. 5. Functional coupling between mitochondria metabolism and neuronal development across species. (**A** and **B**) Representative images (A) and quantification (B) of NNN-labeled human neurons after the indicated treatments. Left: total dendritic length. Middle: Sholl analysis of dendritic branching. Right: cell body area. (**C** and **E**) Representative images of 7 and 13 dp NNN-labeled mouse neurons after treatment with the indicated chemical compounds. (**D** and **F**) Quantification of total dendritic length (top) and Sholl analysis of dendritic branching (bottom) from three biological replicates. For (A) to (F), data are shown as mean ± SEM by unpaired *t* test, Mann-Whitney test, or Dunn's multiple-comparisons test for dendritic length. Two-way ANOVA test was used for Sholl analysis. Tukey's multiple-comparisons test was used for cell body area. **P* < 0.05, ***P* < 0.01, ****P* < 0.001, *****P* < 0.0001, ††††*P* < 0.0001.

inhibitor resulted in decreased dendritic growth, consistent with slower developmental rates (Fig. 5, E and F, and fig. S19).

We tested whether similar effects could be observed in vivo using xenotransplantation of human cortical neurons in the mouse neonatal cortex (*6*–*8*). We performed genetic manipulation of human neuron metabolism by lentiviral overexpression of LDHB or eGFP as a control. LDHB overexpression led to increased neuronal mitochondria OCR in vitro, as expected (Fig. 6A and fig. S20). We xenotransplanted the transduced neurons, which revealed an increased dendritic length and complexity 4 weeks after transplantation (Fig. 6, B to D), corresponding to a pattern found at 2 to 3 months in control conditions (*7*). Functionality was not tested, but these data indicate that increasing mitochondria metabolic activity results in the acceleration of morphological differentiation of human neurons in vivo.

Discussion

We found that mitochondrial metabolic activity sets the species-specific tempo of development of cortical neurons. Enhanced mitochondria metabolism leads to global acceleration of morphological and functional neuron maturation, but it remains to be determined how much it leads to transcriptional, epigenetic, and proteomic changes in developing neurons. AlbuMAX-GSK–treated neurons were still less mature than mouse counterparts at the same age, indicating that other mechanisms contribute to species differences in neuronal developmental timing, including human-specific genes (*34*), RNA or protein turnover (*35*, *36*), and chromatin remodeling (*37*, *38*).

Our transcriptomic analyses suggest that at least part of the temporal differences in mitochondria maturation originate from patterns of mitochondria gene-regulatory mechanisms, but the observed species differences in mitochondria function likely also involve posttranslational mechanisms such as modifications of mitochondrial dynamics and assembly of the ETC (*39*, *40*).

Differences in species-specific metabolic properties of cortical neurons may influence human brain neoteny, which is consistent with previous reports of years-long periods of aerobic glycolysis in the developing human cortex (*41*). Aerobic glycolysis has long been thought to constitute a hallmark of cellular proliferation, as during oncogenesis (*42*). Here, we found that mitochondrial OXPHOS activity influences the speed of postmitotic neuron morphological and functional development and displays species differences. However, alterations in the TCA cycle or other, yet to be explored metabolic pathways may also contribute to determine the timing of neuronal development.

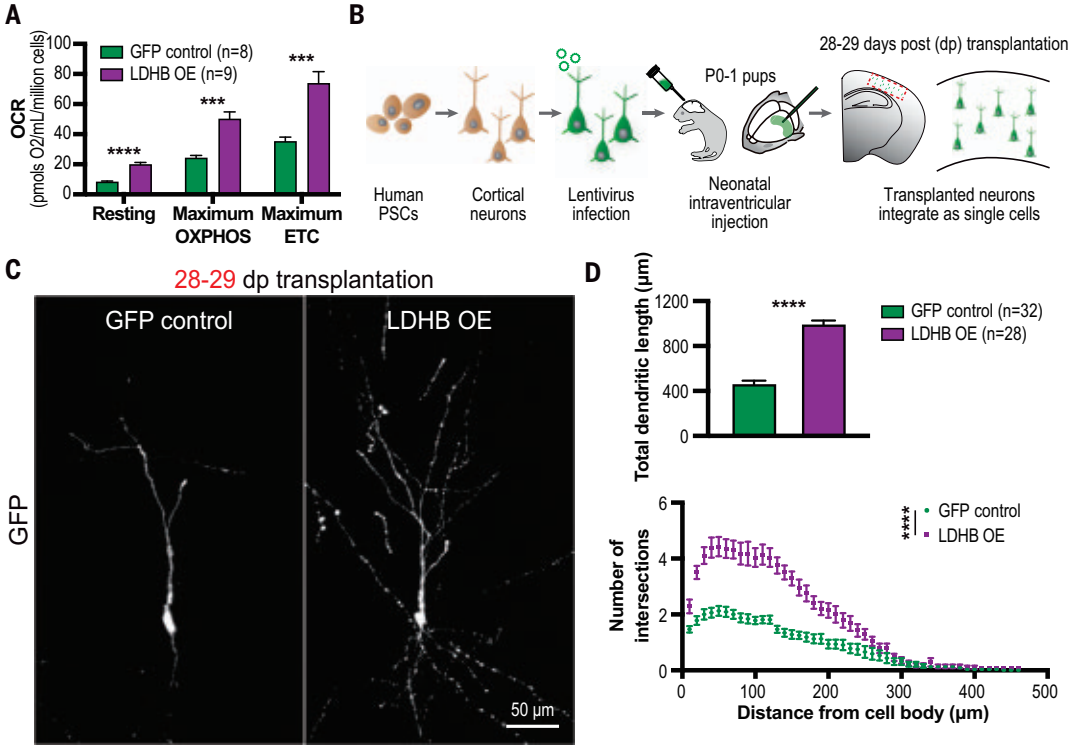

Fig. 6. In vivo maturation of human cortical neurons is enhanced by increased mitochondria function. (**A**) Quantified OCR from three biological replicate experiments. (**B** and **C**) Experimental scheme (B) and representative images (C) of human neurons in mouse cortex at 28 to 29 dp transplantation. (**D**) Quantification of total dendritic length (top) and Sholl analysis of dendritic branching (bottom). All data are shown as mean ± SEM by unpaired *t* test (A). (D) Unpaired *t* test was used for dendritic length. Two-way ANOVA test was used for Sholl analysis. ***$P < 0.001$, ****$P < 0.0001$.

The temporal patterning of mitochondria development is likely an important contributor to the observed species differences in metabolic activity. However, the differences observed in mitochondria function at early stages of neuronal development also suggest that mitochondria from different species may display quantitative or qualitative differences independently of their developmental patterns. This will be important to resolve, because mitochondria and metabolism could contribute to developmental timing in other contexts, from the speed of the somitic clock (*43*) to the maturation of cardiac and pancreas cells (*13*–*15*).

Accelerated human neuronal maturation in vitro might benefit PSC-based modeling of neural diseases, which remains greatly hindered by the slowness of human neuron development. Conversely, human neuronal prolonged development has been long proposed to have a positive role in acquiring human-specific cognitive features (*5*). Tools to accelerate or decelerate neuronal development could allow testing of the impact of neuronal neoteny on brain function, plasticity, and disease.

Materials and methods summary

Detailed information on all materials and methods performed are provided in the supplementary materials.

NeuroD1-dependent NN labeling and purification

Human cortical cell culture was performed as described previously (*20*). Dissociated cells were transduced with the following lentiviruses: LV-NeuroD1 promoter-CreERT2-WPRE and LV-CAG-DIO-Reporter (EGFP and/or truncated CD8)-WPRE. For Cre-dependent recombination, 4-OHT (final concentration: 0.25 µM) was added to the medium for 48 hours. For purification of newborn neurons, cortical cells were dissociated using the NeuroCult Enzymatic Dissociation Kit (STEMCELL Technologies) 48 hours after withdrawal of 4-OHT. The dissociated cells were incubated with magnetic bead–conjugated antihuman CD8 (Miltenyi Biotec) in MACS buffer (Miltenyi Biotec). $CD8^+$ selection was performed with LS columns (Miltenyi Biotec). The sorted cells were plated on mouse astrocyte–coated or poly-L-ornithine-/laminin–coated plates.

Oxygraphy

Cells were dissociated using the NeuroCult Enzymatic Dissociation Kit and resuspended in MiR05 buffer (Oroboros Ecosystem). The cell suspension was injected in a chamber of oxygraphy O2K with subsequent injections of the following chemical compounds to final concentrations as follows (all from Merck except for ADP, which was from Calbiochem): 556 U/ml catalase, 10 µg/ml digitonin, 5 mM pyruvate, 0.5 mM malate, 1 mM ADP, 10 mM glutamate, 10 mM succinate, carbonyl cyanide *m*-chlorophenyl hydrazone (CCCP) Δ1 µM until maximum respiration reached, 75 nM rotenone, 10 mM glycerophosphate, 250 nM antimycin A, 2 mM sodium ascorbate, 0.5 mM N,N,N′,N′-tetramethyl-p-phenylenediamine dihydrochloride, 10 µM cytochrome C, and 200 mM sodium azide. The reported values of maximum OXPHOS (phosphorylating) and ETC (nonphosphorylating) were calculated as succinate minus antimycin A (nonmitochondrial respiration) and CCCP minus antimycin A, respectively (*25*).

Metabolic labeling

One day before the glucose-tracing experiment, the medium was exchanged with Neurobasal/B27 (2.5 mM glucose). After one day, the medium was switched to Neurobasal/B27 (2.5 mM U-^{13}C glucose; Cambridge Isotope Laboratories). After 30 hours of incubation, medium and plates were snap-frozen in liquid nitrogen.

Metabolic modulation by chemical compounds

On the first day of the experiment, the culture medium was removed and replaced by Neurobasal/B27 (2.5 mM glucose) with the indicated chemical compounds: GSK-2837808A (1 to 10 µM; MedChemExpress), PS10 (5 µM; MedChemExpress), AlbuMAX (0.5% w/v; Thermo Fisher Scientific), UK-5099 (2.5 µM; Sigma-Aldrich), and rotenone (21 nM; Sigma-Aldrich). Eighty percent of the culture medium was exchanged with fresh medium and compounds every other day.

Xenotransplantation

Human neuron xenotransplantation was performed as described previously (*7*). On the day of xenotransplantation, cortical cells were dissociated using the NeuroCult Enzymatic Dissociation Kit and resuspended in a solution containing 20 mM EGTA (Merck) and

0.1% Fast Green (Merck) in phosphate-buffered saline at 100,000 to 200,000 cells/μl. Approximately 1 to 2 μl of cell suspension was injected into the lateral ventricles of each hemisphere of postnatal day 0 or 1 mouse brains. At the indicated time points, the mice were sacrificed and perfused with the proper fixative.

REFERENCES AND NOTES

1. M. Ebisuya, J. Briscoe, What does time mean in development? *Development* **145**, dev164368 (2018). doi: 10.1242/dev.164368; pmid: 29945985
2. R. Iwata, Temporal differences of neurodevelopment processes between species. *Neurosci. Res.* **177**, 8–15 (2022). doi: 10.1016/j.neures.2021.08.004; pmid: 34419562
3. R. Iwata, P. Vanderhaeghen, Tempus fugit: How time flies during development. *Science* **369**, 1431–1432 (2020). doi: 10.1126/science.abe0953; pmid: 32943512
4. B. Libé-Philippot, P. Vanderhaeghen, Cellular and molecular mechanisms linking human cortical development and evolution. *Annu. Rev. Genet.* **55**, 555–581 (2021). doi: 10.1146/annurev-genet-071719-020705; pmid: 34535062
5. C. C. Sherwood, A. Gomez-Robles, Brain plasticity and human evolution. *Annu. Rev. Anthropol.* **46**, 399–419 (2017). doi: 10.1146/annurev-anthro-102215-100009
6. I. Espuny-Camacho *et al*., Pyramidal neurons derived from human pluripotent stem cells integrate efficiently into mouse brain circuits in vivo. *Neuron* **77**, 440–456 (2013). doi: 10.1016/j.neuron.2012.12.011; pmid: 23395372
7. D. Linaro *et al*., Xenotransplanted human cortical neurons reveal species-specific development and functional integration into mouse visual circuits. *Neuron* **104**, 972–986.e6 (2019). doi: 10.1016/j.neuron.2019.10.002; pmid: 31761708
8. M. C. Marchetto *et al*., Species-specific maturation profiles of human, chimpanzee and bonobo neural cells. *eLife* **8**, e37527 (2019). doi: 10.7554/eLife.37527; pmid: 30730291
9. M. Knobloch, S. Jessberger, Metabolism and neurogenesis. *Curr. Opin. Neurobiol.* **42**, 45–52 (2017). doi: 10.1016/j.conb.2016.11.006; pmid: 27915086
10. N. Shyh-Chang, G. Q. Daley, L. C. Cantley, Stem cell metabolism in tissue development and aging. *Development* **140**, 2535–2547 (2013). doi: 10.1242/dev.091777; pmid: 23715547
11. L. Pernas, L. Scorrano, Mito-morphosis: Mitochondrial fusion, fission, and cristae remodeling as key mediators of cellular function. *Annu. Rev. Physiol.* **78**, 505–531 (2016). doi: 10.1146/annurev-physiol-021115-105011; pmid: 26667075
12. O. A. Tarazona, O. Pourquié, Exploring the influence of cell metabolism on cell fate through protein post-translational modifications. *Dev. Cell* **54**, 282–292 (2020). doi: 10.1016/j.devcel.2020.06.035; pmid: 32693060
13. X. Yang *et al*., Fatty acids enhance the maturation of cardiomyocytes derived from human pluripotent stem cells. *Stem Cell Reports* **13**, 657–668 (2019). doi: 10.1016/j.stemcr.2019.08.013; pmid: 31564645
14. D. Hu *et al*., Metabolic maturation of human pluripotent stem cellderived cardiomyocytes by inhibition of HIF1α and LDHA. *Circ. Res.* **123**, 1066–1079 (2018). doi: 10.1161/CIRCRESAHA.118.313249; pmid: 30355156
15. E. Yoshihara *et al*., ERRγ is required for the metabolic maturation of therapeutically functional glucose-responsive β cells. *Cell Metab.* **23**, 622–634 (2016). doi: 10.1016/j.cmet.2016.03.005; pmid: 27076077
16. Z. Li, K. Okamoto, Y. Hayashi, M. Sheng, The importance of dendritic mitochondria in the morphogenesis and plasticity of spines and synapses. *Cell* **119**, 873–887 (2004). doi: 10.1016/j.cell.2004.11.003; pmid: 15607982
17. P. Licznerski *et al*., ATP synthase c-subunit leak causes aberrant cellular metabolism in fragile X syndrome. *Cell* **182**, 1170–1185.e9 (2020). doi: 10.1016/j.cell.2020.07.008; pmid: 32795412
18. V. Rangaraju, M. Lauterbach, E. M. Schuman, Spatially stable mitochondrial compartments fuel local translation during plasticity. *Cell* **176**, 73–84.e15 (2019). doi: 10.1016/j.cell.2018.12.013; pmid: 30612742
19. K. Steib, I. Schäffner, R. Jagasia, B. Ebert, D. Chichung Lie, Mitochondria modify exercise-induced development of stem cell-derived neurons in the adult brain. *J. Neurosci.* **34**, 6624–6633 (2014). doi: 10.1523/JNEUROSCI.4972-13.2014; pmid: 24806687
20. R. Iwata, P. Casimir, P. Vanderhaeghen, Mitochondrial dynamics in postmitotic cells regulate neurogenesis. *Science* **369**, 858–862 (2020). doi: 10.1126/science.aba9760; pmid: 32792401
21. R. Iwata, P. Vanderhaeghen, Regulatory roles of mitochondria and metabolism in neurogenesis. *Curr. Opin. Neurobiol.* **69**, 231–240 (2021). doi: 10.1016/j.conb.2021.05.003; pmid: 34171617
22. D. S. Glazier, Is metabolic rate a universal 'pacemaker' for biological processes? *Biol. Rev. Camb. Philos. Soc.* **90**, 377–407 (2015). doi: 10.1111/brv.12115; pmid: 24863680
23. G. B. West, J. H. Brown, B. J. Enquist, A general model for ontogenetic growth. *Nature* **413**, 628–631 (2001). doi: 10.1038/35098076; pmid: 11675785
24. N. Gaspard *et al*., An intrinsic mechanism of corticogenesis from embryonic stem cells. *Nature* **455**, 351–357 (2008). doi: 10.1038/nature07287; pmid: 18716623
25. M. J. Bird *et al*., Oxygraphy versus enzymology for the biochemical diagnosis of primary mitochondrial disease. *Metabolites* **9**, 220 (2019). doi: 10.3390/metabo9100220; pmid: 31658717
26. J. M. Buescher *et al*., A roadmap for interpreting (13)C metabolite labeling patterns from cells. *Curr. Opin. Biotechnol.* **34**, 189–201 (2015). doi: 10.1016/j.copbio.2015.02.003; pmid: 25731751
27. A. Bhaduri *et al*., Cell stress in cortical organoids impairs molecular subtype specification. *Nature* **578**, 142–148 (2020). doi: 10.1038/s41586-020-1962-0; pmid: 31996853
28. D. J. Di Bella *et al*., Molecular logic of cellular diversification in the mouse cerebral cortex. *Nature* **595**, 554–559 (2021). doi: 10.1038/s41586-021-03670-5; pmid: 34163074
29. C. J. Valvona, H. L. Fillmore, P. B. Nunn, G. J. Pilkington, The regulation and function of lactate dehydrogenase A: Therapeutic potential in brain tumor. *Brain Pathol.* **26**, 3–17 (2016). doi: 10.1111/bpa.12299; pmid: 26269128
30. J. Billiard *et al*., Quinoline 3-sulfonamides inhibit lactate dehydrogenase A and reverse aerobic glycolysis in cancer cells. *Cancer Metab.* **1**, 19 (2013). doi: 10.1186/2049-3002-1-19; pmid: 24280423
31. V. R. Fantin, J. St-Pierre, P. Leder, Attenuation of LDH-A expression uncovers a link between glycolysis, mitochondrial physiology, and tumor maintenance. *Cancer Cell* **9**, 425–434 (2006). doi: 10.1016/j.ccr.2006.04.023; pmid: 16766262
32. D. H. Ebert, M. E. Greenberg, Activity-dependent neuronal signalling and autism spectrum disorder. *Nature* **493**, 327–337 (2013). doi: 10.1038/nature11860; pmid: 23325215
33. S. C. Tso *et al*., Structure-guided development of specific pyruvate dehydrogenase kinase inhibitors targeting the ATP-binding pocket. *J. Biol. Chem.* **289**, 4432–4443 (2014). doi: 10.1074/jbc.M113.533885; pmid: 24356970
34. C. Charrier *et al*., Inhibition of SRGAP2 function by its human-specific paralogs induces neoteny during spine maturation. *Cell* **149**, 923–935 (2012). doi: 10.1016/j.cell.2012.03.034; pmid: 22559944
35. M. Matsuda *et al*., Species-specific segmentation clock periods are due to differential biochemical reaction speeds. *Science* **369**, 1450–1455 (2020). doi: 10.1126/science.aba7668; pmid: 32943519
36. T. Rayon *et al*., Species-specific developmental timing is associated with global differences in protein stability in mouse and human. *Science* **3**, (2020). doi: 10.1101/2019.12.29.889543
37. G. Ciceri *et al*., An epigenetic barrier sets the timing of human neuronal maturation. bioRxiv 490114 (2022); https://doi.org/10.1101/2022.06.02.490114.
38. Q. Wu *et al*., Selective translation of epigenetic modifiers affects the temporal pattern and differentiation of neural stem cells. *Nat. Commun.* **13**, 470 (2022). doi: 10.1038/s41467-022-28097-y; pmid: 35078993
39. S. Cogliati, J. L. Cabrera-Alarcón, J. A. Enriquez, Regulation and functional role of the electron transport chain supercomplexes. *Biochem. Soc. Trans.* **49**, 2655–2668 (2021). doi: 10.1042/BST20210460; pmid: 34747989
40. M. Giacomello, A. Pyakurel, C. Glytsou, L. Scorrano, The cell biology of mitochondrial membrane dynamics. *Nat. Rev. Mol. Cell Biol.* **21**, 204–224 (2020). doi: 10.1038/s41580-020-0210-7; pmid: 32071438
41. M. S. Goyal, M. Hawrylycz, J. A. Miller, A. Z. Snyder, M. E. Raichle, Aerobic glycolysis in the human brain is associated with development and neotenous gene expression. *Cell Metab.* **19**, 49–57 (2014). doi: 10.1016/j.cmet.2013.11.020; pmid: 24411938
42. M. G. Vander Heiden, L. C. Cantley, C. B. Thompson, Understanding the Warburg effect: The metabolic requirements of cell proliferation. *Science* **324**, 1029–1033 (2009). doi: 10.1126/science.1160809; pmid: 19460998
43. M. Diaz-Cuadros *et al*., Metabolic regulation of species-specific developmental rates. *Nature* **613**, 550–557 (2023).

ACKNOWLEDGMENTS

We thank the members of P.Va.'s laboratory and F. Polleux for helpful discussions and valuable help. **Funding:** This work was funded by the European Research Council (NEUROTEMPO), the EOS Programme PANDAROME, the Belgian FWO and FRS/FNRS, the Generet Fund (P.Va.), the Belgian Queen Elizabeth Foundation (to R.I. and P.Va.). The authors gratefully acknowledge the VIB Bio Imaging Core for support and assistance in this work. R.I. was supported by a postdoctoral fellowship from the FRS/FNRS. P.C. holds a PhD fellowship of the FWO. L.B. holds a fellowship of the FWO. A.V. holds a PhD fellowship of the FWO (file no. 1176821N). P.Ve. is a senior clinical investigator of the FWO. S.M.F. acknowledges funding from the ERC (ERC Consolidator grant no. 771486–MetaRegulation), FWO, Fonds Baillet Latour, KU Leuven (FTBO and internal funding), and King Baudouin. **Author contributions:** Conceptualization: R.I., P.C., P.Va.; Formal analysis: R.I., P.C., E.E., N.C., S.P., P.Ve., B.G., K.D., B.G., S.M.F., S.C., K.W., P.Va.; Funding acquisition: P.Va.; Investigation: R.I., P.C., E.E., L.B., M.M., M.B., I.G.L., M.D., S.P., B.G., S.E., V.G., S.B., A.V., D.R., N.G., S.C., I.V., E.C., K.W., S.M.F., P.Va.; Methodology: R.I., P.C., P.Va.; Resources: P.Ve., S.A., P.Va.; Supervision: P.Va.; Writing: R.I., P.C., P.Va. **Competing interests:** The authors declare no competing interests. **Data and materials availability:** All data are available in the manuscript or the supplementary materials. All materials are available upon request from P.Va. The single-cell RNA-sequencing data reported in this paper are accessible on NCBI's Gene Expression Omnibus (GEO accession number GSE219253).
License information: Copyright © 2023 the authors, some rights reserved; exclusive licensee American Association for the Advancement of Science. No claim to original US government works. https://www.science.org/about/science-licenses-journal-article-reuse

SUPPLEMENTARY MATERIALS

science.org/doi/10.1126/science.abn4705
Materials and Methods
Figs. S1 to S20
Table S1
References (*44*–*55*)
Data S1 and S2
MDAR Reproducibility Checklist

Submitted 3 December 2021; resubmitted 19 August 2022
Accepted 10 January 2023
Published online 26 January 2023
10.1126/science.abn4705

Pushing the Boundaries of Knowledge

As AAAS's first multidisciplinary, open access journal, *Science Advances* publishes research that reflects the selectivity of high impact, innovative research you expect from the *Science* family of journals, published in an open access format to serve a vast and growing global audience. Check out the latest findings or learn how to submit your research: **ScienceAdvances.org**

Science Advances
AAAS

GOLD OPEN ACCESS, DIGITAL, AND FREE TO ALL READERS

RESEARCH ARTICLE SUMMARY

CORONAVIRUS

Inborn errors of OAS–RNase L in SARS-CoV-2–related multisystem inflammatory syndrome in children

Danyel Lee *et al.*

INTRODUCTION: Multisystem inflammatory syndrome in children (MIS-C) is a severe, unexplained complication of severe acute respiratory syndrome coronavirus 2 (SARS-CoV-2) infection with an estimated prevalence of ~1 per 10,000 infected children. It typically occurs 4 weeks after infection, without hypoxemic pneumonia. Affected children present with fever, rash, abdominal pain, myocarditis, and other clinical features reminiscent of Kawasaki disease, including lymphadenopathy, coronary aneurysm, and high levels of biological markers of acute inflammation. Sustained monocyte activation is consistently reported as a key immunological feature of MIS-C. A more specific immunological abnormality is the polyclonal expansion of $CD4^+$ and $CD8^+$ T cells bearing the T cell receptor Vβ21.3. The root cause of MIS-C and its immunological and clinical features remains unknown.

RATIONALE: We hypothesized that monogenic inborn errors of immunity to SARS-CoV-2 may underlie MIS-C in some children. We further hypothesized that the identification of these inborn errors would provide insights into the molecular and cellular mechanisms underlying its immunological and clinical phenotypes. Finally, we hypothesized that a genetic and mechanistic understanding of a few patients would provide a proof of principle that would facilitate studies in other patients. We performed whole-exome or whole-genome sequencing on 558 internationally recruited patients with MIS-C (aged 3 months to 19 years). We searched for rare nonsynonymous biallelic variants of protein-coding genes, testing a hypothesis of genetic homogeneity.

RESULTS: We found autosomal recessive deficiencies of OAS1 (2′-5′-oligoadenylate synthetase 1), OAS2, or RNase L (ribonuclease L) in five unrelated children of four different ancestries with MIS-C (~1% of our cohort). There were no similar defects in a cohort of 1288 individuals (aged 6 months to 99 years) with asymptomatic or mild infection (P = 0.001) or 334 young patients (aged 0 to 21 years) with asymptomatic or mild infection or COVID-19 pneumonia (P = 0.046). The estimated cumulative frequency of these defects in the general population was ~0.00013. The type I interferon (IFN)–inducible double-stranded RNA (dsRNA)–sensing proteins OAS1 and OAS2 generate 2′-5′-linked oligoadenylates (2-5A), which activate the antiviral single-stranded RNA (ssRNA)–degrading RNase L, particularly in mononuclear phagocytes. Consistent with the absence of pneumonia in these patients, epithelial cells and fibroblasts defective for this pathway restricted SARS-CoV-2 normally. This contrasted with interferon alpha and beta receptor subunit 1 (IFNAR1)–deficient cells from patients prone to hypoxemic pneumonia without MIS-C. Monocytic cell lines with genetic deficiencies of OAS1, OAS2, or RNase L displayed excessive inflammatory cytokine production in response to intracellular dsRNA. Cytokine production by RNase L–deficient cells was impaired by melanoma differentiation-associated protein 5 (MDA5) or retinoic acid–inducible gene I (RIG-I) deficiency and abolished by mitochondrial antiviral-signaling protein (MAVS) deficiency. Exogenous 2-5A suppressed inflammatory responses to these stimuli in control and OAS1-deficient cells but not in RNase L–deficient cells. Finally, monocytic cell lines, primary monocytes, and monocyte-derived dendritic cells with genetic deficiencies of OAS1, OAS2, or RNase L displayed exaggerated inflammatory responses to SARS-CoV-2 as well as SARS-CoV-2–infected cells and their RNA.

CONCLUSION: We report autosomal recessive deficiencies of OAS1, OAS2, or RNase L in ~1% of an international cohort of MIS-C patients. The cytosolic OAS–RNase L pathway suppresses RIG-I/MDA5–MAVS–mediated inflammation in dsRNA-stimulated mononuclear phagocytes. Single-gene recessive inborn errors of the OAS–RNase L pathway unleash the production of SARS-CoV-2–triggered inflammatory cytokines by mononuclear phagocytes, thereby underlying MIS-C. ■

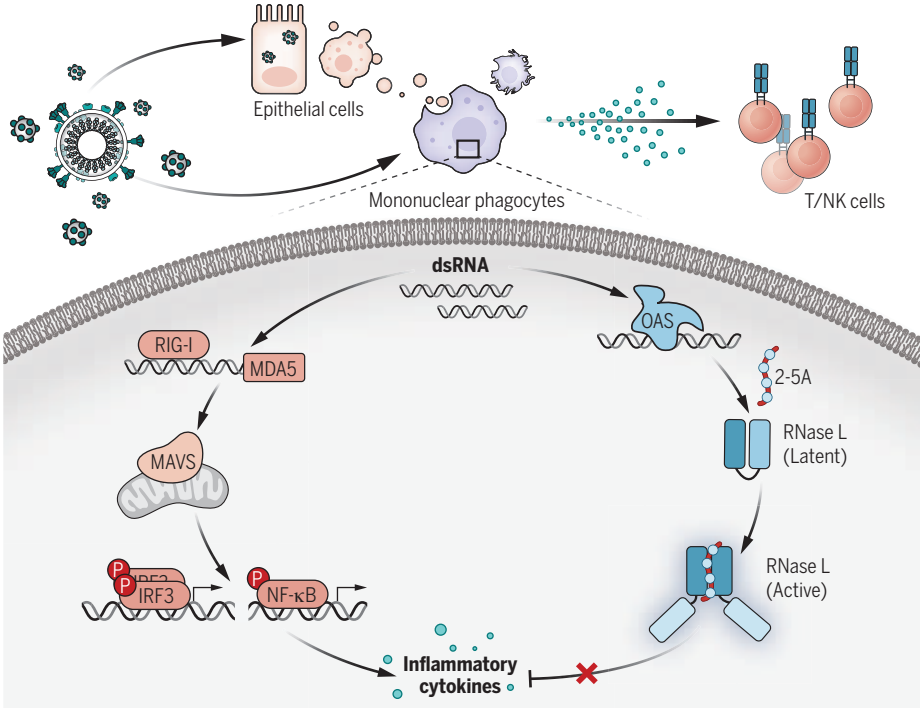

OAS–RNase L deficiency in MIS-C. dsRNAs from SARS-CoV-2 or SARS-CoV-2–permissive cells engulfed by mononuclear phagocytes simultaneously activate the RIG-I/MDA5–MAVS pathway, inducing inflammatory cytokine production, and the OAS–RNase L pathway, exerting posttranscriptional control over inflammatory cytokine production. OAS–RNase L deficiency results in excessive inflammatory cytokine production by myeloid cells, triggering MIS-C, including lymphoid cell activation and multiple tissue lesions. NK, natural killer; IRF3, interferon regulatory factor 3; NF-κB, nuclear factor κB.

All authors and affiliations appear in the full article online.
Corresponding author: Shen-Ying Zhang (shzh289@rockefeller.edu)
This is an open-access article distributed under the terms of the Creative Commons Attribution license (https://creativecommons.org/licenses/by/4.0/), which permits unrestricted use, distribution, and reproduction in any medium, provided the original work is properly cited.
Cite this article as D. Lee *et al.*, *Science* **379**, eabo3627 (2023). DOI: 10.1126/science.abo3627

READ THE FULL ARTICLE AT
https://doi.org/10.1126/science.abo3627

RESEARCH ARTICLE

CORONAVIRUS

Inborn errors of OAS–RNase L in SARS-CoV-2–related multisystem inflammatory syndrome in children

Danyel Lee[1,2,3], Jérémie Le Pen[4]†, Ahmad Yatim[1]†, Beihua Dong[5]†, Yann Aquino[6,7]†, Masato Ogishi[1]†, Rémi Pescarmona[8]†, Estelle Talouarn[2,3]†, Darawan Rinchai[1]‡, Peng Zhang[1]‡, Magali Perret[8]‡, Zhiyong Liu[1], Iolanda Jordan[9,10,11,12,13], Sefika Elmas Bozdemir[14], Gulsum Iclal Bayhan[15], Camille Beaufils[16], Lucy Bizien[2,3], Aurelie Bisiaux[6], Weite Lei[1], Milena Hasan[17], Jie Chen[1], Christina Gaughan[5], Abhishek Asthana[5], Valentina Libri[17], Joseph M. Luna[4,18], Fabrice Jaffré[19], H.-Heinrich Hoffmann[4], Eleftherios Michailidis[4,20], Marion Moreews[21], Yoann Seeleuthner[2,3], Kaya Bilguvar[22,23], Shrikant Mane[24], Carlos Flores[25,26,27], Yu Zhang[29,30], Andrés A. Arias[1,31,32], Rasheed Bailey[1], Agatha Schlüter[33], Baptiste Milisavljevic[1], Benedetta Bigio[1], Tom Le Voyer[2,3], Marie Materna[2,3], Adrian Gervais[2,3], Marcela Moncada-Velez[1], Francesca Pala[29], Tomi Lazarov[34], Romain Levy[2,3], Anna-Lena Neehus[2,3], Jérémie Rosain[2,3], Jessica Peel[1], Yi-Hao Chan[1], Marie-Paule Morin[16], Rosa Maria Pino-Ramirez[35], Serkan Belkaya[36], Lazaro Lorenzo[1], Jordi Anton[12,37,38], Selket Delafontaine[39], Julie Toubiana[40,41], Fanny Bajolle[42], Victoria Fumadó[10,12,43,44], Marta L. DeDiego[45], Nadhira Fidouh[46], Flore Rozenberg[47], Jordi Pérez-Tur[48,49,50], Shuibing Chen[19], Todd Evans[19], Frédéric Geissmann[34], Pierre Lebon[51], Susan R. Weiss[52], Damien Bonnet[42], Xavier Duval[53,54,55,56], CoV-Contact Cohort§, COVID Human Genetic Effort¶, Qiang Pan-Hammarström[57], Anna M. Planas[58,59], Isabelle Meyts[60], Filomeen Haerynck[61], Aurora Pujol[62,63], Vanessa Sancho-Shimizu[64,65], Clifford L. Dalgard[66,67], Jacinta Bustamante[1,2,3,68], Anne Puel[1,2,3], Stéphanie Boisson-Dupuis[1,2,3], Bertrand Boisson[1,2,3], Tom Maniatis[69], Qian Zhang[1,2,3], Paul Bastard[1,2,3,70], Luigi Notarangelo[29], Vivien Béziat[1,2,3], Rebeca Perez de Diego[71,72], Carlos Rodriguez-Gallego[28,73], Helen C. Su[29,30], Richard P. Lifton[24,74], Emmanuelle Jouanguy[1,2,3], Aurélie Cobat[1,2,3]#, Laia Alsina[10,12,38,75]#, Sevgi Keles[76]#, Elie Haddad[77]#, Laurent Abel[1,2,3]**, Alexandre Belot[21,78]**, Lluis Quintana-Murci[6,79]**, Charles M. Rice[4]**, Robert H. Silverman[5]**, Shen-Ying Zhang[1,2,3]*††, Jean-Laurent Casanova[1,2,3,80,81]††

Multisystem inflammatory syndrome in children (MIS-C) is a rare and severe condition that follows benign COVID-19. We report autosomal recessive deficiencies of *OAS1*, *OAS2*, or *RNASEL* in five unrelated children with MIS-C. The cytosolic double-stranded RNA (dsRNA)–sensing OAS1 and OAS2 generate 2′-5′-linked oligoadenylates (2-5A) that activate the single-stranded RNA–degrading ribonuclease L (RNase L). Monocytic cell lines and primary myeloid cells with OAS1, OAS2, or RNase L deficiencies produce excessive amounts of inflammatory cytokines upon dsRNA or severe acute respiratory syndrome coronavirus 2 (SARS-CoV-2) stimulation. Exogenous 2-5A suppresses cytokine production in OAS1-deficient but not RNase L–deficient cells. Cytokine production in RNase L–deficient cells is impaired by MDA5 or RIG-I deficiency and abolished by mitochondrial antiviral-signaling protein (MAVS) deficiency. Recessive OAS–RNase L deficiencies in these patients unleash the production of SARS-CoV-2–triggered, MAVS-mediated inflammatory cytokines by mononuclear phagocytes, thereby underlying MIS-C.

Interindividual clinical variability in the course of primary infection with severe acute respiratory syndrome coronavirus 2 (SARS-CoV-2) is immense in unvaccinated individuals (*1*–*4*). We have shown that inborn errors of type I interferon (IFN) immunity and their phenocopies—autoantibodies against type I IFNs—collectively underlie at least 15% of cases of critical COVID-19 pneumonia in unvaccinated patients (*5*–*9*). Common genetic variants act as more modest risk factors (*10*–*13*). Children were initially thought to be rarely affected by COVID-19, as only 0.001 to 0.005% of infected children had critical pneumonia (*2*). However, another severe SARS-CoV-2–related phenotype, multisystem inflammatory syndrome in children (MIS-C), occurs predominantly in children, typically 4 weeks after infection (*14*–*16*). Its prevalence is estimated at ~1 per 10,000 infected children (*17*–*19*). Children with MIS-C do not suffer from hypoxemic pneumonia and typically display no detectable viral infection of the upper respiratory tract at disease onset. However, most MIS-C cases test positive for anti–SARS-CoV-2 antibodies, and almost all cases have a history of exposure to SARS-CoV-2 (*17*, *20*). Initial reports of MIS-C described it as an atypical form of Kawasaki disease (KD) (*16*, *21*–*25*), as its clinical features include fever, rash, abdominal pain, myocarditis, lymphadenopathy, coronary aneurysm, and elevated biological markers of acute inflammation.

The elevated markers frequently detected in MIS-C patients suggest that inflammation occurs in various organs (*21*, *22*, *26*–*36*). These markers include surrogates of cardiovascular endothelial injury [e.g., troponin and B-type natriuretic peptide (BNP)] and gastrointestinal epithelial injury [e.g., lipopolysaccharide (LPS)–binding protein (LBP) and soluble CD14] (*36*). Various leukocyte subsets are also affected. Sustained monocyte activation has been consistently reported as a key immunological feature of MIS-C, with high levels of proinflammatory markers, including ferritin, interleukin-1 receptor antagonist (IL-1RA), IL-6, IL-10, IL-18, monocyte chemoattractant protein 1 (MCP1, or CCL2), and tumor necrosis factor (TNF) (*21*, *22*, *26*–*36*). In addition, the levels of biomarkers related to type II IFN (IFN-γ) signaling, which are not necessarily specific to monocyte activation, often increase during the early phase of disease (*22*, *31*–*36*). An immunological phenotype specific to MIS-C, observed in ~75% of patients, is the polyclonal expansion of $CD4^+$ and $CD8^+$ T cells bearing the Vβ21.3 segment (*32*, *34*, *36*–*38*). In this multitude of molecular, cellular, and clinical abnormalities, the root cause of MIS-C remains unknown (*39*). We hypothesized that monogenic inborn errors of immunity (IEIs) to SARS-CoV-2 may underlie MIS-C in some children and that the identification of these inborn errors may clarify the molecular, cellular, and immunological basis of disease (*15*, *40*).

Results

Identification of homozygous rare predicted loss-of-function variants of OAS1 *or* RNASEL *in two MIS-C patients*

We performed whole-exome or whole-genome sequencing for 558 patients with MIS-C from the international COVID Human Genetic Effort (CHGE) cohort (https://www.covidhge.com/) (fig. S1). We first searched for homozygous or hemizygous rare predicted loss-of-function (pLOF) variants with a high degree of confidence in human genes with a gene damage index of <13.83 (*41*). We then restricted the list to genes involved in host response to viruses (Gene Ontology term "response to virus," GO:0009615). We identified two unrelated patients homozygous for stop-gain variants, of *OAS1* in one patient (P1, p.R47*) and *RNASEL* in the other (P5, p.E265*) (Fig. 1A, fig. S2A, and Table 1). OAS1 (2′-5′-oligoadenylate synthetase 1) is one of the four members of the OAS family (OAS1, OAS2, OAS3, and the catalytically inactive OASL). These proteins are type I IFN–inducible cytosolic proteins that produce 2′-5′-linked oligoadenylates (2-5A) upon binding to double-stranded RNA (dsRNA). The 2-5A, in turn, induce the dimerization and activation of the latent endoribonuclease RNase L, which degrades single-stranded RNA (ssRNA) of viral or human origin (*42*, *43*). No homozygous variants fulfilling these criteria were identified in any of the 1288 subjects with asymptomatic or mild SARS-CoV-2 infection (SARS-CoV-2–infected controls) in the CHGE database (fig. S1). MIS-C patients therefore display significant

enrichment (P = 0.013) in homozygous pLOF variants of the *OAS1* and *RNASEL* genes, suggesting that these loci are probably relevant to MIS-C pathogenesis. Moreover, although OAS1, OAS2, OAS3, and RNase L are expressed in various cell types in mice and humans, their levels are particularly high in myeloid cells, including monocytes and macrophages (*44*–*46*). Thus, autosomal recessive (AR) deficiencies of the OAS–RNase L pathway may underlie MIS-C by impairing the restriction of viral replication and/or enhancing the virus-triggered inflammatory response in monocytes, macrophages, dendritic cells, or other cell types.

Identification of biallelic rare experimentally deleterious variants of OAS1, OAS2, *or* RNASEL *in five MIS-C patients*

OAS1, *OAS2*, *OAS3*, and *RNASEL* have consensus negative selection (CoNeS) scores for negative selection of 2.25, 0.79, 1.46, and 0.66, respectively, consistent with findings for known monogenic IEIs with an AR mode of inheritance (*47*). We therefore extended our search to all homozygous or potential compound-heterozygous nonsynonymous or essential splicing site variants with a minor allele frequency (MAF) of <0.01 at these four loci in our MIS-C cohort. We identified a total of 12 unrelated patients and 16 different variants of *OAS1*, *OAS2*, *OAS3*, and *RNASEL* (Table 1). To study the expression and function of these 16 variants in vitro, we first analyzed RNase L–mediated ribosomal RNA (rRNA) degradation after the cotransfection of RNase L–deficient HeLa M cells with the corresponding *OAS1*, *OAS2*, *OAS3*, or *RNASEL* cDNAs (*48*–*51*) (Fig. 1, B to D, and fig. S2, B and C). The p.R47* OAS1 (homozygous in P1) mutant protein was not produced and was LOF (Fig. 1B and fig. S2D). The three mutant OAS2 proteins detected (p.R535Q, p.Q258L, and p.V290I) were produced in normal amounts, but p.R535Q (homozygous in P2 and P3) had minimal activity, and p.Q258L and p.V290I (both found in P4) had lower levels of activity than the wild-type (WT) protein (Fig. 1, A and C). All the *OAS3* variants were produced in normal amounts, and all but one (p.R932Q, found in the heterozygous state in one patient) of these variants had normal levels of activity (fig. S2C). The *RNASEL* p.E265* variant (homozygous in P5) was expressed as a truncated protein and was LOF (Fig. 1D and fig. S2E), whereas the p.I264V variant was neutral in expression and function (Fig. 1D). We also quantified the function of the OAS1 and OAS2 mutants in a fluorescence resonance energy transfer (FRET) assay, which confirmed that P1's *OAS1* variant was LOF and that the *OAS2* variants of P2, P3, and P4 were hypomorphic (21 to 43%, 32 to 76%, and 36 to 75% of WT OAS2 activity for p.Q258L, p.V290I, and p.R535Q, respectively) (Fig. 1, E and F). Thus, we identified five unrelated MIS-C patients homozygous or compound heterozygous for rare and deleterious alleles of three of the four genes controlling the OAS–RNase L pathway (Fig. 1A and fig. S2A). The patients' genotypes were confirmed by Sanger sequencing and familial segregation. Their clinical and immunological features were consistent with those previously reported for other MIS-C patients (*21*, *22*, *26*–*36*, *52*) (Fig. 1, G to I, and Table 2).

Enrichment in homozygous deleterious OAS1, OAS2, *and* RNASEL *variants in MIS-C patients*

We found no homozygous rare (MAF < 0.01) deleterious variants of the three genes in the

[1]St. Giles Laboratory of Human Genetics of Infectious Diseases, Rockefeller Branch, The Rockefeller University, New York, NY, USA. [2]Laboratory of Human Genetics of Infectious Diseases, Necker Branch, INSERM U1163, Paris, France. [3]Paris City University, Imagine Institute, Paris, France. [4]Laboratory of Virology and Infectious Disease, The Rockefeller University, New York, NY, USA. [5]Department of Cancer Biology, Lerner Research Institute, Cleveland Clinic, Cleveland, OH, USA. [6]Human Evolutionary Genetics Unit, Institut Pasteur, Paris City University, CNRS UMR 2000, Paris, France. [7]Doctoral College, Sorbonne University, Paris, France. [8]Laboratory of Immunology, Lyon Sud Hospital, Lyon, France. [9]Pediatric Intensive Care Department, Hospital Sant Joan de Déu, Barcelona, Spain. [10]Kids Corona Platform, Barcelona, Spain. [11]Center for Biomedical Network Research on Epidemiology and Public Health (CIBERESP), Instituto de Salud Carlos III, Madrid, Spain. [12]Department of Surgery and Surgical Specializations, Faculty of Medicine and Health Sciences, University of Barcelona, Barcelona, Spain. [13]Respiratory and Immunological Dysfunction in Pediatric Critically Ill Patients, Institute of Recerca Sant Joan de Déu, Barcelona, Spain. [14]Bursa City Hospital, Bursa, Turkey. [15]Ankara City Hospital, Yildirim Beyazit University, Ankara, Turkey. [16]Immunology and Rheumatology Division, Department of Pediatrics, University of Montreal, CHU Sainte-Justine, Montreal, QC, Canada. [17]Center for Translational Research, Institut Pasteur, Paris City University, Paris, France. [18]Department of Biochemistry and Center for RNA Science and Therapeutics, Case Western Reserve University, Cleveland, OH, USA. [19]Department of Surgery, Weill Cornell Medical College, New York, NY, USA. [20]Department of Pediatrics, School of Medicine, Emory University, Atlanta, GA, USA. [21]International Center of Infectiology Research (CIRI), University of Lyon, INSERM U1111, Claude Bernard University, Lyon 1, CNRS, UMR5308, ENS of Lyon, Lyon, France. [22]Departments of Neurosurgery and Genetics and Yale Center for Genome Analysis, Yale School of Medicine, New Haven, CT, USA. [23]Department of Medical Genetics, School of Medicine, Acibadem Mehmet Ali Aydinlar University, Istanbul, Turkey. [24]Department of Genetics, Yale University School of Medicine, New Haven, CT, USA. [25]Research Unit, Nuestra Señora de la Candelaria University Hospital, Santa Cruz de Tenerife, Spain. [26]Genomics Division, Institute of Technology and Renewable Energies (ITER), Granadilla de Abona, Spain. [27]CIBERES, ISCIII, Madrid, Spain. [28]Department of Clinical Sciences, University Fernando Pessoa Canarias, Las Palmas de Gran Canaria, Spain. [29]Laboratory of Clinical Immunology and Microbiology, Division of Intramural Research, NIAID, NIH, Bethesda, MD, USA. [30]NIAID Clinical Genomics Program, NIH, Laboratory of Clinical Immunology and Microbiology, Division of Intramural Research, NIAID, NIH, Bethesda, MD, USA. [31]Primary Immunodeficiencies Group, University of Antioquia (UdeA), Medellin, Colombia. [32]School of Microbiology, University of Antioquia (UdeA), Medellin, Colombia. [33]Neurometabolic Diseases Laboratory, IDIBELL–Hospital Duran I Reynals, CIBERER U759, ISIiii, Madrid, Spain. [34]Immunology Program, Memorial Sloan Kettering Cancer Center, New York, NY, USA. [35]Pediatrics Department, Hospital Sant Joan de Déu, Barcelona, Spain. [36]Department of Molecular Biology and Genetics, Bilkent University, Ankara, Turkey. [37]Pediatric Rheumatology Division, Hospital Sant Joan de Déu, Barcelona, Spain. [38]Study Group for Immune Dysfunction Diseases in Children (GEMDIP), Institute of Recerca Sant Joan de Déu, Barcelona, Spain. [39]Department of Pediatrics, University Hospitals Leuven, Leuven, Belgium. [40]Department of General Pediatrics and Pediatric Infectious Diseases, Necker Hospital for Sick Children, Assistance Publique–Hôpitaux de Paris (AP-HP), Paris City University, Paris, France. [41]Biodiversity and Epidemiology of Bacterial Pathogens, Pasteur Institute, Paris, France. [42]Department of Pediatric Cardiology, Necker Hospital for Sick Children, AP-HP, Paris City University, Paris, France. [43]Pediatrics Infectious Diseases Division, Hospital Sant Joan de Déu, Barcelona, Spain. [44]Infectious Diseases and Microbiome, Institute of Recerca Sant Joan de Déu, Barcelona, Spain. [45]Department of Molecular and Cellular Biology, National Center for Biotechnology (CNB-CSIC), Madrid, Spain. [46]Laboratory of Virology, Bichat–Claude Bernard Hospital, Paris, France. [47]Laboratory of Virology, AP-HP, Cochin Hospital, Paris, France. [48]Molecular Genetics Unit, Institute of Biomedicine of Valencia (IBV-CSIC), Valencia, Spain. [49]CIBERNED, ISCIII, Madrid, Spain. [50]Joint Research Unit in Neurology and Molecular Genetics, Institut of Investigation Sanitaria La Fe, Valencia, Spain. [51]Medical School, Paris City University, Paris, France. [52]Department of Microbiology, Perelman School of Medicine, University of Pennsylvania, Philadelphia, PA, USA. [53]Bichat–Claude Bernard Hospital, Paris, France. [54]University Paris Diderot, Paris 7, UFR of Médecine-Bichat, Paris, France. [55]IAME, INSERM, UMRS1137, Paris City University, Paris, France. [56]Infectious and Tropical Diseases Department, AP-HP, Bichat–Claude Bernard Hospital, Paris, France. [57]Department of Biosciences and Nutrition, Karolinska Institutet, Huddinge, Sweden. [58]Department of Neuroscience and Experimental Therapeutics, Institute for Biomedical Research of Barcelona (IIBB), Spanish National Research Council (CSIC), Barcelona, Spain. [59]Institute for Biomedical Investigations August Pi i Sunyer (IDIBAPS), Barcelona, Spain. [60]Department of Pediatrics, University Hospitals Leuven and Laboratory for Inborn Errors of Immunity, KU Leuven, Leuven, Belgium. [61]Primary Immunodeficiency Research Laboratory, Center for Primary Immunodeficiency Ghent, Ghent University Hospital, Ghent, Belgium. [62]Neurometabolic Diseases Laboratory, IDIBELL–Hospital Duran I Reynals; and Catalan Institution for Research and Advanced Studies (ICREA), Barcelona, Spain. [63]CIBERER U759, ISCiii, Madrid, Spain. [64]Department of Paediatric Infectious Diseases and Virology, Imperial College London, London, UK. [65]Centre for Paediatrics and Child Health, Faculty of Medicine, Imperial College London, London, UK. [66]The American Genome Center, Collaborative Health Initiative Research Program, Uniformed Services University of the Health Sciences, Bethesda, MD, USA. [67]Department of Anatomy, Physiology, and Genetics, Uniformed Services University of the Health Sciences, Bethesda, MD, USA. [68]Study Center for Primary Immunodeficiencies, Necker Hospital for Sick Children, AP-HP, Paris, France. [69]New York Genome Center, New York, NY, USA. [70]Pediatric Hematology-Immunology and Rheumatology Unit, Necker Hospital for Sick Children, AP-HP, Paris, France. [71]Laboratory of Immunogenetics of Human Diseases, Innate Immunity Group, IdiPAZ Institute for Health Research, La Paz Hospital, Madrid, Spain. [72]Interdepartmental Group of Immunodeficiencies, Madrid, Spain. [73]Department of Immunology, University Hospital of Gran Canaria Dr. Negrín, Canarian Health System, Las Palmas de Gran Canaria, Spain. [74]Laboratory of Human Genetics and Genomics, The Rockefeller University, New York, NY, USA. [75]Clinical Immunology and Primary Immunodeficiencies Unit, Pediatric Allergy and Clinical Immunology Department, Hospital Sant Joan de Déu, Barcelona, Spain. [76]Necmettin Erbakan University, Konya, Turkey. [77]Department of Pediatrics, Department of Microbiology, Immunology and Infectious Diseases, University of Montreal, Immunology and Rheumatology Division, CHU Sainte-Justine, Montreal, QC, Canada. [78]National Reference Center for Rheumatic, Autoimmune and Systemic Diseases in Children (RAISE), Pediatric Nephrology, Rheumatology, Dermatology Unit, Hospital of Mother and Child, Hospices Civils of Lyon, Lyon, France. [79]Human Genomics and Evolution, Collège de France, Paris, France. [80]Department of Pediatrics, Necker Hospital for Sick Children, Paris, France. [81]Howard Hughes Medical Institute, The Rockefeller University, New York, NY, USA.
***Corresponding author. Email: shzh289@rockefeller.edu** †These authors contributed equally to this work. ‡These authors contributed equally to this work.
§A full list of CoV-Contact Cohort collaborators and their affiliations is provided at the end of the paper. ¶A full list of COVID Human Genetic Effort collaborators and their affiliations is provided at the end of the paper. #These authors contributed equally to this work. **These authors contributed equally to this work.
††These authors contributed equally to this work.

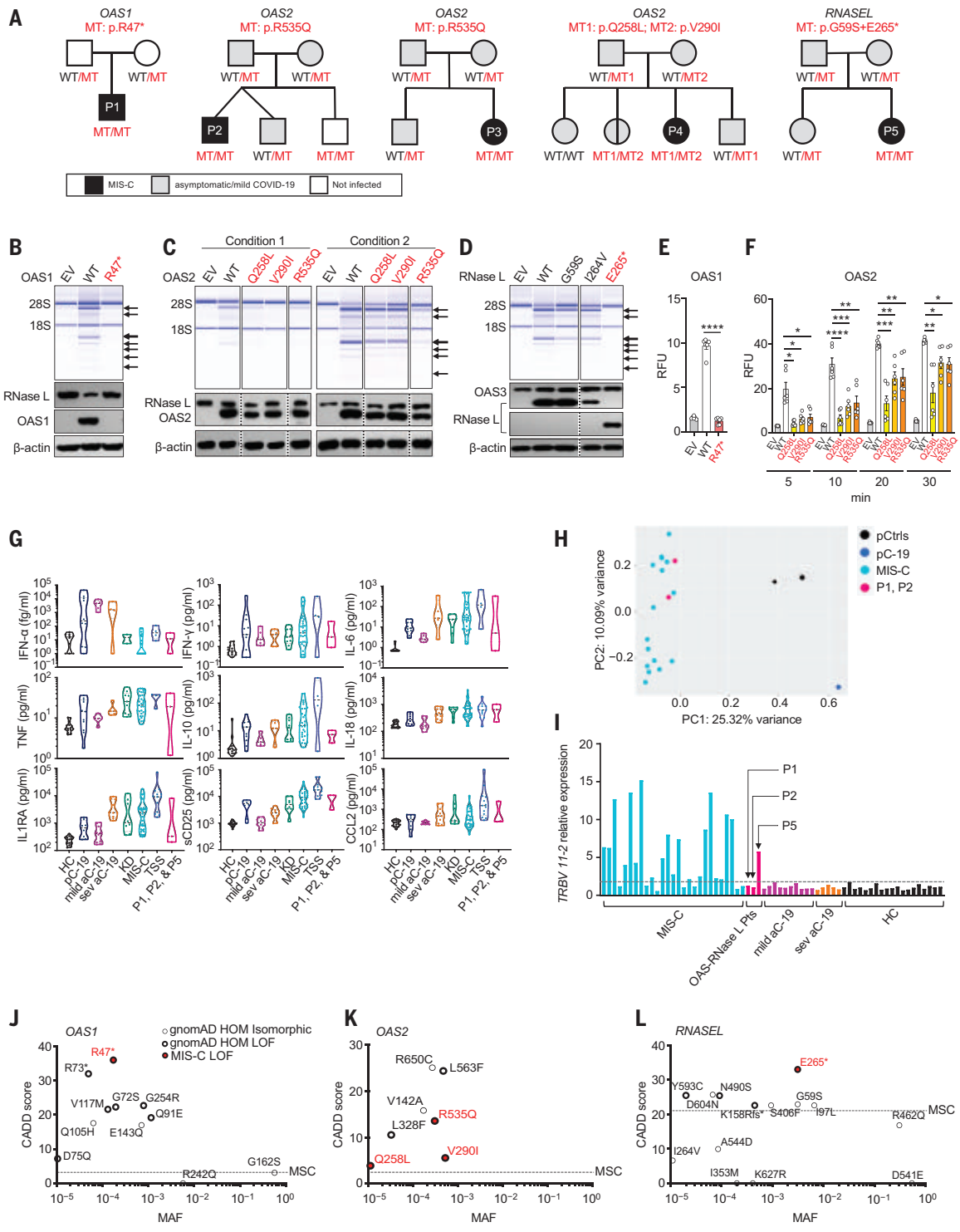

Fig. 1. Biallelic *OAS1*, *OAS2*, and *RNASEL* variants in patients with MIS-C. (**A**) Family pedigrees with allele segregation. Mutant, "MT" in red; wild-type, "WT" in black. (**B** to **D**) Functional assays for WT and mutant OAS1 (B), OAS2 (C), and RNase L (D). Variants for which homozygotes or compound heterozygotes were present in our MIS-C cohort were tested. (Upper panels) RNase L–mediated cleavage of rRNA in a cell-free system based on transfected HeLa M cells. (Lower panels) Immunoblots of the indicated proteins. EV, empty vector. Arrows indicate degraded rRNA species. OAS2 variants (C) were tested under two different sets of conditions (see methods). The results shown in (B) to (D) are representative of three independent experiments. (**E** and **F**) FRET assay of 2-5A synthesized in response to poly(I:C) stimulation by WT and MT OAS1 (E) or OAS2 (F). RFU, relative fluorescence units. The data shown are the means ± SEM of six biological replicates. Statistical analysis was performed as described in the methods. *$P < 0.05$, **$P < 0.01$, ***$P < 0.001$, ****$P < 0.0001$. (**G**) Concentrations of various cytokines in plasma samples from OAS–RNase L–deficient patients during MIS-C (P1, P2, and P5); comparison with those of healthy controls (HC), pediatric (pC-19) or adult COVID-19 pneumonia (aC-19) patients, typical Kawasaki disease patients (KD), other MIS-C patients with no known genetic etiology (MIS-C), and patients with toxic shock syndrome (TSS). (**H**) PCA of gene expression quantified by whole-blood bulk RNA-seq for P1 and

P2 during MIS-C relative to pediatric controls (pCtrls), previously published MIS-C patients, and a pediatric patient with mild COVID-19 (pC-19). (**I**) Relative levels of *TRBV 11-2* (encoding Vβ21.3) RNA in blood samples from P1, P2, and P5 during MIS-C, relative to other MIS-C patients, adults with mild or severe COVID-19 (mild aC-19, sev aC-19), and healthy controls. (**J** to **L**) CADD-MAF graph of *OAS1* (J), *OAS2* (K), and *RNASEL* (L) variants for which homozygotes are reported in gnomAD and/or found in our MIS-C cohort. Single-letter abbreviations for the amino acid residues are as follows: A, Ala; C, Cys; D, Asp; E, Glu; F, Phe; G, Gly; H, His; I, Ile; K, Lys; L, Leu; M, Met; N, Asn; P, Pro; Q, Gln; R, Arg; S, Ser; T, Thr; V, Val; W, Trp; and Y, Tyr.

Table 1. Homozygous or potentially compound-heterozygous rare nonsynonymous variants of the *OAS* and *RNASEL* genes in MIS-C patients. Homozygous or potentially compound-heterozygous nonsynonymous variants with a minor allele frequency (MAF) < 0.01 (gnomAD) found in our cohort of MIS-C patients. CADD_Phred, combined annotation-dependent depletion Phred score; Exp function, experimental function of each variant as tested in the RNase L–dependent rRNA degradation assay (OAS1, OAS2, RNase L) and FRET assay (OAS1, OAS2); Hom, homozygous; Het, heterozygous.

Gene	Nucleotide change	Amino acid change	Zygosity	MAF (gnomAD)	CADD_Phred	Exp function
OAS1	c.139C>T	p.Arg47* (R47*)	Hom	0.00017327	36	LOF
OAS2	c.1604G>A	p.Arg535Gln (R535Q)	Hom	0.00028695	13.58	Hypomorph
OAS2	c.773A>T	p.Gln258Leu (Q258L)	Het	–	3.888	Hypomorph
OAS2	c.868G>A	p.Val290Ile (V290I)	Het	0.0005153	5.585	Hypomorph
OAS3	c.145G>A	p.Ala49Thr (A49T)	Het	0.00243639	9.48	Isomorph
OAS3	c.1475G>A	p.Arg492His (R492H)	Het	0.0054987	9.95	Isomorph
OAS3	c.1703G>A	p.Arg568Lys (R568K)	Het	0.00104951	0.472	Isomorph
OAS3	c.2795G>A	p.Arg932Gln (R932Q)	Het	0.0094	23.2	LOF
OAS3	c.3089A>G	p.Gln1030Arg (Q1030R)	Het	–	23.9	Isomorph
OAS3	c.1586A>G	p.Gln529Arg (Q529R)	Het	0.00000401	5.85	Isomorph
OAS3	c.792C>A	p.His264Gln (H264Q)	Het	0.001001261	0.924	Isomorph
OAS3	c.442C>T	p.Pro148Ser (P148S)	Het	0.000036	22.9	Isomorph
OAS3	c.3259G>A	p.Val1087Met (V1087M)	Het	0.003936537	22.5	Isomorph
RNASEL	c.790A>G	p.Ile264Val (I264V)	Hom	0.00000401	6.597	Isomorph
RNASEL	c.793G>T	p.Glu265* (E265*)†	Hom	0.0031	33	LOF
RNASEL	c.175G>A	p.Gly59Ser (G59S)†	Hom	0.0031	22.9	Isomorph

†*RNASEL* variants p.E265* and p.G59S were in complete linkage disequilibrium (https://www.internationalgenome.org), forming a haplotype.

1288 SARS-CoV-2–infected controls or in a control cohort of 334 patients under the age of 21 years with asymptomatic or mild infection or COVID-19 pneumonia (fig. S1). Thus, there was a significant enrichment in such homozygotes among MIS-C patients relative to infected controls (P = 0.001) or controls under 21 years old (P = 0.046), suggesting that AR deficiencies of three genes of the OAS–RNase L pathway (*OAS1*, *OAS2*, and *RNASEL*) specifically underlie MIS-C. We further assessed the probability of AR deficiencies of these three gene products being causal for MIS-C by evaluating the expression and function of all nonsynonymous variants of *OAS1*, *OAS2*, and *RNASEL* for which homozygotes were reported in the Genome Aggregation Database (gnomAD, v2.1.1 and v3.1.1, 28 variants in total) in our RNase L–mediated rRNA degradation assay (fig. S2, F to H, and table S1). In total, 13 *OAS1*, *OAS2*, or *RNASEL* variants were deleterious and present in the homozygous state in 19 individuals in the gnomAD database (Fig. 1, J to L). The estimated cumulative frequency of homozygous carriers of LOF variants at the three loci was ~0.00013 [95% confidence interval (CI): 7.2×10^{-5} to 20×10^{-5}] in the general population. The rarity of AR OAS–RNase L deficiencies in the general population is therefore consistent with that of MIS-C. Moreover, the enrichment in these deficiencies observed in MIS-C patients relative to the individuals included in gnomAD was highly significant ($P = 2 \times 10^{-6}$). These findings suggest that AR deficiencies of OAS1, OAS2, and RNase L are genetic etiologies of MIS-C.

The expression pattern for the OAS–RNase L pathway implicates mononuclear phagocytes

We studied the basal expression of *OAS1*, *OAS2*, *OAS3*, and *RNASEL* in cells from different tissues. Consistent with data from public databases (*44*), our in-house human cell RNA sequencing (RNA-seq) and reverse transcription–quantitative polymerase chain reaction (RT-qPCR) data showed that myeloid blood cells had higher basal mRNA levels for the four genes than did the tissue-resident cells tested (Fig. 2, A and B). In all cell types studied, both type I and type II IFN treatments up-regulated the levels of mRNA for *OAS1*, *OAS2*, and *OAS3*, whereas the levels of *RNASEL* mRNA were not influenced by these IFNs (fig. S3A). Previous studies reported a relationship between cell type–dependent activation of the OAS–RNase L pathway and basal levels of expression in mice (*45*, *46*). MIS-C occurs 3 to 6 weeks after SARS-CoV-2 infection, but the virus and/or viral proteins may still be detectable in nonrespiratory tissues, such as the intestine or heart, at disease onset in some patients (*32*, *34*, *37*). In addition, $CD4^+$ and $CD8^+$ T cells carrying Vβ21.3 expand, which implies a superantigen-like viral driver of MIS-C (*32*, *34*, *36*–*38*) and suggests that the virus or its antigens persist. Thus, AR deficiencies of the OAS–RNase L pathway may underlie MIS-C by impairing SARS-CoV-2 restriction and/or enhancing virus-triggered inflammatory responses in monocytes and other mononuclear phagocytes.

OAS–RNase L deficiencies have no impact on SARS-CoV-2 replication in A549 epithelial cells and fibroblasts

Previous studies have shown that the overproduction of exogenous OAS1 can result in the restriction of SARS-CoV-2 replication in A549 lung epithelial cells in the absence of exogenous type I IFN (*53*, *54*). However, the five OAS–RNase L–deficient patients had MIS-C without pneumonia. We assessed SARS-CoV-2 replication in A549 cells rendered permissive to SARS-CoV-2 by the stable expression of angiotensin-converting enzyme 2 (ACE2) and transmembrane protease serine 2 (TMPRSS2), which facilitates viral entry. Knockout (KO) of OAS1 or OAS2 did not increase the proportion of SARS-CoV-2–infected cells at 24 or 48 hours relative to that for the parental WT A549 cells, regardless of the presence or absence

Table 2. Demographic and clinical information for MIS-C patients biallelic for deleterious variants of the OAS–RNase L pathway. IEI, inborn error of immunity; SCV2, SARS-CoV-2; IVIG, intravenous immunoglobulins; ND, not determined; CRP, C-reactive protein; sCD25, soluble IL-2Rα.

Patient	P1	P2	P3	P4	P5
IEI (inheritance mode)	*OAS1* (AR)	*OAS2* (AR)	*OAS2* (AR)	*OAS2* (AR)	*RNASEL* (AR)
Age at MIS-C diagnosis	3 months	3 years	14 years	9 years	4 years
Sex	Male	Male	Female	Female	Female
Ethnicity	Filipino	Spanish	Turkish	Turkish	French Canadian
Resident country	Spain	Spain	Turkey	Turkey	Canada
SCV2 virology	Nasal swab PCR (−); blood PCR (−); blood anti-SCV2 IgG (+); blood antigen N (−)	Nasal swab PCR (−); blood PCR (−); blood anti-SCV2 IgG (+); blood antigen N (−)	Nasal swab PCR (−); blood PCR (ND); blood total anti-SCV2 (+); blood antigen N (ND)	Nasal swab PCR (−); blood PCR (ND); blood anti-SCV2 IgM and IgG (+); blood antigen N (ND)	Nasal swab PCR (−); blood PCR (−); blood anti-SCV2 IgG (+); blood antigen N (−)
Hemogram	Normal	Normal	Normal	Normal	Normal
Increased markers of multiorgan inflammation	CRP, ferritin, pro-BNP, GM-CSF, IL-1RA, MCP1, sCD25, IL-18, TNF	CRP, ferritin, pro-BNP, MCP1, sCD25, IL-1RA, IL-18, TNF	CRP, ferritin, troponin	Ferritin, troponin, pro-BNP	sCD25
TRBV 11-2 expansion	(−)	(−)	ND	ND	(+)
Clinical presentation	Kawasaki-like disease: fever, gastrointestinal symptoms, hepatosplenomegaly, aseptic meningitis with neurological symptoms (irritability), peripheral edema, lymphadenopathy, bilateral coronary aneurysm (Z score +8, +8.7), possible cerebral arterial aneurysm	Kawasaki disease: fever, rash, bilateral eyelid edema and erythema, conjunctival hyperemia	Kawasaki-like disease: fever, rash, bilateral nonpurulent conjunctivitis, strawberry tongue, abdominal pain, vomiting, dyspnea, mild mitral insufficiency. One and a half months prior, the patient had fever, headache, and sore throat when her mother had COVID-19. The patient developed oligoarticular juvenile idiopathic arthritis 5 months after MIS-C.	Fever, vomiting, coughing, myocarditis, left ventricular failure, pulmonary edema with paracardiac infiltration, polyneuropathy	Kawasaki disease: fever, rash, erythema and edema of the feet, anterior uveitis, cervical lymphadenopathy
Treatment	IVIG, aspirin, corticosteroids, anticoagulation therapy	IVIG, aspirin	IVIG, methylprednisolone, heparin	IVIG, pulse steroid, anakinra, mechanical ventilation	IVIG
Outcome	Recovery	Recovery	Recovery, but with persistent arthralgia in both knees 1.5 years after MIS-C	Recovery	Recovery

of exogenous IFN-α2b (Fig. 2, C and D, and fig. S3B). Only RNase L KO cells resulted in a mild increase in susceptibility to SARS-CoV-2 relative to WT cells in the absence of IFN-α2b, consistent with previous findings (*55*). We also used patient-specific SV40-transduced human dermal fibroblasts (SV40-fibroblasts) stably expressing ACE2 as a surrogate cell type for studying the impact of OAS–RNase L deficiencies on tissue-resident cell-intrinsic defenses against SARS-CoV-2 (*5*). Consistent with the lack of pneumonia in these patients, no increase in SARS-CoV-2 susceptibility was observed in any of the fibroblasts with *OAS1* (from P1), *OAS2* (P3 and P4), or *RNASEL* (P5) mutations up to 72 hours after infection in the presence or absence of exogenous IFN-α2b, despite the complete loss of expression of OAS1 or RNase L in the cells of P1 and P5, respectively (Fig. 2, E and F). This contrasted with the increased susceptibility reported for fibroblasts from a patient with AR complete IFNAR1 deficiency (*56*) and critical COVID-19 pneumonia.

OAS–RNase L deficiencies have no impact on SARS-CoV-2 replication in THP-1 cells

Only abortive SARS-CoV-2 infection has been reported in human mononuclear phagocytes, including monocytes and macrophages, which express very little to no ACE2 (*57*–*59*). However, basal *Oas* and *Rnasel* expression levels have previously been correlated with murine coronavirus or vesicular stomatitis virus (VSV) restriction in mouse macrophages (*60*). We tested the hypothesis that deficiencies of OAS–RNase L might result in productive SARS-CoV-2 infection in mononuclear phagocytes by assessing the replication of SARS-CoV-2. Unlike WT A549 cells stably transduced with ACE2 and TMPRSS2, in which SARS-CoV-2 can be detected 24 hours after infection, no SARS-CoV-2 was detected in THP-1–derived macrophages (*61*), whether parental or with a KO of OAS1, OAS2, or RNase L (Fig. 2, G and H, and fig. S3C). Thus, no myeloid

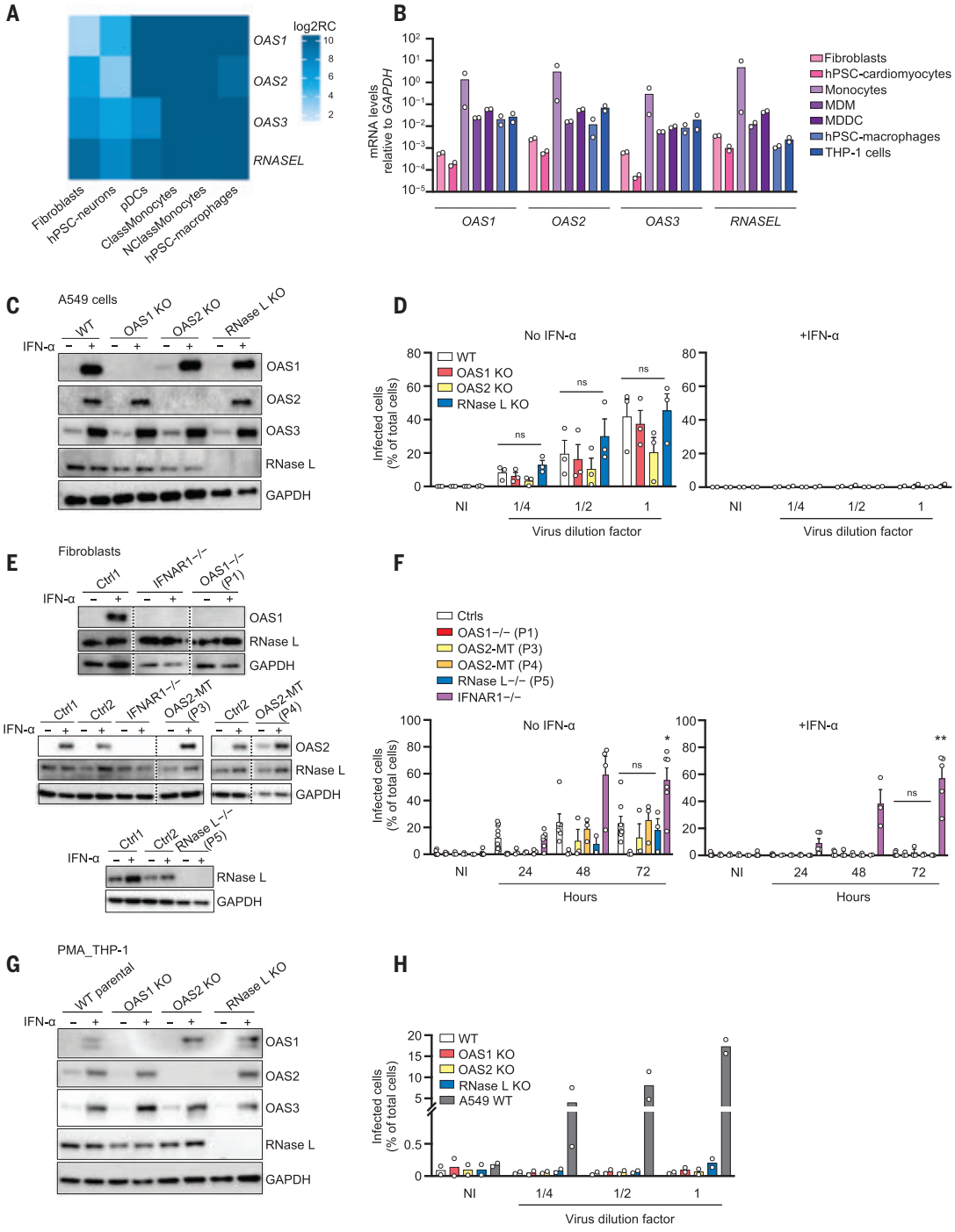

Fig. 2. Expression pattern of the OAS–RNase L pathway genes and their role in SARS-CoV-2 restriction. (**A** and **B**) Relative *OAS1*, *OAS2*, *OAS3*, and *RNASEL* mRNA levels measured by bulk RNA-seq (A) or RT-qPCR (B), in various cell types. hPSC, human pluripotent stem cell; ClassMonocytes, classical monocytes; NClassMonocytes, nonclassical monocytes; MDM, monocyte-derived macrophages; MDDC, monocyte-derived dendritic cells; Log2RC, $\log_2$ read count. (**C** and **D**) Immunoblot of the indicated proteins (C) and immunofluorescence (IF) of SARS-CoV-2 nucleocapsid (N) protein (D) in A549+ACE2/TMPRSS2 cells with and without knockout (KO) of OAS1, OAS2, or RNase L. IF analysis for N protein was performed 24 hours after infection with various dilutions of SARS-CoV-2. Dilution factors of $^1/_4$, $^1/_2$, and 1 correspond to MOI values of 0.0002, 0.0005, and 0.001, respectively. GAPDH, glyceraldehyde-3-phosphate dehydrogenase; NI, noninfected. (**E** and **F**) Immunoblot of the indicated proteins (E) and IF analysis for the SARS-CoV-2 N protein (F) in SV40-fibroblasts +ACE2 from healthy controls (Ctrl1 and Ctrl2), patients with *OAS-RNASEL* mutations (P1, P3, P4, and P5), and a previously reported patient with complete IFNAR1 deficiency (*IFNAR1*$^{-/-}$). IF analysis for N protein was performed at various time points after infection at a MOI of 0.08. (**G** and **H**) Immunoblot of the indicated proteins (G) and IF analysis for the SARS-CoV-2 N protein (H) in THP-1 cells with and without KO of OAS1, OAS2, or RNase L. IF analyses for N protein were performed in PMA-primed THP-1 cells 24 hours after infection with various dilutions of SARS-CoV-2. Dilution factors of $^1/_4$, $^1/_2$, and 1 correspond to MOI values of 0.012, 0.025, and 0.05, respectively. WT A549+ACE2/TMPRSS2 cells were included as a positive control for SARS-CoV-2 infection. The data points are means ± SEM from three [(D) and (F)] or means from two [(B) and (H)] independent experiments with three to six technical replicates per experiment. Statistical analyses were performed as described in the methods. ns, not significant; *P < 0.05, **P < 0.01.

SARS-CoV-2 replication was detected in the presence or absence of deficiencies of the OAS–RNase L pathway, at least in this cellular model of mononuclear phagocytes (*60*).

OAS–RNase L deficiencies result in an exaggerated inflammatory response to intracellular dsRNA in THP-1 cells

Sustained monocyte activation has repeatedly been reported to be a key immunological feature of MIS-C (*22*, *31*–*36*). We studied the impact of OAS–RNase L deficiencies on cellular responses to intracellular (cytosolic) or extracellular (endosomal) stimulation with dsRNA in THP-1 cells. Consistent with a previous study (*62*), THP-1 cells and THP-1–derived macrophages with a KO for OAS1, OAS2, or RNase L displayed enhanced activation, as demonstrated by their higher levels of IFN-λ1, IFN-β, IL-1β, IL-6, CXCL9, CXCL10, and TNF secretion 24 hours after stimulation with various doses of intracellular polyinosinic:polycytidylic acid [poly(I:C)] (Fig. 3A and fig. S4A), as well as higher mRNA induction for *IL6* and *CXCL9* 8 hours after stimulation (fig. S4, B and C). Cell viability was similar to that of WT THP-1 cells after intracellular poly(I:C) stimulation (fig. S4D). Small hairpin RNA–mediated knockdown (KDn) of the expression of *OAS1*, *OAS2*, and *RNASEL* in THP-1 cells confirmed these findings (fig. S4E). The transduction of THP-1 cells with a KO of the corresponding gene with the WT cDNA of *OAS1*, *OAS2*, or *RNASEL*, respectively, resulted in cytokine secretion levels similar to those observed in parental cells, whereas transduction with mutant cDNAs corresponding to the patients' variants had no such effect (*OAS1* variant of P1 and *RNASEL* variant of P5) or a lesser effect (*OAS2* variants of P2, P3, and P4) (Fig. 3B and fig. S5, A to C). Thus, OAS–RNase L deficiencies result in exaggerated inflammatory responses to intracellular dsRNA stimulation in THP-1 cells. Enhanced responses may also occur in the mononuclear phagocytes of our patients, underlying MIS-C.

The inflammatory response to intracellular dsRNA in THP-1 cells is MAVS dependent

Intracellular dsRNA is known to stimulate the RIG-I/MDA5–MAVS pathway (RIG-I, retinoic acid–inducible gene I; MDA5, melanoma differentiation-associated protein 5; MAVS, mitochondrial antiviral-signaling protein), inducing type I IFNs and other cytokines in various cell types (*63*), in addition to the OAS–RNase L pathway (*42*, *64*). Indeed, unlike WT THP-1 cells, MAVS KO THP-1 cells did not respond to intracellular poly(I:C) stimulation, and *RNASEL* gene KDn did not result in enhanced activation (Fig. 3C and fig. S5, D and E), confirming that the response to poly(I:C) is dependent on MAVS-mediated signaling in these cells. The enhancement of the intracellular poly(I:C) response after *RNASEL* KDn was partially attenuated in RIG-I or MDA5 KO THP-1 cells (Fig. 3C and fig. S5, D and E), suggesting that both dsRNA sensors may be involved. Another dsRNA agonist that specifically activates RIG-I, 5′ triphosphate double-stranded RNA (5′ppp-dsRNA), induced enhanced responses in RNase L KO THP-1 cells similar to those seen with poly(I:C) (Fig. 3D). By contrast, the activation of other sensing pathways, including the extracellular ssRNA-sensing toll-like receptor 7 (TLR7) and TLR8 pathways (R848), the TLR4 pathway (LPS), and the intracellular DNA agonist-sensing DAI pathway (ISD), resulted in responses in RNase L KO or KDn THP-1 cells that were similar to those of the parental WT cells (Fig. 3D and fig. S5F). Thus, the exaggerated inflammatory responses to cytosolic dsRNA observed in THP-1 cells deficient for OAS–RNase L appear to require RIG-I/MDA5 sensing and MAVS activation.

Activation of the OAS–RNase L pathway can suppress inflammatory responses in THP-1 cells

Intracellular dsRNA stimulates both the RIG-I/MDA5–MAVS and OAS–RNase L pathways (*42*, *63*, *64*). We therefore investigated whether the dsRNA-sensing MAVS-dependent signaling pathway was itself hyperactivated as a result of OAS–RNase L deficiency. After intracellular poly(I:C) stimulation, interferon regulatory factor 3 (IRF3) and nuclear factor κB (NF-κB) phosphorylation levels were similar in RNase L KO and WT THP-1 cells (Fig. 3E). Thus, the molecular mechanisms by which OAS–RNase L deficiency results in an exaggerated inflammatory response appears to involve an impairment of RNase L activation resulting in a lack of host RNA transcriptional and/or translational inhibition (*65*–*68*), rather than a hyperactivation of the MAVS-dependent pathways. Consistent with this hypothesis, treatment with exogenous 2-5A, which is normally generated by OASs upon dsRNA sensing and activates RNase L (*42*, *43*), rescued the inflammatory phenotype in OAS1 KO THP-1 cells after intracellular poly(I:C) stimulation (Fig. 3F). By contrast, dephosphorylated 2-5A, which is unable to activate RNase L (*69*, *70*), had no such effect (fig. S5G). Moreover, exogenous 2-5A treatment decreased the response to TLR7/8 activation in WT THP-1 cells (Fig. 3G). Treatment with 2-5A had a much weaker effect or even no suppressive effect in RNase L KDn or KO THP-1 cells (Fig. 3F and fig. S5, G and H). Thus, the exaggerated inflammatory response in OAS–RNase L–deficient mononuclear cells appears to result from the activation of the MAVS-dependent pathway (but not of other nucleic acid–sensing pathways) and an impairment of RNase L activation by OAS1- or OAS2-derived 2-5A after dsRNA sensing. This imbalance creates a phenotype that is probably a consequence of an impairment of the posttranscriptional activities of RNase L (*65*–*68*).

OAS–RNase L deficiencies result in an exaggerated inflammatory response to SARS-CoV-2 in THP-1 cells

We investigated whether OAS–RNase L deficiencies resulted in exaggerated inflammatory responses to SARS-CoV-2 in mononuclear phagocytes. Bulk RNA-seq on THP-1 cells with KO of OAS1, OAS2, or RNase L stimulated with intracellular poly(I:C) or SARS-CoV-2 revealed transcriptomic profiles different from those of the parental cells (Fig. 4, A and B, and fig. S6A). Gene set enrichment analysis (GSEA) against Hallmark gene sets (*71*) revealed an enrichment in genes relating to inflammatory responses and IFN-γ signaling in OAS–RNase L–deficient cells, showing that these cells displayed an exacerbated inflammatory response not only to synthetic dsRNA but also to SARS-CoV-2 (Fig. 4, C and D). Moreover, RNase L KO THP-1 cells had higher levels of IL-6 and CXCL10 secretion than WT cells when cocultured with SARS-CoV-2–infected Vero cells, which support SARS-CoV-2 replication (*72*, *73*) (Fig. 4E and fig. S6, B and C). Bulk RNA-seq further confirmed this observation at the transcriptome level (Fig. 4F and fig. S6D), revealing an enrichment in the expression of genes relating to inflammatory responses and IFN-α signaling in RNase L KO cells relative to WT cells (Fig. 4G). In addition, transfection with total RNA from SARS-CoV-2–infected Vero cells, but not from uninfected Vero cells, also induced enhanced responses in RNase L KO THP-1 cells relative to parental WT cells, with an enrichment in genes relating to inflammatory responses and IFN-γ signaling (Fig. 4H and fig. S6E). These findings suggest that OAS–RNase L deficiency results in excessive inflammatory responses in mononuclear phagocytes following both abortive SARS-CoV-2 infection and coculture with SARS-CoV-2–replicating cell types. This is likely due to defective activation of the OAS-RNase L pathway following the engulfment of the virus or infection-related by-products, leading to the release of dsRNA into the cytosol (*73*).

OAS–RNase L deficiencies result in an enhanced inflammatory response to intracellular dsRNA in primary mononuclear cells

We then studied the impact of OAS–RNase L deficiencies on the response to intracellular poly(I:C) stimulation in human peripheral blood mononuclear cells (PBMCs). Routine blood cell counts and immunotyping for the five patients revealed no significant abnormalities in blood leukocyte subsets, a result confirmed by deep immunophenotyping by mass cytometry [cytometry by time of flight (CyTOF)] (fig. S7A and table S2). After intracellular poly(I:C) stimulation, PBMCs from

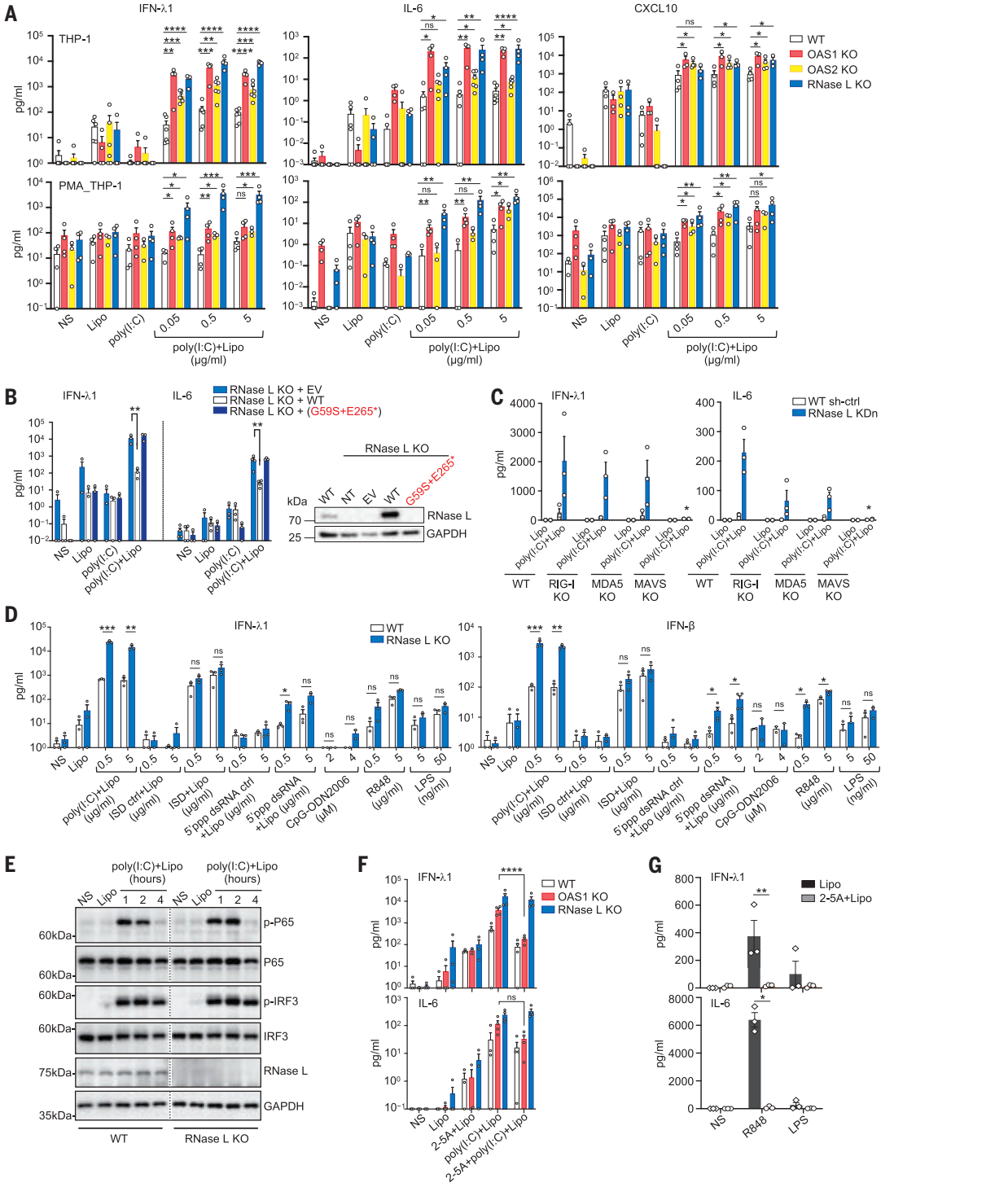

Fig. 3. Exaggerated inflammatory responses of OAS–RNase L-deficient THP-1 cells. (**A**) Concentrations of various cytokines in the supernatant of OAS1 KO, OAS2 KO, RNase L KO, or parental THP-1 cells (upper panels) or PMA-primed THP-1 cells (lower panels) treated as indicated for 24 hours. (**B**) IFN-λ1 and IL-6 concentrations in the supernatant of RNase L KO THP-1 cells transduced with the WT or P5's variant *RNASEL* cDNA, or empty vector (EV), and treated as indicated for 24 hours. On the right, RNase L protein levels, as assessed by immunoblotting. NT, not transfected. (**C**) IFN-λ1 and IL-6 concentrations in the supernatant of parental, RIG-I KO, MDA5 KO, or MAVS KO THP-1 cells with or without (WT sh-ctrl) RNase L knockdown (KDn), treated as indicated for 24 hours. (**D**) IFN-λ1 and IFN-β concentrations in the supernatant of parental or RNase L KO THP-1 cells, treated as indicated for 24 hours. (**E**) Immunoblot of phosphorylated P65 and IRF3 in parental and RNase L KO THP-1 cells treated as indicated. The results shown are representative of two independent experiments. (**F**) IFN-λ1 and IL-6 concentrations in the supernatant of parental, OAS1 KO, or RNase L KO THP-1 cells treated as indicated for 24 hours. (**G**) IFN-λ1 and IL-6 concentrations in WT THP-1 cells treated as indicated for 24 hours. In (A) to (D), (F), and (G), the data points are means ± SEM from three to five independent experiments with one to two technical replicates per experiment. Statistical analysis was performed as described in the methods. ns, not significant; **P* < 0.05, ***P* < 0.01, ****P* < 0.001, *****P* < 0.0001. NS, nonstimulated; Lipo, lipofectamine only; poly(I:C), extracellularly added poly(I:C); poly(I:C)+Lipo, intracellular poly(I:C) in the presence of lipofectamine; 2-5A+Lipo, intracellular 2-5A in the presence of lipofectamine; 2-5A+poly(I:C)+Lipo, intracellular poly(I:C) in addition to intracellular 2-5A.

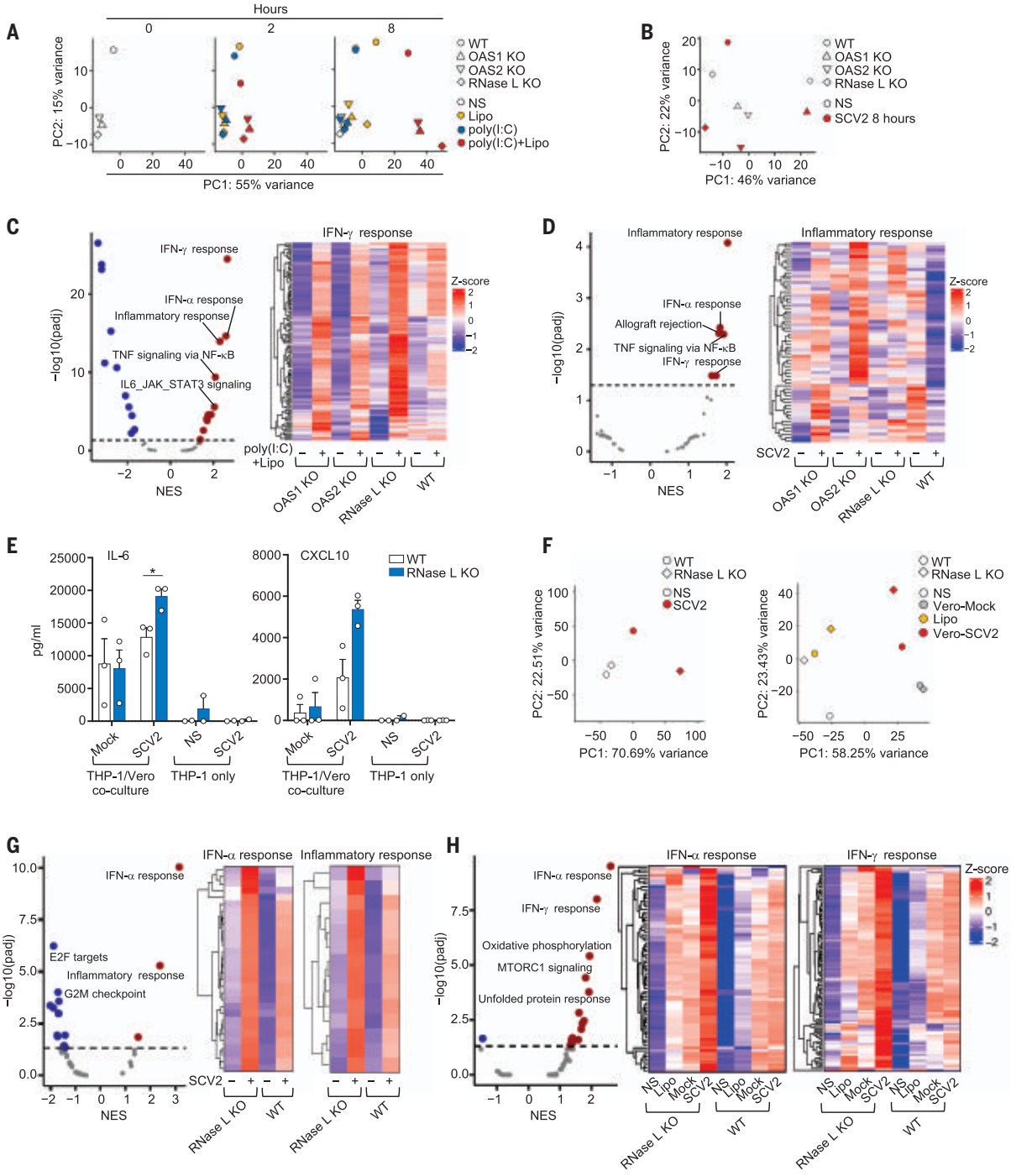

Fig. 4. Exaggerated inflammatory responses to SARS-CoV-2 of OAS–RNase L–deficient THP-1 cells. (**A** and **B**) PCA of RNA-seq–quantified gene expression for OAS1 KO, OAS2 KO, RNase L KO, and parental (WT) THP-1 cells left nonstimulated (NS), treated as indicated for 2 or 8 hours (A), or stimulated with SARS-CoV-2 (SCV2) at a MOI of 0.01 for 8 hours (B). (**C** and **D**) Differential expression analysis (DEA) and gene set enrichment analysis (GSEA) for genes induced by 8 hours of intracellular poly(I:C) stimulation (C) or by 8 hours of SCV2 stimulation (D). The OAS1 KO, OAS2 KO, and RNase L KO THP-1 cells were compared with parental (WT) THP-1 cells. Volcano plots show immune system–related pathways. NES, normalized enrichment score. Heatmaps show gene expression for the "IFN-γ response" (C) or "inflammatory response" (D) Hallmark gene sets. (**E**) IL-6 and CXCL10 concentrations in the supernatant of parental or RNase L KO THP-1 cells treated as indicated for 24 hours. The data points are means ± SEM from three independent experiments with three technical replicates per experiment. Statistical analysis was performed as described in the methods. *$P < 0.05$. (**F**) PCA of RNA-seq–quantified gene expression, for RNase L KO and parental THP-1 cells cocultured with Vero cells with or without SCV2 infection for 24 hours (left) or transfected for 8 hours with RNA from Vero cells with or without SCV2-infection (right). (**G** and **H**) DEA and GSEA for genes induced in RNase L KO THP-1 cells, compared with parental THP-1 cells after 24 hours of coculture with SCV2-infected or mock-infected Vero cells (G), or after 8 hours of transfection with RNA from SCV2-infected or mock-infected Vero cells (H). Volcano plots show immune system–related pathways. Heatmaps show gene expression for the indicated Hallmark gene sets. Heatmaps represent Z-score–scaled $\log_2$ read counts per million. NS, nonstimulated; Lipo, lipofectamine; SCV2, SARS-CoV-2.

P2 (OAS2 deficient), P3 (OAS2 deficient), and P5 (RNase L deficient) secreted larger amounts of the inflammatory cytokines studied than cells from healthy controls (Fig. 5A and fig. S7B). This enhanced inflammatory response to intracellular poly(I:C) stimulation was monocyte dependent, as the depletion of monocytes from the PBMCs of healthy controls strongly decreased this response (fig. S7C). Moreover, the shRNA-mediated KDn of *OAS1*, *OAS2*, or *RNASEL* in monocyte-derived dendritic cells (MDDCs) from healthy controls resulted in an enhanced inflammatory response to intracellular poly(I:C) stimulation, as shown by the higher levels of inflammatory cytokines, including IFN-λ1, IL-6, TNF, and IL-12, than were observed with WT parental cells (Fig. 5B). Thus, deficiencies of the OAS–RNase L pathway also result in exaggerated inflammatory responses to intracellular dsRNA stimulation in primary mononuclear phagocytes, or at least in monocytes and MDDCs.

Enhanced myeloid cell activation by SARS-CoV-2 in patient PBMCs

We studied the impact of OAS–RNase L deficiencies on the responses of the various PBMC populations to SARS-CoV-2 by performing single-cell RNA sequencing (scRNA-seq) on PBMCs from P1 (OAS1), P2 (OAS2), P3 (OAS2), and P5 (RNase L) and comparing the results with those for healthy controls. Regardless of genotype, 6 hours of stimulation with SARS-CoV-2 induced a strong immune response across all five major immune cell types including myeloid, B, $CD4^+$ T, $CD8^+$ T, and natural killer (NK) cells (Fig. 5C), with 1301 unique differentially expressed genes (DEGs) (data S1). OAS–RNase L deficiency significantly changed the response of 48 to 94% of the DEGs in each lineage, with myeloid cells being the most affected. Cellular responses were generally stronger in the OAS–RNase L–deficient patients and were essentially limited to the IFN-α and IFN-γ response pathways. Myeloid cell responses were characterized by a distinct proinflammatory component, such as *IL1B* and *CCL3*, that was stronger in OAS–RNase L–deficient cells (Fig. 5D and data S2). We then calculated pseudobulk estimates by cell type. Consistent with the single-cell observations, genes strongly up-regulated by SARS-CoV-2 in OAS–RNase L–deficient myeloid cells were enriched in types I and II IFN signature genes and TNF signature genes, whereas those strongly up-regulated in $CD4^+$ T cells were enriched in type I IFN signature genes (Fig. 5E). Thus, there is an exaggerated inflammatory response to intracellular dsRNA or extracellular SARS-CoV-2 stimulation in primary monocytes and other mononuclear phagocytes with deficiencies of the OAS–RNase L pathway cultured alone or with other PBMC populations. This provides a plausible pathogenic mechanism for MIS-C, in which this condition is driven by the exacerbated activation of mononuclear phagocytes. This hypothesis is also supported by scRNA-seq on PBMCs from P5 (RNase L deficient) collected during MIS-C and the convalescence period. Enhanced expression levels were observed for IFN-α, IFN-γ, or TNF signature genes in monocytes, myeloid dendritic cells (mDCs), B lymphocytes, plasmacytoid dendritic cells (pDCs), and activated T cells of P5 relative to healthy pediatric controls (Fig. 5, F and G, and fig. S8, A to D). Quantitatively inferred cell–cell communications (*74*) revealed that MIS-C in the RNase L–deficient patient was probably driven by a signal from hyperactivated monocytes and mDCs directed at $CD8^+$ αβ T cells (Fig. 5, H and I, and fig. S8, E to G). This situation differs from that observed in patients with COVID-19 pneumonia without MIS-C but is similar to reports for previously described MIS-C patients (fig. S9) (*33*, *34*, *36*), identifying exaggerated myeloid cell activation due to OAS–RNase L deficiency as the core driver of the immunological and clinical phenotypes of MIS-C in our patients.

Discussion

We report AR deficiencies of OAS1, OAS2, and RNase L as genetic etiologies of MIS-C in five unrelated children, corresponding to ~1% of the international cohort of patients studied. OAS–RNase L–deficient monocytic cell lines, monocyte-derived dendritic cells modeling patient genotypes, and primary monocytes from patients displayed excessive inflammatory responses to intracellular dsRNA, SARS-CoV-2, SARS-CoV-2–infected cells, and their RNA, providing a plausible mechanism for MIS-C. In these patients, MIS-C may result primarily from an excessive response of monocytes and other mononuclear phagocytes to SARS-CoV-2 dsRNA intermediates or by-products, followed by the presentation of a viral superantigen to T cells, resulting in the activation and expansion of $V\beta21.3^+$ $CD4^+$ and $CD8^+$ T cells. The molecular basis of the exacerbated inflammatory response to SARS-CoV-2 due to OAS–RNase L deficiency in mononuclear phagocytes involves an impairment of the activation of RNase L by the dsRNA-sensing molecules OAS1 and OAS2, probably resulting in defective post-transcriptional RNase L activity (*67*, *68*) and the unchecked RIG-I/MDA5–MAVS–mediated production of inflammatory cytokines. Alternative molecular mechanisms cannot be excluded (*64*, *75*). The SARS-CoV-2–related RNA products that trigger phagocyte activation, the viral superantigen(s) that activate T cells, and the human leukocyte antigen (HLA) restriction elements all remain to be discovered. Our findings also do not exclude the possibility that AR OAS–RNase L deficiency additionally affects antiviral responses in cells of other tissues injured during MIS-C, such as cardiomyocytes, enterocytes, and endothelial cells. The role of this pathway in T cells themselves merits further investigation. MIS-C in other patients may result from IEIs that may or may not be related to the OAS–RNase L pathway. Our findings also suggest that other forms of Kawasaki disease may be caused by other virus-specific IEIs in other patients (*15*).

The notion that the OAS–RNase L pathway is essential for antiviral immunity in mononuclear phagocytic cells was first proposed nearly 40 years ago (*60*). Intriguingly, the OAS–RNase L pathway is apparently dispensable for protective immunity to SARS-CoV-2 in the respiratory tract. None of the five MIS-C patients had a pulmonary phenotype, and no viral replication was detectable in the upper respiratory tract of any of the five children at the onset of MIS-C. Nevertheless, genome-wide association studies have suggested that common variants in the vicinity of *OAS1* may be weakly associated with COVID-19 severity (*10*, *11*, *53*, *76*–*79*). Our finding that the human OAS–RNase L pathway is crucial for regulation of the mononuclear phagocyte response to SARS-CoV-2, but not for SARS-CoV-2 restriction in the respiratory tract, suggests that the main protective action of this pathway is mediated by the control of phagocyte-driven systemic inflammation at a later stage of disease rather than viral restriction in the respiratory tract early on. These findings are also consistent with the discovery of germline gain-of-function *OAS1* mutations in humans with an autoinflammatory syndrome involving myeloid cells (*80*, *81*).

The five patients, now aged 1 to 15 years, are normally resistant to diseases caused by other common viruses. Since the discovery of the OAS–RNase L pathway in the 1970s (*65*, *82*, *83*), this pathway has been one of the most intensively studied type I IFN–inducible pathways (*42*, *84*). Biochemically, the three OASs have different subcellular distributions and different dsRNA optima for activation, they synthesize 2-5A of different lengths (*42*, *85*), and they appear to have antiviral activity against different viruses (*86*–*88*). The only well-established function of 2-5A is the activation of RNase L (*66*), and any of the three OASs appears to be sufficient for the biochemical activation of RNase L in human cells in vitro. RNase L has been shown to have antiviral activity against certain viruses (dengue virus and Sindbis virus), but not others (Zika virus), in murine and human cells in vitro (*85*, *89*). In vivo RNase L deficiency in mice drives susceptibility to various viruses (e.g., encephalomyocarditis virus, coxsackievirus B4, murine coronavirus, etc.) (*45*, *85*). Our data suggest that human OAS1, OAS2, and RNase L are each essential for the correct regulation of immunity to SARS-CoV-2 but are otherwise largely redundant in natural conditions of infection. It is also clear that the RNase L–dependent functions of OAS1 and

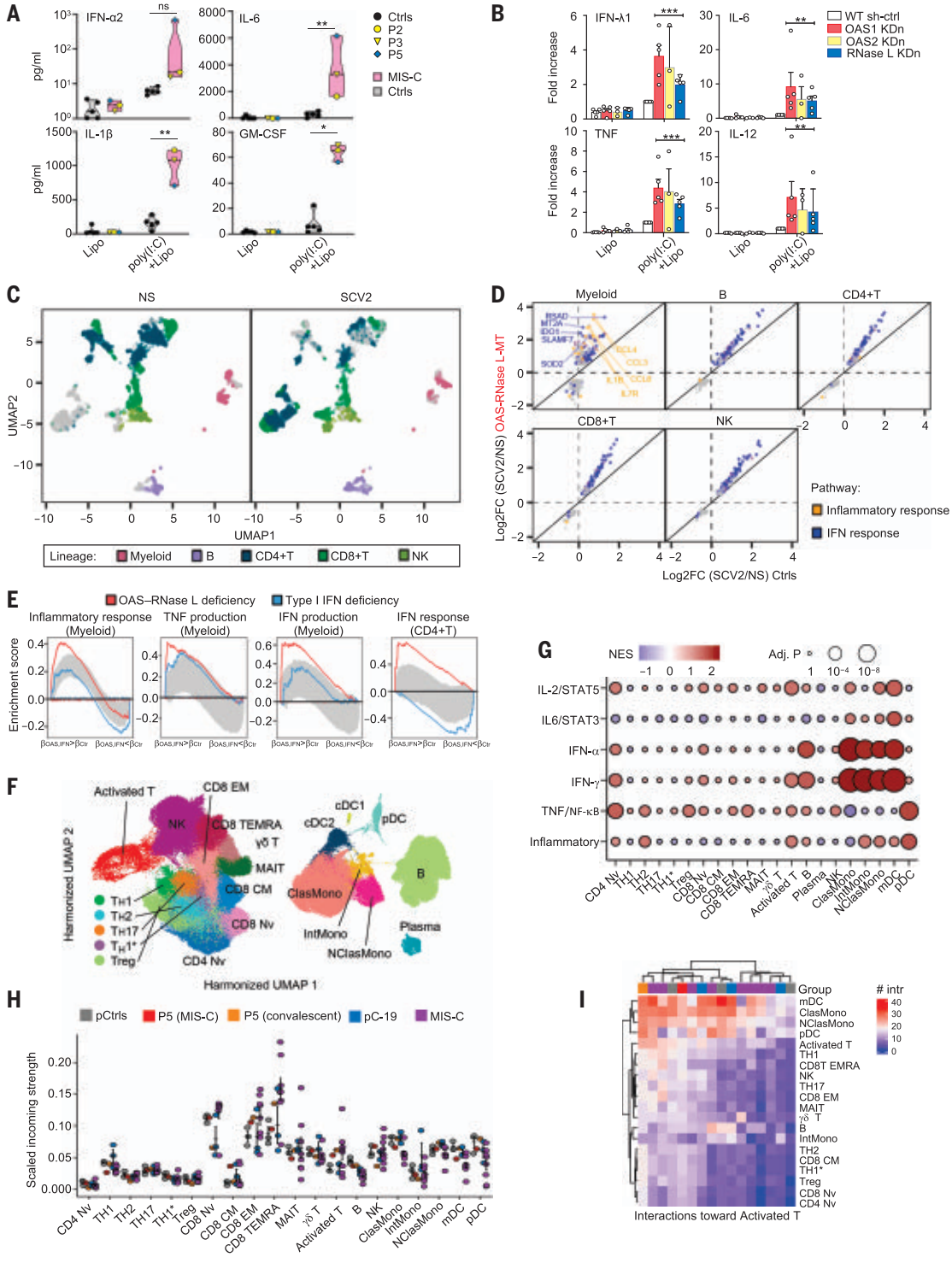

Fig. 5. Exaggerated myeloid cell activation in response to SARS-CoV-2 underlies MIS-C. (**A**) Concentrations of cytokines in the supernatant of PBMCs from OAS–RNase L–deficient patients (grouped in the pink violin zone) and three healthy pediatric and two healthy adult controls (Ctrls; gray violin zone). The data points are means of biological duplicates. (**B**) Fold-increase in the concentrations of cytokines in the supernatant of MDDCs with KDn of OAS1, OAS2, or RNase L, or transduced with control shRNA (WT sh-ctrl). The fold-change is expressed relative to the values for poly(I:C)+lipo-stimulated WT sh-ctrl cells. Data shown are means ± SEM from three independent experiments, with one to two technical replicates per experiment. For (A) and (B), statistical analysis was performed as described in the methods. NS, nonstimulated. ns, not significant; *P < 0.05, **P < 0.01, ***P < 0.001. (**C** to **E**) scRNA-seq of PBMCs from OAS–RNase L–deficient patients (OAS–RNase L-MT) or healthy controls after 6 hours of incubation with SARS-CoV-2 (SCV2) or mock infection (NS). (C) Uniform manifold approximation and projection (UMAP) of single PBMC transcriptomes. (D) Cell type–specific transcriptional responses. Genes passing the FDR < 0.01 and |log2FC| > 0.5 thresholds are shown. (E) GSEA of SCV2-induced genes across immune-related Hallmark gene sets. PBMCs from three patients with type I IFN pathway deficiency are controls for defective type I IFN responses. Gray zone highlights the expected enrichment scores under the null hypothesis (95% CI calculated over 100 randomized genes). (**F** to **I**) scRNA-seq of PBMCs from P5 and from healthy controls. A published dataset for pediatric patients with acute SARS-CoV-2 infection (pC-19) and MIS-C was also integrated. (F) UMAP of clustering analysis. (G) Pseudobulk differential expression analysis with GSEA. P5 (convalescent phase) was compared with local pediatric controls (pCtrls). Immune-related pathways are shown. [(H) and (I)] Intercellular communication analysis with CellChat. (H) Incoming signal strength and (I) the number of interactions for representative cell subsets.

OAS2 are crucial for the regulation of immunity to SARS-CoV-2 within the same cells, as the genetic deficiency of any of these three components results in the same immunological and clinical phenotype, namely MIS-C.

Materials and methods

Patients

We enrolled an international cohort of 558 MIS-C patients (aged 3 months to 19 years, 60.4% boys and 39.6% girls) originating from Europe, Africa, Asia, and America and living in 16 different countries. All patients met the WHO diagnostic criteria for MIS-C (*52*). We focus here on five of these patients (P1 to P5). Written informed consent was obtained

in the country of residence of each patient, in accordance with local regulations and with institutional review board (IRB) approval. Experiments were conducted in the United States and in France, in accordance with local regulations and with the approval of the IRB of the Rockefeller University and the Institut National de la Santé et de la Recherche Médicale, respectively. Approval was obtained from the French Ethics Committee (Comité de Protection des Personnes), the French National Agency for Medicine and Health Product Safety, the Institut National de la Santé et de la Recherche Médicale in Paris, France (protocol no. C10-13), and the Rockefeller University Institutional Review Board in New York, USA (protocol no. JCA-0700). For patients sequenced by National Institute of Allergy and Infectious Diseases (NIAID) through the American Genome Center (TAGC) other than the five patients described in this paper, written informed consent was obtained in the country of residence of each patient, in accordance with local regulations and with IRB approval: Ethics Committee of the Fondazione IRCCS Policlinico San Matteo, Pavia, Italy (protocol 20200037677); Comitato Etico Interaziendale A.O.U. Città della Salute e della Scienza di Torino, Turin, Italy (protocol 00282/2020); and IRB at Children's Hospital of Philadelphia (protocol 18-014863).

The five patients with MIS-C and AR deficiencies of the OAS–RNase L pathway—two boys and three girls—ranged in age from 3 months to 14 years at the time of diagnosis and all fulfilled the WHO criteria for MIS-C (Table 2) (*52*). They originated from the Philippines (P1), Spain (P2), Turkey (P3 and P4), and Canada (of French descent) (P5) and lived in Spain, Turkey, and Canada. P1 (*OAS1* mutation) (*29*), P3 (*OAS2*), and P4 (*OAS2*) had a severe course of MIS-C, with coronary aneurysm, myocarditis, and polyneuropathy, respectively. P2 (*OAS2*) and P5 (*RNASEL*) had a milder course of MIS-C, with a typical Kawasaki disease presentation. None of these patients presented any clinical or radiological evidence of pneumonia. Cytokine profiling of serum obtained from P1, P2, and P5 during MIS-C revealed high levels of IFN-γ, soluble CD25, IL-18, IL-1RA, and MCP1 (CCL2) (Fig. 1G), consistent with previously published immune profiles of MIS-C and in contrast to those for pulmonary COVID-19 (*21*). Bulk mRNA sequencing (RNA-seq) of whole-blood RNA from P1 and P2 collected during the MIS-C phase revealed transcriptomic signatures clearly different from those of healthy controls and a pediatric case of acute COVID-19 pneumonia, but similar to those of previously reported MIS-C patients (Fig. 1H) (*33*). T cell receptor Vβ repertoire analysis confirmed the expansion of *TRBV 11-2* (encoding Vβ21.3) in one of the three MIS-C–phase samples available (P5, with AR RNase L deficiency) (Fig. 1I). The clinical and immunological features of the five patients were, therefore, consistent with those previously reported for other MIS-C patients (*21*, *22*, *26*–*36*).

Whole-exome, whole-genome, and Sanger sequencing

Genomic DNA was extracted from whole blood. Whole-exome sequencing (WES) or whole-genome sequencing (WGS) was performed at several sequencing centers, including the Genomics Core Facility of the Imagine Institute (Paris, France), the Yale Center for Genome Analysis (USA), the New York Genome Center (NY, USA), the American Genome Center (TAGC, Uniformed Services University of the Health Sciences, Bethesda, USA), and the Genomics Division–Institute of Technology and Renewable Energies (ITER) of the Canarian Health System sequencing hub (Canary Islands, Spain). More technical details are provided in the supplementary materials. For the Sanger sequencing of *OAS1*, *OAS2*, and *RNASEL* variants, the relevant regions of *OAS1*, *OAS2*, and *RNASEL* were amplified by PCR, purified by ultracentrifugation through Sephadex G-50 Superfine resin (Amersham-Pharmacia-Biotech), and sequenced with the Big Dye Terminator Cycle Sequencing Kit on an ABI Prism 3700 apparatus (Applied Biosystems).

Whole-exome sequencing data analysis

We performed an enrichment analysis focusing on the three candidate genes in our cohort of 558 MIS-C patients and 1288 children and adults with asymptomatic or paucisymptomatic SARS-CoV-2 infection (controls). We considered variants that were predicted to be loss-of-function or missense, with a highest population MAF < 0.01, not included in segmental duplication regions (gnomAD v2.1.1). We considered genes corresponding to the Gene Ontology term "response to virus" (GO:0009615), with a gene damage index of <13.83 (*41*), corresponding to the 90% least-damaged genes. We searched for all homozygous variants in MIS-C patients, SARS-CoV-2–infected controls, and the gnomAD database. We compared the proportions of patients and controls carrying experimentally confirmed deleterious homozygous variants by means of a logistic regression model, accounting for the ethnic heterogeneity of the cohorts by including the first five principal components of the principal components analysis (PCA), and for data heterogeneity (WGS and WES with various kits and calling processes) by including the two first PCs of a PCA on individual sequence-quality parameters, as previously described (*9*). The PCA for ethnic heterogeneity was performed with PLINK (v1.9) on WES and WGS data, with the 1000 Genomes Project phase 3 public database as a reference, using >15,000 exonic variants with a MAF > 0.01 and a call rate > 0.99. The PCA for data heterogeneity was performed with the R FactoMineR package and the following individual sequence quality parameters calculated with bcftools stats: number of alleles, number of ALT alleles, number of heterozygous variants, Ts/Tv ratio, number of indels, mean depth of coverage, number of singletons, and number of missing genotypes. We also compared the frequency of experimentally confirmed deleterious homozygous variants of the three genes between our MIS-C cohort and gnomAD using Fisher's exact test.

Cell culture

Primary cultures of human fibroblasts were established from skin biopsy specimens from patients or healthy controls. They were transformed with an SV40 vector, as previously described (*56*), to create immortalized SV40-fibroblast cell lines. SV40-fibroblasts, human embryonic kidney 293T (HEK293T) cells, and A549 cells were cultured in Dulbecco's modified essential medium (DMEM; GIBCO) with 10% fetal bovine serum (FBS) (GIBCO). THP-1 cells were cultured in RPMI 1640 medium (GIBCO) with 10% FBS. For the generation of phorbol-12-myristate-13-acetate (PMA)–primed THP-1–derived macrophages, THP-1 cells were incubated with 50 ng/ml of PMA for 48 hours then left without PMA overnight before stimulation. PBMCs were cultured in RPMI 1640 medium (GIBCO) with 10% FBS. For intracellular poly(I:C) or SARS-CoV-2 stimulation of the PBMCs, blood samples were obtained from the OAS–RNase L–deficient patients 2 months to 1 year after acute-phase MIS-C and from five healthy controls with (two pediatric controls and one adult control) or without (one pediatric control and one adult control) prior asymptomatic or mild SARS-CoV-2 infection ~6 months before sample collection. For the differentiation of monocyte-derived dendritic cells, monocytes were isolated from PBMCs with the Pan Monocyte Isolation kit (Miltenyi Biotec) and cultured with 50 ng/ml of recombinant human granulocyte-macrophage colony-stimulating factor (GM-CSF; PeproTech) and 20 ng/ml of recombinant human IL-13 (PeproTech) for 7 days before cell stimulation experiments.

Plasmids

For overexpression studies in HEK293T cells, WT cDNAs for *OAS1* and *RNASEL* in a pCMV6 backbone were purchased from Origene. For rRNA degradation assays, human *OAS1* (GenBank accession no. BC071981.1), *OAS2* (GenBank accession no. BC049215.1), *OAS3* (GenBank accession no. BC113746), and *RNASEL* (GenBank accession no. L10381.1) cDNAs were inserted into p3X-FLAG-CMV-10 (Sigma) as previously described (*75*, *88*). Patient-specific variants or variants from the gnomAD database were

generated by site-directed mutagenesis PCR with the Super Pfx DNA Polymerase (CWbio). For stable lentivirus-mediated transduction with *ACE2* and *RNASEL*, cDNAs for WT and patient-specific *ACE2* or *RNASEL* variants were inserted into pTRIP-SFFV-CD271-P2A, a modified pTRIP-SFFV-mtagBFP-2A (Addgene 102585) in which mtagBFP is replaced with CD271, with InFusion (Takara Bio), according to the manufacturer's instructions. We used the XhoI and BamHI restriction sites. For stable lentivirus-mediated transduction with *OAS1* and *OAS2*, cDNAs for WT and patient-specific *OAS1* or *OAS2* variants were inserted into a modified pSCRPSY vector (KT368137.1) with a PaqCI cutting site expressing blue fluorescent protein (BFP). The PaqCI site was used for cDNA insertion with InFusion. We checked the entire sequences of the *OAS1*, *OAS2*, *OAS3*, and *RNASEL* cDNAs in the plasmids by Sanger sequencing.

Cell-free system assays of OAS and RNase L activity

Assays for OAS and RNase L activity were performed with a modified cell-free system assay based on HeLa M cells (*49*, *50*). The HeLa M cells were cultured in DMEM with 10% FBS, and their identity was confirmed by the presence of short tandem repeat loci with a 94.12% match to HeLa cells (ATCC CCL2, Genetica, Burlington, NC). We previously reported that HeLa M cells have no RNase L expression (*51*). Cells were plated in 24-well dishes (6×10^4 cells per well) with empty vector (p3X-FLAG-CMV-10) or vector containing WT or mutant human *OAS1* (GenBank accession no. BC071981.1), *OAS2* (GenBank accession no. BC049215.1), *OAS3* (GenBank accession no. BC113746), or *RNASEL* (GenBank accession no. L10381.1) cDNAs. HeLa M cells were cotransfected with cDNAs in the presence of Lipofectamine 2000 for 20 hours. Conditions were optimized for each type of enzyme assayed. RNase L assays were performed on cells cotransfected with 300 ng of WT or mutant *RNASEL* cDNA and 100 ng of WT *OAS3* cDNA. *OAS1* assays were performed with 300 ng of *OAS1* cDNA and 100 ng of *RNASEL* cDNA. OAS2 assays were performed with 300 ng (condition 1) or 600 ng (condition 2) of *OAS2* cDNA and 100 ng of *RNASEL* cDNA, and *OAS3* assays were performed with 300 ng of *OAS3* cDNA and 100 ng of *RNASEL* cDNA. The lysis-activation-reaction (LAR) buffer contained 0.1% (by volume) Nonidet P-40, 50 mM Tris-HCl pH 7.5, 0.15 M NaCl, 2 mM EDTA, 10 mM $MgCl_2$, 2 mM ATP, 400 U/ml of RNaseOUT (Thermo Fisher Scientific), and 2.5 μg/ml of poly(I):poly(C) (Millipore catalog no. 528906). LAR buffer (75 μl) was added to each well of cells on ice and the contents of the wells were then transferred to tubes on ice. The lysates were then incubated at 30°C for 30 min, except in OAS2 assays, for which lysates were incubated at 37°C (condition 1) or 30°C (condition 2) for 40 and 50 min, respectively. Total RNA was isolated with RLT buffer supplemented with guanidinium isothiocyanate and the EZ-10 Spin Columns Total RNA Minipreps Super kit (BIO BASIC). RNA was separated on RNA chips with an Agilent Bioanalyzer 2000, from which images and RNA integrity numbers (RINs) were obtained. For immunoblots, aliquots of the lysates (10 μg of protein) were separated by SDS–polyacrylamide gel electrophoresis (SDS-PAGE) in a 7% acrylamide gel. Immunoblots were probed with a monoclonal antibody against the Flag epitope or β-actin (Sigma-Aldrich).

FRET-based OAS enzyme assays

FRET assays of the amount of 2-5A synthesized by WT and mutant isoforms of OAS1 or OAS2 were performed with lysates of transfected HeLa M cells (*90*). Cells were plated in 24-well dishes (6×10^4 cells per well), cultured for 24 hours and transfected for 20 hours with Lipofectamine 2000 transfection reagent (Thermo Fisher Scientific) and 0.5 μg empty vector (p3X-FLAG-CMV-10), or 500 ng of vector containing WT or mutant OAS1 or OAS2. Cells were washed with cold PBS and then lysed with 100 μl of LAR buffer [containing ATP and poly(I:C)] per well on ice. The lysates were transferred to tubes on ice and incubated at 30°C for 50 min before heating at 95°C for 10 min (to stop the reaction and denature proteins) and vortexing twice. The lysates were centrifuged at 12,000*g* for 10 min. The supernatants were then collected and diluted 10-fold in H_2O. Diluted samples (2 μl) were added to 45 μl of cleavage buffer (25 mM Tris-HCl, pH 7.4, 0.1 M KCl, 10 mM $MgCl_2$, 50 μM ATP pH 7.4, and 7 mM β-mercaptoethanol) containing 40 nM RNase L and 135 nM FRET probe in 96-well plates. The probe used was a 36-nucleotide synthetic oligoribonucleotide probe with multiple RNase L cleavage sites, a fluorophore (6-FAM or 6-carboxyfluorescein) at the 5′ terminus, and the black hole quencher-1 (BHQ1) at the 3′ terminus (IDT, Inc.) (*90*). FRET assays were performed at room temperature, every 5 min, for 30 min. Fluorescence was measured in relative fluorescence units (RFU), with excitation at 485 nm and emission at 535 nm, with a Varioskan LUX multimode microplate reader and Skanit version 6.0.1 software (Thermo Fisher Scientific). There were six biological replicates for each treatment group. Standard curves were plotted in triplicate with 0.1 to 30 nM ppp5′A2′p5′A2′p5′A (trimer 2-5A) synthesized with isolated OAS1 and purified by high-performance liquid chromatography (HPLC) (*70*).

Cytokine quantification in plasma samples

Cytokine quantification in plasma samples was performed as previously described (*32*). Briefly, whole blood was sampled into EDTA tubes. The plasma concentrations of IFN-γ, IL-1RA, IL-10, IL-18, IL-6, MCP-1, soluble CD25, and TNF were then determined with Simpleplex technology and an ELLA instrument (Protein Simple) according to the manufacturer's instructions. Plasma IFN-α concentrations were determined with a single-molecule array (Simoa) on an HD-1 Analyzer (Quanterix) with a commercial kit for IFN-α2 quantification (Quanterix). Blood samples from P1, P2, and P5 were obtained on days 7, 4, and 9 after symptom onset, respectively.

TRBV 11-2 relative expression levels

Whole blood was collected into PAXgene (BD Biosciences) or Tempus (Thermo Fisher Scientific) blood RNA tubes or EDTA tubes. RNA was extracted with the corresponding RNA extraction kits or with the Maxwell 16 LEV Blood RNA kit and a Maxwell extractor (Promega) and quantified by spectrometry (Nanovue). For P5, RNA was extracted from sorted T cells with the RNeasy Plus microkit (Qiagen). Relative expression levels were determined for *TRBV 11-2* with nCounter analysis technology (NanoString Technologies), by calculating *TRBV 11-2* mRNA levels relative to other *TRBV* mRNA levels and normalizing against the median value for the healthy volunteer group. Blood samples from P1, P2, and P5 were obtained on days 7, 4, and 9 after symptom onset, respectively.

Immunoblots

Total protein extracts were prepared by lysing cells in NP40 lysis buffer (150 mM NaCl, 50 mM Tris pH 8.0, and 1.0% NP40) supplemented with cOmplete Protease Inhibitor cocktail (Roche, Mannheim, Germany). Equal amounts of protein from each sample were subjected to SDS-PAGE, and the proteins were blotted onto polyvinylidene difluoride membranes (Bio-Rad). The membranes were then probed with the desired primary antibody followed by the appropriate secondary antibody. Primary antibodies against the following targets were used: Flag tag (Sigma-Aldrich, cat: F1804), human OAS1 (Cell Signaling, cat: 14498), OAS2 (Proteintech, cat: 19279-1-AP), RNase L (Cell Signaling, cat: 27281), RIG-I (Cell Signaling, cat: 3743), MDA5 (Cell Signaling, cat: 5321), MAVS (Cell Signaling, cat: 3993), phospho-IRF3 (Cell Signaling, cat: 4947), total IRF3 (Cell Signaling, cat: 11904), phospho-p65 (Cell Signaling, cat: 3033), and total p65 (Santa Cruz, cat: sc-372). Membranes were probed with a horseradish peroxidase (HRP)–conjugated antibody against GAPDH (Proteintech, cat: HRP-60004), as a protein loading control. Antibody binding was detected by enhanced chemiluminescence (Thermo Fisher Scientific).

RT-qPCR

Total RNA was extracted from THP-1 cells and various other cell types with the Quick-RNA MicroPrep kit (Zymo Research). RNA was

reverse-transcribed with random hexamers and the Superscript III first-strand cDNA synthesis system (Invitrogen). Quantitative real-time PCR was then performed with the TaqMan universal PCR master mix (Applied Biosystems). For gene expression assays, TaqMan probes for *OAS1*, *OAS2*, *OAS3*, *RNASEL*, *IL6*, and *CXCL9* were used (Thermo Fisher Scientific). We used β-glucuronidase (*GUSB*) for normalization (Applied Biosystems). The results were analyzed with the ΔCt or ΔΔCt method. For SARS-CoV-2 genomic RNA quantification, RNA was extracted from 3×10^5 THP-1 cells infected with SARS-CoV-2 for 24 hours. Cells were washed three times with PBS and lysed for RNA extraction. Equal amounts of total RNA were reverse-transcribed with random hexamers and the Superscript III first-strand cDNA synthesis kit (Invitrogen). Equal amounts of cDNA were used for the qPCR reaction. Primers and probes for the N gene (N2 region), the RNA-dependent RNA polymerase (RdRP) gene, and their respective standards were purchased from IDT technologies. All qPCR reactions were analyzed with the QuantStudio 3 system.

Gene knockout

OAS1 knockout THP-1 cells and the parental WT cells were kindly provided by W.-B. Lee (*62*). The THP-1 cells with knockouts for RIG-I, MDA5, and MAVS were purchased from Invivogen. A549 KO cells were kindly provided by S. Weiss (*55*). For the generation of OAS2 and RNase L KO THP-1 cells, a set of three single-guide RNAs for *OAS2* or *RNASEL* (Synthego) were combined with TrueCut Cas9 protein v2 (Invitrogen) and used for the nucleofection of the cells with Cell Line Nucleofection kit V (Lonza) and AMAXA Nucleofector 2b (Lonza), according to the manufacturer's instructions. The cells were cultured for several days and then plated at clonal density in 96-well plates and amplified. Genomic DNA was extracted from multiple clones, and genomic regions of ~450 bp around the *OAS2* or *RNASEL* single guide RNAs were subjected to Sanger sequencing. The absence of the protein was confirmed by immunoblotting. The loss of RNase L activity in RNase L KO THP-1 cells was confirmed in an rRNA degradation assay. The sequences of the guide RNAs for OAS2 and RNase L knockouts were 5′-AGCUGAGAGCAAUGGGAAAU-3′, 5′-UCAGACACUGAUCGACGAGA-3′, and 5′-UGCACCAGGGGGAACUGUUC-3′ (*OAS2*); and 5′-GCAGUGGAGAAGAAGCACUU-3′, 5′-GCAGGUGGCAUUUACCGUCA-3′, and 5′-UUUGACCUUACCAUACACAG-3′ (*RNASEL*). The sequencing primers were 5′-CAGTTTCAGTTTCCTGGCTCTGG-3′ and 5′-GCACATAATAGGCACCCAGCAC-3′ for *OAS2* and 5′-CTCTGTTGCCAGAGAATCCCAATTTAC-3′, 5′-CAATCGCTGCGAGGATAAAAGG-3′, 5′-GAGCGTGAAGCTGCTGAAAC-3′, and 5′-TGTACTGGCTCCACGTTTG-3′ for *RNASEL*.

Gene knockdown

The shRNA-mediated silencing experiments were performed with GIPZ (Horizon Discovery) lentiviral vectors encoding microRNA-adapted shRNAs targeting the open reading frame of *OAS1* (catalog nos. 200201641 and 200293786), *OAS2* (200260991 and 200255637), and *RNASEL* (200226261 and 200226578), or a nonsilencing control shRNA (RHS4346). Lentiviral particles encoding shRNA were generated by the transient transfection of HEK293T cells with lentiviral GIPZ vectors and a mixture of packaging plasmids with X-tremeGENE 9 transfection reagent, used according to the manufacturer's instructions. Briefly, HEK293T cells at 80 to 90% confluence in a six-well plate were transfected with 1.5 μg of the lentiviral vector GIPZ, 1 μg of the packaging plasmid (psPAX2, Addgene), and 0.5 μg of the envelope plasmid (pMD2G, Addgene). The medium was changed the following day, and the virus-containing supernatant was collected 48 hours after transfection, passed through a filter with 0.45-μm pores, and used directly for cell transduction or stored at −80°C.

For the transduction of THP-1 cells, the cells were incubated with supernatants containing the lentiviral particles. The medium was replaced with fresh medium the following day, and puromycin was added 3 days after transduction, to a final concentration of 2 μg/ml. Protein production was analyzed by immunoblotting after 4 days of selection. All the experiments were performed between days 7 and 14 after transduction.

For shRNA-mediated knockdown experiments in primary monocyte-derived dendritic cells (MDDCs), a high transduction efficiency (>60% GFP^+ cells) was achieved by cotransduction with shRNA-encoding lentiviral particles and virion-like particles (VLPs) carrying the SIV viral protein Vpx (VLP-Vpx). Vpx suppresses the SAMHD1-mediated restriction of lentiviral reverse transcription in myeloid cells. VLP-Vpx were produced by transfecting HEK293T cells with 1.5 μg of the packaging vector SIV3+ (derived from SIVmac251) and 0.5 μg of the envelope plasmid pMD2G with XtremeGENE9. Monocytes were isolated from PBMCs from healthy donors by negative selection with the Pan Monocyte Isolation Kit (Miltenyi Biotec). Freshly purified monocytes were transduced with shRNA-encoding lentiviral particles and VLP-Vpx in the presence of protamine (8 μg/ml). Transduced cells were allowed to differentiate into MDDCs in the presence of recombinant human GM-CSF (10 ng/ml) and IL-4 (25 ng/ml) for 5 days.

Lentiviral transduction

HEK293T cells were dispensed into a six-well plate at a density of 8×10^5 cells per well. The next day, cells were transfected with pCMV-VSV-G (0.2 μg), pHXB2-env (0.2 μg; NIH-AIDS Reagent Program; 1069), psPAX2 (1 μg; Addgene plasmid no. 12260), and either pTRIP-SFFV-CD271-P2A empty vector or encoding the protein of interest (1.6 μg) in Opti-MEM (Gibco; 300 μl) containing X-tremeGENE 9 (Sigma Aldrich; 10 μl), according to the manufacturer's instructions. After 6 hours, the medium was replaced with 3 ml of fresh culture medium, and the cells were incubated for a further 24 hours for lentiviral particle production. The viral supernatant was collected and passed through a syringe filter with 0.2-μm pores (Pall) to remove debris. Protamine sulfate (Sigma; 10 μg/ml) was added to the supernatant, which was then used immediately or stored at −80°C until use.

For the transduction of THP-1 cells with *OAS1*, *OAS2*, or *RNASEL*, the corresponding gene KO THP-1 cells were dispensed into a 12-well plate at a density of 1×10^6 cells per well, in 500 μl of culture medium per well. Viral supernatant was then added (500 μl per well) the next day. For the transduction of SV40-fibroblasts with ACE2, healthy control or patient-specific SV40-fibroblasts were used to seed six-well plates at a density of 5×10^5 cells per well. Viral supernatant was added (500 μl per well) the next day. The cells were then incubated for a further 48 hours at 37°C. Transduction efficiency was evaluated by surface staining for CD271 (Miltenyi Biotec) for the pTRIP vector, or by flow cytometry to evaluate BFP expression levels for the pSCRPSY vector. MACS column separation was performed with selection beads for CD271-positive cells (Miltenyi Biotec) if the proportion of CD271-positive cells was <80%. Cells transduced with the pSCRPSY vector were selected with puromycin or by flow cytometry. Protein production was subsequently validated by immunoblotting.

SARS-CoV-2 infection

The SARS-CoV-2 NYC isolate was obtained from the saliva of a deidentified patient on 28 July 2020. The sequence of the virus is publicly available (GenBank OM345241). The virus isolate was initially amplified in Caco-2 cells (passage 1, or P#1 stock). For the generation of P#2 and P#3 working stocks, Caco-2 cells were infected with the P#1 and P#2 viruses, respectively, at a multiplicity of infection (MOI) of 0.05 plaque-forming units (PFU)/cell and incubated for 6 and 7 days, respectively, at 37°C. The virus-containing supernatant was then harvested, clarified by centrifugation (3000*g* for 10 min), and filtered through a disposable vacuum filter system with 0.22-μm pores. The P#3 stock used in this study had a titer of 3.4×10^6 PFU/ml determined on Vero E6 cells with a 1% methylcellulose overlay, as previously described (*72*).

A549 + ACE2/TMPSS2 cells, human SV40-fibroblasts + ACE2, or THP-1 cells were used to seed 96-well plates at a density of 1.5×10^4 cells per well, 4×10^3 cells per well, and 1×10^5

cells per well, respectively, in the presence or absence of IFN-α2b at a concentration of 1000 IU/ml. The cells were infected with SARS-CoV-2 24 hours later by directly adding 10 μl of virus stock at various dilutions to the wells (final volume: 110 μl). Cells were infected for 24, 48, or 72 hours. The cells were fixed with neutral buffered formalin at a final concentration of 10% and stained for SARS-CoV-2 with an anti-N antibody (catalog no. GTX135357; GeneTex). An Alexa Fluor 488- or Alexa Fluor 647-conjugated secondary antibody (Invitrogen) was used. Plates were imaged with an ImageXpress micro XL and analyzed with MetaXpress (Molecular Devices).

Cell stimulation

THP-1 cells were used to coat a 96-well plate at a density of 1×10^5 cells per 100 μl of culture medium. For stimulations of PBMCs and MDDCs, we used 1×10^5 cells and 5×10^5 cells per 100 μl of culture medium, respectively. The cells were stimulated with the indicated stimulus at the specified concentrations, with or without lipofectamine 2000 (Invitrogen), according to the manufacturer's instructions. Poly(I:C), 5′ppp-dsRNA, 5′ppp-dsRNA control, ISD, ISD control, R848, CPG-ODN2006, and LPS were purchased from Invivogen. For exogenous 2′5′-linked oligoadenylate (2-5A) or dephosphorylated 2-5A, we used 20 μM of 2-5A for transfection in the presence of lipofectamine simultaneously with the other stimuli [poly(I:C), R848, or LPS]. Dephosphorylated 2-5A (A2′p5′A2′p5′A) was prepared by treating 2-5A with shrimp alkaline phosphatase (SAP) (Thermo Fisher Science) to remove the 5′-triphosphoryl group from 2-5A, rendering it unable to activate RNase L (*69*, *70*). The dephosphorylation reaction mixture contained 5 mM 2-5A incubated with five units of SAP at 37°C for 1 hour, according to the manufacturer's protocol. Samples were denatured by incubation at 95°C for 5 min. Supernatants containing dephosphorylated 2′,5′-A3 were removed after centrifugation at 18,000*g* for 15 min at 4°C. Dephosphorylated 2-5A was then validated by HPLC and FRET assays for RNase L activity. After cell stimulation, the cells or supernatants were harvested, and their cytokine mRNA and protein levels were assessed by RT-qPCR and with a multiplex bead assay (BioLegend), respectively.

Detection of secreted cytokines in a multiplex bead assay

The harvested supernatants of stimulated THP-1 cells, PBMCs, and other types of cells were prepared and used for the LEGENDplex multiplex bead assay (BioLegend), according to the manufacturer's instructions. Samples were analyzed by flow cytometry on an Attune NxT flow cytometer, according to the manufacturer's instructions. Data were analyzed with LEGENDplex Cloud-based Data Analysis Software.

Luciferase assay

THP-1 cells expressing an ISRE-lucia luciferase reporter gene were purchased from Invivogen (THP1-Dual). Cells were stimulated according to the conditions specified above. The supernatant was collected and used for the luciferase assay in accordance with the manufacturer's instructions.

Coculture of THP-1 and SARS-CoV-2–infected cells

Vero cells were plated in a six-well plate and infected at a MOI of 0.05 (as determined by plaque assay on Vero E6 cells) for a total of 48 hours. The supernatant of the infected cells was carefully removed, and the infected cells were then transferred to fresh THP-1 culture medium. A fixed volume of the resulting cell suspension was then dispensed onto WT or RNase L KO THP-1 cells plated in a 96-well plate at a density of 1×10^5 cells in 100 μl. THP-1 cells stimulated with SARS-CoV-2 only were stimulated in parallel for 24 hours. THP-1 cells were stimulated for a total of 24 hours before collection of the supernatant for cytokine determinations and cells for total RNA extraction.

Transfection of THP-1 cells with RNA from SARS-CoV-2–infected cells

Total RNA was extracted from mock-infected Vero cells or Vero cells infected with SARS-CoV-2 at a MOI of 0.05 for a total of 72 hours. THP-1 cells were transfected with 2 μg/ml of total RNA extract for 8 hours. THP-1 cells were then collected for total RNA extraction.

Deep immunophenotyping by mass cytometry (CyTOF)

CyTOF was performed on whole blood with the Maxpar Direct Immune Profiling Assay (Fluidigm), according to the manufacturer's instructions, as previously described (*7*). Cells were frozen at −80°C after overnight staining to eliminate dead cells, and acquisition was performed on a Helios machine (Fluidigm). The antibodies used for staining are listed in table S3. All the samples were processed within 24 hours of sampling. Data analysis was performed with OMIQ software.

Bulk RNA sequencing (RNA-seq)

Total RNA was extracted from THP-1 cells or sorted blood cell populations. Cells were left untreated or were stimulated with poly(I:C) in the presence of lipofectamine or infected with SARS-CoV-2. RNA was extracted with the Quick-RNA MicroPrep kit (Zymo Research) or the RNeasy Micro Kit (Qiagen) and treated with DNase I (Zymo Research and Qiagen) to remove residual genomic DNA. RNA-seq libraries were prepared with the Illumina RiboZero TruSeq Stranded Total RNA Library Prep Kit (Illumina) and sequenced on the Illumina NovaSeq platform in the 100 nucleotide, paired-end configuration. Each library was sequenced twice.

The RNA-seq FASTQ files were first inspected with fastqc to ensure that the raw data were of high quality. The sequencing reads of each FASTQ file were then aligned with the GENCODE human reference genome GRCh37.p13 with STAR aligner v2.6 and the alignment quality of each BAM file was evaluated with RSeQC. Reads were quantified with featureCounts v1.6.0 to generate gene-level feature counts from the read alignment, based on GENCODE GRCh37.p13 gene annotation. The gene-level feature counts were then normalized and $\log_2$-transformed with DESeq2, to obtain gene expression values for all genes and all samples. Differential gene expression analyses were conducted by contrasting the intracellular poly(I:C)-stimulated samples or the SARS-CoV-2–infected samples with the nonstimulated samples. For each gene expression analysis, we performed trimmed mean of M values (TMM) normalization and gene-wise generalized linear model regression by edgeR, and the genes displaying significant differential expression were selected according to the following criteria: FDR ≤ 0.05 and |log2(FoldChange)| ≥ 1. Differential gene expression was plotted as a heatmap with ComplexHeatmap, and genes and samples were clustered according to complete linkage and the Euclidean distances of gene expression values. GSEA was conducted with the fgsea package, by projecting the ranking of fold-change in expression onto the Hallmark gene sets (*71*).

Single-cell RNA sequencing of PBMCs

We performed scRNA-seq on SARS-CoV-2– and mock-stimulated PBMCs sampled from four individuals with inborn errors of the OAS–RNaseL pathway (P1 with OAS1 deficiency, P2 and P3 with OAS2 deficiency, P5 with RNase L deficiency), three individuals with inborn errors of type I IFN immunity, and eight healthy donors—one pediatric control and one adult control with a history of past asymptomatic SARS-CoV-2 infection, and two pediatric controls and four adult controls with no history of prior SARS-CoV-2 infection. The cryopreserved PBMCs were thawed, stimulated, and processed for scRNA-seq. Across all samples, we captured 46,157 high-quality single-cell transcriptomes that were classified into five major immune cell lineages: myeloid, B, $CD4^+$ T, $CD8^+$ T, and NK cells. The data were then analyzed as described in detail in the supplementary materials.

We also performed scRNA-seq on cryopreserved PBMCs from P5 (RNase L–deficient, aged 4 years) sampled during the acute (9 days after MIS-C onset) and convalescent (~1 month after onset) phases, together with cells from one healthy adult and two pediatric controls.

We compared the data obtained with a previously published dataset for patients with pediatric acute SARS-CoV-2 infection or MIS-C (*33*). Clustering analysis showed lower levels of monocytes and type 1 and type 2 conventional dendritic cells (cDCs) in these patients and an expansion of the activated T cell population strongly expressing *MKI67* (Fig. 5F and fig. S8, A and B). Other subsets were largely unaffected. Pseudobulk differential expression analysis was performed at the single-cell level for monocytes, mDCs, B lymphocytes, plasmacytoid dendritic cells (pDCs), and activated T cells. Bulk RNA-seq was performed on sorted nonclassical monocytes and pDCs to further confirm the scRNA-seq findings. We also quantitatively inferred cell–cell communications with CellChat (*74*) to identify the signal-outgoing and the signal-receiving cell subsets. The data generated during this study were analyzed in an integrative manner with historical controls from the laboratory (one pediatric and seven adult controls), publicly available control PBMC datasets downloaded from the 10X Genomics web portal (https://support.10xgenomics.com/single-cell-gene-expression/datasets), and a previously published dataset for patients with acute SARS-CoV-2 infection and MIS-C (GEO accession: GSE167029), as described in detail in the supplementary materials. In addition, two other previously published sets of scRNA-seq data for pediatric healthy controls and children with acute SARS-CoV-2 infection or MIS-C (GSE166489) (*91*) were used for an independent cohort analysis.

Statistical analysis

For experiments performed in vitro, quantitative data were obtained for cells carrying the different mutations and control cells, or cells treated with different stimuli, from at least three biological replicates. For each biological replicate, up to six technical replicates were performed and averaged for downstream analysis. Cytokine determinations were log-transformed after subtracting the limit of detection for the experiment concerned. Mean quantitative values were compared between cells carrying the various mutations and control cells or cells treated with different stimuli in unequal-variance *t* tests. Where relevant, statistical test results are indicated in the corresponding figures (ns, not significant; $*P < 0.05$, $**P < 0.01$, $***P < 0.001$, $****P < 0.0001$).

REFERENCES AND NOTES

1. A. T. Levin *et al*., Assessing the age specificity of infection fatality rates for COVID-19: Systematic review, meta-analysis, and public policy implications. *Eur. J. Epidemiol.* **35**, 1123–1138 (2020). doi: 10.1007/s10654-020-00698-1; pmid: 33289900
2. M. O'Driscoll *et al*., Age-specific mortality and immunity patterns of SARS-CoV-2. *Nature* **590**, 140–145 (2021). doi: 10.1038/s41586-020-2918-0; pmid: 33137809
3. K. Bhaskaran *et al*., Factors associated with deaths due to COVID-19 versus other causes: Population-based cohort analysis of UK primary care data and linked national death registrations within the OpenSAFELY platform. *Lancet Reg. Health Eur.* **6**, 100109 (2021). doi: 10.1016/j.lanepe.2021.100109; pmid: 33997835
4. E. J. Williamson *et al*., Factors associated with COVID-19-related death using OpenSAFELY. *Nature* **584**, 430–436 (2020). doi: 10.1038/s41586-020-2521-4; pmid: 32640463
5. Q. Zhang *et al*., Inborn errors of type I IFN immunity in patients with life-threatening COVID-19. *Science* **370**, eabd4570 (2020). doi: 10.1126/science.abd4570; pmid: 32972995
6. P. Bastard *et al*., Autoantibodies against type I IFNs in patients with life-threatening COVID-19. *Science* **370**, eabd4585 (2020). doi: 10.1126/science.abd4585; pmid: 32972996
7. T. Asano *et al*., X-linked recessive TLR7 deficiency in ~1% of men under 60 years old with life-threatening COVID-19. *Sci. Immunol.* **6**, eabl4348 (2021). doi: 10.1126/sciimmunol.abl4348; pmid: 34413140
8. P. Bastard *et al*., Autoantibodies neutralizing type I IFNs are present in ~4% of uninfected individuals over 70 years old and account for ~20% of COVID-19 deaths. *Sci. Immunol.* **6**, eabl4340 (2021). doi: 10.1126/sciimmunol.abl4340; pmid: 34413139
9. Q. Zhang *et al*., Recessive inborn errors of type I IFN immunity in children with COVID-19 pneumonia. *J. Exp. Med.* **219**, e20220131 (2022). doi: 10.1084/jem.20220131; pmid: 35708626
10. E. Pairo-Castineira *et al*., Genetic mechanisms of critical illness in COVID-19. *Nature* **591**, 92–98 (2021). doi: 10.1038/s41586-020-03065-y; pmid: 33307546
11. H. Zeberg, S. Pääbo, The major genetic risk factor for severe COVID-19 is inherited from Neanderthals. *Nature* **587**, 610–612 (2020). doi: 10.1038/s41586-020-2818-3; pmid: 32998156
12. A. Kousathanas *et al*., Whole-genome sequencing reveals host factors underlying critical COVID-19. *Nature* **607**, 97–103 (2022). doi: 10.1038/s41586-022-04576-6; pmid: 35255492
13. COVID-19 Host Genetics Initiative, Mapping the human genetic architecture of COVID-19. *Nature* **600**, 472–477 (2021). doi: 10.1038/s41586-021-03767-x; pmid: 34237774
14. S. B. Morris *et al*., Case series of multisystem inflammatory syndrome in adults associated with SARS-CoV-2 infection — United Kingdom and United States, March–August 2020. *MMWR Morb. Mortal. Wkly. Rep.* **69**, 1450–1456 (2020). doi: 10.15585/mmwr.mm6940e1; pmid: 33031361
15. V. Sancho-Shimizu *et al*., SARS-CoV-2–related MIS-C: A key to the viral and genetic causes of Kawasaki disease? *J. Exp. Med.* **218**, e20210446 (2021). doi: 10.1084/jem.20210446; pmid: 33904890
16. E. Whittaker *et al*., Clinical characteristics of 58 children with a pediatric inflammatory multisystem syndrome temporally associated with SARS-CoV-2. *JAMA* **324**, 259–269 (2020). doi: 10.1001/jama.2020.10369; pmid: 32511692
17. M. Ahmed *et al*., Multisystem inflammatory syndrome in children: A systematic review. *EClinicalMedicine* **26**, 100527 (2020). doi: 10.1016/j.eclinm.2020.100527; pmid: 32923992
18. E. M. Dufort *et al*., Multisystem inflammatory syndrome in children in New York State. *N. Engl. J. Med.* **383**, 347–358 (2020). doi: 10.1056/NEJMoa2021756; pmid: 32598830
19. A. B. Payne *et al*., Incidence of multisystem inflammatory syndrome in children among US persons infected with SARS-CoV-2. *JAMA Netw. Open* **4**, e2116420 (2021). doi: 10.1001/jamanetworkopen.2021.16420; pmid: 34110391
20. L. R. Feldstein *et al*., Characteristics and outcomes of US children and adolescents with multisystem inflammatory syndrome in children (MIS-C) compared with severe acute COVID-19. *JAMA* **325**, 1074–1087 (2021). doi: 10.1001/jama.2021.2091; pmid: 33625505
21. M. J. Carter *et al*., Peripheral immunophenotypes in children with multisystem inflammatory syndrome associated with SARS-CoV-2 infection. *Nat. Med.* **26**, 1701–1707 (2020). doi: 10.1038/s41591-020-1054-6; pmid: 32812012
22. C. R. Consiglio *et al*., The immunology of multisystem inflammatory syndrome in children with COVID-19. *Cell* **183**, 968–981.e7 (2020). doi: 10.1016/j.cell.2020.09.016; pmid: 32966765
23. L. Hoste, R. Van Paemel, F. Haerynck, Multisystem inflammatory syndrome in children related to COVID-19: A systematic review. *Eur. J. Pediatr.* **180**, 2019–2034 (2021). doi: 10.1007/s00431-021-03993-5; pmid: 33599835
24. J. Toubiana *et al*., Distinctive features of Kawasaki disease following SARS-CoV-2 infection: a controlled study in Paris, France. *J. Clin. Immunol.* **41**, 526–535 (2021). doi: 10.1007/s10875-020-00941-0; pmid: 33394320
25. B. Cherqaoui, I. Koné-Paut, H. Yager, F. L. Bourgeois, M. Piram, Delineating phenotypes of Kawasaki disease and SARS-CoV-2-related inflammatory multisystem syndrome: A French study and literature review. *Rheumatology* **60**, 4530–4537 (2021). doi: 10.1093/rheumatology/keab026; pmid: 33493353
26. C. N. Gruber *et al*., Mapping systemic inflammation and antibody responses in multisystem inflammatory syndrome in children (MIS-C). *Cell* **183**, 982–995.e14 (2020). doi: 10.1016/j.cell.2020.09.034; pmid: 32991843
27. C. Diorio *et al*., Multisystem inflammatory syndrome in children and COVID-19 are distinct presentations of SARS-CoV-2. *J. Clin. Invest.* **130**, 5967–5975 (2020). doi: 10.1172/JCI140970; pmid: 32730233
28. P. Y. Lee *et al*., Distinct clinical and immunological features of SARS-CoV-2-induced multisystem inflammatory syndrome in children. *J. Clin. Invest.* **130**, 5942–5950 (2020). doi: 10.1172/JCI141113; pmid: 32701511
29. A. Esteve-Sole *et al*., Similarities and differences between the immunopathogenesis of COVID-19-related pediatric multisystem inflammatory syndrome and Kawasaki disease. *J. Clin. Invest.* **131**, e144554 (2021). doi: 10.1172/JCI144554; pmid: 33497356
30. H. Bukulmez, Current understanding of multisystem inflammatory syndrome (MIS-C) following COVID-19 and its distinction from Kawasaki disease. *Curr. Rheumatol. Rep.* **23**, 58 (2021). doi: 10.1007/s11926-021-01028-4; pmid: 34216296
31. L. A. Vella *et al*., Deep immune profiling of MIS-C demonstrates marked but transient immune activation compared to adult and pediatric COVID-19. *Sci. Immunol.* **6**, eabf7570 (2021). doi: 10.1126/sciimmunol.abf7570; pmid: 33653907
32. M. Moreews *et al*., Polyclonal expansion of TCR Vβ 21.3$^+$ CD4$^+$ and CD8$^+$ T cells is a hallmark of multisystem inflammatory syndrome in children. *Sci. Immunol.* **6**, eabh1516 (2021). doi: 10.1126/sciimmunol.abh1516; pmid: 34035116
33. C. de Cevins *et al*., A monocyte/dendritic cell molecular signature of SARS-CoV-2-related multisystem inflammatory syndrome in children with severe myocarditis. *Med (N Y)* **2**, 1072–1092.e7 (2021). doi: 10.1016/j.medj.2021.08.002; pmid: 34414385
34. A. Ramaswamy *et al*., Immune dysregulation and autoreactivity correlate with disease severity in SARS-CoV-2-associated multisystem inflammatory syndrome in children. *Immunity* **54**, 1083–1095.e7 (2021). doi: 10.1016/j.immuni.2021.04.003; pmid: 33891889
35. L. A. Vella, A. H. Rowley, Current insights into the pathophysiology of multisystem inflammatory syndrome in children. *Curr. Pediatr. Rep.* **9**, 83–92 (2021). doi: 10.1007/s40124-021-00257-6; pmid: 34692237
36. K. Sacco *et al*., Immunopathological signatures in multisystem inflammatory syndrome in children and pediatric COVID-19. *Nat. Med.* **28**, 1050–1062 (2022). doi: 10.1038/s41591-022-01724-3; pmid: 35177862
37. R. A. Porritt *et al*., HLA class I–associated expansion of TRBV11-2 T cells in multisystem inflammatory syndrome in children. *J. Clin. Invest.* **131**, e146614 (2021). doi: 10.1172/JCI146614; pmid: 33705359
38. L. Hoste *et al*., TIM3$^+$*TRBV11-2* T cells and IFNγ signature in patrolling monocytes and CD16$^+$ NK cells delineate MIS-C. *J. Exp. Med.* **219**, e20211381 (2022). doi: 10.1084/jem.20211381; pmid: 34914824
39. J. L. Casanova, L. Abel, Mechanisms of viral inflammation and disease in humans. *Science* **374**, 1080–1086 (2021). doi: 10.1126/science.abj7965; pmid: 34822298
40. S. Y. Zhang, Q. Zhang, J. L. Casanova, H. C. Su; COVID Team, Severe COVID-19 in the young and healthy: Monogenic inborn errors of immunity? *Nat. Rev. Immunol.* **20**, 455–456 (2020). doi: 10.1038/s41577-020-0373-7; pmid: 32555547
41. Y. Itan *et al*., The human gene damage index as a gene-level approach to prioritizing exome variants. *Proc. Natl. Acad. Sci. U.S.A.* **112**, 13615–13620 (2015). doi: 10.1073/pnas.1518646112; pmid: 26483451
42. S. L. Schwartz, G. L. Conn, RNA regulation of the antiviral protein 2′-5′-oligoadenylate synthetase. *Wiley Interdiscip. Rev. RNA* **10**, e1534 (2019). doi: 10.1002/wrna.1534; pmid: 30989826
43. B. Dong, R. H. Silverman, 2-5A-dependent RNase molecules dimerize during activation by 2-5A. *J. Biol. Chem.* **270**, 4133–4137 (1995). doi: 10.1074/jbc.270.8.4133; pmid: 7876164
44. M. Uhlén *et al*., Tissue-based map of the human proteome. *Science* **347**, 1260419 (2015). doi: 10.1126/science.1260419; pmid: 25613900
45. L. Zhao *et al*., Cell-type-specific activation of the oligoadenylate synthetase–RNase L pathway by a murine coronavirus. *J. Virol.* **87**, 8408–8418 (2013). doi: 10.1128/JVI.00769-13; pmid: 23698313

46. S. Banerjee, A. Chakrabarti, B. K. Jha, S. R. Weiss, R. H. Silverman, Cell-type-specific effects of RNase L on viral induction of beta interferon. *mBio* **5**, e00856-14 (2014). doi: 10.1128/mBio.00856-14; pmid: 24570368
47. F. Rapaport *et al*., Negative selection on human genes underlying inborn errors depends on disease outcome and both the mode and mechanism of inheritance. *Proc. Natl. Acad. Sci. U.S.A.* **118**, e2001248118 (2021). doi: 10.1073/pnas.2001248118; pmid: 33408250
48. B. Dong, M. Niwa, P. Walter, R. H. Silverman, Basis for regulated RNA cleavage by functional analysis of RNase L and Ire1p. *RNA* **7**, 361–373 (2001). doi: 10.1017/S1355838201002230; pmid: 11333017
49. R. H. Silverman, J. J. Skehel, T. C. James, D. H. Wreschner, I. M. Kerr, rRNA cleavage as an index of ppp(A2'p)nA activity in interferon-treated encephalomyocarditis virus-infected cells. *J. Virol.* **46**, 1051–1055 (1983). doi: 10.1128/jvi.46.3.1051-1055.1983; pmid: 6190010
50. D. H. Wreschner, T. C. James, R. H. Silverman, I. M. Kerr, Ribosomal RNA cleavage, nuclease activation and 2-5A ($ppp(A2'p)_nA$) in interferon-treated cells. *Nucleic Acids Res.* **9**, 1571–1581 (1981). doi: 10.1093/nar/9.7.1571; pmid: 6164990
51. Y. Xiang *et al*., Effects of RNase L mutations associated with prostate cancer on apoptosis induced by 2′,5′-oligoadenylates. *Cancer Res.* **63**, 6795–6801 (2003). pmid: 14583476
52. L. A. Henderson *et al*., American College of Rheumatology clinical guidance for multisystem inflammatory syndrome in children associated with SARS-CoV-2 and hyperinflammation in pediatric COVID-19: version 3. *Arthritis Rheumatol.* **74**, e1–e20 (2022). doi: 10.1002/art.42062; pmid: 35118829
53. A. Wickenhagen *et al*., A prenylated dsRNA sensor protects against severe COVID-19. *Science* **374**, eabj3624 (2021). doi: 10.1126/science.abj3624; pmid: 34581622
54. O. Danziger, R. S. Patel, E. J. DeGrace, M. R. Rosen, B. R. Rosenberg, Inducible CRISPR activation screen for interferon-stimulated genes identifies OAS1 as a SARS-CoV-2 restriction factor. *PLOS Pathog.* **18**, e1010464 (2022). doi: 10.1371/journal.ppat.1010464; pmid: 35421191
55. Y. Li *et al*., SARS-CoV-2 induces double-stranded RNA-mediated innate immune responses in respiratory epithelial-derived cells and cardiomyocytes. *Proc. Natl. Acad. Sci. U.S.A.* **118**, e2022643118 (2021). doi: 10.1073/pnas.2022643118; pmid: 33811184
56. P. Bastard *et al*., Herpes simplex encephalitis in a patient with a distinctive form of inherited IFNAR1 deficiency. *J. Clin. Invest.* **131**, e139980 (2021). doi: 10.1172/JCI139980; pmid: 32960813
57. X. Song *et al*., Little to no expression of angiotensin-converting enzyme-2 on most human peripheral blood immune cells but highly expressed on tissue macrophages. *Cytometry A* 10.1002/cyto.a.24285 (2020). doi: 10.1002/cyto.a.24285; pmid: 33280254
58. T. S. Rodrigues *et al*., Inflammasomes are activated in response to SARS-CoV-2 infection and are associated with COVID-19 severity in patients. *J. Exp. Med.* **218**, e20201707 (2021). doi: 10.1084/jem.20201707; pmid: 33231615
59. J. Zheng *et al*., Severe acute respiratory syndrome coronavirus 2–induced immune activation and death of monocyte-derived human macrophages and dendritic cells. *J. Infect. Dis.* **223**, 785–795 (2021). doi: 10.1093/infdis/jiaa753; pmid: 33277988
60. I. Gresser, F. Vignaux, F. Belardelli, M. G. Tovey, M. T. Maunoury, Injection of mice with antibody to mouse interferon alpha/beta decreases the level of 2′-5′ oligoadenylate synthetase in peritoneal macrophages. *J. Virol.* **53**, 221–227 (1985). doi: 10.1128/jvi.53.1.221-227.1985; pmid: 2981340
61. W. Chanput, J. J. Mes, H. J. Wichers, THP-1 cell line: An in vitro cell model for immune modulation approach. *Int. Immunopharmacol.* **23**, 37–45 (2014). doi: 10.1016/j.intimp.2014.08.002; pmid: 25130606
62. W. B. Lee *et al*., OAS1 and OAS3 negatively regulate the expression of chemokines and interferon-responsive genes in human macrophages. *BMB Rep.* **52**, 133–138 (2019). doi: 10.5483/BMBRep.2019.52.2.129; pmid: 30078389
63. T. Kawai, S. Akira, Innate immune recognition of viral infection. *Nat. Immunol.* **7**, 131–137 (2006). doi: 10.1038/ni1303; pmid: 16424890
64. A. Chakrabarti, B. K. Jha, R. H. Silverman, New insights into the role of RNase L in innate immunity. *J. Interferon Cytokine Res.* **31**, 49–57 (2011). doi: 10.1089/jir.2010.0120; pmid: 21190483
65. A. G. Hovanessian, J. Wood, E. Meurs, L. Montagnier, Increased nuclease activity in cells treated with pppA2′p5′A2′p5′ A. *Proc. Natl. Acad. Sci. U.S.A.* **76**, 3261–3265 (1979). doi: 10.1073/pnas.76.7.3261; pmid: 114998
66. A. Zhou, B. A. Hassel, R. H. Silverman, Expression cloning of 2-5A-dependent RNAase: A uniquely regulated mediator of interferon action. *Cell* **72**, 753–765 (1993). doi: 10.1016/0092-8674(93)90403-D; pmid: 7680958
67. K. Malathi *et al*., A transcriptional signaling pathway in the IFN system mediated by 2′-5′-oligoadenylate activation of RNase L. *Proc. Natl. Acad. Sci. U.S.A.* **102**, 14533–14538 (2005). doi: 10.1073/pnas.0507551102; pmid: 16203993
68. J. M. Burke, S. L. Moon, T. Matheny, R. Parker, RNase L reprograms translation by widespread mRNA turnover escaped by antiviral mRNAs. *Mol. Cell* **75**, 1203–1217.e5 (2019). doi: 10.1016/j.molcel.2019.07.029; pmid: 31494035
69. M. Knight *et al*., Radioimmune, radiobinding and HPLC analysis of 2-5A and related oligonucleotides from intact cells. *Nature* **288**, 189–192 (1980). doi: 10.1038/288189a0; pmid: 6159552
70. A. Asthana, C. Gaughan, B. Dong, S. R. Weiss, R. H. Silverman, Specificity and mechanism of coronavirus, rotavirus, and mammalian two-histidine phosphoesterases that antagonize antiviral innate immunity. *mBio* **12**, e0178121 (2021). doi: 10.1128/mBio.01781-21; pmid: 34372695
71. A. Liberzon *et al*., The Molecular Signatures Database (MSigDB) hallmark gene set collection. *Cell Syst.* **1**, 417–425 (2015). doi: 10.1016/j.cels.2015.12.004; pmid: 26771021
72. E. J. Mendoza, K. Manguiat, H. Wood, M. Drebot, Two detailed plaque assay protocols for the quantification of infectious SARS-CoV-2. *Curr. Protoc. Microbiol.* **57**, ecpmc105 (2020). doi: 10.1002/cpmc.105; pmid: 32475066
73. A. C. G. Salina *et al*., Efferocytosis of SARS-CoV-2-infected dying cells impairs macrophage anti-inflammatory functions and clearance of apoptotic cells. *eLife* **11**, e74443 (2022). doi: 10.7554/eLife.74443; pmid: 35666101
74. S. Jin *et al*., Inference and analysis of cell-cell communication using CellChat. *Nat. Commun.* **12**, 1088 (2021). doi: 10.1038/s41467-021-21246-9; pmid: 33597522
75. A. Chakrabarti *et al*., RNase L activates the NLRP3 inflammasome during viral infections. *Cell Host Microbe* **17**, 466–477 (2015). doi: 10.1016/j.chom.2015.02.010; pmid: 25816776
76. N. Magusali *et al*., A genetic link between risk for Alzheimer's disease and severe COVID-19 outcomes via the *OAS1* gene. *Brain* **144**, 3727–3741 (2021). doi: 10.1093/brain/awab337; pmid: 34619763
77. S. Zhou *et al*., A Neanderthal OAS1 isoform protects individuals of European ancestry against COVID-19 susceptibility and severity. *Nat. Med.* **27**, 659–667 (2021). doi: 10.1038/s41591-021-01281-1; pmid: 33633408
78. H. Zeberg, S. Pääbo, A genomic region associated with protection against severe COVID-19 is inherited from Neandertals. *Proc. Natl. Acad. Sci. U.S.A.* **118**, e2026309118 (2021). doi: 10.1073/pnas.2026309118; pmid: 33593941
79. J. E. Huffman *et al*., Multi-ancestry fine mapping implicates *OAS1* splicing in risk of severe COVID-19. *Nat. Genet.* **54**, 125–127 (2022). doi: 10.1038/s41588-021-00996-8; pmid: 35027740
80. K. Cho *et al*., Heterozygous mutations in *OAS1* cause infantile-onset pulmonary alveolar proteinosis with hypogammaglobulinemia. *Am. J. Hum. Genet.* **102**, 480–486 (2018). doi: 10.1016/j.ajhg.2018.01.019; pmid: 29455859
81. T. Magg *et al*., Heterozygous *OAS1* gain-of-function variants cause an autoinflammatory immunodeficiency. *Sci. Immunol.* **6**, eabf9564 (2021). doi: 10.1126/sciimmunol.abf9564; pmid: 34145065
82. A. G. Hovanessian, R. E. Brown, I. M. Kerr, Synthesis of low molecular weight inhibitor of protein synthesis with enzyme from interferon-treated cells. *Nature* **268**, 537–540 (1977). doi: 10.1038/268537a0; pmid: 560630
83. I. M. Kerr, R. E. Brown, pppA2′p5′A2′p5′A: an inhibitor of protein synthesis synthesized with an enzyme fraction from interferon-treated cells. *Proc. Natl. Acad. Sci. U.S.A.* **75**, 256–260 (1978). doi: 10.1073/pnas.75.1.256; pmid: 272640
84. M. Drappier, T. Michiels, Inhibition of the OAS/RNase L pathway by viruses. *Curr. Opin. Virol.* **15**, 19–26 (2015). doi: 10.1016/j.coviro.2015.07.002; pmid: 26231767
85. R. H. Silverman, Viral encounters with 2′,5′-oligoadenylate synthetase and RNase L during the interferon antiviral response. *J. Virol.* **81**, 12720–12729 (2007). doi: 10.1128/JVI.01471-07; pmid: 17804500
86. R. J. Lin *et al*., Distinct antiviral roles for human 2′,5′-oligoadenylate synthetase family members against dengue virus infection. *J. Immunol.* **183**, 8035–8043 (2009). doi: 10.4049/jimmunol.0902728; pmid: 19923450
87. Y. C. Kwon, J. I. Kang, S. B. Hwang, B. Y. Ahn, The ribonuclease L-dependent antiviral roles of human 2′,5′-oligoadenylate synthetase family members against hepatitis C virus. *FEBS Lett.* **587**, 156–164 (2013). doi: 10.1016/j.febslet.2012.11.010; pmid: 23196181
88. Y. Li *et al*., Activation of RNase L is dependent on OAS3 expression during infection with diverse human viruses. *Proc. Natl. Acad. Sci. U.S.A.* **113**, 2241–2246 (2016). doi: 10.1073/pnas.1519657113; pmid: 26858407
89. J. N. Whelan, Y. Li, R. H. Silverman, S. R. Weiss, Zika virus production is resistant to RNase L antiviral activity. *J. Virol.* **93**, e00313-19 (2019). doi: 10.1128/JVI.00313-19; pmid: 31142667
90. C. S. Thakur, Z. Xu, Z. Wang, Z. Novince, R. H. Silverman, A convenient and sensitive fluorescence resonance energy transfer assay for RNase L and 2′,5′ oligoadenylates. *Methods Mol. Med.* **116**, 103–113 (2005). doi: 10.1385/1-59259-939-7:103; pmid: 16000857
91. K. Sacco *et al*, Multiomics approach identifies novel age-, time- and treatment-related immunopathological signatures in MIS-C and pediatric COVID-19, version 1.0.0, Zenodo (2021); https://doi.org/10.5281/zenodo.5524378.

ACKNOWLEDGMENTS

We thank the patients and their families for participating in our research. We thank all members of both branches of the Laboratory of Human Genetics of Infectious Diseases for discussions and technical and administrative support. We thank A. W. Ashbrook for managing the Rice laboratory BSL3 facility. We thank the Memorial Sloan Kettering Cancer Center for help isolating and sequencing the NY SARS-CoV-2 isolate. We thank R. Padgett and G. Stark at the Cleveland Clinic for discussions. We also thank A. Codina and C. Jou from the Biobanc de l'Hospital Infantil Sant Joan de Déu per a la Investigació, which is integrated into the Spanish Biobank Network of ISCIII, for sample and data procurement. **Funding:** The Laboratory of Human Genetics of Infectious Diseases is supported by the Howard Hughes Medical Institute, the Rockefeller University, the St. Giles Foundation, the National Institutes of Health (NIH) (R01AI088364 and R21AI160576), the National Center for Advancing Translational Sciences (NCATS), NIH Clinical and Translational Science Award (CTSA) program (UL1TR001866), the Yale Center for Mendelian Genomics and the GSP Coordinating Center funded by the National Human Genome Research Institute (NHGRI) (UM1HG006504 and U24HG008956), the Yale High-Performance Computing Center (S10OD018521), the Fisher Center for Alzheimer's Research Foundation, the Meyer Foundation, the JBP Foundation, the French National Research Agency (ANR) under the "Investments for the Future" program (ANR-10-IAHU-01), the Integrative Biology of Emerging Infectious Diseases Laboratory of Excellence (ANR-10-LABX-62-IBEID), the French Foundation for Medical Research (FRM) (EQU201903007798), the ANR GenMISC (ANR-21-COVR-039), the ANRS-COV05, ANR GENVIR (ANR-20-CE93-003) and ANR AABIFNCOV (ANR-20-CO11-0001) projects, the ANR-RHU program (ANR-21-RHUS-08), the European Union's Horizon 2020 research and innovation program under grant agreement 824110 (EASI-genomics), the HORIZON-HLTH-2021-DISEASE-04 program under grant agreement 01057100 (UNDINE), the ANR-RHU Program ANR-21-RHUS-08 (COVIFERON), the Square Foundation, Grandir – Fonds de solidarité pour l'enfance, the Fondation du Souffle, the SCOR Corporate Foundation for Science, the French Ministry of Higher Education, Research, and Innovation (MESRI-COVID-19), Institut National de la Santé et de la Recherche Médicale (INSERM), and Paris Cité University. We acknowledge support from the National Institute of Allergy and Infectious Diseases (NIAID) of the NIH under award R01AI104887 to R.H.S. and S.R.W. The Laboratory of Human Evolutionary Genetics (Institut Pasteur) is supported by the Institut Pasteur, the Collège de France, the French Government's Investissement d'Avenir program, Laboratoires d'Excellence "Integrative Biology of Emerging Infectious Diseases" (ANR-10-LABX-62-IBEID) and "Milieu Intérieur" (ANR-10-LABX-69-01), the Fondation de France (no. 00106080), the FRM (Equipe FRM DEQ20180339214 team), and the ANR COVID-19-POPCELL (ANR-21-CO14-0003-01). A.Puj. is supported by ACCI20-759 CIBERER, EasiGenomics H2020 Marató TV3 COVID 2021-31-33, the HORIZON-HLTH-2021-ID: 101057100 (UNDINE), the Horizon 2020 program under grant no. 824110 (EasiGenomics grant no. COVID-19/PID12342), and the CERCA Program/Generalitat de Catalunya. The Canarian Health System sequencing hub was funded by the Instituto de Salud Carlos III (COV20_01333 and COV20_01334), the Spanish Ministry of Science and Innovation (RTC-2017-6471-1; AEI/FEDER, UE), Fundación MAPFRE Guanarteme (OA21/131), and Cabildo Insular de Tenerife (CGIEU0000219140 and "Apuestas científicas del ITER para colaborar

en la lucha contra la COVID-19"). The CoV-Contact Cohort was funded by the French Ministry of Health and the European Commission (RECOVER project). Our studies are also funded by the Ministry of Health of the Czech Republic Conceptual Development of Research Organization (FNBr, 65269705) and ANID COVID0999 funding in Chile. G. Novelli and A. Novelli are supported by Regione Lazio (Research Group Projects 2020) No. A0375-2020-36663, GecoBiomark. A.M.P., M.L.D., and J.P.-T. are supported by the Inmungen-CoV2 project of CSIC. This work was supported in part by the Intramural Research Program of the NIAID, NIH. The research work of A.M..P, M.L.D., and J.P.-T. was funded by the European Commission –NextGenerationEU (Regulation EU 2020/2094), through CSIC's Global Health Platform (PTI Salud Global). I.M. is a senior clinical investigator at FWO Vlaanderen supported by a VIB GC PID grant, by FWO grants G0B5120N (DADA2) and G0E8420N, and by the Jeffrey Modell Foundation. I.M. holds an ERC-StG MORE2ADA2 grant and is also supported by ERN-RITA. A.Y. is supported by fellowships from the European Academy of Dermatology and Venereology and the Swiss National Science Foundation and by an Early Career Award from the Thrasher Research Fund. Y.-H.C. is supported by an A*STAR International Fellowship (AIF). M.O. was supported by the David Rockefeller Graduate Program, the New York Hideyo Noguchi Memorial Society (HNMS), the Funai Foundation for Information Technology (FFIT), the Honjo International Scholarship Foundation (HISF), and the National Cancer Institute (NCI) F99 Award (F99CA274708). A.A.A. was supported by Ministerio de Ciencia Tecnología e Innovación MINCIENCIAS, Colombia (111584467551/CT 415-2020). D.L. is supported by a fellowship from the FRM for medical residents and fellows. E.H. received funding from the Bank of Montreal Chair of Pediatric Immunology, Foundation of CHU Sainte-Justine, CIHR grants PCC-466901 and MM1-181123, and a Canadian Pediatric Society IMPACT study. Q.P.-H. received funding from the European Union's Horizon 2020 research and innovation program (ATAC, 101003650), the Swedish Research Council, and the Knut and Alice Wallenberg Foundation. Work in the Laboratory of Virology and Infectious Disease was supported by NIH grants P01AI138398-S1, 2U19AI111825, R01AI091707-10S1, and R01AI161444; a George Mason University Fast Grant; the G. Harold and Leila Y. Mathers Charitable Foundation; the Meyer Foundation; and the Bawd Foundation. R.P.L. is on the board of directors of both Roche and the Roche subsidiary Genentech. J.L.P. was supported by a Francois Wallace Monahan Postdoctoral Fellowship at the Rockefeller University and by a European Molecular Biology Organization Long-Term Fellowship (ALTF 380-2018). **Author contributions:** D.L., J.L.P., A.Y., B.D., Y.A., M.O., R.P., M.P., Z.L., L.B., A.Bi., W.L., M.H., J.C., C.G., A.A., V.L., J.M.L., F.J., H.-H.H., E.M., M.Mo., K.B., S.M., C.F., Y.Z., A.A.A., R.B., A.S., T.L.V., M.Ma., A.G., M.M.-V., F.P., T.L., R.L., A.-L.N., J.R., J.P., Y.-H.C., M.-P.M., R.M.P.-R., S.B., L.L., M.L.D., N.F., F.R., J.P.-T., S.C., T.E., F.G., P.L., S.R.W., A.M.P., C.L.D., J.B., A.Pue., S.B.-D., B.Bo., T.M., Q.Z., L.N., V.B., R.P.L., E.J., A.Be., L.Q.-M., C.M.R., R.H.S., S.-Y.Z., and J.-L.C. performed or supervised experiments, generated and analyzed data, and contributed to the manuscript by providing figures and tables. E.T., D.R., P.Z., Y.S., B.M., B.Bi., A.C., and L.Ab. performed computational analysis of data. I.J., S.E.B., G.I.B., C.B., J.A., S.D., J.T., F.B., V.F., D.B., X.D., Q.P.-H., I.M., F.H., A.Puj., V.S.-S., P.B., R.P.d.D., C.R.-G., H.C.S., L.Al., S.K., and E.H. evaluated and recruited patients to COVID and/or control cohorts of patients. D.L, S.-Y.Z., and J.-L.C. wrote the manuscript. S.-Y.Z. and J.-L.C. conceptualized and supervised the project. All authors edited the manuscript. **Competing interests:** E.H. received honoraria from CSL-Behring, Takeda, and Octapharma. R.H.S. is a consultant to Laronde, Inc., and Inception Therapeutics, Inc. H.C.S. is also affiliated with the Department of Pathology and Laboratory Medicine, Perelman School of Medicine, University of Pennsylvania, Philadelphia, Pennsylvania. R.H.S. is also affiliated with the Departments of Biochemistry, Molecular Biology and Microbiology, and Molecular Medicine, Cleveland Clinic Lerner College of Medicine of Case Western Reserve University, Cleveland, Ohio; the Departments of Biological, Geological, and Environmental Sciences and Chemistry, Cleveland State University, Cleveland, Ohio; and Ohio School of Biological Sciences, Kent State University, Kent, Ohio. The other authors declare no competing interests. **Data and materials availability:** All data are available in the manuscript or the supplementary materials. The materials and reagents used are commercially available and nonproprietary, with the exception of SARS-CoV-2 working stock and the gene-KO or patient-specific cell lines generated from this study. The SARS-CoV-2 working stock is available from C.M.R. under a material transfer agreement (MTA) with the Rockefeller University. The cell lines generated from this study are available from S.-Y.Z. and J.-L.C. upon request under MTAs from the Rockefeller University and the Imagine Institute. Patient-specific cellular materials from patients enrolled at NIAID are available from H.C.S. under a MTA with the NIH, provided that the request fulfills all articles listed in a MTA with the originating institute where the materials were collected. WGS data for patients sequenced by NIAID through TAGC were deposited under database of Genotypes and Phenotypes (dbGaP) accession number phs002245. Other genomic sequences of the patients reported in this paper are available from the authors upon request under a data transfer agreement. The raw RNA-seq data generated from this study are deposited in the NCBI database under the NCBI-SRA project PRJNA898284. **License information:** This work is licensed under a Creative Commons Attribution 4.0 International (CC BY 4.0) license, which permits unrestricted use, distribution, and reproduction in any medium, provided the original work is properly cited. To view a copy of this license, visit https://creativecommons.org/licenses/by/4.0/. This license does not apply to figures/photos/artwork or other content included in the article that is credited to a third party; obtain authorization from the rights holder before using such material.

CoV-Contact Cohort

Loubna Alavoine[1], Sylvie Behillil[2], Charles Burdet[3], Charlotte Charpentier[3,4], Aline Dechanet[5], Diane Descamps[3,6], Xavier Duval[1,3,7], Jean-Luc Ecobichon[1], Vincent Enouf[8], Wahiba Frezouls[1], Nadhira Houhou[5], Ouifiya Kafif[5], Jonathan Lehacaut[1], Sophie Letrou[1], Bruno Lina[9], Jean-Christophe Lucet[10], Pauline Manchon[5], Mariama Nouroudine[1], Valentine Piquard[5], Caroline Quintin[1], Michael Thy[11], Sarah Tubiana[1], Sylvie van der Werf[8], Valérie Vignali[1], Benoit Visseaux[3,10], Yazdan Yazdanpanah[3,10], Abir Chahine[12], Nawal Waucquier[12], Maria-Claire Migaud[12], Dominique Deplanque[12], Félix Djossou[13], Mayka Mergeay-Fabre[14], Aude Lucarelli[15], Magalie Demar[13], Léa Bruneau[16], Patrick Gérardin[17], Adrien Maillot[16], Christine Payet[18], Bruno Laviolle[19], Fabrice Laine[19], Christophe Paris[19], Mireille Desille-Dugast[19], Julie Fouchard[19], Denis Malvy[20], Duc Nguyen[20], Thierry Pistone[20], Pauline Perreau[20], Valérie Gissot[21], Carole Le Goas[21], Samatha Montagne[22], Lucie Richard[23], Catherine Chirouze[24], Kévin Bouiller[24], Maxime Desmarets[25], Alexandre Meunier[26], Benjamin Lefèvre[27], Hélène Jeulin[28], Karine Legrand[29], Sandra Lomazzi[30], Bernard Tardy[31], Amandine Gagneux-Brunon[32], Frédérique Bertholon[33], Elisabeth Botelho-Nevers[32], Kouakam Christelle[34], Leturque Nicolas[34], Layidé Roufai[34], Karine Amat[35], Sandrine Couffin-Cadiergues[34], Hélène Espérou[36], Samia Hendou[34]

[1]Centre d'Investigation Clinique, INSERM CIC 1425, Hôpital Bichat Claude Bernard, AP-HP, Paris, France. [2]Institut Pasteur, Paris, France. [3]Université de Paris, IAME, INSERM U1137, Paris, France, Hôpital Bichat Claude Bernard, AP-HP, Paris, France. [4]Service de Virologie, Université de Paris, INSERM, IAME, UMR 1137, AP-HP, Hôpital Bichat Claude Bernard, F-75018 Paris, France. [5]Hôpital Bichat Claude Bernard, AP-HP, Paris, France. [6]IAME INSERM U1140, Hôpital Bichat Claude Bernard, AP-HP, Paris, France. [7]Centre d'Investigation Clinique, INSERM CIC 1425, AP-HP, IAME, Paris University, Paris, France. [8]Institut Pasteur, U3569 CNRS, Université de Paris, Paris, France. [9]Virpath Laboratory, International Center of Research in Infectiology, Lyon University, INSERM U1111, CNRS U5308, ENS, UCBL, Lyon, France. [10]IAME INSERM U1138, Hôpital Bichat Claude Bernard, AP-HP, Paris, France. [11]Center for Clinical Investigation, AP-HP, Hôpital Bichat Claude Bernard, Paris, France. [12]Centre d'Investigation Clinique, INSERM CIC 1403, Centre Hospitalo Universitaire de Lille, Lille, France. [13]Service des maladies infectieuses, Centre Hospitalo Universitaire de Cayenne, Guyane, France. [14]Centre d'Investigation Clinique, INSERM CIC 1424, Centre Hospitalier de Cayenne, Cayenne, Guyane Française. [15]Service Hôpital de jour Adulte, Centre Hospitalier de Cayenne, Guyane, France. [16]Centre d'Investigation Clinique, INSERM CIC 1410, Centre Hospitalo universitaire de la Réunion, La Réunion, France. [17]Centre d'Investigation Clinique, INSERM CIC 1410, CHU Reunion, Saint-Pierre, Reunion Island. [18]Centre d'Investigation Clinique, INSERM CIC 1410, Centre de Ressources Biologiques, Centre Hospitalo universitaire de la Réunion, La Réunion, France. [19]Centre d'Investigation Clinique, INSERM CIC 1414, Centre Hospitalo universitaire de Rennes, Rennes, France. [20]Service des maladies infectieuses, Centre Hospitalo universitaire de Bordeaux, Bordeaux, France. [21]Centre d'Investigation Clinique, INSERM CIC 1415, CHRU Tours, Tours, France. [22]CRBT, Centre Hospitalo universitaire de Tours, Tours, France. [23]Pole de Biologie Médicale, Centre Hospitalo universitaire de Tours, Tours, France. [24]Service des maladies infectieuses, Centre Hospitalo universitaire de Besançon, Besançon, France. [25]Service des maladies infectieuses, Centre d'investigation clinique, INSERM CIC1431, Centre Hospitalier Universitaire de Besançon, Besançon, France. [26]Centre de Ressources Biologiques - Filière Microbiologique de Besançon, Centre Hospitalier Universitaire, Besançon, France. [27]Université de Lorraine, CHRU-Nancy and APEMAC, Infectious and Tropical Diseases, Nancy, France. [28]Laboratoire de Virologie, CHRU de Nancy Brabois, Vandoeuvre-lès-Nancy, France. [29]INSERM CIC-EC 1433, Centre Hospitalo universitaire de Nancy, Nancy, France. [30]Centre de ressources Biologiques, Centre Hospitalo universitaire de Nancy, Nancy, France. [31]Centre d'Investigation Clinique, INSERM CIC 1408, Centre Hospitalo universitaire de Saint-Étienne, Saint-Étienne, France. [32]Service des maladies infectieuses, Centre Hospitalo universitaire de Saint-Étienne, Saint-Étienne, France. [33]Service des maladies infectieuses, CRB42-BTK, Centre Hospitalo Universitaire de Saint-Étienne, Saint-Étienne, France. [34]Pole Recherche Clinique, INSERM, Paris, France. [35]IMEA Fondation Léon M'Ba, Paris, France. [36]INSERM Pôle Recherche Clinique, Paris, France.

COVID Human Genetic Effort

Laurent Abel[1], Hassan Abolhassani[2], Sergio Aguilera-Albesa[3], Alessandro Aiuti[4], Ozge Metin Akcan[5], Nihal Akcay[6], Gulsum Alkan[7], Suzan A. Alkhater[8], Luis Miguel Allende[9], Yosunkaya Alper[5], Naima Amenzoui[10], Mark S. Anderson[11], Lisa Arkin[12], Melodie Aubart[13], Iryna Avramenko[14], Şehnaz Aydemir[15], Zeynep Gökçe Gayretli Aydin[16], Caner Aytekin[17], Gökhan Aytekin[18], Selma Erol Aytekin[5], Silvia Yumi Bando[19], Kathie Beland[20], Serkan Belkaya[21], Catherine M. Biggs[22], Agurtzane Bilbao Aburto[23], Geraldine Blanchard-Rohner[24], Daniel Blázquez-Gamero[9], Marketa Bloomfield[25], Dusan Bogunovic[26], Anastasia Bondarenko[27], Alessandro Borghesi[28], Amed Aziz Bousfiha[29], Oksana Boyarchuk[30], Petter Brodin[31], Yenan Bryceson[32], Giorgia Bucciol[33], Valeria Calcaterra[34], Giorgio Casari[4], Andre Cavalcanti[35], Jale Bengi Celik[36], George P. Chrousos[37], Roger Colobran[38], Antonio Condino-Neto[39], Francesca Conti[40], Megan Cooper[41], Taner Coskuner[42], Cyril Cyrus[43], Enza D'Auria[44], Selket Delafontaine[45], Beth A. Drolet[12], Burcu Bursal Duramaz[46], Loubna El Zein[47], Marwa H. Elnagdy[48], Melike Emiroglu[7], Emine Hafize Erdeniz[49], Marianna Fabi[50], Hagit Baris Feldman[51], Jacques Fellay[52], Filip Fencl[25], Filippos Filippatos[53], Julie Freiss[54], Jiri Fremuth[55], Alenka Gagro[56], Blanca Garcia-Solis[57], Gianluca Vergine[58], Rafaela González-Montelongo[59], Yahya Gul[60], Belgin Gülhan[61], Sara Sebnem Kilic Gultekin[62], Marta Gut[63], Rabih Halwani[64], Lennart Hammarström[65], Nevin Hatipoğlu[66], James Heath[67], Sarah E. Henrickson[68], Elisa Hernandez-Brito[69], Ilse Hoffman[70], Levi Hoste[71], Elena Hsieh[72], Antonio Íñigo-Campos[59], Yuval Itan[73], Petr Jabandziev[74], Bahar Kandemir[60], Saliha Kanık-Yüksek[61], Hasan Kapakli[75], Adem Karbuz[76], Ozgur Kasapcopur[77], Robin Kechiche[78], Yasemin Kendir Demirkol[79], Omer Kilic[80], Stella Kim Hansen[81], Adam Klocperk[25], Yu-Lung Lau[82], Jan Leblˇ[25], José M. Lorenzo-Salazar[59], Carrie L. Lucas[83], Majistor Maglorius[84], Laura Marque[85], Yeray Novoa Medina[86], Abián Montesdeoca Melián[87], Alexios-Fotios A. Mentis[37], Michele T. Pato[81], Athanasios Michos[53], Joshua D. Milner[88], Trine H. Mogensen[89], Adrián Muñoz-Barrera[59], Serdar Nepesov[90], João Farela Neves[91], Ashley Ng[12], Lisa F. P. Ng[92], Antonio Novelli[93], Giuseppe Novelli[94], Fatma Nur Oz[95], J. Gonzalo Ocejo-Viñals[96], Satoshi Okada[97], Zerrin Orbak[98], Ahmet Osman Kilic[60], Hind Ouair[29], Şadiye Kübra Tüter Öz[7], Tayfun Özçelik[99], Esra Akyüz Özkan[49], Aslınur Özkaya Parlakay[100], Carlos N. Pato[80], Estela Paz-Artal[9], Simon Pelham[101], Isabelle Pellier[54], Quentin Philippot[84], Laura Planas-Serra[102], Samira Plassart[103], Petra Pokorna[104], Meltem Polat[95], Cecilia Poli[105], Carolina Prando[106], Laurent Renia[107], Jacques G. Rivière[108], Agustí Rodríguez-Palmero[109], Lucie Roussel[110], Luis A. Rubio-Rodriguez[59], Moro Salifu[81], Lumir Sasek[55], Laura Sasia[111], Anna Scherbina[112], Erica Schmitt[41], Anna Sediva[25], Esra Sevketoglu[113], Katerina Slaba[74], Ondrej Slaby[114], Ali Sobh[115], Jordi Solé-Violán[116], Pere Soler-Palacin[108], Lien De Somer[117], Betül Sözeri[42], András N. Spaan[118], Yuriy Stepanovskiy[27], Stuart G. Tangye[119], Gonul Tanir[95], Elizabeth-Barbara Tatsi[53], Christian W. Thorball[120], Selda Hancerli Torun[121], Stuart Turvey[22], Ahmad Abou Tayoun[122], Sathishkumar Ramaswamy[123], Mohammed J. Uddin[124], Emel Uyar[61], Juan Valencia-Ramos[125], Ana Maria Van Den Rym[57], Hulya Vatansev[60], Martín Castillo de Vera[126], François Vermeulen[33], Donald C. Vinh[110], Alla Volokha[27], Horst von Bernuth[127], Carine Wouters[33], Aysun Yahşi[61], Volkan Yarar[75], Osman Yesilbas[128], Mehmet Yıldız[77], Mayana Zatz[129], Pawel Zawadzki[130], Gianvincenzo Zuccotti[131], Shen-Ying Zhang[132], Jean-Laurent Casanova[133]

[1]Laboratory of Human Genetics of Infectious Diseases, Necker Branch, INSERM U1163, Necker Hospital for Sick Children, Paris, France. [2]Department of Biosciences and Nutrition, Karolinska Institutet, SE14183, Huddinge, Sweden.

[3]Pediatrics Department, Navarra Health Service Hospital, Pamplona, Spain. [4]Pediatric Immunohematology, San Raffaele Hospital, Salute San Raffaele University, Italy. [5]Necmettin Erbakan University, Konya, Turkey. [6]Bakirkoy Dr. Sadi Konuk Research and Training Hospital, Pediatric Intensive Care Unit, Istanbul, Turkey. [7]Division of Pediatric Infectious Diseases, Department of Pediatrics, Selcuk University Faculty of Medicine, Konya, Turkey. [8]College of Medicine, Imam Abdulrahman Bin Faisal University, Dammam, Saudi Arabia; Department of Pediatrics, King Fahad Hospital of the University, Al-Khobar, Saudi Arabia. [9]Department of Pediatrics, Hospital Universitario 12 de Octubre, Madrid, Spain. [10]Children Infectious and Clinical Immunology Department, Abderrahim Harouchi Hospital, Faculty of Medicine and Pharmacy, Averroes University Hospital, Hassan 2 University, Casablanca, Morocco. [11]Diabetes Center, University of California, San Francisco, CA, USA. [12]University of Wisconsin School of Medicine, Madison, WI, USA. [13]Laboratory of Human Genetics of Infectious Diseases, Necker Branch, INSERM U1163; Pediatric Neurology Department, Necker-Enfants Malades Hospital, AP-HP, Paris, France. [14]Department of Propedeutics of Pediatrics and Medical Genetics, Danylo Halytsky Lviv National Medical University, Lviv, Ukraine. [15]Dr. Ali Kemal Belviranli State Hospital, Konya Turkey. [16]Department of Pediatrics, Division of Pediatric Infectious Disease, Faculty of Medicine, Karadeniz Technical University, Trabzon, Turkey. [17]Department of Pediatric Immunology, Dr. Sami Ulus Maternity and Children's Health and Diseases Training and Research Hospital, Ankara, Turkey. [18]Konya City Hospital, Konya, Turkey. [19]Laboratory of Pediatric Genomics, Faculty of Medicine, University of Sao Paulo, Sao Paulo, Brazil. [20]CHU Sainte-Justine, Montreal, QC, Canada. [21]Department of Molecular Biology and Genetics, Bilkent University, Ankara, Turkey. [22]Department of Pediatrics, University of British Columbia, Vancouver, BC, Canada; BC Children's Hospital Research Institute, Vancouver, BC, Canada. [23]Servicio de Pediatría, Hospital Universitario Cruces, Spain. [24]Unit of Immunology and Vaccinology, Division of General Pediatrics, Department of Pediatrics, Gynecology and Obstetrics, Geneva University Hospitals, University of Geneva, Geneva, Switzerland. [25]Department of Pediatrics, 2nd Faculty of Medicine, Charles University in Prague and Motol University Hospital, Prague, Czech Republic. [26]Center for Inborn Errors of Immunity, Precision Immunology Institute, Mindich Child Health and Development Institute, Department of Microbiology, Department of Pediatrics, Icahn School of Medicine at Mount Sinai, New York, NY, USA. [27]Pediatric Infectious Disease and Pediatric Immunology Department, Shupyk National Healthcare University of Ukraine, Kyiv, Ukraine. [28]Neonatal Intensive Care Unit, Fondazione IRCCS Policlinico San Matteo, Pavia, Italy; Fellay Lab, Ecole Polytechnique Fédérale de Lausanne (EPFL), Lausanne, Switzerland. [29]Clinical Immunology Unit, Casablanca Children's Hospital, Ibn Rochd Medical School, King Hassan II University, Casablanca, Morocco. [30]Department of Children's Diseases and Pediatric Surgery, I. Horbachevsky Ternopil National Medical University, Ukraine. [31]Science for Life Laboratory, Department of Women's and Children's Health, Karolinska Institutet, Stockholm, Sweden. [32]Center for Hematology and Regenerative Medicine, Department of Medicine, Karolinska Institute, Stockholm, Sweden. [33]Department of Pediatrics, University Hospitals Leuven, Belgium. [34]Department of Pediatrics, Buzzi Children's Hospital, Milan, Italy; Department of Internal Medicine, University of Pavia, Pavia, Italy. [35]Department of Pediatrics, Clinical Hospital of Federal University of Pernambuco, Recife, Brazil. [36]Department of Anesthesiology and Reanimation, Selcuk University Faculty of Medicine, Konya, Turkey. [37]University Research Institute of Maternal and Child Health and Precision Medicine, National and Kapodistrian University of Athens, Athens, Greece. [38]Immunology Division, Genetics Department, Vall d'Hebron Research Institute, Vall d'Hebron Barcelona Hospital Campus, Universitat Autònoma de Barcelona, Barcelona, Spain. [39]Department of Immunology, Institute of Biomedical Sciences, University of Sao Paulo, Sao Paulo, Brazil. [40]Pediatric Unit-IRCCS Azienda Ospedaliero-Universitaria di Bologna, Bologna, Italy. [41]Division of Rheumatology and Immunology, Department of Pediatrics, Washington University in St. Louis, St. Louis, MO, USA. [42]Division of Pediatric Rheumatology, Umraniye Training and Research Hospital, University of Health Sciences, Istanbul, Turkey. [43]Department of Biochemistry, College of Medicine, Imam Abdulrahman Bin Faisal University, Saudi Arabia. [44]Department of Pediatrics, Buzzi Children's Hospital, Milan, Italy. [45]Department of Pediatrics, University Hospitals Leuven, Laboratory for Inborn Errors of Immunity, KU Leuven, Leuven, Belgium. [46]University of Health Sciences, Kanuni Sultan Suleyman Training and Research Hospital, Istanbul, Turkey. [47]Lebanese University, Faculty of Sciences I, Biology Department, Rafic Hariri Campus, Beirut, Lebanon. [48]Medical Biochemistry and Molecular Biology Department, Faculty of Medicine, Mansoura University, Mansoura, Egypt. [49]Ondokuz Mayis University, Samsun, Turkey. [50]Pediatric Emergency Unit, Scientific Institute for Research and Healthcare (IRCCS), Sant'Orsola Hospital, Bologna, Italy. [51]The Genetics Institute, Tel Aviv Sourasky Medical Center and Sackler Faculty of Medicine, Tel Aviv University, Tel Aviv, Israel. [52]School of Life Sciences, École Polytechnique Fédérale de Lausanne, Lausanne, Switzerland; Precision Medicine Unit, Biomedical Data Sciences Center, Lausanne University Hospital and University of Lausanne, Lausanne, Switzerland; Swiss Institute of Bioinformatics, Lausanne, Switzerland. [53]First Department of Pediatrics, National and Kapodistrian University of Athens, Athens, Greece; University Research Institute of Maternal and Child Health and Precision Medicine, National and Kapodistrian University of Athens, Athens, Greece. [54]Unité d'Hématologie-Immunologie-Oncologie Pédiatrique, Centre Hospitalier Universitaire d'Angers, Angers, France. [55]Department of Pediatrics - PICU, Faculty of Medicine in Pilsen, Charles University in Prague, Czech Republic. [56]Department of Pediatrics, University of Zagreb School of Medicine, Children's Hospital Zagreb, Zagreb, Josip Juraj Strossmayer University of Osijek, Medical Faculty Osijek, Osijek, Croatia. [57]Laboratory of Immunogenetics of Human Diseases, IdiPAZ Institute for Health Research, La Paz Hospital, Madrid, Spain. [58]Unità Operativa Complessa Pediatria, Ospedale degli Infermi di Rimini, Rimini, Italy. [59]Genomics Division, Instituto Tecnológico y de Energías Renovables (ITER), Santa Cruz de Tenerife, Spain. [60]Necmettin Erbakan University, Konya, Turkey. [61]Ankara City Hospital, Ankara, Turkey. [62]Pediatric Immunology-Rheumatology Division, Uludag University Medical Faculty, Department of Pediatrics, Bursa, Turkey. [63]CNAG-CRG, Centre for Genomic Regulation (CRG), The Barcelona Institute of Science and Technology (BIST), Barcelona, Spain. [64]College of Medicine, University of Shajah, Shajah, UAE. [65]Division of Clinical Immunology, Department of Laboratory Medicine, Karolinska University Hospital Huddinge, Stockholm, Sweden. [66]Pediatric Infectious Diseases Unit, Bakirkoy Dr. Sadi Konuk Training and Research Hospital, University of Health Sciences, Istanbul, Turkey. [67]Institute of Systems Biology, Seattle, WA, USA. [68]Children's Hospital of Philadelphia, Division of Allergy Immunology, Philadelphia, PA, USA; Department of Microbiology, Perelman School of Medicine, University of Pennsylvania, Philadelphia, PA, USA. [69]Department of Immunology, Hospital Universitario de Gran Canaria Dr. Negrín, Canarian Health System, Las Palmas de Gran Canaria, Spain. [70]Department of Pediatrics, University Hospitals Leuven, Belgium. [71]Primary Immunodeficiency Research Lab, Center for Primary Immunodeficiency Ghent, Ghent University Hospital, Ghent, Belgium. [72]Department of Pediatrics, Section of Allergy and Immunology, Department of Immunology and Microbiology, University of Colorado Anschutz Medical Campus, Children's Hospital Colorado, Aurora, CO, USA. [73]Icahn School of Medicine at Mount Sinai, New York, NY, USA. [74]Department of Pediatrics, University Hospital Brno and Faculty of Medicine, Masaryk University, Brno, Czech Republic. [75]Balikesir City Hospital, Balikesir, Turkey. [76]Prof. Dr. Cemil Taşcıoglu City Hospital, Istanbul, Turkey. [77]Department of Pediatric Rheumatology, Cerrahpasa Medical School, Istanbul University-Cerrahpasa, Istanbul, Turkey. [78]Service de Rhumatologie Pediatrique, CHU Bicetre, France. [79]Department of Pediatric Genetics, Health Sciences University, Umraniye Education and Research Hospital, Istanbul, Turkey. [80]Eskişehir Osmangazi University, Faculty of Medicine, Clinic of Pediatric Infectious Diseases, Eskişehir, Turkey. [81]Institute for Genomic Health, SUNY Downstate, Health Science University, Brooklyn, NY, USA. [82]Department of Paediatrics and Adolescent Medicine, LKS Faculty of Medicine, the University of Hong Kong, Hong Kong. [83]Department of Immunobiology, Yale University School of Medicine, New Haven, CT, USA. [84]Laboratory of Human Genetics of Infectious Diseases, Necker Branch, INSERM U1163, Necker Hospital for Sick Children; Paris Descartes University, Imagine Institute, Paris, France. [85]Immunodeficiencies and Infectious Diseases Unit, Pediatric Department, Centro Materno-Infantil do Norte, Centro Hospitalar Universitario do Porto, Porto, Portugal. [86]Department of Pediatrics, Complejo Hospitalario Universitario Insular-Materno Infantil, Canarian Health System, Las Palmas de Gran Canaria, Spain. [87]Guanarteme Health Care Center, Canarian Health System, Las Palmas de Gran Canaria, Spain. [88]Department of Pediatrics, Columbia University Irving Medical Center, New York, NY, USA. [89]Department of Biomedicine, Aarhus University, Aarhus, Denmark. [90]Pediatric Allergy and Immunology Unit, Istanbul Medipol Üniversity, Istanbul, Turkey. [91]Primary Immunodeficiencies Unit, Hospital Dona Estefânia, CHULC, EPE; CEDOC, Center for Chronic Diseases, Lisbon, Portugal. [92]A*STAR Infectious Disease Labs, Agency for Science, Technology and Research, Singapore. [93]Translational Cytogenomics Research Unit, Bambino Gesù Children's Hospital, IRCCS, Rome, Italy. [94]Department of Biomedicine and Prevention, Tor Vergata University of Rome, Italy. [95]Department of Pediatric Infectious Disease, SBU Ankara Dr. Sami Ulus Maternity Child Health and Diseases Training and Research Hospital, Ankara, Turkey. [96]Department of Immunology, Hospital Marques de Valdecilla, Santander, Spain. [97]Department of Pediatrics, Hiroshima University Graduate School of Biomedical and Health Sciences, Hiroshima, Japan. [98]Department of Pediatrics, Ataturk University, Erzurum, Turkey. [99]Department of Molecular Biology and Genetics, Bilkent University, Ankara, Turkey. [100]Yildirim Beyazit University, Ankara City Hospital, Ankara, Turkey. [101]St. Giles Laboratory of Human Genetics of Infectious Diseases, Rockefeller Branch, The Rockefeller University, New York, NY, USA. [102]Neurometabolic Diseases Laboratory, IDIBELL–Hospital Duran I Reynals; CIBERER U759, ISIiii Madrid, Spain. [103]Service de Rhumatologie pédiatrique, Hôpital Femme-Mère-Enfant, Groupement Hospitalier Est - Bâtiment "Pinel", Bron, France. [104]Central European Institute of Technology, Masaryk University, Brno, Czech Republic. [105]Immunogenetics and Translational Immunology Program, Instituto de Ciencias e Innovación en Medicina (ICIM), School of Medicine, Clínica Alemana-Universidad del Desarrollo, Santiago de Chile, Chile. [106]Faculdades Pequeno Príncipe, Instituto de Pesquisa Pelé Pequeno Príncipe, Curitiba, Brazil. [107]A*STAR Infectious Disease Labs, Agency for Science, Technology and Research, Singapore; Lee Kong Chian School of Medicine, Nanyang Technological University, Singapore; School of Biological Sciences, Nanyang. Technological University, Singapore. [108]Pediatric Infectious Diseases and Immunodeficiencies Unit, Vall d'Hebron Research Institute, Vall d'Hebron Barcelona Hospital Campus, Universitat Autònoma de Barcelona, Barcelona, Spain. [109]Palmero Pediatrics Department, University Hospital Germans Trias i Pujol, Badalona, Barcelona, Spain. [110]Department of Medicine, Division of Infectious Diseases, McGill University Health Centre, Montréal, QC, Canada; Infectious Disease Susceptibility Program, Research Institute, McGill University Health Centre, Montréal, QC, Canada. [111]Hospital Infantil Municipal de Córdoba, Córdoba, Argentina. [112]Dmitry Rogachev National Medical Research Center of Pediatric Hematology, Moscow, Russia. [113]Pediatric Intensive Care Unit, Bakirkoy Dr. Sadi Konuk Training and Research Hospital, University of Health Sciences, Istanbul, Turkey. [114]Department of Biology UKB Kamenice, Masaryk University / Faculty of Medicine, Brno, Czech Republic. [115]Department of Pediatrics, Mansoura University Children's Hospital, Faculty of Medicine, Mansoura University, Mansoura, Egypt. [116]Critical Care Unit, Hospital Universitario de Gran Canaria Dr. Negrín, Canarian Health System, Las Palmas de Gran Canaria, Spain; Universidad Fernando Pessoa, Canarias, Spain; CIBER de Enfermedades Respiratorias. Instituto de Salud Carlos III, Madrid, Spain. [117]Department of Pediatrics, University Hospitals Leuven, Leuven, Belgium. [118]St. Giles Laboratory of Human Genetics of Infectious Diseases, Rockefeller Branch, The Rockefeller University, New York, NY, USA; Department of Medical Microbiology, University Medical Center Utrecht, Utrecht, Netherlands. [119]Garvan Institute of Medical Research, Darlinghurst, NSW, Australia; St Vincent's Clinical School, Faculty of Medicine, UNSW Sydney, Sydney, NSW, Australia. [120]Precision Medicine Unit, Biomedical Data Sciences Center, Lausanne University Hospital and University of Lausanne, Lausanne, Switzerland. [121]Department of Pediatric Infectious Disease, Faculty of Medicine, Istanbul University, Istanbul, Turkey. [122]Genomics Center, Al Jalila Children's Specialty Hospital, Dubai, UAE; Center for Genomic Discovery, Mohammed Bin Rashid University, Dubai, UAE. [123]Genomics Center, Al Jalila Children's Specialty Hospital, Dubai, UAE. [124]College of Medicine, Mohammed Bin Rashid University of Medicine and Health Sciences, Dubai, UAE; Cellular Intelligence (Ci) Lab, GenomeArc Inc., Toronto, ON, Canada. [125]Pediatrics Department, Division Pediatric Intensive Care Unit, Hospital Universitario de Burgos, Burgos, Spain. [126]Doctoral Health Care Center, Canarian Health System, Las Palmas de Gran Canaria, Spain. [127]Department of Pediatric Pneumology, Immunology and Intensive Care, Charité

Universitätsmedizin, Berlin University Hospital Center, Berlin, Germany; Labor Berlin GmbH, Department of Immunology, Berlin, Germany; Berlin Institutes of Health (BIH), Berlin-Brandenburg Center for Regenerative Therapies, Berlin, Germany. [128]Department of Pediatrics, Division of Pediatric Critical Care Medicine, Faculty of Medicine, Karadeniz Technical University, Trabzon, Turkey. [129]Biosciences Institute, University of São Paulo, São Paulo, Brazil. [130]MNM Diagnostics, Poznań, Poland. [131]Department of Pediatrics, Buzzi Children's Hospital, Milan, Italy; Department of Biomedical and Clinical Sciences, University of Milan, Milan, Italy. [132]Laboratory of Human Genetics of Infectious Diseases, Necker Branch, INSERM U1163, Necker Hospital for Sick Children, Paris, France; Laboratory of Human Genetics of Infectious Diseases, Rockefeller Branch, The Rockefeller University, New York, NY, USA. [133]Necker Hospital for Sick Children and INSERM, Paris, France; The Rockefeller University and Howard Hughes Medical Institute, New York, NY, USA.

SUPPLEMENTARY MATERIALS

science.org/doi/10.1126/science.abo3627
Materials and Methods
Figs. S1 to S9
Tables S1 to S3
References (*92*–*100*)
MDAR Reproducibility Checklist
Data S1 and S2

Submitted 29 January 2022; resubmitted 16 August 2022
Accepted 14 December 2022
Published online 20 December 2022
10.1126/science.abo3627

RESEARCH ARTICLES

NANOPHOTONICS

Negative refraction in hyperbolic hetero-bicrystals

A. J. Sternbach[1]*, S. L. Moore[1], A. Rikhter[2], S. Zhang[1], R. Jing[1], Y. Shao[1], B. S. Y. Kim[3], S. Xu[1], S. Liu[3,4], J. H. Edgar[4], A. Rubio[5,6], C. Dean[1], J. Hone[3], M. M. Fogler[2], D. N. Basov[1]

We visualized negative refraction of phonon polaritons, which occurs at the interface between two natural crystals. The polaritons—hybrids of infrared photons and lattice vibrations—form collimated rays that display negative refraction when passing through a planar interface between the two hyperbolic van der Waals materials: molybdenum oxide (MoO_3) and isotopically pure hexagonal boron nitride ($h^{11}BN$). At a special frequency ω_0, these rays can circulate along closed diamond-shaped trajectories. We have shown that polariton eigenmodes display regions of both positive and negative dispersion interrupted by multiple gaps that result from polaritonic-level repulsion and strong coupling.

Refraction is an elemental phenomenon in optics, in which a ray of light changes direction after traveling across an interface between two media (*1*). Refraction is considered "negative" if the refracted beam emerges on the same side of the interface normal as the incident one. This uncommon occurrence was demonstrated in artificial metamaterials (*2*) and superlattices (*3*) whose permittivity ε and permeability μ are simultaneously negative. Negative refraction alters light amplification and emission (*4*, *5*) as well as nonlinear optics (*6*) and may also cause trapped light (*7*, *8*) as well as "perfect" lensing (*9*). Interfaces between anisotropic meta-structures with rotationally misaligned principal axes can also enable negative refraction (*10*–*12*). Extreme anisotropy is offered by hyperbolic materials (HMs), whose hybrid light-matter modes—polaritons—are predicted to exhibit all-angle negative refraction at carefully crafted interfaces (*11*, *13*). In this work, we studied polaritons in a previously unexplored class of hyperbolic hetero-bicrystals made of two thin crystals, molybdenum oxide (MoO_3) (*14*–*18*) and isotopically pure hexagonal boron nitride ($h^{11}BN$) (*19*–*21*). Our hyperspectral nano-imaging data reveal localization, negative refraction, and closed-loop circulation of polaritonic rays inside $h^{11}BN$-MoO_3 hetero-bicrystals. Central to the observed effects is the gap in the polaritonic dispersion, which we extracted from hyperspectral images of polaritonic waves.

The hyperbolic electrodynamics of both $h^{11}BN$ (crystal A) and MoO_3 (crystal B) is born out of strong dipole active phonons (*22*). These resonances drive the permittivity negative along at least one principal axis, whereas positive "dielectric-like" positive permittivity is preserved along the remaining principal direction(s). Our results can be understood by focusing on the x-z plane (Fig. 1) for frequencies at which the phonon (Reststrahlen) bands of the constituent crystals overlap, 740 $cm^{-1} < \omega < 822\ cm^{-1}$. At these frequencies, the permittivity of $h^{11}BN$ is positive along $\hat{x}$ and negative along $\hat{z}$, $\varepsilon_A^x(\omega) > 0$, and $\varepsilon_A^z(\omega) < 0$ (type-I hyperbolicity). In MoO_3, the signs are reversed, $\varepsilon_B^x(\omega) < 0$ and $\varepsilon_B^z(\omega) > 0$ (type-II hyperbolicity) (Fig. 1A) in the same frequency range.

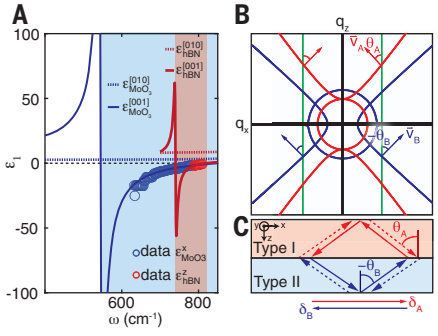

Fig. 1. Polaritons in hyperbolic hetero-bicrystals. (**A**) Real components of the permittivity, ε_1, of $h^{11}BN$ and MoO_3. The dots are experimental data. The parameters for the calculations, indicated with solid lines, are extracted from our data (table S1). (**B**) Schematic showing $q_y = 0$ cuts of the polariton isofrequency surfaces of type-I (crystal A, red) and type-II (crystal B, blue) HMs (supplementary text, section S1). The group velocities $\vec{v}_{A,B}$ and their tilt angles $\theta_A > 0$, $\theta_B < 0$ are indicated. (**C**) Schematic of the polariton rays in a bicrystal assembled from a type-I HM (crystal A, $h^{11}BN$) and a type-II HM (crystal B, MoO_3). The lateral shifts inside the crystals $\delta_A > 0$, $\delta_B < 0$ are indicated with arrows. The ray paths are closed if $\delta_A + \delta_B = 0$.

It is customary to refer to electromagnetic modes of polar materials as polaritons. The polariton dispersion assumes a simple form $(q_x^2/\varepsilon^z) + (q_z^2/\varepsilon^x) = \omega^2/c^2$ when the polariton momentum $\vec{q} = (q_x, q_y, q_z)$ is in the x-z plane, $q_y = 0$. In HMs, the polariton isofrequency lines are hyperbolas (Fig. 1B) (*14*, *19*, *20*, *23*). The asymptotes of these hyperbolas are inclined by the angle ±θ with respect to the x axis, where $\theta = \theta(\omega)$, defined by $\tan\theta = i\sqrt{\varepsilon^x}/\sqrt{\varepsilon^z}$, is positive for type-I and negative for type-II HMs. In the high-q limit, probed in our near-field experiments, the polariton group velocity $\vec{v} = \nabla_{\vec{q}}\omega$ becomes orthogonal to $\vec{q}$ (*24*). Because the angles $\theta_A > 0$ and $\theta_B < 0$ have opposite signs while momentum q_x is conserved, the tangential velocity $v_x = -|v|\mathrm{sgn}\, q_x \sin\theta$ changes sign in refraction at the A-B interface. The net effect is that polaritons exhibit negative refraction (supplementary text, section S1).

We report on a new class of hyperbolic hetero-bicrystal structures that reveal negative refraction of polaritons. If a hyperbolic ray emerges on the B-side of the A-B interface, the ray will be laterally displaced by a distance $\delta_B/2 < 0$ after propagating through crystal B. Negative refraction occurs at the interface with crystal A, prompting an additional displacement $\delta_A/2 > 0$. At a frequency ω_0, at which the condition $\delta_A(\omega_0) + \delta_B(\omega_0) = 0$ is satisfied, the polaritons travel in closed trajectories (Fig. 1C, ray construction). Experimental signatures of the closed-cycle electrodynamics near ω_0 are evident in our data (Figs. 2 and 3). However, these observations cannot be explained by polaritonic ray optics alone. We have shown that the principal modes of crystals A and B hybridize into a single strongly coupled eigenmode at ω_0, leading to prominent gaps in frequency-momentum dispersion.

To visualize polaritons, we used scanning near-field optical microscopy (SNOM). In SNOM measurements, the metalized tip of an atomic force microscope probes optical effects with subdiffractional spatial resolution, roughly given by the tip's radius, which is about 20 nm (*25*). To meet the demand for quasi-monochromatic excitation at frequencies within the overlapping Reststrahlen bands of $h^{11}BN$ and MoO_3 (Fig. 1A) (*26*), we generated ultranarrowband mid-infrared pulses with the spectral bandwidth <4 cm^{-1} (supplementary text, section S2.5).

Nano-imaging data unequivocally demonstrated negative refraction in $h^{11}BN$-MoO_3 hetero-bicrystals (Fig. 2). We patterned a gold strip with a width of $2w \approx 750$ nm on the surface of silicon dioxide (SiO_2). The sharp edges of the strip along the y axis enhance the infrared field and excite polaritons in the bicrystal with $q_y \approx 0$ (*27*). A MoO_3 crystal was placed on top of the launcher with its c axis perpendicular to the strip (fig. S7). We obtained images of the scattering amplitude, $|s|$, at temperature

[1]Department of Physics, Columbia University, New York, NY, USA. [2]Department of Physics, University of California San Diego, San Diego, CA, USA. [3]Department of Mechanical Engineering, Columbia University, New York, NY, USA. [4]Tim Taylor Department of Chemical Engineering, Kansas State University, Manhattan, KS, USA. [5]Center for Computational Quantum Physics (CCQ), Flatiron Institute, New York, NY, USA. [6]Max Planck Institute for the Structure and Dynamics of Matter, Luruper Chaussee, Hamburg, Germany.
*Corresponding author. Email: as5049@columbia.edu

T = 99 K to minimize losses. Images of $|s|$, collected at the surface of MoO_3 (Fig. 2B), reveal a pair of characteristic twin-peak profiles near the edges of the launching strip (Fig. 2C, inset; marked 1, 2, 3, and 4). The separation, δ_B, between peaks 1 and 2, or equivalently 3 and 4, is consistent with the directional propagation of hyperbolic rays introduced in Fig. 1 (*14*). Further, the magnitude of δ_B increases as the infrared frequency decreases (fig. S8), which also supports the notion of conical ray propagation in MoO_3 that is characteristic for a hyperbolic medium.

Next, we placed a crystal of $h^{11}BN$ on top of the MoO_3-Au (gold) assembly and visualized the nano-optical intensity at the top of the hetero-bicrystal. We observed a single peak of $|s|$ in relation to each edge of the Au strip at ω_0 = 787 cm^{-1} (Fig. 2, A and C). We also detected a considerable intensity between the two peaks (supplementary text, sections S1 and S2.6). Our observations, augmented with modeling, are consistent with negative refraction guiding the hyperbolic rays to the same lateral positions at the top and bottom surfaces of the bicrystal (Fig. 2C, top inset). Effectively, negative refraction delivers a projection of

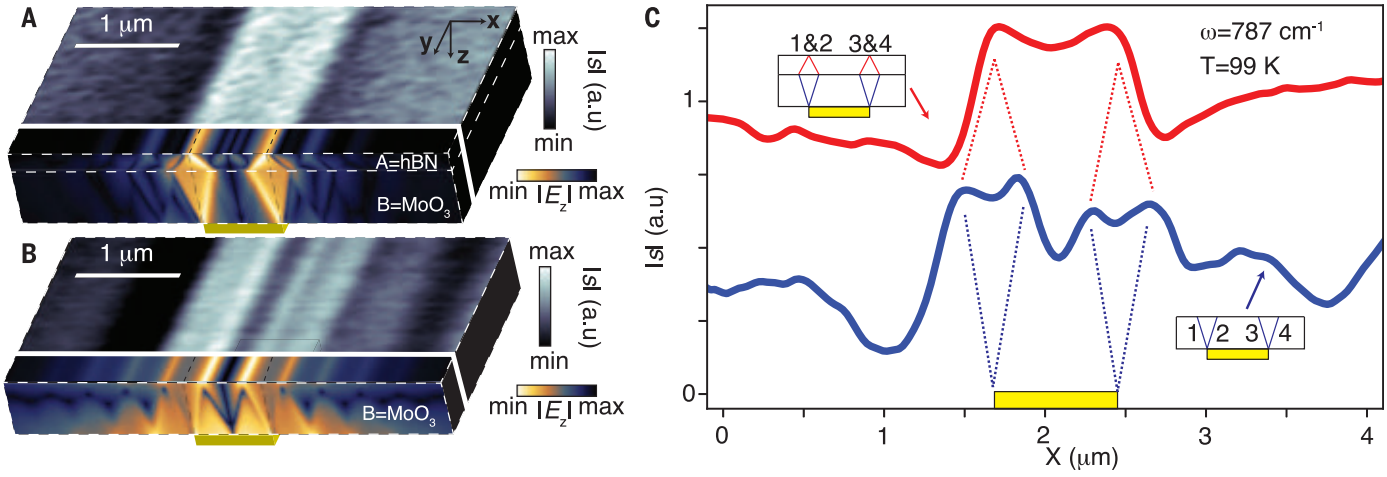

Fig. 2. Negative refraction of polaritons. Near-field amplitude data, $|s|$, obtained at various surfaces in the x-y plane of an $h^{11}BN$-MoO_3-Au stack. All data were obtained with ω = 787 cm^{-1} at temperature T = 99K, with thicknesses d_{hBN} = 98 nm on d_{MoO3} = 290 nm A = $h^{11}BN$ and B = MoO_3 crystals, respectively. (**A**) Imaging data of $|s|$ in perspective at the top surface of $h^{11}BN$-MoO_3-Au. (**B**) Data obtained at the surface of MoO_3-Au, displayed in an identical manner to that of (A). Calculations of $|E_z|$ in the x-z plane, and a strip in the x-y plane, are also shown in false color (supplementary text, section S1) in (A) and (B). Yellow rectangles indicate gold bars, beneath the HMs, and black dashed lines indicate the strip's edges. (**C**) Line profiles of $|s|$ as a function of the real-space coordinate, X. (Insets) The geometry in the x-z plane. Two pairs of hyperbolic rays—1 and 2, and 3 and 4—launched by the two edges of the Au strip are labeled.

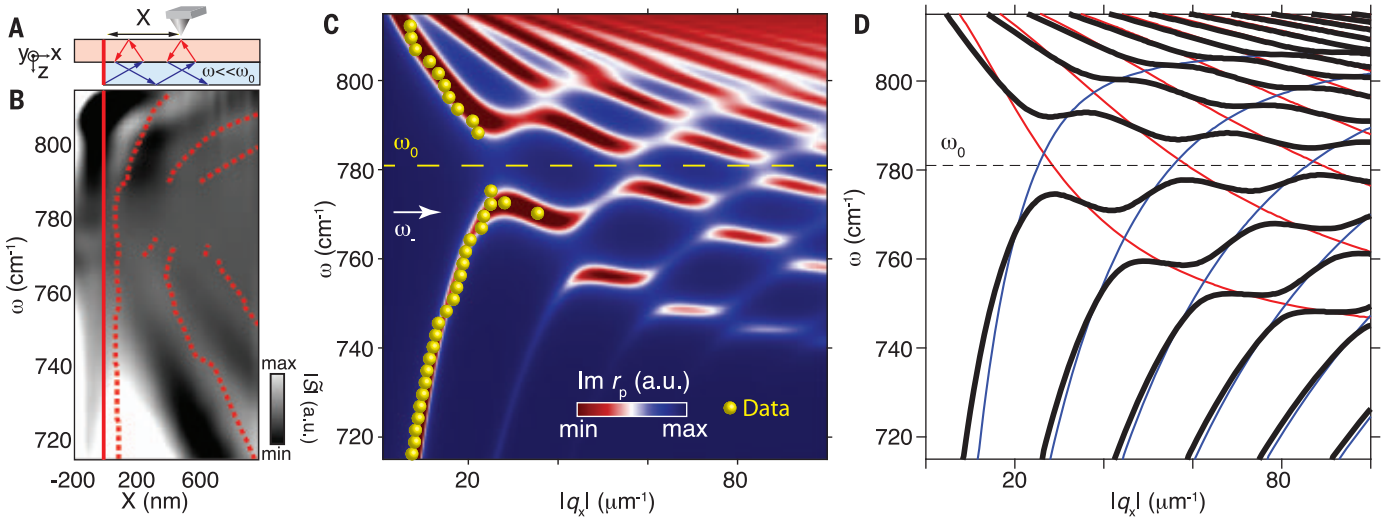

Fig. 3. Spectral gaps in the hetero-bicrystal dispersion. All data were obtained on a $h^{11}BN$-MoO_3 bicrystal with thicknesses of d_{hBN} = 58 nm and d_{MoO3} = 150 nm at ambient temperature. (**A**) Schematic illustrating ray trajectories in $h^{11}BN$ (red) and MoO_3 (blue) for $\omega \gg \omega_0$. (**B**) Amplitude data, $|S(X,\omega)|$ as a function of the distance X between the tip and bicrystal edge (solid red line). The edge of $h^{11}BN$ is located at X = −700 nm (supplementary text, section S1). The red dashed lines indicate locations where maxima are observed in our calculations (fig. S6D). (**C**) The imaginary part of the p-polarized reflection coefficient (Im r_p) is shown as a function of ω and the absolute value of the momentum component, $|q_x|$. The calculation uses realistic room-temperature losses of $h^{11}BN$ and MoO_3 (table S1). Data points are indicated with yellow dots (fig. S6). (**D**) The bicrystal dispersion is indicated with black lines for the idealized case with vanishing losses. Thin color traces indicate the dispersions of the parent crystals, MoO_3 (blue), and $h^{11}BN$ (red) calculated by using parameters in table S1.

the Au strip to the top surface of the bicrystal through diverging and converging trajectories of the hyperbolic rays inside the bicrystal. Numerical simulations capture gross features of the data in Fig. 2, A and B (analysis of subtle differences between the model and experiments is provided in the supplementary text, section S1.3). The totality of data in Fig. 2 and fig. S8 establishes negative refraction at the $h^{11}BN$-MoO_3 interface.

We then inquired into the frequency-momentum (ω, q_x) dispersion of the hetero-bicrystal polaritons and its implications for the observed negative refraction. We collected hyperspectral data of the frequency-dependent near-field amplitude $|\tilde{S}(X,\omega)|$ as a function of the distance X from the bicrystal edge, following established procedures (*20*, *25*, *28*). Except for a narrow window of frequencies around $\omega_0 = 787\ cm^{-1}$, we witnessed oscillations (or fringes) of $|\tilde{S}(X,\omega)|$ in our hyperspectral data (Fig. 3B). The period of the oscillations identified in Fig. 3B systematically varies with ω. Thus, our observations revealed how the wavelength of polaritonic waves, $\lambda_p(\omega)$, evolves with the frequency of incident infrared light. The data in Fig. 3B provide access to the polaritonic $(\omega, |q_x|)$ dispersion because $\lambda_p(\omega) = 2\pi/|q_x(\omega)|$ (Fig. 3C). We stress a nonmonotonic trend of $\lambda_p(\omega)$. Indeed, $\lambda_p(\omega)$ decreased when the frequency was near the lower bound of the overlapping Reststrahlen bands, but then reversed the trend near the upper bound of this frequency range. Near the frequency $\omega_- = 773\ cm^{-1}$, we detected two different fringe periods; hence, there are two sets of q_x points in the vicinity of ω_- in Fig. 3C (fig. S6). These features, at ω_0 and ω_-, are not present in the dispersions of constituent crystals (fig. S11). Thus, the hyperspectral data in Fig. 3 indicate that polaritons in the bicrystal are coupled modes.

A standard method for calculating the polariton dispersion involves finding the maxima of the reflection coefficient $r_p = r_p(\omega, |q_x|)$ of a *p*-polarized plane wave (*20*, *28*–*30*). The results for the imaginary part of the *p*-polarized reflection coefficient (Im r_p) (Fig. 3) reveal the existence of multiple dispersion branches. The data points match the calculated branches with the smallest q_x, the so-called principal modes. The full dispersion of the bicrystal displays a nonmonotonic $|q_x(\omega)|$ punctuated by spectral gaps (Fig. 3C). This dispersion can be understood as the family of avoided crossings exhibited by the modes of the constituent crystals. The polariton branches shown in Fig. 3D have a negative dispersion in crystal A (Fig. 3D, red curves) and positive dispersion in crystal B (Fig. 3D, blue curves) (fig. S11). Accordingly, the dispersion of the coupled modes of the bicrystal alternates in sign each time $|q_x|$ passes through an avoided crossing. The locations of the crossings are determined by a Bohr-Sommerfeld–like quantization condition

$$(\delta_A + \delta_B)q_x = \pi n + \text{const} \qquad (1)$$

where n is an integer. Equation 1 implies that the frequency ω_0, at which $\delta_A + \delta_B$ vanishes, is typically gapped at all q_x, which is in agreement with Fig. 3C. Our modeling predicts that the magnitude of these gaps scales with the polariton's velocity. Therefore, the gap decreases as $\sim 1/|q_x|$, at large $|q_x|$ (supplementary text, section S1). Within the gaps, the pole of $r_p(\omega, q_x)$ occurs at a complex q_x with a nonzero imaginary part even in the absence of dissipation. Thus, exactly at ω_0 the polaritonic modes are evanescent—exponentially localized near a launcher because of the combined effects of negative refraction and wave interference. We observed a gap near ω_0 (Fig. 3C) situated near $|q_x| = 24\ \mu m^{-1}$ with the size $\Delta\omega = 13 \pm 3\ cm^{-1}$, which is in good agreement with the calculated value of $\Delta\omega(|q_x| = 26\ \mu m^{-1}) = 16\ cm^{-1}$ (Fig. 3, C and D). The hetero-bicrystal polaritons visualized here comply with the definition of the strong mode coupling: The magnitude of the gap exceeds the linewidth of the mode (supplementary text, section S1).

In this work, we introduced hyperbolic hetero-bicrystal polaritons. We showed that the interface polaritons in $h^{11}BN$-MoO_3 can display negative refraction, spectral gaps, strong coupling, and localization. These attributes of hetero-bicrystals are broadly relevant to photonic applications (*31*, *32*) by using HMs. Moreover, polaritons in hetero-bicrystals can be focused to subdiffraction-limited spot sizes (*18*, *33*, *34*), which can enable perfect lensing by means of negative refraction (*9*). The attainable focal spots can, however, be limited by extrinsic factors, including crystal losses and imperfect polaritonic launchers (fig. S15). Further, similar to Fabry-Pérot cavities, negative refraction can cause radiation to propagate in closed cycles in our hetero-bicrystal nanocavities. Dielectric losses remain a challenge but could possibly be mitigated with active loss compensation (*4*, *5*, *35*).

REFERENCES AND NOTES

1. N. Yu *et al*., *Science* **334**, 333–337 (2011).
2. R. A. Shelby, D. R. Smith, S. Schultz, *Science* **292**, 77–79 (2001).
3. A. Pimenov, A. Loidl, P. Przyslupski, B. Dabrowski, *Phys. Rev. Lett.* **95**, 247009 (2005).
4. S. Xiao *et al*., *Nature* **466**, 735–738 (2010).
5. T. Pickering, J. M. Hamm, A. F. Page, S. Wuestner, O. Hess, *Nat. Commun.* **5**, 4972 (2014).
6. A. K. Popov, V. M. Shalaev, *Opt. Lett.* **31**, 2169–2171 (2006).
7. K. L. Tsakmakidis, A. D. Boardman, O. Hess, *Nature* **450**, 397–401 (2007).
8. K. L. Tsakmakidis, O. Hess, R. W. Boyd, X. Zhang, *Science* **358**, eaan5196 (2017).
9. J. B. Pendry, *Phys. Rev. Lett.* **85**, 3966–3969 (2000).
10. Y. Zhang, B. Fluegel, A. Mascarenhas, *Phys. Rev. Lett.* **91**, 157404 (2003).
11. X. Lin *et al*., *Proc. Natl. Acad. Sci. U.S.A.* **114**, 6717–6721 (2017).
12. A. J. Hoffman *et al*., *Nat. Mater.* **6**, 946–950 (2007).
13. J. Jiang, X. Lin, B. Zhang, *Research* **2018**, 2532819 (2018).
14. W. Ma *et al*., *Nature* **562**, 557–562 (2018).
15. G. Álvarez-Pérez *et al*., *Sci. Adv.* **8**, eabp8486 (2022).
16. G. Hu *et al*., *Nature* **582**, 209–213 (2020).
17. M. Chen *et al*., *Nat. Mater.* **19**, 1307–1311 (2020).
18. J. Duan *et al*., *Nat. Commun.* **12**, 4325 (2021).
19. A. J. Giles *et al*., *Nat. Mater.* **17**, 134–139 (2018).
20. S. Dai *et al*., *Science* **343**, 1125–1129 (2014).
21. H. Herzig Sheinfux *et al*., Multimodal interference and bound in the continuum modes in indirectly-patterned hyperbolic cavities. arXiv:2202.08611 [physics.optics] (2022).
22. Q. Zhang *et al*., *Nature* **597**, 187–195 (2021).
23. Z. Jacob *et al*., *Appl. Phys. B* **100**, 215–218 (2010).
24. R. K. Fisher, R. W. Gould, *Phys. Rev. Lett.* **22**, 1093–1095 (1969).
25. Materials and methods are available as supplementary materials.
26. A. J. Sternbach *et al*., *Nat. Commun.* **11**, 3567 (2020).
27. P. Li *et al*., *Nat. Commun.* **6**, 7507 (2015).
28. E. Yoxall *et al*., *Nat. Photonics* **9**, 674–678 (2015).
29. T. Low *et al*., *Nat. Mater.* **16**, 182–194 (2017).
30. H. N. S. Krishnamoorthy, Z. Jacob, E. Narimanov, I. Kretzschmar, V. M. Menon, *Science* **336**, 205–209 (2012).
31. G. Lu *et al*., *Nano Lett.* **21**, 1831–1838 (2021).
32. A. Yariv, *IEEE J. Quantum Electron.* **9**, 919–933 (1973).
33. Z. Zheng *et al*., *Adv. Mater.* **34**, e2104164 (2022).
34. Q. Chen *et al*., *Photon. Res.* **9**, 1540–1549 (2021).
35. S. Wuestner, A. Pusch, K. L. Tsakmakidis, J. M. Hamm, O. Hess, *Phys. Rev. Lett.* **105**, 127401 (2010).

ACKNOWLEDGMENTS

Funding: Research on polaritons in van der Waals materials is supported as part of Programmable Quantum Materials, an Energy Frontier Research Center funded by the US Department of Energy (DOE), Office of Science, Basic Energy Sciences (BES), under award DE-SC0019443. Work on negative refraction is supported through the Vannevar Bush Faculty Fellow program ONR-VB: N00014-19-1-2630. D.N.B. is a Moore Investigator in Quantum Materials EPIQS GBMF9455. The development of nanophotonics methods is supported by DOE-BES grant DE-SC0018426. Support for the $h^{11}BN$ crystal growth comes from the Office of Naval Research, award N00014-20-1-2474. **Author contributions:** A.J.S. conceived of the study. A.J.S. recorded and analyzed the near-field data, with assistance from S.Z., S.X., S.M., and R.J.; S.M., B.S.Y.K., and S.L. prepared the samples, with guidance from J.H.E., C.D., and J.H.; Y.S. performed far-field measurements. A.R. and M.M.F. performed theoretical calculations, with assistance from A.J.S.; A.J.S., D.N.B., and M.M.F. wrote the manuscript, with input from all the coauthors. **Competing interests:** The authors declare that they have no competing interests. **Data and materials availability:** All data are available in the main text or the supplementary materials. **License information:** Copyright © 2023 the authors, some rights reserved; exclusive licensee American Association for the Advancement of Science. No claim to original US government works. https://www.science.org/about/science-licenses-journal-article-reuse

SUPPLEMENTARY MATERIALS

science.org/doi/10.1126/science.adf1065
Materials and Methods
Supplementary Text
Figs. S1 to S15
Table S1
References (*36*–*45*)

Submitted 30 September 2022; accepted 13 January 2023
10.1126/science.adf1065

NANOPHOTONICS

Gate-tunable negative refraction of mid-infrared polaritons

Hai Hu[1,2]†*, Na Chen[1,2]†, Hanchao Teng[1,2]†, Renwen Yu[3], Mengfei Xue[6], Ke Chen[1,2], Yuchuan Xiao[1,2], Yunpeng Qu[1,2], Debo Hu[1,2], Jianing Chen[6], Zhipei Sun[7], Peining Li[8], F. Javier García de Abajo[4,5]*, Qing Dai[1,2]*

Negative refraction provides a platform to manipulate mid-infrared and terahertz radiation for molecular sensing and thermal emission applications. However, its implementation based on metamaterials and plasmonic media presents challenges with optical losses, limited spatial confinement, and lack of active tunability in this spectral range. We demonstrate gate-tunable negative refraction at mid-infrared frequencies using hybrid topological polaritons in van der Waals heterostructures. Specifically, we visualize wide-angle negatively refracted polaritons in α-MoO_3 films partially decorated with graphene, undergoing reversible planar nanoscale focusing. Our atomically thick heterostructures weaken scattering losses at the interface while enabling an actively tunable transition of normal to negative refraction through electrical gating. We propose polaritonic negative refraction as a promising platform for infrared applications such as electrically tunable super-resolution imaging, nanoscale thermal manipulation, enhanced molecular sensing, and on-chip optical circuitry.

Negative refraction has been extensively investigated in optics (*1*–*3*), nanoelectronics (*4*), acoustics (*5*), and magnetism (*6*) as a counter-intuitive physical phenomenon that holds strong potential for applications such as subwavelength imaging and cloaking (*7*). The past two decades have witnessed substantial progress in this field, with negative refraction demonstrations typically implemented using metallic metamaterials (*8*, *9*), dielectric photonic crystals (*10*, *11*), and hyperbolic metamaterials (*12*–*14*), composed of periodic arrays of subwavelength unit cells. The metamaterials invoked in these structures restrict their ability to strongly confine light. As an alternative, metal plasmons have also demonstrated negative refraction in the ultraviolet (*15*), visible (*16*), and near-infrared regions (*17*). This approach is limited by ohmic losses at visible and higher frequencies as well as by poor spatial confinement in the infrared range. Deep subwavelength negative refraction in the mid-infrared and terahertz domains has therefore remained a challenge despite its potential for sampling and controlling molecular vibrations and thermal radiation.

The emergence of van der Waals (vdW) materials has introduced a new degree of freedom in controlling light at the nanoscale over a wide spectral range by leveraging the strong optical confinement of their polaritonic modes (*18*–*22*). Recent theoretical studies have proposed the use of vdW polaritons to achieve deep subwavelength mid-infrared negative refraction, for example, in periodic arrays of graphene (*23*), or using planar graphene and hexagonal boron nitride (*h*-BN) heterostructures (*24*). Nevertheless, the extreme spatial confinement of polaritons in these structures hinders tailoring of their dispersions; reflection and scattering losses inherent to such structures also complicate the realization of theoretical concepts.

Results and discussion

We demonstrate deep subwavelength mid-infrared negative refraction by constructing a vdW heterostructure consisting of an α-MoO_3 film partially covered by monolayer graphene. Phonon polaritons (PhPs) in α-MoO_3 exhibit in-plane hyperbolic dispersion in the Reststrahlen band II from 816 to 972 cm^{-1}, where the permittivity components along the [100], [001], and [010] crystal directions satisfy $\varepsilon_x < 0$, $\varepsilon_y > 0$, and $\varepsilon_z > 0$, respectively (*25*–*28*) (note S1 and fig. S1). By contrast, graphene supports highly confined isotropic plasmons in this spectral region (*29*, *30*), such that anisotropic hyperbolic PhPs in the α-MoO_3 couple to graphene plasmons and results in an optical topological transition that allows us to flexibly engineer dispersion and isofrequency contours (IFCs) (*31*–*34*) (fig. S2).

By conserving the polariton wave vector along the direction of the interface (i.e., the

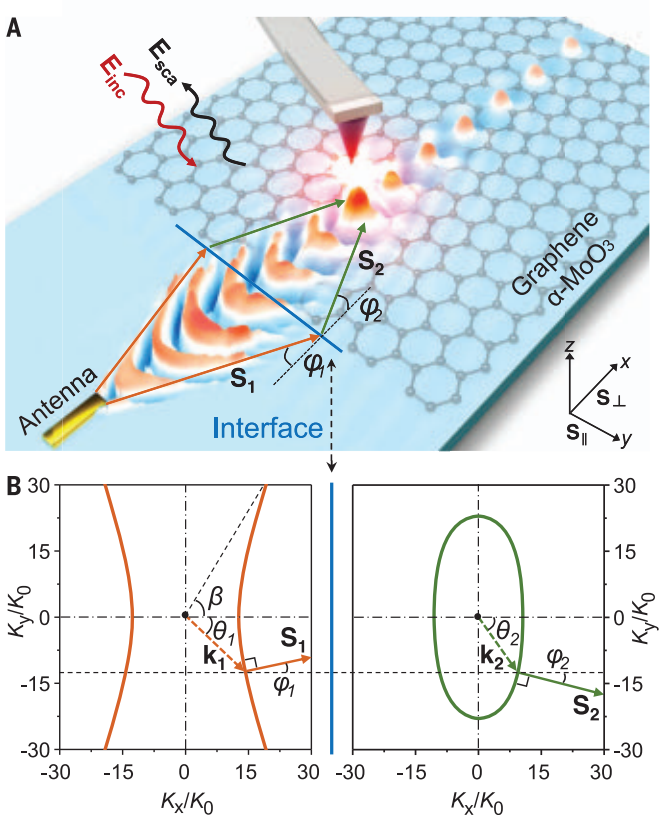

Fig. 1. Negative refraction of polaritons in two dimensions. (**A**) Schematics of the device. (**B**) IFCs of polaritons in hyperbolic (α-MoO_3) and elliptic (graphene/α-MoO_3) media. Negative refraction takes place at the interface between the two media as a result of conservation of the tangential wave vector. We define incidence and refraction angles θ_1 and θ_2 of the polaritons with wave vectors k_1 and k_2, respectively, as well as incidence and refraction angles φ_1 and φ_2 of the corresponding Poynting vectors S_1 and S_2, respectively. Angles are defined as positive (negative) on the upside (downside) of the direction normal to the interface.

[1]CAS Key Laboratory of Nanophotonic Materials and Devices, CAS Key Laboratory of Standardization and Measurement for Nanotechnology, CAS Center for Excellence in Nanoscience, National Center for Nanoscience and Technology, Beijing 100190, China. [2]Center of Materials Science and Optoelectronics Engineering, University of Chinese Academy of Sciences, Beijing 100049, China. [3]Department of Electrical Engineering, Ginzton Laboratory, Stanford University, Stanford, CA, USA. [4]ICFO-Institut de Ciencies Fotoniques, The Barcelona Institute of Science and Technology, 08860 Castelldefels (Barcelona), Spain. [5]ICREA-Institució Catalana de Recerca i Estudis Avançats, Passeig Lluís Companys 23, 08010 Barcelona, Spain. [6]The Institute of Physics, Chinese Academy of Sciences, P.O. Box 603, Beijing, China. [7]QTF Centre of Excellence, Department of Electronics and Nanoengineering, Aalto University, FI-02150 Espoo, Finland. [8]Wuhan National Laboratory for Optoelectronics and School of Optical and Electronic Information, Huazhong University of Science and Technology, Wuhan, China.
*Corresponding author. Email: daiq@nanoctr.cn, javier.garciadeabajo@nanophotonics.es, huh@nanoctr.cn
†These authors contributed equally to this work.

graphene edge), negative refraction is shown to take place when polaritons traverse the in-plane interface between the two regions (Fig. 1A). The Poynting vector S (directed along the energy flow, which is normal to the IFC) and the wave vector k are not collinear for non-circular IFCs (fig. S3 and note S2), such as those of hyperbolic polaritons in α-MoO_3 (Fig. 1B) (*35*). Because the boundary conditions at the interface (between α-MoO_3 with and without covering graphene) only require conservation of the tangential wave vector component $k_{\parallel} = k \sin\theta$, where θ is the angle between the wave vector and the direction normal to the interface, the refracted wave can exhibit normal (positive) refraction for k, but negative refraction for S (with $S_{\parallel} = S \sin\varphi$, where φ is the angle between the Poynting vector and the interface normal). Additional explanations regarding negative refraction are shown in fig. S4.

Negative refraction transforms the linear interface into a lens capable of focusing at a position determined from the relation between incidence and refraction angles, which can in turn be obtained by inspecting the distribution of the *z*-*z* component of the Dyadic Green function in real space and then comparing the Poynting vector S to the IFCs (see details in fig. S5 and note S3). Notably, because the IFCs possess inversion symmetry with respect to the graphene edge, negative refraction occurs reversibly when crossing the interface in both directions (i.e., to or from bare α-MoO_3).

For an experimental demonstration of negative refraction, we fabricated a gold antenna on one side of the interface (fig. S6) to serve as an excitation source of polaritons. Features of negative refraction are revealed by a scattering-type scanning near-field optical microscope equipped with a tunable quantum cascade laser (*36*, *37*). When hyperbolic PhPs are launched on the bare α-MoO_3 side and propagate toward the region covered by graphene, negative refraction occurs and the transmitted concave wavefront is observed to shrink sharply (Fig. 2, A and C). The focal point is situated at the fringe with the smallest full width at half maximum [(FWHM), the fifth fringe], yielding foci of FWHM as small as 373 nm (i.e., 1/30 of the free-space light wavelength) (Fig. 2E, right panel). After passing the focal spot, the wavefront begins to spread slightly in a diffractive fashion (sixth and higher order fringes).

We also demonstrate negative refraction when reversing the propagation direction by placing the launching antenna on the graphene/α-MoO_3 side (fig. S7), so that the diverging elliptic polaritons in such a medium are transmitted into converging hyperbolic PhPs in bare α-MoO_3 (Fig. 2, B and D), and a tightly squeezed focal spot (FWHM = 303 nm) is produced (Fig. 2E, right panel). After passing the focal point, the wavefront begins to spread slightly, but now with a hyperbolic wavefront. For a given set of polariton IFCs, the focusing effect can be modulated by moving the launching source, which produces a phase shift of the entire propagation wave (fig. S8).

The focusing concentrates the energy carried by polaritons to enhance the field intensity. Indeed, the square of the ratio of the electrical field at the focal spot to that without focusing yields an intensity increase by a factor of 10 (Fig. 2E and fig. S9). We note that losses related to refraction at the interface—which involve modal-profile mismatch between PhPs in α-MoO_3 and hybrid polaritons in graphene/α-MoO_3, as well as additional losses at the graphene edge—are relatively low (see details in figs. S10 and S11). Our experimental measurements agree well with simulated near-field distributions of Re{E_z} (Fig. 2, A and D) and the extracted simulation near-field profile also quantitatively matches the experimental data (fig. S9).

The reported in-plane negative refraction takes place over a wide range of incidence angles (Fig. 2F) as well as a wide spectral range, where the opening angle β of PhPs in α-MoO_3 increases with the illumination frequency, and the focal length varies in opposite ways with frequency for the two reversed refraction scenarios (figs. S12 and S13). For incidence or refraction in bare α-MoO_3, the incidence and refraction angles are both limited by the opening angle β as a result of PhPs propagation being prohibited beyond the IFC hyperbolic region, whereas negative refraction can be generated for a wide-angle range. Notably, in the Reststrahlen band III (higher light frequency from 958 to 1010 cm^{-1}), a lateral heterostructure can also achieve nanoscale negative refraction arising from the negative group velocity in the reversed dispersion of PhPs in α-MoO_3, whereas the actual experiment must take the impact of interface losses into account (*24*).

Active control and dynamic switching of negative refraction can be gained through electrostatic gating by varying the graphene chemical potential. We have demonstrated this possibility by preparing samples with a SiO_2/doped-Si substrate instead of Au, such that

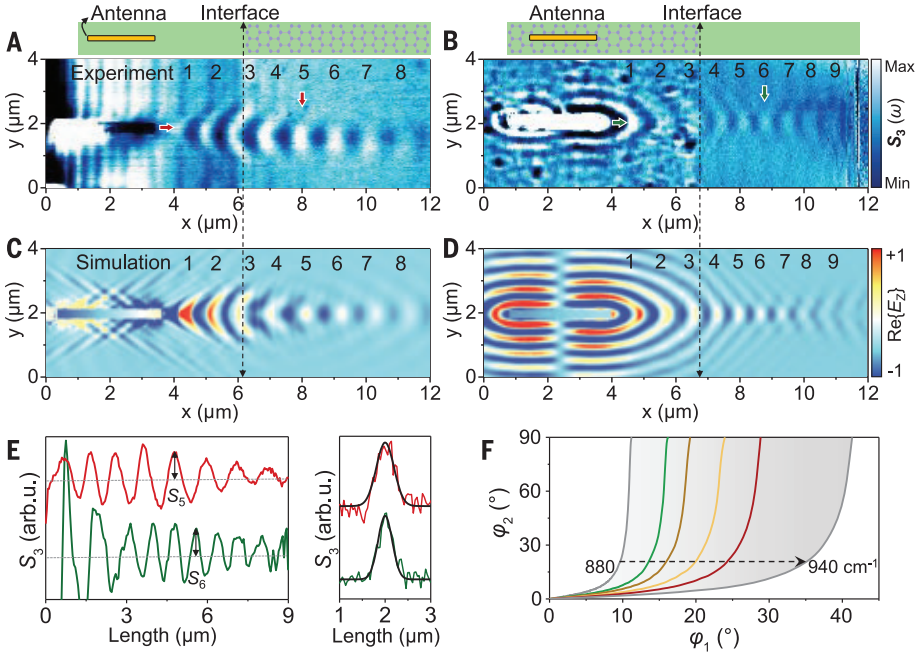

Fig. 2. Direct observation of nanoscale negative refraction. (**A** and **C**) Experimental (A) and simulated (C) near-field images illustrating negative refraction from a hyperbolic wave in α-MoO_3 to an elliptic wave in a graphene/α-MoO_3 heterostructure. (**B** and **D**) Negative refraction from elliptic to hyperbolic waves with the antenna now placed on the graphene/α-MoO_3 side. (**E**) Near-field profiles along the *x* (left) and *y* (right) directions [see red and green arrows in panels (A) and (B)]. Black curves in the latter are Gaussian fits of the transverse focal profile. All experimental results are measured from an in situ sample. The α-MoO_3 thickness is d = 242 nm. The graphene is mechanically exfoliated and statically doped to E_F = 0.5 eV by coverage with monolayer α-$RuCl_3$. The illumination frequency is ω_0 = 893 cm^{-1} (A) and 900 cm^{-1} (B), respectively. (**F**) Refraction (incidence) angle φ_2 in graphene/α-MoO_3 as a function of incidence (refraction) angle φ_1 in α-MoO_3 for various illumination frequencies from 880 to 940 cm^{-1} (gray shaded area). Color curves represent specific frequencies measured in our experiments.

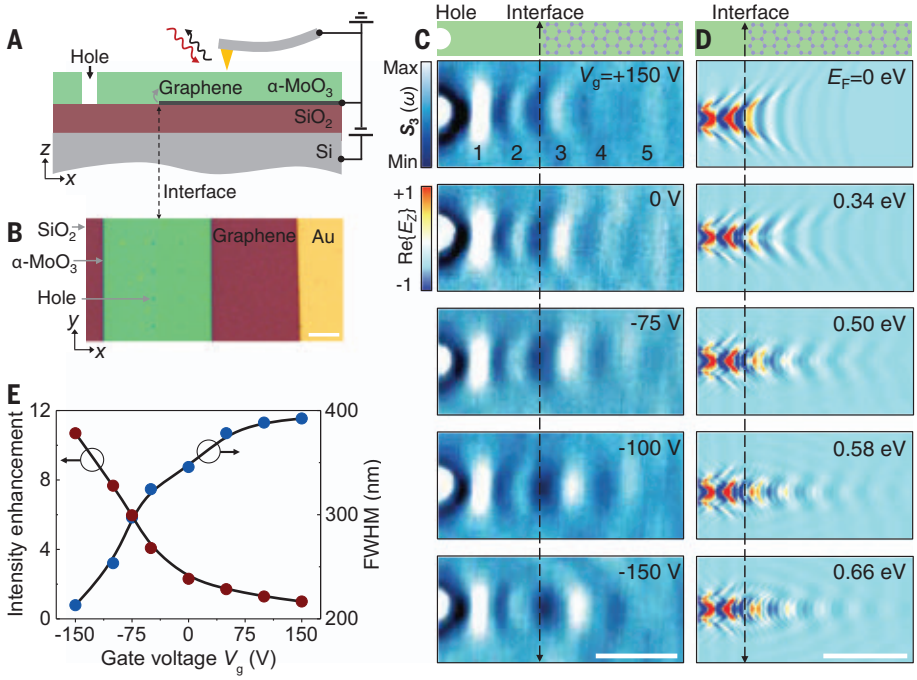

Fig. 3. Gate-tunable negative refraction. (**A**) Scheme of the gate-tunable device. (**B**) Optical image of a device consisting of an α-MoO_3 film, double-layer graphene, and SiO_2 substrate (from top to bottom). The diameter of the circular holes is 400 nm. (**C**) Experimentally measured near-field images of the transition from normal to negative refraction with gate voltages varying from +150 to −150 V. The vertical black dashed line represents the interface defined by the graphene edge. (**D**) Numerically simulated negative refraction with various Fermi energies of graphene from E_F = 0 to 0.66 eV, corresponding to the applied gate voltages. (**E**) Intensity enhancement (left) and FWHM (right) of the focal spots for various gate voltages, taken from the experimental measurements in (C). The α-MoO_3 thickness is d = 60 nm and the illumination frequency is fixed at 893 cm^{-1}. The scale bar indicates 10 μm (A), 0.5 μm (C), and 2.5 μm (D), respectively.

we can apply a perpendicular electric field to graphene through a SiO_2 dielectric layer coating a Si backgate (Fig. 3A). To obtain a clean interface, we have directly transferred an α-MoO_3 film with through holes on the graphene with prefabricated electrodes (Fig. 3B), where polaritons are excited by the tip and subsequently reflected by the hole edge.

The effect of changing gating voltage V_g on the polaritons is shown in Fig. 3C and fig. S15, where the Fermi energy is tuned over a wide range from E_F = 0 to ~0.66 electron volts (eV). By decreasing V_g, the open angle of the hyperbolic wavefront continues to shrink toward the canalization point for the graphene/α-MoO_3 region (figs. S15 and S16 and Fig. 3C), whereas the hyperbolic polaritons in bare α-MoO_3 show no response to the gate voltage (fig. S16A). This is attributable to a gradual switch on of negative refraction that originates in the topological transition of hybrid polaritons as holes are increasingly injected into graphene by lowering V_g. Our simulations further reproduce the continuous switching of negative refraction with varying doping levels of graphene (Fig. 3D and fig. S16B).

This gate-tunable negative refraction provides the capability to actively control the wavefront of polaritons in situ and change the focusing position and the corresponding optical fields at the nanoscale (Fig. 3, C and D). As the gate voltage changes from +150 to −150 V, the FWHM transverse size of the focal spot decreases and the focal field intensity increases by more than one order of magnitude (Fig. 3E and fig. S17). Figure S18 shows our gate-tunable negative refraction of another sample with monolayer graphene and thinner α-MoO_3, where the FWHM of the focal point reaches sizes as small as 185 nm (i.e., ~1/60 or 1.6% of the free-space light wavelength).

Negative refraction achieved by engaging topological polaritons with different IFC shapes is distinct from that attained by using bulk materials with a negative index of refraction (*8*). We are essentially relying on a homogeneous film (α-MoO_3) in which the addition of an atomically thin layer (graphene) radically changes the polaritonic mode characteristics to enable negative refraction. By changing the Fermi energy of graphene (and correspondingly, the composition of the topological hybrid polaritons), we can actively and continuously transition from normal to negative refraction (figs. S19 and S20 show how gate tuning of graphene affects negative refraction), whereas control of bulk materials remains a challenge. Note that, to achieve a high degree of negative refraction, the required doping level is relatively high. Therefore, we use double-layer graphene and adopt thinner α-MoO_3 films in Fig. 3 to decrease the demand for gate voltages, although this results in a shorter propagation distance than in the thicker sample in Fig. 2. To balance propagation distance and tunability range, more efficient double (top-and-back) gates (*38*) are promising for future investigations, possibly in combination with glass or ion gel spacers.

Conclusion

We have experimentally demonstrated a transition from normal to negative refraction in the mid-infrared spectral region by designing a vdW heterostructure consisting of an extended α-MoO_3 film that is half covered by monolayer graphene. The observed negative refraction over a wide range of incidence angles, which relies on topological polaritons with tunable dispersion curves, is revealed through real-space nanoimaging based on infrared nanoscopy. We leverage reversible negative refraction to demonstrate nanoscale focusing with either concave or convex wavefronts, which—because of the high spatial confinement of polaritons and the atomic thickness of the employed vdW structures—results in deep subwavelength focal spots with highly squeezed sizes of less than 60 times that of the corresponding illumination wavelength, more than tenfold intensity enhancement, and ~90% transmission of negatively refracted energy. Notably, we show that the transition from normal to negative refraction can be actively tuned by an electrostatic gate, resulting in the ability to control the wavefront of polaritons in situ and change focal spots and their nanoscale optical fields.

Considering the vast range of freshly available two-dimensional polaritonic materials, we anticipate negative refraction of polaritons in other vdW heterostructures involving, for example, α-V_2O_5, black phosphorus, and nanostructured metasurfaces (e.g., based on isotopically pure *h*-BN). The broad suite of existing materials could lead to polaritonic negative refraction covering the entire mid-infrared and terahertz region. The combined advantage of strong polariton-field confinement, flexible control over anisotropic polariton propagation and focusing, and tunability by material stacking as well as electric gating opens exciting avenues for negative refraction in optical and thermal applications.

REFERENCES AND NOTES

1. J. B. Pendry, *Phys. Rev. Lett.* **85**, 3966–3969 (2000).
2. R. A. Shelby, D. R. Smith, S. Schultz, *Science* **292**, 77–79 (2001).
3. J. Yao *et al.*, *Science* **321**, 930 (2008).

4. G.-H. Lee, G.-H. Park, H.-J. Lee, *Nat. Phys.* **11**, 925–929 (2015).
5. H. He *et al.*, *Nature* **560**, 61–64 (2018).
6. A. Pimenov, A. Loidl, P. Przyslupski, B. Dabrowski, *Phys. Rev. Lett.* **95**, 247009 (2005).
7. W. Cai, U. K. Chettiar, A. V. Kildishev, V. M. Shalaev, *Nat. Photonics* **1**, 224–227 (2007).
8. D. R. Smith, J. B. Pendry, M. C. Wiltshire, *Science* **305**, 788–792 (2004).
9. K. L. Tsakmakidis, A. D. Boardman, O. Hess, *Nature* **450**, 397–401 (2007).
10. E. Cubukcu, K. Aydin, E. Ozbay, S. Foteinopoulou, C. M. Soukoulis, *Nature* **423**, 604–605 (2003).
11. P. V. Parimi, W. T. Lu, P. Vodo, S. Sridhar, *Nature* **426**, 404 (2003).
12. A. Poddubny, I. Iorsh, P. Belov, Y. Kivshar, *Nat. Photonics* **7**, 948–957 (2013).
13. J. S. Gomez-Diaz, A. Alù, *ACS Photonics* **3**, 2211–2224 (2016).
14. Q. Chen *et al.*, *Photon. Res.* **9**, 1540–1549 (2021).
15. T. Xu, A. Agrawal, M. Abashin, K. J. Chau, H. J. Lezec, *Nature* **497**, 470–474 (2013).
16. H. J. Lezec, J. A. Dionne, H. A. Atwater, *Science* **316**, 430–432 (2007).
17. V. Podolskiy, A. Sarychev, V. Shalaev, *Opt. Express* **11**, 735–745 (2003).
18. A. Vakil, N. Engheta, *Science* **332**, 1291–1294 (2011).
19. D. N. Basov, M. M. Fogler, F. J. García de Abajo, *Science* **354**, aag1992 (2016).
20. T. Low *et al.*, *Nat. Mater.* **16**, 182–194 (2017).
21. Q. Zhang *et al.*, *Nature* **597**, 187–195 (2021).
22. Y. Wu *et al.*, *Nat. Rev. Phys.* **4**, 578–594 (2022).
23. K. V. Sreekanth, A. De Luca, G. Strangi, *Appl. Phys. Lett.* **103**, 023107 (2013).
24. X. Lin *et al.*, *Proc. Natl. Acad. Sci. U.S.A.* **114**, 6717–6721 (2017).
25. W. Ma *et al.*, *Nature* **562**, 557–562 (2018).
26. Z. Zheng *et al.*, *Sci. Adv.* **5**, eaav8690 (2019).
27. G. Hu *et al.*, *Nature* **582**, 209–213 (2020).
28. M. Chen *et al.*, *Nat. Mater.* **19**, 1307–1311 (2020).
29. J. Chen *et al.*, *Nature* **487**, 77–81 (2012).
30. Z. Fei *et al.*, *Nature* **487**, 82–85 (2012).
31. G. Álvarez-Pérez *et al.*, *ACS Photonics* **9**, 383–390 (2022).
32. Y. Zeng *et al.*, *Nano Lett.* **22**, 4260–4268 (2022).
33. F. L. Ruta *et al.*, *Nat. Commun.* **13**, 3719 (2022).
34. H. Hu *et al.*, *Nat. Nanotechnol.* **17**, 940–946 (2022).
35. G. Álvarez-Pérez *et al.*, *Sci. Adv.* **8**, eabp8486 (2022).
36. P. Alonso-González *et al.*, *Science* **344**, 1369–1373 (2014).
37. P. Li *et al.*, *Science* **359**, 892–896 (2018).
38. Y. Zhang *et al.*, *Nature* **459**, 820–823 (2009).

ACKNOWLEDGMENTS

This work was completed especially for the 20th anniversary of the National Center for Nanoscience and Technology, Beijing. The authors acknowledge the Nanofabrication Lab of NCNST for assistance in sample fabrication. **Funding:** This work was funded by the following: National Key Research and Development Program of China grant 2021YFA1201500 (to Q.D.); National Key Research and Development Program of China grant 2020YFB2205701 (to H.H.); National Natural Science Foundation of China grants 51902065 and 52172139 (to H.H.); National Natural Science Foundation of China grants 51925203 and U2032206 (to Q.D.); National Natural Science Foundation of China grant U2032206 (to Q.D.); National Natural Science Foundation of China grant 52072083 (to D.B.H.); National Natural Science Foundation of China grant 62075070 (to P.N.L.); Beijing Municipal Natural Science Foundation grant 2202062 (to H.H.); Beijing Nova Program grant 2022012 (to H.H.); Strategic Priority Research Program of Chinese Academy of Sciences grant XDB36000000 (to Q.D.); ERC grant 789104-eNANO (to F.J.G.A.); Spanish MICINN grants PID2020-112625GB-I00 and SEV2015-0522 (to F.J.G.A.); Academy of Finland grants 314810, 333982, 336144, 352780, 352930, and 353364 (to Z.P.S.); Academy of Finland Flagship Programme grant 320167, PREIN (to Z.P.S.); EU H2020-MSCA-RISE-872049 (IPN-Bio) (to Z.P.S.); ERC grant 834742 (to Z.P.S.). **Author contributions:** Conceptualization: Q.D., F.J.G.A., and H.H. Supervision: Q.D. and F.J.G.A. Funding acquisition: Q.D., H.H., F.J.G.A., Z.P.S., P.N.L., and D.B.H. Experimentation: H.H. and N.C. Theory and simulation: H.C.T., R.W.Y., and F.J.G.A. Data Analysis: H.H., N.C., and H.C.T. Writing – original draft: H.H., N.C., H.C.T., and Q.D. Writing – review and editing: H.H., N.C., H.C.T., Q.D., F.J.G.A., Z.P.S., P.N.L., J.N.C., R.W.Y., D.B.H., Y.P.Q., M.F.X., K.C., and Y.C.X. **Competing interests:** The authors declare no competing interests. **Data and materials availability:** The data that support the findings of this study are all available and archived in the main text or the supplementary materials.

License information: Copyright © 2023 the authors, some rights reserved; exclusive licensee American Association for the Advancement of Science. No claim to original US government works. https://www.sciencemag.org/about/science-licenses-journal-article-reuse

SUPPLEMENTARY MATERIALS

science.org/doi/10.1126/science.adf1251
Materials and Methods
Notes S1 to S3
Figs. S1 to S21
Table S1
References (*39*–*44*)

Submitted 30 September 2022; accepted 13 January 2023
10.1126/science.adf1251

HOMININ EVOLUTION

Expanded geographic distribution and dietary strategies of the earliest Oldowan hominins and *Paranthropus*

Thomas W. Plummer[1,2,3,4]*, James S. Oliver[5], Emma M. Finestone[6,7], Peter W. Ditchfield[8], Laura C. Bishop[9,10], Scott A. Blumenthal[4,11,12], Cristina Lemorini[13], Isabella Caricola[13,14], Shara E. Bailey[3,15], Andy I. R. Herries[16,17], Jennifer A. Parkinson[4,18], Elizabeth Whitfield[9], Fritz Hertel[19], Rahab N. Kinyanjui[4,20,21], Thomas H. Vincent[9], Youjuan Li[22,23], Julien Louys[24], Stephen R. Frost[11], David R. Braun[25,26], Jonathan S. Reeves[26], Emily D. G. Early[4,27], Blasto Onyango[20], Raquel Lamela-Lopez[2,3], Frances L. Forrest[28,29], Huaiyu He[30], Timothy P. Lane[9], Marine Frouin[31], Sébastien Nomade[32,33], Evan P. Wilson[2,3], Simion K. Bartilol[34], Nelson Kiprono Rotich[35], Richard Potts[4,20]

The oldest Oldowan tool sites, from around 2.6 million years ago, have previously been confined to Ethiopia's Afar Triangle. We describe sites at Nyayanga, Kenya, dated to 3.032 to 2.581 million years ago and expand this distribution by over 1300 kilometers. Furthermore, we found two hippopotamid butchery sites associated with mosaic vegetation and a C_4 grazer–dominated fauna. Tool flaking proficiency was comparable with that of younger Oldowan assemblages, but pounding activities were more common. Tool use-wear and bone damage indicate plant and animal tissue processing. *Paranthropus* sp. teeth, the first from southwestern Kenya, possessed carbon isotopic values indicative of a diet rich in C_4 foods. We argue that the earliest Oldowan was more widespread than previously known, used to process diverse foods including megafauna, and associated with *Paranthropus* from its onset.

The appearance of Oldowan tools around 2.6 million years ago (Ma) was a technological breakthrough that used systematically produced, sharp-edged flakes for cutting and cobbles or cores for percussion (*1*). Although the Oldowan is often attributed to the genus *Homo*, multiple hominin taxa overlapped temporally and geographically with these early tools, and it is possible that other genera, such as *Paranthropus*, made and/or used them. Some have linked emergent Oldowan technology to the first access to or more efficient processing of nutrient-rich animal carcasses [for example, (*2*, *3*)]. Others have argued that plant food processing was the primary goal of early Oldowan stone tool usage, with increased carnivory (and butchery with stone tools) being added to the behavioral repertoire after 2 Ma (*4*, *5*). The evolutionary benefits connected with the emergence of Oldowan technology are unclear because of the paucity of late Pliocene Oldowan sites, hitherto known only from the Afar Triangle of Ethiopia at Gona and Ledi-Geraru, localities found approximately 50 km away from each other (*6*, *7*). In this study, we report 3.032–2.595 Ma deposits at Nyayanga, Kenya, that expand the geographic range of the earliest Oldowan by more than 1300 km and the range of *Paranthropus* by approximately 230 km to southwestern Kenya. Archeological findings demonstrate that hominins used tools to butcher a variety of animals, including megafauna, and process diverse plants at the Oldowan's inception.

Nyayanga (0° 23.909'S, 34° 27.115'E) is an archeological and paleontological locality on the western shoreline of the Homa Peninsula (Fig. 1A) [(*8*), section 1]. The peninsula is located on the southern margin of the Winam Gulf of Lake Victoria, within the east-west–oriented Nyanza Rift between the two main branches of the East African Rift System (*9*). It is dominated by the Homa Mountain carbonatite complex, which on its flanks bears alluvial, fluvial, and lacustrine sediments that range in age from 6 Ma through the Holocene (*10*–*13*). Sediments at Nyayanga are exposed in a 40,000 m^2 amphitheater and a gully that can be traced for 500 m upslope (Fig. 1). Excavations and surface collection focused on the top half of the oldest bed (Fig. 1, NY-1),

which yielded Oldowan artifacts, *Paranthropus* sp. fossils, and faunal fossils in overbank deposits from a westward-flowing paleochannel [(*8*), section 2].

The age of the Nyayanga Beds is constrained by (U-Th)/He dating of apatite crystals, magnetostratigraphy, lithostratigraphic correlation with the Rawi Fm (*11*, *13*) deposited north of Homa Mountain, and biostratigraphy. The (U-Th)/He dating of apatite crystals yielded ages of 2.87 ± 0.79 Ma and 2.98 ± 0.50 Ma from two tuffaceous silts in NY-1 (fig. S1 and table S1) [(*8*), section 3]. Magnetostratigraphic sampling was carried out on the excavation 3 slope and in trenches 9 and 11 (Fig. 1) [(*8*), section 4]. The Nyayanga sequence shows reversed polarity in unit A, intermediate-normal to normal polarity from basal to middle NY-1, normal polarity from middle NY-1 through NY-2, intermediate normal polarity in the base of NY-3, and reversed polarity at the top of NY-3 (Fig. 1, fig. S2, and table S2). The (U-Th)/He apatite crystal dates suggest that the normal interval corresponds to the C2An.1n Subchron between 3.032 and 2.595 Ma (*14*). This is similarly indicated by the lithostratigraphic correlation of the Nyayanga Beds with the Rawi Fm (*11*, *13*), which was also deposited during the C2An.1n Subchron. Biostratigraphy [(*8*), section 6] is consistent with a late Pliocene age, including more archaic examples of two pig species, the suine *Metridiochoerus andrewsi* and the tetraconodont *Notochoerus* cf. *scotti*, than the nearby locality of Kanjera South from 2 Ma (*13*), as well as an equid sample composed exclusively of hipparionin (*Eurygnathohippus* sp.) fossils. The latter indicates a date earlier than the 2.3 Ma dispersal of *Equus* across Africa (*15*). Acknowledging the wide 1σ uncertainty, the combination of (U-Th)/He apatite crystal dates, biostratigraphy, and the transitional nature of the magnetostratigraphy of lower NY-1 supports deposition early in the temporal range of the C2An.1n Subchron.

We recovered 330 artifacts from the upper half of NY-1; 135 were recovered in situ from excavations 3 and 5, and 195 were recovered from the surface [(*8*), section 7]. The overall technological attributes of tools, such as core and flake sizes and the number of flake scars on cores, are similar to other Oldowan assemblages (Fig. 2A and table S4). Nyayanga hominins efficiently removed flakes from cores using unifacial, bifacial, and multifacial reduction that is also comparable with technology at other Oldowan localities (*7*). The presence of cortical flakes and hammerstones with battering damage is consistent with on-site flake production through hard hammer percussion. Artifacts were manufactured from a diverse array of raw materials, including rhyolite, quartzite, and quartz. The Nyayanga assemblage is distinct in containing a high frequency of cores (20.6%, n = 68) (Fig. 2B) and a large percentage of artifacts preserving evidence of percussive activities (7.0%, n = 23) (Fig. 2C).

A total of 1776 bones were recovered in situ from NY-1 in excavation 3 (n = 1580) and excavation 5 (n = 196). The most common taxa in excavations 3 and 5 are hippopotamids [57.1 and 61.9% of the number of identified specimens (NISP), respectively] followed by bovids (19.2 and 22.2% of the NISP, respectively) (fig. S4 and tables S5 and S6) [(*8*), section 8]. The high in situ frequencies of animals preferring near-water habitats [such as hippopotamids, turtles, crocodilians, and cane rats (*Thryonomyidae*)] reflect a riparian depositional context. Bone surface preservation was highly variable, but more than 85% of the sample in both excavations showed no or minimal weathering, which is consistent with the results of rapid burial by fluvial sediments (fig. S7).

Hippopotamid butchery is documented in both excavation 3 and excavation 5. A minimum of two hippopotamid individuals were recovered from excavation 3 (fig. S5). The more complete individual is composed of 241 bone fragments from across the skeleton, including a large axial bone concentration likely marking its death site. Stone tools (n = 42) were closely associated with the skeleton, including several tools recovered in direct physical contact with hippopotamid bones. Despite the varied bone preservation, one hippopotamid rib fragment exhibits a deep cutmark with clearly preserved internal striations (Fig. 3B), and three stone flakes (detached pieces) exhibit use-wear indicative of butchery.

In excavation 5, 39 hippopotamid bones, likely from a single individual, were found spatially associated with 14 artifacts (fig. S6). One cluster of bones consisted of girdle elements (scapula, innominate), appendicular elements (proximal half of tibia, calcaneum), a flake, and a split cobble with percussion damage. The anterior tuberosity of the tibia has a series of four short, parallel cutmarks (Fig. 3A). A second cluster of bones, located 2 m away, consists of a broken humerus, a flake, a rib fragment, and a manuport. The nonanatomical placement of these bones, some with hominin damage, and associated artifacts (one with use-wear indicative of butchery) in a fine silt suggests that the bones may have been moved by hominins while butchering the carcass.

Tool-damaged bones of nonhippopotamid taxa were also found in the excavations and eroding out of NY-1 in the amphitheater. A size three bovid scapular spine fragment with cut marks was found eroding from an in-situ context at about the same level as the excavation 5 hippopotamid (Fig. 3C). Other bones from NY-1 with cut marks or percussion damage show that hominins were consuming both meat and marrow (Fig. 3D), a finding supported by use-wear analysis. Overall frequencies of hominin damage from the excavations are low: 0.9 and 1.9% at excavations 3 and 5, respectively (table S7). In part, this reflects poor surface preservation of many of the fossils as well as fragmentation of ribs.

Use-wear observed on 30 quartz, quartzite, granite, carbonatite, and rhyolite tools from NY-1 confirm hominin processing of faunal remains and plant tissue [(*8*), section 9]. Use-wear found on six pounded pieces (*16*) and 17 flaked pieces (cores) show macro- and microtraces related to pounding activities (fig. S8). Percussive stone tools were heavily used, showing deep pits and developed polishes and striations at low and high magnification, which, based on modern experiments, require at least several hours of use to emerge. On the

[1]Department of Anthropology, Queens College, Flushing, NY, USA. [2]The CUNY Graduate Center, New York, NY, USA. [3]New York Consortium in Evolutionary Primatology, New York, NY, USA. [4]Human Origins Program, National Museum of Natural History, Smithsonian Institution, Washington, DC, USA. [5]Anthropology Section, Illinois State Museum Springfield, IL, USA. [6]The Cleveland Museum of Natural History, Cleveland, OH, USA. [7]Department of Archeology, Max Planck Institute for the Science of Human History, Jena, Germany. [8]School of Archeology, University of Oxford, Oxford, UK. [9]Research Centre in Evolutionary Anthropology and Paleoecology, School of Biological and Environmental Sciences, Liverpool John Moores University, Liverpool, UK. [10]The Sino-British College, University of Shanghai for Science and Technology, Shanghai, China. [11]Department of Anthropology, University of Oregon, Eugene, OR, USA. [12]University of British Columbia, Vancouver, BC, Canada. [13]LTFAPA Laboratory, Department of Classics, Sapienza University of Rome, Rome, Italy. [14]School of History, Classics and Archeology, Newcastle University, Newcastle upon Tyne, UK. [15]Department of Anthropology, New York University, New York, NY, USA. [16]The Australian Archaeomagnetism Laboratory, Dept. Archaeology and History, La Trobe University, Melbourne Campus, 3086 Bundoora, Victoria, Australia. [17]Paleo-Research Institute, University of Johannesburg, Johannesburg, South Africa. [18]Department of Anthropology, University of San Diego, San Diego, CA, USA. [19]Department of Biology, California State University, Northridge, CA, USA. [20]National Museums of Kenya, Nairobi, Kenya. [21]Max Planck Institute for Geoanthropology, Jena, Germany. [22]Department of Geoscience, University of Wisconsin-Madison, Madison, WI, USA. [23]Institute of Geology, China Earthquake Administration, Beijing, China. [24]Australian Research Centre for Human Evolution, Griffith University, Brisbane, Australia. [25]Department of Anthropology, George Washington University, Washington, DC, USA. [26]Max Planck Institute for Evolutionary Anthropology, Leipzig, Germany. [27]Arizona Museum of Natural History, Mesa, AZ, USA. [28]Department of Sociology and Anthropology, Fairfield University, Fairfield, CT, USA. [29]American Museum of Natural History, New York, NY, USA. [30]Institute of Geology and Geophysics, Chinese Academy of Sciences, Beijing, China. [31]Department of Geosciences, Stony Brook University, Stony Brook, NY, USA. [32]Laboratoire des Sciences du Climat et de l'Environnement, Université de Versailles Saint-Quentin and Paris Saclay, Gif Sur Yvette, France. [33]Institut Pierre Simon Laplace, Guyancourt, France. [34]Institute of Nuclear Science and Technology, University of Nairobi, Nairobi, Kenya. [35]Institute of Nuclear Chemistry and Technology, Warsaw, Poland.
***Corresponding author. Email: thomas.plummer@qc.cuny.edu**

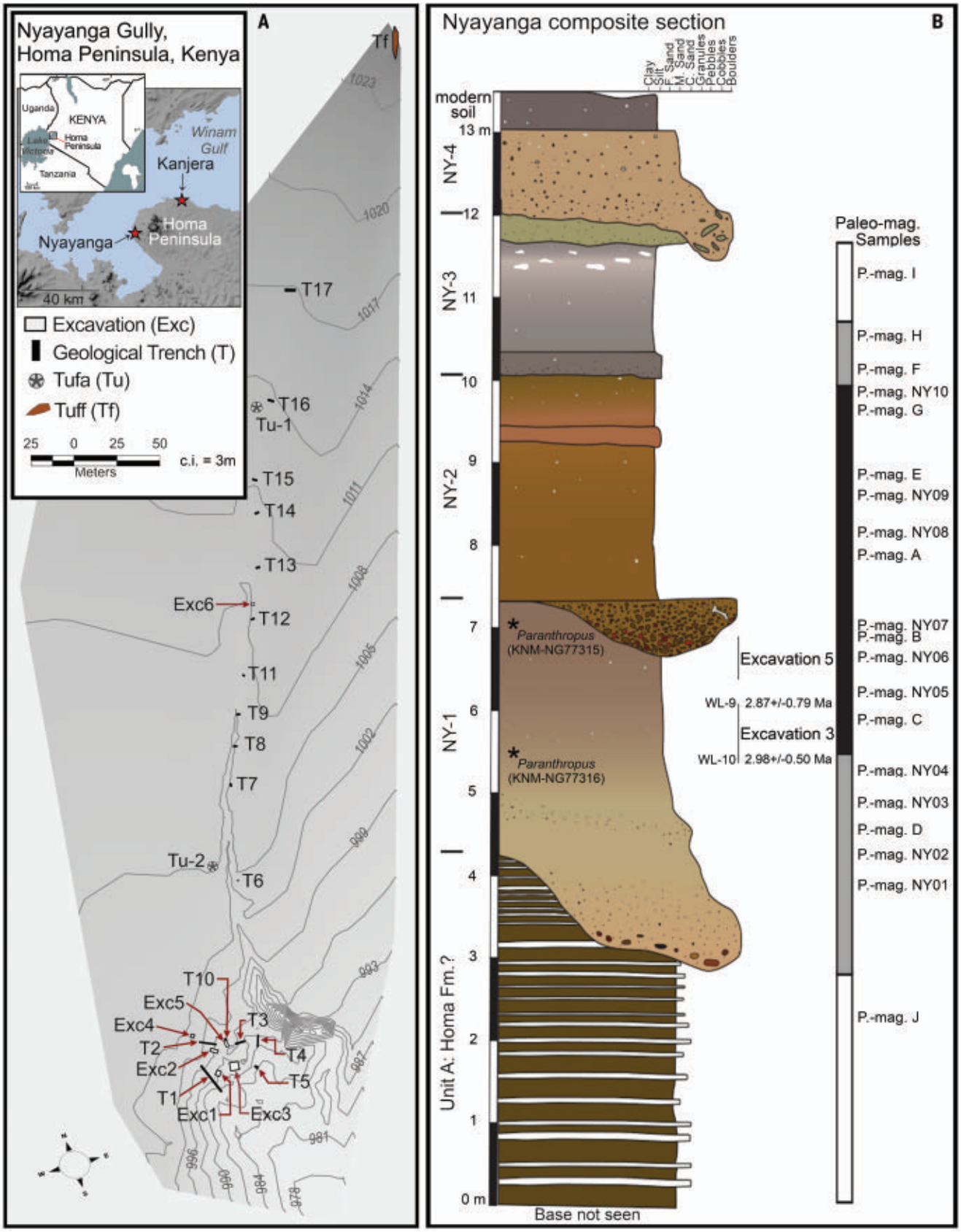

Fig. 1. Nyayanga gully, stratigraphy, magnetostratigraphic data, and apatite crystal dating results. (**A**) Topographic map of the gully system showing the locations of geologic trenches and excavations. (**B**) Composite stratigraphic column of the Nyayanga Beds showing the stratigraphic placement of excavations 3 and 5 and the magnetostratigraphic profile. Reversed polarity is shown in white, intermediate normal polarity in gray, and normal polarity in black.

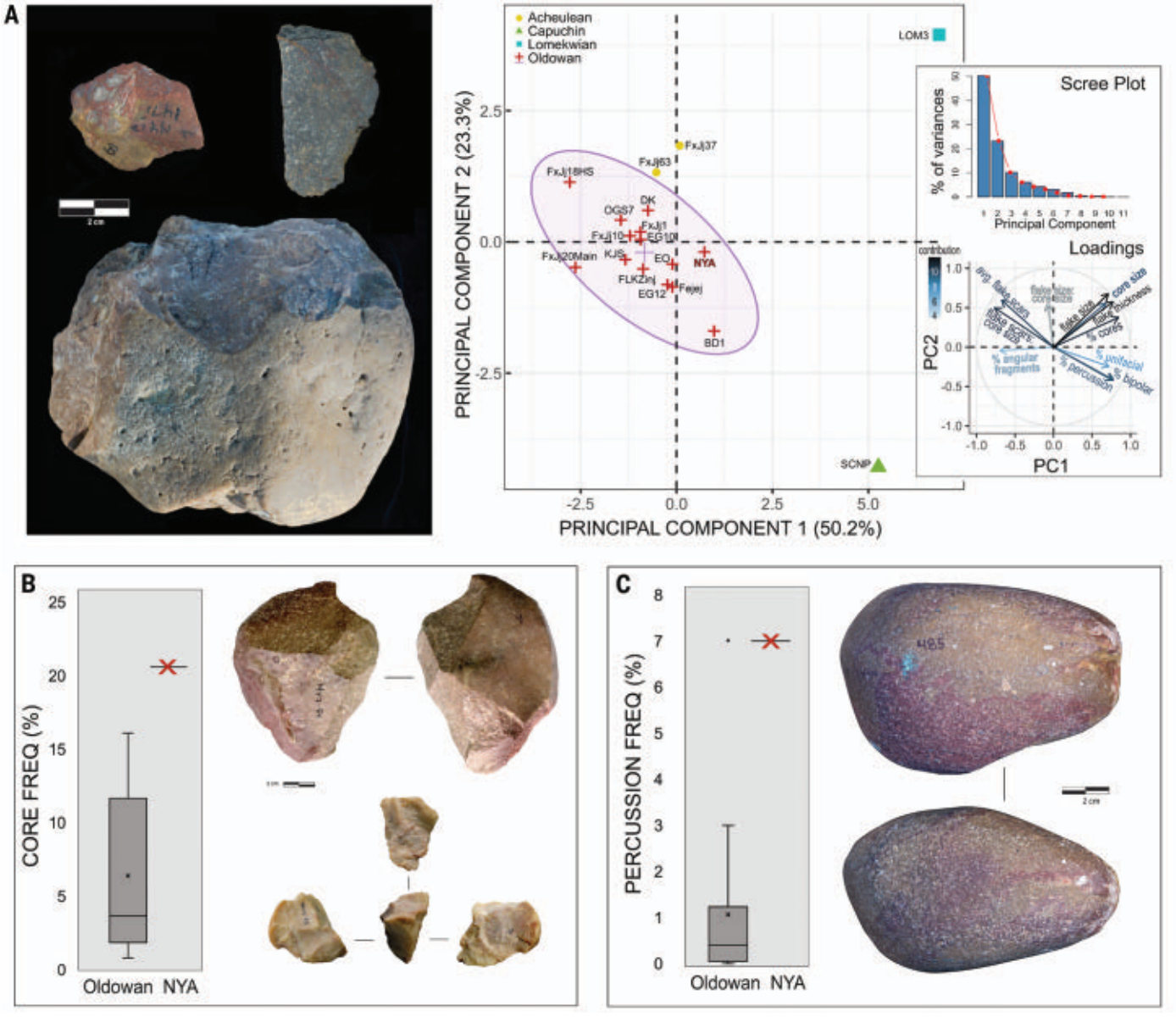

Fig. 2. Oldowan artifact technological analysis. (**A**) Photos of a dorsal flake (Exc3-1475), ventral flake (Exc3-1413), and core (NY17-128) from Nyayanga next to a principal component analysis based on major technological attributes of Early Stone Age artifact assemblages and a capuchin-derived assemblage (table S4) [(*8*), section 9]. Assemblages are plotted according to principal component 1 (*x* axis) and principal component 2 (*y* axis). The Nyayanga assemblage (NYA) falls within the shaded ellipse that represents the 95% confidence interval for Oldowan sites. A scree plot with eigenvalue percentage of variance for principal components 1 through 11, and a loadings plot showing the contribution of each variable are shown to the right. (**B**) The frequency of cores in other Oldowan assemblages compared with those of Nyayanga (table S4) and photos of two Nyayanga cores (NY17-54, top; NY17-55, bottom). (**C**) The frequency of artifacts with percussion damage in other Oldowan assemblages compared with those of Nyayanga (table S4) with photos of a Nyayanga pounded piece (Exc3-485).

basis of experimental analogs (figs. S9 and S10 and tables S8 and S10), the quartzite and rhyolite Oldowan percussive tools at Nyayanga were used to process soft (such as soft tubers, vegetables, or fruits) and hard (such as fibrous tubers or woody parts) plant tissues (fig. S11 and table S11). Macro- and microtraces related to cutting and scraping on six detached pieces (flakes) and one flaked piece show that similar materials were being cut and pounded (fig. S12 and tables S9 and S12). Five quartz detached pieces from excavation 3 show traces indicative of underground storage organ, wood, and animal processing. A rhyolite flaked piece from excavation 5 and a NY-1 surface collected detached piece also have use-wear related to butchery (fig. S12 and table S12).

Stable carbon isotopic analysis of pedogenic carbonates, dietary reconstruction by using tooth enamel isotopes, and bovid taxonomic frequencies indicate that hominin activities took place in a wooded grassland to grassy woodland, bushland, or shrubland along a stream channel within a mesic savanna biome characterized by an abundance of C_4 grasses and herbaceous plants (figs. S13 to S17 and tables S13 and S14) [(*8*), sections 10 to 12]. Similar C_4 grazer–dominated ecosystems are documented at the Ethiopian sites of Ledi-Geraru (~2.8 Ma) (*17*) and Mille-Logya (~2.8 to ~2.4 Ma) (*18*), indicating that early representatives of both *Paranthropus* and *Homo* were found in substantially open ecosystems. The

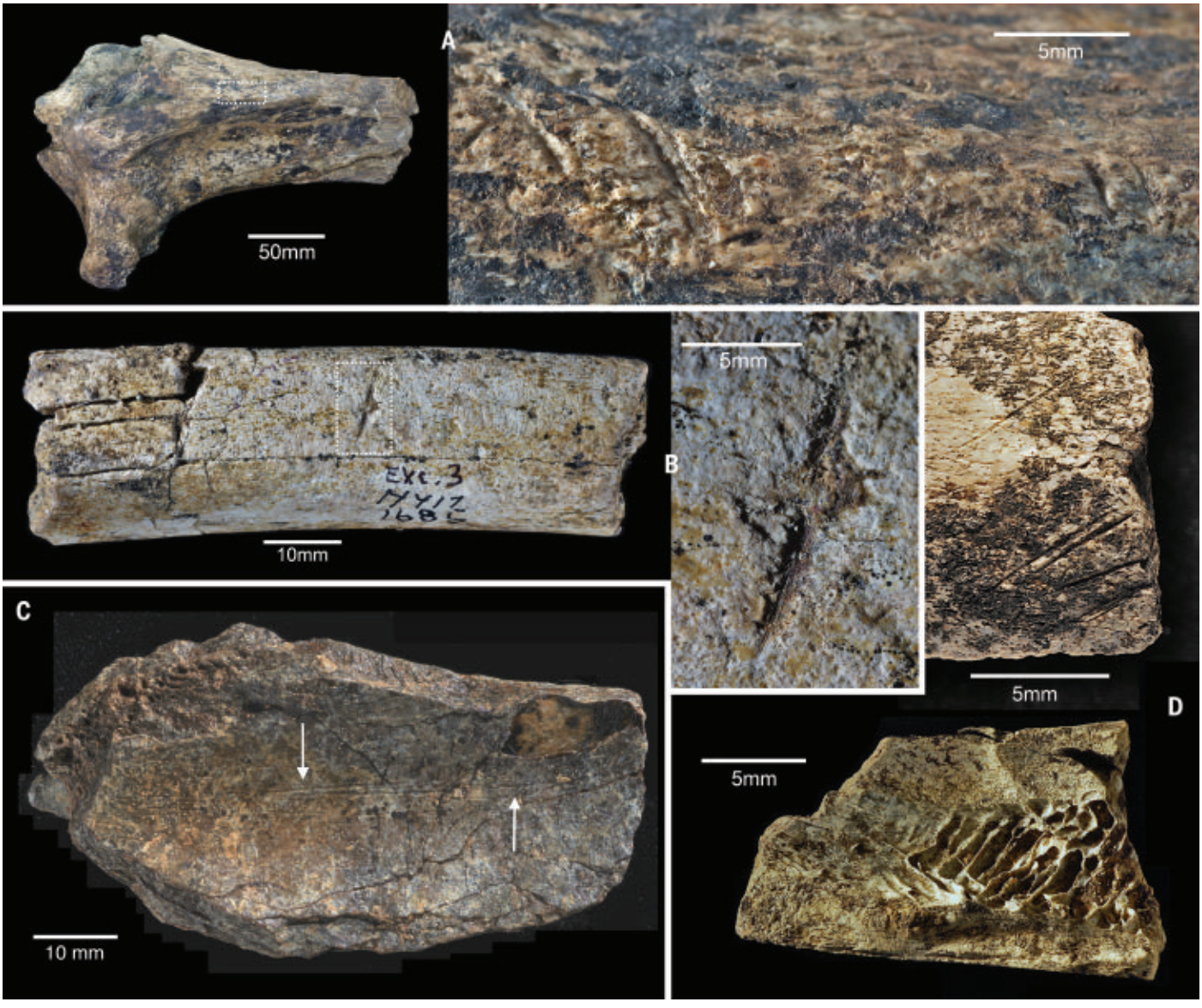

Fig. 3. Stone tool–damaged fossilized bones from Bed NY-1. (**A**) Hippopotamid tibia (Exc5-170, proximal end oriented to left) displaying a series of identically oriented cut marks with striae on anterior tibial crest. (**B**) Cut mark on a hippopotamid rib (Exc3-1685) displaying striae and a concretion filling the middle of the mark. (**C**) Parallel cut marks extending along the spine of size three bovid scapula NY17-1. (**D**) A series of parallel cut marks (top) as well as percussion load points and flake scars created during marrow processing (bottom) visible on a size three bovid long bone shaft fragment (NY15-61).

riparian setting, nearby freshwater spring, and ecotone with open habitats provided Nyayanga hominins with a diverse array of plant and animal foods, shelter, and potable water.

Two hominin individuals from Bed NY-1 are assigned to *Paranthropus* sp. (Fig. 4) [(*8*), section 13]. KNM-NG 77315 is a relatively complete left upper molar, probably M^2 (second upper molar), from surface collection, with a crown area above the range of that of *P. boisei* and *P. robustus* samples (tables S17 and S18). KNM-NG 77316 is a nearly complete lingual portion of a left lower molar, probably M_1 (first lower molar), found in situ in excavation 3, spatially associated with Oldowan artifacts and a butchered hippopotamid. The Nyayanga *Paranthropus* teeth have an average $\delta^{13}C_{enamel}$ value of −0.7 ± 0.4‰ (Fig. 4C), which demonstrates a heavy reliance on C_4 foods. Thus, the emergence of C_4 specialist diets coincided with the appearance of at least one major aspect of robust masticatory morphology (large postcanine teeth) relatively early in the evolution of *Paranthropus* [as opposed to (*19*)].

Paranthropus molar KNM-NG 77316 from the excavation 3 hippopotamid butchery site is a clear association of a hominin fossil with artifacts, raising the possibility that *Paranthropus* made and/or co-opted stone tools. Although its skull anatomy was not preserved, Nyayanga *Paranthropus* was megadont and had flat molars with poor shearing capability. However, its specialized gnathic morphology may not have precluded tool use. Extraoral cutting and pounding with stone tools could have provided access to carcasses and within bone nutrients, and made plant and animal tissue easier to chew and digest (*20*), potentially allowing *Paranthropus* to expand its diet. Although not found at Nyayanga, *Homo* was also present in eastern Africa at about the time of Nyayanga deposition (*21*), so the Nyayanga artifacts cannot be definitively attributed to a specific hominin genus.

Deposits at Nyayanga dated between 3.032 and 2.581 Ma show that at its earliest onset the Oldowan was geographically more widely dispersed than previously known, a finding consistent with a recently described Oldowan site

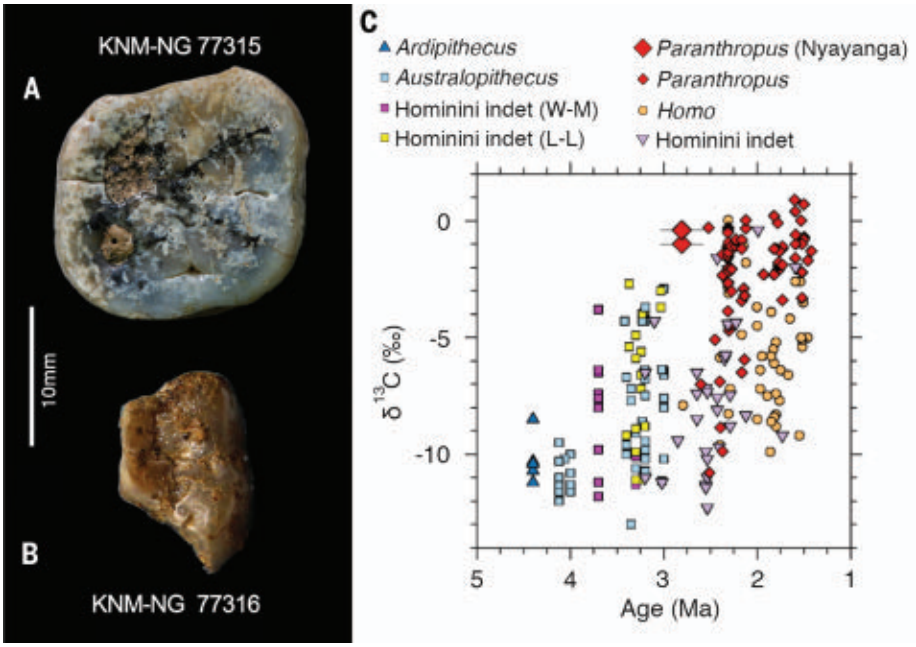

Fig. 4. *Paranthropus* finds from Nyayanga. (**A**) *Paranthropus* sp. left upper molar KNM-NG 77315 found on the surface of NY-1. (**B**) *Paranthropus* sp. left lower molar KNM-NG 77316 found in situ in NY-1 in excavation 3. (**C**) Tooth enamel $\delta^{13}C$ of Nyayanga hominins and previously published $\delta^{13}C$ data from eastern African hominins (*19*, *25*–*34*). Pliocene hominin teeth from Woranso-Mille are identified as "hominini indet (W-M)." Mid-Pliocene hominin teeth from Lomekwi and Lothagam in the Turkana Basin previously attributed to *K. platyops* (*28*) are identified here as "hominini indet (L-L)" (*35*). Hominin teeth from other areas of the Omo-Turkana Basin that cannot be confidently attributed to a genus are identified as "hominini indet."

from around 2.4 Ma in North Africa (*22*). Nyayanga artifacts were used to cut, scrape, and pound large mammal and plant tissue, demonstrating that at their emergence Oldowan tools were used in a variety of actions to access a broad array of food types. By 2 Ma, Oldowan sites are found from northern to southern Africa in both grassy and wooded habitats (*23*), suggesting that one of the key attributes of the technology was the flexibility to process foods with different physical properties in a diversity of habitats.

The behaviors preserved at Nyayanga are at least 600,000 years older than prior evidence of megafaunal carcass and plant processing and substantially predate the increase in absolute brain size documented in the genus *Homo* after 2 Ma (*24*). The late Pliocene expanded geography of the earliest Oldowan, and new evidence of its use in diverse tasks amplifies our understanding of the adaptive advantage of early stone technology in hominin diet and foraging ecology.

REFERENCES AND NOTES

1. N. Toth, K. Schick, *Azania* **53**, 3–39 (2018).
2. M. J. Rogers, S. Semaw, in *Sourcebook of Paleolithic Transitions* (Springer, 2009), pp. 155–171.
3. I. Cáceres, N. Kandi, M. Sahnouni, Z. Harichane, J. van der Made, *Proceedings of the II Meeting of African Prehistory: Burgos 15–16 April, 2015* (Consorcio CENIEH, Burgos, Spain, 2017), pp. 173–196.
4. M. Domínguez-Rodrigo, B. Martínez-Navarro, *J. Hum. Evol.* **62**, 315–327 (2012).
5. E. Hovers, in *Developments in Quaternary Sciences* (Elsevier, 2012), vol. 16, pp. 51–68.
6. S. Semaw *et al*., *Nature* **385**, 333–336 (1997).
7. D. R. Braun *et al*., *Proc. Natl. Acad. Sci. U.S.A.* **116**, 11712–11717 (2019).
8. Materials and methods are available as supplementary materials.
9. M. J. Le Bas, *Carbonatite-Nephelinite Volcanism: an African Case History* (Wiley London, 1977).
10. A. K. Behrensmeyer *et al*., *J. Hum. Evol.* **29**, 247–274 (1995).
11. P. Ditchfield, J. Hicks, T. Plummer, L. C. Bishop, R. Potts, *J. Hum. Evol.* **36**, 123–150 (1999).
12. T. Plummer, L. C. Bishop, P. Ditchfield, J. Hicks, *J. Hum. Evol.* **36**, 151–170 (1999).
13. L. C. Bishop *et al*., in *African Palaeoecology and Human Evolution*, S. C. Reynolds, R. Bobe, Eds. (Cambridge Univ. Press, 2022), pp. 360–375.
14. J. G. Ogg, in *Geologic Time Scale 2020* (Elsevier, 2020), pp. 159–192.
15. R. L. Bernor, M. J. Armour-Chelu, H. Gilbert, T. M. Kaiser, E. Schulz, in *Cenozoic mammals of Africa*, L. Werdelin, B. Sanders, Eds. (Univ. California Press, 2010), pp. 685–722.
16. G. L. Isaac, J. W. K. Harris, E. M. Kroll, in *Koobi Fora Research Project, Volume 5: Plio-Pleistocene Archaeology* (Clarendon Press, 1997).
17. E. N. DiMaggio *et al*., *Science* **347**, 1355–1359 (2015).
18. Z. Alemseged *et al*., *Nat. Commun.* **11**, 2480 (2020).
19. J. G. Wynn *et al*., *Proc. Natl. Acad. Sci. U.S.A.* **117**, 21978–21984 (2020).
20. K. D. Zink, D. E. Lieberman, *Nature* **531**, 500–503 (2016).
21. B. Villmoare *et al*., *Science* **347**, 1352–1355 (2015).
22. M. Sahnouni *et al*., *Science* **362**, 1297–1301 (2018).
23. T. Plummer, *Am. J. Phys. Anthropol.* **125**, 118–164 (2004).
24. S. C. Antón, R. Potts, L. C. Aiello, *Science* **345**, (2014).
25. N. J. Van der Merwe, F. T. Masao, M. K. Bamford, *S. Af. J. Sci.* **104**, 153–155 (2008).
26. T. D. White *et al*., *Science* **326**, 87–93 (2009).
27. T. E. Cerling *et al*., *Proc. Natl. Acad. Sci. U.S.A.* **108**, 9337–9341 (2011).
28. T. E. Cerling *et al*., *Proc. Natl. Acad. Sci. U.S.A.* **110**, 10501–10506 (2013).
29. M. Sponheimer *et al*., *Proc. Natl. Acad. Sci. U.S.A.* **110**, 10513–10518 (2013).
30. N. E. Levin, Y. Haile-Selassie, S. R. Frost, B. Z. Saylor, *Proc. Natl. Acad. Sci. U.S.A.* **112**, 12304–12309 (2015).
31. J. R. Robinson, J. Rowan, C. J. Campisano, J. G. Wynn, K. E. Reed, *Nat. Ecol. Evol.* **1**, 159 (2017).
32. T. Lüdecke *et al*., *Proc. Natl. Acad. Sci. U.S.A.* **115**, 13330–13335 (2018).
33. J. E. Martin, T. Tacail, J. Braga, T. E. Cerling, V. Balter, *Nat. Commun.* **11**, 3587 (2020).
34. S. Semaw *et al*., *Sci. Adv.* **6**, eaaw4694 (2020).
35. M. M. Skinner, M. G. Leakey, L. N. Leakey, F. K. Manthi, F. Spoor, *J. Hum. Evol.* **145**, 102820 (2020).

ACKNOWLEDGMENTS

The authors thank the National Museums of Kenya and M. Kibunjia, F. K. Manthi, J. Kibii, and E. Ndiema for support and acknowledge Kenya government permission granted by the Ministry of Sports, Culture, and the Arts and by NACOSTI permit P/14/7709/701. We thank P. Onyango for bringing the Nyayanga exposures to our attention. N. Todd assisted with elephant tooth identification. **Funding:** Funding from the L.S.B. Leakey Foundation (award 35805), the National Science Foundation (award 1327047), the Wenner-Gren Foundation (award 9428), and the Professional Staff Congress City University of New York Research Award Program (award 60589-00 48) to T.P., and funding from the William H. Donner Foundation and the Peter Buck Fund for Human Origins Research to R.P., is gratefully acknowledged. **Author contributions:** T.W.P., L.C.B., E.M.F., J.S.O., B.O., and R.P. contributed to excavation strategy and research design. Magnetostratigraphy sampling was conducted by P.W.D. and analysis of samples and magnetostratigraphic interpretation was undertaken by A.I.R.H. Sampling for (U-Th)/He apatite crystal dates was undertaken by H.H. and Y.L. carried out (U-Th)/He analysis. T.P.L., S.N., and M.F. provided additional geochronological analysis and contributed to the geochronological framework. Lithostratigraphy and sedimentology was conducted by P.W.D., E.W., and T.H.V. Paleosol carbonates were sampled and analyzed for stable isotopic composition by P.W.D. and S.A.B.: P.W.D. interpreted paleosol carbonate results, and S.A.B. sampled and carried out stable isotopic analysis of tooth enamel. B.O., T.W.P., J.S.O., E.M.F., L.C.B., R.L.-L., F.L.F., J.L., F.H., and J.A.P. contributed to field direction and data collection during field work. S.A.B., T.W.P., P.W.D., R.N.K., E.W., L.C.B., T.H.V., S.R.F., and R.P. contributed to the paleoenvironmental interpretation. S.E.B. analyzed and described the hominin teeth, and S.R.F. analyzed the monkey fossils. Other taxa were studied by F.H., J.L., E.D.G.E., L.C.B., T.W.P., and J.S.O. Bone identification and surface damage were conducted by J.A.P., J.S.O., and T.W.P. Lithic technology was studied by E.M.F. Additional insights on the lithic technology were provided by D.R.B., J.S.R., C.L., I.C., S.K.B., N.K.R., and E.P.W.; C.L. and I.C. conducted use-wear and residue analyses. T.W.P. wrote the article with contributions from J.S.O., E.M.F., P.W.D., L.C.B., C.L., I.C., S.E.B., A.I.R.H., E.W., F.H., and Y.L. All authors contributed editorial comments to the manuscript. **Competing Interests:** The authors declare no competing interests. **Data and materials availability:** All data supporting the findings of this study are available within the paper and its supplementary materials. All archeological and paleontological collections and field records are archived in the Department of Earth Sciences in the National Museums of Kenya in Nairobi.

License information: Copyright © 2023 the authors, some rights reserved; exclusive licensee American Association for the Advancement of Science. No claim to original US government works. https://www.science.org/about/science-licenses-journal-article-reuse

SUPPLEMENTARY MATERIALS

science.org/doi/10.1126/science.abo7452
Materials and Methods
Figs. S1 to S17
Tables S1 to S21
References (*36*–*135*)

Submitted 22 February 2022; accepted 4 January 2023
10.1126/science.abo7452

PALEONTOLOGY

A Mesozoic fossil lagerstätte from 250.8 million years ago shows a modern-type marine ecosystem

Xu Dai[1,2], Joshua H. F. L. Davies[3], Zhiwei Yuan[1], Arnaud Brayard[2], Maria Ovtcharova[4], Guanghui Xu[5,6], Xiaokang Liu[1], Christopher P. A. Smith[2], Carrie E. Schweitzer[7], Mingtao Li[8], Morgann G. Perrot[3,9], Shouyi Jiang[1], Luyi Miao[1], Yiran Cao[1], Jia Yan[1], Ruoyu Bai[10], Fengyu Wang[1], Wei Guo[1], Huyue Song[1], Li Tian[1], Jacopo Dal Corso[1], Yuting Liu[1], Daoliang Chu[1], Haijun Song[1]*

Finely preserved fossil assemblages (lagerstätten) provide crucial insights into evolutionary innovations in deep time. We report an exceptionally preserved Early Triassic fossil assemblage, the Guiyang Biota, from the Daye Formation near Guiyang, South China. High-precision uranium-lead dating shows that the age of the Guiyang Biota is 250.83 +0.07/−0.06 million years ago. This is only 1.08 ± 0.08 million years after the severe Permian-Triassic mass extinction, and this assemblage therefore represents the oldest known Mesozoic lagerstätte found so far. The Guiyang Biota comprises at least 12 classes and 19 orders, including diverse fish fauna and malacostracans, revealing a trophically complex marine ecosystem. Therefore, this assemblage demonstrates the rapid rise of modern-type marine ecosystems after the Permian-Triassic mass extinction.

Phanerozoic marine organisms can be divided into three great evolutionary faunas: (i) the trilobite-dominated Cambrian evolutionary fauna, (ii) the brachiopod-dominated Paleozoic evolutionary fauna, and (iii) the mollusk-dominated modern evolutionary fauna, which still thrive in present-day oceans (*1*). The rise to dominance of the modern evolutionary fauna happened after the Permian-Triassic mass extinction (PTME), also known as the "great dying," around the Permian-Triassic boundary ~251.9 million years ago (Ma) (*2*), which wiped out >80% of marine species (*3*, *4*). The subsequent recovery was a major period of evolutionary changes, during which not only did modern marine ecosystems emerge (*5*), but the Triassic Revolution began (*6*). However, because of the relative scarcity of Early Triassic fossil records for many marine groups, and especially the lack of exceptionally preserved fossil assemblages, the timing and processes of the rise of modern-type marine ecosystems remain poorly understood (*5*).

[1]State Key Laboratory of Biogeology and Environmental Geology, School of Earth Sciences, China University of Geosciences, Wuhan 430074, China. [2]Biogéosciences, UMR 6282, CNRS, Université de Bourgogne, 21000 Dijon, France. [3]Département des Sciences de la Terre et de l'atmosphère, Université du Québec à Montréal/GEOTOP, Montréal, Quebec H2X 3Y7, Canada. [4]Department of Earth Sciences, University of Geneva, CH-1205 Geneva, Switzerland. [5]Key Laboratory of Vertebrate Evolution and Human Origins of Chinese Academy of Sciences, Institute of Vertebrate Paleontology and Paleoanthropology, Chinese Academy of Sciences, Beijing 100044, China. [6]CAS Center for Excellence in Life and Paleoenvironment, Beijing 100044, China. [7]Department of Earth Sciences, Kent State University at Stark, North Canton, OH 44720, USA. [8]Institute of Geology and Paleontology, Linyi University, Linyi 276005, China. [9]Department of Earth and Planetary Sciences/GEOTOP, McGill University, Montréal, Quebec H3A 0E8, Canada. [10]Henan University of Engineering, Zhengzhou 451191, China.
*Corresponding author. Email: haijunsong@cug.edu.cn

After the PTME, Early Triassic marine fossil communities were thought to be depauperate, poorly diversified, and dominated by abundant and cosmopolitan disaster or opportunistic taxa (*7*–*11*). A slow, trophically stepwise recovery model, from bottom-level primary producers to topmost predators, has been proposed (*7*), but this pattern is highly debated (*12*). Full reestablishment of complex marine ecosystems was thought to have not occurred until ~10 million years (Myr) after the PTME, being represented by the Luoping Biota (*13*). However, recent fossil finds, for instance, the Spathian Paris Biota (~3 Myr after the PTME) from the Western United States (*5*, *14*) and the Spathian Chaohu Biota (~4 Myr after the PTME) from South China (*15*–*19*), indicate that diverse and trophically complex marine ecosystems occurred in the late Early Triassic. Despite these late Early Triassic biotas, a 3-Myr gap still exists after the PTME with no such biotas. This gap could be the consequence of recurrent environmental stresses, including high sea surface temperature (*20*, *21*), episodes of oceanic acidification (*22*), and anoxic or euxinic events (*23*, *24*) mainly occurring during the Permian-Triassic transition, the late Dienerian, and the late Smithian. Alternatively, it may also result from preservation and sampling biases, which are often neglected in many previous works (*5*, *9*).

Here, we report an exceptionally preserved fossil assemblage named Guiyang Biota from Guizhou Province, South China, which is late Dienerian in age (~1 Myr after the PTME) and is therefore the oldest known Mesozoic fossil lagerstätte. The Guiyang Biota represents a diverse and trophically complex marine ecosystem and partially fills the 3-Myr gap of complex marine faunas, indicating a rapid rise of modern-type marine ecosystems after the PTME despite global sea-surface temperatures remaining high.

Geological setting

Specimens of the Guiyang Biota were found in the middle unit of the Lower Triassic Daye Formation at six sections near Guiyang, Guizhou Province, China (Fig. 1, B and C). All of these sections were located on the northern margin of the Nanpanjiang Basin, which was located in the eastern Tethys, near the equator, during the Early Triassic (Fig. 1A). The three best-exposed sections were measured and sampled at a high resolution (fig. S1). The middle unit of the Daye Formation is characterized by alternating finely laminated black shales and thin- to medium-bedded limestones (figs. S2 and S3). Carbonate concretions are also common and usually rich in pyrite framboids. No bioturbation has been observed within this interval. Microfacies analyses show that the thin-bedded limestones are pelagic wackestones with occasional occurrences of small foraminifers and ostracods (fig. S4). There is no major difference in facies among the studied sections. The middle unit of the Daye Formation is thus interpreted to have been deposited in a deep shelf region of the northern Nanpanjiang Basin, where oxygen-depleted environments frequently occurred (*25*).

Age of the Guiyang Biota

The age of the Guiyang Biota is constrained to the late Dienerian by three independent methods (Fig. 1D): (i) ammonoid and conodont biostratigraphy, (ii) carbon isotope chemostratigraphy (table S1), and (iii) high-precision U-Pb dating (table S2). The assemblage of ammonoids (*Radioceras* sp.) and conodonts (*Neospathodus cristagalli* and *N. dieneri*) indicates a late Dienerian age (fig. S5). The Early Triassic carbon isotope curve displays four negative (N1 to N4) and three positive (P1 to P3) excursions, which can be correlated globally (*26*). At Gujiao, a carbon isotope curve with biostratigraphic calibration indicates that the Guiyang Biota corresponds to the N2 (Fig. 1D), again supporting a late Dienerian age. Finally, high-precision chemical abrasion isotope dilution–thermal ionization mass spectrometry (CA-ID-TIMS) zircon U-Pb ages from two ash beds at Gujiao provide absolute time constraints for the Guiyang Biota. Zircons from sample GJ-ASH-134, ~3 m below the fossil interval, yield an age of 250.92 ± 0.15 Ma (2σ). The second ash sample, GJ-ASH-157, occurring within the fossil interval at Gujiao, yields an age of 250.766 ± 0.084 Ma (2σ). An age-depth model using the ages from these ash beds indicates that the lower and upper age limits of the Guiyang Biota are 250.83 +0.07/−0.06 and 250.72 +0.09/−0.21 Ma, respectively. Thus,

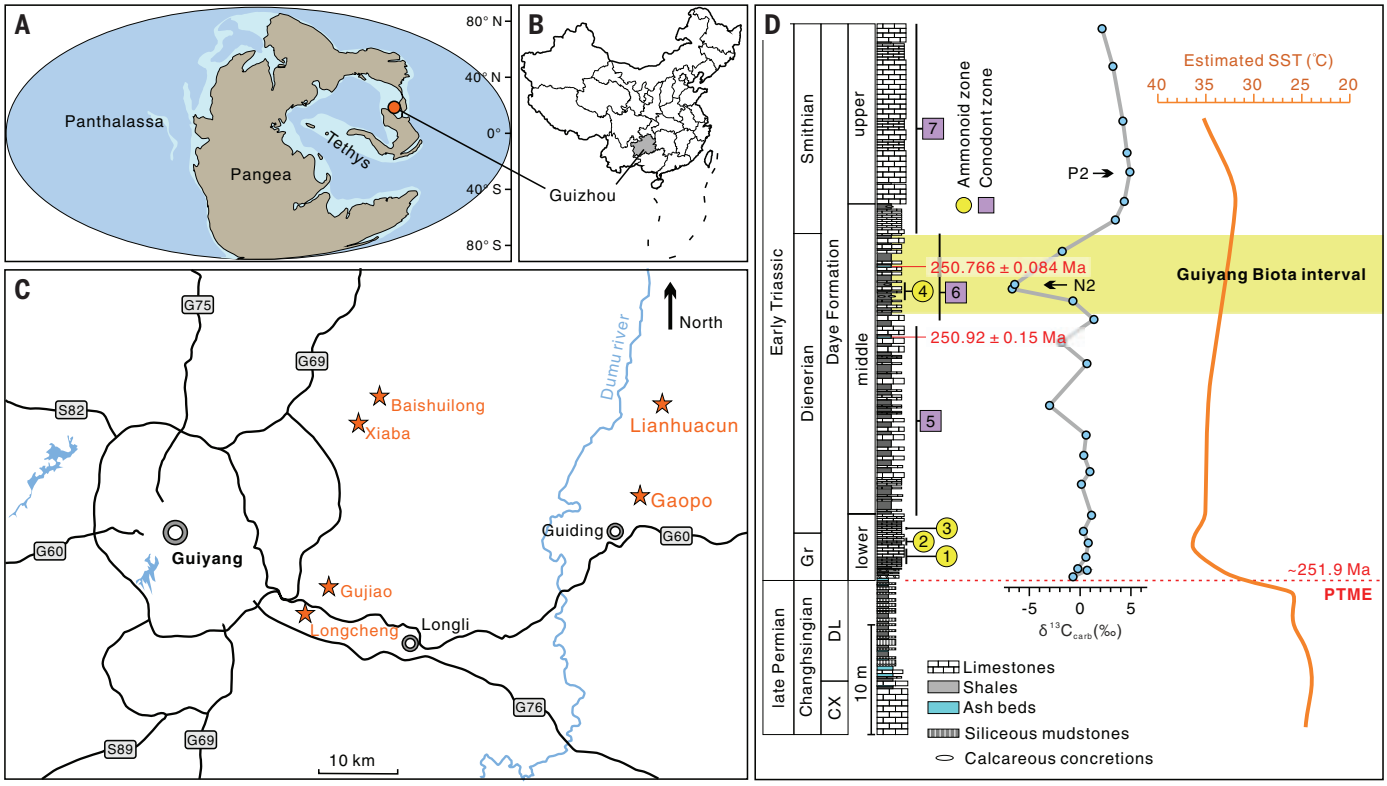

Fig. 1. Geological context of the Guiyang Biota. (**A** to **C**) Early Triassic and present-day locations of the studied exposures. The Early Triassic paleogeographic map was modified from Scotese (*42*). (**D**) Synthetic regional lithological succession with associated carbon isotopic trend (analyzed in this study) and simplified estimated sea surface temperature (SST) modified from (*20*). Gr, Griesbachian; CX, Changxing Formation; DL: Dalong Formation. The yellow band indicates the stratigraphic position of the Guiyang Biota. Ammonoid zonation is after (*43*): 1, *Ophiceras medium* beds; 2, *Jieshaniceras guizhouense* beds; 3, *Ambites radiatus* bed; 4, *Radioceras* sp. beds. Conodont zones: 5, *Neospathodus dieneri* zone; 6, *Neospathodus cristagalli* zone; 7, *Novispathodus waageni* zone. The definitions of N2 and P2 of the carbon isotope curve refer to (*26*).

the Guiyang Biota spans an interval of 0.11 +0.21/−0.06 Myr and is 1.08 ± 0.08 Myr after the PTME (fig. S6).

Taxonomic composition

One million years after the PTME, the Guiyang Biota showed an unexpectedly diversified assemblage, including coelacanths, actinopterygians, decapods, Cyclida, ammonoids, bivalves, conodonts, foraminifers, ostracods, sponges, radiolarians, and coprolites (Figs. 2 and 3, figs. S7 to S10, and table S3). Sampled specimens are usually compressed in two dimensions, except for some bony fishes and ammonoids from calcareous concretions, which retain three-dimensional structures. Fishes, decapods, Cyclida, and coprolites are all preserved in calcium phosphate (figs. S11 to S15). Sponge spicules and radiolarians are silicified. Foraminifers are usually calcareous, but some of them are pyritized (Fig. 3P).

Osteichthyes are the main component of the biota and occur in two main groups, Actinistia (Fig. 2A) and Actinopterygii (Fig. 2, B to F). Two different coelacanth species have been found so far and are the largest macrofossils in the Guiyang Biota. All of these specimens show an estimated body length of >0.5 m, with the largest specimen reaching a body length of ~1 m. More than 10 species of at least six actinopterygian orders have been identified, including stem actinopterygians (Palaeonisciformes and Ptycholepiformes), chondrosteans (Acipenseriformes), stem neopterygians [Perleidiformes (*27*) and Polzbergiiformes], and holosteans (Parasemionotiformes). Additionally, Chondrichthyes, represented by hybodontiform teeth, have also been found (Fig. 2, G and H).

Arthropods are the most abundant group. They are represented by malacostracans (Decapoda), ostracods, and Cyclida, which is an enigmatic crustacean group with a scarce fossil record and uncertain phylogeny. Among the decapods, two shrimp taxa are recognized as *Anisaeger* sp. (Fig. 3, J and K) and an undetermined Aegeridae (Fig. 3, E to I, and figs. S8 and S13), which extend the temporal range of this family by 1.5 Myr to the Dienerian (*28*). The Aegeridae are thought to be the basal group for most modern shrimps (*28*). Therefore, the fossils of the Guiyang Biota represent some of the oldest known shrimps. One specimen of an undetermined litogastrid lobster (Fig. 3L) was also found, predating the previously oldest report of this group by nearly 1.5 Myr (*28*). Overall, this decapod fauna is the oldest known among the Early Triassic fauna documented so far (*5*, *28*, *29*). In addition, one specimen of Cyclida has been found (Fig. 3, M and N, and fig. S14), which shows a close morphological affinity to *Yunnanocyclus nodosus* reported from the Anisian Luoping Biota (*30*) but differs mainly by shorter thoracic segmentations. This specimen represents the third reported occurrence of Early Triassic Cyclida, the others being from the Induan of Madagascar and the Olenekian of Germany (*31*).

At least two ammonoid taxa were found in the Guiyang Biota, *Pseudosageceras* sp. and *Radioceras* sp. (Fig. 3, A and B, and fig. S9). Four bivalve genera were also recognized, *Eumorphotis*, *Claraia*, *Scythentolium*, and *Modiolus* (Fig. 3, C and D, and fig. S9). Isolated sponge spicules are common in some beds in the fossiliferous interval (Fig. 3Q and fig. S10). One radiolarian taxon was found, *Latentifistula* sp. (fig. S10), a long-ranging genus that lived from the Permian to the Triassic. Foraminifers are also common (Fig. 3P and fig. S10), with

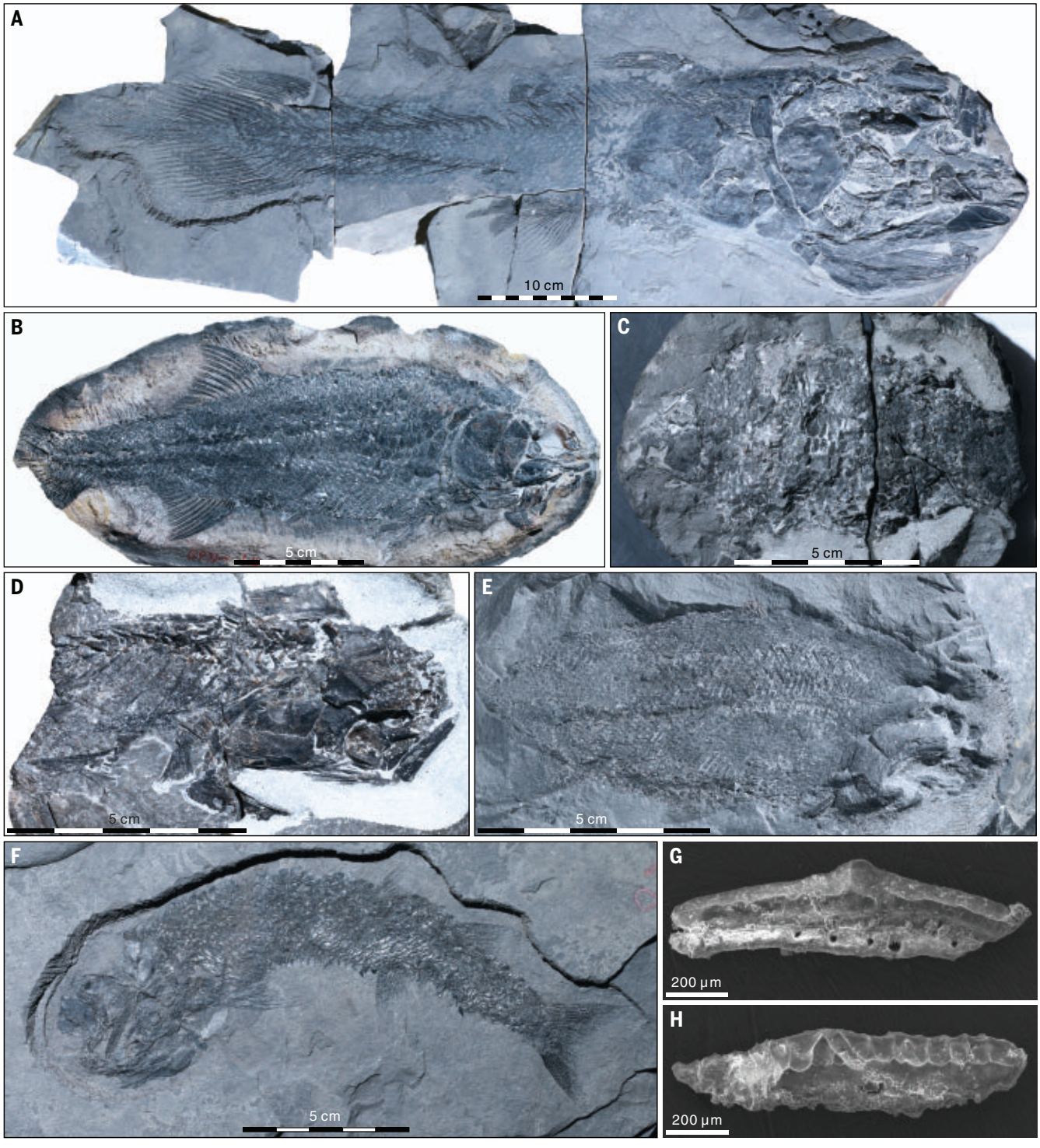

Fig. 2. Osteichthyes and Chondrichthyes from the Guiyang Biota. (**A**) Coelacanthiformes indet A., CUGM 00343, Gujiao. (**B**) Parasemionotiformes *Watsonulus* sp., CUGM 00344, Gaopo. (**C**) Polzbergiformes indet., CUGM 00345, Gujiao. (**D**) Acipenseriformes *Errolichthys* sp., CUGM 00346, Gujiao. (**E**) Palaeonisciformes indet., CUGM 00347, Gujiao. (**F**) Perleidiformes *Teffichthys elegans*, CUGM 00348, Gujiao. (**G** and **H**) Hybodontiformes teeth, Gujiao, CUGM 00349 (G) and CUGM 00350 (H).

seven species recognized (table S3), of which *Postcladella kalhori* is the most abundant. This foraminifer fauna appears to be one of the richest known so far for the Dienerian (*32*). Three conodont species, *Neospathodus kristagalli*, *Neospathodus dieneri*, and *Novispathodus posterolongatus*, were found within the fossiliferous interval at Gujiao (fig. S5).

Trophic and ecological structure

This new assemblage is trophically complex, including various representative species ranging from primary consumers such as foraminifers to large predators such as coelacanths. On the basis of the trophic pyramid model of a fossilized marine ecosystem (*7*), the Guiyang Biota contains representatives of all trophic levels and represents a complete trophic pyramid

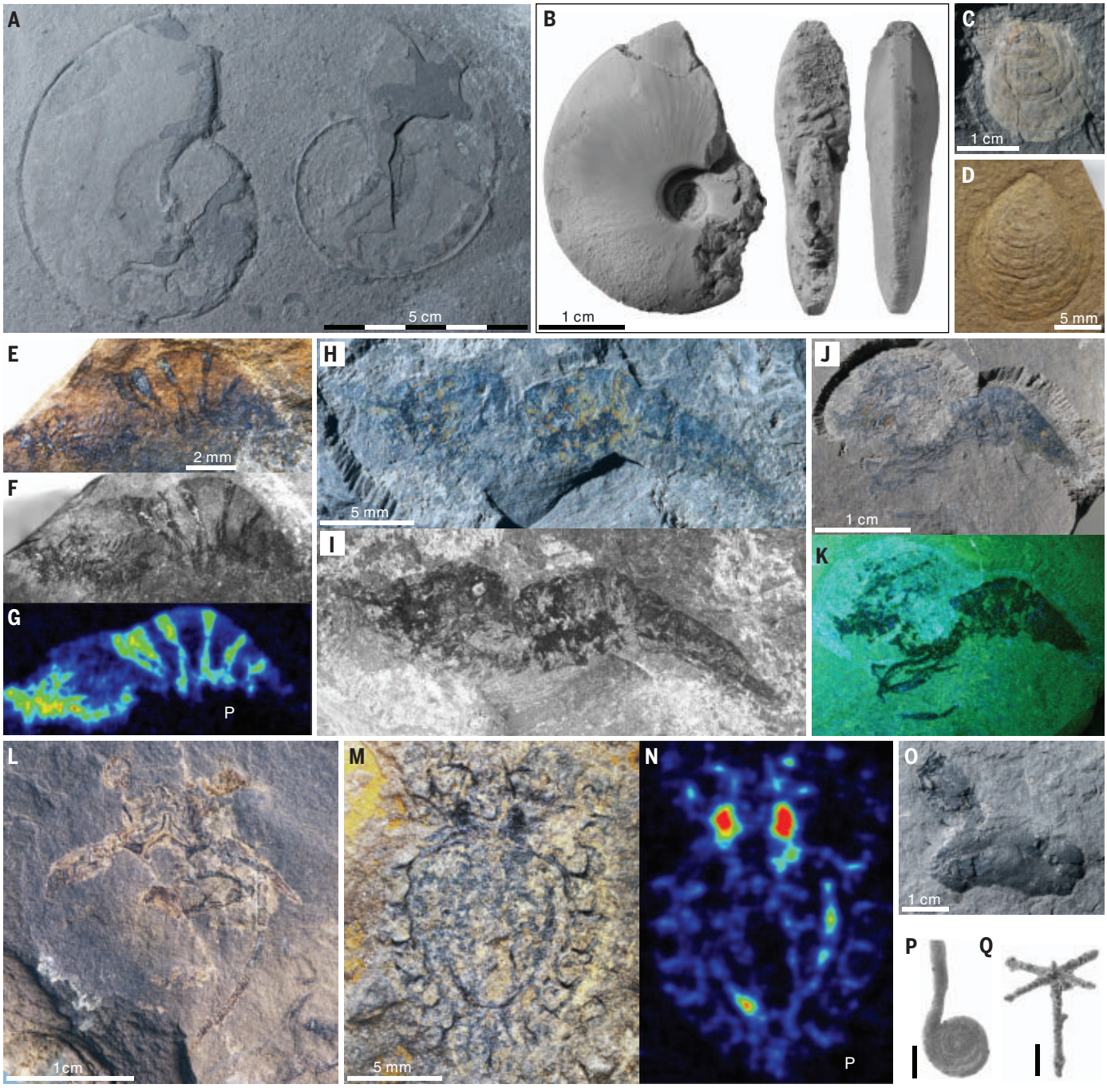

Fig. 3. Invertebrates from the Guiyang Biota. (**A**) Ammonoid *Pseudosageceras* sp., CUGM 00351, Gujiao. (**B**) Ammonoid *Radioceras* sp., CUGM 00352, Lianhuachun. (**C**) Bivalve *Eumorphotis hinnitidae*, CUGM 00353, Gujiao. (**D**) Bivalve *Scythentolium* sp., CUGM 00354, Xiaba. (**E** to **G**) Shrimp Aegeridae indet., CUGM 00355, Baishuilong, under natural light (E), in a fluorescence photograph (F), and in a micro–x-ray fluorescence (μXRF) phosphorus elemental map (G). (**H** and **I**) Shrimp Aegeridae indet., CUGM 00356, Baishuilong, under natural light (H) and in a fluorescence photograph (I). (**J** and **K**) Shrimp *Anisaeger* sp., CUGM 00357, Baishuilong, under natural light (J) and shown by composite multispectral imaging (K). (**L**) Litogastrid lobster, CUGM 00358, Xiaba. (**M** and **N**) Cyclida, CUGM 00359, Xiaba section, under natural light (M) and in a μXRF phosphorus elemental map (N). (**O**) Coprolites, CUGM 00360, Gujiao. (**P**) Foraminifer *Postcladella kalhori,* CUGM 00361, Gujiao. (**Q**) Sponge spicule, CUGM 00362, Gujiao. Scale bars in (P) and (Q), 100 μm.

(Fig. 4C). Although fossils of primary producers such as algae have not been found in the Guiyang Biota, their presence may be inferred because they are at the base of trophic networks. Primary consumers found in the biota consist of at least seven species of foraminifers, one genus of radiolarians, and one taxon of sponges. Bivalves, including at least four genera, represent mesoconsumers. Ammonoids and decapods are likely to have been predatory. Predatory fishes, represented mainly by coelacanths, are at the apex of trophic network of the Guiyang Biota. Conodonts may have acted as predators or scavengers in marine ecosystems (*33*). Additionally, the occurrence of vertebrate coprolites ranging from 1 to 3 cm in diameter (Fig. 3O) confirms a complex trophic network. According to the

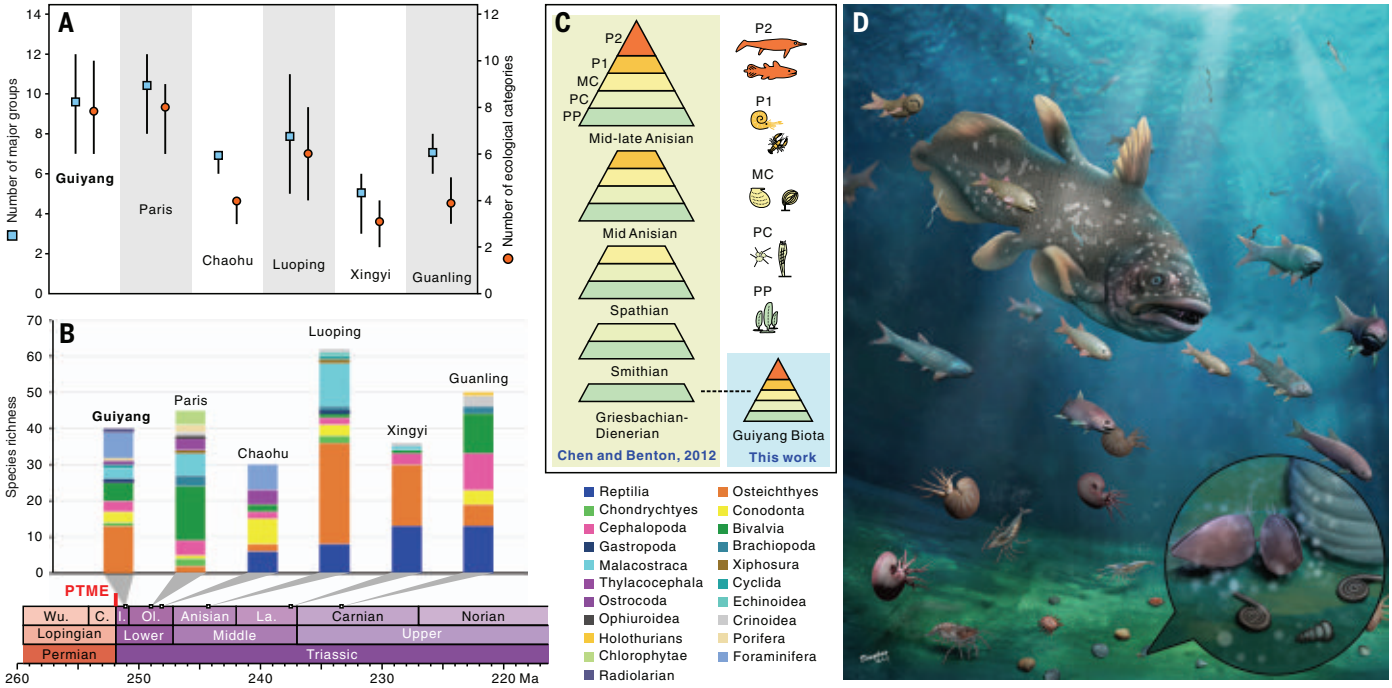

Fig. 4. Taxonomic and ecological features of the Guiyang Biota and comparison with other main biotas after the PTME. (**A**) Number of major groups and ecological categories of main Triassic biotas. See fig. S12 for the definition of ecological categories. The fossil data for each biota are available in data S1. Vertical bars indicate 95% confidence intervals based on rarefaction analyses (n = 25). (**B**) Taxonomic composition and species richness of the main Triassic biotas. The lack of Permian lagerstätte (*44*) prevents a direct comparison of lagerstätten before and after the PTME. Wu., Wuchiapingian; C., Changhsingian; I., Induan (= Griesbachian + Dienerian); Ol., Olenekian (= Smithian + Spathian); and La., Ladinian. (**C**) Previously hypothesized trophically stepwise model of the recovery after the PTME (*7*). The diversity of the Dienerian Guiyang Biota contrasts with this model. From bottom to top, the trophic levels include primary producers (PP) such as algae, primary consumers (PC) such as foraminifers and sponges, mesoconsumers (MC) such as bivalves and brachiopods, predatory invertebrates (P1) such as ammonoids and decapods, and predatory fishes and reptiles (P2). (**D**) Artistic reconstruction of the Guiyang Biota (illustration by Dinghua Yang).

theoretical ecospace model (*34*), which is based on six tiering positions, six motility levels, and six feeding strategies for marine organisms, the Guiyang Biota includes at least 10 ecological modes (fig. S16) that are similar to those of younger renowned Triassic biotas (Fig. 4A and tables S4 and S5).

Discussion

The Guiyang Biota contains a diverse and trophically complex marine ecosystem and extends the occurrence of complex marine ecosystems to ~1 Myr after the PTME (Fig. 4, B and C), representing the oldest Mesozoic lagerstätte known to date. The Guiyang Biota shows that some significant groups of modern marine ecosystems, such as decapod arthropods and actinopterygian fishes, experienced a more rapid post-PTME diversification than was previously thought (*15*, *28*, *35*). Preservation and sampling biases have distorted our current understanding of the post-PTME recovery, and this report of a complex biota from even closer to this event forces us to rethink interpretations of this recovery. The Guiyang Biota suggests that higher trophic levels either were not completely eliminated by the PTME or recovered rapidly driven by biotic interactions such as interspecific competition (*36*).

The Early Triassic is often portrayed as a super-greenhouse world (*20*, *21*) in which life was expelled from the tropics, leading to a poleward shift of tetrapods and a near absence of fish faunas within the tropics (*20*, *37*, *38*). On the basis of the new data from the Guiyang Biota, in the middle unit of the Daye Formation, the supposed tropical fish gap appears to be solely a product of sampling bias. The presence of fishes in the late Dienerian Guiyang Biota and in the late Smithian of South China (*39*) and the Western United States basin (*40*) filled the tropical fish gap at least during these two periods of relative cooling (*20*, *21*). Therefore, this suggests that the supposed tropical lethally hot temperature was at least not consistent throughout the entire Early Triassic and likely fluctuated, with some cooler periods corresponding to the thermal tolerances of marine fishes.

Although the Guiyang Biota remains incompletely sampled, it highlights that the slow and stepwise recovery model (*7*) after the PTME is not applicable. Further, it fills part of a wide knowledge gap regarding the rise of modern marine ecosystems after the PTME by documenting the early diversification of fishes and decapods, two groups playing a substantial role in present-day marine ecosystems and in prey-predator interactions during the Mesozoic marine revolution (*6*, *41*).

REFERENCES AND NOTES

1. J. J. Sepkoski Jr., *Paleobiology* **7**, 36–53 (1981).
2. S. D. Burgess, S. Bowring, S.-Z. Shen, *Proc. Natl. Acad. Sci. U.S.A.* **111**, 3316–3321 (2014).
3. D. M. Raup, *Science* **206**, 217–218 (1979).
4. S. M. Stanley, *Proc. Natl. Acad. Sci. U.S.A.* **113**, E6325–E6334 (2016).
5. A. Brayard *et al.*, *Sci. Adv.* **3**, e1602159 (2017).
6. M. J. Benton, F. Wu, *Front. Earth Sci. (Lausanne)* **10**, 899541 (2022).
7. Z.-Q. Chen, M. J. Benton, *Nat. Geosci.* **5**, 375–383 (2012).
8. D. J. Bottjer, M. E. Clapham, M. L. Fraiser, C. M. Powers, *GSA Today* **18**, 4–10 (2008).
9. A. Hallam, *Hist. Biol.* **5**, 257–262 (1991).
10. W. J. Foster, S. Danise, G. D. Price, R. J. Twitchett, *PLOS ONE* **12**, e0172321 (2017).
11. E. Petsios, D. J. Bottjer, *Paleobiology* **42**, 380–393 (2016).
12. T. M. Scheyer, C. Romano, J. Jenks, H. Bucher, *PLOS ONE* **9**, e88987 (2014).
13. S. X. Hu *et al.*, *Proc. Biol. Sci.* **278**, 2274–2282 (2011).
14. C. P. A. Smith *et al.*, *Sci. Rep.* **11**, 19657 (2021).
15. M. J. Benton *et al.*, *Earth Sci. Rev.* **125**, 199–243 (2013).
16. C. Ji, A. Tintori, D. Jiang, R. Motani, F. Confortini, *J. Paleontol.* **95**, 305–319 (2020).
17. D.-Y. Jiang *et al.*, *Sci. Rep.* **6**, 26232 (2016).
18. R. Motani *et al.*, *Nature* **517**, 485–488 (2015).
19. A. Tintori *et al.*, *Riv. Ital. Paleontol. Stratigr.* **120**, 157–164 (2014).
20. Y. Sun *et al.*, *Science* **338**, 366–370 (2012).
21. C. Romano *et al.*, *Nat. Geosci.* **6**, 57–60 (2013).

22. H. Song *et al*., *Chem. Geol.* **562**, 120038 (2021).
23. P. B. Wignall, R. J. Twitchett, *Science* **272**, 1155–1158 (1996).
24. S. E. Grasby, B. Beauchamp, A. Embry, H. Sanei, *Geology* **41**, 175–178 (2013).
25. L. Tian *et al*., *Palaeogeogr. Palaeoclimatol. Palaeoecol.* **412**, 68–79 (2014).
26. H. Song *et al*., *Global Planet. Change* **105**, 7–20 (2013).
27. Z. Yuan *et al*., *PeerJ* **10**, e13448 (2022).
28. C. P. A. Smith *et al*., *J. Paleontol.* **96**, 1235–1263 (2022).
29. A. Garassino, G. Pasini, G. Teruzzi, *Contrib. Zool.* **72**, 137–139 (2003).
30. R. M. Feldmann *et al*., *J. Crustac. Biol.* **37**, 406–412 (2017).
31. C. E. Schweitzer, E. V. Mychko, R. M. Feldmann, *Neues Jahrb. Geol. Paläontol. Abh.* **296**, 245–303 (2020).
32. H. Song *et al*., *Geology* **39**, 739–742 (2011).
33. M. A. Purnell, *Nature* **374**, 798–800 (1995).
34. R. K. Bambach, A. M. Bush, D. H. Erwin, *Palaeontology* **50**, 1–22 (2007).
35. C. Romano *et al*., *Biol. Rev. Camb. Philos. Soc.* **91**, 106–147 (2016).
36. M. Hautmann *et al*., *Palaeontology* **58**, 871–901 (2015).
37. B. J. Allen, P. B. Wignall, D. J. Hill, E. E. Saupe, A. M. Dunhill, *Proc. Biol. Sci.* **287**, 20201125 (2020).
38. M. Bernardi, F. M. Petti, M. J. Benton, *Proc. Biol. Sci.* **285**, 20172331 (2018).
39. J. Tong, X. Zhou, D. H. Erwin, J. Zuo, L. Zhao, *J. Paleontol.* **80**, 146–161 (2006).
40. C. Romano *et al*., *J. Paleontol.* **91**, 1025–1046 (2017).
41. G. J. Vermeij, *Palaeogeogr. Palaeoclimatol. Palaeoecol.* **263**, 3–8 (2008).
42. C. R. Scotese, "Atlas of Middle & Late Permian and Triassic Paleogeographic maps, maps 43–48 from volume 3 of the PALEOMAP Atlas for ArcGIS (Jurassic and Triassic) and maps 49–52 from volume 4 of the PALEOMAP PaleoAtlas for ArcGIS (Late Paleozoic)" (Mollweide Projection, PALEOMAP Project, 2014); https://doi.org/10.13140/2.1.2609.9209.
43. X. Dai, H. Song, A. Brayard, D. Ware, *J. Paleontol.* **93**, 48–71 (2019).
44. A. D. Muscente *et al*., *Gondwana Res.* **48**, 164–188 (2017).
45. X. Dai *et al*., R scripts for: A Mesozoic fossil lagerstätte from 250.8 Ma showing a modern-type marine ecosystem, Zenodo (2022); https://doi.org/10.5281/zenodo.7466123.

ACKNOWLEDGMENTS

We thank W. Guo and Y. Ma for assistance in zircon analyses, Y. Wang for assistance in the field, and D. Zhai and Q. Wang for help in taking fluorescence photographs at Yunnan University. **Funding:** This work was supported by the National Natural Science Foundation of China (grants 92155201, 41821001, and 92255303); the Strategic Priority Research Program of the Chinese Academy of Sciences (grant XDB26000000); the 111 Project (grant B08030); Fundamental Research Funds for National University, China University of Geosciences (Wuhan); the China Scholarship Council (grant 202006410051); Programme TelluS of the INSU, CNRS (A.B.); French "Investissements d'Avenir" program (project ISITE-BFC: ANR-15-IDEX-03 to A.B.); and BQR of the Université de Bourgogne (X.D. and A.B.). **Author contributions:** Conceptualization: X.D., Ha.S.; Funding acquisition: Ha.S., X.D., A.B.; Investigation: X.D., X.L., L.M., Y.C., S.J., D.C., Z.Y., Ha.S.; Methodology: X.D., J.H.F.L.D., Z.Y., M.O., M.G.P., W.G., Hu.S., X.L., A.B., G.X., C.P.A.S., C.E.S., J.Y., R.B., Y.L.; Supervision: Ha.S., A.B.; Visualization: X.D., Z.Y., J.H.F.L.D., R.B., Y.L.; Writing – original draft: X.D., Ha.S., A.B.; Writing – review and editing: X.D., Ha.S., A.B., J.D.C., J.H.F.L.D., Hu.S., W.G., L.T., D.C. with other input from all authors. **Competing interests:** The authors declare no competing interests. **Data and materials availability:** Data and code for rarefaction analysis are available at (*45*); all other data are available in the main text or the supplementary materials. All figured specimens are housed at the Yifu Museum of China University of Geosciences (CUGM) and can be accessed by contacting the curator, Jing Chen, at jingchen@cug.edu.cn; accession numbers can be found in the materials and methods in the supplementary materials. **License information:** Copyright © 2023 the authors, some rights reserved; exclusive licensee American Association for the Advancement of Science. No claim to original US government works. https://www.science.org/about/science-licenses-journal-article-reuse

SUPPLEMENTARY MATERIALS

science.org/doi/10.1126/science.adf1622
Materials and Methods
Figs. S1 to S16
Tables S1 to S6
References (*46*–*58*)
Data S1
MDAR Reproducibility Checklist

Submitted 5 October 2022; accepted 10 January 2023
10.1126/science.adf1622

FISH EVOLUTION

Genome structures resolve the early diversification of teleost fishes

Elise Parey[1,2]†, Alexandra Louis[1], Jerome Montfort[2], Olivier Bouchez[3], Céline Roques[3], Carole Iampietro[3], Jerome Lluch[3], Adrien Castinel[3], Cécile Donnadieu[3], Thomas Desvignes[4], Christabel Floi Bucao[5,6], Elodie Jouanno[2], Ming Wen[2,7], Sahar Mejri[8], Ron Dirks[9], Hans Jansen[9], Christiaan Henkel[10,11], Wei-Jen Chen[12], Margot Zahm[13], Cédric Cabau[13], Christophe Klopp[13,14], Andrew Thompson[15,16], Marc Robinson-Rechavi[5], Ingo Braasch[15,16], Guillaume Lecointre[17], Julien Bobe[2], John H. Postlethwait[4], Camille Berthelot[1,18]*‡, Hugues Roest Crollius[1]*‡, Yann Guiguen[2]*‡

Accurate species phylogenies are a prerequisite for all evolutionary research. Teleosts are the largest and most diversified group of extant vertebrates, but relationships among their three oldest extant lineages remain unresolved. On the basis of seven high-quality new genome assemblies in Elopomorpha (tarpons, eels), we revisited the topology of the deepest branches of the teleost phylogeny using independent gene sequence and chromosomal rearrangement phylogenomic approaches. These analyses converged to a single scenario that unambiguously places the Elopomorpha and Osteoglossomorpha (arapaima, elephantnose fish) in a monophyletic sister group to all other teleosts, i.e., the Clupeocephala lineage (zebrafish, medaka). This finding resolves more than 50 years of controversy on the evolutionary relationships of these lineages and highlights the power of combining different levels of genome-wide information to solve complex phylogenies.

Species phylogenies retrace evolutionary relationships among extant species (*1*). Accurate species trees are important for our understanding and representation of the evolution of life on earth, but they are also a fundamental prerequisite for evolutionary analyses at the developmental, anatomical, genetic, and species levels.

Comprising more than 30,000 species, teleost fishes account for roughly half of all extant vertebrates (*2*). Their phylogeny has been, and is still, subject to many disputes at different taxonomic levels (*2*, *3*). Among these debates, a long-standing and major unresolved question concerns the topology of the earliest-branching clades of crown teleosts, which diverged ~250 million years (Myr) ago (*4*, *5*). These earliest-branching clades of crown teleosts are the Elopomorpha (including tarpon, bonefish, and eels), the Osteoglossomorpha (named after "bony tongues" and including goldeye, arapaima, and elephantnose fishes), and all the remaining extant teleosts in the Clupeocephala lineage (including, e.g., zebrafish, a model organism for biomedical research) (*3*, *6*).

Because of their anatomical and morphological characters, elopiforms (tarpons and ladyfishes) were first suggested to be the most "primitive living teleosts" nearly 100 years ago (*7*). Since then, Elopomorpha and Osteoglossomorpha have been alternatively placed as the earliest-branching clade of teleosts. The first of these scenarios, proposed in 1977 (*8*), placed the Osteoglossomorpha as the sister group to the Elopocephala, which consists of Elopomorpha and Clupeocephala (Fig. 1A). This scenario was later challenged in 1997 (*9*, *10*) by the placement of Elopomorpha as the earliest-branching clade of teleosts, with Osteoglossomorpha and Clupeocephala composing the Osteoglossocephala clade (Fig. 1B). These early controversies were based on morphological evidence and remained largely unsolved, but a recent compendium on fish systematics still considers the Elopomorpha as the earliest-branching clade of crown teleosts (*2*).

With the emergence of molecular phylogenetic approaches in the 1990s, this question was extensively revisited using gene-sequence phylogeny reconstruction [reviewed in (*3*, *11*)]. However, despite extensive efforts, including several large-scale multilocus approaches (*4*, *5*, *12*), no consensus has been reached in favor of either

[1]Institut de Biologie de l'ENS (IBENS), Département de Biologie, École Normale Supérieure, CNRS, INSERM, Université PSL, Paris, France. [2]INRAE, LPGP, Rennes, France. [3]GeT-PlaGe, INRAE, Genotoul, Castanet-Tolosan, France. [4]Institute of Neuroscience, University of Oregon, Eugene, OR, USA. [5]Department of Ecology and Evolution, University of Lausanne, Lausanne, Switzerland. [6]SIB Swiss Institute of Bioinformatics, Lausanne, Switzerland. [7]State Key Laboratory of Developmental Biology of Freshwater Fish, College of Life Science, Hunan Normal University, Changsha, China. [8]Florida Atlantic University, Harbor Branch Oceanographic Institute, Fort Pierce, FL, USA. [9]Future Genomics Technologies, Leiden, Netherlands. [10]Institute of Biology, University of Leiden, Leiden, Netherlands. [11]Faculty of Veterinary Medicine, Norwegian University of Life Sciences, Ås, Norway. [12]Institute of Oceanography, National Taiwan University, Taipei 10617, Taiwan. [13]Sigenae, GenPhySE, INRAE, ENVT, Université de Toulouse, Castanet Tolosan, France. [14]Sigenae, Genotoul Bioinfo, MIAT UR875, INRAE, Castanet Tolosan, France. [15]Department of Integrative Biology, Michigan State University, East Lansing, MI, USA. [16]Ecology, Evolution, and Behavior Program, Michigan State University, East Lansing, MI, USA. [17]Institut Systématique, Evolution, Biodiversité (ISYEB), Muséum national d'Histoire naturelle, CNRS, SU, EPHE, UA, Paris, France. [18]Institut Pasteur, Université Paris Cité, CNRS UMR 3525, INSERM UA12, Comparative Functional Genomics group, F-75015 Paris, France.
***Corresponding author. Email: camille.berthelot@pasteur.fr (C.B.); hrc@bio.ens.psl.eu (H.R.C.); yann.guiguen@inrae.fr (Y.G.)**
†Present address: Department of Genetics, Evolution and Environment, University College London, London WC1E 6BT, UK.
‡These authors contributed equally to this work.

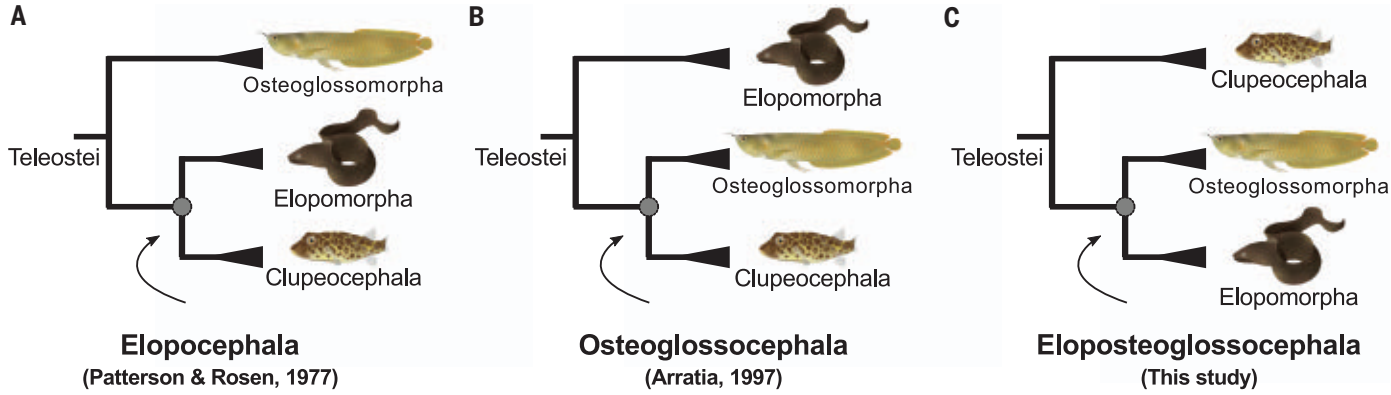

Fig. 1. Proposed scenarios for the topology of the earliest-branching teleost clades. The Elopocephala (*8*) (**A**), Osteoglossocephala (*9*) (**B**), and Eloposteoglossocephala (**C**) scenarios respectively propose Clupeocephala and Elopomorpha, Clupeocephala and Osteglossomorpha, or Osteglossomorpha and Elopomorpha as sister groups (see text for details).

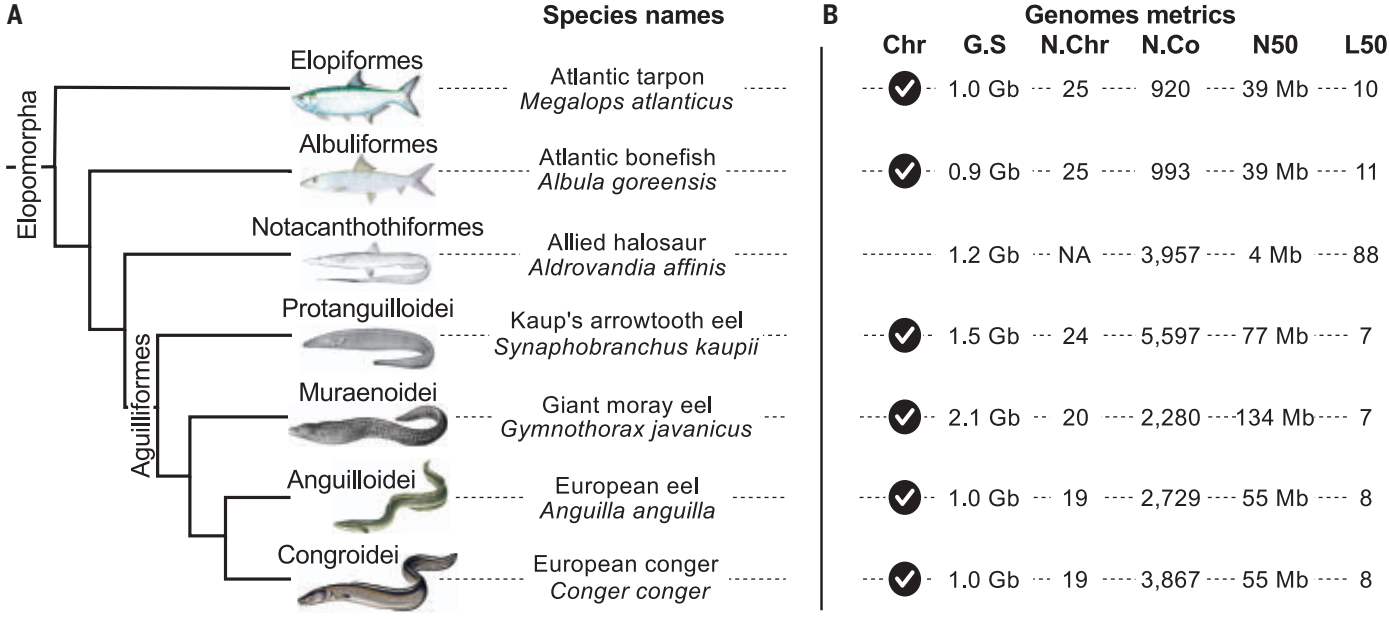

Fig. 2. Schematic phylogeny of representative Elopomorpha species. (**A**) This tree topology is based on (*29*) and includes each species for which we provide new whole-genome assemblies. (**B**) Six of these seven genomes were assembled at chromosome scale (Chr) with high-quality genome assembly metrics. G.S, genome size; N.Chr, haploid chromosome number; N.Co, number of contigs; N50, sequence length at which half of the genome assembly is covered by longer sequences; L50, smallest number of scaffolds needed to sum to half of the predicted genome size.

the Elopocephala or the Osteoglossocephala hypothesis. In addition, a third topology, placing Elopomorpha and Osteoglossomorpha as sister groups (Fig. 1C), was suggested in the early 1990s (*13*) and since then has been supported by a few more recent studies (*4*, *14*–*19*). This clade, which we tentatively named the Eloposteoglossocephala (Fig. 1C), was not formally retained, probably because this topology was not supported by any morphological evidence (*3*). The prevailing hypothesis, confirmed by a recent reanalysis of gene sequence phylogenetic studies (*11*), thus remains the Osteoglossocephala hypothesis, which places Elopomorpha as the earliest-branching clade of extant teleosts (*5*). However, the precise phylogenetic relationships of these major teleost lineages are still debated and have been recently reviewed by Dornburg and Near (*3*) as one of the major unresolved questions of the 21st century regarding the evolution of actinopterygian fishes. To promote a reexamination of this problem, they proposed to retain "the unconventional and intriguing possibility of an osteoglossomorph and elopomorph sister group relationship" (*3*).

A multiscale genomic approach for phylogenetic analyses

To resolve the phylogenetic relationships of these early-branching teleost clades, we first sequenced, assembled, and annotated high-quality reference genome sequences of 7 species that represent major Elopomorpha orders or families (Fig. 2 and table S1) for which chromosome-level whole-genome resources were lacking. We combined genome information from these seven Elopomorpha species with 18 additional publicly available genome assemblies including four Osteoglossomorpha, 10 Clupeocephala, and four vertebrate outgroups, including the spotted gar and bowfin nonteleost fishes, to perform phylogenomic analyses.

A major challenge for achieving accurate phylogenetic analysis of teleost genes is their high number of duplicate (paralogous) gene copies. Many of these paralogs are inherited from a whole-genome duplication (WGD) that occurred in a last common ancestor, 50 to

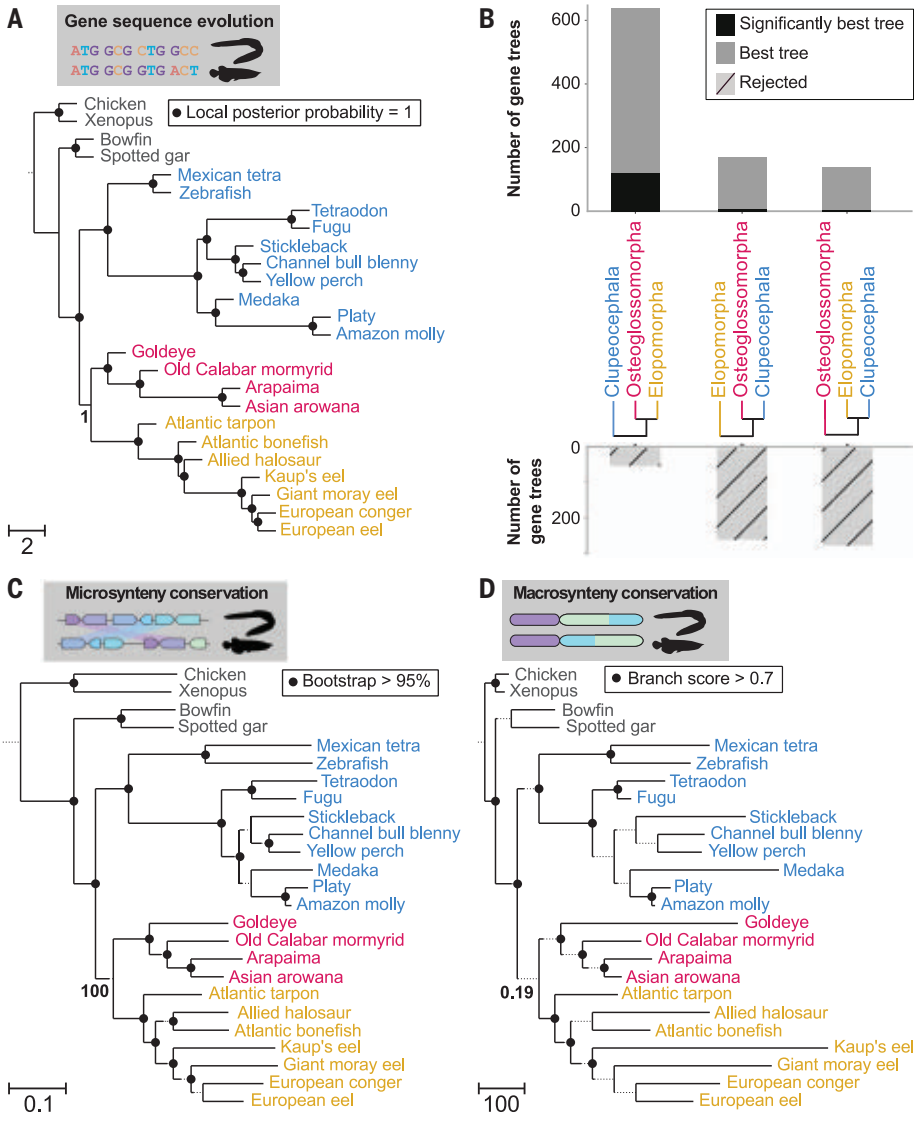

Fig. 3. Different phylogenomic reconstruction methods converge to support Osteoglossomorpha and Elopomorpha as sister groups. (**A**) Species tree inferred with ASTRAL under the multispecies coalescent model (*30*) from 955 single-copy gene trees. This method measures internal branch lengths in coalescent units; lengths at terminal branches are represented as equal and arbitrary. Node support is calculated as a local posterior probability. (**B**) Molecular gene genealogy interrogation: number of gene trees supporting each hypothesis (top, gray bars), significantly supporting each hypothesis (top, black bars), and number of significantly rejected gene trees (bottom, dashed bar). (**C**) Neighbor-joining species tree estimated from gene adjacencies between 3041 marker genes. Branch lengths represent the proportion of broken adjacencies, and nodes are supported by bootstrap values. (**D**) Best-supported species tree based on shared synteny breakpoints, reconstructed with PhyChro, a phylogenomics method based on partial split distances (*21*, *23*). Branch lengths are an estimate of the number of breakpoints. Branch scores correspond to the fraction of informative breakpoints that support the clade. Note that branch scores are different from bootstrap scores (*21*). (A to D) Very short branches have been extended with a dotted line for visualization purposes. Solid lines report the true branch lengths.

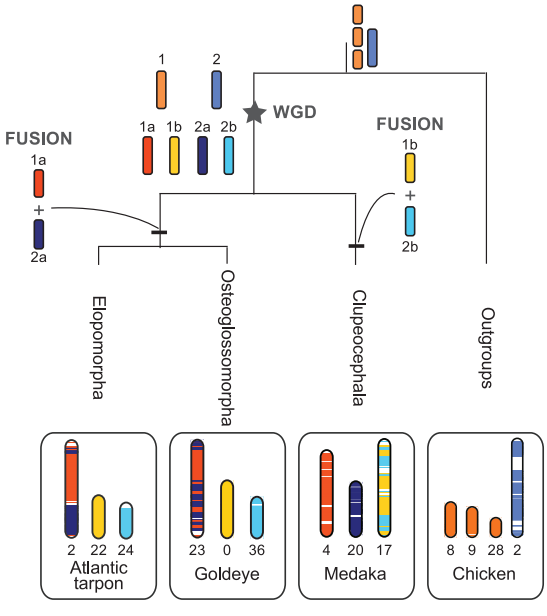

Fig. 4. Chromosomal rearrangements shared within the Eloposteoglossocephala clade. Inferred rearrangement scenario for two pairs of duplicated chromosomes (1a-1b and 2a-2b) in teleosts. Osteoglossomorpha and Elopomorpha share the 1a-2a chromosomal fusion, while Clupeocephala experienced an independent fusion between 1b and 2b (see fig. S7 for scenario support based on gene trees, fig. S8 for results on all studied genomes, and fig. S9 for discussion of an alternative ancestral scenario also supporting the monophyly of Elopomorpha and Osteoglossomorpha).

70 Myr before the diversification of extant teleost lineages (*20*). These WGD paralogs are known to mislead phylogenetic reconstructions (*4*). To mitigate the effect of paralog inclusion, we applied a WGD-tailored pipeline leveraging gene sequences and synteny conservation (*21*) to select 955 high-confidence 1-to-1 orthologous genes across all the 25 genomes that we analyzed. This list represents by far the largest molecular dataset considered for teleost phylogeny reconstruction, in terms of both sampled Elopomorpha genomes and total alignment size (fig. S1). We then performed phylogenetic reconstructions on the basis of these 955 individual gene trees, using coalescent-based summary analyses with ASTRAL [Accurate Species Tree Algorithm (Fig. 3A; fig. S2 for protein trees)], as well as maximum likelihood analyses of their concatenated sequences at both the nucleotide and protein levels (figs. S3 and S4). These analyses all provided support for the Eloposteoglossocephala

hypothesis, which places Osteoglossomorpha and Elopomorpha as sister groups. Additionally, this Eloposteoglossocephala clade was further supported by gene–genealogy interrogation, which directly compares the likelihood of each of the three evolutionary scenarios based on individual gene sequence alignments (Fig. 3B). These results are robust to the marker-selection methodology that we used (fig. S5 and table S2).

However, because previous sequence-based studies have yielded opposing results to resolve the three early-diverging teleost branches (*4*, *11*), we also used two innovative genome-wide methods to infer species trees based on conservation of genome structures. First, we analyzed the conservation of gene adjacencies between 3041 orthologous marker genes covering 57 to 98% of each teleost genome, and inferred a neighbor-joining species tree from local microsyntenic conservation (*22*). Second, we also analyzed macrosyntenic evolution by measuring the fraction of shared chromosomal breakpoints between species with PhyChro (*23*), on the basis of a set of independent, large-scale orthologous markers identified with SynChro (*24*). These two complementary approaches (Fig. 3, C and D; fig. S6; and table S2) also provided congruent support for the Eloposteoglossocephala scenario, confirming the results from gene sequence phylogenies.

Moreover, by looking at all potential chromosomal macrorearrangements, we identified a single chromosomal fusion exclusively shared between karyotypes of Osteoglossomorpha and Elopomorpha species (Fig. 4 and figs. S7 to S9). Together with the absence of other rearrangements that would be consistent with alternative groupings, this identical chromosomal macrorearrangement further supports our finding indicating that the two groups descend from a common ancestor, strengthening the phylogenomic evidence for the Eloposteoglossocephala clade.

Using a combination of new whole-genome resources for Elopomorpha and an array of independent phylogenomic reconstruction methods, we resolved long-standing questions regarding the early evolution of teleost fishes. This achievement highlights the power of genome-wide methods to resolve complex and ancient evolutionary histories, especially when these methods integrate a variety of informative evolutionary characters in complement to sequence information. Chromosome rearrangements, in particular, are fixed at a low rate and thus are less prone to mutational saturation and character reversal, which can occur in sequence-based phylogenies (*25*).

Eloposteoglossocephala is a new and unexpected clade

Our results resolve more than 50 years of controversy and show that Elopomorpha and Osteoglossomorpha constitute a monophyletic clade for which we suggest the name Eloposteoglossocephala (*21*). This conclusion raises questions about the paucity of anatomical evidence in favor of this scenario despite more than 70 years of extensive research (*3*, *6*). We carefully reexamined the available literature on these anatomical characters in light of our results, and we could not find a morphological character exclusively and unambiguously shared by Elopomorpha and Osteoglossomorpha. However, the fusion of the retroarticular with the angular and/or the articular, a derived character previously considered a synapomorphy of the Elopomorpha (*26*, *27*), has been shown to be shared at least with mormyrids among Osteoglossomorpha (*27*, *28*). Even if this character is described as either present (*28*) or ambiguous in goldeye *Hiodon alosoides*, and absent in two other Osteoglossomorpha (*27*), we propose this derived state as a morphological synapomorphy of the Eloposteoglossocephala, which was secondarily lost in some Osteoglossomorpha. We anticipate that as a result of our findings, more character mapping and new targeted anatomical and morphological searches will soon provide nonambiguous synapomorphies shared by the Eloposteoglossocephala.

By resolving the relationships of the three earliest-branching clades of crown teleosts, our results highlight the power of combining different levels of genome-wide information to solve complex phylogenies. This accurate topology of early teleost diversification will serve as a basis for new investigations into their genomic and functional evolution.

REFERENCES AND NOTES

1. F. Delsuc, H. Brinkmann, H. Philippe, *Nat. Rev. Genet.* **6**, 361–375 (2005).
2. J. S. Nelson, T. C. Grande, M. V. H. Wilson, *Fishes of the World* (Wiley, 2016).
3. A. Dornburg, T. J. Near, *Annu. Rev. Ecol. Evol. Syst.* **52**, 427–452 (2021).
4. L. C. Hughes *et al*., *Proc. Natl. Acad. Sci. U.S.A.* **115**, 6249–6254 (2018).
5. R. Betancur-R *et al*., *BMC Evol. Biol.* **17**, 162 (2017).
6. G. Arratia, *Estud. Oceanol.* **19**, 19–51 (2000).
7. C. T. Regan, *Proc. Zool. Soc. Lond.* **93**, 445–461 (1923).
8. C. Patterson, D. E. Rosen, *Bull. Am. Mus. Nat. Hist.* **158**, 81-172 (1977).
9. G. Arratia, *Basal Teleosts and Teleostean Phylogeny. Paleo Ichtyologica* 7, 1–168 (Dr. Friedrich Pfeil, 1997).
10. G. Arratia, *Copeia* **1998**, 1109–1113 (1998).
11. N. Takezaki, *Genome Biol. Evol.* **13**, evab052 (2021).
12. T. J. Near *et al*., *Proc. Natl. Acad. Sci. U.S.A.* **109**, 13698–13703 (2012).
13. H. L. Le, G. Lecointre, R. Perasso, *Mol. Phylogenet. Evol.* **2**, 31–51 (1993).
14. I. A. Hurley *et al*., *Proc. Biol. Sci.* **274**, 489–498 (2007).
15. R. Broughton, in *Origin and Phylogenetic Interrelationships of Teleosts*, J. S. Nelson, H.-P. Schultze, M. V. H. Wilson., Eds. (Dr. Friedrich Pfeil, 2010), pp. 61–76.
16. M.-Y. Chen, D. Liang, P. Zhang, *Syst. Biol.* **64**, 1104–1120 (2015).
17. C. Bian *et al*., *Sci. Rep.* **6**, 24501 (2016).
18. R. A. Vialle *et al*., *Genome Biol. Evol.* **10**, 2366–2379 (2018).
19. Z. Musilova *et al*., *Science* **364**, 588–592 (2019).
20. I. Braasch, J. H. Postlethwait, in *Polyploidy and Genome Evolution*, P. S. Soltis, D. E. Soltis, Eds. (Springer, Berlin, Heidelberg, 2012; https://doi.org/), pp. 341–383.
21. Materials and methods are available as supplementary materials at the *Science* website.
22. A. W. Thompson *et al*., *Nat. Genet.* **53**, 1373–1384 (2021).
23. G. Drillon, R. Champeimont, F. Oteri, G. Fischer, A. Carbone, *Mol. Biol. Evol.* **37**, 2747–2762 (2020).
24. G. Drillon, A. Carbone, G. Fischer, *PLOS ONE* **9**, e92621 (2014).
25. B. M. E. Moret, J. Tang, L.-S. Wang, T. Warnow, *J. Comput. Syst. Sci.* **65**, 508–525 (2002).
26. C. Patterson, in *Major Patterns in Vertebrate Evolution*, M. K. Hecht, P. C. Goody, B. M. Hecht, Eds. (NATO Advanced Study Institutes Series, Springer US, 1977), pp. 579–643.
27. R. Diogo, I. Doadrio, P. Vandewalle, *Int. J. Morphol.* **26**, (2008).
28. E. J. Hilton, *Zool. J. Linn. Soc.* **137**, 1–100 (2003).
29. J.-N. Chen, J. A. López, S. Lavoué, M. Miya, W.-J. Chen, *Mol. Phylogenet. Evol.* **70**, 152–161 (2014).
30. C. Zhang, M. Rabiee, E. Sayyari, S. Mirarab, *BMC Bioinformatics* **19** (suppl. 6), 153 (2018).
31. Y. Guiguen, Genomes assemblies and annotations of some Elopomorpha and Osteglossomorpha fish species, version 2.0, Omics Dataverse (2022); https://doi.org/10.15454/GWL0GP.
32. E. Parey *et al*., Code archive: Phylogeny of early teleost lineages, version 2, Zenodo (2022); https://doi.org/10.5281/zenodo.7303906.

ACKNOWLEDGMENTS

We thank Y. Guilloux, F. Quendo, and A. J. Adams for their help in providing fish samples. We also thank the leaders of the oceanography cruises and the crew of the RV *Atalante*, France, and ORI, Taiwan, in organizing the survey and helping to collect the deep-sea fish samples under the TDSB-TFDeepEvo joint program. **Funding:** This work was supported by the Agence Nationale de la Recherche, France (ANR) on the GenoFish project, 2016–2021 (grant No. ANR-16-CE12-003) to H.R.C., C.B., J.B., J.H.P., M.R.C., and Y.G., and by France Génomique National infrastructure, funded as part of "Investissement d'avenir" program managed by ANR (grant No. ANR-10-INBS-09) to C.D. Part of the fellowship to E.P. was supported by funds from the European Union Horizon 2020 research and innovation program under Grant Agreement No 817923 (AQUA-FAANG). M.R.-R. was supported by the Swiss National Science Foundation grant 31003A_173048. J.H.P and I.B were supported by the National Institutes of Health under grant agreement No. R01OD011116. W.J.C. was supported by MOST grants No. 111-2611-M-002-025, 110-2611-M-002-013, and 108-2611-M-002-012-MY2. **Author contributions:** Conceptualization: C.B., J.B., I.B., Y.G., C.K., A.L., J.H.P., M.R.R., H.R.C. Software: C.B., A.L., E.P., H.R.C. Formal analysis: C.B., A.L., E.P., H.R.C. Investigation: C.B., O.B., C.C., A.C., C.D., R.D., C.F., Y.G., C.I., H.J., E.J., C.K., G.L., J.L., A.L., J.M., E.P., H.R.C., C.R., M.W., M.Z. Resources: J.B., I.B., W.J.C., R.D., Y.G., C.H., H.J., S.M., J.H.P., A.T., M.W. Data curation: C.B., C.C., Y.G., C.K., A.L., J.M., M.Z. Visualization: C.B., Y.G., A.L., E.P. Funding acquisition: C.B., J.B., C.D., Y.G., J.H.P., M.R.R., H.R.C. Project administration: Y.G. Supervision: C.B., Y.G., H.R.C. Writing – original draft: C.B., Y.G., E.P., H.R.C. Writing – review and editing: C.B., J.B., I.B., C.C., T.D., Y.G., G.L., E.P., H.R.C., C.R., M.R.R. **Competing interests:** Authors declare that they have no competing interests. **Data and materials availability:** The Whole Genome Shotgun projects for the seven Elopomorpha species are available in the Sequence Read Archive (SRA) under the following BioProject references: PRJNA702045 (*Conger conger*), PRJNA692825 (*Albula goreensis*), PRJNA743502 (*Aldrovandia affinis*), PRJNA690086 (*Megalops atlanticus*), PRJNA693699 (*Anguilla anguilla*), PRJNA743503 (*Synaphobranchus kaupii*), and PRJNA702255 (*Gymnothorax javanicus*). All genome assemblies plus their annotations are also available in the Omics Dataverse (open source research data repository) server (*31*). All input data (sets of orthologous marker genes, CDS codons alignments, gene coordinates files) and the generated reconstructed species phylogenies have been deposited in Zenodo (*32*), along with all scripts and environments necessary to reproduce the analyses.

License information: Copyright © 2023 the authors, some rights reserved; exclusive licensee American Association for the Advancement of Science. No claim to original US government works. https://www.science.org/about/science-licenses-journal-article-reuse

SUPPLEMENTARY MATERIALS

science.org/doi/10.1126/science.abq4257
Materials and Methods
Supplementary Text
Figs. S1 to S9
Tables S1 to S5
References (*33*–*77*)
MDAR Reproducibility Checklist

Submitted 7 April 2022; accepted 6 January 2023
10.1126/science.abq4257

PLANT SCIENCE

Taxon-specific, phased siRNAs underlie a speciation locus in monkeyflowers

Mei Liang[1]*, Wenjie Chen[1,2], Amy M. LaFountain[1], Yuanlong Liu[3], Foen Peng[4,5], Rui Xia[3], H. D. Bradshaw[4], Yao-Wu Yuan[1,6]*

Taxon-specific small RNA loci are widespread in eukaryotic genomes, yet their role in lineage-specific adaptation, phenotypic diversification, and speciation is poorly understood. Here, we report that a speciation locus in monkeyflowers (*Mimulus*), *YELLOW UPPER* (*YUP*), contains an inverted repeat region that produces small interfering RNAs (siRNAs) in a phased pattern. Although the inverted repeat is derived from a partial duplication of a protein-coding gene that is not involved in flower pigmentation, one of the siRNAs targets and represses a master regulator of floral carotenoid pigmentation. *YUP* emerged with two protein-coding genes that control other aspects of flower coloration as a "superlocus" in a subclade of *Mimulus* and has contributed to subsequent phenotypic diversification and pollinator-mediated speciation in the descendant species.

Related organisms share developmental regulatory genes; morphological diversity is often generated by changes in function or expression patterns of these shared genes (*1*–*5*). However, whole-genome sequencing across the tree of life has revealed that new genes do evolve in specific groups of organisms (*6*–*13*). What is less clear is whether these "taxon-restricted" genes affect the subsequent evolution of the organisms that inherit them, including lineage-specific adaptation, morphological diversification, and speciation. Here, we report that a speciation locus in monkeyflowers (*Mimulus*) produces phased small interfering RNAs (siRNAs) that regulate floral carotenoid pigmentation. This noncoding gene evolved with two adjacent protein-coding genes that control other aspects of flower coloration as a "superlocus" that is restricted to a subclade of *Mimulus*.

The *Mimulus lewisii* complex contains several closely related species with three distinct pollination syndromes, including the bumble bee–pollinated *M. lewisii*, the self-pollinated *Mimulus parishii*, and the hummingbird-pollinated *Mimulus cardinalis* (Fig. 1, A to C). Where *M. lewisii* and *M. cardinalis* coflower in sympatry, they are reproductively isolated by pollinator preference (*14*, *15*). The flower color locus *YELLOW UPPER* (*YUP*) was shown to be a major contributor to pollinator choice in the natural habitat: Substitution of the *M. lewisii YUP* allele by the *M. cardinalis* version in a near-isogenic line (NIL) decreased bumble bee visitation and increased hummingbird visitation, producing a pollinator shift (*16*). As such, *YUP* is an example of a single locus causing pollinator-mediated reproductive isolation and speciation.

YUP determines the presence or absence of yellow carotenoid pigments in the petal upper epidermis (*17*). Previous genetic analyses using crosses between *M. lewisii* and *M. cardinalis* (*17*–*20*) suggested that the dominant *M. lewisii* YUP^L allele suppresses carotenoid accumulation in the pink corolla, except in the yellow nectar guides (Fig. 1A) where *YUP* is presumably not expressed. The recessive *M. cardinalis* yup^C allele allows carotenoid deposition in the entire corolla; this produces the bright red color in conjunction with a high concentration of anthocyanins (Fig. 1C), which is regulated by the *R2R3-MYB* gene *PETAL LOBE ANTHOCYANIN* (*PELAN*). Fine-scale genetic mapping of *YUP* using the *M. lewisii*–*M. cardinalis* species pair has been impeded by the lack of recombination around the *YUP* region between the two species (*19*, *20*).

Results

YUP *is a noncoding locus that produces siRNAs*

Here, we explored the possibility of using *M. parishii* as one of the parents for genetic mapping. As in *M. lewisii*, the YUP^P allele in *M. parishii* is dominant and the F_1 hybrid between *M. parishii* and *M. cardinalis* lacks carotenoid accumulation in the petal lobes (fig. S1). We first generated a crude $yup^{C/C}$ NIL in the *M. parishii* background by introgressing the *M. cardinalis* yup^C allele into *M. parishii* through two rounds of backcrossing and selfing. A resulting BC_2S_1 individual that was most similar to *M. parishii* in both vegetative and reproductive morphology but with yellow flowers was selected for the third round of backcrossing and selfing. Genotyping ~3000 BC_3S_1 and BC_3S_2 individuals delimited *YUP* to a 70-kb interval (Fig. 1I and fig. S2) and resulted in a refined Mpar_$yup^{C/C}$ NIL with petal lobe carotenoid accumulation (Fig. 1E).

This 70-kb candidate interval is part of the 337-kb chromosome fragment introgressed from *M. cardinalis* to *M. parishii* in the previously generated *DARK PINK* (*DPK*) NIL (*21*). The Mpar_$DPK^{C/C}$ NIL (Fig. 1F) accumulates more petal lobe anthocyanins than the wild-type *M. parishii* because it contains the semi-dominant *M. cardinalis PELAN* allele. The colocalization of *YUP* and *PELAN* in the *DPK* fragment explains the color hue difference between the *DPK* NILs in the heterozygous and homozygous states (dark pink versus orange) because the latter accumulates carotenoids in the petal lobes, whereas the former does not (Fig. 1, F to H). The 70-kb introgressed fragment in the Mpar_$yup^{C/C}$ NIL resulted from a rare recombination between *YUP* and *PELAN* (Fig. 1I). As such, this NIL carries the *M. cardinalis* yup^C allele but still has the *M. parishii* $pelan^P$ allele (Fig. 1H). We also introgressed the yup^C-$pelan^P$ fragment from the Mpar_$yup^{C/C}$ NIL into *M. lewisii*, which resulted in a Mlew_$yup^{C/C}$ NIL that resembles *M. lewisii* but with yellow flowers (Fig. 1D).

The 70-kb candidate interval contains eight protein-coding genes (Fig. 1I). However, RNA interference experiments of these genes in *M. lewisii* produced no phenotypic changes in carotenoid pigmentation (fig. S3), which prompted us to search for noncoding genes in this region. Examination of RNA sequencing reads mapped to this interval revealed a ~1.3-kb transcript (fig. S4A) that contains no open reading frames conserved between the dominant YUP^L and YUP^P alleles (fig. S4B) but includes an inverted repeat that could fold into a stable hairpin structure with an arm length of ~250 base pairs (fig. S5). Comparing this transcript against the genome using the Basic Local Alignment Search Tool (BLAST) revealed that the 5′-tail and left arm contiguously matched the 5′ untranslated region (5′UTR) and the first exon of a *CYP450* gene that is ~5 Mb away (Fig. 2A and fig. S6). Given that hairpin structures are often substrates for small RNA (sRNA) production (*22*), we sequenced sRNA libraries prepared from the whole corollas of wild-type *M. lewisii* and *M. parishii* as well as the Mpar_$yup^{C/C}$ NIL.

The sRNA sequencing data showed that this inverted repeat region in *M. lewisii* and *M. parishii* produced abundant 21–nucleotide (nt) siRNAs in a phased pattern (Fig. 2A), with the siRNAs generated from a specific starting position in a regular, head-to-tail arrangement (fig. S5) (*23*, *24*). By contrast, the siRNAs from the *M. cardinalis* allele, as expressed in the Mpar_$yup^{C/C}$ NIL, showed a different profile—the most abundant siRNA produced by the

[1]Department of Ecology and Evolutionary Biology, University of Connecticut, Storrs, CT 06269, USA. [2]Qinghai Provincial Key Laboratory of Crop Molecular Breeding and Key Laboratory of Adaptation and Evolution of Plateau Biota, Northwest Institute of Plateau Biology, Chinese Academy of Sciences, Xining 810008, Qinghai, China. [3]State Key Laboratory for Conservation and Utilization of Subtropical Agro-Bioresources, South China Agricultural University, Guangzhou, Guangdong 510642, China. [4]Department of Biology, University of Washington, Seattle, WA 98195, USA. [5]Department of Biology, Haverford College, Haverford, PA 19041, USA. [6]Institute for Systems Genomics, University of Connecticut, Storrs, CT 06269, USA.
*Corresponding author. Email: mei.liang@uconn.edu (M.L.); yaowu.yuan@uconn.edu (Y.-W.Y.)

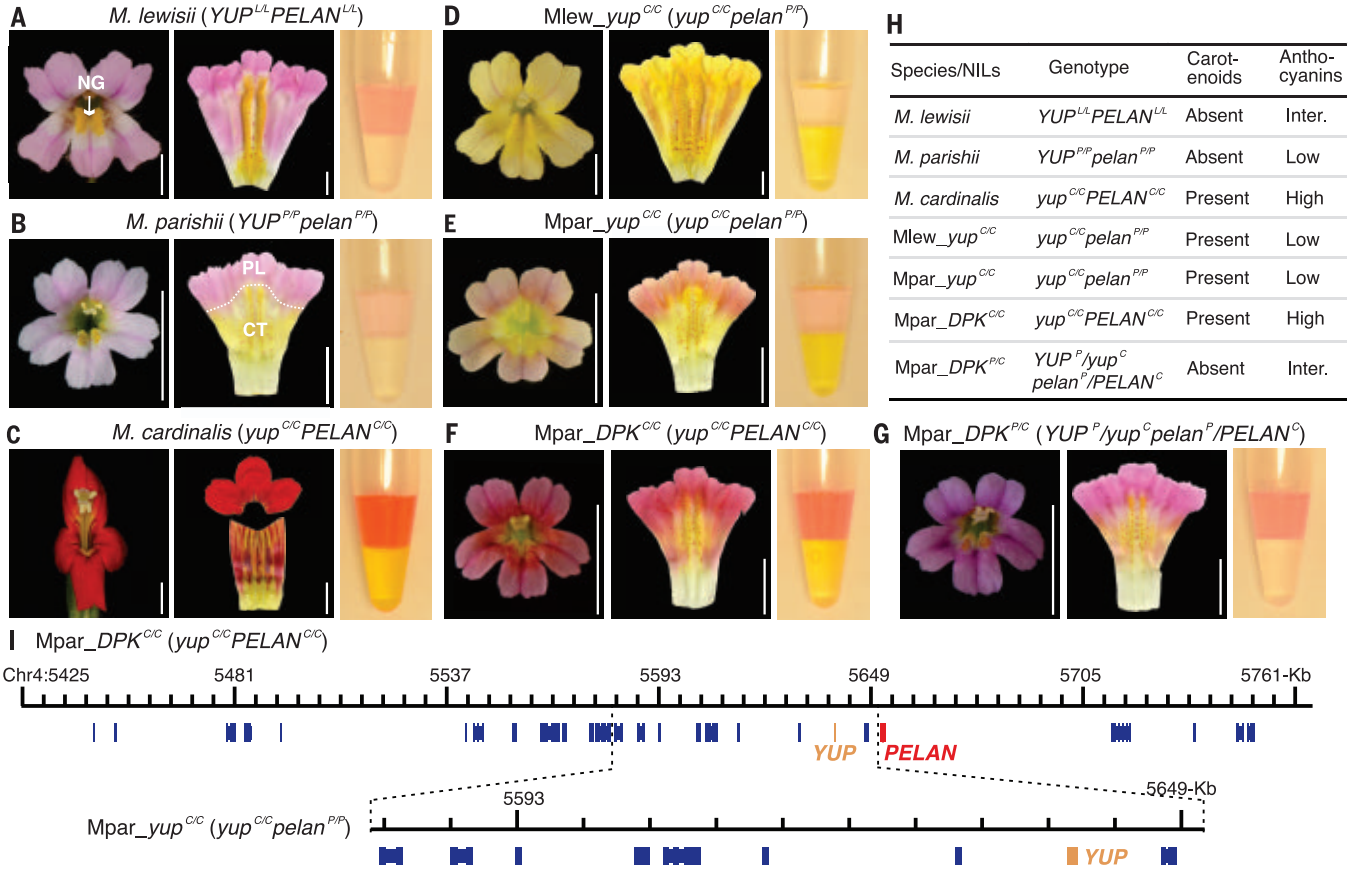

H

Species/NILs	Genotype	Carot-enoids	Antho-cyanins
M. lewisii	$YUP^{L/L}PELAN^{L/L}$	Absent	Inter.
M. parishii	$YUP^{P/P}pelan^{P/P}$	Absent	Low
M. cardinalis	$yup^{C/C}PELAN^{C/C}$	Present	High
Mlew_*yup*$^{C/C}$	$yup^{C/C}pelan^{P/P}$	Present	Low
Mpar_*yup*$^{C/C}$	$yup^{C/C}pelan^{P/P}$	Present	Low
Mpar_*DPK*$^{C/C}$	$yup^{C/C}PELAN^{C/C}$	Present	High
Mpar_*DPK*$^{P/C}$	YUP^{P}/yup^{C} $pelan^{P}/PELAN^{C}$	Absent	Inter.

Fig. 1. Flower color phenotypes of different genotypic combinations of *YUP* and *PELAN*. (**A** to **G**) The front view (left image) and dissected view (middle image) of the corollas of the three parental species [(A) to (C)] and various NILs [(D) to (G)]. The dissected view was produced by cutting the corolla along the junction between the two dorsal (upper) petals 1 day before anthesis. The white arrow in (A) indicates the yellow nectar guides (NG) of *M. lewisii*; the dashed line in (B) marks the boundary between the petal lobes (PL) and corolla tube (CT). Phase separation of pigment extracts from petal lobes of equal area are also shown (right image). Anthocyanins and carotenoids were separated into the upper and lower layer, respectively, following the protocol described in (*25*). The Mpar_*DPK*$^{C/C}$ homozygous NIL (F) accumulates more anthocyanins than the Mpar_*DPK*$^{P/C}$ heterozygous NIL (G) in the petal lobes because the *PELAN*^{C} allele is semidominant (*21*). Scale bars are 10 mm. (**H**) Genotypic combinations of *YUP* and *PELAN* and pigment compositions of the parental species and NILs shown in (A) to (G). Inter, intermediate. (**I**) The 70-kb candidate interval for *YUP* is part of the 337-kb introgressed fragment in the Mpar_*DPK*$^{C/C}$ NIL. Chr4, chromosome 4.

M. parishii YUP^{P} allele had much lower accumulation in the Mpar_*yup*$^{C/C}$ NIL (Fig. 2A and fig. S5). We named the most abundant siRNA from *YUP*^{P} as *YUP_siR1* and used its accumulation as a proxy to assess the total siRNA expression level from the inverted repeat region. Quantitative reverse transcription polymerase chain reaction (qRT-PCR) across multiple stages of flower development confirmed that the abundance of *YUP_siR1* in *M. parishii* was higher than that in *M. cardinalis* (Fig. 2B). Further qRT-PCR of different floral organs of the wild-type *M. parishii* at the peak expression stage (9 mm) showed that *YUP_siR1* accumulation is restricted to the corolla and is ~7-fold higher in the petal lobes than in the corolla tube (Fig. 2C).

To test whether this sRNA locus is *YUP*, we transformed the orange-flowered Mpar_*DPK*$^{C/C}$ NIL with the ~1.3-kb transcript from *M. lewisii*, *M. parishii*, and *M. cardinalis* driven by the constitutive *CaMV 35S* promoter. All of the 30 independent transgenic lines that overexpressed the *M. lewisii* transcript showed dark pink flowers that resembled those of the heterozygous Mpar_*DPK*$^{P/C}$ NIL, with no carotenoid accumulation (Fig. 2D and figs. S7A and S8A). Transformation of the *M. parishii* transcript (35 lines) produced the same results (Fig. 2E and figs. S7A and S8B). By contrast, no phenotypic change was observed among the 41 lines that were transformed with the *M. cardinalis* allele (Fig. 2F and figs. S7A and S8C). These results confirmed that this noncoding gene is indeed *YUP*.

Although the *35S:yup*^{C} lines had similar transcript levels of the transgene as the *35S:YUP*^{L} and *35S:YUP*^{P} lines (fig. S7B), the *35S:yup*^{C} lines produced conspicuously less *YUP_siR1* (Fig. 2G). Taking this finding together with the observation that the endogenous *yup*^{C} allele does produce abundant total siRNAs (Fig. 2A), just not *YUP_siR1* per se, we conclude that the recessive *yup*^{C} allele is due to mutations that disrupt the original phased pattern (fig. S5), which leads to accumulations of different siRNA species than those produced by the dominant *YUP* alleles.

YUP *represses carotenoid accumulation through* RCP2

To explore the molecular mechanism through which the dominant *YUP* allele represses carotenoid accumulation, we queried the siRNAs derived from the dominant *YUP* allele against the sequences of all known carotenoid biosynthesis genes and their regulators in *Mimulus*. Three forms of *YUP_siR1*, two 21-nt forms and one 22-nt form, were predicted to target *REDUCED CAROTENOID PIGMENTATION2* (*RCP2*) (Fig. 3A and fig. S9A), which encodes a tetratricopeptide repeat protein that is required for carotenoid accumulation in *Mimulus* (*25*). RNA ligase–mediated 5′ rapid amplification of cDNA ends (5′ RLM RACE) confirmed that *RCP2* transcripts could be cleaved at the predicted target site in *M. lewisii* (Fig. 3A).

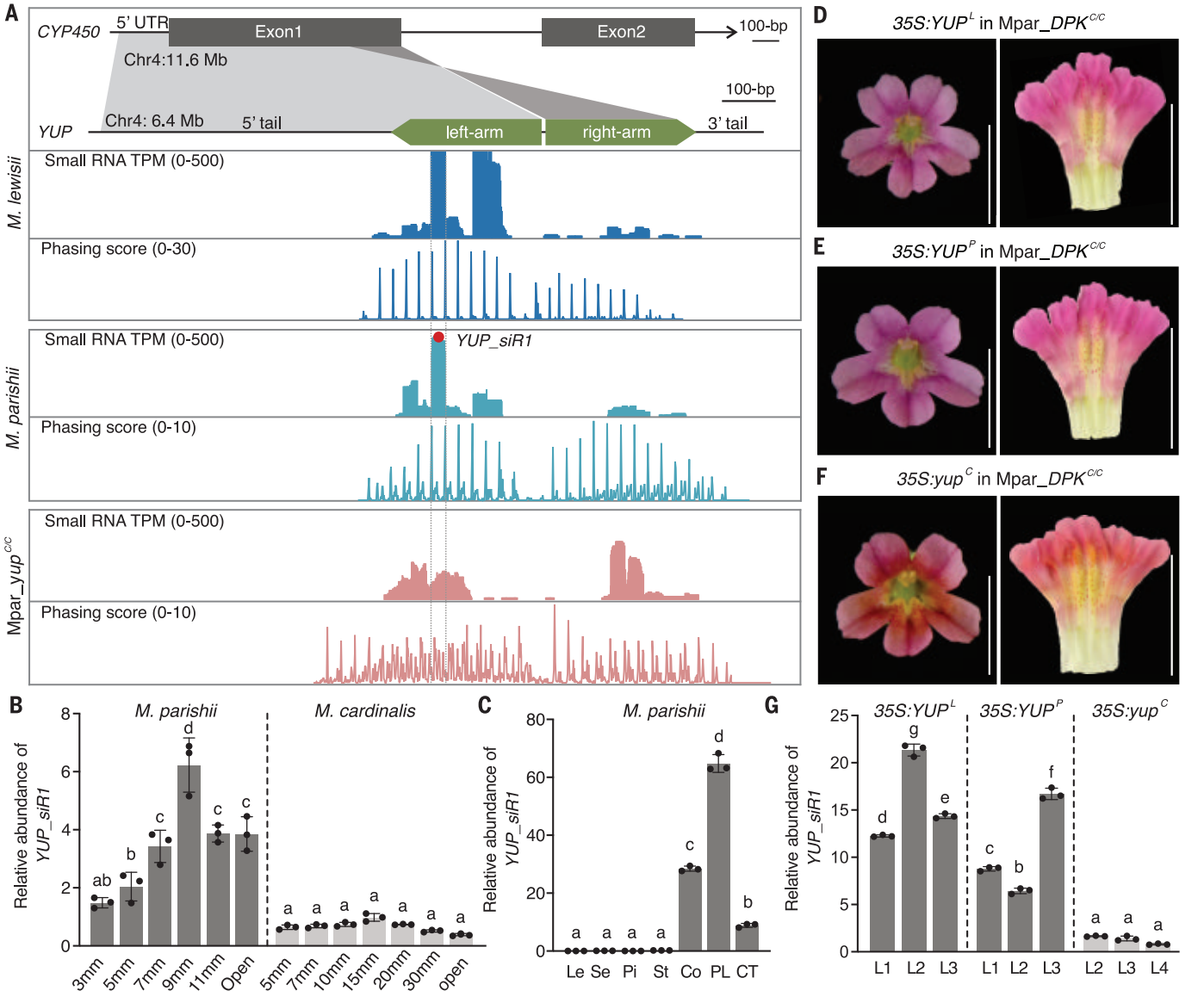

Fig. 2. *YUP* is an inverted repeat that produces phased siRNAs and represses carotenoid accumulation. (**A**) Integrative Genomics Viewer (IGV) view of the sRNA reads mapped to *YUP* and the siRNA phasing score. Sequencing data were generated from the 15-mm corolla of *M. lewisii* and the 5-mm corollas of *M. parishii* and the Mpar_*yup*$^{C/C}$ NIL and were mapped to the *M. lewisii*, *M. parishii*, and *M. cardinalis* genomes, respectively. The phasing score was calculated as in (*35*) and indicates the strength of the phasing pattern of siRNA distribution (higher score and less noise around the peaks indicate a stronger phasing pattern). The red dot indicates *YUP_siR1*, the most abundant siRNA from the *YUP*^{P} allele. TPM, tags per million. (**B**) Relative abundance of *YUP_siR1* across multiple corolla developmental stages, as measured by qRT-PCR. (**C**) Relative abundance of *YUP_siR1* in the leaf and different floral organs of *M. parishii* at the 9-mm corolla stage. Le, leaf; Se, sepal; Pi, pistil; St, stamen; Co, corolla; PL, petal lobe; CT, corolla tube. (**D** to **F**) The front view (left) and dissected view (right) of the corollas of *35S:YUP*^{L} (D), *35S:YUP*^{P} (E), and *35S:yup*^{C} (F) transgenic lines in the Mpar_*DPK*$^{C/C}$ NIL background. Scale bars are 10 mm. Also see pigment quantification in fig. S8, A to C. (**G**) Relative abundance of *YUP_siR1* in various transgenic lines. Error bars in (B), (C), and (G) are one standard deviation from three technical replicates. Different letters denote significant differences [$P < 0.01$, one-way analysis of variance (ANOVA)].

Furthermore, by examining the *M. lewisii* sRNA sequencing reads, we found that *YUP_siR1* also triggered the production of secondary siRNAs from the 5′ cleavage fragment of *RCP2* (fig. S9B). These results demonstrate that *YUP_siR1* indeed targets *RCP2*, and hereafter we will refer to it as *siR-RCP2*.

To determine whether *siR-RCP2* is sufficient to suppress carotenoid accumulation, we transformed the orange-flowered Mpar_*DPK*$^{C/C}$ NIL with an artificial *siR-RCP2* overexpression construct (*35S:amiR-RCP2*; fig. S9C). Multiple *35S:amiR-RCP2* transgenic lines (6 of 21 total lines) displayed dark pink flowers without carotenoid accumulation (Fig. 3B and fig. S8D) that were indistinguishable from those of the *35S:YUP*^{L} or *35S:YUP*^{P} lines. Further qRT-PCR analysis of three strong *35S:amiR-RCP2* lines showed a 17- to 43-fold increase in *siR-RCP2* abundance compared with the Mpar_*DPK*$^{C/C}$ NIL (Fig. 3C). However, we found that the transcript levels of *RCP2* in these lines only moderately decreased (Fig. 3D), indicating that *siR-RCP2* may also act on *RCP2* through translational inhibition.

To test the translational inhibition hypothesis, we generated transgenic *M. parishii* that overexpressed the coding sequences of *RCP2* with a C-terminal yellow fluorescent protein (YFP) fusion (fig. S10A). None of the 71 resulting transgenic lines that expressed *35S:RCP2-YFP* showed

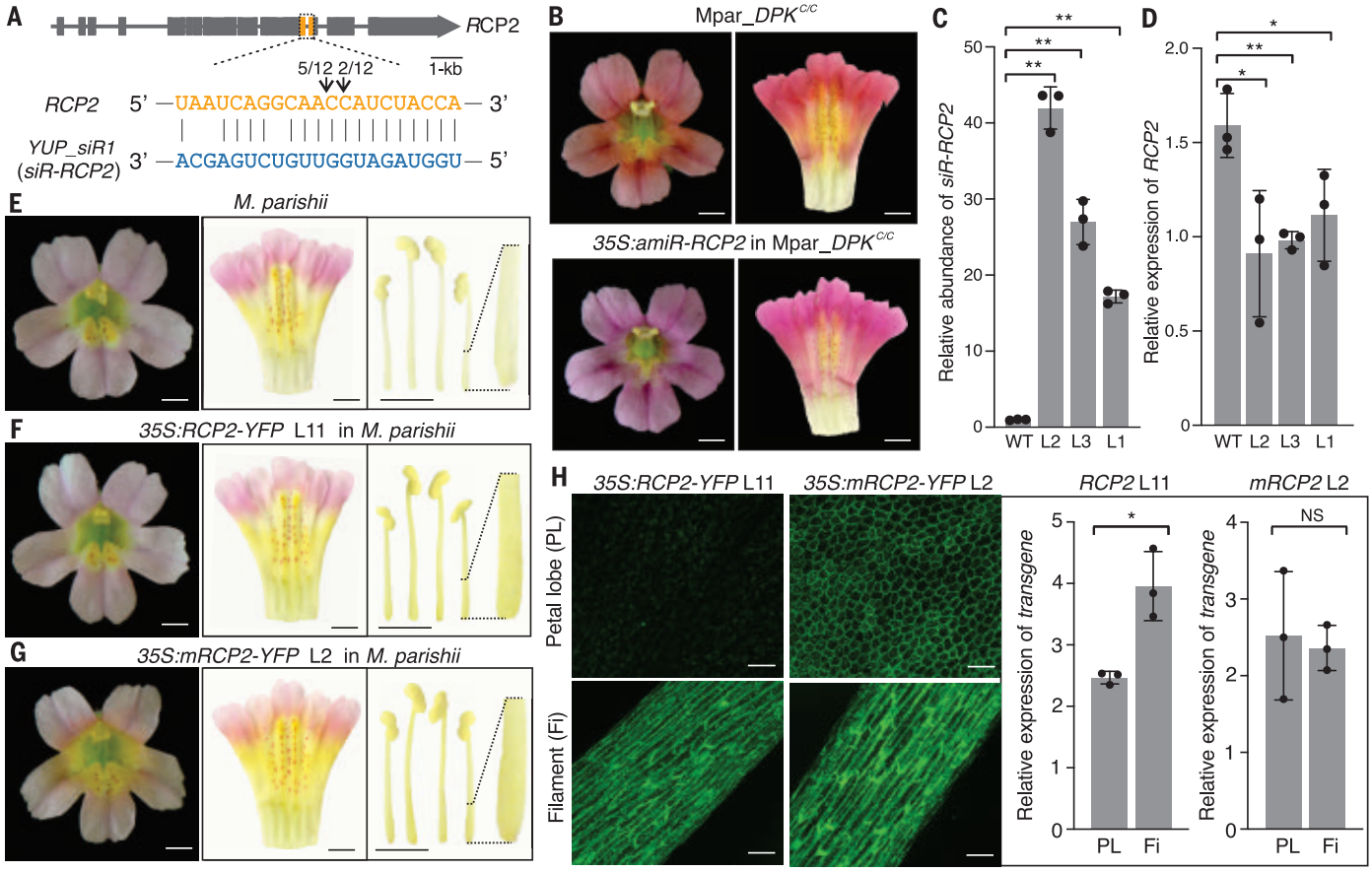

Fig. 3. *siR-RCP2* targets and represses *RCP2* through both transcript cleavage and translational inhibition. (**A**) The *siR-RCP2* target site on *RCP2* identified by 5′ RLM RACE assay. The cleavage positions are indicated by arrows, with the proportion of sequenced clones noted. (**B**) Overexpression of *siR-RCP2* in the Mpar_*DPK*$^{C/C}$ NIL resulted in a flower color shift from orange to pink. Scale bars are 2 mm. Also see pigment quantification in fig. S8D. (**C** and **D**) Relative abundance of *siR-RCP2* (C) and the transcript level of *RCP2* (D) in 9-mm corollas of the wild type (Mpar_*DPK*$^{C/C}$ NIL) and *35S:amiR-RCP2* transgenic lines, as measured by qRT-PCR. (**E** to **G**) Overexpression of the wild-type *RCP2* in *M. parishii* (E) resulted in ectopic accumulation of carotenoids in the stamen filaments but not in the corolla (F), whereas the *siR-RCP2*–insensitive *RCP2* (*mRCP2*) increased carotenoid accumulation in both organs (G). Scale bars are 2 mm. Also see pigment quantification in fig. S8, E and F, and the light microscope images of the filaments in fig. S10B. (**H**) The *35S:RCP2-YFP* transgene showed a slight decrease in petal lobes (PL) compared with the filament (Fi) at the transcript level, as measured by qRT-PCR, but a marked decrease at the protein level, as reflected by YFP fluorescent signals (left image and left graph). By contrast, the *35S:mRCP2-YFP* transgene showed similar levels of expression in petal lobes and filament at both the transcript and protein levels (right image and right graph). The YFP signals were confirmed in at least three flowers per line. Scale bars are 50 μm. Error bars in all qRT-PCR graphs [(C), (D), and (H)] are one standard deviation from three biological replicates. NS is not significant, $*P < 0.05$, and $**P < 0.01$ (Student's *t* test).

any change in corolla pigmentation, whereas many of the lines had increased carotenoid pigmentation in the stamen filament (Fig. 3, E and F, and figs. S8E and S10B). This was expected because, in the wild-type *M. parishii*, *siR-RCP2* is expressed in the corolla but not in stamens (Fig. 2C). The relative transcript and protein levels of the *RCP2-YFP* transgene in petal lobes and filaments were then assessed using qRT-PCR and confocal microscopy, respectively. qRT-PCR detected only a moderate difference in the transcript level between petal lobes and filaments (Fig. 3H). By contrast, confocal imaging revealed a conspicuous difference in the YFP fluorescence signal, which was hardly detectable in the petal lobes but was prominent in the filaments (Fig. 3H). These observations suggest that the *RCP2-YFP* reporter gene was translated in the filaments in the absence of *YUP* expression but that the translation was repressed in the petal lobes, which supports the translational inhibition hypothesis. This hypothesis also predicts that a *siR-RCP2*–resistant version of *RCP2* should result in protein translation in both the petal lobes and filaments. We thus transformed *M. parishii* with a *35S:mRCP2-YFP* construct by replacing the *siR-RCP2* target site with silent mutations (fig. S10A). Indeed, 11 of the 41 resulting lines showed increased carotenoid accumulation in both corolla and filament (Fig. 3G and fig. S8F) and comparable YFP signals in the two organs (Fig. 3H). In addition, the petal lobe of a *35S:mRCP2-YFP* line showed threefold higher YFP intensity than that of a *35S:RCP2-YFP* line with a very similar steady-state mRNA level of the transgene (fig. S10C), further suggesting that the *mRCP2-YFP* transcript is translated more efficiently than the *siR-RCP2*–sensitive version.

RCP1 *patterns nectar guides by repressing* YUP

The spatial segregation of carotenoids in the corolla is pronounced in the bumble bee–pollinated *M. lewisii*, where the yellow pigments accumulate only in the ventral part of the corolla tube (Fig. 1A), which serves as the nectar guides for bumble bee visitation (*26*). We found that *siR-RCP2* accumulation in *M. lewisii* is high in the petal lobes but low in the yellow nectar guides (Fig. 4A). This spatial pattern of *YUP* expression is complementary to that of *REDUCED CAROTENOID PIGMENTATION1* (*RCP1*) (Fig. 4B), a previously characterized

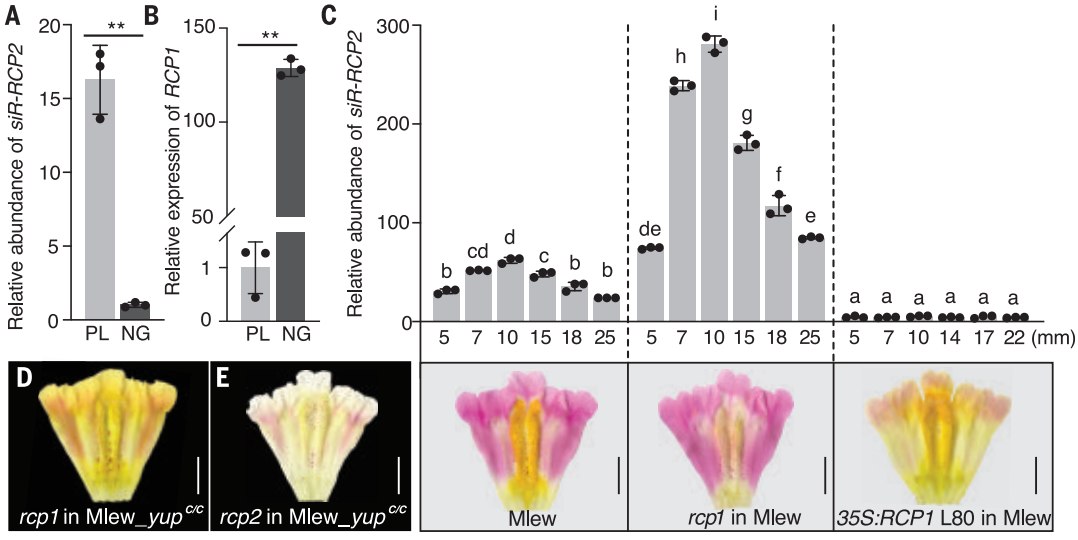

Fig. 4. *RCP1* represses *YUP* expression. (**A** and **B**) qRT-PCR assays of *siR-RCP2* (A) and *RCP1* (B) on the petal lobe (PL) and nectar guide (NG) tissue of a 10-mm *M. lewisii* corolla. Error bars are one standard deviation from three biological replicates. $^{**}P < 0.01$ (Student's *t* test). (**C**) qRT-PCR assay of *siR-RCP2* across multiple corolla stages in the wild-type *M. lewisii*, the *rcp1* mutant, and an *RCP1* overexpression line. Error bars are one standard deviation from three technical replicates. Different letters denote significant differences ($P < 0.01$, one-way ANOVA). The dissected corollas are shown below each bar graph. Scale bars are 5 mm. (**D** and **E**) Carotenoid accumulation in the corolla of Mlew_$yup^{C/C}$ NIL is not affected by the *rcp1* loss-of-function mutation (left) but is abolished by the *rcp2* mutation (right). Scale bars are 5 mm.

R2R3-MYB gene that is required for carotenoid pigmentation in the nectar guides of *M. lewisii* (*27*). We thus reasoned that *RCP1* may repress the expression of *YUP*. We performed qRT-PCR of *siR-RCP2* across multiple stages of corolla development in the wild-type *M. lewisii*, the previously characterized *rcp1* mutant, and a *35S:RCP1* overexpression line (*27*). We found that *siR-RCP2* accumulation increased in the *rcp1* mutant compared with the wild type at all corresponding stages and decreased in the *RCP1* overexpression line (Fig. 4C). These results suggest that *RCP1* represses *YUP* expression in the nectar guides, thereby allowing carotenoid accumulation in a tissue-specific fashion to promote bumble bee pollination in *M. lewisii*.

To further confirm the regulatory relationship among *RCP1*, *YUP*, and *RCP2* in the same genetic background, we crossed the loss-of-function *M. lewisii* mutants, *rcp1* and *rcp2* (*25*, *27*), with the Mlew_$yup^{C/C}$ NIL (Fig. 1B) to generate the "double mutants" *rcp1* $yup^{C/C}$ and *rcp2* $yup^{C/C}$; the former had yellow flowers with carotenoids in both the petal lobes and nectar guides (Fig. 4D), similar to the Mlew_$yup^{C/C}$ NIL, whereas the latter showed little carotenoid accumulation (Fig. 4E). These observations support the model that *RCP1* acts upstream of *YUP* and *YUP* acts upstream of *RCP2*.

Origin and evolution of the YUP-SOLAR-PELAN *superlocus*

Sequence homology indicates that *YUP* has originated from a partial duplication of the *CYP450* gene (Fig. 2A), although the source gene itself has no known function in carotenoid pigmentation and has negligible expression in the corolla of both *M. parishii* and the orange-flowered Mpar_$yup^{C/C}$ NIL (fig. S11). To determine the evolutionary timing of *YUP* origin, we first compared the synteny around *YUP* among our focal species and two distantly related *Mimulus* species with chromosome-level genome assemblies, *Mimulus guttatus* and *Mimulus aurantiacus* (*28*, *29*). Whereas the genomic region encompassing ~10 genes upstream and ~10 genes downstream of *YUP* showed great collinearity among these species, *M. guttatus* and *M. aurantiacus* lacked *YUP*, *PELAN*, and the one gene between them (Fig. 5A). The gene between *YUP* and *PELAN* is paralogous to *LIGHT AREAS1* (fig. S13), which is a subgroup-7 *R2R3-MYB* known to activate *FLAVONOL SYNTHASE* in *M. lewisii* (*30*), and is thus named *SISTER OF LIGHT AREAS1* (*SOLAR*) here. Knockdown of *SOLAR* by RNA interference resulted in reduced floral anthocyanin pigmentation (fig. S3E), suggesting that *SOLAR* is also involved in the regulation of flower coloration. We note that the source genes for *YUP*, *SOLAR*, and *PELAN* are far apart from each other in the *Mimulus* genomes (fig. S13).

The synteny analysis indicates that the *YUP-SOLAR-PELAN* "superlocus" originated after the split between the lineage that gave rise to the *M. guttatus* group and the one that gave rise to the *M. lewisii* complex (section Erythranthe) and the three closely related sections (*31*) (Fig. 5A). To pin down the evolutionary origin of this superlocus, we sequenced the genomes of four additional species that represent sections Monimanthe, Monantha, and Paradantha. Examining contigs that contain the ~20 genes surrounding *YUP* revealed that the three genes are only present in section Monimanthe, suggesting that the *YUP-SOLAR-PELAN* superlocus arose in the common ancestor of sections Erythranthe and Monimanthe ~5 million years ago (Fig. 5A).

Overexpression of the dominant YUP^{L} allele in four additional *Mimulus* species representing Erythranthe and the distantly related *M. guttatus* group all resulted in reduced flower carotenoid accumulation (Fig. 5, B to E, and fig. S14, A to D), indicating that the common ancestor of these *Mimulus* species was already predisposed to *YUP* action. Indeed, the *siR-RCP2* target site in the *RCP2* orthologs is highly conserved not only within *Mimulus* but also among a wide range of angiosperm species (fig. S14E).

Discussion

In this study, we isolated the speciation locus in *Mimulus*, *YUP*, as a taxon-restricted noncoding gene that produces phased siRNAs. One of these siRNAs represses *RCP2*, a master regulator of carotenoid accumulation, through both transcript cleavage and translational inhibition. Since its origin ~5 million years ago, the *YUP-SOLAR-PELAN* superlocus has contributed to flower color diversification and adaptation to different pollination modes in the descendant species (Fig. 5F).

Another example of a regulatory sRNA locus derived from inverted duplication underlying phenotypic variation with clear ecological importance is the *SULF* locus in the snapdragon *Antirrhinum majus* (*22*). In monkeyflowers, *YUP* shows the following distinguishing features: (i) the target of *YUP* siRNA (i.e., *RCP2*) has no phylogenetic affinity to the *CYP450* source gene; (ii) production of this *RCP2*-targeting siRNA relies on a particular mode of hairpin processing to generate siRNAs in a phased pattern, likely by DICER-LIKE 4 on the basis of our current understanding of the

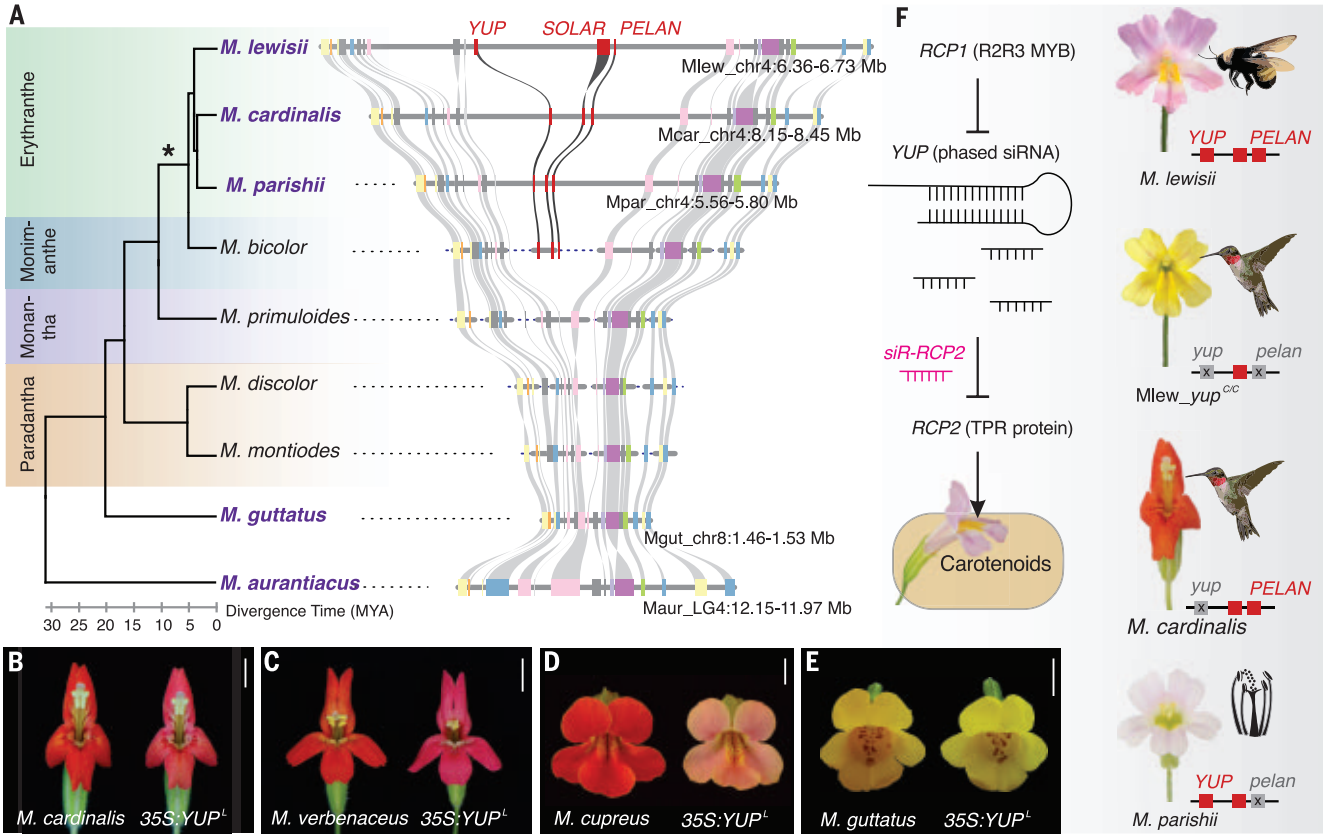

Fig. 5. The *YUP-SOLAR-PELAN* superlocus evolved in a subclade of *Mimulus* and contributed to flower color diversification. (**A**) Syntenic relationships of the *YUP* region encompassing ~10 flanking genes on each side of the *YUP-SOLAR-PELAN* superlocus. The time tree shown on the left is based on the maximum likelihood phylogeny (fig. S12) with the divergence time between the *M. guttatus* group and "*M. lewisii* + *M. bicolor*" clade as the calibration point. The species highlighted in bold have chromosome-level genome assemblies, where the *YUP* region is contiguously assembled. The other four species have fragmentary genome assemblies, and their contigs that match the *YUP* region are manually linked, as indicated by the dashed lines. The asterisk marks the node where *YUP*, *SOLAR*, and *PELAN* originated. The exceptionally large size of the *M. lewisii SOLAR* gene is due to a long intron. MYA, million years ago. (**B** to **E**) Overexpression of the *M. lewisii* YUP^{L} allele in various *Mimulus* species results in reduced petal carotenoid accumulation. Scale bars are 10 mm. Also see pigment quantification in fig. S14. (**F**) Summary of the regulatory relationships among *RCP1*, *YUP*, and *RCP2* (left) and flower color diversity generated by different *YUP* and *PELAN* genotypic combinations (right). Flower size in (F) is not scaled in proportion. All species listed in (A) to (F) are genus *Mimulus*. TPR, tetratricopeptide repeat.

DICER-like proteins in *Arabidopsis* (*24*); and (iii) *YUP* evolved as part of the *YUP-SOLAR-PELAN* superlocus. It is difficult to envision how these three genes were brought together in the first place because their source genes are far apart in all the available *Mimulus* genomes (fig. S13). Given that all three genes are involved in flower coloration, it is tempting to speculate that this superlocus was maintained by pollinator-mediated selection after its emergence. Each of these three features alone seems to render *YUP* origination improbable; the odds are even smaller with all three combined. Yet, not only was *YUP* generated de novo, but it also has been subsequently maintained in the descendant species, contributing to flower color variation and speciation by evolving tissue specific expression patterns (e.g., as in *M. lewisii*) or loss-of-function mutations that disrupt the phased pattern of siRNA production (e.g., as in *M. cardinalis*).

Our results highlight the role of taxon-restricted regulatory sRNAs in species diversification. That these taxon-restricted sRNAs have not garnered as much attention as transcription factors and structural genes is perhaps due more to the practical challenges of their identification and functional characterization than to any difference in their relevance to phenotypic evolution.

The *M. lewisii* complex has served as a laboratory and field model in our quest to understand the molecular basis of phenotypic diversification, adaptation, and speciation (*32*). The common ancestor of the *M. lewisii* complex most likely had dark pink flowers (*21*, *33*). The bumble bee–pollinated *M. lewisii* evolved light pink flowers because of cis-regulatory mutations that up-regulated the transcription of *ROSE INTENSITY1* (*ROI1*), a conserved anthocyanin-repressing *R3-MYB* gene (*34*), which conforms to the widely accepted paradigm for the molecular basis of phenotypic evolution (*2*–*5*). By contrast, the self-pollinated *M. parishii* convergently evolved pale pink flowers because of a single nucleotide substitution in the 5′UTR of the anthocyanin-activating *R2R3-MYB* gene *PELAN* that inhibits protein translation (*21*), a type of mutation rarely considered when investigating phenotypic variation. Our results here show that the hummingbird-pollinated *M. cardinalis* evolved red flowers using a third mechanism that involved taxon-restricted phased siRNA derived from an inverted duplication of a gene that is not even part of the pigmentation pathway. We expect that further studies of this system will likely reveal additional molecular mechanisms of adaptive genetic variation.

REFERENCES AND NOTES

1. M. C. King, A. C. Wilson, *Science* **188**, 107–116 (1975).
2. H. E. Hoekstra, J. A. Coyne, *Evolution* **61**, 995–1016 (2007).

3. S. B. Carroll, *Cell* **134**, 25–36 (2008).
4. D. L. Stern, V. Orgogozo, *Science* **323**, 746–751 (2009).
5. V. Courtier-Orgogozo, L. Arnoult, S. R. Prigent, S. Wiltgen, A. Martin, *Nucleic Acids Res.* **48**, D696–D703 (2020).
6. K. Khalturin, G. Hemmrich, S. Fraune, R. Augustin, T. C. G. Bosch, *Trends Genet.* **25**, 404–413 (2009).
7. H. Kaessmann, *Genome Res.* **20**, 1313–1326 (2010).
8. S. Chen, B. H. Krinsky, M. Long, *Nat. Rev. Genet.* **14**, 645–660 (2013).
9. R. Neme, D. Tautz, *BMC Genomics* **14**, 117 (2013).
10. M. E. Santos, A. Le Bouquin, A. J. J. Crumière, A. Khila, *Science* **358**, 386–390 (2017).
11. J. Paps, P. W. H. Holland, *Nat. Commun.* **9**, 1730 (2018).
12. S. Xia *et al.*, *PLOS Genet.* **17**, e1009654 (2021).
13. L. Wu, J. D. Lambert, *Semin. Cell Dev. Biol.* S1084-9521 (22) 00183-5 (2022).
14. D. W. Schemske, H. D. Bradshaw Jr., *Proc. Natl. Acad. Sci. U.S.A.* **96**, 11910–11915 (1999).
15. J. Ramsey, H. D. Bradshaw Jr., D. W. Schemske, *Evolution* **57**, 1520–1534 (2003).
16. H. D. Bradshaw Jr., D. W. Schemske, *Nature* **426**, 176–178 (2003).
17. W. M. Hiesey, M. A. Nobs, O. Björkman, *Experimental Studies on the Nature of Species: V. Biosystematics, Genetics and Physiological Ecology of the Erythranthe Section of the Erythranthe Section of* Mimulus (Publication 628, Carnegie Institute of Washington, 1971).
18. H. D. Bradshaw Jr., S. M. Wilbert, K. G. Otto, D. W. Schemske, *Nature* **376**, 762–765 (1995).
19. C. R. Pince, thesis, University of Washington (2009).
20. L. Fishman, A. Stathos, P. M. Beardsley, C. F. Williams, J. P. Hill, *Evolution* **67**, 2547–2560 (2013).
21. M. Liang, C. E. Foster, Y. W. Yuan, *Sci. Adv.* **8**, eabo1113 (2022).
22. D. Bradley *et al.*, *Science* **358**, 925–928 (2017).
23. Q. Fei, R. Xia, B. C. Meyers, *Plant Cell* **25**, 2400–2415 (2013).
24. Y. Liu, C. Teng, R. Xia, B. C. Meyers, *Plant Cell* **32**, 3059–3080 (2020).
25. L. E. Stanley *et al.*, *Plant Cell* **32**, 1536–1555 (2020).
26. C. R. Owen, H. D. Bradshaw, *Arthropod-Plant Interact.* **5**, 235–244 (2011).
27. J. M. Sagawa *et al.*, *New Phytol.* **209**, 1049–1057 (2016).
28. U. Hellsten *et al.*, *Proc. Natl. Acad. Sci. U.S.A.* **110**, 19478–19482 (2013).
29. S. Stankowski *et al.*, *PLOS Biol.* **17**, e3000391 (2019).
30. Y. W. Yuan, A. B. Rebocho, J. M. Sagawa, L. E. Stanley, H. D. Bradshaw Jr., *Proc. Natl. Acad. Sci. U.S.A.* **113**, 2448–2453 (2016).
31. W. R. Barker, G. L. Nesom, P. M. Beardsley, N. S. Fraga, *Phytoneuron* **39**, 1–60 (2012).
32. Y. W. Yuan, *New Phytol.* **222**, 694–700 (2019).
33. T. C. Nelson *et al.*, *PLOS Genet.* **17**, e1009095 (2021).
34. Y. W. Yuan, J. M. Sagawa, R. C. Young, B. J. Christensen, H. D. Bradshaw Jr., *Genetics* **194**, 255–263 (2013).
35. R. Xia *et al.*, *Plant Cell* **25**, 1555–1572 (2013).

ACKNOWLEDGMENTS

We thank M. Opel, M. Moriarty, A. Garchow, and C. Liu for excellent plant care in the University of Connecticut EEB research greenhouses. We thank D. Grossenbacher for providing the *Mimulus bicolor* seeds; A. Cooley for the *Mimulus cupreus* seeds; L. Fishman for the *Mimulus primuloides* tissue; and L. Stanley for the *Mimulus discolor* and *Mimulus montioides* tissues. We thank members of the Yuan laboratory for comments on the manuscript and thank D. Schemske, B. Watson, J. Sagawa, L. Fishman, L. Stanley, Q. Lin, and B. Ding for discussion and assistance during the hunt for *YUP* over the years. **Funding:** This work was supported by an NSF grant (IOS-1827645) and an NIH grant (R01GM140092) to Y.-W.Y. and an NIH grant (R01GM088805) to H.D.B. **Author contributions:** M.L., H.D.B., and Y.-W.Y. designed the research; M.L., W.C., A.M.L., F.P., H.D.B., and Y.-W.Y. performed the research; M.L., Y.L., R.X., and Y.-W.Y. analyzed data; and M.L. and Y.-W.Y. wrote the paper with input from all authors. **Competing interests:** The authors declare that they have no competing interests. **Data and materials availability:** All the data required to evaluate and extend the conclusions in the paper are present in the paper and/or the supplementary materials. The Illumina sequencing data (sRNA sequencing, whole-genome sequencing) have been deposited to the National Center for Biotechnology Information (NCBI) under BioProject numbers PRJNA882815 and PRJNA882787. The described biological material can be obtained from Y.-W.Y. **License information:**

Copyright © 2023 the authors, some rights reserved; exclusive licensee American Association for the Advancement of Science. No claim to original US government works. https://www.science.org/about/science-licenses-journal-article-reuse

SUPPLEMENTARY MATERIALS

science.org/doi/10.1126/science.adf1323
Materials and Methods
Figs. S1 to S14
Table S1
References (*36*–*56*)
MDAR Reproducibility Checklist

Submitted 30 September 2022; accepted 6 December 2022
10.1126/science.adf1323

GEOCHEMISTRY

Relatively oxidized fluids fed Earth's earliest hydrothermal systems

Dustin Trail[1]* and Thomas M. McCollom[2]

The properties of high-temperature lithospheric fluids within the early Earth are poorly known, yet many origin-of-life scenarios depend upon their characteristics. These fluids represent a key communication pathway between Earth's interior and hydrothermal pools. We use zircon chemistry, experiments, and modeling to infer the character of lithospheric fluids approaching 4 billion years. We constrain oxygen fugacity, chlorine content, and temperature, which allow us to model the solubility and transport of metals that are hypothesized to be crucial for the origin of life. We show that these fluids were more oxidized than the terrestrial mantle during this time and that they were interacting with near-surface aqueous systems, possibly subaerial hydrothermal pools, amplifying redox gradients in a location attractive for prebiotic molecular synthesis or sustained microbial activity.

High-temperature fluids constitute a bridge between the solid earth and shallow subsurface hydrothermal systems; i.e., they transport solubilized rock components to the surface. The properties of high-temperature lithospheric fluids are broadly constrained for the modern Earth, but the characteristics of these fluids during the first 700 million years of our planet's history remain largely unknown. The problem is that mineral proxies that can record subsolidus fluid-rock interactions during the Eoarchean and Hadean [>3.6 billion years (Ga) ago] are sparse or altogether absent, leaving the chemical and physical properties of hydrothermal fluids largely uncertain. In the past several years, key discoveries have revealed a handful of ~4-Ga-old zircons ($ZrSiO_4$) that record temperatures too low to be directly attributable to crystallization from igneous magma, and therefore must have formed from aqueous fluid interactions within the crust (*1*, *2*). This presents an opportunity to explore—by zircon proxy—the properties of ancient lithosphere fluids interacting with rock.

Here, we show that zircon trace-element and isotope characteristics frame a geologic environment where the fluids are connected to subaerial hydrothermal systems. We also present a zircon experimental calibration to quantify the oxygen fugacity (fO_2) of the fluid(s). When the calibration is applied to zircons approaching 4 Ga old, it reveals oxidized conditions relative to recent high-precision fO_2 sensors applied to mantle rocks of similar age (*3*). The fO_2 is an important variable to quantify because it affects the stability of minerals, as well as the composition of the coexisting fluid. For redox-sensitive elements (e.g., Fe, Zn, S, C), fO_2 also regulates the solubility and speciation of the constituents in the fluid. Moreover, an enormous amount of geochemical energy is potentially available from redox disequilibria that may arise during buoyant fluid transport and chemical interactions between the solid earth and surface fluids. When available chemical constraints are considered, our preferred model is that relatively oxidized hydrothermal fluids fed subaerial hydrothermal pools nearly 4 Ga ago. Complementary geochemical rock-fluid modeling reveals that Mn, Zn, and Fe were more available than Cu to participate as inorganic metal catalysts in prebiotic chemistry or to support an already established biome if life was present.

[1]Department of Earth and Environmental Sciences, University of Rochester, Rochester, NY 14627, USA. [2]Laboratory for Atmospheric and Space Physics, University of Colorado, Boulder, CO 80309, USA.
*Corresponding author. Email: dtrail@ur.rochester.edu

Oxidation state of hydrothermal fluids

As a first step, we constrain fluid oxidation state using zircon chemistry as a proxy. In terrestrial systems, Ce is found as either a trivalent or

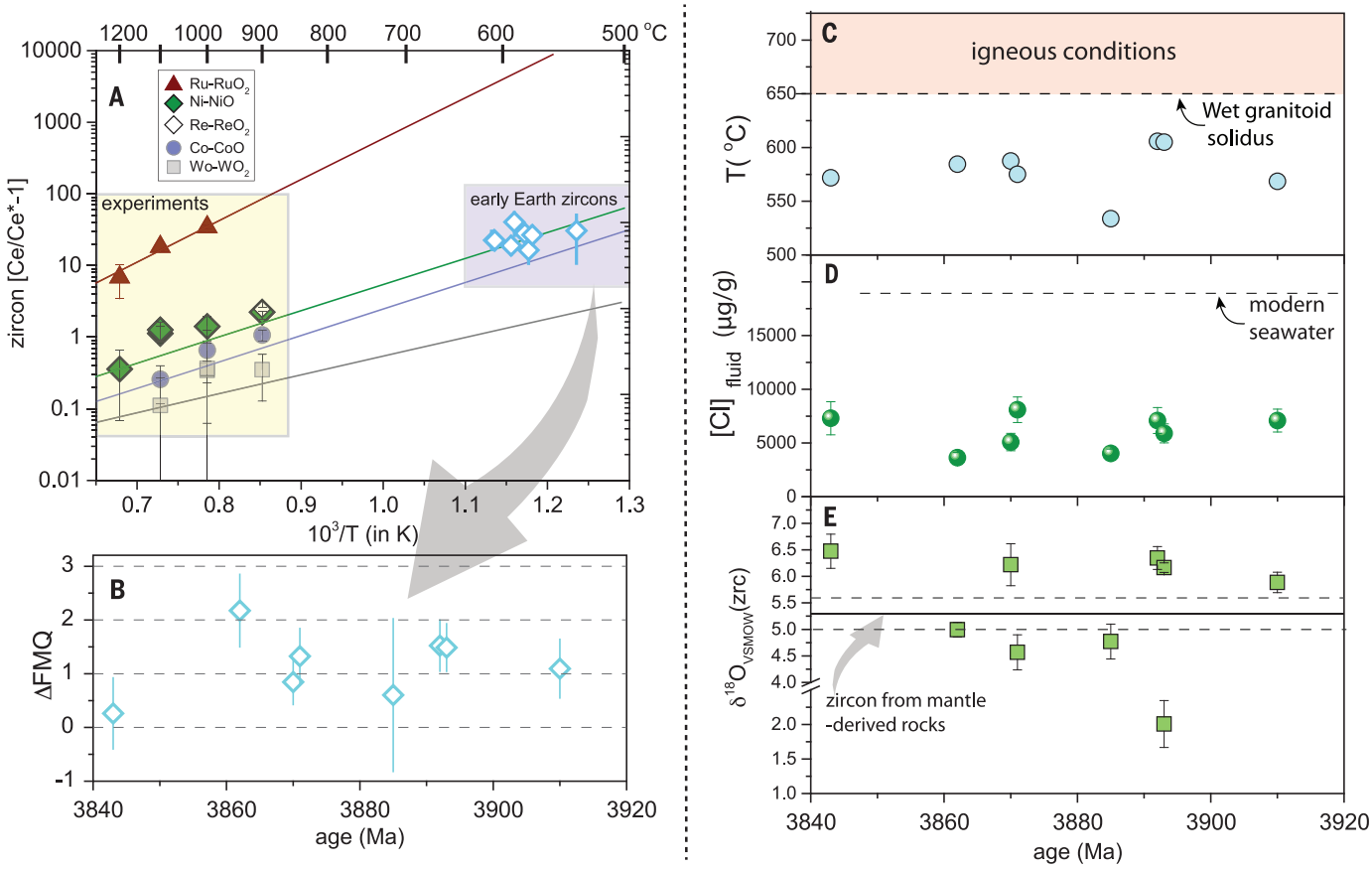

Fig. 1. Zircon trace-element and stable-isotope data. (**A**) Experimental calibration showing zircon Ce anomalies (plotted as Ce/Ce* − 1) for zircon-fluid REE partitioning from 16 experiments using five different metal-metal oxide fo_2 buffers (tables S3 to S6). Ce anomalies are positively correlated with fo_2 and inversely correlated with temperature (T). To apply this calibration to natural samples, Ce anomalies for the Jack Hills zircons are calculated by normalizing to the chondritic uniform reservoir (*32*), and T is derived using the Ti-in-zircon thermometer (*33*). (**B**) The calculated fo_2 of the fluids is relatively oxidized, i.e., ΔFMQ = 1.1. (**C**) Ti-in-zircon crystallization temperatures (*33*) plot below the wet granite solidus indicative of a nonmagmatic environment; here, equal titania and silica activities are assumed to calculate temperature (*1*, *9*). (**D**) Calculated fluid Cl content ($[Cl]_{fluid}$) using the measured Cl content in natural zircons ($[Cl]_{zircon}$) and zircon-fluid partitioning for Cl (*1*) give average values for $[Cl]_{fluid}$ of 6000 ± 1600 µg/g (1 SD; µg/g = mg/liter). (**E**) The $\delta^{18}O_{VSMOW}(zrc)$ values are defined as $([^{18}O/^{16}O]_{zircon}/[^{18}O/^{16}O]_{VSMOW} - 1) \times 1000‰$, where VSMOW is the Vienna standard mean ocean water standard.

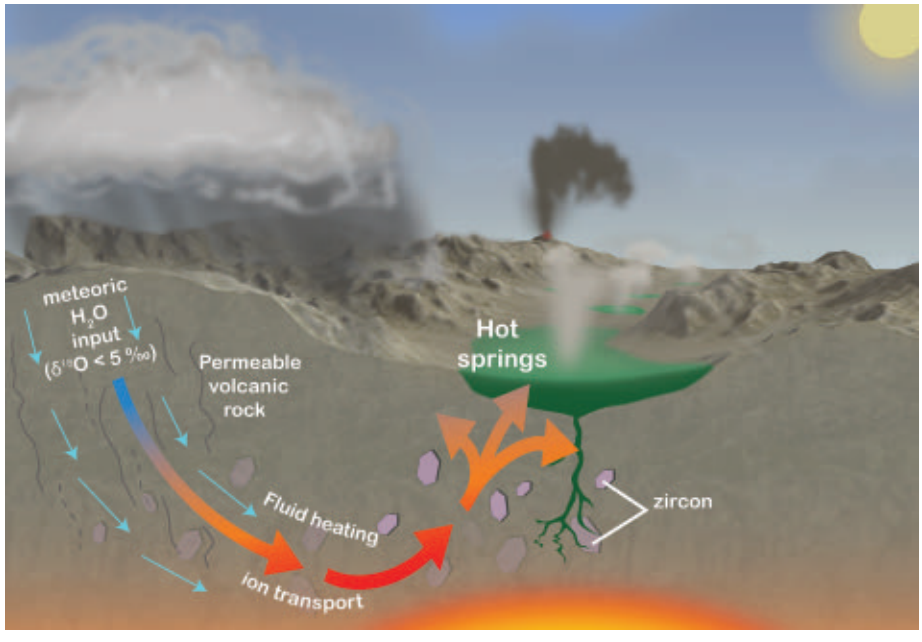

Fig. 2. A model geologic environment, constrained by zircon chemistry. Hydrothermal fields, driven by magmatic heat, are replenished by meteoric water (*4*). The meteoric water is responsible for the subset of the zircons with submantle $\delta^{18}O$ values (Fig. 1E), and low $[Cl]_{fluid}$ when compared to seawater (Fig. 1D). Both are indicators of subaerial environments. Zircons with $\delta^{18}O$ values above that of the mantle field (Fig. 1E) interacted with a comparatively smaller fraction of meteoric water, possibly owing to formation at greater depths (*7*). Hydrothermal activity can last >10^6 years; systems may wane, followed by rejuvenation with later magma pulses (*34*).

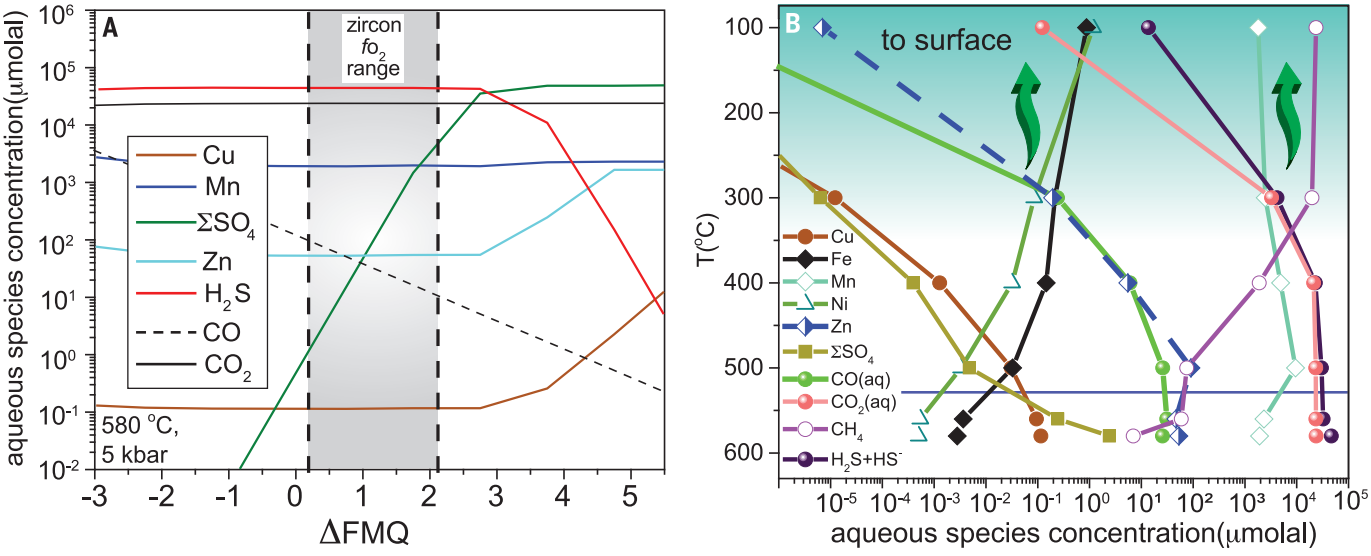

Fig. 3. Early Earth fluid properties determined from reaction path models. (**A**) Predicted equilibrium abundances of total dissolved metals, carbon, and sulfur species from the models constrained by zircon chemistry. Sulfate-bearing species are present across the entire fo_2 range predicted here, though the total concentration ($\sum SO_4$) decreases by about three orders of magnitude across this range. Not shown are Fe and Ni, whose concentrations are $<10^{-2}$ μmolal (*4*) and are thus off the scale. (**B**) A model that tracks metal solubility in the fluid during buoyant rise en route to the surface. Temperatures lower than the solid purple line (~530°C) are model extrapolations that extend to lower temperatures than the zircon data. These models were executed at average fo_2 values of ΔFMQ = 1 (*4*). Methane exhibits increasing abundance at lower *T*, reflecting the increased thermodynamic stability of reduced carbon species. At 100°C Cu, $\sum SO_4$, and CO(aq) plot off the scale and have respective concentrations of ~10^{-11}, ~10^{-9}, and ~10^{-8} μmolal. The models do not take into consideration that fluids that transition rapidly from high to low *T* may carry higher loads of dissolved solutes than those predicted by the discrete equilibrium steps. Also, the models do not take into consideration complexation of metals with organic compounds, which may inhibit the formation of metal precipitates at lower temperature near the surface and enhance the concentration of some dissolved metals in hydrothermal fluids (*35*).

tetravalent cation, with the latter exhibiting better compatibility in the Zr^{4+} site of zircon. The more oxidized the fluid, the greater the fraction of Ce^{4+} in the system, the consequence of which is a higher concentration of Ce in zircon. This is quantified through a partition coefficient, which represents the concentration of Ce in zircon divided by the Ce concentration in the fluid ($D_{Ce}^{zrc/fluid}$). Zircon-fluid partitioning experiments (fig. S1) were conducted as a function of fo_2 and temperature for Ce and other non–redox sensitive trivalent rare earth elements (REEs) (e.g., La, Pr, Sm, etc.). The Ce compatibility in zircon is presented relative to neighboring REEs by calculating a Ce anomaly:

$$\left(\frac{Ce}{Ce^*}\right)_D = \frac{D_{Ce}^{zircon/fluid}}{\sqrt{D_{La}^{zircon/fluid} \times D_{Pr}^{zircon/fluid}}} \quad (1)$$

where the subscript "D" indicates that the Ce anomaly is calculated with the partition coefficients. The Ce anomaly represents the deviation from a ~Ce^{3+}-only system. The Ce^{3+}-only partition coefficient is represented by the denominator of Eq. 1 and requires $D_{La}^{zrc/fluid}$ and $D_{Pr}^{zrc/fluid}$ to quantify. As defined, the higher the fo_2, the larger the Ce anomaly becomes in zircon. Five different fo_2 buffers were imposed upon zircon-fluid REE partitioning experiments to characterize the zircon Ce anomaly as a function of fo_2 and *T* (fig. S1), resulting in the following empirical calibration:

$$\log\left[\left(\frac{Ce}{Ce^*}\right)_D - 1\right] = (0.237 \pm 0.040) \times \log(fO_2) + \frac{9437 \pm 640}{T(K)} - 5.02 \pm 0.38 \quad (2)$$

If $(Ce/Ce^*)_D = 1$ (Eq. 1), the presence of only Ce^{3+} is implied, and so a Ce redox exchange reaction cannot be written, and the fo_2 cannot be calculated. More generally, if $(Ce/Ce^*) \leq 1$, the result is undefined, which is reflected by the term on the left-hand side of Eq. 2. We apply this calibration to detrital zircons from the Jack Hills, Western Australia, with crystallization temperatures below the granite solidus (*1*). The relative fo_2 for the fluids is reported with respect to the fayalite-magnetite-quartz (FMQ) equilibrium. That is, ΔFMQ is defined as the $\log_{10}[fo_2(\text{fluid})] - \log_{10}[fo_2(\text{FMQ})]$ at the zircon crystallization temperature. The fluid fo_2 ranges from ΔFMQ = 0.2 to 2.1, with an average ΔFMQ value of 1.1 (±0.6, 1 SD) (Fig. 1, A and B). These eight zircons were formed under unexpectedly oxidizing conditions and furthermore represent the oldest quantified fo_2 of terrestrial fluids, with U-Pb ages from 3840 to 3910 million years.

Subaerial environments on early Earth

Complementary chemical tracers (Fig. 1) help frame a local geologic environment. First, we emphasize that the above-mentioned zircons formed 50° to 100°C lower than magma solidification temperatures (Fig. 1C) (*4*). Second, $[Cl]_{zircon}$ and $D_{Cl}^{zrc/fluid}$ (*1*) give an average $[Cl]_{fluid}$ ~3 times lower than that of modern seawater (Fig. 1D). The salinity of Archean seawater and submarine hydrothermal fluids is thought to be comparable to modern values or higher (*5*, *6*), providing geochemical support that these zircons formed outside of a submarine environment. Thus, to explain $[Cl]_{fluid}$ values requires another source of fluids, such as meteoric water or volatile inputs from magma sources (*7*, *8*). Third, the local environment is further constrained from the zircon $\delta^{18}O$ values (*1*, *9*). Some grains are depleted in ^{18}O relative to zircon derived from mantle melts (*10*), a chemical feature that is consistent with input of meteoric water into the system. Similar oxygen isotope signatures, resulting from assimilation of crust that has been hydrothermally altered by surface waters, are common in modern hotspot settings such as Iceland and Yellowstone (*11*). Moreover, complementary ^{18}O-enriched and -depleted zircon, relative to the mantle (Fig. 1E), has also been argued to be a chemical feature of early Earth Iceland-like systems

(*7*), similar to the environment that we propose here (*4*). To summarize, the zircon geochemistry requires relatively oxidized lithospheric fluids (~580°C), shallow subsurface water-rock interactions, fluid derived from meteoric sources, and restricted input of Cl-rich fluid into the source, where the latter two constraints are consistent with a subaerial environment (Fig. 2).

These fluid-rock interactions represent a more enclosed environment—compared to a substantially larger body of water such as a global ocean (*12*)—which likely helps concentrate and enhance the participation of metals in prebiotic reactions. To explore the behavior of metals, minerals, and other volatiles in the environment inferred above, we implement reaction path models using the software package EQ3/6 (*13*) to calculate equilibrium fluid and mineral compositions for a representative rock composition over a range of fO_2, $[Cl]_{fluid}$, and T (*4*). The starting rock is based on the average composition for icelandites from the GEOROC database (n = 123 rock samples, where the average SiO_2 content is 57.6 ± 5 wt %, 1 SD) (*4*).

We show the abundances of metals and predominant sulfur and carbon species from 580°C in models across a range of fO_2 conditions (Fig. 3A), with corresponding mineralogy and additional model results (fig. S2). Our modeling demonstrates that the three most abundant metals in the fluid (at 580°C) are Mn, Zn, and Cu. The dominant S-bearing species across the fO_2 range predicted by the zircon data is H_2S at 580°C, whereas the concentration of SO_4-bearing species ($\sum SO_4$) only dominates at fO_2 values more oxidizing than those predicted here (i.e., ΔFMQ ≥ 3). Carbon dioxide is two to three orders of magnitude more abundant than CO across the same fO_2 range. We now turn to a simple observation: Hot fluids are buoyant and lower in density than the rock in which they tend to interact. We now model the solubility changes with decreasing temperature and pressure during transport of the fluid to the surface (Fig. 3B).

Availability of metals for prebiotic chemistry

With these model results, we can infer the relative abundances of metals and explore the viability of their role in the local early Earth environment that may have been suitable for life or the emergence of life. This objective shares some commonalities with metallomics, a concept developed to recognize the importance of metal-assisted function in modern cellular reactions (*14*). For instance, enzyme metal cofactors such as Cu, Fe, and Zn are common in modern proteins (*15*), and some ribozymes require the presence of metal cations for catalysis (*16*). The metallome certainly evolved though time, regulated by metal availability owing to solid earth processes and biome feedback, resulting in amplified or muted biological function (*17*). The identity of metals associated with Paleoarchean carbonaceous residue, for example, has been used to infer ancient biological function and the chemical selectivity of ancient cells (*18*). Even further back in time, metal ions may have served an essential role as primitive catalysts (*19*) before life arose on Earth. Metals may thus function as key intermediaries between emerging biologic and prebiotic systems and the environment, providing strong motivation to explore metal-specific prebiotic paths using our results to provide context.

Copper-cyanometallates, for example, were shown to be a key component of one hypothesized reaction path for abiotic synthesis of glycolaldehyde and glyceraldehyde, under experimental conditions designed to emulate a subaerial environment exposed to ultraviolet radiation (*20*). However, our water-rock modeling yields very low Cu fluid concentrations that call into question the availability of Cu to catalyze the production of these simple sugars or other organic compounds (Fig. 3B).

On the other end of the spectrum, Mn has the highest concentration of metallic solutes inferred for the hydrothermal fluids (Fig. 3B), yet this metal is only rarely considered in origin-of-life scenarios (*21*). The high predicted $[Mn]_{fluid}$ is nevertheless consistent with Mn enrichments documented in the remains of younger subaerial Archean hot springs (*22*). Zinc and Ni concentrations are on the order of ~1 μmolal at 100° to 300°C (Fig. 3B), which is >5 orders of magnitude more abundant than Cu under the same conditions. Zinc, and to a minor extent Ni, are known to increase the adsorption of nucleotides and adenosine onto clays, and crucially, both elements are more effective at doing so than Na, Mg, and Ca, which are major cations in modern seawater (*23*). Enhanced Zn- and Ni-mediated absorption of biomolecules onto mineral surfaces can help concentrate simple organics for subsequent polymerization steps, potentially in the presence of sheet silicate minerals such as muscovite, tremolite, and prehnite, which all have stability fields that exist below 400°C (fig. S2).

The relatively oxidizing conditions seen in this study also result in a mixture of Fe^{2+} and Fe^{3+} in the fluid and minerals. At 580°C, magnetite ($Fe_2^{3+}Fe^{2+}O_4$) and pyroxenes are predicted to be the stable Fe-bearing minerals, whereas from 400° to 100°C epidote ($Ca_2Fe^{3+}Al_2Si_3O_{12}[OH]$) and annite ($KFe_3^{2+}AlSi_3O_{10}[OH]_2$) represent the equilibrium minerals. This is a key observation, given that the presence of mixed-valence Fe-hydroxides (versus Fe^{2+} or Fe^{3+} only) may enhance amino acid formation in synthetic hydrothermal vent systems (*24*). In addition, although Fe^{3+} is relatively insoluble in aqueous fluids, it is present with H_2S; both are thought to be requisites to form Fe-S clusters (*25*), hypothesized by some to be among the most ancient metal-based cofactors in primitive metabolic networks (*26*, *27*). Finally, methane becomes increasingly stable at lower temperatures; this component is frequently used as a reactant in experiments that seek to produce primitive prebiotic compounds, such as nucleic and amino acids (*28*).

With the model results presented (Fig. 3B), we assume an evolution of buoyant fluids along an fO_2 of ~ΔFMQ+1, independent of temperature, though hydrothermal systems are inherently in a state of disequilibrium and fluids may evolve along different fO_2 paths. We cannot exclude the possibility that fluids entered into a more reducing (or oxidizing) environment that is at or near the surface of Earth, which would produce a redox gradient. This intriguing scenario may also solve a paradox in prebiotic chemistry in which oxidizing and reducing conditions are "simultaneously" required (*29*) to increase molecular complexity to obtain prebiochemistry molecules such as aspartate and pyrimidines (*30*, *31*). Although the fluids constrained here would most likely represent a subset of the diversity of early terrestrial hydrothermal systems, our results mark the oldest quantified fO_2 of fluids in Earth's crust, which may have fed hydrothermal systems capable of concentrating and fractionating metals and other raw ingredients necessary for "productive" prebiotic activity.

REFERENCES AND NOTES

1. H. Tang, D. Trail, E. A. Bell, T. M. Harrison, *Geochem. Perspect. Lett.* **9**, 49–53 (2019).
2. T. M. Harrison, *Hadean Earth* (Springer, ed. 1, 2020).
3. L. Gao *et al*., *Nat. Commun.* **13**, 3283 (2022).
4. Materials and methods are available as supplementary materials.
5. B. Marty, G. Avice, D. V. Bekaert, M. W. Broadley, *C. R. Geosci.* **350**, 154–163 (2018).
6. R. Burgess *et al*., *Am. Mineral.* **105**, 1317–1325 (2020).
7. J. R. Reimink, T. Chacko, R. A. Stern, L. M. Heaman, *Nat. Geosci.* **7**, 529–533 (2014).
8. S. Arnórsson, A. Andrésdóttir, *Geochim. Cosmochim. Acta* **59**, 4125–4146 (1995).
9. E. A. Bell, T. M. Harrison, *Earth Planet. Sci. Lett.* **364**, 1–11 (2013).
10. J. W. Valley *et al*., *Contrib. Mineral. Petrol.* **150**, 561–580 (2005).
11. I. Bindeman *et al*., *Terra Nova* **24**, 227–232 (2012).
12. B. Damer, D. Deamer, *Astrobiology* **20**, 429–452 (2020).
13. T. J. Wolery, R. L. Jarek, *Software User's Manual: EQ3/6, Version 8.0* (Lawrence Livermore National Laboratory, 2003).
14. J. J. R. Fraústo da Silva, R. J. P. Williams, *The Biological Chemistry of the Elements: The Inorganic Chemistry of Life* (Oxford Univ. Press, ed. 2, 2001).
15. J. A. Tainer, V. A. Roberts, E. D. Getzoff, *Curr. Opin. Biotechnol.* **2**, 582–591 (1991).
16. R. K. O. Sigel, A. M. Pyle, *Chem. Rev.* **107**, 97–113 (2007).
17. A. L. Zerkle, C. H. House, S. L. Brantley, *Am. J. Sci.* **305**, 467–502 (2005).
18. K. Hickman-Lewis *et al*., *Sci. Rep.* **10**, 4965 (2020).
19. B. C. Clark, V. M. Kolb, *Life* **10**, 278 (2020).
20. D. Ritson, J. D. Sutherland, *Nat. Chem.* **4**, 895–899 (2012).
21. B. Bhushan, U. Shanker, Kamaluddin, *Orig. Life Evol. Biosph.* **41**, 469–482 (2011).
22. M. J. Van Kranendonk *et al*., *Astrobiology* **21**, 39–59 (2021).
23. J. Hao, M. Mokhtari, U. Pedreira-Segade, L. J. Michot, I. Daniel, *ACS Earth Space Chem.* **3**, 109–119 (2019).
24. L. M. Barge, E. Flores, M. M. Baum, D. G. VanderVelde, M. J. Russell, *Proc. Natl. Acad. Sci. U.S.A.* **116**, 4828–4833 (2019).
25. C. Bonfio *et al*., *Nat. Chem.* **9**, 1229–1234 (2017).

26. J. E. Goldford, H. Hartman, T. F. Smith, D. Segrè, *Cell* **168**, 1126–1134.e9 (2017).
27. E. K. Moore, B. I. Jelen, D. Giovannelli, H. Raanan, P. G. Falkowski, *Nat. Geosci.* **10**, 629–636 (2017).
28. T. M. McCollom, *Annu. Rev. Earth Planet. Sci.* **41**, 207–229 (2013).
29. S. A. Benner *et al.*, *ChemSystemsChem* **2**, (2020).
30. G. D. Cody *et al.*, *Geochim. Cosmochim. Acta* **68**, 2185–2196 (2004).
31. M. Yadav, R. Kumar, R. Krishnamurthy, *Chem. Rev.* **120**, 4766–4805 (2020).
32. D. Trail, E. B. Watson, N. D. Tailby, *Nature* **480**, 79–82 (2011).
33. J. M. Ferry, E. B. Watson, *Contrib. Mineral. Petrol.* **154**, 429–437 (2007).
34. E. Martin, O. Sigmarsson, *Lithos* **116**, 129–144 (2010).
35. S. G. Sander, A. Koschinsky, *Nat. Geosci.* **4**, 145–150 (2011).

ACKNOWLEDGMENTS

We thank Y. Wang, J. Buettner, and K. Johnston for technical assistance and three reviewers for constructive comments. **Funding:** This work was supported by NSF EAR-175190 and NASA grant 80NSSC19M0069. **Author contributions:** Conceptualization: D.T. Methodology: D.T., T.M.M. Investigation: D.T., T.M.M. Visualization: D.T., T.M.M. Funding acquisition: D.T., T.M.M. Project administration: D.T., T.M.M. Supervision: D.T., T.M.M. Writing – original draft: D.T. Writing – review and editing: D.T., T.M.M. **Competing interests:** The authors declare that they have no competing interests. **Data and materials availability:** All experimental data are available in the main text or the supplementary materials. EQ3/6 model outputs are included in the supplementary materials. **License information:** Copyright © 2023 the authors, some rights reserved; exclusive licensee American Association for the Advancement of Science. No claim to original US government works. https://www.sciencemag.org/about/science-licenses-journal-article-reuse

SUPPLEMENTARY MATERIALS

science.org/doi/10.1126/science.adc8751
Materials and Methods
Supplementary Text
Figs. S1 to S8
Tables S1 to S8
References (*36*–*57*)
Data S1

Submitted 5 May 2022; accepted 6 December 2022
10.1126/science.adc8751

VIROLOGY

Inhibition of cellular RNA methyltransferase abrogates influenza virus capping and replication

Yuta Tsukamoto[1], Takahiro Hiono[2,3], Shintaro Yamada[1], Keita Matsuno[2,4,5], Aileen Faist[6,7], Tobias Claff[8], Jianyu Hou[8], Vigneshwaran Namasivayam[8], Anja vom Hemdt[9], Satoko Sugimoto[10], Jin Ying Ng[1], Maria H. Christensen[11], Yonas M. Tesfamariam[11], Steven Wolter[12], Stefan Juranek[13], Thomas Zillinger[12,14,15], Stefan Bauer[14], Takatsugu Hirokawa[16,17,18], Florian I. Schmidt[11,19], Georg Kochs[20,21], Masayuki Shimojima[10], Yi-Shuian Huang[22,23], Andreas Pichlmair[24,25], Beate M. Kümmerer[9,26], Yoshihiro Sakoda[2,3], Martin Schlee[12], Linda Brunotte[6,27], Christa E. Müller[8], Manabu Igarashi[2,28]*, Hiroki Kato[1]*

Orthomyxo- and bunyaviruses steal the 5′ cap portion of host RNAs to prime their own transcription in a process called "cap snatching." We report that RNA modification of the cap portion by host 2′-O-ribose methyltransferase 1 (MTr1) is essential for the initiation of influenza A and B virus replication, but not for other cap-snatching viruses. We identified with in silico compound screening and functional analysis a derivative of a natural product from *Streptomyces*, called trifluoromethyl-tubercidin (TFMT), that inhibits MTr1 through interaction at its *S*-adenosyl-L-methionine binding pocket to restrict influenza virus replication. Mechanistically, TFMT impairs the association of host cap RNAs with the viral polymerase basic protein 2 subunit in human lung explants and in vivo in mice. TFMT acts synergistically with approved anti-influenza drugs.

Mammalian mRNAs and small nuclear RNAs (snRNAs) are capped at their respective 5′ ends with 7-methylguanosine (m^7G) and 2,2,7-trimethylguanosine (Gm3) (*1*), which are linked to the RNA by a triphosphate bridge and called cap0. The RNA methyltransferase (MTase) known as 2′-O-ribose methyltransferase MTr1 (CMTR1/FTSJD2) is mainly localized in the nucleus and catalyzes 2′-O-methylation of the first nucleotide (N1-2′-O-Me) of cap0 mRNA and snRNA to generate mature cap1 (*2*). The cap structure on host RNAs is crucial for stability and translation. Unmethylated immature RNAs, including cap0 RNAs, are recognized as a non-self RNA signature by retinoic acid–inducible gene-I (RIG-I)–like receptors for interferon (IFN) induction, and by interferon-induced protein with tetratricopeptide repeats 1 (IFIT1) for translational suppression (*3*, *4*). By contrast, the fully methylated cap1 RNA escapes innate immune mechanisms. Viruses commonly appropriate or imitate the mature cap structure of cellular RNAs to avoid triggering an immune response. Bunyaviruses, as well as orthomyxoviruses including influenza A virus (IAV) and influenza B virus (IBV), use a strategy called "cap snatching," in which the 5′ end of fully capped cellular RNA is removed and attached to viral mRNAs. For example, IAV polymerase consists of three subunits: polymerase acidic protein (PA), polymerase basic protein 1 (PB1), and polymerase basic protein 2 (PB2). The PB2 subunit of the trimeric polymerase binds to the cap structure of host RNAs to initiate RNA cleavage by the PA endonuclease at 10 to 13 nucleotides downstream of the cap structure. Viral mRNA is synthesized by PB1 by using the cleaved host-derived nucleotides with cap as a primer (*5*, *6*). By contrast, non–cap-snatching viruses such as coronaviruses, poxviruses, and flaviviruses encode their own cap-binding 2′-O-MTases and mediate 2′-O-methylation of their RNA to imitate the cellular cap and evade recognition by antiviral sensors (*7*, *8*). Cellular MTr1 deficiency leads to the accumulation of host cap0 RNAs in the cytoplasm (*2*) and potentially activates RIG-I and IFIT1 (*3*, *4*). This deficiency indicates that the methylation status of endogenous capped mRNAs at the first nucleotide is important for preventing immune activation. However, MTr1 deficiency enhances antiviral IFN responses to IAV and reduces its cap-snatching efficacy and impairs replication (*9*). Thus, MTr1 could be

[1]Institute of Cardiovascular Immunology, Medical Faculty, University Hospital Bonn, University of Bonn, Bonn, Germany. [2]International Collaboration Unit, International Institute for Zoonosis Control, Hokkaido University, Sapporo, Hokkaido, Japan. [3]Laboratory of Microbiology, Department of Disease Control, Faculty of Veterinary Medicine, Hokkaido University, Sapporo, Hokkaido, Japan. [4]Division of Risk Analysis and Management, International Institute for Zoonosis Control, Hokkaido University, Sapporo, Hokkaido, Japan. [5]One Health Research Center, Hokkaido University, Sapporo, Hokkaido, Japan. [6]Institute of Virology Muenster, Westfaelische Wilhelms–University, Muenster, Germany. [7]CiM-IMPRS, Westfaelische Wilhelms–University Muenster, International Max Planck Research School – Molecular Biomedicine, Muenster, Germany. [8]PharmaCenter Bonn and Pharmaceutical Institute, Pharmaceutical and Medicinal Chemistry, University of Bonn, Bonn, Germany. [9]Institute of Virology, Medical Faculty, University Hospital Bonn, University of Bonn, Bonn, Germany. [10]Department of Virology I, National Institute of Infectious Diseases, Tokyo, Japan. [11]Institute of Innate Immunity, Medical Faculty, University Hospital Bonn, University of Bonn, Bonn, Germany. [12]Institute of Clinical Chemistry and Clinical Pharmacology, Medical Faculty, University Hospital Bonn, Bonn, Germany. [13]Department of Oncology, Hematology, Rheumatology and Immune-Oncology, University Hospital Bonn, University of Bonn, Bonn, Germany. [14]Institute of Immunology, Philipps–University Marburg, Marburg, Germany. [15]Department of Biomedicine, Aarhus University, Aarhus, Denmark. [16]Transborder Medical Research Center, University of Tsukuba, Tsukuba, Japan. [17]Division of Biomedical Science, University of Tsukuba, Tsukuba, Japan. [18]Cellular and Molecular Biotechnology Research Institute, National Institute of Advanced Industrial Science and Technology, Tokyo, Japan. [19]Core Facility Nanobodies, Medical Faculty, University Hospital Bonn, University of Bonn, Bonn, Germany. [20]Institute of Virology, Medical Center, University of Freiburg, Freiburg, Germany. [21]Faculty of Medicine, University of Freiburg, Freiburg, Germany. [22]Institute of Biomedical Sciences, Academia Sinica, Taipei, Taiwan. [23]Neuroscience Program of Academia Sinica, Academia Sinica, Taipei, Taiwan. [24]Institute of Virology, School of Medicine, Technical University of Munich, Munich, Germany. [25]German Center for Infection Research (DZIF), Munich Partner Site, Munich, Germany. [26]German Center for Infection Research (DZIF), partner site Bonn-Cologne, Bonn, Germany. [27]Interdisciplinary Center for Medical Research, Medical Faculty Muenster, Germany. [28]Division of Global Epidemiology, International Institute for Zoonosis Control, Hokkaido University, Sapporo, Hokkaido, Japan.
***Corresponding authors. Email: hkato@uni-bonn.de (H.K.); igarashi@czc.hokudai.ac.jp (M.I.)**

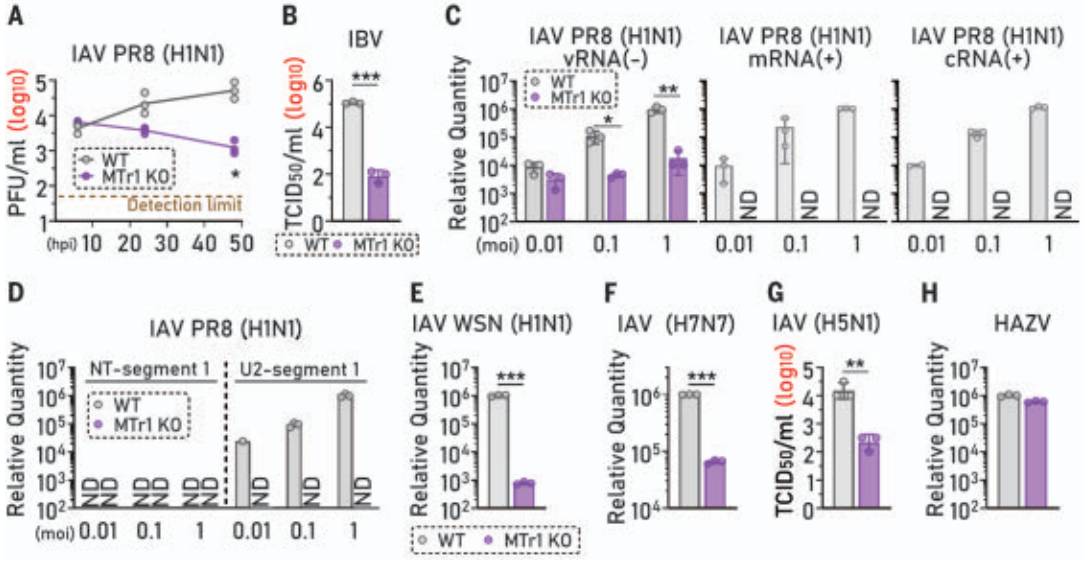

Fig. 1. Characterization of the requirement of host MTr1 for the replication of cap-snatching orthomyxoviruses and bunyaviruses. (**A**) Viral growth of IAV (H1N1, PR8) in WT and MTr1 KO A549 cells. After infection at multiplicity of infection (MOI) of 1, supernatants were taken at the indicated time points as hours after infection, and virus titers were determined as PFU/ml by means of plaque assay. The detection limit is indicated as a brown dotted line. hpi, hours postinfection. (**B**) Virus yield in the supernatant from WT and MTr1 KO A549 cells infected with IBV for 48 hours at moi of 0.1. Virus titers were determined as median tissue culture infection dose ($TCID_{50}$)/ml. (**C**) Strand-specific qRT-PCR analysis for relative RNA quantity of IAV vRNA, mRNA, and cRNA (segment 5) in the WT and MTr1 KO A549 cells infected with IAV PR8 for 24 hours at the indicated MOI. (**D**) qRT-PCR analysis for relative RNA quantity of NT/U2-IAV hybrid RNA in WT and MTr1 KO A549 cells infected with IAV PR8 for 24 hours at the indicated MOI. (**E** and **F**) qRT-PCR analysis for relative RNA quantity of IAV RNA (segment 7) or GFP (green fluorescent protein) RNA (inserted in segment 8) in WT and MTr1 KO A549 cells infected with (E) IAV WSN or (F) IAV SC35M-GFP (H7N7) for 24 hours at one infectious particle per cell. (**G**) Virus yield in the supernatant of WT and MTr1 KO A549 cells infected with IAV HK483 (H5N1) for 48 hours at MOI of 0.1. Virus titers were determined as $TCID_{50}$/ml. (**H**) qRT-PCR analysis for relative RNA quantity of the indicated viral RNA in WT and MTr1 KO A549 cells infected with HAZV at MOI of 0.1 for 24 hours. Statistics were calculated with Student's two-sided *t* test (*$P < 0.05$, **$P < 0.01$, ***$P < 0.001$). ND, not detected.

an interesting host-directed target for anti-IAV drugs and possibly for drugs against other cap-snatching viruses. Currently, no MTr1 inhibitors have been reported, and their potential as antiviral agonists remains unexplored.

MTr1 is specifically essential for IAV and IBV

To establish a functional antiviral screening system for MTr1 inhibitors, we first characterized the requirement of MTr1 for the replication of various cap-snatching viruses. We used CRISPR/Cas9 to generate A549 cells in which MTr1 was deleted (MTr1 KO cells) (fig. S1F). Consistent with a previous study that shows that MTr1 deficiency accumulates cap0 RNAs (*2*), we confirmed that recombinant MTr1 protein exhibited cap0-dependent MTase activity (fig. S1A) and that total and small RNA from MTr1 KO cells induced higher activity compared with that of control cells (fig. S1, B and C). These cells were infected with two orthomyxoviruses, IAV (PR8 strain, H1N1) and IBV (Victoria lineage Hokkaido strain), and viral replication levels were monitored. Accumulation of IAV and IBV was impaired in MTr1 KO cells compared with that in controls (Fig. 1, A and B). Consistent with this observation, we observed suppression of viral RNA levels and viral protein expression in MTr1 KO cells (fig. S1, D to I). IAV replication in MTr1 KO cells was rescued by retroviral reexpressing of MTr1, but not of MTr1 K239A, a catalytically inactive mutant (*2*) (fig. S2). Strand-specific quantitative reverse-transcription polymerase chain reaction (qRT-PCR) (*10*) revealed that only IAV viral RNA (vRNA), but not mRNA or complementary RNA (cRNA), was detected in MTr1 KO cells (Fig. 1C and fig. S3). In accordance with previous work (*9*), we confirmed the defect in the cap-snatching step of IAV replication in MTr1 KO cells by quantifying the level of IAV mRNA (segment 1) snatched specifically from U2 spliceosomal snRNA by means of qRT-PCR with the U2–segment 1 (PB2) hybrid primer (*5*, *11*) (Fig. 1D and fig. S4).

To explore whether MTr1 is only required for the PR8 strain of IAV (H1N1) or whether other orthomyxoviruses are similarly dependent on this host enzyme, we tested the replication efficacy of different IAV strains and other orthomyxoviruses. Not only PR8 (H1N1), but also WSN (H1N1), SC35M (H7N7), and a highly pathogenic avian IAV HK483 (H5N1) showed replication defects in MTr1 KO cells (Fig. 1, E to G, and fig. S5, A and B). MTr1 deficiency had minimal or no effect on the production of virus particles and the RNA replication of two other orthomyxoviruses, influenza D virus (IDV) and Thogoto virus (THOV) (fig. S5, C and D), suggesting distinct requirements for MTr1 among orthomyxoviruses. We next asked whether MTr1 serves as a general host factor for cap-snatching viruses. Besides orthomyxoviruses, bunyaviruses are also known to perform cap-snatching (*12*). Therefore, we examined a variety of bunyaviruses, including Rift Valley fever virus (RVFV), Hazara virus (HAZV), Issyk-Kul virus (ISKV), Soft tick bunyavirus (STBV), and Dugbe virus (DUGV). The RNA replication levels and virus yields in the supernatants of MTr1 KO cells infected with these bunyaviruses exhibited minimal to no difference compared with those of wild-type (WT) cells (Fig. 1H and fig. S6, A to E). These data suggest that the cap-snatching activity of these bunyaviruses, as well as of the two orthomyxoviruses IDV and THOV, is independent of MTr1-dependent cap modification. Moreover, our data indicate that host-directed inhibitors for MTr1 will specifically inhibit IAV and IBV among cap-snatching viruses, independent of subtype and strain (fig. S6F).

Identification of trifluoromethyl-tubercidin as an MTr1 inhibitor

Considering the specific and potent restriction of IAV and IBV replication by MTr1 deficiency, MTr1 is potentially a target for anti-IAV and anti-IBV drugs, including highly pathogenic avian IAV strains such as H5N1 (Fig. 1G). Because MTr1 transfers a methyl group from the methyl donor *S*-adenosyl-L-methionine (SAM) to a cap0 RNA recipient, producing cap1 RNA and *S*-adenosyl-L-homocysteine (SAH) as a by-product (*2*), we assumed that compounds that specifically bind to the SAM-binding pocket of MTr1 could act as inhibitors. We performed an in silico screening to search for potential MTr1 inhibitors (fig. S7, A and B). We screened 5597 compounds from a chemical database (DrugBank; https://go.drugbank.com/) and used the crystal structure of MTr1 [Protein

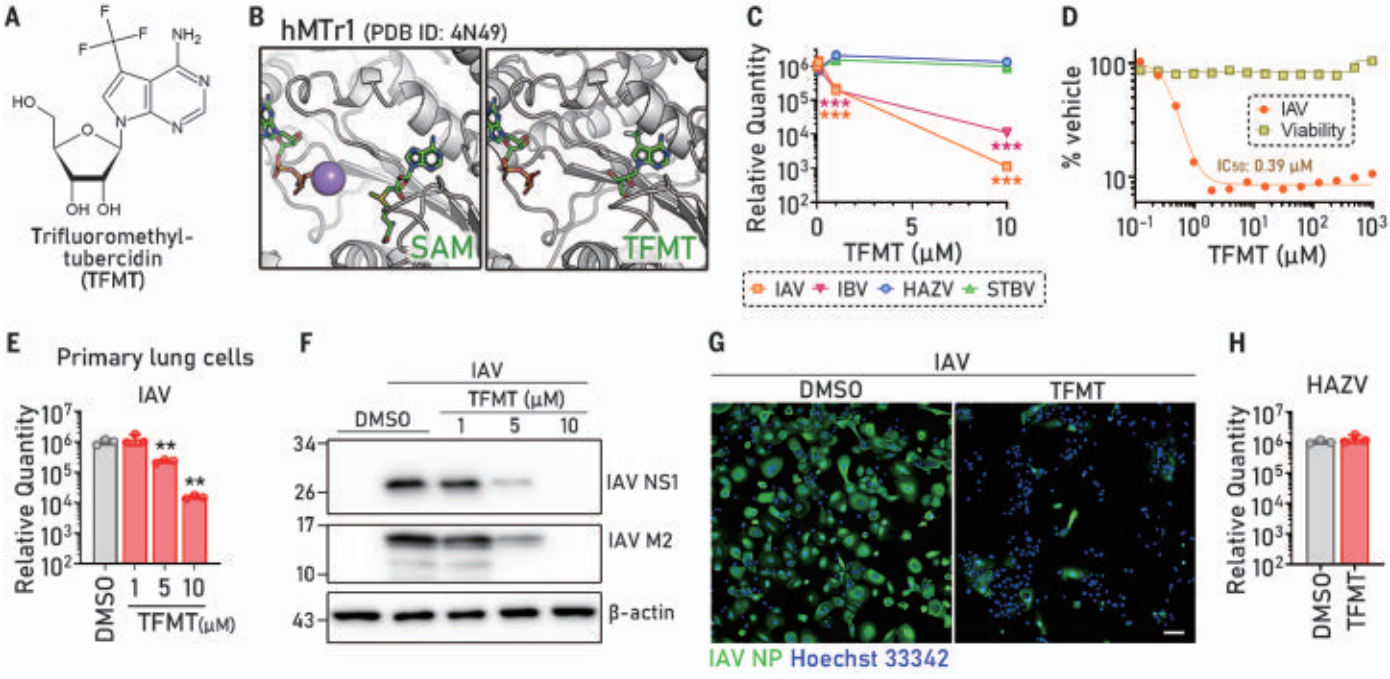

Fig. 2. Identification of TFMT as an MTr1 inhibitor with specific anti-IAV and anti-IBV efficacy. (**A**) Chemical structure of TFMT. (**B**) The docking poses of TFMT in the SAM-binding pocket of human MTr1. (**C**) qRT-PCR analysis for relative RNA quantity of the indicated viral RNA in A549 cells infected with IAV (MOI, 1), IBV (MOI, 1), HAZV (MOI, 0.1), and STBV (MOI, 0.1) for 24 hours. (**D**) GFP level quantification for IAV replication level and cytotoxicity test (WST-8 assay) of A549 cells infected with IAV-GFP (MOI, 0.1) for 19 hours. (**E**) qRT-PCR analysis for relative RNA quantity of IAV RNA (segment 7) in NHBE cells infected with IAV PR8 strain for 24 hours at MOI of 1. (**F**) Western blot analysis of the indicated proteins in NHBE cells infected with IAV PR8 strain for 24 hours at MOI of 1. (**G**) Immunostaining of the IAV NP in NHBE cells infected with IAV PR8 strain for 24 hours at MOI of 2 in the presence of 10 μM TFMT or vehicle. Scale bar, 100 μm. (**H**) qRT-PCR analysis for relative RNA quantity of HAZV RNA in NHBE cells infected with HAZV for 24 hours at MOI of 0.1 in the presence of 10 μM TFMT or vehicle. TFMT was added 3 hours before infection in (C) to (H). Statistics were calculated with Student's two-sided *t* test (***P* < 0.01, ****P* < 0.001).

Data Bank identifier (PDB ID): 4N49] (fig. S7, A and B) (*13*) for the molecular docking studies. We listed compounds in the order of calculated affinity scores and confirmed that SAM, SAH, and the SAM analog sinefungin ranked among the top 10 high-affinity binders identified with our in silico screening method (fig. S7C) (*14*, *15*). Next, 12 commercially available compounds with high affinity scores among the top 30 were examined for their anti-IAV activity in cells. We identified a natural product from *Streptomyces*—an adenosine analog, tubercidin—as the most effective compound and confirmed its dose-dependent inhibition from 0.1 to 100 μM with minor cytotoxicity (fig. S7, D to H). Tubercidin was also effective against IBV infection (fig. S7I). Moreover, we confirmed the direct binding of tubercidin to recombinant MTr1 by thermal shift assay (fig. S7, J and K). Tubercidin inhibited the MTase activity of recombinant MTr1 protein in a dose-dependent manner (fig. S7, L and M), indicating that tubercidin is an MTr1 inhibitor capable of suppressing IAV replication.

Tubercidin is known to have antiviral and anticancer activity (*16*, *17*) and exhibits toxicity in vivo (*8*, *18*). Thus, we evaluated 115 tubercidin-related compounds with antiviral drug assays in a three-step screening procedure to identify an alternative compound with specific anti-IAV and anti-IBV activity, and which displays minimal or no toxicity in vitro and in vivo (fig. S8A). In step one, we infected cells with IAV in the presence of each tubercidin-related compound and identified 13 compounds with anti-IAV efficacy (fig. S8A). In step two, we investigated anti-IAV activity at a lower concentration and counterscreened for activity against HAZV to rule out off-target inhibition of virus infection or toxicity. We found four compounds in step two that inhibited IAV replication without showing any reduction of HAZV replication (fig. S8A), which was similar to the results we obtained in MTr1 KO cells (Fig. 1H). In step three, we evaluated which of the identified compounds had an inhibitory effect at the lowest concentration and finally identified trifluoromethyl-tubercidin (TFMT) as the most effective compound (Fig. 2A and fig. S8, A and B). We confirmed the binding of TFMT to the SAM binding pocket of MTr1 and recombinant MTr1 with in silico docking and in vitro thermal shift assay (Fig. 2B and fig. S8C), respectively. Furthermore, we confirmed TFMT inhibition of the MTase activity of the recombinant MTr1 protein (fig. S8D). We also confirmed TFMT was active against IAV and IBV but not HAZV or STBV (Fig. 2C), exactly matching the phenotypes of MTr1 deficiency shown in Fig. 1 and fig. S6. The median inhibitory concentration (IC_{50}) for TFMT against IAV infection was 0.30 μM, and no notable in vitro toxicity was observed in the range of effective concentrations, as measured with water-soluble tetrazolium (WST)–8 cell viability assay (Fig. 2D). TFMT treatment also greatly inhibited IAV replication when administered 3 to 4 hours after infection; however, the effect was reduced or not visible if the drug was administered later (fig. S8E).

Anti-influenza efficacy of TFMT

Next, we examined the anti-IAV activity of TFMT in normal human bronchial epithelial (NHBE) cells. The RNA and protein levels of IAV (H1N1, PR8) were significantly reduced by TFMT treatment in a dose-dependent manner (Fig. 2, E and F). Histological analysis also revealed a profound reduction of the IAV NP levels in TFMT-treated NHBE cells without cytotoxicity (Fig. 2G). TFMT treatment did not inhibit HAZV replication (Fig. 2H), indicating that specific efficacy against certain viruses by this compound was retained even in human primary cells. Because this compound was effective in human NHBE cells, this prompted us to evaluate TFMT in human lung explants

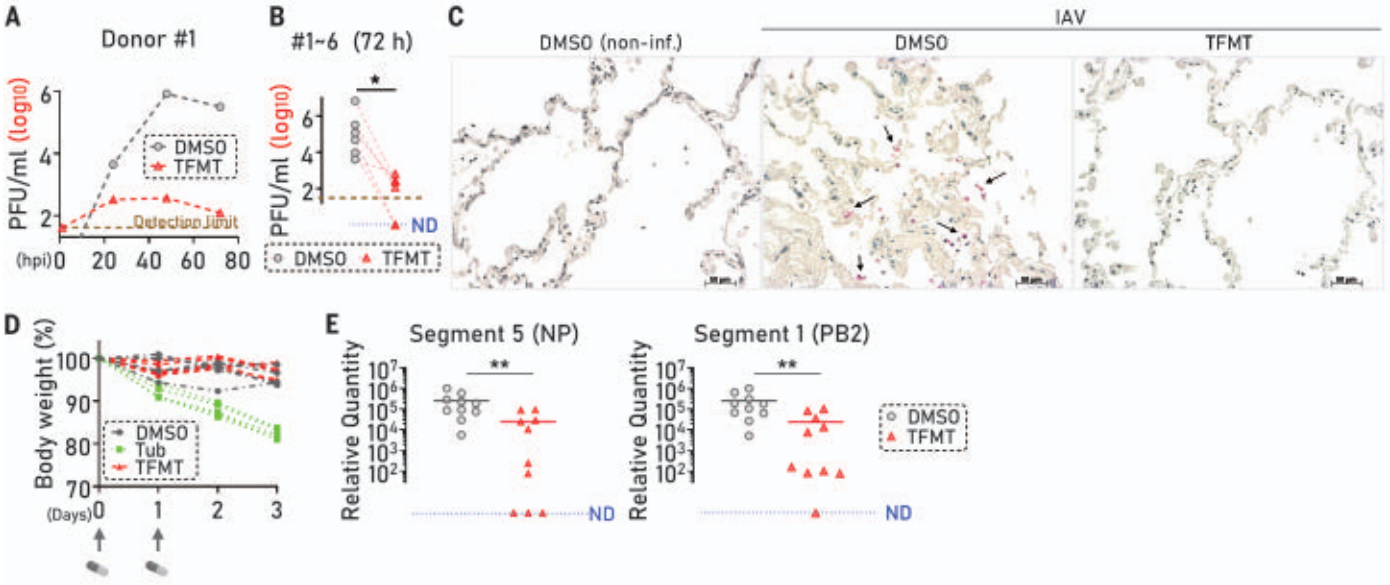

Fig. 3. IAV replication was inhibited by TFMT treatment in ex vivo human lung explants and in vivo mouse systems. (**A** to **C**) Virus growth and immunohistochemistry of a seasonal IAV (H1N1 from 2019) protein in human lung tissue. Upon infection, supernatants were taken at the indicated time points postinfection, and virus titers were determined as PFU/ml by plaque assay. The detection limit is indicated as a brown dotted line. We stained the tissues using anti-NP antibody. Before and after infection, TFMT was added at 10 μM. (**D**) Body weight of C57BL/6 mice. At days 0 and 1, 2 mg/kg of TFMT or tubercidin were intranasally administered. (**E**) qRT-PCR analysis for relative RNA quantity of IAV RNA (segments 5 and 1) in the lung tissues from IAV-infected C57BL/6 mice at day 2 (5×10^3 PFU). At day 0 and day 1 of infection, 2 mg/kg of TFMT (n = 10) or dimethyl sulfoxide (DMSO) (n = 10) were intranasally administered. Statistics were calculated with the Mann-Whitney test for the mouse in vivo assay, and the Wilcoxon matched-pair signed-rank test for the human lung ex vivo assay (*P < 0.05, **P < 0.01). ND, not detected.

as an ex vivo setting (fig. S9A). We infected lung tissues with IAV (H1N1, seasonal isolate in 2019), and the viral titer in the supernatant was determined with plaque assay at 1, 24, 48, and 72 hours after infection. As shown in Fig. 3A, the titer in the nontreated samples increased >10^5 plaque-forming units (PFU)/ml at 48 or 72 hours after infection, whereas the titer from the TFMT-treated lung explants remained <10^3 PFU/ml, indicating 100- to 1000-fold suppression by the treatment. The sum of the titers of all six independent donors revealed differences between the control and TFMT treatment–reduced IAV titers in culture supernatants (Fig. 3B and fig. S9B). TFMT treatment at 12 hours IAV after infection significantly impaired virus growth in human lung explants (fig. S9C). Consistent with virus titers observed, no IAV NP–positive cells or morphological changes were observed in IAV-infected lung tissues treated with TFMT (Fig. 3C and fig. S9D). These results indicate that TFMT inhibits replication of the seasonal IAV isolate ex vivo and shows potential for clinical translation.

We tested the in vivo efficacy of this compound in mice. We first confirmed that TFMT showed inhibitory activity in the IAV-infected mouse cell line LA-4, albeit with lower potency (IC_{50} = 7.7 μM) than in human cells (fig. S10A). Next, we assessed in vivo toxicity in mice with intranasal inoculation once a day for 2 days. Although treatment with the parental compound tubercidin caused substantial weight loss of mice, we did not observe any weight loss or cytotoxicity in lungs with the selected derivative TFMT (Fig. 3D and fig. S10B). Last, we examined the effect of TFMT treatment at 2 days after infection with IAV. At this point, NP and PB2 mRNA levels were significantly reduced by TFMT treatment in mouse lungs, indicating that the trifluoromethyl substitution of tubercidin reduces in vivo toxicity to levels we could not detect, but retains anti-IAV efficacy (Fig. 3E). We also confirmed the antiviral efficacy of baloxavir marboxil (BXM) in vivo in this setting (fig. S10C). Taken together, TFMT shows potential to inhibit IAV replication in all tested systems, including a human cell line and NHBE cells in vitro, human lung explants ex vivo, and mice in vivo.

TFMT inhibits IAV cap snatching

As shown in Fig. 4A, the effect of TFMT treatment on IAV replication was independent of IFIT1-dependent sequestration of RNA or RIG-I or MDA5 signaling. We found no replication of IAV in RIG-I–MTr1 double KO cells or IFIT1-MTr1 double KO cells, similarly to MTr1 KO cells (fig. S11, A and B). In addition, IFN signaling blockade by JAK inhibitor tofacitinib was not accompanied by IAV replication in MTr1 KO cells (fig. S12, C and D). Influenza A virus with a deletion of nonstructural protein 1 (IAVΔNS1) is known to induce high IFN responses, and its replication was prevented in MTr1-deficient cells without IFN and ISG (interferon-stimulated gene) induction but was rescued by MTr1 overexpression (fig. S2, D and E). TFMT treatment did not induce IFN-β or antiviral ISGs in A549 cells nor in PBMC (Fig. 4B and fig. S12). These results confirm that the observed antiviral effect does not depend on activation of antiviral IFN responses. Replication of IFN-sensitive non–cap-snatching RNA viruses such as Sendai virus (SeV), vesicular stomatitis virus (VSV), and encephalomyocarditis virus (EMCV) were not altered by TFMT treatment (Fig. 4C)—likewise, in MTr1 KO cells (fig. S13). Expression of IAV mRNA (segment 1) snatched specifically from U2 spliceosomal snRNA was impaired by TFMT treatment (Fig. 4D), similar to the effect of MTr1 deficiency (Fig. 1D). Hence, we conclude that TFMT treatment inhibits IAV replication by directly affecting the cap-snatching activity of IAV and not through immune modulation.

To elucidate the cap-snatching defect caused by TFMT, we examined the site of interaction of N1-2′-O-Me in the IAV polymerase PB2 subunit. On the basis of the reported structure of the IAV polymerase complex with cap0 RNA (PDB ID: 6RR7) (*19*), structural modeling predicted that N1-2′-O-Me (Fig. 4E, red circle) located in close proximity (within 3 Å distance) to two amino acids, Q257 and I261, in the alpha helix structure of PB2 (fig. S14A). Methylation is therefore estimated to increase the affinity between the helix of PB2 and the host mRNA

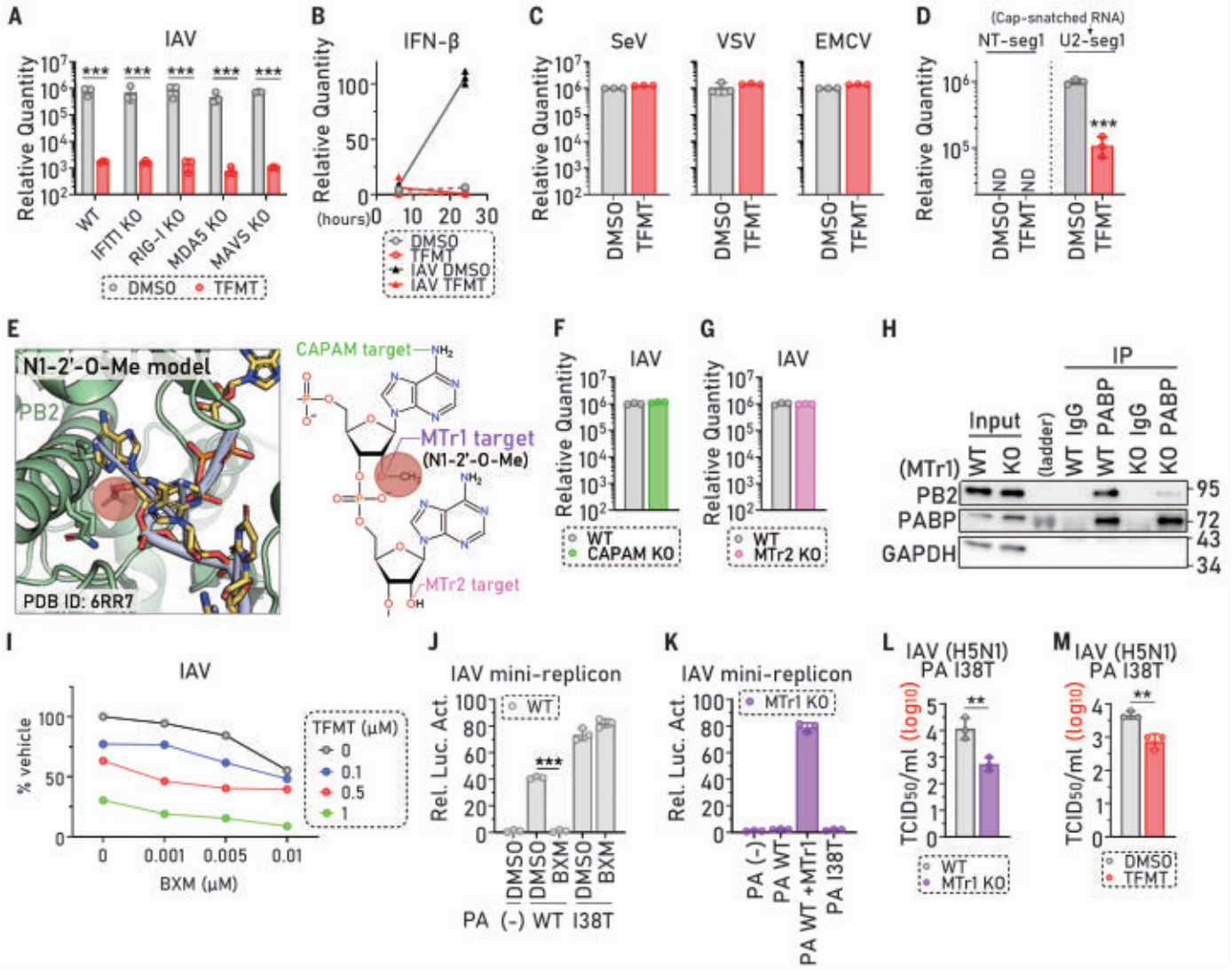

Fig. 4. TFMT inhibits IAV replication independently of innate immune responses, targets the interaction between IAV polymerase subunit PB2 and capped RNA, and exhibits synergistic effects with BXM. (**A**) qRT-PCR analysis for relative RNA quantity of IAV RNA (segment 7) in A549 cells infected with IAV PR8 strain for 24 hours at MOI of 1. Relative qantity was calculated as $10^6 \times 2^{-\Delta\Delta CT}$ by the $\Delta\Delta C_T$ method (C_T, cycle threshold). $\Delta\Delta C_T$, each ΔC_T minus the ΔC_T of WT DMSO. ΔC_T equals each target gene C_T minus each 18S rRNA C_T. (**B**) qRT-PCR analysis for relative RNA quantity of IFN-β RNA in A549 cells with or without 10 μM TFMT. IAV PR8 strain infection for indicated timepoint at MOI of 1. (**C**) qRT-PCR analysis for relative RNA quantity of SeV, VSV, or EMCV RNA in A549 cells infected with SeV [1×10^{-6} hemagglutination unit (HAU)/cell], VSV-GFP (MOI, 1), or EMCV (MOI, 0.01) for 24 hours. (**D**) qRT-PCR analysis for relative RNA quantity of NT/U2–IAV hybrid RNA in A549 cells infected with IAV PR8 for 24 hours at MOI of 1. TFMT was added at 10 μM at 3 hours before infection in (A), (C), and (D). (**E**) (Left) Structural model of N1-2'-O-Me in the RNA bound to IAV PB2 (PDB ID: 6RR7). The red circle indicates the methyl group at N1-2'-O position. (Right) Structure of N1 and N2 of cap1 RNA. The red circle indicates N1-2'-O-Me. (**F** and **G**) qRT-PCR analysis for relative RNA quantity of IAV RNA (segment 7) in the indicated genotypes of A549 cells infected with IAV PR8 for 24 hours at MOI of 1. (**H**) Western blot analysis of indicated input and immunoprecipitated proteins in PB2-expressing WT and MTr1 KO HEK-293T cells. (**I**) Relative fluorescent units of GFP in A549 cells infected with IAV SC35M–GFP for 19 hours at 0.1 infectious particle per cell. At 3 hours before infection, TFMT and/or BXM were added at the indicated concentrations. (**J** and **K**) Luciferase reporter assay of IAV PR8 minireplicon in (J) WT and (K) MTr1 KO HEK-293T cells overexpressing IAV PB2, PB1, NP, and the indicated PA. In (J), at 1 hour before transfection, 0.1 μM BXM was added. (**L**) Virus yield in the supernatant of WT and MTr1 KO A549 cells infected with IAV HK483 PA I38T, a BXM-resistant virus, for 48 hours at MOI of 0.1. (**M**) Virus yield in the supernatant of A549 cells infected with IAV HK483 PA I38T for 48 hours at MOI of 0.1. TFMT was added at 10 μM at 3 hours prior to infection. Statistics were calculated with Student's two-sided *t* test (***P* < 0.01, ****P* < 0.001). ND, not detected.

through hydrophobic effects and van der Waals interactions between hydrophobic amino acids, I260 and I261. Thus, the absence of the N1-2'-O-methyl group of capped RNAs in MTr1 KO cells would hinder interaction with the PB2 subunit of the IAV polymerase. Other cap methylation reactions are catalyzed by the methyltransferases MTr2 and cap-specific adenosine methyltransferase (CAPAM, PCIF1) to create N2-2′-O-Me and N1-m^{6}A, respectively. We did not observe the interaction between PB2 and N2-2′-O-Me or N1-m^{6}A (fig. S14, C and D). Consistent with this, no IAV replication defect was observed in CAPAM or MTr2 KO cells (Fig. 4, F and G).

We performed cap RNA poly(A)-binding protein (PABP) immunoprecipitation using IAV PB2-overexpressing control or MTr1 KO

cells (fig. S15, A and B). In MTr1-deficient cells, the amount of PB2 that coprecipitated with PABP diminished (Fig. 4H). IAV RNA-dependent RNA polymerases (RdRps) are also reported to bind host RNA polymerase II (Pol II) and snatch the cap portion from the nascent RNA. Immunoprecipitation of IAV PB2 and Pol II showed that the interaction was impaired in MTr1 KO cells (fig. S15C), indicating that MTr1-dependent N1-2′-O-Me increases the affinity of PB2 for cap mRNAs within the cell, which is consistent with our structural modeling. We also enriched capped RNAs with immunoprecipitation using the antibody to Gm3 (m^7G) and examined the relative quantity of virus mRNA. IAV mRNA, but not HAZV or STBV mRNA, was significantly diminished in the enriched capped RNAs of MTr1 KO and TFMT-treated cells (fig. S15, D and E), also indicating virus-specific cap snatching defect by MTr1 depletion.

BXM is an approved anti-IAV drug targeting the active site of the polymerase PA subunit (*20*, *21*). We found that this drug acted in synergy with TFMT, which inhibits the cap binding activity of the distinct PB2 subunit of the IAV polymerase and showed no cytotoxicity in vitro (Fig. 4I and fig. S16). Furthermore, the combination of TFMT and oseltamivir, a neuraminidase inhibitor (*22*), also showed synergism (fig. S17). These data indicate potential use for TFMT in combination therapy. A BXM-resistant IAV bearing an I38T mutant in the PA subunit (*20*) could not replicate in MTr1 KO cells, and we confirmed that TFMT treatment was effective in suppressing replication of BXM-resistant IAV in cells (Fig. 4, J to M). Given the sensitivity of the viral polymerase activity to MTr1 deficiency, we wondered whether some IAV strains might overcome the specific requirement for N1-2′-O-Me in the cap-binding site of PB2. None of the mutants Q257, I260, I261, nor R264 supported IAV replication in MTr1 KO cells (fig. S18). Our modeling indicated that conserved amino acids are critical for IAV replication in WT cells, suggesting that the IAV PB2 subunit is unlikely to be able to overcome the absence of the N1-2′-O-Me cap RNA structure for efficient replication.

Discussion

Currently approved drugs for IAV treatment against viral proteins are available; however, drug-resistant virus mutants have been reported for all. Host-directed antiviral drugs are less likely to induce resistance, and the host mitogen-activated protein kinase inhibitor ATR-002 has been shown to have broad efficacy against RNA viruses, including influenza viruses and SARS-CoV-2, by inhibiting viral replication and modulating inflammation (*23*, *24*). In this study, we show the anti-influenza efficacy of a cellular RNA methyltransferase inhibitor TFMT. Considering possible toxicity through long-term targeting of host factors, it will be practical to minimize the dose and combine with other approved virus-directed drugs such as BXM and oseltamivir.

We found that TFMT is a highly specific and nontoxic MTr1 inhibitor that specifically restricts replication of the cap snatching–dependent viruses, IAV and IBV (fig. S19). Collectively, our data show that suppression of MTr1 cap snatching by TFMT specifically inhibits replication of several strains of IAV and IBV, including a seasonal H1N1 isolate and a highly pathogenic and BXM-resistant avian IAV. Mechanistically, TFMT causes MTr1 disfunction and cap0 RNA accumulation, which impairs binding of the viral polymerase subunit PB2 to host cap RNAs and thereby hinders IAV polymerase–mediated cap snatching and viral RNA synthesis. TFMT acts in synergy with BXM because the drugs target distinct polymerase subunits PB2 and PA, respectively. TFMT-dependent restriction of IAV is independent of innate immune responses by RIG-I and IFIT1, and TFMT has no effect on the replication of interferon-sensitive viruses, such as VSV and EMCV. Comparison of PB2 subunits of influenza viruses and THOV showed that the primary structure of the cap RNA–binding region (such as N1-2′-O-Me–interactive amino acids) of IAV PB2 is conserved in IBV PB2 but not in ICV, IDV, or THOV PB2 (fig. S14B). Moreover, IAV requires 10 to 13 nucleotides for cap snatching, whereas THOV is reported to snatch the 5′-terminal m^7G cap residue (*25*). Mechanistic differences among viral polymerases for cap snatching may explain the specificity of TFMT-restriction for IAV and IBV.

REFERENCES AND NOTES

1. R. Reddy, R. Singh, S. Shimba, *Pharmacol. Ther.* **54**, 249–267 (1992).
2. F. Bélanger, J. Stepinski, E. Darzynkiewicz, J. Pelletier, *J. Biol. Chem.* **285**, 33037–33044 (2010).
3. C. Schuberth-Wagner *et al*., *Immunity* **43**, 41–51 (2015).
4. M. Habjan *et al*., *PLOS Pathog.* **9**, e1003663 (2013).
5. D. Koppstein, J. Ashour, D. P. Bartel, *Nucleic Acids Res.* **43**, 5052–5064 (2015).
6. D. Sikora, L. Rocheleau, E. G. Brown, M. Pelchat, *Sci. Rep.* **4**, 6181 (2014).
7. S. Daffis *et al*., *Nature* **468**, 452–456 (2010).
8. V. Bergant *et al*., *EMBO J.* **41**, e111608 (2022).
9. B. Li *et al*., *Nat. Commun.* **11**, 164 (2020).
10. E. Kawakami *et al*., *J. Virol. Methods* **173**, 1–6 (2011).
11. W. Gu *et al*., *RNA* **21**, 2067–2075 (2015).
12. S. Olschewski, S. Cusack, M. Rosenthal, *Trends Microbiol.* **28**, 293–303 (2020).
13. M. Smietanski *et al*., *Nat. Commun.* **5**, 3004 (2014).
14. R. A. Friesner *et al*., *J. Med. Chem.* **47**, 1739–1749 (2004).
15. T. A. Halgren *et al*., *J. Med. Chem.* **47**, 1750–1759 (2004).
16. D. C. Schultz *et al*., *Nature* **604**, 134–140 (2022).
17. J. Chen *et al*., *J. Cell. Mol. Med.* **26**, 2557–2565 (2022).
18. T. P. Lynch, E. S. Jakobs, J. H. Paran, A. R. Paterson, *Cancer Res.* **41**, 3200–3204 (1981).
19. H. Fan *et al*., *Nature* **573**, 287–290 (2019).
20. N. Hirotsu *et al*., *Clin. Infect. Dis.* **71**, 971–981 (2020).
21. A. Dias *et al*., *Nature* **458**, 914–918 (2009).
22. K. McClellan, C. M. Perry, *Drugs* **61**, 263–283 (2001).
23. H. Hamza, M. M. Shehata, A. Mostafa, S. Pleschka, O. Planz, *Front. Microbiol.* **12**, 611958 (2021).
24. A. Schreiber *et al*., *Cell. Mol. Life Sci.* **79**, 65 (2022).
25. F. Weber, O. Haller, G. Kochs, *J. Virol.* **70**, 8361–8367 (1996).
26. Y. Tsukamoto, H. Kato, Inhibition of cellular RNA methyltransferase abrogates influenza virus capping and replication. Zenodo (2023); doi:10.5281/zenodo.7503461.
27. Gene alignment data are available at https://purl.org/phylo/treebase/phylows/study/TB2:S30042 (2023).

ACKNOWLEDGMENTS

The authors thank the following: Microscopy Core Facility (MCF) and the Flow Cytometry Core Facility (FCCF) of the Medical Faculty at the University of Bonn for providing help, services, and devices; K. P. Hopfner, P. A. König, S. Jung, and V. Schütte for scientific suggestions; and T. Wadenpohl, A. Limbach, Y. Hu, D. Luca, B. Sivri, H. Miyamoto, J. Heuser, and J. Wieseler for technical assistance. PDB DOIs: 10.2210/pdb4N49/pdb (MTr1) and 10.2210/pdb6RR7/pdb (IAV RdRP). Approve numbers: 2022-1-78 (HPAIVs), 2Uke-Monkashin652 (genetically modified HPAIVs), AZ:2016-265-f-S (human lung explants), and 81-02.04.2021.A219 (mice experiment). All animal experiments with IAV were performed in a biosafety level 3 facility at University Hospital Bonn according to institutional and governmental guidelines of animal welfare. Breeding and housing as well as the euthanasia of the animals are fully compliant with all German (German Animal Welfare Act) and European Union (Directive 2010/63/EU) applicable laws and regulations concerning the care and use of laboratory animals. Details can be found in the Materials and Methods in the Supplementary Materials. **Funding:** Deutsche Forschungsgemeinschaft (DFG, German Research Foundation) EXC 2151: ImmunoSensation2, Project 390873048 was awarded to H.K.; DFG TRR 237, Project number 369799452 was awarded to F.I.S. (A01), S.B. (A02), M.Sc. (A04), B.M.K. (A04), A.P. (A07), H.K. (B22), and T.Z. (J02); DFG TRR 179 (TP11) was awarded to A.P.; European Research Council (ERC-CoG), Grant 817798 was awarded to A.P.; DFG – CRU 342, Grant BR5189/3-1 to L.B.; JSPS – Fund for the Promotion of Joint International Research [Fostering Joint International Research (B)], JP22KK0094 was awarded to M.I.; DFG – Emmy Noether Programme (322568668) was awarded to F.I.S.; DFG – Project number 388159768 (Devices of MCF); and DFG – Project number 216372545 (Devices of FCCF). **Author contributions:** Conceptualization, supervision, writing, funding acquisition: H.K. Formal analysis and visualization: T.Hir., M.I. Investigation and methodology: Y.T. Investigation: T.Hio., S.Y., K.M., A.F., T.C., A.v.H., and J.Y.N. Resources: J.H., V.N., S.S., M.H.C., Y.M.T., S.W., S.J., T.Z., S.B., F.I.S., G.K., M.Sh., Y.-S.H., A.P., B.M.K., Y.S., M.Sc., L.B., and C.E.M. **Competing interests:** The patent application number is US63/412,884. F.I.S. is a cofounder and shareholder of Dioscure Therapeutics SE and Odyssey Therapeutics. F.I.S. and H.K. are paid consultants of Odyssey Therapeutics. **Data and materials availability:** All data are available in the main text or in the supplementary materials. All raw data are provided in (*26*, *27*).

License information: Copyright © 2023 the authors, some rights reserved; exclusive licensee American Association for the Advancement of Science. No claim to original US government works. https://www.science.org/about/science-licenses-journal-article-reuse

SUPPLEMENTARY MATERIALS

science.org/doi/10.1126/science.add0875
Materials and Methods
Figs. S1 to S20
Tables S1 to S3
References (*28*–*37*)

Submitted 30 May 2022; resubmitted 18 October 2022
Accepted 9 January 2023
10.1126/science.add0875

Discussion leaders are noted in bold italics.

Advanced Cell and Tissue Biomanufacturing NEW!

Accelerating Cell and Tissue Manufacturing Technology Development and Innovation Through Convergence

JUN 25-30, 2023

GRAND SUMMIT HOTEL AT SUNDAY RIVER, NEWRY, ME

CHAIRS: Kaiming Ye and Paul Goodwin

VICE CHAIRS: Gang Bao and James Hoying

- **Keynote Session: Manufacturing Cell and Tissue Products at Scale** *Rosemarie Hunziker,* Kam Leong, Matt Udelhofen
- **Cell and Material Sourcing** *Sha Jin,* David Kaplan, Mark Powers, Sean Palecek
- **Process Modeling, Simulation, and Scale-Up/Out** *Pinar Zorlutuna,* John Wikswo, Emmanuel Tzanakakis, Sakis Mantalaris
- **Tissue Biofabrication Monitoring, Measurement, and Tools** *Greta Babakhanova,* John Fisher, Michael Golway
- **Industrial Scale Bioreactor Design and System Integration** *Tracy Hookway,* Thomas Bollenbach, Sarindr "Ik" Bhumiratana, Jordan Miller
- **Functional Determination and Readiness Assessment of Tissue Maturation** *Guohao Dai,* Roger Kamm, Milica Radisic
- **Cell and Tissue Preservation, Logistics, and Distribution** *Julie Allickson,* Mehmet Toner, Chelsea White
- **Regulation and Standardization of Tissue Biofabrication** *Richard McFarland,* Carl Simon, Barbara Boyan
- **Keynote Session: Moving From the Bench to Bedside: Lessons Learned and the Promise of Regenerative Medicine** *Larry Nagahara,* Beth Ripley, Krishnendu Roy, John Schiel
- **The GRC Power Hour™** *Tracy Hookway*

Amygdala Function in Emotion, Cognition and Disease +GRS

Exploring the Amygdala in Pathology and Physiology

JUL 9-14, 2023

REY DON JAIME GRAND HOTEL, CASTELLDEFELS, SPAIN

CHAIR: Thomas Kash

VICE CHAIR: Kate Wassum

- **Keynote Session: Dissecting Amygdala Function Across Translational Scales** *Josh Johansen,* Elizabeth Phelps, Kay Tye
- **The Stressed Amygdala** *Marisa Roberto,* Christine Rabinak, Rosenkranz Amiel, Nate Harnett, Jackie Giovanniello
- **Sex Differences in the Amygdala** *Kristen Pleil,* Raul Andero, Deena Walker, Jessica Tollkuhn, Jennifer Blackford
- **Value, Decision Making and the Amygdala** *Nadine Gogolla,* Caitlin Orsini, Mimi Liljeholm, Fabricio Do Monte, Jan Gründemann
- **Microcircuitry and Modulation in the Amygdala** *Mario Penzo,* Larry Zweifel, Andrew Holmes, Jin-Hee Han, Ayako M. Watabe
- **Appetitive Learning and the Amygdala** *Susan Sangha,* Andreas Luthi, Mihaela Iordanova, Anna Beyeler, Melissa Sharpe
- **Appetitive Learning and the Amygdala** *Stephen Maren,* Vincent Laurent, Paul Frankland, Vincent Costa
- **Developing Amygdala** *Steve Ramirez,* Ned Kalin, Dylan Gee, Maithe Arruda-Carvalho
- **Pain and the Amygdala** *Yarimar Carrasquillo,* Fusao Kato, Nicholas Gilpin, Denise Cai
- **The GRC Power Hour™** *Nicholas Gilpin*

Amyotrophic Lateral Sclerosis (ALS) and Related Motor Neuron Diseases +GRS

Mechanisms, Modeling and Translational Therapeutics

JUL 2-7, 2023

LES DIABLERETS CONFERENCE CENTER, LES DIABLERETS, SWITZERLAND

CHAIRS: Robert Baloh and Cat Lutz

VICE CHAIRS: Ludo Van Den Bosch and Christine Vande Velde

- **Translational Science and Therapeutic Landscape** *Charlotte Sumner,* John Day, Don Cleveland
- **TDP-43 and Neurodegeneration: Loss of Function, Cryptic Splicing, and Therapeutics** *Emanuele Buratti,* Pietro Fratta, Clotilde Lagier-Tourenne, Magdalini Polymenidou
- **Emerging Genetic and Mechanistic Modifiers of ALS and FTD** *Rosa Rademakers,* Leonard Petrucelli, Benjamin Ryskeldi-Falcon, Dorothee Dormann
- **Axonal and Synapse Biology: Degeneration in Motor Neuron Diseases** *Jeroen Pasterkamp,* Alison Twelvetrees, Robert Burgess, Eran Perlson, Sandrine Da Cruz
- **Neuroinflammation and Vascular Biology in ALS and FTD** *Severine Boilee,* Eric Huang, Renzo Mancuso
- **Astrocyte Biology in ALS and FTD** *Jeffrey Rothstein,* Brigitte Van Zundert, Kristine Freude, Shane Liddelow
- **Translational Biomarkers** *Lucie Bruijn,* David Owen, Sanjay Kalra, Andrea Malaspina
- **Translational Science in ALS and FTD** *David Taylor,* Timothy Miller, Neil Shneider
- **Late-Breaking Topics** *Don Cleveland,* Michael Ward, Chris Henderson, Christopher Pearson, Aaron Gitler
- **The GRC Power Hour™** *Aarti Sharma*

Angiogenesis +GRS

Angiogenesis and Angiostability in Development, Disease and Engineered Tissues

JUL 30 - AUG 4, 2023

SALVE REGINA UNIVERSITY, NEWPORT, RI

CHAIR: Ondine Cleaver

VICE CHAIR: Karina Yaniv

- **Keynote Session: Angiogenesis and Beyond: Building Vessels in Healthy and Diseased Tissues** *Luisa Iruela-Arispe,* Eli Keshet, Jennifer Lewis, Josef Penninger
- **Endothelial Control of Stem Cell Quiescence, Proliferation and Differentiation** *Anna Randi,* Shahin Rafii, Shiri Gur-Cohen, Stefania Nicoli
- **Building Vessels in Tissues and Organoids** *Napoleone Ferrara,* Ying Zheng, Lena Claesson-Welsh, Milica Radisic
- **Angiostability: Vessels in Aging, Inflammation and Disease** Laura Benjamin, Hellmut Augustin, Yoshiaki Kubota, Yuval Dor, Christer Betsholtz
- **Deciphering Molecular Mechanisms of Vascular Anomalies** Rong Wang, Miikka Vikkula, Mariona Graupera, Elisabeth Tournier-Lasserve
- **Building Vessels in The Embryo** *Victoria Bautch,* Carmen Ruiz de Almodovar, Brant Weinstein, Anne Eichmann, Amber Stratman
- **Mechanotransduction and Blood Vessels: Structure, Mechanics and Adaptation** *Mary Dickinson,* Luisa Iruela-Arispe, Salim Seyfried, Julia Mack, Li-Kun Phng
- **Organotypic Specialization of Endothelial Cells** *Nathan Lawson,* Ralf Adams, Mark Kahn, Rui Benedito
- **New Frontiers in Cardiovascular Regeneration** *Stefanie Dimmeler,* Brian Black, Miguel Torres, Ruben Marin Juez
- **The GRC Power Hour™** *Karina Yaniv*

Animal-Microbe Symbioses +GRS

Recent Advances in Evolutionary and Functional Analyses of Symbiotic Interactions

JUN 18-23, 2023

RENAISSANCE TUSCANY IL CIOCCO, LUCCA (BARGA), ITALY

CHAIR: Thomas Bosch

VICE CHAIR: Martin Kaltenpoth

- **Manipulating the Microbiome** *Bärbel Stecher,* Filipe Cabreiro, Takema Fukatsu
- **Microbial Community Assembly** *Koty Sharp,* Itzhak Mizrahi, Alecia Septer, Christian Voolstra
- **Chemical Ecology of Interspecies Interactions** *Nancy Moran,* Helge Bode, Mônica Pupo
- **Eco-Evolutionary Dynamics in Host-Microbe Interactions** *Ute Hentschel,* Ellen Decaestecker, Gillian Gile, Seth Rudman
- **Microbial Impact on Host Development and Behavior** *Margaret McFall-Ngai,* Sahar El Aidy, Karen Guillemin
- **The Role of the Environment in Shaping Symbiotic Partnerships** *Ulisse Cardini,* Kerri Coon, Andrew Goodman, Francois Leulier
- **Conceptional Frameworks and Novel Tools to Decipher Metaorganismic Complexity** *Katharine Coyte,* Nancy Obeng, Sara Mitri
- **Learning From Non-Model Metaorganisms** *Nancy Obeng,* Deepa Agashe, Mohamed Donia, Jean-Baptiste Raina
- **Innovative Approaches to Address Basic Questions in Symbiosis Research** *Alejandro Manzano Marín,* Martin Kaltenpoth, Ute Hentschel
- **The GRC Power Hour™** *Nancy Obeng, Stephanie McClelland*

Applied and Environmental Microbiology +GRS

Writing the Microbial Constitution

JUL 16-21, 2023

MOUNT HOLYOKE COLLEGE, SOUTH HADLEY, MA

CHAIR: Joel Kostka

VICE CHAIR: Denise Akob

- **Keynote Session: Core Principles that Govern Life** *John Spear,* Eric Boyd, Donato Giovannelli
- **Biodiversity and Ecosystem Function** *Thulani Makhalanyane,* A. Murat Eren, Cristina Dorador, Peter Girguis
- **Ecoengineering, Applications and Emerging Contaminants** *Rup Lal,* Casey Hubert, Xiaoxu Sun, Amelia-Elena Rotaru
- **Ecology and Evolution of Holobionts** *Gabriele Berg,* Choong-Min Ryu, Dilfuza Egamberdieva, Mohamed Donia
- **Transitioning Human Microbiome Research into Health Outcomes** *Rosa Krajmalnik-Brown,* Marvin Whiteley, Paul Turner
- **Probing Microbial Phenotypes In Situ** *Roland Hatzenpichler,* Fatima Pereira, Kimberly Halsey, Marcel Kuypers
- **Microbial Mediation of Biogeochemical Cycles** *Kirsten Küsel,* Laura Lehtovirta-Morley, Josh Neufeld, J. Colin Murrell
- **Microbes and Climate Change** *Jennifer Pett-Ridge,* Kristen Deangelis, Chris Greening, Alexander Tveit
- **Symbiosis in Ecosystems** *Jillian Petersen,* Caitlin Petro, Meghan Duffy
- **The GRC Power Hour™** *Deirdre Mikkelsen*

Archaea: Ecology, Metabolism and Molecular Biology +GRS

The Root and Branch of Discovery: Lessons on Life From the Archaea

JUL 23-28, 2023

MOUNT SNOW, WEST DOVER, VT

CHAIRS: Amy Schmid and Thorsten Allers

VICE CHAIRS: Kira Makarova and Tessa Quax

- **Keynote Session: New Perspectives on the Tree of Life: From Life's Origins to Modern Ecosystems** *Uri Gophna,* Puri Lopez-Garcia
- **Recent Progress on the Metagenomics and Molecular Biology of the ASGARD, DPANN and Other New Lineages** *Christa Schleper,* Laura Eme, Christine Moissl-Eichinger, Masaru Nobu, Olga Golyshina
- **New Technologies Lead to New Discoveries in Cell Biology** *Mechthild Pohlschroder,* Alex Bisson, Yoshiaki Kinoshita
- **Information Processing and Regulation Provide Insights into the Central Dogma** *Eveline Peeters,* Ruth Schmitz-Streit, Jocelyne DiRuggiero
- **Connecting Geochemical Cycles with Metabolic Networks** *Tristan Wagner,* Kiran Patil, Annette Rowe
- **The Dynamic Genome: Recombination, Repair and Structural Variation of Archaeal Genomes** *Dennis Grogan,* Roxane Lestini, Steve Bell, Daniela Barillà, Nick Robinson
- **Biotechnology and Bioinformatics Databases, Genomic Methods and Visualization Tools** *Zvi Kelman,* Kelly Zatopek, Stefan Schulze, Guillaume Borrel

- **Cell-Virus Interactions and Defense Mechanisms Including Viruses, CRISPR, Cell Surfaces and Mobile Elements** *Sonja-Verena Albers*, Eugene Koonin, David Prangishvili, Hanna Oksanen, Adi Millman, Mart Krupovic
- **Current Phylogenomic Drafts of the Tree of Life** *Thijs Ettema,* Brett Baker, Tom Williams, Laura Villanueva, Anja Spang
- **The GRC Power Hour™** *Kira Makarova*

Artificial Molecular Switches and Motors +GRS

Design, Synthesis, Power and Control

JUN 18-23, 2023

COLBY-SAWYER COLLEGE, NEW LONDON, NH

CHAIRS: Dirk Trauner and Stefan Hecht

VICE CHAIRS: Alex Lippert and Mindy Levine

- **From Small Molecules to Complex Tasks** *James Cooper,* Nathalie Katsonis, Javier Read de Alaniz
- **Early-Career Investigator Presentations** *Angelique Y. Louie,* Olalla Vázquez, Ximin He, Lauren Zarzar, Julia Kalow, Grace Han
- **Molecular Switches and Motors at Surfaces** *Oliver Thorn-Seshold,* Leo Gross, Paul S. Weiss
- **Designing Molecular Switches** *Henry Dube,* Ivan Aprahamian, Matthew Fuchter, Steven Lopez
- **Switches, Motors and Their Environment** *Natia Frank,* Noboyuki Tamaoki, Pance Naumov
- **Taking Molecular Switches and Motors From and to Biology** *Laura Na Liu,* Davita Watkins, Friedrich Simmel, Rebecca Schulman, Stefan Raunser
- **Topological Molecular Switches** *Michael Kathan*, Steve Goldup, Rainer Herges
- **Soft Materials and Robotics** *Jennifer Lu,* Yanlei Yu, Arri Priimägi, Rebecca Taylor
- **Molecules in Action** *Jonathan Sessler,* Rafal Klajn
- **The GRC Power Hour™** *Natia Frank*

Assisted Circulation +GRS

Future of Mechanically Assisted Circulatory Support Therapy

MAY 28 - JUN 2, 2023

WATERVILLE VALLEY, WATERVILLE VALLEY, NH

CHAIRS: Kurt Dasse and Robert Kormos

VICE CHAIRS: Francis Pagani and Steven Koenig

- **MCS: Defining Metrics for Success** *JoAnn Lindenfeld, Scott Silvestry,* Maria Generosa Crespo-Leiro, Heinrich Schima, James Long
- **Expanding MCS Therapy to Under-Represented Populations** *Kavitha Muthiah, Melvin Echols*, Khadijah Breathett, K.R. Balakrishnan, Alanna Morris, Jane Wilcox
- **Informative Approaches to Support Decision-Making for MCS** *Tim Baldwin, Angela Lorts,* Valluvan Jeevanandam, Mark Slaughter, Kevin Veen
- **Identifying Optimal MCS Designs with Pre-Clinical Testing** *Karen May-Newman, Bart Meyns,* Diane de Zélicourt, Shaun Gregory, Ellen Roche, Christina Vanderpluym, Bettina Wiegmann
- **Pump Designs, Patient Management and Clinical Trial Designs for Pediatric MCS** *Harvey Borovetz, Antonio Amodeo,* Christina Vanderpluym, Peta Alexander, Marianne Schmid Daners, Mark Rodefeld
- **Identifying Opportunities for Improvement in MCS Outcomes** *Ivan Netuka, Thomas Schloeglhofer,* Ryan Tedford, Ulrich Steinseifer, Seraina Dual, Stavros Drakos, Melana Yuzefpolskaya
- **How Novel Engineering Solutions Can Optimize MCS Devices** *Robert Dowling, Sonna Patel-Raman,* Trevor Snyder, Stephane Garrigue, Daniel Timms, Chen Chen, Kevin Bourque
- **Novel Technologies or Biological Approaches to Improve MCS Outcomes** *Manreet Kanwar, Jennifer Cowger,* Bengt Bern, Michael Zilbershlag, Nir Uriel
- **Real-World Issues Impacting the Choice for MCS** *Nir Uriel,* Ivan Netuka, Arman Kilic, Douglas Horstmanshof
- **The GRC Power Hour™** *Priscilla Petit*

Atherosclerosis +GRS

Molecular Mechanisms, Genomic Modifiers and Emerging Therapies

JUN 18-23, 2023

REY DON JAIME GRAND HOTEL, CASTELLDEFELS, SPAIN

CHAIRS: Filip Swirski and Kathryn Moore

VICE CHAIRS: Esther Lutgens and Nick Leeper

- **Keynote Session: Atherosclerosis and Heart Disease: From Population Science to Molecular Mechanisms** *Masanori Aikawa,* Valentin Fuster, Anne Tybjærg-Hansen, Goran Hansson, Peter Libby
- **Systems in Context** *José Gabriel Barcia Durán,* Claudia Monaco, Edward Fisher, Max Nieuwdorp, Gabrielle Fredman, Thomas Vallim, Atsushi Anzai
- **The Single Cell Resolution Revolution** *Vesna Todorovic,* Andres Hidalgo, Willem Mulder, Paul Kubes, Chiara Giannarelli
- **Genetics and Epigenetics** *Muredach Reilly,* Heribert Schunkert, Casey Romanoski, Andreas Zirlik, Menno de Winther, Catherine 'Lynn' Hedrick
- **Epigenetics and Reprogramming** *Hanrui Zhang,* Siddhartha Jaiswal, Yajaira Suarez, Ivan Zanoni, Kathleen Martin
- **Vascular and Hematopoietic Systems** *Michelle Olive,* Delphine Gomez, Clinton Robbins, Andrew Murphy, Daniela Cihakova, Mihai Netea, Dimitrios Tsiantoulas, Noemi Rotllan Vila
- **The Immune System** *Esther Lutgens,* Oliver Soehnlein, Florent Ginhoux, Christoph Binder, Elena Galkina
- **Metabolism, Metabolites and Mitochondria** *Carlos Fernandez-Hernando,* Eicke Latz, Ebru Erbay, Babak Razani, Ira Tabas, E. Dale Abel, Mireille Ouimet, Leigh Goedeke
- **Immunometabolism** *Klaus Ley,* Musa Mhlanga, Marit Westerterp, Katey Rayner, Luke O'Neill
- **The GRC Power Hour™** *Daisy Sahoo, Elizabeth Tarling*

Atmospheric Chemistry

Fundamental Chemistry and Societal Changes: Shaping Air Quality and Climate From the Molecular to the Planetary Scale

JUL 30 - AUG 4, 2023

GRAND SUMMIT HOTEL AT SUNDAY RIVER, NEWRY, ME

CHAIRS: Annmarie Carlton and Joel Thornton

VICE CHAIRS: Colette Heald and Sergey Nizkorodov

- **Keynote Session: Atmospheric Chemistry and Policy** *Sherri Hunt,* Paulo Saldiva, Arlene Fiore
- **Chemistry of Aerosol Formation** *Jim Smith,* Mikael Ehn, Astrid Kiendler-Scharr, Marianne Glasius
- **The Evolving Urban Atmosphere** *Drew Gentner*, Joost de Gouw, Aijun Ding
- **Aerosol-Cloud-Chemistry Interactions** *Hartmut Herrmann,* Mary Barth, Susannah Burrows, Tran Nguyen
- **Aerosol Particle Chemistry and Properties** *Andrew Ault,* Miriam Freedman, Kevin Wilson
- **Remote Environments From the Ocean Surface to Saturn's Moons** *V. Faye McNeill,* Sarah Horst, Lucy Carpenter
- **Climate-Chemistry Interactions** *Havala Pye,* Mathew Evans, Hamish Gordon
- **Advancing Models of Short-Lived Climate Forcings** *Glenn Wolfe,* Loretta Mickley, Alexander Turner
- **New Remote Sensing Methods** *Jenny Stavrakou,* Sally Pusede, Daniel Cusworth
- **The GRC Power Hour™** *Colette Heald, Sergey Nizkorodov*

Atomic Physics +GRS

Precision Measurements, Quantum Science and Ultracold Phenomena in Atomic and Molecular Physics

JUN 11-16, 2023

SALVE REGINA UNIVERSITY, NEWPORT, RI

CHAIR: Derek Jackson Kimball

VICE CHAIR: Heather Lewandowski

- **Frontiers of AMO Physics: The Next 50 Years** *Dmitry Budker,* Eric Cornell, John Doyle, Ana Maria Rey
- **Quantum Control, Entanglement and Computing** *Christopher Monroe,* Dietrich Leibfried, Monika Schleier-Smith, Crystal Senko, Ofer Firstenberg
- **Probes of Gravity** *Hendrik Ulbricht,* Jun Ye, Brian D'Urso, Markus Aspelmeyer
- **Tests of Fundamental Physics** *Tanya Zelevinsky,* Alexander Sushkov, Ronald F Garcia Ruiz, Swati Singh, Andrew Jayich
- **Clocks and the Nature of Time** *Marianna Safronova,* Shimon Kolkowitz, Tara Fortier, Marcus Huber
- **Quantum Sensors and Metrology** *Mikhail Lukin,* Thad Walker, Victor Acosta, Danielle Braje, Manuel Endres
- **Cold Chemistry and Molecules** *Brianna Heazlewood,* Kang-Kuen Ni, Wes Campbell, Marissa Weichman
- **Novel Phases and Properties of Ultracold Matter** *Silke Ospelkaus,* Caroline Champenois, Leticia Tarruell, Tim Langen, Charles Brown
- **Quantum and Nonlinear Optics** *Christiane Koch,* James Thompson, Ana Asenjo-Garcia, Elizabeth Goldschmidt
- **The GRC Power Hour™** *Heather Lewandowski*

Bacterial Cell Biology and Development NEW!

Structure, Dynamics and Development of Bacterial Cells

JUN 4-9, 2023

SOUTHERN NEW HAMPSHIRE UNIVERSITY, MANCHESTER, NH

CHAIRS: Mark Buttner and Erin Goley

VICE CHAIRS: Ethan Garner and Pamela Brown

- **Keynote Session: Signaling and Regulation** *Peter Chien,* Michael Laub, Marie Elliot
- **Cell Division** *Seamus Holden,* Mariana Pinho, Susan Schlimpert, Silvia Bulgheresi
- **Cellular Decision-Making** *Patrick Viollier,* Karine Gibbs, Urs Jenal
- **Cell Morphology and Dynamics** *Srividya Iyer-Biswas,* Christine Jacobs-Wagner, Elitza Tocheva, Lotte Sogaard-Andersen
- **Structure and Transport of Genetic Material** *Jan-Willem Veening,* Briana Burton, Martin Thanbichler, Joe Pogliano
- **Cell Wall and Cell Envelope** *Cara Boutte,* Sloan Siegrist, Enrique Rojas, Thomas Bernhardt
- **Motility** *Daniel Kearns,* Tam Mignot, Gladys Alexandre
- **Cell Biology and Interspecies Interactions** *Kristina Jonas,* Andrew Lovering, Jeanne Salje, Kerwyn Huang
- **Cellular Organization and Structure** *Jennifer Herman,* Jan Löwe, Anthony Vecchiarelli, Arash Komeili

Barrier Function of Mammalian Skin +GRS

An Intelligent and Personalized Skin Barrier: Integration and Translation of Cell and Molecular Biology, Bioengineering and Physical Chemistry

AUG 6-11, 2023

WATERVILLE VALLEY, WATERVILLE VALLEY, NH

CHAIRS: Marjana Tomic-Canic and M. Begona Delgado-Charro

VICE CHAIRS: Nicole Brogden and Pankaj Karande

- **Keynote Session: The Effects of Aging and Environment on the Skin Barrier** *Theodora Mauro,* Anna Celli, Elena Goleva, Elizabeth Kovacs
- **Skin Colonizers: Making or Breaking the Barrier** *Lindsay Kalan,* Elizabeth Grice, Heidi Kong, Irena Pastar, Stuart Jones
- **Inflammation in Barrier Function and Dysfunction** *Johann Gudjonsson,* Shruti Naik, Luisa DiPietro, Maria Morasso
- **Optimizing Dermatological Therapies** *David Moore,* Rosalind Hannen, Jon Lenn, Audra Stinchcomb
- **Big Data to Knowledge: Models, Diagnostics and Therapies** *Nicole Brogden,* Cristina Strong, Tesfaye Mersha, Florian Gruber
- **Predicting Permeation Through the Skin Barrier: Chemical Exposure and Risk Assessment** *Annette Bunge,* John Troutman, Peter Olmsted, John Kissel
- **Applied Knowledge of Skin Barrier: From Discovery to Recovery** *Anna De Benedetto,* Marianne Lind, Chandan K Sen, Dan Kaplan
- **Imaging the Skin Barrier: Seeing the Previously Unseen** *Richard Guy,* Sebastien Gregoire, Conor Evans, Maxim Darvin, Natalie Belsey
- **The "Next Big Question" on the Skin Barrier** *Pankaj Karande,* Johann Gudjonsson, Amanda MacLeod
- **The GRC Power Hour™** *Elizabeth Grice*

Basic Mechanisms to Clinical Trials in Brain Tumors NEW!

Advances In Brain Tumor Research and Therapy

JUN 25-30, 2023

BRYANT UNIVERSITY, SMITHFIELD, RI

CHAIR: Sadhan Majumder

VICE CHAIR: Eric Holland

- **Neuropathology, Neurosurgery, and Health Disparities** *Priscilla Brastianos, Patrick Wen,* Charles Eberhart, Nduka Amankulor, Melissa Bondy
- **Developmental Biology of the Brain and Cancer** *Martine Roussel, Charles Eberhart,* Michael Taylor, Mariella Filbin, Peter Dirks, Hongjun Song, Frank Winkler
- **Meningioma, Brain Metastasis and Diffuse Intrinsic Pontine Glioma** *Mariella Filbin, Nduka Amankulor,* Priscilla Brastianos, Benjamin Izar, Suzanne Baker
- **Genomics and Tumor Microenvironment** *Peter Dirks, Michael Taylor,* Mario Suva, Antonio Iavarone, Rakesh Jain, Candece Gladson
- **Mechanisms** *Candece Gladson, Suzanne Baker,* Vidya Gopalakrishnan, Anna Lasorella
- **Immunotherapy** *Rakesh Jain, E. Antonio Chiocca,* Duane Mitchell, Kai Wucherpfennig
- **Virus-Mediated Therapeutics** *Duane Mitchell, E. Antonio Chiocca,* Frederick F. Lang
- **Preclinical Modeling, Gene-Fusion and Mechanism-Based Therapeutics** *Frank Winkler, Antonio Iavarone,* Taran Gujral, Frank Furnari, Martine Roussel, Frank Szulzewsky
- **Clinical Trials** *Frederick F. Lang, Kai Wucherpfennig,* Patrick Wen, Marta Alonso
- **The GRC Power Hour™** *Melissa Bondy, Vidya Gopalakrishnan, Anna Lasorella*

Bioelectronics

Discovering Fundamental Principles and Engineering Electrical Communication Across The Cell-Materials Interface

JUN 4-9, 2023

PROCTOR ACADEMY, ANDOVER, NH

CHAIRS: Alberto Salleo and Caroline Ajo-Franklin

VICE CHAIRS: Leonard Tender and Markita Landry

- **Keynote Session: Innovations in Bioelectronic Devices and Applications** *Khalil Ramadi,* Bianxiao Cui
- **Engineering Biology for Bioelectronic Applications** *Susan Daniel,* Jonathan (Joff) Silberg, Sarah Glaven
- **From Molecules to Electrons: Different Bioelectronic Modes of Detection** *Rafael Verduzco*, Sahika Inal, Luisa Torsi
- **Engineering Materials, Processes and Interfaces for Bioelectronics** *Alexandra Rutz,* Francesca Santoro, Rafael Verduzco, Benjamin Keitz, Nurit Ashkenasy, Xuanhe Zhao
- **Neurobioelectronic Devices** *Jonathan Rivnay,* Dion Khodagholy, Guosong Hong
- **Emerging Characterization Techniques** *Lars Jeuken,* Ardemis Boghossian, Cullen Buie
- **Selected Poster Presentations** *Jonathan (Joff) Silberg*

- **Fundamentals of Ion and Electron Transport** *Leonard Tender,* Moh El-Naggar, Paul Meredith, Daniel Bond, Akihiro Okamoto
- **Applications and Commercialization of Bioelectronics** *Christopher Bettinger,* Susan Daniel, Sameer Sonkusale
- **The GRC Power Hour™**

Bioenergetics +GRS

Application of Mechanism, Structure and Cellular Function in Bioenergetics of Health and Disease

JUN 25-30, 2023

PROCTOR ACADEMY, ANDOVER, NH

CHAIR: Greg Cook

VICE CHAIRS: Susanne Arnold and Thomas Meier

- **ATP Synthase in Health and Disease** *Alastair Stewart,* John Rubinstein, Leonid Sazanov
- **Structures and Functions of Supercomplex Assemblies** *Werner Kühlbrandt,* Bonnie Murphy, James Letts, Lilach Sheiner
- **The Diversity and Complexity of Complex I** *Ulrich Brandt,* Judy Hirst, Janet Vonck
- **Structures and Mechanisms of Complex Redox Enzymes** *Robert Gennis,* Schara Safarian, Peter Brzezinski, Chris Greening
- **Disruption of Bioenergetic Networks to Combat Drug Resistance** *Jamie Blaza,* Tom Duncan, Daniel Ken Inaoka
- **Late-Breaking Topics** *Manuela Pereira,* Douglas Kell, Bianca Introini
- **Mitochondria Function in Health and Disease, and New Strategies for Therapy** *Susanne Arnold,* Vamsi Mootha, Eric Schon, Erika Fernandez-Vizarra
- **V-type ATPases: Molecular Machines and Drug Targets** *Michael Forgac,* Patricia Kane, Rajini Rao
- **Bioenergetics on the Single Molecule Level** *Wayne Frasch,* Hiroyuki Noji, Navish Wadhwa
- **The GRC Power Hour™** *Karlett Parra*

Biology of Aging +GRS

Evolving Concepts of Organismal Aging

JUL 2-7, 2023

REY DON JAIME GRAND HOTEL, CASTELLDEFELS, SPAIN

CHAIRS: Tony Wyss-Coray and Dario Riccardo Valenzano

VICE CHAIRS: Vera Gorbunova and Jennifer Garrison

- **Keynote Session: Environment and Stem Cell Aging** *Vera Gorbunova,* Anne Brunet
- **Microbiome Dynamics During Aging** *Bali Pulendran,* Michelle Linterman, Filipe Cabreiro, Isabel Gordo
- **Immune Aging** *Michelle Linterman,* María Mittelbrunn, Naomi Habib, Andrea Ablasser
- **Comparative Biology of Aging** *Isabel Gordo,* Peter Sudmant, Kyoko Miura, Alessandro Ori
- **New Technologies to Study Aging** *Sara Wickstrom,* Xiao Wang, Alex Cagan
- **Cell Intrinsic Versus Extrinsic Aging** *Richard Miller,* Sara Wickstrom, Eva Hoffmann, Saul Villeda
- **Systems Biology of Aging** *Peter Sudmant,* Uri Alon, Keenan Walker
- **Immune Interventions, Vaccines and Aging** *Andrea Ablasser,* Benoit Lehallier, Arne Akbar, Bali Pulendran
- **Keynote Session: Aging Mosaicism** *Jennifer Garrison,* Corina Amor, Martin Hetzer
- **The GRC Power Hour™** *Samir Morsli*

Biomass to Biobased Chemicals and Materials +GRS

Combining Biotechnologies, Green Chemistry and Downstream Process to Convert Biomass into Biobased Products

MAY 28 - JUN 2, 2023

GRAND SUMMIT HOTEL AT SUNDAY RIVER, NEWRY, ME

CHAIR: Florent Allais

VICE CHAIR: Seema Singh

- **Biorefinery and Bioeconomy Concepts** *Honorine Katir,* Ed de Jong, Eric Olivier, Corinne Scown
- **Biorefinery Processes: Terrestrial Biomass and Microalgae** *Karin Odelius,* Sonja Salmon, Madeleine Bussemaker, Katalin Barta, Jean Francois Sassi, Lieve Laurens
- **Lignin Upgrading** *Mika Sipponen,* Jeremy Luterbacher, Ning Yan
- **(Hemi)Cellulose Upgrading** *Katalin Barta,* Karine De Oliveira Vigier, Youssef Habibi, Gil Garnier, Carl Houtman
- **Downstream Processing and Process Intensification** *Sankar Nair,* Marianthi Ierapetritou, Nolan Wilson
- **Biocatalysts and Heterogeneous Catalysts for Biomass Conversion** *Michael Bott,* Tim Bugg, Damien Debecker, Rafael Luque, Adam Lee
- **Whole Cell and Plant-Based Chemical and Material Production Platforms** *Gregg Beckham,* Jenny Mortimer, Kevin O'Connor
- **Biomass-Derived Sustainable Polymers and Materials** *Karen Wooley,* Karin Odelius, Megan Robertson, Sylvain Caillol, Joseph Stanzione, Thomas Farmer
- **Biomass-Derived Interfacial Chemicals and Green Solvents** *George John,* Richard Gross, John Warner
- **The GRC Power Hour™** *Katalin Barta, Ezinne Achinivu*

Biomaterials and Tissue Engineering +GRS

Design, Function and Translation of Instructive Materials

JUL 16-21, 2023

HOLDERNESS SCHOOL, HOLDERNESS, NH

CHAIRS: Tatiana Segura and Andrew Putnam

VICE CHAIRS: Benjamin Keselowsky and Omolola Eniola-Adefeso

- **Keynote Session: Design, Function, and Translation of Instructive Materials** *Andres Garcia,* Jeffrey Hubbell, David Mooney
- **Materials for Brain Repair and Regeneration** *Shelly Sakiyama-Elbert,* S. Thomas Carmichael, Molly Shoichet, David Nisbet
- **New Biomaterial Design** *Jennifer West,* Donald Griffin, Cole DeForest
- **Biomaterials for Drug and Gene Delivery** *Craig Duvall,* Angela Pannier, Phillip Messersmith, Paula Hammond
- **Materials for Stem Cell Engineering** *Brendan Harley,* Yuguo Lei, Ke Cheng
- **Immune Engineering: Vaccine, Cancer, and Tolerance** *Joel Collier,* Darrell Irvine, Kristy Ainslie, Lonnie Shea
- **Engineering Microenviroment for Regeneration** *Edward Botchwey,* Jennifer Elisseeff, Karen Christman
- **Building Vasculature Across Length Scales** *Sharon Gerecht,* Juan Melero-Martin, Christopher Breuer, Shulamit Levenberg
- **Innovation in Biomaterials and Tissue Engineering: Short Talks Selected From Poster Abstracts** *Benjamin Keselowsky,* Omolola Eniola-Adefeso
- **The GRC Power Hour™** *Omolola Eniola-Adefeso*

Biomechanics in Vascular Biology and Disease NEW!

Integrating Vascular Mechanics, Biology and Medicine

AUG 6-11, 2023

MOUNT HOLYOKE COLLEGE, SOUTH HADLEY, MA

CHAIR: Hanjoong Jo

VICE CHAIRS: Kim Van Der Heiden and Tzung Hsiai

- **Keynote Session: Mechanosensing and Mechanotransduction** *Bradford Berk,* Ellie Tzima, Christopher Chen
- **Mechanosensing** *Rob Krams,* Martin Schwartz, David Beech, Cheng Zhu, Irena Levitan
- **Plaque Dynamics and Hemodynamics** *Stephanie Lehoux,* Lucas Timmins, Noelia Grande Gutiérrez
- **Aneurysms Dynamics and Hemodynamics** *Brenda R. Kwak,* Jay Humphrey, W. Robert Taylor, Frank Gijsen, Anne Robertson, Alison Marsden
- **Mechanical Forces and Atherosclerosis** *John Shyy,* Paul Evans, Yun Fang, Wayne Orr
- **Mechanosignal Transduction** *Guillermo Garcia-Cardena,* Ingrid Fleming, Luke Brewster, Manu Platt, Yingxiao Wang, Stephen White
- **Plaque, Aneurysm Rupture, and Cardivascular Events** *Ton van der Steen,* Tríona Lally, Jolanda Wentzel
- **Cardiovascular Biomechanics: Emerging Topics** *John Oshinski,* Peter Weinberg, Craig Goergen, Elizabeth Jones, Stefania Nicoli
- **Young Investigators in Cardiovascular Biomechanics and Mechanobiomedicine** *Zorina Galis,* Mabruka Alfaidi, Juan Jiménez
- **The GRC Power Hour™** *Eno Ebong, Manu Platt*

Bioorganic Chemistry +GRS

Catalyzing Fundamental and Translational Discoveries with Chemical Biology

JUN 11-16, 2023

PROCTOR ACADEMY, ANDOVER, NH

CHAIRS: Daniel Nomura and Jason Thomas

VICE CHAIRS: Amanda Hargrove and Jeremy Baryza

- **Keynote Session: Translational Chemical Biology** *Ziyang Zhang,* Stuart Schreiber, James Wells
- **Targeted Protein Degradation and Induced Proximity** *Ekaterina (Katya) Vinogradova,* Philip Chamberlain, Ryan Potts
- **Cellular Imaging Probes** *Sierra Williams,* Yamuna Krishnan, Alanna Schepartz
- **Using Chemical Biology for Serendipitous Discoveries** *Laura Dassama,* Jack Taunton, Michelle Arkin, Jonathan Long
- **Nucleic Acids Chemical Biology** *Nathanael Lintner,* Kevin Weeks, Ming Hammond, John Schneekloth, Jr.
- **Omics in Disease Biology** *Euna Yoo,* Keriann Backus, Eranthie Weerapana
- **Glycobiology** *Steven Banik,* Catherine Leimkuhler Grimes, Michael Boyce
- **New Therapeutic Modalities and Emerging Technologies** *Fleur Ferguson,* Michael Erb, Jamie Cate
- **Computational Chemical Biology** *Karsten Krug,* Nir London, John Irwin
- **The GRC Power Hour™** *Catherine Leimkuhler Grimes*

CAG Triplet Repeat Disorders +GRS

Common Themes in Diverse Diseases: From Molecular Mechanisms to Therapeutic Strategies

JUN 11-16, 2023

MOUNT SNOW, WEST DOVER, VT

CHAIR: Vanessa Wheeler

VICE CHAIR: Frederic Saudou

- **Keynote Session: The Pathway From the Lab to the Clinic** *Diane Merry,* Sarah Tabrizi, Kenneth (Kurt) Fischbeck
- **Dynamic Repeat Mutations** *Christopher Pearson,* Melissa Gymrek, Marc Ciosi
- **DNA and Chromatin Effects** *Jeff Carroll,* Anna Pluciennik, Vincent Dion, Albert La Spada
- **Toxic RNA and Protein Species** *Laura Ranum,* Gillian Bates, Eric Wang
- **Dissecting Disease Mechanisms: From Networks to Cells** *Harry Orr,* Janghoo Lim, Myriam Heiman
- **Protein Function and Dysfunction** *Erich Wanker,* Baskar Bakthavachalu, Sandrine Humbert, Patrícia Maciel
- **Beyond CAG: Other Repeats and Intersecting Mechanisms** *Henry Paulson,* Henry Houlden, Alice Davidson, Nicolas Charlet
- **Therapeutics: Strategies and Developments** *Beverly Davidson,* Caroline Benn, Anastasia Khvorova
- **Late-Breaking Topics** *Anne Rosser,* Paul Lockhart, Steve McCarroll
- **The GRC Power Hour™** *Ghazaleh Sadri-Vakili, Michelle Gray*

Cancer Genetics and Epigenetics +GRS

Precision Cancer Medicine for the Evolving Cancer Genome and Epigenome

MAY 21-26, 2023

RENAISSANCE TUSCANY IL CIOCCO, LUCCA (BARGA), ITALY

CHAIR: Ting Wang

VICE CHAIR: Mathieu Lupien

- **Keynote Session: Integrative Cancer Genetics and Epigenetics in Precision Cancer Therapy** *Hui Shen,* Kathleen Burns, Joseph Costello, Jonathan Licht
- **Cancer and Non-Coding Genome** *Feng Yue,* Hui Shen, Nada Jabado, Danny Leung, Peter Scacheri
- **New Technologies to Interrogate Cancer Genome, Epigenome and 3D Chromatin** *Guillaume Bourque,* Chia-Lin Wei, Feng Yue, Elisa Oricchio, Juanma Vaquerizas
- **Transposable Elements and Immune Response** *Danny Leung,* Katherine Chiappinelli, Guillaume Bourque, Zuzana Tothova, Didier Trono
- **Intratumoral Heterogeneity** *Yun Nancy Huang,* Sarah Aitken, Bing Ren, Celine Vallot, Luca Magnani
- **Cancer Systems Biology** *Sarah Aitken,* Martin Hirst, Peter Jones, Han Liang
- **Beyond the Tumor Cells: Microenvironment and Macroenvironment** *Daniel De Carvalho,* Yvonne Fondufe-Mittendorf, Cheryl Walker, Marisa Bartolomei, Toshikazu Ushijima
- **Translational Epigenetics: Detection and Therapy** *Zuzana Tothova,* Daniel De Carvalho, Susan Clark, Stephen Baylin
- **Cancer Genome, Epigenome and Epi-Transcriptome Engineering** *Martin Hirst,* Housheng He, Yun Nancy Huang, Christopher Vakoc
- **The GRC Power Hour™** *Katherine Chiappinelli*

Cancer Nanotechnology +GRS

Imaging, Editing and Immunomodulating the Tumor Microenvironment

JUN 11-16, 2023

WATERVILLE VALLEY, WATERVILLE VALLEY, NH

CHAIR: Darrell Irvine

VICE CHAIR: Daniel Heller

- **Keynote Session: Imaging Cancer with Nanotechnology** *Darrell Irvine,* Michelle Bradbury, Ulrich Wiesner
- **Interactions of Nanomaterials with the Tumor Microenvironment** *James Moon,* Paula Hammond, Kostas Kostarelos, Ronit Satchi-Fainaro
- **New Materials for Cancer Therapy and Diagnostics** *Ronit Satchi-Fainaro,* Michael Mitchell, Yeongseon Jang
- **Nanotechnology in Cancer Immunotherapy** Junsang Doh, *John Wilson,* Li Tang, Susan Thomas
- **Nanomedicine Therapeutics** *Tom Anchordoquy,* Emily Day, Samir Mitragotri
- **Diagnostics, Imaging, and Nanomaterial-Cell Interactions** *Debra Auguste,* ERic Huang, Christopher Alabi, Yana Reshetnyak
- **Gene Therapy and Gene Editing for Cancer** *Susan Thomas,* James Dahlman, Debra Auguste
- **Novel Nanotechnology Platforms Moving into the Clinic** *Marianne Ashford,* Geoffrey Lynn, Nicole Steinmetz
- **Short Talks Selected From Posters** *Daniel Heller*
- **The GRC Power Hour™** *Marianne Ashford, Daniel Heller*

Cannabinoid Function in the CNS +GRS

Charting the Course to Novel Therapeutics From a Fundamental Understanding of Cannabinoid Neurobiology

JUL 16-21, 2023

REY DON JAIME GRAND HOTEL, CASTELLDEFELS, SPAIN

CHAIRS: Miriam Melis and Mario van der Stelt

VICE CHAIRS: Cecilia Hillard and Jibran Khokhar

- **Keynote Session: Endocannabinoid Signalling and Neuroinflammation** *Andrea Hohmann,* Beth Stevens
- **Probes to Modulate and Visualize the Endocannabinoid System** *Istvan Katona,* Yulong Li, Uwe Grether, James Frank, Elizabeth Liedhegner
- **Endocannabinoid Trafficking and Signaling** *Michelle Glass,* Ruth Ross, Jürg Gertsch, Giovanni Marsicano, Pal Pacher

- **Endocannabinoids and Neurodevelopment** *Tiziana Rubino,* Yasmin Hurd, Pier Vincenzo Piazza, Viviana Trezza, Davide Dulcis
- **Synaptic Effects of Endocannabinoids** *Bradley Alger,* Stephanie Cragg, Raffaella Tonini, Barna Dudok
- **Endocannabinoids in Emotional Homeostasis** *Patrizia Campolongo,* Carmen Sandi, Joseph Cheer, Giuseppe Gangarossa
- **Endocannabinoids as Stepping-Stones to the Processes of Deregulated Cell Behavior** *Manuel Guzman,* Leila Akkari, Laura Heitman
- **Neuroprotective Effects of Endocannabinoids** *Mauro Maccarrone,* Inge Huitinga, Emma Puighermanal, Nephi Stella, Elizabeth Thiele
- **Inhibition of Endocannabinoid Metabolism as Potential Therapy** *Daniele Piomelli,* Sachin Patel, Matthew Hill
- **The GRC Power Hour™** *Giuseppe Gangarossa, Leah Mayo*

Carbohydrate-Active Enzymes for Glycan Conversions +GRS

CAZymes for Environmental Sustainability and Human Health

JUL 23-28, 2023
PROCTOR ACADEMY, ANDOVER, NH
CHAIRS: Tina Jeoh and Nicole Koropatkin
VICE CHAIR: Paul Walton

- **Keynote Session: CAZymes for Environmental Sustainability and Human Health** *Emma Master,* Breeanna Urbanowicz, Matthew Redinbo
- **Molecular Mechanisms of Complex Carbohydrate Degradation** *Bernd Nidetzky,* Zarah Forsberg, Jeremy Luterbacher, Elisabeth Lowe, Roland Ludwig
- **Visualizing CAZyme-Substrate Interactions** *Steve Decker,* Shishir Chundawat, William Hancock
- **Bacterial CAZymes Targeting Human Host Glycans** *Mario Murakami,* Alisdair Boraston, Marcelo Guerin, Tracey Gloster
- **CAZymes Prospecting and Discovery** *Michelle O'Malley,* Yanbin Yin, Robert Gruninger, Lauren McKee
- **Plant Cell Wall Construction and Deconstruction** *Debra Mohnen,* Charles Anderson, Kevin Solomon
- **CAZymes for Novel Glycan Synthesis** *Kiyohiko Igarashi,* Sabine Flitsch, Carme Rovira
- **CAZyme-Based Biotherapeutic Design** *Romina Rodríguez Sanoja,* Darrell Cockburn, Isaac Cann
- **CAZyme-Assisted Biomaterial Production** *Anne S. Meyer,* Bryan Berger, Olanrewaju Raji
- **The GRC Power Hour™** *Paul Walton*

Carbohydrates +GRS

Basic and Translational Glycoscience for Human Health and Diseases

JUN 18-23, 2023
HOLDERNESS SCHOOL, HOLDERNESS, NH
CHAIRS: Peter Andreana and Xuefei Huang
VICE CHAIRS: Jennifer Kohler and Xing Chen

- **Glycans in COVID-19 and Other Emerging Diseases** *Steven Townsend,* Max Crispin, Jason McLellan, Catherine Leimkuhler Grimes
- **Chemical Synthesis of Complex Glycans** *Pavel Nagorny,* M. Carmen Galan, Laurence Mulard
- **Glycoimmunology and Vaccines** *Steven Sucheck,* Zhongwu Guo, James Paulson, Edward Ryan
- **Industrial Applications of Glycoscience** *Jennifer Koviach-Cote,* Muthiah (Mano) Manoharan, John Magnani, Francesca Micoli
- **Chemical Glycobiology** *Lina Cui,* Stephen Withers, Linda Hsieh-Wilson, Hung-Wen Liu
- **Glycoanalysis and Glycomics** *Joseph Barchi Jr.,* Anne Dell, Jesus Jimenez-Barbero, Ten Feizi, Lara Mahal, Maren Roman
- **Glycans and Therapeutics** *Weiping Tang,* Todd Lowary, David Vocadlo
- **Enzymatic and Glycoconjugate Synthesis** *Lai-Xi Wang,* Xi Chen, Yasuhiro Kajihara, Jian Liu
- **Glycans in Host-Microbe Interactions** *Danielle Dube,* Gerald Pier, Willie Vann
- **The GRC Power Hour™** *Nicole Snyder*

Carbon Capture, Utilization and Storage +GRS

Transformative Science for the New Carbon Economy

MAY 28 - JUN 2, 2023
LES DIABLERETS CONFERENCE CENTER, LES DIABLERETS, SWITZERLAND
CHAIR: Andre Bardow
VICE CHAIR: Greeshma Gadikota

- **Fast-Tracking CCUS From Lab to Innovation** *Andrea Ramirez Ramirez,* George Shimizu, Charlotte Williams
- **Converting CO_2 into Products** *Christoph Guertler,* Boon Siang Yeo, Aldo Steinfeld, Emily Carter
- **Moving From Technical Feasibility to Societal Impact** *Holly Buck,* Elisabeth (Beth Rose) Middleton Manning, Benjamin Sovacool
- **Innovation in CO_2 Capture** *Kristin Jordal,* Susana Garcia, Harry Atwater
- **The Systems Challenge of the Carbon Transition** *Heleen de Coninck,* Mischa Repmann, Massimo Tavoni
- **Learning From Deployment** *Frauke Kracke,* Jannicke Gerner Bjerkås, Nathalie Casas, Noah McQueen
- **Greenhouse Gas Removal Harnessing Ocean, Land and Forests** *Yiwen Pan,* Andreas Oschlies, Lydie Stella Koutika, Stephanie Roe
- **Permanently Storing CO_2 in Minerals and Underground** *Greeshma Gadikota,* Douglas Wicks, Sarah Gasda, Herbert Todd Schaef
- **Unlocking Value Chains for Negative Emissions** *Sandra Osk Snaebjornsdottir,* Heinz Felder, Viola Becattini, Oliver Geden
- **The GRC Power Hour™** *Frances Wang, Caroline Normile*

Catchment Science: Interactions of Hydrology, Biology and Geochemistry +GRS

Challenges and Uncertainty in Predicting Catchment Responses to Stress

JUN 18-23, 2023
PROCTOR ACADEMY, ANDOVER, NH
CHAIRS: Sarah Godsey and Julian Klaus
VICE CHAIRS: Hilary McMillan and Ingo Heidbuechel

- **Keynote Session: Diverse Catchment Stressors Across Climates and Landscapes** *David Hannah,* Li Li
- **Catchment Processes in Vulnerable Landscapes** *Rachel Gabor,* Holly Barnard, Eugenia Marti, Ilja van Meerveld, Ellen Wohl
- **Predicting Dynamic Catchment Processes** *Christian Birkel,* Reed Maxwell
- **Drivers of Systems Under Stress: Integrating Observations, Models and Experiments** *Christa Kelleher,* Julien Bouchez, Ciaran Harman, Catalina Segura, Kei Yoshimura
- **Connecting Groundwater and Surface Water in Drying Landscapes** *Andreas Hartmann,* Margaret Shanafield
- **Humans as Stressors and Solvers: Changing Boundary Conditions and Changing Processes** *Anna Lintern,* Björn Guse, Sujay Kaushal, Arial Shogren, Kevin Devito
- **Cascading Effects of Pervasive Contaminants in Catchment Science** *Jay Zarnetske,* Timothy Hoellein
- **Integrating Tools Across Disciplines to Address Emerging Stressors** *Martyn Clark,* Steven Holbrook, Youri Rothfuss, Wouter Buytaert, Di Long
- **Keynote Session: Uncertainty in Understanding Catchments as Complex Systems** *Nandita Basu,* Diane McKnight
- **The GRC Power Hour™** *Christa Kelleher*

Catecholamines +GRS

Bridging Molecules, Circuits and Behavior

AUG 13-18, 2023
REY DON JAIME GRAND HOTEL, CASTELLDEFELS, SPAIN
CHAIR: Garret Stuber
VICE CHAIR: Mary Kay Lobo

- **Keynote Session: Catecholaminergic Signaling During Behavior** *Michael Bruchas,* Carmen Sandi, Naoshige Uchida
- **Molecular Genetics and Epigenetics of Catecholamine Neurons** *Zoe McElligott,* Ian Maze, Jeremy Day, Catherine Pena, Keri Martinowich
- **Molecular Pharmacology and Signaling in Catecholamine Systems** *Erin Calipari,* Bryan Roth, Michelle Mazei-Robison
- **New Tools to Probe Catecholaminergic Functions** *Stephan Lammel,* Tommaso Patriarchi, Yao Chen, Abraham Beyene
- **Catecholamine Signaling in Naturalistic Behaviors** *Michael Krashes,* Camilla Bellone, Annegret Falkner
- **Diversity of Catecholamine Encoding of Learned Behaviors** *Christian Lüscher,* Larry Zweifel, Ilya Monosov
- **Catecholamines, Actions, and Movements** *David Weinshenker,* Josh Berke, Susan Ferguson
- **The Role of Catecholamines in Pain and Addiction** *Paul Phillips,* Julia Lemos, Meaghan Creed
- **Early-Career Investigator Presentations** *Lex Kravitz*
- **The GRC Power Hour™** *Susan Ferguson*

Cell Biology of Metals +GRS

Biological Impacts of Metals: From the Environment to Human Health

JUL 30 - AUG 4, 2023
MOUNT SNOW, WEST DOVER, VT
CHAIRS: Angela Wilks and Kerry Kornfeld
VICE CHAIRS: Erin Connolly and Tom Bartnikas

- **Metal Nutrition From Plants to Humans** *Mary Lou Guerinot,* Wolfgang Busch, David Mendoza-Cozatl, Martin Warren
- **Metals in Metabolic Disorders and Disease** *Valeria Culotta,* Donita Brady, Iqbal Hamza, Svetlana Lutsenko, Fanis Missirlis
- **The Environmental Impact of Metals** *Mak Saito,* Jaclyn Saunders, Joseph Cotruvo, Jr., Rene Boiteau
- **Metal Clusters, Cofactors and Catalysis** *Ralf R. Mendel,* Caryn Outten, Kurt Warnhoff, Jennifer Bridwell-Rabb, Alejandro Vila
- **Metal Homeostasis in Cell Death and Aging** *Patricia Muller,* Michael Petris, Marcus Conrad, Peter Tsvetkov
- **Metal Trafficking, Storage and Regulation** *Celia Goulding,* Andrew Hudson, Crysten Blaby-Haas, Sabeeha Merchant, David Giedroc
- **Metals and Developmental Biology** *Thomas O'Halloran,* Adelita Mendoza, Teresa Woodruff
- **Metals at the Host Pathogen Interface** *Amanda Oglesby,* Jeffrey Henderson, Mario Rivera, Philippe Bouloc, Elizabeth Nolan
- **Keynote Session: Imaging Metal Trafficking, Signaling and Reactivity** *Amit Reddi,* Christopher Chang, Amy Palmer
- **The GRC Power Hour™** *Erin Connolly*

Cell Contact and Adhesion +GRS

Cell-Cell Junctions: Integrating Cell Signals and Mechanical Force in Development and Disease

JUN 25-30, 2023
COLBY-SAWYER COLLEGE, NEW LONDON, NH
CHAIR: Kris DeMali
VICE CHAIR: Mark Peifer

- **Keynote Session: The Molecular Basis of Vascular Intercellular Adhesion** *Mark Peifer,* Martin Schwartz, Jaap van Buul
- **New Insights into the Molecular Composition of Cell Contacts** *Yulia Komarova,* Alf Honigmann, Lindsay Case, Gregory Alushin
- **Cell Interactions at Desmosomes, Tight Junctions and Beyond** *Carien Niessen,* Andrew Kowalczyk, Mikio Furuse, Alexa Mattheyses
- **Exploring Cell Interactions** *Adam Kwiatkowski,* Ana Suncana Smith, Ann Miller
- **Cell Interactions as Integrators of Mechanical Signals** *Tristan Driscoll,* Alpha Yap, Benoit Ladoux, Jennifer Zallen
- **Cell Interactions as Integrators of Cell Signaling** *Cara Gottardi,* Gaudenz Danuser, Marcos Simoes-Costa
- **Cell Interactions During Morphogenesis** *Rashmi Priya,* Adam Martin, Crystal Rogers
- **Tissue Engineering and Tissue Models of Organoids** *Sara Stahley,* Sara Wickstrom, Ulrich Tepass
- **Cell Interactions in Tumor Cell Invasion and Metastasis** *Gaudenz Danuser,* Andrew Ewald, Patrick Derksen, Jing Yang
- **The GRC Power Hour™** *Andrew Kowalczyk, Cara Gottardi*

Cell Growth and Proliferation +GRS

Cell Cycle and Cell Proliferation in Development and Disease

JUL 9-14, 2023
MOUNT SNOW, WEST DOVER, VT
CHAIR: Martine Roussel
VICE CHAIR: Prasad Jallepalli

- **Keynote Session: Protein Degradation in Development and Disease** *Anwesha Dey,* Michael Rape, Ryan Potts
- **Core Cell Cycle Machinery and Cell Division** *Laura Buttitta,* Min Wu, Sue Biggins, Melissa Kemp
- **Proliferation and Genome Stability** *Laura Attardi,* Geert Kops, Andrea Ventura, David Gallo
- **Mechanisms of Cell Cycle Progression and Quiescence** *Stefano Di Talia,* Laura Buttitta, Gustavo Leone, Ryan Rountree
- **Driving the Cell Cycle** *Sabrina Spencer,* Jennifer Benanti, Bruce Clurman, Stefano Di Talia
- **Targeting Cyclin-Dependent Kinases** *Jennifer Benanti,* Geoffrey Shapiro, Sabrina Spencer, Peter Sicinski
- **Signaling Pathways in Development and Cancer** *Min Wu,* Amaia Lujambio, Julien Sage, Anwesha Dey
- **Genome Integrity and Immunity** *Elham Azizi,* Teresa Davoli, Samuel Bakhoum
- **System Biology and Genomics** *Amaia Lujambio,* Elham Azizi, M. Madan Babu
- **The GRC Power Hour™** *Anwesha Dey*

Cellular and Molecular Mechanisms of Toxicity +GRS

Modernized Approaches to Mechanistic Toxicology Investigations

AUG 13-18, 2023
PROCTOR ACADEMY, ANDOVER, NH
CHAIR: Rhiannon Hardwick
VICE CHAIR: Heather Wallace

- **Keynote Session: Gene Essentiality and Functional Genomics for Mechanistic Toxicology** *Muireann Coen,* Jason Sheltzer, Keren Carss
- **Artificial Intelligence in Toxicology and its Role in Decision Making** *Ruth Roberts,* Shraddha Thakkar, Ronald Tjalkens, Matthew Martin
- **The Cellular Microenvironment in Tissue Health, Disease and Toxic Exposure Outcomes** *Shaun McCullough, Kymberly Gowdy,* Ana Mora, Matthew Campen, Stavros Garantziotis
- **New Modalities, Mechanisms and Methods in Neurotoxicity** *Matthew Wagoner, James (Eric) McDuffie,* Timothy Shafer, Mohamed Kreir, Nibha Mishra
- **Novel Mechanisms Regulating Environmental Toxicant Metabolism** *Danielle Carlin, Lauren Aleksunes,* Jamie Bernard, Weston Porter, Jonathan Doorn
- **Modern Approaches in Developmental Toxicity Testing** *Kari Sant, Jessica LaRocca,* George Daston, Maria Bondesson, Thomas Knudsen
- **A Mechanistic View of Mixtures Toxicology From Human Health to Ecological Health** *Phillip Wages,* Cynthia Rider, Paul Price, Rolf Altenburger
- **Early-Career Investigator Presentations** *Cassandra Meakin, Katelyn Lavrich,* Cody Smith, Mohit Jain

THE GRC POWER HOUR™

The GRC Power Hour is designed to address ways to improve diversity and inclusion in science by providing a safe environment for informal and meaningful conversations amongst colleagues of all career stages.

- **Keynote Session: Mechanisms of Protein Degradation by Immunomodulatory Drugs and Targeted Protein Degraders** *Pete Newham,* Eric Fischer, Kevin Moreau
- **The GRC Power Hour™** *Samantha Snow, Sarah Lacher*

Central Nervous System Injury and Repair +GFS

Spinal Cord Injury and Repair: From Mechanisms to Translation

JUL 9-14, 2023
RENAISSANCE TUSCANY IL CIOCCO, LUCCA (BARGA), ITALY
CHAIRS: Elizabeth Bradbury and Yishi Jin
VICE CHAIRS: Victoria Abraira and Binhai Zheng

- **Keynote Session: Neuronal Circuit Mechanisms of Movement** *Victoria Abraira,* Martyn Goulding
- **Cervical and Respiratory Plasticity** *Gordon Mitchell,* Erica Dale, Philippa Warren, Florence Bareyre
- **Genomics Approaches to Axon Regeneration** *Binhai Zheng,* Simone Di Giovanni, Murray Blackmore, Claire Le Pichon, Zhigang He
- **Roles of Glia and Matrix in Spinal Cord Repair** *Catherina Becker,* Yimin Zou, Alyson Fournier, Linda Hsieh-Wilson, Jerry Silver
- **Animal Models for Axon Regeneration** *Britta Eickholt,* Catherina Becker, Alexandra Byrne, Catherine Collins, Monica Sousa
- **Translational Research to Inform Practice (TRIP)** *Linda Jones,* John Gensel, Mariel Purcell, Martin Schwab
- **Motor Plasticity** *Megan Detloff,* Karim Fouad, Tuan Bui, Aya Takeoka, Wolfram Tetzlaff
- **Neuronal Cell Biology of Axon Regeneration** *Hongyan (Jenny) Zou,* Frank Bradke, Kai Liu, Homaira Nawabi, Britta Eickholt
- **Keynote Session: Stem Cells in CNS Repair** *Mark Tuszynski,* Magdalena Goetz
- **The GRC Power Hour™** *Angela Filous, Simone Di Giovanni*

Cerebellum +GFS

Integrating Cerebellar Neurobiology, Neurocomputation and Neurotherapeutics

AUG 6-11, 2023
BATES COLLEGE, LEWISTON, ME
CHAIRS: Roy Sillitoe and Daniela Popa
VICE CHAIRS: Alanna Watt and Samuel Wang

- **Keynote Session: Cerebello-Forebrain Circuitry and Function** *Joshua White,* Kamran Khodakhah
- **Cerebellum in Motor and Non-Motor Pathologies** *Amy Bastian,* Dagmar Timmann, Cécile Gallea, Cherie Marvel, Esther Krook-Magnuson
- **Expression of Cellular and Functional Diversity** *Sascha du Lac,* Kathleen Millen, James Li, Janelle Pakan, Adam Hantman, Detlef Heck
- **Integration of Synaptic Mechanisms During Behavior** *Jennifer Raymond,* Nidia Quillinan, Taro Ishikawa, Marylka Yoe Uusisaari, Sachiko Tsuda, Volker Steuber
- **Linking Cerebellar Structure and Function** *Alexandra Joyner,* Richard Wingate, Sarah Goetz, Julie Lefebvre, Erik De Schutter
- **Mechanistic Roles of Cerebellar Circuits During Skilled Movement** *Eiman Azim,* Abigail Person, Justus Kebschull, Mark Blumberg, Helen Lai
- **Error and Reward as Cerebellar Learning Mechanisms** *Chris De Zeeuw,* Reza Shadmehr, Yifat Prut, Angus Silver, Kazuo Kitamura
- **Cerebello-Forebrain Interactions and Behavior** *Christelle Rochefort,* Clément Léna, Laure Rondi-Reig, Jessica Verpeut, Wade Regehr, Jörn Diedrichsen
- **Cerebellum as a Target for Therapy** *Freek Hoebeek,* Traian Popa, Hsiao-Tuan Chao, Stefan Pulst
- **The GRC Power Hour™** *Huda Zoghbi*

Chemical Imaging NEW!

Molecular Machinery in Real Time and Space

JUL 30 - AUG 4, 2023
STONEHILL COLLEGE, EASTON, MA
CHAIRS: Ji-Xin Cheng and Ning Fang
VICE CHAIRS: Lane Baker and Livia Eberlin

- **Keynote Session: Visualizing the Invisible From Single Molecules to Whole Organs** *Ashok Ajoy,* Xiaowei Zhuang, Lihong Wang
- **Breaking Physical Limitations in Sensitivity, Multiplexing and Resolution** *Christy Landes,* Ara Apkarian, Julia Laskin, Wei Min, Sylvie Roke
- **Unveiling Molecular Machinery Inside the Cell** *Lane Baker,* Katsumasa Fujita, Irene Georgakoudi, Meng Wang
- **Visualizing Chemical Transformations** *Caroline Karanja,* Libai Huang, Bo Zhang, Warren Warren
- **Translating Imaging Technologies into Clinical Practice** *Sixian You,* Rohit Bhargava, Jeffrey Spraggins, Dieter Henrik Heiland
- **Imaging of Materials and Interfaces** *Chi Zhang,* Peng Chen, Amber Krummel, Joaquin Rodriguez-Lopez, Katherine Willets
- **Molecules Inside the Brain** *Boone Prentice,* Maria Angela Franceschini, Na Ji, Daniel Razansky
- **Big Data, AI and Computational Imaging** *Garth Simpson,* Charles Bouman, Vivek Goyal, Aydogan Ozcan, Lei Tian
- **Short Talks Selected From Poster Abstracts** *Livia Eberlin,* Ed Boyden
- **The GRC Power Hour™** *Livia Eberlin, Ji-Xin Cheng*

Chemical Oceanography +GFS

Chemical Tracers in the Sea

JUL 16-21, 2023
SOUTHERN NEW HAMPSHIRE UNIVERSITY, MANCHESTER, NH
CHAIR: Lihini Aluwihare
VICE CHAIR: Phoebe Lam

- **Keynote Session: Diverse Tracers of Biogeochemical Processes in the Sea** *Ann Pearson,* Ellen Druffel, Mak Saito
- **Geochemical Proxies** *Youngsook Huh,* Alex Gagnon, Chandranath Basak, Morgan Raven
- **New Perspectives on Vertical Expor** *Bethanie Edwards,* Jan-Hendrik Hehemann, Kimberlee Thamatrakoln
- **Life at the Margins and its Influence on Ocean Chemistry** *Sunita Walter,* Anne Dekas, Clara Fuchsman, Susan Lang
- **Emerging Anthropogenic Impacts on Ocean Chemistry** *Jessica Fitzsimmons,* David Ho, Amy Gartman
- **Anthropogenic Tracers in the Sea** *Penny Vlahos,* Collin Ward, Amina Schartup, Maxi Castrillejo
- **Late-Breaking Topics** *Claudia Benitez-Nelson*
- **Gasses in the Ocean's Interior** *Roberta Hamme,* Alan Seltzer, Seth Bushinsky, Allison Moreno
- **Organic Matter Cycling** *Elizabeth Minor,* Daniel Repeta
- **The GRC Power Hour™** *Claudia Benitez-Nelson*

Chemistry and Physics of Liquids +GFS

Structural, Dynamic and Reactive Properties in the Liquid Phase

JUL 30 - AUG 4, 2023
HOLDERNESS SCHOOL, HOLDERNESS, NH
CHAIR: Nancy Levinger
VICE CHAIR: Christopher Mundy

- **Liquids at Soft Interfaces: Nanobubbles and Self Assembly** *David Limmer,* Valeria Molinero, Carlos Baiz
- **Liquids at Hard Interfaces: Water, Mineral and Organic Interactions** *Richard Remsing, Franz Geiger,* Julianne Gibbs, Sapna Sarupria, Ian Bourg
- **Complex Solutions: Ions, Osmolytes and Electrolytes** *Elise Duboué-Dijon,* Paul Cremer, Barbara Kirchner
- **Solvation Structure and Dynamics: Liquid Response to Invaders** *Greg Schenter,* Pavel Jungwirth, Susan Rempe, Martina Havenith
- **Liquids in Motion: Transport and Flow** *Jaehun Chun,* David Weitz, Clare McCabe
- **Motion in Liquids: From Ultrafast to Very Slow** *Steven Corcelli,* Mark Berg, Klaas Wynne, Lu Wang
- **Liquids in Biology: Biological Mimics, Materials and Polymers** *Jean Chung, Eva Pluharova,* Joan-Emma Shea, Christine Keating
- **Glasses, Ice, Vitrification and Coacervates** *Laura Kaufman,* Grzegorz Szamel, Jennifer Laaser, Amir Haji-Akbari
- **Keynote Session: Liquids in Layers and Early-Career Investigator Presentations** *Shuwen Yue,* Zahra Fakhraai, Bruce Kay
- **The GRC Power Hour™** *Zahra Fakhraai, Sapna Sarupria*

Chemistry Education Research and Practice +GFS

Coordinating the Production and Consumption of Knowledge on Chemistry Teaching and Learning

JUL 9-14, 2023
BATES COLLEGE, LEWISTON, ME
CHAIR: Ellen Yezierski
VICE CHAIR: Michael Seery

- **Chemical Thinking** *Alison Flynn,* Nathaniel Grove, Christina Schwarz
- **Science Practices** *Nicole Graulich,* Erin Dolan, Alena Moon, Joi Walker
- **Key K-12 Connections** *Marilyne Stains,* Brian Reiser, Wendy Adams
- **Students' Self-Theories** *Jeffrey Raker,* John Hutchinson, W. Stephen McNeil
- **Fostering More Inclusive Chemistry Cultures** *Gwendolyn Lawrie,* Minjung Ryu, Geraldine Richmond
- **Advancing Equity** *Sam Pazicni,* Aurora Kamimura, Zakiya Wilson-Kennedy, Tim McKay
- **Strengthening Feelings of Belonging** *Maria Oliver-Hoyo,* Regina Frey, Jean Stockard
- **Language and Learning** *Stacey Lowery Bretz,* Kimberly Tanner, Simon Rees, James Nyachwaya
- **Online and Hybrid Innovation** *Thomas Holme,* Jack Eichler, Deborah Herrington
- **The GRC Power Hour™** *Brittland DeKorver*

Chromosome Dynamics +GFS

Chromosome Biology From Cellular, Molecular and Physical Perspectives

JUN 25-30, 2023
RENAISSANCE TUSCANY IL CIOCCO, LUCCA (BARGA), ITALY
CHAIR: Camilla Björkegren
VICE CHAIR: Steve Bell

- **Keynote Session: Chromosomes: From Molecules to Cells and Organisms** *John Marko,* Susan Gasser, Geeta Narlikar, Romain Koszul
- **Chromosome Organization and Gene Regulation** *Katsuhiko Shirahige,* Wendy Bickmore, Hitoshi Kurumizaka, Barbara Meyer, Ana Losada
- **Chromosome Replication** *Susan Lovett,* Rodrigo Reyes Lamothe, John Diffley, James Berger, Karim Labib
- **Chromosome Instability and Repair** *Julia Cooper,* Karlene Cimprich, Houra Merrikh, Gaelle Legube, Eric Greene

"At the core of any GRC is exceptional technical programming and a vibrant scientific community."

DR. KRISTI ANSETH, University of Colorado Boulder

- **Meiotic Chromosomes** *Abby Dernburg,* Scott Keeney, Franz K. Klein, Jennifer Fung
- **Genome Organization** *Christian Haering,* Karolin Luger, Xindan Wang
- **Centromere Structure and Function** *Aaron Straight,* Robin Allshire, Jennifer Gerton
- **Chromosomes, DNA and Supercoiling** *Adele Marston,* Marco Foiani, Laura Baranello, Nynke Dekker
- **Structural Maintenance of Chromosomes** *Frank Uhlmann,* Benjamin Rowland, Tatsuya Hirano, Stephan Gruber, Jan-Michael Peters
- **The GRC Power Hour™** *Coral Zhou, Susan Gasser*

CO_2 Assimilation in Plants From Genome to Biome +GRS

Photosynthetic Efficiency in a Changing Climate

MAY 7-12, 2023

RENAISSANCE TUSCANY IL CIOCCO, LUCCA (BARGA), ITALY

CHAIRS: Asaph Cousins and Tracy Lawson

VICE CHAIRS: Elizabeth Ainsworth and Andrea Braeutigam

- **Keynote Session: Photosynthesis for Food and Fuel Security** *Oula Ghannoum,* Christine Raines, Ana Lobo, Michele Faralli
- **Carbon Metabolism** *Thomas Sharkey,* Tobias Erb, Michael Hodges, Stéphanie Arrivault, Amanda De Souza
- **Genomic Regulation of CO_2 Assimilation** *Julian Hibberd,* Pallavi Singh, Anthony Studer, Karolina Heyduk
- **Carboxylation Reactions and Photorespiration** *Oliver Mueller-Cajar,* Laura Gunn, Urte Schlueter, Patrick Shih, Veronica Maurino
- **Structure and Function of Photosynthesis** *Ichiro Terashima,* Craig Brodersen, Shan He, Florence Danila
- **Stomatal and Mesophyll Conductance** *Jaume Flexas,* Andrew Leakey, Michael Blatt, Yusuke Mizokami, Guillaume Théroux-Rancourt
- **Short Talks Selected From Poster Abstracts** *Lisa Ainsworth*
- **CO_2 Concentrating Mechanisms** *Howard Griffiths,* Gitanjali Yadav, David Savage, Steve Kelly, Erika Edwards
- **Keynote Session: Photosynthesis and Climate Change** *Danielle Way,* Jennifer Johnson, Jennifer McElwain, Johannes Kromdijk
- **The GRC Power Hour™** *Amanda Cavanagh, Donald Ort*

Coastal Ocean Dynamics +GRS

Coastal Ocean Physics and its Connections to Marine Ecosystems

JUN 18-23, 2023

BRYANT UNIVERSITY, SMITHFIELD, RI

CHAIRS: Kristen Davis and Weifeng (Gordon) Zhang

VICE CHAIRS: Hans Burchard and Melanie Fewings

- **Dynamics of Tropical and Temperate Estuaries** *Geno Pawlak,* Arnoldo Valle-Levinson, Yoeri Dijkstra
- **Nearshore Dynamics** *H Tuba Ozkan-Haller,* Julie Pietrzak, Jacqueline McSweeney, Jim Thomson
- **Predictability of the Coastal Ocean** *Pierre De Mey-Frémaux,* John Wilkin, Mercedes Pozo Buil
- **Exchange Between Continental Shelves and the Deep Ocean** *Catherine Edwards,* John Huthnance, Moninya Roughan, Andrew Stewart
- **Connecting Coastal Physics, Biogeochemical Dynamics, and Climate Impacts** *Samantha Siedlecki,* Susan Allen, Moritz Mathis
- **Coastal Sea Level Variability** *Rick Luettich,* Sönke Dangendorf, Charitha Pattiaratchi, Talea Mayo
- **Subterranean Estuaries and Groundwater Exchange** *Britt Raubenheimer,* David Brankovits, Gudrun Massmann
- **High-Latitude Shelf Dynamics** *Rebecca Jackson,* Laura Herraiz Borreguero, Fiamma Straneo, Maddie Smith
- **Novel Approaches to Observing in Coastal Systems** *Melissa Moulton,* Jessica Garwood, Margaret Palmsten
- **The GRC Power Hour™** *H Tuba Ozkan-Haller*

Collagen +GRS

Physiological and Disease Relevance and the Underlying Molecular Properties of Collagens

JUL 9-14, 2023

COLBY-SAWYER COLLEGE, NEW LONDON, NH

CHAIR: Taina Pihlajaniemi

VICE CHAIR: Douglas Gould

- **Keynote Session: ECM Dynamics in Development and Disease** *Johanna Myllyharju,* Irit Sagi, Ernestina Schipani
- **Functional Effects and Translational Potential of Mutations in Collagens** *Florence Ruggiero,* Billy Hudson, Paolo Bonaldo, Fransiska Malfait
- **Collagen Transport, Turnover and Homeostasis** *Yoshihiro Ishikawa,* Suneel Apte, Joan Chang
- **Collagens and Related Molecules in Stem Cell Regulation** *Leena Bruckner-Tuderman,* Sara Wickstrom, Danny Chan
- **Bioengineering and Materials Design** *Nancy Forde,* Jeffrey Hartgerink, Fei Xu, Matthew Harrington
- **Tumor Growth and Metastasis** *Raphael Reuten,* Cynthia Reinhart-King, Alexandra Naba, Kandice Tanner, Thomas Cox
- **Collagens: Systems Approaches, Networks and Interactomes** *Delfien Syx,* Sylvie Ricard-Blum, Valerio Izzi, Collin Ewald
- **Fibrosis and Tissue Repair** *Sergey Leikin,* Boris Hinz, Alexander Nystrom, Jagdeep Nanchahal
- **Musculoskeletal Development and Pathology** *Antonella Forlino,* Shireen Lamande, Paul Eckhard Witten
- **The GRC Power Hour™** *Rachel Lennon*

Collective Behavior NEW!

Mechanisms of Social Communication in all Kingdoms

AUG 13-18, 2023

GRAND SUMMIT HOTEL AT SUNDAY RIVER, NEWRY, ME

CHAIR: Jonathan Arnold

VICE CHAIRS: Heidi Kaplan and Stephen Pratt

- **Keynote Session: Insect Societies: The Roots of Collective Behavior** *Oleg Igoshin,* Deborah M Gordon
- **Quorum Sensing** *Art Edison,* Michael Judge, Asher Leeks, Grace Beggs
- **Collective Cell Movement** *Corina Tarnita,* Allyson Sgro, Daniel Cohen
- **Synthetic Collective Behavior** *Shufan Zhang,* William Bentley, Naomi Leonard
- **Collective Exchange Between Plants and Fungi** *Stephen Pratt,* Nancy Johnson, Vasilis Kokkoris, Corey Wilson
- **Cell-to-Cell Interactions** *Alexander Bucksch,* Zev Gartner, Lorenz Fenk
- **Collective Behavior of Biological Oscillators** *Jia Hwei Cheong,* Heinz-Bernd Schüttler, Felix Naef, Yuanzhao Zhang
- **Flocks, Schools, and Armies** *Liliana Salvador,* Colin Torney, Jerome Buhl
- **Collective Decision Making** *Juan B. Gutiérrez,* Ariana Strandburg-Peshkin, Erik Bollt
- **The GRC Power Hour™** *Graciela Lorca*

Computational Aspects of Biomolecular NMR +GRS

From Spins to Cells: Biological Mechanism in Space and Time

JUN 18-23, 2023

MOUNT SNOW, WEST DOVER, VT

CHAIR: Arthur Palmer

VICE CHAIR: Katja Petzold

- **Keynote Session: Dynamics Take the Stage From NMR Spectroscopy to Biological Function** *Adriaan Bax,* Hashim Al-Hashimi, Dorothee Kern
- **Theory, Calculations, and Experiments** *Ilya Kuprov,* David Case, Lucio Frydman
- **Structures and Dynamics of Nucleic Acids** *Qi Zhang,* Sarah Keane, Yi Xue
- **Protein Dynamics in Solution and Solids** *Patrick Loria,* Mikael Akke, Józef Lewandowski
- **MD Simulations Integrated with NMR Experiments** *Francesca Massi,* Paul Robustelli, Birgit Strodel
- **IDPs and Non-Globular States** *Paul Robustelli,* Jean Baum, Martin Blackledge, Roberta Pierattelli
- **Data Acquisition and Interpretation** *Haribabu Arthanari,* Rafael Bruschweiler, Vladislav Orekhov
- **Approaches for Large Systems in Solution and Solid States** *Francesca Marassi,* Tatyana Polenova, Dominique Frueh, Rina Rosenzweig
- **New Experimental and Theoretical Approaches** *Angela Gronenborn,* Mei Hong, Matthias Ernst
- **The GRC Power Hour™** *Linda Nicholson*

Computer Aided Drug Design +GRS

Data Analytics and Computational Modeling for Next Generation Molecular Design

JUL 16-21, 2023

MOUNT SNOW, WEST DOVER, VT

CHAIR: Georgia McGaughey

VICE CHAIR: Matthias Rarey

- **Keynote Session: Emerging Technologies and Covid-19 Research** *Clara Christ,* John Chodera, Qingyi Yang
- **Computational Exploration of New Modalities** *Michelle Lamb,* Amber Balazs, Dahlia Weiss
- **Modeling of Chemical Reactions on a Large Scale** *Rajarshi Guha,* Lee Cronin, Anat Milo
- **Next-Generation Machine Learning in Drug Discovery** *Steven Kearnes,* Daniel Reker, Francesca Grisoni, Lucy Colwell
- **Computational Molecular Design in Pharmaceutical Research** *Melissa Landon,* Kelly Ganamet, Aysegul Ozen, Frank Pickard
- **Protein Structures, Dynamics and Design** *Sereina Riniker,* Charlotte Deane, Steffen Lindert, Dominik Oberthuer, Gregory Bowman
- **ADMET Modeling Beyond QSAR** *Andrea Volkamer,* Floriane Montanari, Matthew Danielson, Ying-Duo Gao
- **Navigating Chemical Space** *Christos Nicolaou,* Jeffrey Messer, Paul Beroza, Christian Kramer, Ola Engkvist
- **Keynote Session: Open Challenges in CADD: A Vision for the Next Decade** *Barbara Zdrazil,* Connor Coley, Nadine Schneider, Robert Glen
- **The GRC Power Hour™** *Fiorella Ruggiu*

Consciousness, Anesthesia and Evolutionary Biology NEW!

Anesthetic Insights into the Unconscious State Across Species

JUN 11-16, 2023

STONEHILL COLLEGE, EASTON, MA

CHAIR: Max Kelz

VICE CHAIR: Ken Solt

- **Keynote Session: The Genesis of Consciousness** *George Mashour,* Theofanis Panagiotaropoulos, Biyu He
- **Consciousness and Model Organisms** *Phil Morgan,* Colin Klein, Paco Calvo, Margaret Sedensky
- **Phylogenetically Conserved Molecular Targets of Anesthesia** *Hugh Hemmings,* Bruno van Swinderen, Slobodan Todorovic
- **Anesthetic Effects on Model Organisms** *Mike Crowder,* Andy Adamatzky, Chris Connor, Stu Forman
- **Cortical Signaling in Anesthetic States** *Robert Sanders,* Aeyal Raz, Dinesh Pal
- **Subcortical Targets of Anesthetic Hypnosis and Sleep** *Nick Franks,* Christa Nehs (Van Dort), Giancarlo Vanini, William Wisden
- **Sensory Signaling in Anesthetic States** *Peter Goldstein,* Matthew Banks, Alexander Proekt
- **Dynamics of Anesthetics and Unconsciousness in Non-human Primates** *Yuri Saalmann,* Michelle Redinbaugh, Yumiko Ishizawa, Bechir Jarraya
- **The Unconscious State in Humans** *Seun Johnson-Akeju,* Harry Scheinin, Katie Warnaby, Marcello Massimini
- **The GRC Power Hour™** *Christa Nehs (Van Dort)*

Crystal Growth and Assembly +GRS

Mechanistic Understanding of the Growth and Assembly of Ordered Materials

JUN 18-23, 2023

SOUTHERN NEW HAMPSHIRE UNIVERSITY, MANCHESTER, NH

CHAIR: Kristen Fichthorn

VICE CHAIR: Willem Noorduin

- **Keynote Session: Hierarchical Assembly of Functional Materials** *Jim De Yoreo,* Sharon Glotzer, Chad Mirkin
- **Nanocrystal Growth** *Xingchen Ye,* Raymond Schaak, Riccardo Ferrando, Matthew Jones
- **Non-Classical Crystal Growth** *Xin Zhang,* Dongsheng Li, Helmut Cölfen
- **Understanding Nucleation** *Jerome Delhommelle,* Pablo Piaggi, Nadine Candoni, James Evans, Ute Kaiser
- **Molecular-Level Understanding of Organic Crystal Growth** *Stephanie Lee,* Matteo Salvalaglio, Sarah (Sally) Price
- **Synthesis Science of Crystalline Materials** *Xin Qi,* Jeffrey Rimer, Miaofang Chi, Robert Macfarlane
- **Assembly in Action: Mechanisms and Dynamics** *Asaph Widmer-Cooper,* Qian Chen, Michael Grünwald
- **Organic and Biogenic Crystals** *Peter Vekilov,* Lia Addadi, Fiona Meldrum, Paolo Raiteri
- **Keynote Session: Directing Growth and Assembly From the Bottom Up** *Elias Vlieg,* Frances Ross, Nicholas Kotov
- **The GRC Power Hour™** *Bryan Alamani, Christine Orme*

Developmental Biology +GRS

Developmental Origin of Form and Function

JUN 25-30, 2023

MOUNT HOLYOKE COLLEGE, SOUTH HADLEY, MA

CHAIRS: James Briscoe and Anne Grapin-Botton

VICE CHAIR: Swathi Arur

- **Keynote Session: Cell Diversity and Embryonic Patterning** *Swathi Arur,* Claudio Stern, Anna Kicheva
- **Metabolic Fluxes in Development** *Marianne Bronner,* Aurelio Teleman, Jason Tennessen, Tina Mukherjee
- **Gene Regulation** *Anna Kicheva,* Samantha Morris, Martha Bulyk
- **Dynamic Signaling at Tissue Scale** *Sally Dunwoodie,* Daniel Ríos Barrera, Ajay Chitnis
- **Regeneration** *Claudio Stern,* Mansi Srivastava, Ken Poss, Dasaradhi Palakodeti

- **Lineage Tracing Revisited in the Age of Single Cell Genomics** *Samantha Morris,* Marianne Bronner, Celina Juliano, Allon Klein
- **Tissue Mechanics and Morphogenesis** *Daniel Ríos Barrera,* Charlotte Kirchhelle, Madhav Mani, Miltos Tsiantis
- **Developmental Origin of Disease** *Martha Bulyk,* Richard Gilbertson, Sally Dunwoodie, Anwesha Dey
- **Transgenerational Inheritance** *Ajay Chitnis,* Eric Miska, Xiaoqi Feng, Shosei Yoshida
- **The GRC Power Hour™** *Marianne Bronner, Ken Poss*

Drug Metabolism +GRS

Diversity and Connectivity in Progressing ADME Science: Novel Approaches and Emerging Technologies In Silico, In Vitro and In Vivo

JUL 9-14, 2023
HOLDERNESS SCHOOL, HOLDERNESS, NH
CHAIR: Jane Kenny
VICE CHAIR: John Harrelson

- **Keynote Session: Translation of *In Silico, In Vitro and In Vivo* ADME Data Through Mechanistic Understanding and Modelling and Simulation** *John Harrelson,* K Sandy Pang
- **The Power of Computational ADME in Drug Discovery and Development** *Prashant Desai,* Christopher Keefer, Susanne Winiwarter, Maria Posada, Giulia Caron
- **Expanding ADME Capabilities Through New Laboratory Techniques** *Bernard Murray,* Graeme Young, Dylan Ross
- **Mechanistic ADME: Metabolism, Biotransformation, Transport, and IVIVE** *Klarissa Jackson, J*acqueline Tiley, Bhagwat Prasad, Matthew Cerny
- **Clinical Approaches and Investigations Expanding Our Translational ADME Understanding** *Mary Paine,* Nathan Cherrington, Stephani Stancil, Janne Backman
- **Advances in Mechanistic Modelling and Simulation of ADME Properties and PKPD Relationships** *Yuching Yang,* Nina Isoherranen, Kate Gill, Xiling Jiang, Lara Clemens
- **Early-Career Investigator Presentations** *Swati Nagar*
- **Mechanistic Drug Discovery and Development Problem Solving Beyond Small and Large Molecules** *Anshul Gupta,* Nancy Chen, Jimit Raghav, Prathap Nagaraja Shastri, Carina Cantrill
- **Regulatory and DDI Clinical Problem Solving** *Aleksandra Galetin,* Karen Rowland-Yeo, Xinning Yang, Carolina Säll
- **The GRC Power Hour™** *Netz Arroyo*

Ecological and Evolutionary Genomics +GRS

Dynamics of Ecological and Evolutionary Change

JUL 30 - AUG 4, 2023
BRYANT UNIVERSITY, SMITHFIELD, RI
CHAIRS: Camille Berthelot and Sarah Kocher
VICE CHAIRS: Sam Yeaman and Irene Newton

- **Experimental Evolution** *Arnaud Martin,* Christian Schlötterer, Megan Frederickson
- **Adaptation and Evolutionary Innovations** *Elizabeth Heath-Heckman,* Hopi Hoekstra, Arnaud Martin, Paul Magwene
- **Rapid Evolutionary Change, Climate and Biodiversity** *Sam Yeaman,* Moises Exposito-Alonso, David Enard
- **Population and Community Genomics** *Vera Domingues,* Julia Saltz, A. Murat Eren, Manon Morin
- **Comparative Genomics** *Ines Drinnenberg,* Priya Moorjani, Dmitri Petrov, Kirsten Bomblies
- **Biodiversity in the Omics Era** *Adam Siepel,* Rachel Meyer, Aude Bernheim, Tim Sackton
- **Dark Side of the Genome** *Julien Ayroles,* Ines Drinnenberg, Alexander Suh
- **Methodological Innovation, Machine Learning and Big Data** *Priya Moorjani,* Adam Siepel, Erin Molloy, Andrew Kern
- **The Future of Ecological and Evolutionary Genomics** *Moises Exposito-Alonso,* Olivia Harringmeyer, Ioannis Sarropoulos
- **The GRC Power Hour™** *Irene Newton*

Elastin, Elastic Fibers and Microfibrils +GRS

Elastic Tissues and Regulation of Cellular Signaling in Development, Homeostasis and Disease

JUL 23-28, 2023
SOUTHERN NEW HAMPSHIRE UNIVERSITY, MANCHESTER, NH
CHAIR: Dianna Milewicz
VICE CHAIR: Beth Kozel

- **Elastin Properties and Assembly** *Katherine Zhang,* Brigida Bochicchio, Christian Schmelzer, Anna Tarakanova
- **Elastin and Vascular Inflammation** *Ying Shen,* Hiromi Yanagisawa, George Tellides
- **Structural Roles of Elastin and Microfibril Associated Proteins** *Hiromi Yanagisawa,* Dieter Reinhardt, Clair Baldock, Robert Mecham, Gerhard Sengle, Suneel Apte
- **Signaling in Elastin Rich Tissues** *David Dichek,* Elena Gallo MacFarlane, Juan Miguel Redondo
- **Elastin and Microfibril Modifiers, Assembly, and Development** *Katja Schenke-Layland,* Anthony (Tony) Weiss, Dirk Hubmacher, Dieter Reinhardt, Daniel Greif
- **Elastin and Microfibril Matrix: Multi-Omics Approaches** *Clair Baldock,* Sara Procknow, Scott LeMaire
- **Aortic Structure and Biomechanics in Health and Disease** *Julie Phillippi,* Bart Spronck, Jay Humphrey, Shaine Morris
- **Elastic Fibers in Tissue Engineering and Regenerative Medicine** *Ying Shen,* Alan Daugherty, Katja Schenke-Layland, Sanjay Sinha, Naren Vyavahare
- **Elastin Structural Integrity with Aging and Environmental Damage** *Carmen Halabi,* Andrea Heinz, Monzur Murshed, Daniel Goldstein
- **The GRC Power Hour™** *Hiromi Yanagisawa, Ying Shen, Jessica Wagenseil*

Electron Spin Interactions with Chiral Molecules and Materials NEW!

Chiral Spin Filtering and its Manifestations From Molecules to Devices

JUL 30 - AUG 4, 2023
SOUTHERN NEW HAMPSHIRE UNIVERSITY, MANCHESTER, NH
CHAIRS: Karen Michaeli and David Waldeck
VICE CHAIRS: Carmen Herrmann and Yossi Paltiel

- **Chiral Molecules and Magnetism** *Paul S. Weiss,* Roberta Sessoli, John Abendroth
- **Spin Transport in a Chiral Potential** *Ora Entin-Wohlman,* Solmar Varela, Hiroshi Yamamoto, Mikhail Lemeshko
- **Chirality and Spin in Chemical Systems** *Francesco Tassinari,* Magalí Lingenfelder, Michael Wasielewski
- **Chiral Interfaces of Electronic Materials** *Bart Van Wees,* Jeremy Levy, Peng Xiong, Binghai Yan
- **Spin and Chirality in Perovskite Materials** *Zeev Valy Vardeny,* Matthew Beard, Dali Sun
- **Chiral Induced Spin Selectivity in Chiral Materials** *Jeanne Crassous,* Michael Therien, Helmut Zacharias, Shira Yochelis
- **Chirality and Spin in Biological and Biomimetic Systems** *Clarice Aiello,* Moh El-Naggar, Ron Naaman
- **Interaction Effects on CISS** *Per Hedegård,* Vladimiro Mujica, Jonas Fransson, Elena Díaz
- **New Avenues in CISS** *David Beratan,* Joseph Subotnik
- **The GRC Power Hour™** *Karen Michaeli*

Enzymes, Coenzymes and Metabolic Pathways +GRS

Biosynthesis, Biocatalysis, and New Methods in Enzymology

JUL 16-21, 2023
WATERVILLE VALLEY, WATERVILLE VALLEY, NH
CHAIRS: Satish Nair and Luiz Pedro Carvalho
VICE CHAIRS: Pablo Sobrado and Erika Taylor

- **Enzyme Function and Mechanism** *Vinayak Agarwal,* Karen Allen, Wen Shan Yew, Wilfred van der Donk
- **Enzymology of Complex Systems** *Y. Jessie Zhang,* Matthias Wilmanns, Heather Hundley, Andrew Hanson, Rafael da Silva
- **Biocatalysis and Synthetic Biology** *Sara Cortese,* Yifan Wang, John McIntosh, Todd Hyster
- **Anti-Infective Biosynthesis** *Hua Wang,* Jaclyn Winter, Jesko Koehnke, David Christianson, Ikuro Abe
- **Metals in Biochemistry** *Jennifer Bridwell-Rabb,* N. Cecilia Martinez-Gomez, Akif Tezcan, Bo Li
- **Principles of Enzyme Catalysis** *James Errey,* Clarissa Czekster, Courtney Aldrich, Randy Kipp
- **Enzyme Function and Engineering** *Andrea Mattevi,* Joelle Pelletier, Michelle Chang, Marcus Hartmann
- **Emerging New Methods in Enzymology** *Michelle Bond,* Margaux Pinney, Lynn Kamerlin, Mohammad Seyedsayamdost
- **Keynote Session: Biocatalysis and Enzymology for Translational Biochemistry** *Andrew Gulick,* Chaitan Khosla, Ruma Banerjee
- **The GRC Power Hour™** *Pablo Sobrado, Erika Taylor*

Epigenetic Regulation of Cardiovascular Disease +GRS

From Mechanism to Therapy At Chromatin and Beyond

JUN 18-23, 2023
FOUR POINTS SHERATON / HOLIDAY INN EXPRESS, VENTURA, CA
CHAIR: Yibin Wang
VICE CHAIRS: Johannes Backs and Federica Accornero

- **Keynote Session: Single Cell Resolution of Cardiac Epigenetic Landscape** *Thomas Vondriska,* Bing Ren
- **Epigenetics in Development and Congenital Heart Diseases** *Maha Abdellatif,* Richard Harvey, Deepak Srivastava, Ali Marian
- **Epigenetic Landscape in CV System** *Gergana Dobreva,* Kaifu Chen, Li Qian
- **Novel Players and Mechanisms in CV Epigenetic Regulatory Network** *Assam El-Osta,* Nathan Palpant, Matthew Stratton, Vincent Christoffels, Ivan Moskowitz
- **Metabolism and Epigenetics** *John Elrod,* Tamer Sallam, Thomas Braun, Anja Karlstaedt, Timothy McKinsey
- **Epigenetics in Cardiovascular Precision Medicine** *Gianluigi Condorelli,* W. H. Wilson Tang, Danny Leung, Elisabeth Zeisberg, Helle Jorgensen
- **Epigenetic Regulation Beyond Chromatin** *Ralf Gilsbach,* Guo Huang, Mirko Völkers
- **Epigenetic Regulation of Cardiomyocyte Reprogramming** *Sarah Franklin,* Sebastian Preissl, Llewelyn Roderick, Aaron Goldman, William Pu, Roger Foo
- **Keynote Session: New Insights into Heart Development, Disease and Regeneration** *Johannes Backs,* Eric Olson
- **The GRC Power Hour™** *Sarah Franklin*

Epigenetics +GRS

Epigenetic Information: Mechanisms, Memory and Inheritance

AUG 6-11, 2023
HOLDERNESS SCHOOL, HOLDERNESS, NH
CHAIRS: Mary Gehring and Petra Hajkova
VICE CHAIRS: Mary Goll and Robin Allshire

- **Chromatin Structure** *Maria-Elena Torres-Padilla,* Ting (C-ting) Wu, Genevieve Almouzni, Giacomo Cavalli
- **RNA-Directed Processes** *R. Keith Slotkin,* Blake Meyers, Eric Miska, Hailing Jin, Chuan He
- **Heterochromatin** *Susan Gasser,* Shiv Grewal, Bas van Steensel, Jerome Dejardin
- **Epigenome Maintenance** *Steve Jacobsen,* Anja Groth, Julie Law, Sophie Polo, Hiten Madhani
- **Transposable Elements Shaping the Genome** *Mary Goll,* Deborah Bourc'his, Vincent Colot, Robert Martienssen
- **Epigenetic Information in Development** *Haruhiko Koseki,* Wolf Reik, Camila dos Santos, Ryan Lister, Edith Heard
- **Programming and Reprogramming for the Next Generation** *Frederic Berger,* Bradley Cairns, Xiaoqi Feng, Eugene Gladyshev
- **Epigenetic Inheritance Between Generations** *Ueli Grossniklaus,* Scott Kennedy, Bluma Lesch, Danesh Moazed
- **Epigenetics at the Interface Between the Genome and the Environment** *Robin Allshire,* Jose Gutierrez-Marcos, Jason Locasale, Anne Ferguson-Smith
- **The GRC Power Hour™** *Mary Goll, Robin Allshire*

Epithelial Differentiation and Keratinization +GRS

Novel Mechanisms of Regulation of Epithelial Biology and Their Implication in Physiology, Aging and Disease

JUN 4-9, 2023
REY DON JAIME GRAND HOTEL, CASTELLDEFELS, SPAIN
CHAIR: Salvador Aznar Benitah
VICE CHAIRS: Maria Kasper and Elena Ezhkova

- **Keynote Session: Principles of Epidermal and Immune Physiology** *Pierre Coulombe,* Paul Khavari, Jennifer Elisseeff
- **Stem Cells and Homeostasis** *Pritinder Kaur,* Valentina Greco, Benjamin Simons, Fiona Watt, Elaine Fuchs, Yasmine Belkaid
- **Aging and Stress** *Desmond Tobin,* Emi Nishimura, Vladimir Botchkarev, Ya-chieh Hsu, Kim Jensen
- **Epithelial-Environment and Niche Interactions** *Guiomar Solanas,* Julie Segre, Michael Rendl, Yuval Rinkevich, Jessica Strid
- **Epigenetics** *Philip Jones,* Tudorita (Doina) Tumbar, Anthony Oro, Sara Wickstrom
- **Tissue Architecture and Niche Interactions** *Kathleen Green,* Muzlifah Haniffa, Shalev Itzkovitz, Valerie Horsley, Sarah-Maria Fendt
- **Tissue Regeneration** *Bogi Andersen,* Ophir Klein, George Cotsarelis, Carien Niessen
- **Cancer Genetics, Epigenetics and Signalling** *Srikala Raghavan,* Cedric Blanpain, Andrzej Dlugosz, Nuria Lopez-Bigas, Michaela Frye
- **Epithelial Therapeutics** *Terry Lechler,* Michele De Luca, Maria Alcolea
- **The GRC Power Hour™** *Sarah Millar*

Excitatory Synapses and Brain Function +GRS

Synapses and Circuits in Health and Disease

JUN 4-9, 2023
LES DIABLERETS CONFERENCE CENTER, LES DIABLERETS, SWITZERLAND
CHAIRS: Pablo Castillo and Camilla Bellone
VICE CHAIRS: Hey-Kyoung Lee and Juan Lerma

- **Keynote Session: Synaptic, Plasticity and Behavior** *Alison Barth,* Christian Lüscher, Gina Turrigiano
- **Excitatory Synapses as Key Regulators of Neural Circuits** *Christian Lüscher,* Manuel Mameli, Stephan Lammel, Ofer Yizhar, Marisela Morales
- **Excitatory Synapses in Learning and Memory** *Richard Huganir,* Sheena Josselyn, Yingxi Lin, Attila Losonczy, Alfonso Araque
- **Experience-Dependent Synaptic Plasticity** *Gina Turrigiano,* Jackie Schiller, Haruo Kasai, Judit Makara
- **New Imaging Tools to Study Synapses** *Daniel Choquet,* Alison Barth, Na Ji, Valentin Nägerl, Joshua Levitz

- **Synaptic Dysfunction in Brain Disorders** *Isabel Perez-Otaño,* Ana Luisa Carvalho, Tara Spires-Jones, Mauro Costa-Mattioli, Hailan Hu
- **Glutamate Receptors: Structure and Function** *Hailan Hu,* Pierre Paoletti, Fabrizio Gardoni, Gabriela Popescu, Karen Zito
- **Synapse Specification and Transsynaptic Signaling** *Peter Scheiffele,* Eunjoon Kim, Scott Soderling, Joris de Wit, Thomas Blanpied
- **Gene Transcription in Neural Circuit Function** *Karen Zito,* Brenda Bloodgood, Denis Jabaudon, Hongkui Zeng, Sacha Nelson
- **The GRC Power Hour™** *Hey-Kyoung Lee*

Eye Movements +GFS

A Model System for Sensory, Motor and Cognitive Function

JUL 9-14, 2023

MOUNT HOLYOKE COLLEGE, SOUTH HADLEY, MA

CHAIRS: Jacqueline Gottlieb and Miguel Eckstein

VICE CHAIRS: Richard Krauzlis and Linda McLoon

- **Keynote Session: Goal-Directed Eye Movement Control** *Michael Goldberg,* Okihide Hikosaka, Mary Hayhoe
- **Extraocular Muscles and Cranial Motor Neuron Development** *Fatima Pedrosa-Domellof,* Chrissa Kioussi, Sarah Guthrie, David Schoppik, Mary Whitman
- **Brainstem Control of Eye Movements** *Michael Mustari,* Yoshiko Kojima, Aristides Arrenberg, Vallabh Das
- **Eye Movements in Exploration and Free Visual Search** *Vincent Ferrera,* Mark Segraves, Georgia Gregoriou, Suliann Ben Hamed, Becket Ebitz
- **Basal Ganglia: Circuits, Computations and Pathophysiology** *Michele A Basso,* Long Ding, Masaki Tanaka, Anne Sereno
- **Multi-Sensory Integration in Oculomotor Control** *Dora Angelaki,* Maria Chait, Jennifer Groh, Henrik Mouritsen
- **Reference Frames for Visual Perception and Motor Control Across Saccades** *Julie Golomb,* Douglas Crawford, Katja Fiehler, John Pezaris, Stefan Van der Stigchel
- **Navigation, Memory and the Hippocampus** *Kathleen Cullen,* Jennifer Ryan, Matt van der Meer, Christian Doeller, Elizabeth Buffalo
- **Predicting Fixation Properties From Neural Activity** *Ueli Rutishauser,* Stefan Pollmann, Avniel Ghuman, Katalin Gothard
- **The GRC Power Hour™** *Jolande Fooken*

Fertilization and Activation of Development +GFS

The Basics of Gamete Biology and Early Development and Their Clinical Implications

JUL 23-28, 2023

HOLDERNESS SCHOOL, HOLDERNESS, NH

CHAIR: Celia Santi

VICE CHAIR: Rafael Fissore

- **Embryo Development** *Anna-Katerina Hadjantonakis,* Kikue Tachibana, Magdalena Zernicka-Goetz, Eszter Posfai
- **Oocyte Maturation and Preparation for Fertilization** *Karen Schindler,* Suzanne Madgwick, Swathi Arur, Ahmed Balboula, Binyam Mogessie
- **Reproductive Environment and Gamete Maturation** *Sylvie Breton,* Irina Larina, Steve Dorus
- **Molecular Mechanisms Involved in Acquisition of Sperm Fertilization Competence** *Mariano Buffone,* Tzviya Zeev-Ben-Mordehai, Rossana Sapiro
- **Identification of Novel Contraceptive Targets and New Platforms for Contraceptive Screening** *Gregory Kopf,* David Pepin, Lonny Levin, Jianjun Sun
- **The Molecular Basis of Sperm-Egg Recognition** *Luca Jovine,* Naokazu Inoue, Jennifer Pinello, Li-Jia Qu, Katerina Komrskova
- **The Genetics and Epigenetics of Fertilization and Embryo Development** *Steven L'Hernault,* Rafael Oliva, Julie Brind'Amour, Bradley Cairns
- **Short Talks Selected From Poster Abstracts** *Rafael Fissore,* Ruth Lehmann
- **Evolution of Reproductive Mechanisms and Behaviors** *Mariana Wolfner,* Katie Barott, Irem Sepil
- **The GRC Power Hour™** *Farners Amargant i Riera*

Genome Architecture in Cell Fate and Disease +GFS

Deciphering the Mechanisms and Functions of Chromatin Organization in Eukaryotic Genomes

JUN 11-16, 2023

FOUR POINTS SHERATON / HOLIDAY INN EXPRESS, VENTURA, CA

CHAIRS: Victor Corces and Danny Leung

VICE CHAIRS: Ana Pombo and Wei Xie

- **Epigenomics and Chromatin Architecture** *Kathrin Plath,* Bing Ren, Jennifer Philips-Cremins, Alistair Boettiger
- **Chromatin Organization in the Brain** *Jennifer Philips-Cremins,* Yin Shen, Daniele Canzio
- **Nuclear Organization in Stem Cells and Development** *Maria Cristina Gambetta,* Maria-Elena Torres-Padilla, Kathrin Plath
- **Emerging Technologies** *Jian Yan,* Steven Henikoff, Philippe Collas

- **Computational Analysis of Chromatin Structures** *Inkyung Jung,* Yuk-Lap (Kevin) Yip, Mitch Guttman, Elzo de Wit
- **Epigenetic and Transcriptional Regulation** *Yuk-Lap (Kevin) Yip,* Chia-Lin Wei, Mayra Furlan-Magaril
- **Dynamics in Genome Organization** *Ichiro Hiratani,* David Gilbert, Maria Cristina Gambetta
- **Repetitive Elements** *Yin Shen,* Ting Wang, Yoichi Shinkai
- **Chromatin Regulation in Disease** *Mayra Furlan-Magaril,* Eric Joyce, Marieke Oudelaar, Giacomo Cavalli
- **The GRC Power Hour™** *Maria-Elena Torres-Padilla, Chia-Lin Wei*

Geochronology +GFS

Timing, Tempo and Drivers of Lithospheric Evolution

AUG 13-18, 2023

MOUNT SNOW, WEST DOVER, VT

CHAIRS: Blair Schoene and Leah Morgan

VICE CHAIRS: Ann Bauer and Klaudia Kuiper

- **Growth and Stabilization of Continents** *Vickie Bennett,* Chris Spencer, Jun Korenaga
- **Large Igneous Provinces** *Joshua Davies,* Jill VanTongeren, Leif Karlstrom
- **Collisional Orogens** *Clare Warren,* Nadine McQuarrie, Chris Mark
- **Landscape Evolution** *Marissa Tremblay,* Paulo Vasconcelos, Georgina King
- **Basin Evolution** *George Gehrels,* Julie Fosdick, Francis Macdonald
- **Subduction Zones** *Kari Cooper,* Whitney Behr, Benjamin Klein, Christy Till
- **Tectonics and Paleogeography** *C. Brenhin Keller,* David Evans, Craig O'Neill, Cris Lana
- **Batholiths and Super Eruptions** *Jorge Vazquez,* Drew Coleman, Xiaolei Wang, Patricia Gregg
- **Mantle Lithosphere** *Graham Pearson,* Emily Chin, Sonja Aulbach
- **The GRC Power Hour™** *Rebecca Flowers*

Germinal Stem Cell Biology +GFS

Induction and Programming of the Germ Cell Lineage

MAY 7-12, 2023

REY DON JAIME GRAND HOTEL, CASTELLDEFELS, SPAIN

CHAIR: Blanche Capel

VICE CHAIR: Mitinori Saitou

- **Germline Specification and Pre-Specification Events** *Mitinori Saitou,* Katsuhiko Hayashi, Shankar Srinivas, Azim Surani
- **Synthetic Primate Embryology** *Monika Ward,* Ge Guo, Amander Clark, Kyle Orwig
- **Synthetic Biology and Genome Editing** *James Turner,* Misao Fujita, Insoo Hyun
- **Signals to the Germline** *Josephine Bowles,* Shosei Yoshida, Tessa Lord, Diana Laird
- **Silencing Events in the Germline** *Jon Oatley,* Bernhard Payer, Paula Cohen, Satoshi Namekawa
- **Environmental Effects on Epigenetic Programming** *Patrick Allard,* Folami Ideraabdullah, Sarah Kimmins, Wei Xie
- **RNA Metabolism and Translational Control** *Victor Ruthig,* Miguel Ramalho-Santos, Donal O'Carroll, Mofang Liu
- **Mutation and Aneuploidy in the Germline** *Ignasi Roig,* Melina Schuh, Eva Hoffmann, Aurora Ruiz-Herrera
- **Meiosis** *Paula Cohen,* Jesus Page, Peter Fraser, Bernard de Massy, Devanshi Jain
- **The GRC Power Hour™** *Paula Cohen*

Heterocyclic Compounds

Creating Connections with Heterocycles

JUN 18-23, 2023

SALVE REGINA UNIVERSITY, NEWPORT, RI

CHAIR: Catharine Larsen

VICE CHAIR: Eric Voight

- **Creative Approaches to Heterocyclic Targets** *Florence Williams,* Lisa Marcaurelle, Andrew Parsons
- **Heterocycles to Probe Biological Activity** *Jeanne Bolliger,* Charles Yeung, Ying Wang, Maryll Geherty
- **Advances in Catalytic Methods and Mechanisms** *Zarko Boskovic,* Helma Wennemers, Travis Williams, Andrew McNally, Anna Wenzel
- **Exploring Heterocyclic Chemistry** *Christine Le,* Jeffrey Aubé, Courtney Roberts, Mark Levin, Mary Watson
- **Heterocyclic Natural Products** *Kevin Kou,* Jon Njardarson, Victoria Piunova, Tadeusz Molinski
- **Novel Strategies of Construction with Heterocycles** *Cheyenne Brindle,* Donald Watson, Corinna Schindler, Hosea Nelson
- **Harnessing Heterocyclic Compounds as Therapeutics** *Dave Martin,* Sabine Hadida, Francisco Gonzalez-Bobes, Dani Schultz
- **Transforming Heterocycles** *Myles Smith,* Vanessa Marx, Thomas Beauchamp
- **Keynote Session: Innovations Fueled by Heterocycles** *Sophie Rousseaux,* Stefan France, Alison Wendlandt, Dean Toste
- **The GRC Power Hour™** *Florence Williams, Stefan France*

High Temperature Corrosion +GFS

Degradation Mechanisms, Life Prediction and Improved Materials for Application in Extreme Environments

JUL 16-21, 2023

COLBY-SAWYER COLLEGE, NEW LONDON, NH

CHAIR: Bruce Pint

VICE CHAIR: Shigenari Hayashi

- **New Insights into the Reactive Element Effect** *Christine Geers,* Mike Finnis, Satoshi Kitaoka
- **Modeling High Temperature Corrosion Processes** *Peter Tortorelli,* Rishi Pillai, Yilun Gong, Itai Panas
- **ICME for High Temperature Corrosion** *Clara Desgranges,* Ji-Cheng (JC) Zhao, Adrien Couet
- **Progress in Understanding H2O Mechanisms** *David Young,* Michihisa Fukumoto, Anton Chyrkin
- **New Alloys and Processes for High Temperature** *Masao Takeyama,* Daniel Monceau, Zachary Cordero
- **Development of Environmental Barrier Coatings** *Elizabeth Opila,* Rebekah Webster, David Poerschke
- **Coatings: Laboratory and Field Studies** *Alina Aguero,* Xuan Liu, Elisa Zaleski, Voramon Dheeradhada
- **Deposit-Induced Corrosion** *Brian Gleeson,* Simon Gray, Dmitry Naumenko, Xabier Montero
- **Keynote Session: The Low Carbon Future** *John Shingledecker,* Neva Espinoza
- **The GRC Power Hour™** *Mike Maloney*

High Throughput Chemistry and Chemical Biology +GFS

Employing Fundamental Biology and Chemical Space to Probe Cellular Homeostasis

JUL 30 - AUG 4, 2023

COLBY-SAWYER COLLEGE, NEW LONDON, NH

CHAIR: Ann Rowley

VICE CHAIRS: Deborah Rothman and Brian Paegel

- **Keynote Session: Analysis of Chemical and Biological Complexity at Scale** *Jay Schneekloth,* Petra Dittrich, Polly Fordyce
- **RNA: Structure and Drug Discovery** *MariJean Eggen,* Amanda Hargrove, Kerrie Spencer, Jessica Brown
- **Leveraging Artificial Intelligence for Privileged Tool Development** *William Pomerantz,* Jean-Louis Reymond, Nessa Carson, Thomas Grike
- **Reaction Scouting for High-Throughput Chemistry and DELs** *Alexander Satz,* Dennis Gillingham, Iulia Strambeanu
- **Expanding and Understanding Diversity: DELs and Cheminformatics** *Zhicai Shi,* Anokha Ratnayake
- **Chemical Probes and Phenotypic Cellular Assays** *Damian Young,* Jason Sello, Jennifer Heemstra, Jacquin Niles, Heidi Greulich
- **Inflammasomes: Dissecting and Interrogating Inflammasome Pathways** *Amber Hackler,* Rebecca Coll, Arturo Zychlinsky, Daniel Bachovchin
- **Cutting-Edge Omics Tools and Integration into Drug Discovery** *Albert Bowers,* Christian Münch, Keriann Backus, Christopher Parker
- **Keynote Session: Expanding Novel Platforms to Probe Biological Pathways** *Mark Fitzgerald,* Stacy Malaker, Ingrid Wertz, Sara Buhrlage
- **The GRC Power Hour™** *Jennifer Heemstra, Kerrie Spencer*

Histone and DNA Modifications NEW!

Chromatin Modifications in Health and Disease

JUN 11-16, 2023

BRYANT UNIVERSITY, SMITHFIELD, RI

CHAIRS: Tatiana Kutateladze and Tom Muir

VICE CHAIRS: Cheryl Arrowsmith and Robert Schneider

- **Discoveries of Epigenetic Modifications** *Cheryl Arrowsmith,* Robert Roeder, Dinshaw Patel
- **Histone Lysine Methylation: Biology and Molecular Mechanisms** *Xiaobing Shi,* Or Gozani, Juerg Mueller, Yang Shi, Kai Ge
- **Biological Role of Histone Lysine Acylation** *Mark Bedford,* Xiaobing Shi, Jacques Cote, Hong Wen, Benjamin Garcia
- **Histone lysine Acylation: Molecular Mechanisms** *Hong Wen,* Ming-Ming Zhou, John Denu, Philip Cole, Haitao Li, Wenshe Liu, Christopher Schofield
- **Crosstalk of Histone PTMs** *Ming-Ming Zhou,* Alessio Ciulli, Erin Green, Mark Bedford
- **Chromatin Biology and DNA and RNA Modifications** *Brian Strahl,* Steve Jacobsen, Peter Jones, Joshua Black, Shannon Lauberth, Scott Rothbart, Daniel Panne
- **Nucleosome Modifications: Molecular Mechanisms** *Steve Jacobsen,* Xiaodong Cheng, Brian Strahl, Beat Fierz
- **Histone, DNA and RNA Modifications and Human Disease** *Danica Fujimori,* Greg Wang, Ian Maze, Johnathan Whetstine, Akihiko Yokoyama
- **Epigenetic Therapeutics** *Alessio Ciulli,* Lindsey James, Danica Fujimori
- **The GRC Power Hour™** *Robert Schneider, Shannon Lauberth*

Hormone-Dependent Cancers +GRS

Understanding and Exploiting Genomic Aberrations and Microenvironmental Adaptations

AUG 6-11, 2023

GRAND SUMMIT HOTEL AT SUNDAY RIVER, NEWRY, ME

CHAIR: Felix Feng

VICE CHAIR: Leonie Young

- **Keynote Session: Advances in Targeting Steroid Receptors** *Wayne Tilley,* Geoffrey Greene, Steffi Oesterreich, Karen Knudsen
- **DNA Repair Deficiency in Hormone-Dependent Cancers** *Steve Balk,* Luc Furic, Peter Nelson, Robert Bristow
- **Cancer Genomics and Genetics** *Alex Swarbrick,* Scott Dehm, Adrian Lee, David Quigley, Housheng He, Jay Gertz
- **Drivers of Heterogeneity and Progression in Hormone-Dependent Cancers** *Charlotte Bevan,* Wilbert Zwart, Theresa Hickey, Myles Brown
- **Tumor Immunology and Dormancy** *Luke Selth,* Katherine Aird, John Lee, Maria Vivanco
- **The Evolving Role of Tumor Microenvironment in Cancer Progression** *Daniel Frigo,* Saraswati Sukumar, Karen Blyth, Walid Khaled, Leigh Ellis, Joshua Lang
- **Novel Targets and Clinical Trials in Hormone-Related Cancers** *Carlo Palmieri,* Elgene Lim, Amina Zoubeidi
- **Defining and Addressing the Next Big Question in Hormone-Related Cancers** *Luca Magnani,* Christopher Sweeney, Damir Varešlija
- **Translating Novel Targets in Hormone-Related Cancers into the Industry Setting** *Jennifer Richer,* Massimo Loda, Ciara Metcalfe, Scott Tomlins
- **The GRC Power Hour™** *Karen Knudsen*

Human Genetics and Genomics +GRS

Human Genetics: Advances to Support Scalability

JUL 9-14, 2023

WATERVILLE VALLEY, WATERVILLE VALLEY, NH

CHAIR: Wendy Chung

VICE CHAIR: Shamil Sunyaev

- **Learning From Large Cohorts** *Jennifer Posey,* Richard Scott, Anastasia Wise, Anjene Musick
- **Mendelian Genetics and Clinical Implementation** *Yufeng Shen,* Jennifer Posey, Nara Lygia Sobreira, Shinya Yamamoto, Sharon Plon
- **Use of Human Genetics in Drug Development** *John Stamatoyannopoulos,* Emmanouil Dermitzakis, Stella Aslibekyan
- **Novel Statistical Methods Using Large Data Sets** *Eimear Kenny,* Manuel Rivas, Jonathan Marchini, Benjamin Neale, Eleazar Eskin, Po-Ru Loh
- **Treatments for Rare Genetic Diseases** *Sharon Plon,* Stanley Crooke, Yael Weiss
- **Population Genetics Using Large Data Sets** *Shamil Sunyaev,* Michael Talkowski, Jeremy Berg, Kelley Harris, John Novembre, Mashaal Sohail
- **Genetics of Structural Anomalies** *Michael Talkowski,* Sarah Morton, Yufeng Shen
- **Genome Function and Regulation** *Manuel Rivas,* Barak Cohen, Peter Kharchenko, Len Pennacchio, John Stamatoyannopoulos, Nicole Soranzo
- **Power of Diverse Population Cohorts** *Benjamin Neale,* Nicholas Katsanis, Eimear Kenny
- **The GRC Power Hour™** *Susan Slaugenhaupt*

Hydrogen-Metal Systems +GRS

Dynamics of Hydrogen in Materials and Molecules

JUN 25-30, 2023

LES DIABLERETS CONFERENCE CENTER, LES DIABLERETS, SWITZERLAND

CHAIRS: Tom Autrey and Ping Chen

VICE CHAIRS: Rana Mohtadi and Yaroslav Filinchuk

- **Dynamics of Transport and Utilization of Hydrogen** *Martin Dornheim,* Hanna Breunig, Bill David
- **Hydrogen Carriers: Energy Storage in Chemical Bonds** *Craig Buckley,* Todd Brix, Mark Bowden, Hyangsoo Jeong
- **Selected Poster Presentations** *Chiara Milanese*
- **Catalysis and Hydrides in Chemical Conversions** *Petra De Jongh,* Long Qi, Zhaomin Hou, Christophe Coperet
- **Hydrogen Adsorption** *Thomas Gennett,* Valeska Ting, Martin Head-Gordon
- **Ion Conduction: Hydrides, Protons, Anions and Cations** *Shin-ichi Orimo,* Ryan O'Hayre, Bernard Dam, Soshi Iimura
- **Hydrides Under Pressure** *Claudia Zlotea,* Paul Loubeyre, ChangQing Jin
- **Borides and Clusters: Synthesis, Characterization and Energy Storage** *Beth Bosley,* Alexander Spokoyny, Takahiro Kondo
- **Keynote Session: Forty Years of Hydrogen Metal Systems and the Dynamic Future** *Ned Stetson,* Michael Felderhoff, Etsuo Akiba, Paul Lucchese
- **The GRC Power Hour™** *Sarah Shulda*

Inhibition in the CNS +GRS

Assembly and Function of Inhibitory Neurons in Health and Disease

JUL 16-21, 2023

LES DIABLERETS CONFERENCE CENTER, LES DIABLERETS, SWITZERLAND

CHAIRS: Beatriz Rico and Marlene Bartos

VICE CHAIRS: Gordon Fishell and Attila Losonczy

- **Keynote Session: Interneuron and Principal Cell Signaling During the Sensory Experience and Spatial Coding** *Gordon Fishell,* Gina Turrigiano, Ivan Soltesz
- **Excitation Inhibition Balance in Developing and Mature Circuits** *Rosa Cossart,* Sonia Garel, Linda Van Aelst, Natalia De Marco Garcia, Nathalie Rochefort
- **Functional and Structural Plasticity of GABAergic Cells** *Alberto Bacci,* Juan Burrone, Elly Nedivi, Pico Caroni, Daniel Feldman
- **Inhibition and Sensory Information Processing in the Somatosensory Cortex** *Alison Barth,* Johannes Letzkus, Carl Petersen, James Poulet
- **Inhibition and Network Dynamics in Prefrontal Cortex: Decision-Making, Enhanced Attention and Gambling** *Attila Losonczy,* Thomas Klausberger, Adam Kepecs, Ofer Yizhar, Marie Carlen
- **Inhibitory Subnetworks During Learning** *Liset Menendez de la Prida,* Hannah Monyer, David Dupret, Vikaas Sohal, Lisa Topolnik
- **Modulation of Inhibition, Memory and Sleep** *Imre Vida,* Liping Wang, Gábor Nyiri, Dilja Krueger-Burg, Joshua Trachtenberg
- **Influence of Inhibition on Coding and Network Synchronization in Diseases** *Chris McBain,* Carlos Portera-Cailliau, Claudia Bagni, Peyman Golshani, Jorge Palop
- **Inhibition in Human: Molecular Programs, Circuitries and Networks** *Zoltan Nusser,* Nenad Sestan, Caroline Robertson, David Lewis, Dimitri Kullmann
- **The GRC Power Hour™** *Rosa Cossart*

Interior of the Earth +GRS

Material Properties of the Mantle and Core and their Constraints, Causes and Consequences for Earth Evolution

JUN 18-23, 2023

MOUNT HOLYOKE COLLEGE, SOUTH HADLEY, MA

CHAIR: Maureen Long

VICE CHAIR: Karen Fischer

- **Stability of Melt in the Mantle** *Joe Byrnes,* Jie Deng, Sanne Cottaar
- **The Upper Mantle: Rheology, Conductivity and (An)elasticity** *Colleen Dalton,* Kristel Chanard, Elvira Mulyukova, Samer Naif
- **Mantle Convection and Mixing and the Role of the Transition Zone** *Abby Kavner,* Tauzin Benoit, Matthew Jackson
- **Physical and Chemical Heterogeneity and the Dynamics of the Lower Mantle** *Vedran Lekic,* Harriet Lau, Jennifer Jackson, Juliane Dannberg
- **The Lithosphere-Asthenosphere System and D" as Mantle Boundary Layers** *Maxim Ballmer,* Zach Eilon, Carolina Lithgow-Bertelloni
- **Journey to the Center of the Earth: The Core** *Peter Driscoll,* Daniel Frost, Jonathan Aurnou
- **Probing the Material Properties of Planetary Interiors** *Bradford Foley,* Alex Evans, Caroline Beghein
- **The Early Earth and Controls on Earth Evolution** *Rita Parai,* Jesse Reimink, Peng Ni, Yoshinori Miyazaki
- **Keynote Session: Future Directions in Earth's Interior Research** *Rachel Bernard,* Mark Panning
- **The GRC Power Hour™** *Karen Fischer*

Lactic Acid Bacteria Biology, Symbioses and Applications NEW!

Beneficial Microbes in the Environment and Health

JUL 23-28, 2023

FOUR POINTS SHERATON / HOLIDAY INN EXPRESS, VENTURA, CA

CHAIRS: Maria Marco and Robert Britton

VICE CHAIRS: William Ludington and Jan Peter van Pijkeren

- **Keynote Session: Evolution** *Giovanna Felis,* Rodolphe Barrangou, Paul O'Toole
- **Metabolism** *Sybille Tachon,* Michiel Kleerebezem, Herwig Bachmann
- **Bacteriophages** *Jan Peter van Pijkeren,* Breck Duerkop, Sylvain Moineau
- **Cell Surface** *Robert Scheffler,* Kimberly Kline, Oscar Kuipers, Marie-Pierre Chapot-Chartier
- **Intestinal Symbioses** *Anthony Shiver,* Satya Dandekar, Francois Leulier
- **Food Ecosystems** *Bob Hutkins,* Michael Gänzle, Benjamin Wolfe
- **Vaginal Symbioses** *Katy Patras,* Jacques Ravel, Sarah Lebeer
- **Biotherapeutics** *Sara Di Rienzi,* Christine Beeton, Mindy Engevik, Yvonne Kapila
- **Synthetic Biology** *William Ludington,* Caroline Ajo-Franklin, Nikhil (Nik) Nair
- **The GRC Power Hour™** *Sarah Lebeer*

Laser Diagnostics in Energy and Combustion Science +GRS

Advancing Optical Diagnostics for Future Energy Systems

JUL 9-14, 2023

GRAND SUMMIT HOTEL AT SUNDAY RIVER, NEWRY, ME

CHAIR: Terrence Meyer

VICE CHAIR: Simone Hochgreb

- **Keynote Session: Prospects in Ultrafast Lasers and Spectroscopy** *Simone Hochgreb,* Ursula Keller
- **New Light Sources for High-Speed Imaging and Spectroscopy** *Ursula Keller,* Mikhail Slipchenko, Mitchell Spearrin, James Michael
- **Diagnostics for Electrochemical Energy Conversion and Storage** *Claire Villevieille,* Eugene Smotkin, Christian Brackmann
- **Advances in Measurements for High-Speed Flows** *Paul Danehy,* Yi Mazumdar, Timothy Fahringer, Naibo Jiang
- **Interrogating Droplets, Aerosols, and Particulates** *Yannis Hardalupas,* Carmela Russo, Lars Zigan
- **In Situ Diagnostics for Engine Applications** *Mitchell Spearrin,* Gaetano Magnotti, Venkat Athmanathan, Julien Manin
- **High-Resolution Particle Image Velocimetry** *Daniel Schanz,* Jerry Westerweel, Jeffrey Sutton
- **Advances in Ultrafast Laser Spectroscopy** *Sean Kearney,* Ali Hosseinnia, Chloe Dedic, Daniel Richardson
- **Optical Diagnostics for Surface and Near-Surface Reactions** *Johan Zetterberg,* Christian Hess, Benoit Fond
- **The GRC Power Hour™** *Francesca De Domenico,* Jacqueline O'Connor

Lasers in Micro, Nano and Bio Systems +GRS

Emerging Platforms, Concepts and Materials for Small(er) Lasers and New Applications of Small Lasers

JUN 4-9, 2023

MOUNT SNOW, WEST DOVER, VT

CHAIR: Malte Gather

VICE CHAIRS: Teri Odom and Lan Yang

- **Natural and Bioinspired Resonant Photonics** *Alon Gorodetsky,* Mathias Kolle, Silvia Vignolini
- **Miniaturization of Lasers and Resonant Structures** *Lan Yang,* Arseniy Kuznetsov, Peidong Yang, Hong-Gyu Park
- **Biointegrated Lasers** *Andrea Armani,* Seok-Hyun Andy Yun, Marcel Schubert
- **Emerging Materials and Platforms for Optical Gain: Organics and Perovskites** *Graham Turnbull,* Chihaya Adachi, Letian Dou, Yohei Yamamoto
- **Lasing in Living Systems** *Xudong (Sherman) Fan,* Yu-Cheng Chen, Matjaz Humar
- **Resonators and Lasers for Biosensing** *Sile Nic Chormaic,* Laura Lechuga, Thomas Krauss
- **Advances in Resonator Geometries** *Hui Cao,* Riccardo Sapienza, Femi Ojambati
- **Polaritonic and Toplogical Lasers** *Vinod Menon,* Hui Deng, Mercedeh Khajavikhan, Sebastian Klembt
- **Emerging Materials and Platforms for Optical Gain: Inorganics** *Teri Odom,* Emory Chan, Detlev Grützmacher
- **The GRC Power Hour™** *Lan Yang, Teri Odom*

Liquid Crystals +GRS

Learning From Nature to Transform Technology through Liquid Crystal Science

JUN 25-30, 2023

SOUTHERN NEW HAMPSHIRE UNIVERSITY, MANCHESTER, NH

CHAIRS: Jan Lagerwall and Cecilia Leal

VICE CHAIRS: Elda Hegmann and Timothy Atherton

- **Liquid Crystalline Arrangements in Nature and From Bioderived Components** *Irena Drevensek-Olenik,* Mohan Srinivasarao, Silvia Vignolini
- **Self-Assembly in Lyotropic Liquid Crystals, Colloids and Polymers** *Ivan Smalyukh,* Helen Gleeson, Daniel Hammer, Johanna R. Bruckner, Mahesh Mahanthappa, Evan Scott, Matthew Helgeson
- **Living Liquid Crystals** *Chenhui Zhu,* Alison Sweeney, Nikta Fakhri
- **Pushing the Boundaries of Active Matter Research** *Andreas Menzel,* Douglas Cleaver, Anupam Sengupta, Francesca Serra, Linda Hirst, Daniel Beller, Margaret Gardel
- **The Benefits of Polymerizing Liquid Crystals** *Chinedum Osuji,* Arri Priimägi, Julie Kornfield, Emily Davidson, Jonathan Whitmer
- **Power of Liquid Crystals: Industry and Defense Perspectives** *Dirk Broer,* Jennifer Schaefer, Timothy White, Danqing Liu, Kristopher Lavery, Lu Lu, Timothy Bunning
- **Early-Career Investigator Presentations** *Taylor Ware,* Randall Kamien
- **Geometry, Confinement and Chirality** *Verena Gortz,* David Walba, Teresa Lopez Leon, Apala Majumdar, Sabetta Matsumoto, Yuka Tabe, Torsten Hegmann
- **Application Opportunities Through Unconventional Liquid Crystal Science** *Xiaoguang Wang,* Cecilia Roque, Santanu Kumar Pal, Young-Ki Kim, Nicholas Abbott
- **The GRC Power Hour™** *Timothy Atherton, Shu Yang*

Lung Development, Injury and Repair +GRS

Post-COVID Return to Respiratory Health

AUG 13-18, 2023

WATERVILLE VALLEY, WATERVILLE VALLEY, NH

CHAIRS: Rory Morty and Xin Sun

VICE CHAIRS: Darrell Kotton and Susan Majka

- **Keynote Session: Post-COVID Opportunities to Broaden Lung Biology** *Justinn Barr,* James Kiley
- **Post-COVID Priorities in Lung Injury Repair** *Lynn Schnapp,* Edward Morrisey, Enid Neptune, Jianwen Que
- **Tipping the Balance From Dysplastic to Regenerative Repair** *Stijn De Langhe,* Anny Zhou, Zea Borok, Peter Chen
- **An Ageless Lung** *Wellington Cardoso,* Daniel Swarr, Jichao Chen, Anne-Karina Perl, Jennifer Sucre
- **Insights From Single Cell Resolution** *Gloria Pryhuber,* Maya Kumar, John Engelhardt, Kerstin Meyer
- **Fibroblasts** *Daniel Tschumperlin,* Rachel Knipe, Jonathan Kropski, Tien Peng, Elie El Agha
- **The Lung as a Sensory Organ** *Jie Sun,* Christin Kuo, Nora Barrett, Andrew Vaughan, Leah Reznikov, Sara Prescott
- **Circulating Cells in the Lung-Body Dialogue** *Laura Crotty Alexander,* Eniko Sajti, G.R. Scott Budinger, William Janssen, Nicholas Lukacs, Mark Looney
- **The Rules and Exceptions of Pulmonary Vessels** *Jaymin Kathiriya,* Harry Karmouty Quintana, Grazyna Kwapiszewska, Larissa Shimoda
- **The GRC Power Hour™** *Denise Al Alam, Laura Crotty Alexander*

Lysosomal Diseases +GRS

Connecting Function to Pathophysiology for Innovative Therapies

MAY 14-19, 2023

REY DON JAIME GRAND HOTEL, CASTELLDEFELS, SPAIN

CHAIRS: Timothy Cox and Volkmar Gieselmann

VICE CHAIRS: Cynthia Tifft and Paul Saftig

- **Keynote Session: Lysosomal Function in Health and Disease** *Tony Futerman,* Frances Platt, Alessandra D'Azzo
- **Newly Identified Disease Mechanisms and Protein Function** *Steven Walkley,* Bruno Gasnier, Alessia Calcagni, Sabrina Jabs, Joseph Mindell, Shawn Ferguson, Markus Damme, Judith Klumperman
- **Lysosomal Cross Talk with Other Organelles** *Andrea Ballabio,* Rosa Puertollano Moro, Lalita Ramakrishnan, Meng Wang
- **Mechanistic Aspects of Lysosomal Diseases and Lysosomal Protein Function** *Frances Platt,* Hans Aerts, Dominic Winter, Volker Haucke, Gennaro Napolitano, Emil Gustavsson, Nouf Laqtom
- **Function of Lysosomal Enzymes In The Immune System** *Lalita Ramakrishnan,* Jutta Gärtner, Elena Pavlova, Nan Yan
- **Incoming Therapies** *Hans Aerts,* Derralynn Hughes, Anna Bakardjiev, Ulrich Matzner
- **Late-Breaking Topics** *Thomas Braulke,* Alessandra D'Azzo
- **Gene Therapy of Lysosomal Diseases** *Jeffrey Medin,* Patricia Dickson, Jacinthe Gingras, James Wilson
- **Small Molecule Therapies for Lysosomal Diseases** *James Shayman,* S Pablo Sardi, Giancarlo Parenti, Raphael Schiffmann, Lars Schlotawa
- **The GRC Power Hour™** *Cynthia Tifft*

Malaria +GRS

Reinvigorating Malaria Control, Prevention and Treatment: From Bench to Bedside to Bednets

MAY 28 - JUN 2, 2023

REY DON JAIME GRAND HOTEL, CASTELLDEFELS, SPAIN

CHAIR: Terrie Taylor

VICE CHAIR: Faith Osier

- **Keynote Session: A Pivot Point for Malaria Treatment, Control and Eradication** *Faith Osier,* Abdisalan Noor, Kevin Marsh, Ify Aniebo

> ***"GRCs are an excellent mechanism for building communities that support career advancement for junior and senior scientists alike. GRCs in recent years have helped promote diversity and inclusion among their participants."***
>
> DR. CYNTHIA BURROWS, University of Utah

- **Visualizing Malaria Pathogenesis: The Real Deal versus Model Systems** *Himanshu Gupta,* Christopher Moxon, Mara Lawniczak, Chet Joyner, Kevin Couper, Maria Bernabeu
- **Malaria Pathogenesis** *Arjen M Dondorp,* Kamija Phiri, Andrea Conroy, Richard Idro, Julie Gutman
- **Enhancing Antimalarial Immunity, Up to But Not Including Vaccines** *Yaw Bediako,* Prasanna Jagannathan, Francis Ndungu, Teun Bousema, Hedda Wardemann
- **Vaccine-Mediated Immunity** *Ashley Birkett,* Simon Draper, Adrian Hill, Georgia Tomaras, Ally Olotu, Neville Kisalu, Michelle Boyle
- **Advances in Vector Biology** *Charles Wondji,* Marta Ferreira Maia, Elena Levashina, Fredros Okumu, Flaminia Catteruccia
- **Identifying, Tracking and Treating Silent Reservoirs of Infection** *Brian Greenwood,* Lauren Cohee, Steven Kho, Alassane Dicko, Photini Sinnis
- **Malaria Morbidity: The Burden of Disease in Survivors** *Ruth Namazzi,* Chandy John, Gretchen Birbeck, Paul Bangirana, Amina Abubakar, Ryan D'Arcy
- **Keynote Session: Anticipating Opportunities and Challenges** *Ify Aniebo,* Abdoulaye Djimde, Don Mathanga, Kenny Evans
- **The GRC Power Hour™** *Kim Lindblade, Amy Bei*

Mammary Gland Biology +GRS

Molecules and Mechanisms From Normal Biology to Cancer

MAY 28 - JUN 2, 2023

MOUNT SNOW, WEST DOVER, VT

CHAIRS: Russell Hovey and Senthil Muthuswamy

VICE CHAIRS: Walid Khaled and Leonie Young

- **Keynote Session: Phenotypic and Genetic Approaches for Personalized Treatment** *Jeffrey Rosen,* D. Joseph Jerry
- **Mapping Normal and Diseased States** *Geoffrey Wahl,* Nienke Bosschaart, Nicholas Navin, Kornelia Polyak
- **Nutrients and Metabolism in Normal and Cancer** *Jenifer Monks,* Alex Toker, John Wysolmerski, Erik Nelson
- **Hormonal and Systemic Regulation of Normal Biology and Cancer** *Leonie Young,* Lindsay Hinck, Pepper Schedin, Myles Brown
- **Microbiome and Inflammation in Normal Biology and Cancer** *Walid Khaled,* David Mills, Dipali Sharma, Mikala Egeblad
- **Microenvironmental Modulation of Development, Function and Cancer** *Heather Machado,* Xiang Zhang, Philipp Scherer, Michael Angelo
- **Immune Modulation in Normal Biology and Cancer** *Kaylee Schwertfeger,* Forest White, Marcia Haigis, Tomonori Nochi
- **Epigenetics and Plasticity During Normal Biology and Cancer** *Heide Ford,* Jayanta Debnath, Min Yu, Yibin Kang
- **Keynote Session: Lifestyle, Genetic Factors and Breast Cancer Etiology** *D. Joseph Jerry,* A. Heather Eliassen
- **The GRC Power Hour™** *Lindsay Hinck, Jeffrey Rosen*

Mechanisms of Membrane Transport +GRS

Unraveling the Mechanisms of Membrane Transport: Structure, Dynamics and Allosteric Regulation

JUN 18-23, 2023

LES DIABLERETS CONFERENCE CENTER, LES DIABLERETS, SWITZERLAND

CHAIRS: Janice Robertson and David Drew

VICE CHAIRS: Vera Moiseenkova-Bell and Robert Tampé

- **Ultrastructure and Macromolecular Assemblies in the Membrane** *Jianping Wu,* Justin Taraska, Simon Scheuring
- **Mechanisms of Secondary Active Transporters** *Nicolas Reyes,* Lucy Forrest, Liang Feng, Simon Newstead, Gary Rudnick
- **Interrogating Dynamic Transport** *Claus Loland,* Katherine Henzler-Wildman, Olga Boudker
- **Membrane-Dependent Regulation of Transport** *Lucie Delemotte,* Grace Brannigan, Jose Faraldo-Gomez, Sara Liin, Joseph Mindell
- **Design and Folding of Membrane Transporters** *Karen Fleming,* Peilong Lu, Nir Fluman, Bil Clemons
- **The New World of Hybrid Transport** *Cristina Paulino,* Show-Ling Shyng, Raimund Dutzler, Harley Kurata
- **Mechanisms of ATP Coupled Transport** *Kaspar Locher,* Heather Pinkett, Bert Poolman
- **Structure, Dynamics and Allostery of Ion Channels** *Crina Nimigean,* Ann McDermott, Anna Stary-Weinzinger, Cedric Govaerts, Zhen Yan
- **Physiological Connections to Transport Mechanisms** *David Clapham,* Rajini Rao, Thomas Jentsch, Robert Edwards
- **The GRC Power Hour™** *Lucy Forrest*

Mechanisms of Microbial Transcription +GRS

Microbial Transcription From Atomic Resolution to Cellular Landscapes

JUN 11-16, 2023

SOUTHERN NEW HAMPSHIRE UNIVERSITY, MANCHESTER, NH

CHAIRS: Ramesh Wigneshweraraj and Bryce Nickels

VICE CHAIRS: Scarlet Shell and Sean Crosson

- **Keynote Session: Emerging Insights into Microbial RNA Polymerase Structure, Function and Regulation** *Steve Busby,* Robert Landick, Xiaodong Zhang
- **Structural and Mechanistic Basis of Microbial Transcription** *Katsuhiko Murakami,* Seth Darst, Albert Weixlbaumer
- **Single Molecules Studies on Microbial Transcription** *Irina Artsimovitch,* Achillefs Kapanidis, Terence Strick, Jeff Gelles
- **Transcription Control in Microbes** *Deborah Hinton,* Richard Gourse, Wilma Ross, Paul Babitzke
- **Microbial Transcription at Systems Level** *Carol Gross,* Joseph Wade, Patrick Viollier, Teresa Cortes Mendez, Kathryn Ramsey
- **Microbial Transcription From Systems to Molecules** *Megan Bergkessel,* David Grainger, Tatiana Mishanina, Nikolay Zenkin
- **Spatial Transcription Regulation in Microbes** *Ramesh Wigneshweraraj,* Orna Amster-Choder, Jared Schrader, Stephanie Weber
- **RNA Regulation in Microbes** *Katharina Höfer,* Kristine Arnvig, Kathrin Fröhlich, Sine Lo Svenningsen
- **Post-Transcriptional Regulation in Microbes** *Masatoshi Miyakoshi,* Katharina Höfer, Kai Papenfort
- **The GRC Power Hour™** *Scarlet Shell*

Medicinal Chemistry +GRS

Emerging Science to Enable Drug Discovery

AUG 6-11, 2023

COLBY-SAWYER COLLEGE, NEW LONDON, NH

CHAIR: Michael Ellis

VICE CHAIR: Erin DiMauro

- **Tackling Mutants and Difficult to Drug Targets** *Callie Bryan,* Jennifer Allen, Kelley Shortsleeves
- **Covalent Approaches to Challenging Targets** *Joachim Rudolph,* Hasnain Malik, Jason Green
- **Breakthroughs** *Meredeth McGowan,* Christopher Bungard
- **Platform-Based Approaches to Empower Drug Discovery** *Julia Haas,* Elena Koltun, Manj Lall
- **First in Class** *Amy Hart,* Beth Thomas
- **Lessons Learned From Discontinued Leads** *Yue-Mei Zhang,* David Weinstein, Emily Peterson, Xueqing Wang
- **Advances in Screening and Lead Generation** *Thomas Durand-Reville,* Petrina Kamya, Joseph Carpenter
- **Late-Breaking Topics: First Disclosures of Clinical Candidates** *H. Rachel Lagiakos,* Dean Brown
- **Keynote Session: Activity-Based Proteomics: Protein and Ligand Discovery on a Global Scale** *Michael Ellis, Benjamin Cravatt*
- **The GRC Power Hour™** *Emily Peterson, David Marcoux*

Membrane Protein Folding +GRS

Linking Fundamental Principles to Cellular Biosynthesis

JUN 25-30, 2023

REY DON JAIME GRAND HOTEL, CASTELLDEFELS, SPAIN

CHAIR: Paula Booth

VICE CHAIR: Linda Columbus

- **Membrane Systems: Proteins, Lipids and Organization** *Liz Miller,* M. Madan Babu, Robert Ernst
- **Protein Insertion, Translocons and Regulation** *Nir Fluman,* Ramanujan Hegde, Rebecca Voorhees, Jan Kubicek
- **Co-Translational Folding, Misfolding, Aggregation and Disease** *Jonathan Schlebach,* Alina Guna, Sonya Neal
- **Membrane Protein Organization and Lipid Regulation** *Heather Pinkett,* Barbara Imperiali, Mikhail Bogdanov, Steven Harborne
- **Folding and Assembly of Beta Barrels** *Anastassia Vorobieva,* Taylor Devlin, Meagan Belcher Dufrisne
- **Emerging Methods, Cell Free Approaches, Cell Mimicry and Synthetic Biology** *Kalina Hristova,* Neha Kamat, Tomoaki Matsuura
- **Insights into Folding and Misfolding Mechanisms Linked to Disease** *Heedeok Hong,* Vlad Ladizhansky, Charles Sanders

- **Computational Approaches to Folding, Design and New Therapeutics** *Martin Ulmschneider,* Robert Jefferson, Huong Kratochvil, Alan Mark, Peter Bond
- **Simulations of Spatial Organization and Signaling in the Membrane** *Sarah Veatch,* Jay Groves, Irina Moreira
- **The GRC Power Hour™** *Jonathan Schlebach, Anastassia Vorobieva*

Microbial Adhesion and Signal Transduction +GRS

Microbial Responses to Complex Environments

JUL 16-21, 2023

SALVE REGINA UNIVERSITY, NEWPORT, RI

CHAIRS: Raphael Valdivia and Melanie Blokesch

VICE CHAIRS: Fitnat Yildiz and Tracy Palmer

- **Bacterial Cell Surface Structures** *Tracy Palmer,* Guillaume Dumenil, Joanne Engel, M. Stephen Trent
- **Application of Imaging and Visualization Techniques** *Nina Salama,* Manuela Hospenthal, Ariane Briegel
- **Host-Microbe Interactions** *Fitnat Yildiz,* Renee Tsolis, John Mekalanos
- **Colonization, Adhesion and Host Impact** *Hank Seifert,* Kimberly Kline, Aimee Shen, Karen Guillemin
- **Bacteriophage and Host Defense** *Wai-Leung Ng,* Joseph Bondy-Denomy, Alexander Harms, Aude Bernheim
- **New Frontiers in Antimicrobials** *Mario Feldman,* Zemer Gitai, Ana Rita Brochado
- **Functional Microbiomes** *Andreas Baumler,* Eric Martens, Kerwyn Huang, Neil Surana, Karina Xavier
- **Signal Transduction** *Shumin Tan,* Petra Dersch, Andres Vazquez-Torres, Christopher Sassetti, Urs Jenal
- **Intracellular Infection** *Craig Roy,* Ralph Isberg, Heran Darwin, Sophie Helaine
- **The GRC Power Hour™** *Karen Ottemann*

Microbial Population Biology +GRS

Evolution and Ecology of Natural Microbial Communities

JUL 9-14, 2023

PROCTOR ACADEMY, ANDOVER, NH

CHAIRS: Rosie Redfield and Vaughn Cooper

VICE CHAIRS: Christina Burch and Rees Kassen

- **Microbial Communities of Fermented Foods** *Sijmen Schoustra,* Benjamin Wolfe, Delphine Sicard, Bernard Moonga
- **Intermicrobial Warfare** *Kevin Foster,* Melanie Blokesch, William Smith, Thierry Soldati
- **Origins and Evolution of Animal Epidemics and Pandemics** *Raina Plowright,* Jeff Foster, Kathryn Hanley, Wendy Turner
- **Origins and Evolution of Human Epidemics and Pandemics** *Bill Hanage,* Emma Hodcroft, Nathan Grubaugh, Judith Breuer, David Kennedy
- **Metabolic Interdependencies in Symbioses** *Nicole Dubilier,* Toby Spribille, Lee Henry, Nicole Gerardo
- **Interactions in Polymicrobial Infections** *Michael Surette,* Joao Xavier, Michel Koo, Katrine Whiteson, Chelsie Armbruster
- **COVID-19** *Bruce Levin,* Marc Lipsitch, Frank Snowden
- **Viruses as Drivers of Microbial Dynamics** *Maureen Coleman,* Debbie Lindell, Gil Amitai, Eugene Koonin, Matthew Sullivan
- **Planetary-Scale Microbiomes** *Paul Falkowski,* Valeria Souza, Naomi Levine, Alyson Santoro
- **The GRC Power Hour™** *Christina Burch*

Modulation of Neural Circuits and Behavior +GRS

Mechanisms that Underlie Flexible Neural Coding

MAY 21-26, 2023

LES DIABLERETS CONFERENCE CENTER, LES DIABLERETS, SWITZERLAND

CHAIRS: Mario De Bono and Lisa Stowers

VICE CHAIRS: Ilona Grunwald Kadow and Dayu Lin

- **Sensory Motor Systems** *Eugenia Chiappe,* Thomas Clandinin, Yvette Fisher, Megan Carey, Sophie Steculorum
- **Regulation and Function of Brain States** *Luis De Lecea,* Gilles Laurent, Steven Flavell
- **Flexible Regulation of Basic Biological Functions** *Adrienne Fairhall,* Kay Tye, Mala Murthy, Timothy O'Leary, Stephan Lammel
- **Modulation of Cells, Circuits and Behaviors** *Rainer Friedrich,* Tiago Branco, Isabel Beets, Cori Bargmann
- **Neuromodulation and Computation** *Tiago Branco,* Liqun Luo, Monica Dus, Yuki Oka
- **Sensory Modulation of Brain Functions** *Ilona Grunwald Kadow,* Nadine Gogolla, Michael Bruchas, Andreas Luthi, Garret Stuber
- **Social Behavior** *Dayu Lin,* Nirao Shah, Susana Lima, Bianca Jones Marlin, David Anderson
- **Mechanisms of Neuromodulation Beyond CNS Neurons** *Christian Lüscher,* Kira Poskanzer, Misha Ahrens, Inbal Goshen, Luis De Lecea
- **Principles of Neuromodulation Across Organisms** *Gilles Laurent,* Tessa Montague, Zachary Mainen, Rainer Friedrich
- **The GRC Power Hour™** *Kay Tye*

Molecular and Cellular Biology of Lipids +GRS

Regulation of the Structure and Function of Lipids and Lipid Metabolizing Enzymes in Signaling and Metabolism

JUL 23-28, 2023

WATERVILLE VALLEY, WATERVILLE VALLEY, NH

CHAIR: Daniel Raben

VICE CHAIR: Miriam Greenberg

- **Keynote Session: Dynamic Regulation of Lipid Metabolizing Enzymes** *Julie Saba,* Roger Williams
- **Membrane Architecture and Signaling** *Vytas Bankaitis,* Karin Reinisch, Nicolas Vitale, Tamas Balla, Patricia Bassereau
- **Physiology and Pathophysiology of Membrane Lipid Metabolism** *Raymond Blind,* Joost Holthuis, Lucio Cocco
- **Sensors and Analyses of Lipid Diversity and Dynamics** *Sandra Gabelli,* John Burke, Wonhwa Cho, Tatyana Igumenova, Jeremy Baskin
- **Lipid Droplets and Systemic Lipid Metabolism** *Michael Wolfgang,* James Olzmann, Karen Reue
- **Regulation of Membrane Lipids and Lipid Metabolites** *Binks Wattenberg,* Shamshad Cockcroft, Teresa Dunn, Michael Airola, Brooke Emerling
- **Lipid Metabolism in Yeast and Prokaryotes** *Eric Klein,* Shu-Sin Chng, Robert Ernst
- **Structure and Biochemistry of Lipid Metabolizing Enzymes** *Michael Airola,* Angeline Lyon, Sandra Gabelli, Fumio Sakane, Ku-Lung Hsu
- **Keynote Session: Lipid Metabolizing Enzymes: From Biochemistry to Physiology** *Miriam Greenberg,* Julie Saba
- **The GRC Power Hour™** *Julie Saba, Judith Storch*

Molecular Mechanisms in Evolution +GRS

Genetic and Phenotypic Evolution at the Organismal, Cellular and Molecular Levels

JUN 25-30, 2023

STONEHILL COLLEGE, EASTON, MA

CHAIRS: Judith Berman and Olivier Tenaillon

VICE CHAIRS: Daniel Jarosz and Shelley Copley

- **Keynote Session: Principles and Mechanisms of Genome Evolution** *Daniel Jarosz,* Rong Li, Eugene Koonin
- **Mechanistic Control of Molecular Evolution: A Tale of Mutation and Recombination Rates** *Ivan Matic,* Jade Wang, Nadia Singh
- **Evolution Beyond Single Nucleotide Variants: The Evolution of Genome Architecture** *Anna Selmecki,* Jef Boeke, Audrey Gasch, Adi Stern
- **Molecular Determinants of Atypical Heredity** *Mia Levine,* Sarah Zanders, Upasna Sharma
- **Protein Evolution: Lessons From Deep Scans and Large Databases** *Nobuhiko Tokuriki,* Martin Weigt, Douglas Fowler, Marc Ostermeier
- **Metabolism Evolution, Natural and Engineered Innovations** *Anne-Ruxandra Carvunis,* Markus Ralser, Bas Teusink, Julia Vorholt
- **Drugs, Germs and Genes: Evolution in Response to Stress and Drugs** *Jan Michiels,* Nathalie Balaban, Ran Friedman, Pleuni Pennings
- **Somatic and Cancer Evolution** *Jamie Blundell,* Ashby Morrison, Uri Ben-David, Dmitri Petrov
- **Epistasis and The Evolution of Complex Traits** *Nathan Springer,* Emma Farley, Mark Siegal, Gael Yvert
- **The GRC Power Hour™** *Nandini Krishnamurthy*

Molecular Membrane Biology +GRS

Function of Proteins and Lipids at Organelle Membranes in Health and Disease

JUL 16-21, 2023

PROCTOR ACADEMY, ANDOVER, NH

CHAIR: Christian Ungermann

VICE CHAIR: Maya Schuldiner

- **Keynote Session: Biogenesis and Function of Membranes** *Suzanne Pfeffer,* Tom Rapoport, Gillian Griffiths, Ramanujan Hegde
- **Connecting Membranes** *Lilach Sheiner, Jennifer Lippincott-Schwartz,* Robin Klemm, Maria Bohnert, William Prinz, Gia Voeltz
- **Metabolism and Signaling at Membranes** *Scott Emr,* Claudio De Virgilio, Rosa Puertollano Moro, Monther Abu-Ramaileh, Ralf Erdmann
- **Protein Biogenesis and Quality Control at Membranes** *Liz Miller, Rebecca Voorhees,* David Teis, Sonya Neal, Agnieszka Chacinska, Johannes Herrmann
- **Lipid Homeostasis at Membranes** *Randy Schekman,* Elina Ikonen, Christopher Stefan, Chris Loewen, Abdou Rachid Thiam
- **Membrane Remodeling, Fission and Fusion** *Jodi Nunnari, William Wickner,* Josep Rizo, Andreas Mayer, Heike Folsch, John Briggs
- **Disease, Infections and Treatments** *Fulvio Reggiori,* Lena Pernas, Neta Regev-Rudzki, Jens Brüning, Noboru Mizushima
- **Mechanisms of Organelle Identity** *Chris Fromme, Anne Spang,* Elvan Böke, Adam Hughes, Sean Munro, Jared Rutter
- **Novel Techniques in Molecular Membrane Biology** *Adam Frost,* Jeanne Stachowiak, Alanna Schepartz, Florian Fröhlich
- **The GRC Power Hour™** *Lois Weisman, Mary Munson*

Molecular Pharmacology +GRS

Progressive Technologies and Approaches Revealing Novel GPCR Biology and Drug Development Potential

JUN 11-16, 2023

LES DIABLERETS CONFERENCE CENTER, LES DIABLERETS, SWITZERLAND

CHAIRS: Andrew Tobin and Martine Smit

VICE CHAIRS: Marta Filizola and J. Silvio Gutkind

- **Keynote Session: Future Prospects in GPCR-Biology and Drug Discovery** *Marta Filizola,* Fiona Marshall, Arthur Christopoulos
- **Systems Biology and AI in GPCR-Based Disease and Treatments** *Martin Lohse,* Michel Bouvier, Graham Ladds, Jana Selent, Aurélien Rizk
- **Emerging GPCR Drug Targets** *J. Silvio Gutkind,* Aashish Manglik, Gunnar Schulte, Chloe Peach, Thomas Sakmar
- **Structural Basis of Receptor Function** *Patrick Sexton,* Denise Wootten, Sebastien Granier, Brian Volkman, Christopher Tate, Gebhard Schertler
- **GPCR Pharmacogenetics** *David Gloriam,* Maria Marti Solano, Alexander Hauser
- **Intelligent Drug Design** *Fiona Marshall,* Alastair Brown, Brian Shoichet, Graeme Milligan, Bryan Roth, David Gloriam, Lora Heisler
- **GPCR Signal Transduction** *JoAnn Trejo,* Jean Philippe Pin, Miriam Stoeber, Brian Kobilka, Julia Drube
- **Advanced Approaches in GPCR Research** *Roger Sunahara,* Davide Calebiro, Andrea Kliewer, Stefan Schulz, Jin Zhang, John Tesmer, Louis Dwomoh, Caitrin Crudden, Martha Sommer
- **Advances in Receptor Physiology and Translation** *Graeme Milligan,* Carrie Jones, Stephen Ferguson, Laura Bohn, Yamina Berchiche
- **The GRC Power Hour™** *Meritxell Canals, JoAnn Trejo*

Movement Ecology of Animals +GRS

Proximate and Ultimate Drivers of Animal Movement

MAY 28 - JUN 2, 2023

RENAISSANCE TUSCANY IL CIOCCO, LUCCA (BARGA), ITALY

CHAIR: Karen McCoy

VICE CHAIR: Francesca Cagnacci

- **Evolutionary Drivers of Animal Movement** *Emanuel Fronhofer,* Sutirth Dey, Hanna Kokko, Marjo Saastamoinen
- **Origins of Individual Variation in Movement Strategies** *Judy Shamoun-Baranes,* Susan Lowerre-Barbieri, Samantha Patrick, Dries Bonte, Anne Hertel, Jerod Merkle
- **Interspecific Interactions that Motivate Movement** *Meggan Craft,* Sandra Binning, Emily Cohen, Allison Shaw
- **Cues to Decide When and Where to Move** *Mark Hebblewhite,* Autumn-Lynn Harrison, Briana Abrahms, Guillaume Bastille-Rousseau, Brett Jesmer, Emily Bennitt
- **Modelling Space Use: From the Individual to the Population** *Juan Morales,* Jonathan Potts, Nathan Ranc, Louise Riotte-Lambert
- **Compiling Big Data to Understand the Movement Process** *Ana Sequeira,* Ran Nathan, Luca Boerger, Ryan Reisinger, Marie Auger-Méthé, Marius Somveille
- **Responses to a Changing Environment** *Julie Young,* Christopher Wilmers, Simon Chamaillé-Jammes, Akinori Takahashi
- **Invasions and Outbreaks** *Richard Hall,* Ceridwen Fraser, Gao Hu, Adele Mennerat, Atle Mysterud, Claire Teitelbaum
- **Keynote Session: Emerging Movement Patterns and Conservation Issues** *John Fryxell,* Ulrike Schlaegel, Oswald Schmitz
- **The GRC Power Hour™** *Francesca Cagnacci*

Muscle: Excitation-Contraction Coupling +GRS

Nanodomain Signaling Controls Muscle Function

JUN 4-9, 2023

COLBY-SAWYER COLLEGE, NEW LONDON, NH

CHAIRS: Donald Bers and Ana Gomez

VICE CHAIRS: Montserrat Samso and Laszlo Csernoch

- **L-Type Ca Channels** *Riccardo Olcese,* Steven Marx, Manuel Navedo, Ivy Dick, Anamika Dayal
- **Ryanodine Receptor** *Xander Wehrens,* Parisa Asghari, Wayne Chen, Mark Nelson, Robyn Rebbeck
- **InsP3 Receptors-Nuclear Signaling** *Enrique Jaimovich,* Senka Holzer, Marcel Egger, Irina Serysheva
- **Malignant Hyperthermia and CPVT** *Hector Valdivia,* Vincent Jacquemond, Francisco Alvarado
- **Store-Operated Ca Entry, TRP and SAC** *Isabelle Marty,* Feliciano Protasi, Ingrid Bonilla, David Beech, Mohamed Trebak
- **Muscular Dystrophy and Diabetes** *Madeline Nieves-Cintron,* Dawn Lowe, Scott Earley, Jeff Erickson, Eduardo Rios
- **Nanodomain Structure-Function** *Peter Lipp,* Mark Cannell, William Louch, Julia Gorelik, TingTing Hong
- **Heart Failure and Skeletal Muscle Fatigue** *Bjorn Knollmann,* Katharine Dibb, Long-Sheng Song, Llewelyn Roderick
- **Keynote Session: Structure-Function of the Ca Release Channels** *W. Jonathan Lederer,* Filip Van Petegem
- **The GRC Power Hour™** *Susan Treves, Michelle Munro*

Myogenesis +GRS

Intrinsic and Extrinsic Control of Myogenesis Under Physiological and Pathological Conditions

JUN 11-16, 2023

RENAISSANCE TUSCANY IL CIOCCO, LUCCA (BARGA), ITALY

CHAIRS: Jeffrey Dilworth and Clarissa Henry

VICE CHAIR: Zhenguo Wu

- **Keynote Session: Single Cell Transcriptomics** *Stephen Tapscott,* Ibrahim Cisse, Omid Mashinchian
- **Latest Advances in Understanding Muscle Development** *Gabrielle Kardon,* Peter Currie, Talila Volk, Krzysztof Jagla, Erika Geisbrecht, Simon Hughes
- **Intrinsic and Extrinsic Factor Controlling Satellite Cell Function** *Carmen Birchmeier,* Foteini Mourkioti, Jerome Feige, D Cornelison
- **Maintaining Myofiber Function** *David Glass,* Karyn Esser, Mary Baylies, Peleg Hasson, Delphine Duprez, Rachelle Crosbie
- **Satellite Cell Quiescence** *Bénédicte Chazaud,* Thomas Rando, Philippos Mourikis, Colin Crist
- **Mechanisms Driving Disease Pathology** *Peter Currie,* Jim Dowling, Ping Hu, Stephen Tapscott, Michael Kyba, Gabrielle Kardon
- **Metabolic Regulation of Muscle** *Rachelle Crosbie,* Clara Peek, Katrien De Bock, Mireille Khacho
- **Epigenetic Control of Muscle Development and Regeneration** *D. Cornelison,* Chiara Lanzuolo, Michael Rudnicki, Huating Wang, Carmen Birchmeier, Hiu Cheung
- **Contributions of the Niche to Satellite Cell Function** *Peleg Hasson,* Shahragim Tajbakhsh, Bénédicte Chazaud, Florian Bentzinger, David Glass
- **The GRC Power Hour™** *Clarissa Henry*

Nanoporous Materials and Their Applications +GRS

Expanding the Horizons of Porous Materials Design and Applications

AUG 6-11, 2023

PROCTOR ACADEMY, ANDOVER, NH

CHAIR: Jeffrey Rimer

VICE CHAIR: Christopher Lew

- **Keynote Session: Breakthroughs in Nanoporous Materials Applications** *Mircea Dinca,* Jeffrey Long, Manuel Moliner
- **Fundamentals of Materials Assembly** *Toru Wakihara,* Donglin Jiang, Valentin Valtchev, Wendy Queen
- **Elucidating the Interplay Between Structure and Function** *Psaras McGrier,* Hong-Cai Zhou, William Schneider
- **Advancements in Materials Synthesis and Characterization** *Svetlana Mintova,* Shengqian Ma, Xiaodong Zou
- **Exploiting Activity in Porous Materials** *J.R. Schmidt,* Amanda Morris, Javier Garcia Martinez
- **Enhanced Functionality of Nanoporous Materials** *Gregory Lewis,* Paul Wright, Francois-Xavier Coudert, Omar Farha
- **New Paradigms in Heterogeneous Catalysis** *Jihong Yu,* Veronique Van Speybroeck, Jeroen A. van Bokhoven
- **Engineering Multifunctional Porous Materials** *Dana Medina-Tautz,* Katherine Mirica, Kumar Varoon Agrawal
- **Keynote Session: New Frontiers in Nanoporous Materials Design** *Ahmad Moini,* Bettina Lotsch, William Dichtel
- **The GRC Power Hour™** *Tendai Gadzikwa*

Natural Products and Bioactive Compounds +GRS

Natural Products: Inspiring Innovation in Chemistry, Biology and the Discovery of New Medicines

JUL 30 - AUG 4, 2023

PROCTOR ACADEMY, ANDOVER, NH

CHAIR: Philip Kym

VICE CHAIR: Dirk Trauner

- **Keynote Session: Chemical Biology of Natural Products and Bioactive Compounds** *Ian Seiple,* Stuart Schreiber, Benjamin Cravatt
- **Target Oriented Synthesis of Bioactive Compounds** *Jennifer Frost,* Cheryl Hayward, Jamie McCabe Dunn
- **Strategies and Tactics for Complex Natural Product Total Synthesis** *Joshua Pierce,* David Sarlah, Keisuke Suzuki, Vy Dong
- **Synthetic Biology and Biosynthesis of Natural Products** *Ruijie Zhang,* Alessandra Eustaquio, Michelle Chang, Sarah O'Connor, Chaitan Khosla
- **Paradigm Shifting Technology** *Lisa Marcaurelle,* Neil Kelleher, Daniel Nocera
- **Discovery of Natural Products and Their Signaling Pathways** *Matthew Bertin,* Marcy Balunas, J. P. Gerdt, Sandra Loesgen, Elizabeth Nolan
- **Medicinal Chemistry of Natural Products and Bioactive Compounds** *Marie-Priscille Brun,* Christopher Marvin, Paul Hergenrother, Stephen Martin
- **Novel Synthetic Strategies and Methodologies** *Jeff Ciavarri,* Jennifer Schomaker, Ryan Looper, David Nagib, Janine Cossy
- **Keynote Session: Total Synthesis of Complex Natural Products** *Uttam Tambar,* Justin Du Bois, Sarah Reisman
- **The GRC Power Hour™** *Jennifer Frost*

Neuroethology: Behavior, Evolution and Neurobiology +GRS

Linking Diversity in Cells, Circuits, and Brain Architecture to Ecologically Relevant Behaviors

AUG 6-11, 2023

MOUNT SNOW, WEST DOVER, VT

CHAIRS: Kim Hoke and Stefan Schuster

VICE CHAIRS: Julie Simpson and Miriam Liedvogel

- **Keynote Session: Evolution and Plasticity of Neural Circuit Computations Underlying Behavior** *Harold Zakon,* Vanessa Ruta
- **Energetic Constraints on Circuits and Behavioral Strategies** *Mark Shein-Idelson,* Clare Rittschof, Michael Markham
- **Cell Type Identification and Function in an Evolutionary Context** *Eva K Fischer,* David Schulz, Maria Antonietta Tosches
- **Stabilizing Circuit and Behavioral Function Across Environments** *Eileen Hebets,* Gina Turrigiano, Michael Dickinson
- **Evolution of Sleep: Why Neural Circuits Need a Break** *Adriana Migliaro,* Jerome Siegel, Niels Rattenborg, David Raizen
- **Neuroethology of Temporal Precision** *Erik Zornik,* Michael Brainard, Kate Feller, Herwig Baier
- **Constraints on Localization** *Ximena Bernal,* Catherine Carr, Ysabel Giraldo, Venkatesh Gopal
- **Integrating Circuit Elements Across Ontogeny and Evolution** *Vatsala Thirumalai,* Eve Schneider, Osama Ahmed, Keith Sillar
- **Modulation and State Dependence of Communication** *Sara Wasserman,* Laura Quintana, Stephanie Campos, Cory Miller
- **The GRC Power Hour™** *Nicole Baran*

Neurotrophic Mechanisms in Health and Disease +GRS

Neurotrophic Factor Functions in Development, Plasticity, Regeneration and Disease

MAY 28 - JUN 2, 2023

SALVE REGINA UNIVERSITY, NEWPORT, RI

CHAIR: Rejji Kuruvilla

VICE CHAIR: Elizabeth Coulson

- **Neurotrophic Factors in Circuit Development** *Christopher Deppmann,* Freda Miller, Debby Silver
- **Synaptic Connectivity and Plasticity** *Francisca Bronfman,* Michael Greenberg, Barbara Hempstead, Stephanie Gupton, Alexis Stranahan
- **Neurotrophic Factors in Stress, Mood, Depression and Physiology** *Francis Lee,* Mary Kay Lobo, Keri Martinowich, Carlos Ibanez
- **Sensory Signaling** *Wenquin Luo,* Lauren Orefice, David Ginty, Eli Zunder
- **Neurotrophic Factors in Disease and Therapy** *Mark Bothwell,* Eero Castren, Susan Croll
- **Neuronal Morphology, Cytoskeleton and Organelle Transport** *Sandra Maday,* Ai Yamamoto, Rosalind Segal, Bettina Winckler, Lilian Kisiswa, Damaris Lorenzo
- **Axon Degeneration and Regeneration** *Eran Perlson,* Mike Fainzilber, Gareth Thomas, Warren Tourtellotte
- **Neuron-Glia and Immune Interactions** *Bruce Carter,* Ya-chieh Hsu, Cagla Eroglu, Meng-meng Fu, Henrique Veiga-Fernandes, Aaron James
- **Toolkits in Neurotrophic Factor Biology** *Katrin Deinhardt,* Ryohei Yasuda, Won Do Heo, Liting Duan
- **The GRC Power Hour™** *Rosalind Segal*

Neutron Scattering +GRS

Neutron Scattering for a Sustainable Society

JUN 25-30, 2023

FOUR POINTS SHERATON / HOLIDAY INN EXPRESS, VENTURA, CA

CHAIRS: Victoria Garcia Sakai and Collin Broholm

VICE CHAIRS: Pascale Deen and Dongfeng Chen

- **Sustainable Cities and Transport** *Ken Andersen,* Hassina Bilheux, Peter Dowding, Bing Li, Tad Koga
- **Healthy Living** *Jill Trewhella, Yun Liu,* Andrey Kovalevsky, Judith Peters, Andy Stephen, Luis Fernandez Barquin
- **Food for the Future and Sustainable Agriculture** *Elliot Gilbert,* Drew Marquardt, Genoveva Burca, Gyozo Garab
- **Quantum Materials for Energy and Information Technology** *Victor Balédent,* Radu Coldea, Efrain Rodriguez, Shan Wu
- **Infrastructure and Construction Materials** *Anna Paradowska,* Peter Hedstrom, Claire White, Stefanus Harjo
- **Neutron Scattering for a Curiosity Driven Society** *Helmut Schober,* Liang Hong, Helen Fraser, Joseph Bevitt, Maria Paula Marques, Grace Causer
- **Sustainable Use of Nature's Resources** *Peter Müller-Buschbaum,* Lilo Pozzo, Indri Adilina, Daniel Söderberg
- **Advanced Materials for Clean Energy** *Kristina Edstrom, Vanessa Peterson,* Peter Müller-Buschbaum, Sandrine Lyonnard, Genki Kobayashi, Nikolay Kardjilov, Kanishka Biswas
- **Fighting Climate Change** *Craig Brown,* Konstantinos Stefanopoulos, Sihai Yang
- **The GRC Power Hour™** *Anna Paradowska, Kristina Edstrom*

Nonproliferation, Counterproliferation and Disarmament Science NEW!

Cross-Cutting Science Facilitating Collaboration Across the Threat-Science Research Community

JUL 9-14, 2023

FOUR POINTS SHERATON / HOLIDAY INN EXPRESS, VENTURA, CA

CHAIR: Peter Hotchkiss

VICE CHAIR: Anna Erickson

- **Implications of WMD CBRNE Science on Policy** *James Revill,* Margaret Kosal, Bradley Dickerson
- **Approaches to Counterproliferation and Trafficking** *George Moore,* Stefano Costanzi, AJ Cadeau
- **Science for Verification** *Jennifer Ladd-Lively,* John Mattingly, Areg Danagoulian
- **Detection and Monitoring of CBRNE Materials** *Mitaire Ojaruega,* Gerardine Botte, Igor Jovanovic, Gary Sutlieff
- **Emerging Science and Technologies** *Patricia McDaniel,* David Mascarenas, Becky Hess
- **Approaches to Provenancing** *Cindi Corbett,* Jenifer Shafer, Josh Dettman, Hanna Hakulinen
- **The Role of Reference Labs** *Graeme Clark,* Audrey Williams, Brigitte Dorner
- **Creative Approaches to WMD CBRNE Science** *Jonathan Forman,* Greg Gillen, Mirjam de Bruin-Hoegée
- **Data Mining for Detection** *Richard Cupitt,* Erin Dumbacher, Patrick Boyle
- **The GRC Power Hour™** *Patricia McDaniel*

Nuclear Chemistry +GRS

Patterns and Reactions of Exotic Nuclei

JUN 11-16, 2023

COLBY-SAWYER COLLEGE, NEW LONDON, NH

CHAIR: Ingo Wiedenhoever

VICE CHAIR: Iris Dillmann

- **Science Opportunities From New Facilities for Exotic Nuclei** *Alexandra Gade, Wolfram Korten,* Kei Minamisono, Jan Glorius
- **Experiments Redefining Shell Structure at the Extremes** *Vandana Tripathi, Kathrin Wimmer,* David Sharp, Robert Grzywacz, Olivier Sorlin, Andrea Gottardo, Vladimir Manea, Freddy Flavigny
- **Nuclear Structure of Heavy Nuclei** *Roderick Clark, Rolf-Dietmar Herzberg,* Dirk Rudolph, Jennifer Pore, Dariusz Seweryniak, Francesca Giacoppo, Araceli Lopez-Martens
- **The Origin of the Chemical Elements** *Artemis Spyrou, Marialuisa Aliotta,* Rosanna Depalo, Melina Avila, Chris Wrede, Amanda Karakas, Dennis Muecher, Matthew Mumpower
- **Angular Momenta of Fission Fragments** *Aurel Bulgac, Jonathan Wilson,* Antoine Lemasson, Ionel Stetcu, Cedric Simenel, Matt Devlin
- **Precision Computations for Nuclear Structure and Reactions** *Elena Litvinova, Yutaka Utsuno,* Noritaka Shimizu, Kyle Wendt, Sebastian Koenig, Jie Meng
- **Fundamentals with Stored Ions** *Yuri Litvinov, Stephan Malbrunot-Ettenauer,* Ronald F Garcia Ruiz, Erich Leistenschneider
- **Collective Nuclear Structure and Emergent Phenomena** *Magda Zielinska, Mitch Allmond,* Akaa Daniel Ayangeakaa, David O'Donnell, Tomas R. Rodriguez, Ben Kay
- **Late-Breaking Topics** *Iris Dillmann,* Roman Gernhäuser, Stefanos Paschalis
- **The GRC Power Hour™** *Artemis Spyrou, Shelly Lesher*

Nucleic Acids +GRS

Structural, Functional and Mechanistic Behavior of DNA, RNA and Nucleic Acid Processing Enzymes

JUN 18-23, 2023

GRAND SUMMIT HOTEL AT SUNDAY RIVER, NEWRY, ME

CHAIRS: Anna Marie Pyle and James Berger

VICE CHAIRS: Brandt Eichman and Jane Jackman

- **Keynote Session: Frontiers in Nucleic Acid Science** *Philip Kranzusch,* Andrei Korostelev, Agata Smogorzewska
- **Re-Engineering the Central Dogma** *Hashim Al-Hashimi,* Chang Liu, Farren Isaacs, Yamuna Krishnan, David Lilley
- **RNA and DNA Viruses** *Stewart Shuman,* Andrea Gamarnik, Philip Kranzusch
- **Nucleic Acid Processing Machines: Regulation and Structure** *Rui Zhao,* Yuan He, Yunsun Nam, Ailong Ke, Kristen Lynch, Caroline Kisker
- **Regulatory Modifications in Nucleic Acids and Immune Sensing** *David Lilley,* Peter Beal, Kate Meyer, Stacy Horner
- **Nucleic Acid Processing Machines: New Systems and Biophysics** *Ailong Ke,* Michelle Wang, Stewart Shuman, Kathleen Collins, Rui Zhao, Stephen P. Bell
- **Overcoming RNA, DNA, and Nucleotide Damage** *Tanya Paull,* Catherine Freudenreich, Puck Knipscheer
- **Exploiting and Targeting Nucleic Acids in Therapeutics** *Chang Liu,* Amanda Hargrove, Hashim Al-Hashimi, Anastasia Khvorova, Elizabeth Garner, Kari Efferen

- **Nucleic Acids in Phase Condensation and Genome and Subcellular Localization** *Michelle Wang,* Sua Myong, Marina Feric, Job Dekker, Tanya Paull
- **The GRC Power Hour™** *Jane Jackman, Brandt Eichman*

Nucleosides, Nucleotides and Oligonucleotides +GRS

Chemical Biology of Nucleosides and Nucleic Acids Towards Human Therapeutics

JUN 25-30, 2023

SALVE REGINA UNIVERSITY, NEWPORT, RI

CHAIRS: Kathie Seley-Radtke and Muthiah (Mano) Manoharan

VICE CHAIRS: Eriks Rozners and John Randolph

- **Keynote Session: Nucleic Acid Medicine Reaches Home** *David Corey,* Stanley Crooke, Laura Sepp-Lorenzino, Raymond Schinazi
- **Structural Chemistry of Nucleic Acids** *Dinshaw Patel,* Blanton Tolbert, Martin Egli, Leemor Joshua-Tor
- **Nucleoside and Nucleotide Natural Products** *Christian Ducho,* Steven Van Lanen, Rebecca Goss, Seok-Yong Lee, Yana Cen
- **Challenges and Opportunities for Nucleic Acid Therapeutics** *Steven Dowdy,* Joanna Kowalska, Rakesh Veedu, Hiroshi Abe
- **Oligonucleotide Therapeutics** *Krishna Ganesh,* Isabel Aznarez, Maja Janas De Angelis, Arthur Levin
- **Small Molecules: Chemistry and Applications** *Bruce Armitage,* Amanda Bryant-Friedrich, Harry De Koning, Andrea Brancale, Zlatko Janeba
- **Therapeutics for Coronaviruses** *Joy Feng,* Luis M Schang, Bruno Canard, Mattias Gotte, Chris Meier
- **Chemical Biology and Nucleic Acid-Based Diagnostics** *Piet Herdewijn,* Mehnaaz Ali, Sabine Muller, Andrea Rentmeister, Yi Xiao
- **RNA-Targeting and Epitranscriptomes** *Maureen McKeague,* Amanda Garner, Ronald Micura, Satoshi Obika, Christopher Brown, Ken Yamada
- **The GRC Power Hour™** *Amanda Bryant-Friedrich*

Organellar Channels and Transporters +GRS

Molecular Mechanisms and Parallels Between Intracellular Transport in Eukaryotes

AUG 6-11, 2023

REY DON JAIME GRAND HOTEL, CASTELLDEFELS, SPAIN

CHAIRS: Dale Sanders and Harpreet Singh

VICE CHAIRS: Elizabeth Jonas and Myriam Charpentier

- **Keynote Session: Groundbreaking Discoveries in Organellar Channels and Transporters** *Bruno Gasnier,* Yuriy Kirichok, Barbara Ann Halkier, Douglas Wallace
- **The Dynamic Mitochondrion and Chloroplasts** *Adam Szewczyk,* Dipayan Chaudhuri, Ildiko Szabo, Ute Armbruster, Markus Schwarzlander, Radhakrishnan Mahalakshmi
- **The Physiology of Mitochondrion and Chloroplasts** *Andrea Bruggemann,* Erin Connolly, Isabella Grumbach, Katrin Philippar
- **The Master Regulator of Membrane Trafficking and Cellular Calcium: Endoplasmic Reticulum and Golgi Apparatus** *Sheng Luan,* Montserrat Samso, Klaus Groschner, Gyorgy Hajnoczky, Yanzhuang Wang
- **The Physiology of Endoplasmic Reticulum and Golgi Apparatus** *Amalia Dolga,* Mohamed Trebak, Christian Grimm
- **Emerging Concepts: Vesicle and Vacuoles** *Thomas Jentsch,* Suresh Damodaran, Yi-Fang Tsay, Rainer Hedrich, Karin Schumacher, Bruno André
- **The Physiology of Vesicle and Vacuoles** *Michael Zhu,* Haoxing Xu, Ran Tivony, Zhaozhu Qiu
- **Nuclear Ion Channels** *Damian Bell,* Stanley Nattel, Michele Mazzanti, Youxing Jiang
- **Intracellular Ion Channel Physiology and Novel techniques** *Yamuna Krishnan,* Pinaki Talukdar, Antonio Felipe, Menachem Moshelion
- **The GRC Power Hour™** *Shubha Gururaja Rao*

Organic Reactions and Processes

Catalysis, Methods and Strategies Empowering Organic Synthesis

JUL 16-21, 2023

BRYANT UNIVERSITY, SMITHFIELD, RI

CHAIRS: Craig Merlic and Michael Zacuto

VICE CHAIRS: Philip Wheeler and Alexander Grenning

- **Stereochemical Control in Organic Synthesis** *Alexander Grenning,* Cathleen Crudden, Jonathan Ellman
- **Organometallic Catalysis and Mechanisms** *Sasha Sundstrom,* Peng Liu, Martin Oestreich
- **Synthesis of Complex Bioactive Molecules** *Jean Suffert,* Mathias Christmann, Timothy Newhouse
- **Catalysis and Process Chemistry** *Dave Martin,* Dawei Ma, Dean Toste, Qi-Lin Zhou
- **New Oxidative Transformations to Generate Molecular Complexity** *Jennifer Albaneze-Walker,* Andrew McNally, Laurel Schafer, Paolo Melchiorre
- **Novel Strategies and Methodologies for Synthesis** *Andrew Harned,* Janine Cossy, Jennifer Schomaker

- **Advances in Alkene- and Aromatic- Functionalization Reactions** *Kana Yamamoto,* Alison Narayan, Song Lin, Ohyun Kwon
- **Process Chemistry Research for the Synthesis of Pharmaceuticals** *Jesse McAtee,* Theodore Martinot, Denise Andersen
- **Metal Catalyzed Reactions and Complex Molecule Synthesis** *Philip Wheeler,* Varinder Aggarwal, Shu Kobayashi, Barry Trost
- **The GRC Power Hour™** *Laurel Schafer*

Organometallic Chemistry +GRS

New Frontiers in Synthesis, Catalysis and Materials Chemistry

JUL 9-14, 2023

SALVE REGINA UNIVERSITY, NEWPORT, RI

CHAIR: Heather Spinney

VICE CHAIR: Paula Diaconescu

- **Organometallic Chemistry of the Lanthanides and Actinides** *Stosh Kozimor,* Suzanne Bart, Karsten Meyer
- **Early-Career Investigator Presentations** *Neal Mankad,* Alex Nett, Amanda Cook, Robert Comito
- **Energy and the Environment** *Max Delferro,* Caroline Saouma, Susannah Scott
- **Applications of Organometallic Chemistry in Organic Synthesis** *Jessica Klinkenberg,* Melanie Sanford, Caleb Hethcox, Sophie Rousseaux
- **Main Group Chemistry and Catalysis** *Parisa Mehrkhodavandi,* Robert Gilliard, Roland Roesler
- **Ligand Design** *Christopher Uyeda,* Kensha Clark, Ba Tran, Natalie Fey, Tiow-Gan Ong
- **Transition Metal Chemistry and Catalysis** *Maurice Brookhart,* Kyoko Nozaki, Stefan Mecking
- **Organometallic Materials and Polymers** *Mari Rosen,* Alexandra Velian, Ian Manners, David Kaphan
- **Keynote Session: Mechanistic Organometallic Chemistry** *Paula Diaconescu,* Clark Landis, Karen Goldberg
- **The GRC Power Hour™** *Nancy Williams*

Origins of Solar Systems +GRS

Chemical and Dynamical Constraints on Planet Formation

JUN 11-16, 2023

MOUNT HOLYOKE COLLEGE, SOUTH HADLEY, MA

CHAIR: Alycia Weinberger

VICE CHAIR: Maria Schönbächler

- **Ice lines and Dust Migration: Planet Formation Cause or Effect** *Ilse Cleeves,* Ke Zhang, Joanna Drazkowska
- **Chemical Diversity in Inner-Disks and the Planetesimals and Planets That Form There** *Ramon Brasser,* Colette Salyk, Martin Bizzarro, Miki Nakajima
- **The Cometary and Asteroidal Record of Early Solar System Chemical Inventories and Transport** *Andrew Rivkin,* Stefanie Milam, Curtis Williams
- **What Asteroid Missions and Sample Return Tell Us About Planetary Building Blocks** *Linda Elkins-Tanton,* Hannah Kaplan, Hikaru Yabuta, Shogo Tachibana
- **What ALMA and JWST Reveal About Disk: Exoplanet Connections** *Eve Lee,* Laura Pérez, Christine Chen
- **Connections Between Rocky Planet Formation and Their Interiors and Atmospheres** *Laura Schaefer,* Tim Lichtenberg, Siyi Xu, Myriam Telus
- **How Planets Do or Don't Accrete Water and Carbon** *Michael Meyer,* Lars Borg, Melissa McClure
- **Jupiter and Giant Planet Formation** *Kevin Schlaufman,* Ravit Helled, Richard Teague, Konstatin Batygin
- **How Inevitable is Water on Rocky Planets** *Francis McCubbin,* Jessica Barnes, Rhian Jones
- **The GRC Power Hour™** *Linda Elkins-Tanton*

Pancreatic Diseases +GRS

Understanding Cell Behavior and Communication

APR 30 - MAY 5, 2023

RENAISSANCE TUSCANY IL CIOCCO, LUCCA (BARGA), ITALY

CHAIRS: Francisco Real and Nabeel Bardeesy

VICE CHAIRS: Maureen Gannon and Carmella Evans-Molina

- **A High-Level View of Pancreatic Diseases** *Steven Leach, Lori Sussel,* Prof. Dr. med. Markus Maximilian Lerch, Antoinette Moran
- **Intra-Pancreas Communication** *Limor Landsman, Farzad Esni,* James Wells, Peter Thompson, Joana Almaça
- **Inter-Organ Communication** *Amelia Linnemann, Matthias Hebrok,* Mehboob Hussain, Emilyn Alejandro, Clotilde Théry
- **Cross Talk Between Exocrine Disease and Endocrine Dysregulation** *Ilse Rooman, Jorge Ferrer,* Teresa Mastracci, Rohit Kulkarni, Jack Virostko
- **Recapitulating Cell Interactions In Vitro, Niche and Pancreatic Organoids** *Anne Grapin-Botton, Seung Kim,* Fanny Mann, Daniel Öhlund, Cristina Nostro
- **Organellar Function in Pancreatic Homeostasis and Disease** *Cosimo Commisso, Miriam Cnop,* Orian Shirihai, Christine Chio, Rushika Perera
- **The Pancreatic Microenvironment** *Decio Eizirik, Corinne Bousquet,* Roberto Mallone, Claus Jorgensen, Mara Sherman
- **Genomics of Pancreatic Diseases** *Lorenzo Pasquali, Julie Sneddon,* Jonas Rosendahl, Yan Li, Gioacchino Natoli
- **Modeling Pancreatic Diseases** *Françoise Carlotti, Scott Lowe,* Roland Rad, Maike Sander, Alexander Kleger
- **The GRC Power Hour™** *Nabeel Bardeesy, Maureen Gannon*

Parkinson's Disease +GRS

Proteins, Pathway, and Pathophysiology in Parkinson's

MAY 7-12, 2023

LES DIABLERETS CONFERENCE CENTER, LES DIABLERETS, SWITZERLAND

CHAIR: Malu Tansey

VICE CHAIR: Alexandra Nelson

- **Keynote Session: Matching Therapies to Disease** *J. Timothy Greenamyre,* Glenda Halliday
- **Complex Genetics of Parkinsonism and Related Disorders** *Vincenzo Bonifati,* Sonja Scholz, Huw Morris, Sara Bandres Ciga, Mina Ryten, Alice Chen-Plotkin
- **Physiology of Non-Motor Systems Relevant To PD** *Benjamin Wolozin,* Michael Burton, Karen Gamble, Yang Dan
- **Non-Nigral and Mixed Pathology in PD** *Alexandra Nelson,* Vincenzo Bonifati, Lorraine Kalia, Le Zhang, Michael Henderson, Caleb Webber
- **Vesicular Sorting** *Sabine Hilfiker,* Darren Moore, Sreeganga Chandra, Hilal Lashuel
- **Lysosomal Function** *Darren Moore,* Peter Vangheluwe, Monther Abu-Ramaileh, Matthew LaVoie, Aimee Kao, Shawn Ferguson
- **Neuroinflammation and Glial Cell Interactions** *Matthew LaVoie,* Shane Liddelow, Max Gutierrez, Ashley Harms
- **Cellular and Intracellular Parkinson's Disease Pathways** *Peter Vangheluwe,* J. David Beckham, Luis Bonet-Ponce, Miratul Muqit, Lindsay De Biase, Sabine Hilfiker
- **Emerging Topics in Neurodegeneration** *Shalini Padmanabhan,* Wilma van de Berg, James Shorter, Benjamin Wolozin
- **The GRC Power Hour™** *Alexandra Nelson, Shalini Padmanabhan*

Phagocytes +GRS

Molecular and Cellular Diversity in Host Defense and Inflammation

JUN 4-9, 2023

WATERVILLE VALLEY, WATERVILLE VALLEY, NH

CHAIR: Sergio Catz

VICE CHAIR: Alison Criss

- **Keynote Session: Adhesion Molecules in Leukocyte Activation** *William Nauseef,* Klaus Ley
- **Phagocyte Function, Immunity and Disease** *Silvia Uriarte,* Ivan Zanoni, Markus Sperandio, Catherine Hedrick, Emanuela Bruscia
- **Phagocytes in Inflammatory Disease** *Florence Niedergang,* Marco Antonio Cassatella, Veronique Witko-Sarsat
- **Myeloid Cellular Immunity, Autophagy and Cell Death** *Gustavo Menezes,* Mordecahy Gerlic, Sanja Arandjelovic, Sussan Nourshargh, Sergio Grinstein
- **Neutrophils in Immunity and Inflammation** *Daniel Irimia,* Gustavo Menezes, Arturo Zychlinsky, Carole Parent
- **Mechanisms of Phagocytosis in Macrophages and Dendritic Cells** *Mallary Greenlee-Wacker,* Julie Magarian Blander, Johnathan Canton, Roberto Botelho, Ana-Maria Lennon-Dumenil
- **Microglia and the Regulation of Inflammation** *Ivan Zanoni,* Dorothy Schafer, Anna Victoria Molofsky
- **Phagocytes in Host-Pathogen Interaction** *Roberto Botelho,* Sunny Shin, Juhi Bagaitkar, Jorge Galan, Keke Fairfax
- **Phagocytes, Mucosal Immunity and the Microbiota** *Sanja Arandjelovic,* Gretchen Diehl, Niki Moutsopoulos
- **The GRC Power Hour™** *Silvia Uriarte, Mallary Greenlee-Wacker*

Photochemistry +GRS

Using Light to Advance Discovery in Chemistry, Physics and Biology

JUL 30 - AUG 4, 2023

BATES COLLEGE, LEWISTON, ME

CHAIRS: James McCusker and Elizabeth Harbron

VICE CHAIRS: Valentine Vullev and Amanda Morris

- **Advanced Spectroscopic Methods** *Theodore Goodson,* Renee Frontiera, Kelly Gaffney, Elad Harel
- **The Photophysics and Photochemistry of Solar Energy Conversion** *Leif Hammarstrom,* Dorthe Eisele, Osamu Ishitani, Hemamala Karunadasa, Daniel Nocera
- **Photons in Medicine and Biology** *Claudia Turro,* Ivan Dmochowski, Antonin Vlcek, Daniela Buccella
- **Photoredox Catalysis: Mechanism and Function** *Tehshik Yoon,* Beth Elacqua, Kaid Harper, Todd Hyster, John Swierk
- **Coherence in Chemistry** *Gregory Scholes,* Warren Beck, Alexandra Olaya-Castro, Elisabetta Collini
- **Photochemical Foundations for Light-Activated Molecular Devices** *Francisco M. Raymo,* Olof Johansson, Grace Han, Natia Frank, Alex Lippert
- **Optical Materials** *Mark Thompson,* Robert Gilliard, Julia Kalow, Roy Weinstain
- **Emergent Photophysics of the First Transition Series** *Oliver Wenger,* Elena Jakubikova, Kenneth Wärnmark, Ryan Hadt, David Herbert
- **Keynote Session: Frontiers in Photochemical Sciences** *Amanda Morris,* Vivian Yam
- **The GRC Power Hour™** *Elizabeth Harbron*

Photosynthesis +GRS

From Molecular Structure Function to Systems Integration

JUL 23-28, 2023

GRAND SUMMIT HOTEL AT SUNDAY RIVER, NEWRY, ME

CHAIR: Robert Burnap

VICE CHAIR: Kevin Redding

- **Keynote Session: Photosynthetic Systems: Integration Across Scales From Molecular to Cellular** *Roberta Croce,* David Kramer, Neil Hunter, Abhishek Singharoy
- **Light Harvesting, Energy Transfer, and Charge Separation** *Jessica Anna,* Gabriela Schlau-Cohen, Cheryl Kerfeld, Howe-Siang Tan, Dimitrios Pantazis, Doran Bennett Raccah
- **Diversity and Adaptation of the Photosynthetic Apparatus** *Arthur Grossman,* Christopher Gisriel, Jindong Zhao, Benjamin Bailleul
- **Advances in the Mechanism of Water Oxidation** *Gary Brudvig,* Michi Suga, Junko Yano, Holger Dau, Richard Debus
- **Electron and Proton Fluxes in Photosynthesis** *A. William Rutherford,* Marilyn Gunner, Hiroshi Ishikita
- **Structure and Dynamics Photosynthetic Membranes** *Emilie Wientjes,* Matt Johnson, Luning Liu, Jeffrey Cameron, David Vinyard
- **Manipulation of Photosynthesis for Energy and Products** *Jianping Yu,* Matthew Posewitz, Paul Hudson, Angad Mehta
- **Photoprotection, and Integration of the Energy Generating and Utilizing Pathways** *Yagut Allahverdiyeva-Rinne,* Tomas Morosinotto, Adrien Burlacot, Alizée Malnoë, Daniel Ducat
- **Evolution of Photosynthesis** *Tanai Cardona,* Patricia Sanchez-Baracaldo, Woodward Fischer
- **The GRC Power Hour™** *Roberta Croce, Tanai Cardona*

Physical Metallurgy +GRS

Metallurgy Matters for Creating a Sustainable World

JUL 9-14, 2023

STONEHILL COLLEGE, EASTON, MA

CHAIRS: Suveen Mathaudhu and William Curtin

VICE CHAIRS: Dallas Trinkle and Emmanuelle Marquis

- **Keynote Session: Prospects for Sustainable Metallurgy** *Anthony Rollett,* Dierk Raabe, Jonah Erlebacher
- **Functional Metallic Materials** *Matthew Willard,* Laura Lewis, A. Lindsay Greer, Jason Trelewicz
- **Metallurgy in the Hydrogen Economy** *Jimmy Burns,* Sabrina Sartori, Vikram Deshpande
- **Nucleation and Interfaces** *Carol Handwerker,* Bi-Cheng Zhou, Xiaochun Li, John Martin
- **Additive Manufacturing** *Allison Beese,* Amy Clarke, Greta Lindwall
- **High Entropy Alloys** *Daniel Miracle,* Tresa Pollock, Maryam Ghazisaeidi, Easo George
- **Innovative Steels** *John Lewandowski,* Mingxin Huang, Stuart Maloy
- **Lightweight Metals (Mg, Al, Ti)** *Warren Poole,* Amit Misra, María Teresa Pérez-Prado, Igor Abrikosov
- **Nanocrystalline Materials** *Erica Lilleodden,* Christopher Schuh, Yuntian Zhu
- **The GRC Power Hour™** *Jennifer Carter, Kristina Maria Kareh*

Physical Organic Chemistry +GRS

Analyzing, Understanding and Predicting Organic Reactivity

JUN 25-30, 2023

HOLDERNESS SCHOOL, HOLDERNESS, NH

CHAIRS: Burkhard Koenig and Cornelia Bohne

VICE CHAIRS: Malcolm Forbes and Kathleen Kilway

- **Mechanisms and Kinetics in Catalysis** *Peng Liu,* Jordi Bures, Hosea Nelson, Deryn Fogg
- **Electrons and Photons in Organic Chemistry** *Anna Gudmundsdottir,* Zhiwei Zuo, Ksenija Glusac, Thorsten Bach, Dirk Trauner
- **Methods at the Interfaces** *Uta Wille,* Gonzalo Cosa, Monica Olvera de la Cruz, David Hickey
- **Methods and Computations in Materials** *Colleen Scott,* Pance Naumov, Toby Nelson, Eva Hemmer, Renana Poranne
- **Organic Chemistry in Complex Systems** *Jana Roithová,* Joseph Moran, Valentine Ananikov, Sijbren Otto
- **Controlling Reactivity in Organic Synthesis** *Ruth Gschwind,* Nuno Maulide, David Leitch, Osvaldo Gutierrez, Igor Alabugin
- **Shaping Large Molecules Through Supramolecular Chemistry** *Davita Watkins,* Melanie Chiu, Xiaopeng Li, Christina Thiele
- **Computational Chemistry Addressing Dynamic and Large Systems** *Robert Paton,* Peter Schreiner, Fernanda Duarte, Dean Tantillo, Anat Milo
- **Selected Poster Presentations** *Kathleen Kilway, Malcolm Forbes*
- **The GRC Power Hour™** *Kathleen Kilway*

Physics and Chemistry of Microfluidics +GRS

Microscale Systems: From Physical Phenomena to Biological Applications

JUN 4-9, 2023

RENAISSANCE TUSCANY IL CIOCCO, LUCCA (BARGA), ITALY

CHAIRS: Ashleigh Theberge and Charles Henry

VICE CHAIRS: Katherine Elvira and Polly Fordyce

- **Organs on a Chip** *Cinzia Silvestri,* Rebecca Pompano, Roisin Owens, Stephanie Descroix
- **Clinical Applications of Microfluidics** *Aman Russom,* Martyn Boutelle, Sabeth Verpoorte, Stefano Cinti
- **Single Cell Analysis** *Petra Dittrich,* Aaron Streets, Angela Wu, Julea Vlassakis
- **Open Microfluidics** *Noo Li Jeon,* Jean Berthier, Ayokunle Olanrewaju
- **Fundamentals of Flow** *Rosanne Guijt,* Thomas Gervais, Moran Bercovici, Burcu Gumuscu
- **Point-of-Care Diagnostics and Capillary Microfluidics** *Hadley Sikes,* Daniel Citterio, Jacqueline Linnes, Bhushan Toley
- **Cell Microenvironment** *Maribel Vazquez,* Yi-Chin Toh, David Beebe, Sally Peyman
- **New Materials and Biosensing** *Netz Arroyo,* Shana Kelley, Alberto Escarpa, Robbyn Anand
- **Droplet and Multiphase Microfluidics** *Jean-Christophe Baret,* John Oakey, Christopher Easley, Paul Abbyad
- **The GRC Power Hour™** *Yi-Chin Toh, Aaron Streets*

Plant Metabolic Engineering +GRS

Metabolic Engineering in Plants: Sustainability Through Innovation

JUN 11-16, 2023

REY DON JAIME GRAND HOTEL, CASTELLDEFELS, SPAIN

CHAIRS: Katrina Cornish and Andreas Weber

VICE CHAIRS: Jing-Ke Weng and Dominique Van Der Straeten

- **Keynote Session: Plant Metabolism** *Andreas Weber,* Asaph Aharoni
- **Photosynthesis: Light-Powered Carbon Sequestration** *Quentin Dudley,* Manajit Hayer-Hartl, Megan Matthews
- **Balancing Metabolism and Homeostasis** *Erich Grotewold,* Adriano Nunes-Nesi, Björn Hamberger, Shashi Kumar
- **Evolution as a Blueprint for Engineering** *Douglas Orr,* Sibongile Mafu, Gaurav Moghe, Alvaro L Pérez-Quintero
- **From CRISPR to Chromosomes: Engineering at the Genome Scale** *Elizabeth Hood,* Magdy Mahfouz, Holger Puchta
- **Engineering the Metabolic Landscape to Control Plant-Microbe Interactions** *David Mackey,* Giles Oldroyd, Kenichi Tsuda, John McDowell
- **Making Medicines in Plants** *Jing-Ke Weng,* Jessica Cooperstone, Andrea Doseff, Renier van der Hoorn, Elizabeth Sattely
- **Sustainability: Crop Production and Products for the Bioeconomy** *Patrick Shih,* Elizabeth Hood, Madhu Khanna, Takalani Mulaudzi-Masuku, Damar Lopez-Arredondo, Wolfgang Busch, Hiroshi Maeda
- **Translating Research into Commercial Viability** *Madhu Khanna,* Walter Acosta, CJ Schwartz, Frank Röber
- **The GRC Power Hour™** *Jessica Cooperstone*

Plant Proteolysis NEW!

Integrating Our Understanding of Proteolysis in Plant Biology

AUG 6-11, 2023

BRYANT UNIVERSITY, SMITHFIELD, RI

CHAIRS: Klaas Van Wijk and Marco Trujillo

VICE CHAIRS: Andreas Schaller and Marisa Otegui

- **Proteolytic Systems and Their Study in Plant Biology** *Judy Callis,* Pascal Genschik, Diane Bassham
- **Ubiquitin, Ub-like Modification Systems and the Proteasome** *Steven Spoel,* Libo Shan, Nitzan Shabek, Ullas Pedmale, Yangnan Gu
- **Proteolysis Technology and Degrons** *Pitter Huesgen,* Christopher Overall, A. Harvey Millar, Tim Clausen
- **Autophagy: The ATG Machinery, Receptors and Functions** *Liwen Jiang,* Tamar Avin-Wittenberg, Yasin Dagdas, Eleazar Rodriguez
- **Organellar Proteases and Proteostasis** *Bonnie Bartel,* Jianming Li, Paul Jarvis, Monika Murcha
- **Autophagy of Organelles (Pexophagy, Chlorophagy, Mitophagy) and Endocytic Degradation** *Yasin Dagdas,* Bonnie Bartel, Erika Isono
- **Proteolysis in Abiotic and Biotic Defense** *Zach Adam,* Johana Misas Villamil, Ari Sadanandom, Xin Li
- **Proteolysis in Plant Development, Senescence and Programmed Cell Death** *Nuria S. Coll,* Pitter Huesgen, Frank Van Breusegem, Annick Stintzi
- **Proteolysis in Biotechnology** *David Craik,* Renier van der Hoorn
- **The GRC Power Hour™** *Marisa Otegui*

Plasmonically Powered Processes +GRS

Plasmonic Control of Photons, Charges and Phonons

JUN 4-9, 2023

FOUR POINTS SHERATON / HOLIDAY INN EXPRESS, VENTURA, CA

CHAIRS: Jianfang Wang and Suljo Linic

VICE CHAIRS: Xing Yi Ling and Mikael Kall

- **Keynote Session: Opportunities and Challenges in Plasmonically Powered Processes** *Prashant Jain,* Jeremy Baumberg, Stephan Link
- **Coupling with Excitons in Molecules and QDs** *Jing Zhao,* Gilad Haran, Christoph Lienau, Jino George, Stefano Corni
- **Plasmon-Induced Forces** *Zijie Yan,* Yuebing Zheng, Kenneth Crozier, Yongmin Liu
- **Plasmon-Driven Reactions** *Yadong Yin,* Emiliano Cortés, David Nesbitt, Katherine Willets, Emiko Kazuma
- **Ultrasensitive Sensing** *Laura Fabris,* Frank Vollmer, Francesco De Angelis, Joel Villatoro, Raffaele Velotta
- **Coupling with 2D Excitons** *Dangyuan Lei,* Qing-Hua Xu, Shangjr Gwo, Markus Raschke, Jao van de Lagemaat
- **Thermoplasmonics** *Ramon Alvarez-Puebla,* Tadaaki Nagao, Guillaume Baffou, Frank Cichos
- **Optical and Optoelectronic Devices** *Sang-Hyun Oh,* Zhaowei Liu, Sergey Bozhevolnyi, Elizabeth Boer-Duchemin, Richard Wilson
- **Chiroptical Responses** *Zachary Schultz, Michelle Personick,* Ki Tae Nam, Laurens Kuipers, Miguel A. Correa-Duarte
- **The GRC Power Hour™** *Christy Landes*

Plastics Recycling and Upcycling NEW!

Towards Viable Interdisciplinary Solutions for Plastics Recycling and Redesign

JUL 9-14, 2023

SOUTHERN NEW HAMPSHIRE UNIVERSITY, MANCHESTER, NH

CHAIRS: Gregg Beckham and John McGeehan

VICE CHAIRS: Kathryn Beers and Nick Wierckx

- **Keynote Session: Framing the Challenges and Opportunities in Plastics Recycling, Upcycling, and Redesign** *Jenna Jambeck,* Kara Lavender Law, Andre Bardow, LaShanda Korley
- **Heterogeneous Catalysis for Plastics Deconstruction** *Yuriy Román,* Kevin Van Geem, Julie Rorrer, Aaron Sadow, Bert Weckhuysen
- **Homogeneous Catalysis for Plastics Deconstruction** *Haritz Sardon,* Megan Fieser, John Hartwig, Tobin Marks
- **Biological Deconstruction and Upcycling of Plastics** *Sierin Lim,* Peter Westh, Uwe Bornscheuer, Karine Auclair, Federica Bertocchini, Lars M. Blank

- **Mechanical and Solvent-Based Methods for Plastics Recycling** *Jason Hallett,* Michael Shaver, George Huber
- **Polymer Redesign for Circularity** *Brett Helms,* Karen Wooley, Charlotte Williams, Geoffrey Coates, Andrew Dove, Paul Chirik
- **Polymer Functionalization for Upcycling** *Margaret Sobkowicz,* Brent Sumerlin, Anne McNeil, Karen Winey
- **Advances in Tools Development for Polymer Recycling, Upcycling, and Redesign** *Timothy Long,* Sanat Kumar, Linda Broadbelt, Elsa Olivetti, Christopher Tassone
- **Plastics Recycling, Upcycling, and Redesign in Industry** *Jill Martin,* Brian Schmatz
- **The GRC Power Hour™** *Rachel Segalman, Gayle Bentley*

Polyamines +GFS

Polyamines in Cancer, Medical Genetics, Aging, Pathogens and Plants

JUN 25-30, 2023
WATERVILLE VALLEY, WATERVILLE VALLEY, NH
CHAIRS: Andre Bachmann and Gianluca Canettieri
VICE CHAIRS: Stephan Sigrist and Sigrid Roberts

- **Late-Breaking Discoveries in Polyamine Research** *John Cleveland,* Daniel Puleston
- **Translational Regulation by Polyamines** *Thomas Dever,* Katja Simon, Teresa Mastracci, Sebastian Hofer, Duojia Pan, Sonia Coni
- **Polyamines and Metabolism** *Dominic Smiraglia,* Tracy Murray Stewart, Frederic Bost, Leah Vardy
- **Inborn Metabolic Diseases and Polyamines in Medical Genetics** *Charles Schwartz,* Caleb Bupp, Alban Ziegler, Angela Peron, Siddharth Banka
- **Polyamines and Oxidative Stress in Degenerative Diseases** *Manuela Cervelli,* Peter Vangheluwe, Kenneth Lee, Laura Ciapponi
- **Clinical Prevention and Treatment of Cancer and Other Diseases** *Heather Wallace,* Kelly Goldsmith, Noymi Yam, Elizabeth Bruckheimer, Linda DiMeglio
- **Medicinal Chemistry and Pharmacological Targeting of Polyamines** *Takami Oka,* Patrick Woster, Mark Burns, Edmund Ellsworth
- **Polyamines in Plants and Pathogens** *Subhash Minocha,* Keith Wilson, Autar Mattoo, Bryan Mounce, Annette Kaiser
- **Early-Career Investigator Presentations** *Susan Gilmour,* Robert Casero
- **The GRC Power Hour™** *Heather Wallace, Leah Vardy, Manuela Cervelli*

Polymers +GFS

Synthesis, Structure, Sustainability and Function

JUN 4-9, 2023
MOUNT HOLYOKE COLLEGE, SOUTH HADLEY, MA
CHAIRS: Tara Meyer and Robert Grubbs
VICE CHAIRS: Emily Pentzer and Thomas Epps

- **Synthesis: New Routes to Precisely Controlled Structures** *Jimmy Lawrence,* Garret Miyake, Makoto Ouchi
- **Polymers Against Pathogens** *Abigail Knight, Sarah Goh,* Laura Kiessling, Christopher Alabi
- **Sustainable Polymers** *Kathryn Beers,* Megan Robertson, Scott Trenor
- **Continuous Flow Reactors, Machine Learning and Other Tools for Designing and Controlling Polymer Structure and Properties** *Melanie Chiu,* Frank Leibfarth, Tanja Junkers
- **New Concepts for Sustainable Polymers** *Aleksandr Zhukhovitskiy,* Paula Diaconescu, Elizabeth Gillies
- **Late-Breaking Topics** *Lei Fang,* Will Gutekunst, Jennifer Laaser, Maxwell Robb, Adrianne Rosales
- **Designing New Polymer Structures** *Jia Niu,* Tae-Lim Choi, Julia Kalow
- **Polymers for Energy Applications** *Helen Tran,* Joaquin Rodriguez-Lopez, Rebekka Klausen
- **Stimuli-responsive Polymer Materials** *Rachel Letteri,* Zhibo Li, Brent Sumerlin
- **The GRC Power Hour™** *Kathryn Beers*

Preclinical Form and Formulation for Drug Discovery +GFS

Form and Formulation Development for Novel and Unmet Medical Needs

JUN 25-30, 2023
MOUNT SNOW, WEST DOVER, VT
CHAIRS: Annette Bak and Julie Champion
VICE CHAIRS: Erica Schlesinger and Lynne Taylor

- **Keynote Session: Gaps in Disease Treatment Impacting Large and Small Patient Populations** *Allen Templeton,* Jennifer Dent, Federico Mingozzi
- **Next Generation Formulation Strategies for New Modalities** *Grace Okoh,* Kathryn Whitehead, Wenzhan Yang, Mansoor Amiji
- **New Frontiers of Gene Based Therapies** *Gregg Duncan,* Millicent Sullivan, Ramesh Gupta, David Schaffer
- **Characterization Techniques Applicable Across Small and Large Molecules** *Li Di,* Boris Rybtchinski, Mei Hong, Karen Edler
- **In Silico Methodologies Applied on Form and Formulation** *Siladitya Ray Chaudhuri,* John Shelley, Gabriele Sadowski, Carlos Borca
- **Microbial Therapies: Design and Characterization** *Susan Joyce, Shannon Sirk,* Nancy Allbritton, James Moon, Tal Danino
- **Solubility and Permeability Challenges for Oral Delivery of Large Molecules** *Freddy Arce, Geoff Zhang,* Vincent Jannin, Christel Bergstrom, David Brayden
- **Advanced Manufacturing to Deliver Therapies From One to Billions** *Brenda Carrillo-Conde, Matt Defrese,* Theodore Randolph, Alvaro Goyanes
- **Drug Design and Delivery for Global Health Medicines** *Lia Bersin,* Niya Bowers, Mark Prausnitz, Michael Jewett
- **The GRC Power Hour™** *Christel Bergstrom, Lauren Austin*

Predictive Ecology NEW!

Temporal, Spatial or Phylogenetic Forecasting

JUN 4-9, 2023
STONEHILL COLLEGE, EASTON, MA
CHAIRS: Jeff Houlahan and Marie-Josée Fortin
VICE CHAIR: Shannon LaDeau

- **Prediction and Decision Support** *Brian McGill,* Michael Runge, Carl Boettiger
- **Perspectives From Ecosystem Science** *Shawn Leroux,* Laurel Larsen, Serguei Saavedra, Anna Trugman, Winslow Hansen
- **Predictive Modelling Techniques** *Eliot McIntire,* Vishwesha Guttal, Christina Semeniuk
- **Complexity, Stochasticity and Limits to Predictive Ability** *Korryn Bodner,* Benjamin Blonder, Beth Fulton
- **Mechanistic Versus Phenomenological Models** *James Grace,* Ryan Chisholm, Leah Johnson
- **Spatial and Temporal Transferability of Predictive Models** *Kim Cuddington,* Robert Freckleton, Barbara Han
- **Problems of Prediction at Different Scales of Time, Space and Ecological Organization** *Jennifer Sunday,* Peter Adler, Jackie Matthes
- **Prediction and Causal Inference** *Shannon LaDeau,* Paul Ferraro, Alkistis Elliott-Graves
- **Accelerating Research Synthesis in Predictive Ecology** *Michael Dietze,* Michael Dietze, Christine Laney
- **The GRC Power Hour™** *Marie-Josée Fortin, Shannon LaDeau*

Protein Engineering NEW!

Expanding the Boundaries of Protein Engineering

JUL 23-28, 2023
BRYANT UNIVERSITY, SMITHFIELD, RI
CHAIR: Huimin Zhao
VICE CHAIRS: Yvonne Chen and Dunming Zhu

- **Keynote Session: Fundamental Principles of Protein Engineering** *Yvonne Chen,* Donald Hilvert, James Wells
- **Protein Engineering for Biocatalysis** *Stephanie Galanie,* Stefan Lutz, Uwe Bornscheuer, Pimchai Chaiyen
- **Engineering Proteins with Novel Functions** *Vesna Mitchell,* Takashi Hayashi, Jacob Bale
- **Protein Engineering for Flux Control and Biosynthesis** *Ee Lui Ang,* Claudia Schmidt-Dannert, Danielle Tullman-Ercek
- **Machine Learning in Protein Engineering** *Philip Romero,* Jiri Damborsky, Possu Huang
- **Protein Engineering for Therapeutic Applications** *Jennifer Maynard,* Jennifer Cochran, Michael Birnbaum
- **Protein Engineering for Bioimaging** *Yingxiao Wang,* Jennifer Prescher, Anna Wu
- **Engineering Immunomodulatory Proteins** *Annie Gai,* Robbie Majzner, K. Dane Wittrup, Cristina Puig Saus
- **Emerging Tools for Protein Engineering** *Miguel Alcalde,* Jean-Louis Reymond, Florian Hollfelder
- **The GRC Power Hour™**

Proteins +GFS

Complexity in Proteins

JUN 11-16, 2023
HOLDERNESS SCHOOL, HOLDERNESS, NH
CHAIRS: Joan-Emma Shea and Josh Wand
VICE CHAIRS: Erin Dueber and Michael Harms

- **Keynote Session: Complexity in Proteins** *Erin Dueber,* Wah Chiu, Karen Fleming
- **Membrane Proteins** *Karen Fleming,* Benoit Roux, Stephen Sligar, Linda Columbus
- **Biologics and Drug Discovery** *James Kranz,* K. Dane Wittrup, John Karanicolas
- **The Protein Ensemble** *Jeetain Mittal,* Nicolas Lux Fawzi, Ken Dill, Vincent Hilser
- **Protein Aggregation and Phase Separation** *Shana Elbaum-Garfinkle,* Jeetain Mittal, Robert Tycko, Martin Blackledge
- **Enzymology** *Giulia Palermo,* Emily Parker, Elizabeth Komives, Lynn Kamerlin
- **Complex Proteins** *Martin Blackledge,* James Shorter, Giulia Palermo
- **Protein Complexes** *Eva Nogales,* Gabriela Schlau-Cohen, Charles Brooks, Martin Gruebele
- **Keynote Session: Macromolecular Complexes** *Michael Harms, Erin Dueber,* Eva Nogales, Juli Feigon
- **The GRC Power Hour™** *Erin Dueber*

Quantum Control of Light and Matter +GFS

Diversity and Synergetic in Quantum Control and Quantum Technology

AUG 6-11, 2023
SALVE REGINA UNIVERSITY, NEWPORT, RI
CHAIRS: Kenji Ohmori and Regina de Vivie-Riedle
VICE CHAIRS: Ben Sussman and Ignacio Franco

- **Electron Dynamics** *David Tannor,* Peter Hommelhoff, Hans Jakob Wörner
- **Quantum Control for Quantum Computing** *Daniel Lidar,* John Martinis, Rainer Blatt, Mark Saffman, Mikhail Lukin
- **Solid-State Control** *Stefanie Gräfe,* Achim Hartschuh, Hanyu Zhu
- **Quantum Many-Body Systems** *Richard Harris,* Immanuel Bloch, Tommaso Calarco, Antoine Browaeys, Ronnie Kosloff
- **Bimolecular Control** *Christiane Koch,* Rosario Gonzalez-Ferez, Oliver Kühn
- **Cavity-Based Control** *Monika Schleier-Smith,* Markus Kowalewski, Vladan Vuletic, Agnes Vibok
- **Quantum Control for Quantum Sensing** *Mikio Kozuma,* Mark Kasevich, Philippe Bouyer
- **Polyatomic Molecular Systems** *Patrick Nuernberger,* John Doyle, Robert Levis, Paul Brumer, Herschel Rabitz
- **Chiral Molecules and Chiral Light** *Ilya Averbukh,* Thomas Baumert, Valery Milner
- **The GRC Power Hour™** *Patricia Vindel Zandbergen*

Quantum Sensing +GFS

Frontiers of Sensing in the Quantum Regime with Atomic, Solid-State and Photonic Systems

JUL 23-28, 2023
LES DIABLERETS CONFERENCE CENTER, LES DIABLERETS, SWITZERLAND
CHAIRS: Michael Trupke and Jiangfeng Du
VICE CHAIRS: Isabelle Philip and Marcus Doherty

- **Keynote Session: Frontiers of Precision and Coherence** *Jiangfeng Du,* David Awschalom, Jun Ye
- **Solid-State Sensors** *Ronald Walsworth,* Milos Nesladek, Jörg Wrachtrup, Abdelghani Laraoui
- **Nanoscale Sensors** *Adam Gali,* Andreas Heinrich, Zhen-Chao Dong, Elke Neu-Ruffing
- **Electron Spin and Nuclear Magnetic Resonance** *Jörg Wrachtrup,* Martin Plenio, Nir Bar-Gill, Cristian Bonato
- **Light, Sound, and 2D Materials** *Lukas Novotny,* Jack Harris, Igor Aharonovich, Warwick Bowen
- **Biomedical Sensors** *Isabelle Philip,* Quan Li, Philipp Neumann
- **Time, Space, and Gravity** *Michael Trupke,* Mark Kasevich, Raghavendra Srinivas
- **Magnetometry and AC Field Sensing** *Marcus Doherty,* Paola Cappellaro, Fazhan Shi, Kai-Mei Fu
- **Inertial Sensing and Navigation** *Warwick Bowen,* Kai Bongs, Robert Scholten, Alexey Akimov
- **The GRC Power Hour™** *Elke Neu-Ruffing*

Radiation and Climate +GFS

Theoretical and Observational Constraints on Climate System Behavior

JUL 23-28, 2023
BATES COLLEGE, LEWISTON, ME
CHAIRS: Patrick Taylor and Allison McComiskey
VICE CHAIRS: Philip Stier and Christine Chiu

- **The Role of Radiation and Climate Science in Society** *Bruce Wielicki,* Elizabeth Weatherhead
- **Energy Constraints on Climate System Behavior** *Maria Rugenstein,* Eli Mlawer, Aaron Donohoe, Angeline Pendergrass
- **Data-Driven Prediction** *Amy Braverman,* Peter Ukkonen, Maria Molina
- **Emerging Observational Techniques** *Laura Riihimaki,* Xianglei Huang, Meghan Cronin, Belay Demoz
- **The Spectral Dimension** *Nadir Jeevanjee,* David Paynter, Maria Hakuba
- **Radiative Forcing of Climate** *Chris Smith,* Vaishali Naik, Duncan Watson-Parris, Ryan Kramer
- **Constraining Climate Models with Observations** *Mark Zelinka,* Isla Simpson, Alex Hall
- **Resolving Climate Complexity with Model Hierarchy** *Wendy Parker,* Kevin Reed, Adele Igel
- **Early-Career Investigator Presentations** *Mikael Witte*
- **The GRC Power Hour™** *Tim Carlsen*

Red Cells

Erythropoiesis: Development, Function and Disease

JUN 4-9, 2023

SALVE REGINA UNIVERSITY, NEWPORT, RI

CHAIRS: Naomi Taylor and Robert Paulson

VICE CHAIRS: Laurie Steiner and Emery Bresnick

- **Keynote Session: Developmental Hematopoiesis and Stem Cells** *Irene Roberts, Leonard Zon,* Kyunghee Choi, Leal Oburoglu
- **Single Cell Analysis in Erythropoiesis and Hematopoiesis** *Merav Socolovsky, Vince Schulz,* Janis Abkowitz, Leila Perié
- **Erythrocyte Cell Biology and Regulation of Homeostasis** *Olivier Hermine, Tracey Rouault,* Patrick Gallagher, Yvette Yien
- **Iron, Inflammation and Infection** *Hal Drakesmith,* Lionel Blanc, Catherine Lavazec, Philip Low
- **Physiology of Normal and Perturbed Erythropoiesis** *Esther Obeng, Marjorie Brand,* Christian Babbs, Jian Xu, Pedro Gonzalez-Menendez
- **Emerging Treatments and Therapeutics to Treat Erythroid Disorders** *Russell Ware,* Charles Quinn, Sara El Hoss
- **Congenital and Acquired Diseases of Erythrocytes** *Lydie Da Costa, Peng Ji,* Xiuli An, Katie Seu, Deena Iskander
- **Novel Insights into Erythroid Genome Organization** *Marieke Oudelaar,* Vijay Sankaran, Yong Cheng, Sherry Lee, Marit Vermunt
- **Gene Regulation in Erythroid Development and Differentiation** *Gerd Blobel, Kyle Hewitt,* Scott Peslak, Mitchell Weiss
- **The GRC Power Hour™** *Sandrina Kinet, Velia Fowler*

Salmonella Biology and Pathogenesis +GRS

Salmonella: From Basic Biology to Complex Pathogen-Host Interactions

JUL 23-28, 2023

RENAISSANCE TUSCANY IL CIOCCO, LUCCA (BARGA), ITALY

CHAIRS: Michael Hensel and Renee Tsolis

VICE CHAIRS: Leigh Knodler and Dirk Bumann

- **New Insights into Salmonella Epidemiology, Drug Resistance and Vaccines** *Cal MacLennan,* Samuel Kariuki, Melita Gordon
- **Molecular Mechanisms of Host-Pathogen Interactions** *Andres Vazquez-Torres,* Olivia Steele-Mortimer, William Navarre, Stéphane Méresse, Marc Erhardt
- **Interactions Between Salmonella and Host Cells** *Leigh Knodler,* Beth McCormick, Mahak Sharma, Jost Enninga, John Brumell
- **Salmonella Interactions in the Intestine** *Cagla Tukel,* Manuela Raffatellu, Shipra Vaishnava, Judith Behnsen, Mikael Sellin
- **Innate Immunity During Bacterial Infection** *Denise Monack,* Sunny Shin, Mathias Hornef, Petr Broz, Edward Miao
- **Gene Regulation and Bacterial Signaling Networks** *James Slauch,* Cari Vanderpool, Ute Romling, Joerg Vogel
- **Novel Approaches to Antimicrobial Resistance** *Robert Kingsley,* Corrella Detweiler, Brian Coombes, Mederic Diard
- **Evolution and Genomics of Salmonella-Host Interactions** *Wolf-Dietrich Hardt,* Helene Andrews-Polymenis, Alexander Herbig
- **Emerging Technologies and New Challenges** *Jay Hinton,* Athanasios Typas, Howard Hang, Emmanuel Saliba
- **The GRC Power Hour™** *Sophie Helaine*

Science of Adhesion +GRS

Deterministic Control of Adhesion Across Length Scales: Fundamentals to Applications

JUL 23-28, 2023

MOUNT HOLYOKE COLLEGE, SOUTH HADLEY, MA

CHAIR: Kevin Turner

VICE CHAIR: Niels Holten-Andersen

- **Opportunities in Adhesion Science and Soft Matter** *Joelle Frechette,* Costantino Creton, Alfred Crosby
- **Soft Contacts and Interfaces** *Anand Jagota,* Tal Cohen, Katharine Jensen, Rosa M. Espinosa-Marzal
- **Active Control of Adhesion for Robotics** *Wanliang Shan,* Ryan Hayward, Michael Bartlett
- **Soft Materials and Adhesives for Health and Medicine** *Kenneth Shull,* Marleen Kamperman, Jianyu Li
- **Adhesion and Fracture of Soft Biomaterials** *Thao (Vicky) Nguyen,* Prashant Purohit, Michelle Oyen
- **Composites and Heterogenous Materials** *Michal Budzik,* Chelsea Davis, Grace Gu, Ange-Therese Akono
- **Tactile Contacts** *Cynthia Hipwell,* Lilian Hsiao, Charles Dhong
- **Interfaces between the Body and Engineered Devices** *Niels Holten-Andersen,* Shaoyi Jiang, Nanshu Lu
- **Keynote Session: Understanding and Engineering Adhesive Contacts** *Kathryn Wahl,* Kevin Kendall, Eduard Arzt
- **The GRC Power Hour™** *Jingjie Hu*

Self-Assembly and Supramolecular Chemistry +GRS

Structure and Motion Across Length Scales

MAY 14-19, 2023

LES DIABLERETS CONFERENCE CENTER, LES DIABLERETS, SWITZERLAND

CHAIRS: Rafal Klajn and Nathalie Katsonis

VICE CHAIRS: Rein Ulijn and Thomas Hermans

- **Keynote Session: Structures and Functions Over Multiple Length Scales** *Rein Ulijn, Thomas Hermans,* E.W. "Bert" Meijer, Molly Stevens
- **Self-Assembly in Polymeric Systems** *Tom Russell,* Alfredo Alexander-Katz, Ting Xu, Roxanne Kieltyka
- **Metal–Organic Architectures** *Partha Sarathi Mukherjee,* Natalia Shustova, Shuhei Furukawa, Kim Jelfs
- **Nanoparticulate Building Blocks** *Nicholas Kotov,* Elena Shevchenko, Benjamin Abécassis, Euan Kay
- **Biomolecular Building Blocks** *Tanja Weil,* Ronit Bitton, So-Jung Park, Dora Tang
- **Light-Responsive Systems** *Alberta Ferrarini,* Ben Feringa, Jonathon Beves, Yanlei Yu, Seraphine Wegner
- **Dynamics of Self-Assembled Systems** *Steven De Feyter,* Subi J. George, Giovanni M. Pavan, Shiki Yagai
- **Motile Systems** *Ayusman Sen,* Lauren Zarzar, Kyle Bishop, Stephen Fletcher
- **Keynote Session: Motion within Synthetic Molecules and Materials** *Matthew Tirrell,* Joanna Aizenberg, Fraser Stoddart
- **The GRC Power Hour™** *Molly Stevens, Thomas Hermans*

Silk Proteins and the Transition to Biotechnologies NEW!

Impact of Natural and Synthetic Silk-Based Materials on Technology Development in the Biomedical Field and Beyond

JUL 9-14, 2023

BRYANT UNIVERSITY, SMITHFIELD, RI

CHAIRS: David Kaplan and Antonella Motta

VICE CHAIRS: Chris Holland and Keiji Numata

- **Nanostructures, Molecular Assembly and Mechanical Properties of Silk Macromolecules** *Fritz Vollrath,* Cedric Dicko, Shengjie Ling, Gregory Holland
- **Artificial (Recombinant) Silks** *Auxiliadora Prieto, Thomas Scheibel,* Anna Rising, Xiaoxia Xia, David Breslauer
- **Biochemistry, Biocompatibility and Chemistry with Silk** *Rosalyn Abbott, Amanda Baryshyan,* Chunmei Li, Amanda Murphy, Kelly Burke
- **Silk Purification: Quality Control** *Lorenz Meinel,* Jeannine Coburn, Jonathan Kluge, Rangam Rajkhowa
- **Advanced Processing Strategies** *Anthony Weiss, Evangelia Bellas,* Jelena Rnjak-Kovacina, Vladimir Tsukruk
- **Tissue Engineering with Silk** *Joshua Mauney,* Whitney Stoppel, Chiara Ghezzi, Biman Mandal
- **Optical and Electronic Sensors with Silk** *Christopher Bettinger, Vamsi Yadavalli,* Fiorenzo Omenetto
- **Regulatory and Commercialization for Silk-Based Materials** *Monica Serban, Randy Lewis,* Chanhum Park, Joseph Brown, Andreas Teuschl
- **Next Generation Silk-Based Materials: Future Designs and Functions** *Jessica Garb, Alessandra Balduini,* Benedetto Marelli, J. Miguel Oliveira, Markus Buehler
- **The GRC Power Hour™** *Whitney Stoppel, Hanna Dams-Kozlowska*

Single-Cell Approaches in Plant Biology NEW!

Understanding Functions and Behaviors of Individual Plant Cells in Space and Time

JUL 30 - AUG 4, 2023

FOUR POINTS SHERATON / HOLIDAY INN EXPRESS, VENTURA, CA

CHAIRS: Seung Rhee and Ken Birnbaum

VICE CHAIRS: Marisa Otegui and Nicholas Provart

- **Vision for the Plant Cell Atlas** *Samuel Leiboff,* Ru Gunawardane, Philip Benfey
- **Characterizing Plant Developmental Programs at the Single-Cell Level** *Marc Libault, Benjamin Cole,* Joseph Ecker, Jennifer Nemhauser, Cole Trapnell
- **Multiscale and Quantitative Imaging for Single Cells** *David Ehrhardt,* Sylvia Rodrigues da Silveira, Florent Waltz
- **Spatially Defining the Proteome Landscape in Plant Cells** *R. Glen Uhrig*, Sixue Chen, Amir Ahkami, Justin Walley
- **Spatially Resolved Single Cell Metabolomics** *Christopher Anderton,* Asaph Aharoni, Aleksandra Skirycz
- **Automating Phenotyping at Cellular, Organ, and Whole Organism Levels** *Margaret Frank,* Malia Gehan, Siobhan Braybrook, Anne-Lise Routier-Kierzkowska
- **Single Cell Comparative Plant Cell Biology and Evolution** *Michelle Facette,* Joyce Onyenedum, Masayuki Onishi
- **Systems and Synthetic Biology Approaches for Enabling Single Cell Biology** *Jenn Brophy,* Christine Queitsch, Aditya Kunjapur, Sean Cutler
- **Modeling and Data Integration for Knowledge Synthesis From Single Cell Datasets** *Noah Fahlgren,* Robert Schmitz, Shao-shan Carol Huang
- **The GRC Power Hour™** *Yoselin Benitez Alfonso,* Noah Fahlgren, Rachel Shahan

Spin Dynamics in Nanostructures +GRS

Spin Dynamics and Manipulation Near and Far From Equilibrium in New Materials, Scales and Geometries

JUL 9-14, 2023

LES DIABLERETS CONFERENCE CENTER, LES DIABLERETS, SWITZERLAND

CHAIR: Jairo Sinova

VICE CHAIRS: Alexey Kimel and Alexandra Kalashnikova

- **Magnetism and Spintronics in 2-Dimensional Materials and Devices** *Bart Van Wees,* Jie Shan, Talieh Ghiasi, Kin Fai Mak
- **Spin Dynamics at the Time, Length and Energy Scales of Fundamental Interactions** *Martin Aeschlimann,* Andrei Kirilyuk, Andrea Cavalleri, Markus Münzenberg
- **Hidden Magnetism: Antiferromagnetic Spintronics and Altermagnetism** *Tomas Jungwirth,* Joerg Wunderlich, Libor Smejkal, Enrique Del Barco
- **Spintronics for Non-Conventional Computation** *Mark Stiles,* Alice Mizrahi, Shunsuke Fukami
- **Spin-Orbitronics and Topological Matter in Spintronics** *Claudia Felser,* Stefan Bluegel, Christopher Marrows
- **Magnetism and Spin Dynamics at the Interface** *Christian Back,* Stuart Parkin, Mirko Cinchetti
- **Magnonics At the Edge** *Gerrit Bauer,* Sergej Demokritov, Dirk Grundler, Ilya Krivorotov
- **New Magnetic Imaging Techniques** *Angela Wittmann,* Claus Ropers, Amir Yacoby, Claire Donnelly
- **Emerging Applications Paradigms: Present and Future of Spintronics in Technology, the Cloud, and the Internet of Things** *Axel Hoffmann,* Ursula Ebels, Pietro Gambardella
- **The GRC Power Hour™** *Helena Reichlova*

Staphylococcal Diseases +GRS

New Insights into Staphylococcal Biology, Disease Mechanisms and Treatment

JUL 30 - AUG 4, 2023

WATERVILLE VALLEY, WATERVILLE VALLEY, NH

CHAIRS: Alexander Horswill and Juliane Bubeck Wardenburg

VICE CHAIRS: Joan Geoghegan and Barbara Kahl

- **Keynote Session: Fundamental Properties of Staphylococci** *Jose Penades,* John Chen, Andreas Peschel, Dominique Missiakas, Suzanne Walker
- **Staphylococcal Interactions within the Microbial Community** *Katherine Lemon,* Hanne Ingmer, Elizabeth Grice, Julia Oh, Tami Lieberman, Jennifer Ronholm
- **Interconnections Between Staphylococcal Metabolism and Virulence** *Alice Prince,* Francis Alonzo, Anthony Richardson, Paul Fey
- **Signaling and Gene Regulation in Staphylococci** *Jeffrey Bose,* Lindsey Shaw, Andrew Herr, Adriana Rosato, Rebecca Corrigan
- **Host-Pathogen Interactions** *Neal Hammer,* Jim Cassat, Isaac Chiu, Suzan Rooijakkers
- **Immune Responses to Staphylococcal Infections** *Jos van Strijp,* Barbara Broeker, Rachel McLoughlin, George Liu, Bas Surewaard
- **Genomics and Molecular Epidemiology of Staphylococcal Disease** *Paul Planet,* Ross Fitzgerald, Timothy Read, Ruth Massey, Jodi Lindsay, Maria Miragaia
- **Clinical Staphylococcal Disease** *George Sakoulas,* Jaime Hook, Bo Shopsin, Aaron Milstone, Stephanie Fritz
- **Late-Breaking Topics** *Joan Geoghegan, Barbara Kahl*

Stem Cells and Cancer +GRS

Strategies for Controlling Development, Tissue Homeostasis and Cancer

- May 14-19, 2023

RENAISSANCE TUSCANY IL CIOCCO, LUCCA (BARGA), ITALY

CHAIR: Cedric Blanpain

VICE CHAIRS: Leanne Jones and Kathrin Plath

- **Cancer and Stem Cell Metabolism** *Emmanuelle Passegue,* Salvador Aznar Benitah, William Lowry, Sean Morrison
- **Development** *Elly Tanaka,* Anna-Katerina Hadjantonakis, Kathy Niakan, James Briscoe, Wei Xie
- **Cell Competition and Cancer Initiation** *Elaine Fuchs,* Cristina Lo Celso, Eduardo Moreno Lampaya, Leonard Zon
- **Stem Cell Plasticity** *Sara Wickstrom,* Ophir Klein, Prisca Liberali, Elaine Fuchs, Benjamin Simons
- **Aging** *Salvador Aznar Benitah,* Amy Wagers, Anne Brunet, Konrad Hochedlinger
- **Novel Therapy in Stem Cells and Cancer** *Sean Morrison,* Anwesha Dey, Michele De Luca, Ross Cagan, Sohail Tavazoie

- **Tumor Heterogeneity** *Eduard Batlle,* Sara Wickstrom, Ilaria Malanchi, Eduard Batlle
- **Stem Cells During Regeneration and Tissue Repair** *Prisca Liberali,* Elly Tanaka, Emmanuelle Passegue, Alexander van Oudenaarden
- **Keynote Session: Mechanisms Regulating Stem Cells and Cancer** *Ilaria Malanchi,* Magdalena Goetz, Karen Vousden
- **The GRC Power Hour™** *Amy Wagers*

Stress Proteins in Growth, Development and Disease +GRS

Protein Homeostasis and the Challenges of Environment, Aging and Disease

JUL 2-7, 2023

RENAISSANCE TUSCANY IL CIOCCO, LUCCA (BARGA), ITALY

CHAIR: Brian Freeman

VICE CHAIR: Harm Kampinga

- **Keynote Session: From the Decline of Proteostasis with Aging to the Protein Machines Supporting Proteostasis** *Harm Kampinga,* Johannes Buchner, Susan Ackerman
- **Signaling Systems Governing the Protein Homeostasis Network** *Monica Driscoll,* Chengkai Dai, Patricija van Oosten-Hawle, Heinrich Jasper, Vladimir Denic
- **Gene Regulatory Responses to Stress and Aging** *Richard Morimoto,* John Lis, Lea Sistonen, Kevin Morano
- **Translation Events Maintaining Protein Homeostasis** *Judith Frydman,* Jonathan Weissman, Elke Deuerling, W. Lee Kraus
- **Molecular Chaperone Machines** *F. Ulrich Hartl,* Justin Benesch, Lila Gierasch, Didier Picard
- **Stress Responses of the Endoplasmic Reticulum with Age** *Jeffrey Brodsky,* Anne Bertolotti, Maho Niwa, Peter Walter
- **Mitochondrial Function During Aging and Stress** *Andrew Dillin,* Liza Pon, Xinnan Wang, Marcia Haigis
- **Protein Aggregation and Phase Transitions During Health, Aging, and Disease** *Jeffery Kelly,* Simon Alberti, Manajit Hayer-Hartl, James Shorter
- **Protein Ubiquitination and Degradation** *Bernd Bukau,* Rachel Klevit, Wade Harper, Malene Hansen
- **The GRC Power Hour™** *Patricija van Oosten-Hawle*

Superconductivity +GRS

Interactions, Topology and Applications

APR 30 - MAY 5, 2023

LES DIABLERETS CONFERENCE CENTER, LES DIABLERETS, SWITZERLAND

CHAIRS: Joerg Schmalian and Stuart Brown

VICE CHAIRS: Hong Ding and Dung-Hai Lee

- **Low Density Superconductors** *Kamran Behnia,* Susanne Stemmer, Andrew Millis, Yasuhide Tomioka
- **Two-Dimensional Superconductors** *Eva Andrei,* Philip Kim, Oskar Vafek, Ali Yazdani, Abhay Pasupathy
- **Pairing with Momentum** *Bernhard Keimer,* Peter Abbamonte, J.C. Seamus Davis, Vidya Madhavan
- **Multicomponent Superconductors** *Aline Ramires,* Daniel Agterberg, Elena Hassinger, Priscila Rosa, Clifford Hicks, Hae-Young Kee
- **Superconducting Applications** *Gregory Boebinger,* David Larbalestier, Tabea Arndt, David Divincenzo
- **Superconductivity and Quantum Criticality** *Antoine Georges,* Subir Sachdev, Steven Kivelson, Andrey Chubukov, Dirk Van Der Marel, Louis Taillefer
- **Topological Superconductivity** *Carlo Beenakker,* Yoichi Ando, Erez Berg, Ashvin Vishwanath
- **Superconducting Materials** *Paul Canfield,* Stephen Wilson, Rafael Fernandes, Andrew Mackenzie, Antia Botana, Ariando Ariando
- **Hydride Superconductivity** *Peter Hirschfeld,* Mikhail Eremets, Eva Zurek, James Hamlin
- **The GRC Power Hour™** *Priscila Rosa, Vidya Madhavan*

Synthetic Biology +GRS

Transforming Biology into a Technology to Solve Global Challenges

JUL 16-21, 2023

GRAND SUMMIT HOTEL AT SUNDAY RIVER, NEWRY, ME

CHAIRS: Ahmad Khalil and Ann Marie Faust

VICE CHAIRS: Karen Polizzi and Grant Murphy

- **Keynote Session: Genome Design** *Caleb Bashor,* Jason Chin, Hiroaki Suga, Yue Shen
- **Genetic Circuit Design** *Jamie Spangler,* Caleb Bashor, Lacramioara Bintu
- **Biomolecule Design** *Elizabeth Wayne,* Jamie Spangler, Ming Hammond, Justin English, Xiaojing Gao
- **Synthetic Immunology** *Evan Scott,* Elizabeth Wayne, Kole Roybal, Sai Reddy, Evan Scott
- **Molecules and Medicines** *Pulin Li,* Narendra Maheshri, Emily Derbyshire
- **Microbial Cell Engineering** *Mark Mimee*, Kevin Solomon, Elizabeth Onderko
- **Multicellular and Tissue Design** *Justin English,* Pulin Li, Miki Ebisuya, John Ngo
- **Microbiomes** *Miki Ebisuya,* Matthew Chang, Mark Mimee, Seth Rakoff-Nahoum
- **Keynote Session: Plant Tools and Pathways** *Elizabeth Onderko,* Elizabeth Sattely, Yanran Li, Jing-Ke Weng
- **The GRC Power Hour™** *Una Nattermann*

Three Dimensional Electron Microscopy +GRS

Expanding the Frontiers of Cryo-EM Towards More Challenging Targets

JUN 11-16, 2023

GRAND SUMMIT HOTEL AT SUNDAY RIVER, NEWRY, ME

CHAIR: Radostin Danev

VICE CHAIR: Sriram Subramaniam

- **Keynote Session: 3DEM and Frontiers in Structural Biology** *Bridget Carragher,* Julia Mahamid, Elizabeth Campbell, Nigel Unwin
- **The In Situ Revolution: Recent Breakthroughs and Innovations** *Elizabeth Villa,* Gaia Pigino, Digvijay Singh, Bronwyn Lucas, Benjamin Engel, Zhen Chen
- **Integrative and Correlative Approaches** *Naoko Mizuno,* Jan Schuller, Wanda Kukulski, Clemens Plaschka
- **Pushing Performance Limits with Challenging Samples** *John Rubinstein,* Claire Coupland, Oliver Clarke, Alexey Amunts, Yanyan Zhao, Halil Aydin
- **Selected Poster Presentations: New Developments in 3DEM** *Masahide Kikkawa*
- **New Algorithms and AI Methods** *Nikolaus Grigorieff,* Bertram Daum, Slavica Jonic, Barrett Powell, Kiarash Jamali, Daisuke Kihara
- **3DEM in Translational Research** *Georgios Skiniotis,* Victoria Cushing, Xin Zhang, Cornelius Gati
- **Advances in Hardware and Imaging** *Christopher Russo,* Priya Ramakrishna, Anthony Fitzpatrick, Juergen Plitzko, Radu Aricescu, Peiyi Wang
- **Selected Poster Presentations: New Developments in 3DEM** *Elizabeth Kellogg*

Tissue Microstructure Imaging +GRS

Developing Synergies Between Microstructure Imaging Modalities

JUL 16-21, 2023

STONEHILL COLLEGE, EASTON, MA

CHAIR: Dmitry Novikov

VICE CHAIR: Olivier Couture

- **Single Cells** *Lakiesha Williams,* Denis Grebenkov, Ronald Walsworth
- **Beating the Diffraction Limit** *Ali Ertürk*, Harald Hess, Pengfei Song, Edward Boyden
- **Making Use of Diffraction** *Georges Chabouh,* Alexandre Aubry, Ana Diaz
- **MRI as an In Vivo Microscope** Ileana Jelescu, Sune Jespersen, Peter Basser, Evgeniya Kirilina
- **Imaging Brain Structure** *Wei-Chung Allen Lee,* Kwanghun Chung, Viren Jain
- **Imaging Brain Function** *Jin Hyung Lee,* Gero Miesenboeck, Anna Devor, Mickael Tanter
- **Brain Microstructure and Behavior** *Olivier Couture,* Anton Arkhipov, Denis Le Bihan
- **Synergies Between Imaging Modalities** *Derek Jones,* David Kleinfeld, Daniel Razansky, Elisa Konofagou
- **Microstructure in Medicine and in Everyday Life** *Joseph Ackerman,* Susie Huang, David Weitz
- **The GRC Power Hour™** *Ileana Jelescu, Lakiesha Williams*

Tissue Repair and Regeneration +GRS

From Model Organisms to Translational Science: Exploring How Tissues Repair and Regenerate

MAY 28 - JUN 2, 2023

COLBY-SAWYER COLLEGE, NEW LONDON, NH

CHAIR: Kimberly Mace

VICE CHAIR: Tanya Shaw

- **Keynote Session: Progress in Stem and Progenitor Cell Biology in Tissue Regeneration** *Valerie Horsley,* Ken Poss, Stuart Forbes
- **Evolution of Tissue Repair and Regeneration** *Matthew Ronshaugen,* Alejandro Sanchez Alvarado, Mansi Srivastava, Rachel Smith-Bolton, B. Duygu Ozpolat
- **The Role of Metabolism and ROS in Healing** *Philipp Niethammer,* Enrique Amaya, Sabine Werner
- **Immunity and Infection in Repair** *Luisa DiPietro*, Judith Allen, Christopher Hernandez
- **Tissue Engineering and Regenerative Medicine** *Joel Boerckel,* Kelly Stevens, Daniel Cohen, Jeroen Eyckmans
- **Modelling Regeneration** *Brian Stramer,* Julia Cordero, Maksim Pilkus, Will Wood
- **Cell Signalling and Gene Regulation in Wound Healing and Regeneration** *Brigitte Galliot,* Katherine Gallagher, Andrea Wills
- **Tissue Scarring and Remodeling** *Tanya Shaw,* Boris Hinz, Ellen Pure, Paul Martin, Thomas Fabre
- **Translational Medicine and Clinical Strategies** *Marjana Tomic-Canic,* Geoffrey Gurtner, Rivkah Isseroff
- **The GRC Power Hour™** *Mansi Srivastava, Tanya Shaw*

Topological and Correlated Matter +GRS

Mapping a Landscape of Novel Unexpected States

MAY 28 - JUN 2, 2023

FOUR POINTS SHERATON / HOLIDAY INN EXPRESS, VENTURA, CA

CHAIRS: Xi Dai and Hidenori Takagi

VICE CHAIRS: Pablo Jarillo-Herrero and Ady Stern

- **Emergent Topological Materials** *Claudia Felser,* Takeshi Kondo, Yuanbo Zhang
- **Majorana Search Toward Quantum Computation** *Sankar Das Sarma,* Tetsuo Hanaguri, Vidya Madhavan, Chetan Nayak
- **Dirac and Weyl Semimetals and Axion Insulators** *Leslie Schoop,* Ho Nyung Lee, Collin Broholm, Zhijun Wang
- **Superconductivity and Topology** *Ziqiang Wang,* Johnpierre Paglione, Stephen Wilson, Ilija Zeljkovic, Aharon Kapitulnik
- **Emergent Approach to New Materials** *Bogdan Bernevig,* Maia Vergniory, Andreas Schnyder, Zhida Song
- **Recent Progress in Graphene Moire Superlattices** *Pablo Jarillo-Herrero,* Biao Lian, Qiong Ma, Stevan Nadj-Perge, Amir Yacoby
- **Non-Equilibrium Topological System** *Yong-Baek Kim,* Masatoshi Sato, Shinsei Ryu, Tilman Esslinger
- **Electromagnetic Response and Tuning of Topological Matter** *Joseph Orenstein,* Satoru Nakatsuji, Liang Wu, Shambhu Ghimire, Fumitaka Kagawa
- **Twistronics in Transition Metal Dichalcogenides** *Philip Kim,* Feng Wang, Abhay Pasupathy, Jie Shan
- **The GRC Power Hour™** *Claudia Felser*

Tuberculosis Drug Discovery and Development +GRS

Leads, Technologies and Clinical Trials for New TB Drug Regimens

JUL 23-28, 2023

REY DON JAIME GRAND HOTEL, CASTELLDEFELS, SPAIN

CHAIRS: Anna Upton and Dirk Schnappinger

VICE CHAIRS: Christina Stallings and Joel Lelievre

- **Keynote Session: Applying New Technologies and Recent Learnings From TB Drug Discovery and Development, Towards Next Generation Treatments** *Sarah Fortune,* Stewart Cole, Anastasia Koch
- **Improving TB Chemotherapy Through Translational Science and Clinical Trial Design** *Kelly Dooley,* Rada Savic, Robert J Wilkinson, Nicholas Walter
- **Designing and Evaluating TB Drug Combinations Using Preclinical Data** *Jurriaan De Steenwinkel,* Bree Aldridge, Alexander Berg
- **Finding and Optimizing New Lead Compounds** *Brendan Crowley,* Laura Cleghorn, Elena Fonfria, Natalya Serbina, Kamel Djaout
- **Profiling Drugs and Leads** *Khisimuzi Mdluli,* Max Gutierrez, Neeraj Dhar, Laura Kiessling
- **Approaches to Seeking New Chemical Matter** *Christine Roubert,* Anthony Keefe, Deborah Hung, Robert Abramovitch
- **Alternative Strategies to Cure TB** *Thomas Dick,* Graham Hatfull, Francesca Ester Morreale
- **Advancing Our Understanding of TB and Mtb to Improve TB Chemotherapy** *Luiz Pedro Carvalho,* Jeremy Rock, Michael Glickman, Greg Cook
- **Drug Tolerance, Resilience, and Resistance** *Valerie Mizrahi,* Qingyun Liu, David Alland
- **The GRC Power Hour™** *Bree Aldridge*

Undergraduate Biology Education Research +GRS

A New Vision for Change: Re-Imagining Biology Education Through Social Justice

JUN 25-30, 2023

BATES COLLEGE, LEWISTON, ME

CHAIRS: Stanley Lo and Carrie Diaz Eaton

VICE CHAIRS: Paula Lemons and Heather Seitz

- **Keynote Session: Reshaping the Landscape of Biology Education: Social Justice at the Forefront** *Bryan Dewsbury,* Beronda Montgomery, Edna Tan
- **Centering People and Communities: Identity and Intersectionality in the Foreground** *Elli Theobald,* Jeffrey Maloy, Derek Braun, Jonita Kerr, Jannelle Couret
- **Centering People and Communities: Critical Voice and Epistemology in STEM** *Joshua Reid,* Terrell Morton, Nancy Acevedo, Jessica Hernandez
- **Collaborating Across Disciplines: Future of Data Science in Biology Education** *Juan Ramirez-Lugo,* Krystal Tsosie, Jayson Nissen, Mentewab Ayalew

- **Collaborating Across Communities: Partnerships Beyond Outreach and Service** *Sunshine Brosi,* Vivian Carter, Mike Gil
- **Fostering Systemic Change: Policies and Structures Toward Common Goals** *Starlette Sharp,* Richelle Tanner, Samiksha Raut, Miriam Segura-Totten, Mike Wilton, Jason Williams
- **Fostering Systemic Change: New and Critical Lenses for Curricula and Programs** *Carlos Goller,* Dennis Lee, Ashley Juavinett, Naneh Apkarian
- **Disruptions Toward Justice: Changing Culture and Discourse in Biology Education** *Kaitlin Bonner,* Karen Cangialosi, Rou-Jia Sung, Sam Long, Desiree Forsythe
- **Keynote Session: Disruptions Toward Justice: Moving Forward as a Community** *Gloriana Trujillo,* Heidi Schweingruber, April Hill
- **The GRC Power Hour™** *Shuang Lim, Erin Dolan, Stacey Kiser*

Upconverting Nanoparticles NEW!

Upconverting and Related Light-Conversion Materials Aimed at Biomedical, Energy and Quantum Applications

JUN 18-23, 2023

WATERVILLE VALLEY, WATERVILLE VALLEY, NH

CHAIR: P. James Schuck

VICE CHAIR: Yung Doug Suh

- **Keynote Session: Pushing the Limits of Bio-Imaging with UCNPs** *Yung Doug Suh,* Xiaogang Liu, Andries Meijerink
- **Hybrid Upconverters** *Laura Francés Soriano,* Rebecca Abergel, Dan Congreve, Niko Hildebrandt, Fiorenzo Vetrone
- **Nanoscale Heating, Cooling and Thermometry** *Damien Hudry,* Eva Hemmer, Peter Pauzauskie, Andrea Pickel
- **UCNP Sensing, Diagnostics and Therapeutics** *Bruce Cohen,* Hans H. Gorris, Jennifer Dionne, John Capobianco, Julia Perez-Prieto
- **Upconverting Nano and Microphotonics** *Kees (J.C.) Hummelen,* Reuven Gordon, Guanying Chen, Daniel Jaque García
- **Synthesis, Functionalization, and Application-Driven Design** *Emory Chan,* Markus Haase, Christopher Murray, Gang Han, Damien Hudry
- **Bio and Superresolution Imaging** *Eva Hemmer,* Yong Il Park, Sam Peng, Bruce Cohen
- **Energy Transfer Enhancement, Avalanching, and Superfluorescence** *Stanley May,* Emory Chan, Mary Berry, Shuang Lim, Won Park
- **Future Directions and Visions** *Yung Doug Suh,* Artur Bednarkiewicz, Dayong Jin
- **The GRC Power Hour™** *Rebecca Abergel*

Urbanization, Water and Food Security

One Health Approaches to Urbanization, Water and Food Security

JUL 16-21, 2023

RENAISSANCE TUSCANY IL CIOCCO, LUCCA (BARGA), ITALY

CHAIRS: Kenneth Leung and Ceri Lewis

VICE CHAIRS: Carla Ng and William Cheung

- **Keynote Session: One Health Approaches to Urbanization, Water and Food Security** *Kyungho Choi,* Bryan Brooks, Leah Gerber
- **Environmental Contaminants of Concern** *Rudolf Wu,* Tong Zhang, Jessica Ray, Jing You, Scott Belcher
- **Innovations for Combating Water Pollution** *Klara Hilscherova,* Carsten Prasse, William Tarpeh
- **Food Security in a Changing World** *Wanxin Li,* Benjamin Ryan, Rebecca Short, Laura Carter
- **Climate Change Impacts** *Joleah Lamb,* Drew Harvell, Kathryn Smith
- **Sustainable Aquaculture and Fisheries** *Yangfan LI,* Grant Stentiford, Rebecca Selden, Easton White
- **Life Cycle Analysis and Sustainable Materials** *Leo Yeung,* Rachael Floreani, Vikas Khanna
- **Blue Carbon and Ecological Restoration** *Michael Warne,* Katherine Dafforn, Jong Seong Khim, Mandy Meng Fang
- **Global Initiative for Sustainability** *Elvis Genbo Xu,* Zhanyun Wang, Charles Goddard
- **The GRC Power Hour™** *Ceri Lewis, Carla Ng*

Viruses and Cells +GRS

The Biology of Viral Infection: Replication, Host Interactions and Pathogenesis

MAY 21-26, 2023

REY DON JAIME GRAND HOTEL, CASTELLDEFELS, SPAIN

CHAIR: Britt Glaunsinger

VICE CHAIR: Ana Fernandez-Sesma

- **Entry and Egress** *Jonathan Abraham,* David Veesler, Nicole Tischler, Hector Aguilar-Carreno
- **Gene Regulation** *Mandy Muller,* Noam Stern-Ginossar, Ian Mohr
- **Viral Evolution and Adaptation** *Albert Bosch,* Julie Pfeiffer, Jesse Bloom, Theodora Hatziioannou
- **Replication and Cellular Reorganization** *Montserrat Barcena,* Joe Pogliano, Urs Greber, Volker Thiel
- **Immune System Activation and Viral Immune Evasion** *Kellie Jurado,* Olivier Schwartz, Yan Xiang, Laurie Krug
- **Pathogenesis** *Sumana Sanyal,* Eva Harris, Stanley Lemon, César Muñoz-Fontela
- **Latency, Persistence and Oncogenesis** *Robert Kalejta,* Päivi Ojala, Micah Luftig
- **Virus-Host Interactions** *Carolina Arias,* Maya Shmulevitz, Karen Maxwell, Mary Estes, Christopher Sullivan
- **Therapeutic Strategies** *Justin Richner,* Ilhem Messaoudi, Sabra Klein
- **The GRC Power Hour™** *Julie Pfeiffer*

Volume Electron Microscopy NEW!

Capturing Subcellular Architecture From Organelles to Organisms

JUL 16-21, 2023

FOUR POINTS SHERATON / HOLIDAY INN EXPRESS, VENTURA, CA

CHAIRS: Paul Verkade and Lucy Collinson

VICE CHAIRS: Kedar Narayan and Yannick Schwab

- **Keynote Session: Key vEM Technologies** *Yannick Schwab,* C. Shan Xu, Christel Genoud, Jeff Lichtman
- **Key Applications of vEM** *Saskia Lippens,* Claudia Lopez, Moritz Helmstaedter
- **Tackling Sample Preparation Challenges for vEM** *Nicole L. Schieber,* Thomas Templier, Emily Benson
- **Molecular Labelling Strategies for vEM** *Ben Giepmans,* Kristina Micheva, Maria Paez Segala, Kara Fulton
- **High-Speed, High-Volume vEM Imaging** *Nalan Liv,* Alex de Marco, Meike Sievers, Martina Schifferer
- **Tools for Acquiring, Processing and Analysing vEM Data** *Erin Tranfield,* John Bogovic, Anna Kreshuk
- **Visualizing and Sharing Big vEM Data** *Aubrey Weigel,* Gerard Kleywegt, Josh Moore
- **Volume Correlative Microscopy** *Kedar Narayan,* Eija Jokitalo, Kimberly Meechan, Jurgen Kriel
- **Latest Developments in the vEM Field** *Song Pang,* Jacob Hoogenboom, Alexandra Pacureanu, Rob Parton
- **The GRC Power Hour™** *Nalan Liv, Erin Tranfield, Song Pang*

Water Disinfection, Byproducts and Health +GRS

Options and Limitations of Disinfection and Oxidation Processes for Water Safety

JUL 30 - AUG 4, 2023

MOUNT HOLYOKE COLLEGE, SOUTH HADLEY, MA

CHAIR: Urs von Gunten

VICE CHAIR: John Sivey

- **Challenges in Water Management and Drinking Water Provision** *David Sedlak,* Thomas Ternes, Peter Grevatt
- **Microbiological Contaminants and Disinfection** *Tamar Kohn,* Lutgarde Raskin, Daniele Lantagne, Frederik Hammes
- **Natural Organic Matter: Dealing with Complexity and Environmental Changes** *Fernando Rosario-Ortiz,* Christy Remucal, Alex Chow, Robert Spencer
- **Mechanistic Studies in Oxidation and Disinfection Processes** *Susana Kimura,* Carsten Prasse, Yunho Lee, Daniel McCurry, Holger Lutze
- **Surveillance of DBP Fluxes and Infectious Diseases** *Matthias Grote,* Alexandria Boehm
- **Water Quality in Distribution Systems: Chemical and Microbiological Issues** *Emmanuelle Prest,* Haizhou Liu, Kat Fish, Wenhai Chu, Ameet Pinto
- **Disinfection Byproducts: Detection, Occurrence, Exposure and Epidemiology** *Cristina Villanueva,* Maria José Farré, Qiang Zeng, Manuel Rodriguez
- **Toxicity of Disinfection By-Products** *Richard Bull,* Yang Pan, Mengting Yang, Gloria Jahnke, Cécile Vignal
- **Disinfection By-Products: Practical Approaches for Risk Reduction** *Eric Dickenson,* Russell Ford, Eugene Leung
- **The GRC Power Hour™** *John Sivey, Susana Kimura*

Wnt Signaling +GRS

Molecular Mechanisms, Embryonic Development and Adult Tissue Homeostasis and Therapeutics

JUL 30 - AUG 4, 2023

REY DON JAIME GRAND HOTEL, CASTELLDEFELS, SPAIN

CHAIRS: Stephane Angers and Mariann Bienz

VICE CHAIRS: Madelon Maurice and Ken Cadigan

- **Keynote Session: Structure and Function of Wnt Signaling** *Madelon Maurice,* Rami Hannoush, Sebastian Guettler, Yvonne Jones

- **Mechanisms of Wnt Signal Transduction** *Xi He,* Feng Cong, Renee Van Amerongen, Akira Kikuchi
- **Wnt Signaling in Diseases** *Yi Arial Zeng,* Owen Sansom, Kaitlin Basham, Bruno Reversade
- **Wnt Signaling in Tissue Engineering and Organoids** *Elizabeth Vincan,* Toshiro Sato, Vivian Li
- **Wnt Signaling and Development** *Christof Niehrs,* Terry Yamaguchi, Bart Williams, Aaron Zorn
- **ßcatenin-Independent Signaling** *David Strutt,* Yingzi Yang, Vitezslav Bryja, Danelle Devenport, Ashani Weeraratna
- **Wnt Secretion, Regulation of Gene Expression and Nuclear Mechanisms** *Ken Cadigan,* David Virshup, Michael Boutros, Jean-Paul Vincent, Marian Waterman
- **Therapeutic Targeting of Wnt Signaling** *Rami Hannoush,* Lukas Dow, Harald Junge, Karl Willert
- **Wnt Signaling in Stem Cells, Tissue Homeostasis and Regeneration** *Renee Van Amerongen,* Christian Petersen, Yi Arial Zeng, Maria Cosma, Roeland Nusse
- **The GRC Power Hour™** *Michael Ranes*

X-Ray Science +GRS

Observing Complex Systems in Space and Time with Tailormade X-Rays From Next-Generation Sources

JUL 23-28, 2023

STONEHILL COLLEGE, EASTON, MA

CHAIR: Christian Schroer

VICE CHAIR: Makina Yabashi

- **Tailormade X-Rays From Next-Generation Sources and Their Detection** *Chris Jacobsen,* Jumpei Yamada, Anna Bergamaschi
- **Microscopy and Imaging** *Andrej Singer,* Manuel Guizar Sicairos, Felix Buettner
- **Light-Matter Interaction and Non-Linear X-Ray Optics** *Nina Rohringer,* Ichiro Inoue, György Vankó
- **From Data to Knowledge** *Vincent Favre-Nicolin,* Doga Gursoy, Martin Burger
- **X-Rays for Life Science** *Gwyndaf Evans,* Alexandra Pacureanu, Sarah Bowman
- **Following Physical and Chemical Processes Under In-Situ and Operando Conditions** *Claire Donnelly,* Florian Meirer, Dorota Koziej, Phillip Maffettone
- **Dynamics and Ultrafast Phenomena** *Markus Guehr,* Anders Madsen, Agostino Marinelli
- **Complex States of Matter and Quantum Materials** *Hyunjung Kim,* Aaron Bostwick, Norimasa Ozaki
- **Keynote Session: How Future X-Ray Sources Contribute to Solving Grand Societal Challenges** *Caterina Biscari,* Francesco Sette
- **The GRC Power Hour™** *Bridget Murphy*

Science
JOURNALS AAAS

Publish your research in the *Science* family of journals

The *Science* family of journals (*Science, Science Advances*, *Science Immunology, Science Robotics*, *Science Signaling*, and *Science Translational Medicine)* are among the most highly-regarded journals in the world for quality and selectivity. Our peer-reviewed journals are committed to publishing cutting-edge research, incisive scientific commentary, and insights on what's important to the scientific world at the highest standards.

Submit your research today!

Learn more at **Science.org/journals**

hhmi

POSTDOCTORAL POSITIONS

Several postdoctoral researcher positions are available in Dr. Xin Chen's laboratory at Johns Hopkins University. We are interested in how epigenetic mechanisms regulate cell fate determination, maintenance and change during development, homeostasis and disease in multicellular organisms. We use several model organisms, including Drosophila, C. elegans and mouse, and apply interdisciplinary approaches using genetics, molecular biology, cell biology, genomics and biophysics approaches. Details of our research can be found at: **https://bio.jhu.edu/directory/xin-chen/** and **https://www.hhmi.org/scientists/xin-chen**.

The candidate should have a Ph.D. in Molecular and Cell Biology, Developmental Biology, Genetics, Biochemistry, or related areas. The candidate who has biophysics, bioinformatics, or systems biology background will be a plus. The candidate is expected to have good communication and scientific writing skills.

Salary and benefit are commensurate with research experience and accomplishments.

For interested candidates, please send your curriculum vitae and contact information of three referees to Dr. Xin Chen by email at **xchen32@jhu.edu**.

HHMI and Johns Hopkins University are affirmation action/equal opportunity employers, and applications from women and members of underrepresented groups are very encouraged.

THE UNIVERSITY OF CHICAGO

DESCRIPTION - The Neuroscience Institute and the Biological Sciences Collegiate Division at the University of Chicago are accepting applications for an open rank **Instructional Professor** position in neuroscience. This is a full-time teaching position beginning on or after **September 1, 2023**. The appointment will be for an initial term of at least two years with reappointment and progression possible following review.

Responsibilities include teaching undergraduate neuroscience and general biological science courses. Some courses include both lecture and lab components, and some are taught in partnership with university faculty. Therefore, the Instructional Professor must be able to teach a course independently and to function well as a member of a teaching team in both a lecture and laboratory teaching setting. Additional duties include hiring, training, and supervising teaching assistants. Instructional Professors of all ranks are required to engage in regular professional development.

QUALIFICATIONS - Applicants must have a PhD in Neuroscience or related field prior to start date and at least one year of teaching university level lecture and/or laboratory courses.

APPLICATION INSTRUCTIONS - To apply for this position, candidates must submit their application through the University of Chicago's Interfolio jobs board at **apply.interfolio.com/120742** and upload the following: **1)** a cover letter that addresses professional and teaching experience; **2)** a curriculum vitae; **3)** a teaching statement which should include information about the candidate's teaching philosophy and goals; **4)** a sample course syllabus; **5)** course evaluations or evidence of past teaching performance; **6)** the names and contact information (including email addresses) for three references whose letters of recommendation may be solicited

Review of applications will begin on **March 17, 2023** and will continue until the position is filled or the search is closed.

The position will be part of the Service Employees International Union.

EQUAL EMPLOYMENT OPPORTUNITY STATEMENT - All University departments and institutes are charged with building a faculty from a diversity of backgrounds and with diverse viewpoints; with cultivating an inclusive community that values freedom of expression; and with welcoming and supporting all their members. We seek a diverse pool of applicants who wish to join an academic community that places the highest value on rigorous inquiry and encourages diverse perspectives, experiences, groups of individuals, and ideas to inform and stimulate intellectual challenge, engagement, and exchange. The University's Statements on Diversity are at https://provost.uchicago.edu/statements-diversity.

The University of Chicago is an Affirmative Action/Equal Opportunity /Disabled/Veterans Employer and does not discriminate on the basis of race, color, religion, sex, sexual orientation, gender identity, national or ethnic origin, age, status as an individual with a disability, protected veteran status, genetic information, or other protected classes under the law. For additional information please see the University's Notice of Nondiscrimination.

Job seekers in need of a reasonable accommodation to complete the application process should call 773-834-3988 or email equalopportunity@uchicago.edu with their request.

Features in myIDP include:

- Exercises to help you examine your skills, interests, and values.
- A list of 20 scientific career paths with a prediction of which ones best fit your skills and interests.

myIDP

Visit the website and start planning today!
myIDP.sciencecareers.org

Science Careers | AAAS In partnership with:

FASEB Federation of American Societies for Experimental Biology
University of Massachusetts Medical School
UMASS
UCSF University of California San Francisco
UIC
BURROUGHS WELLCOME FUND

ScienceCareers online @sciencecareers.org

ARE YOU THE KIND WHO WORKS TO HELP ALL HUMANKIND?

Find your next job at ScienceCareers.org

The relevance of science is at an all-time high these days. For anyone who's looking to get ahead in —or just plain get into— science, there's no better, more trusted resource or authority on the subject than *Science* Careers. Here you'll find opportunities and savvy advice across all disciplines and levels. There's no shortage of global problems today that science can't solve. Be part of the solution.

ScienceCareers

FROM THE JOURNAL SCIENCE AAAS

What's Your Next Career Move?

From networking to mentoring to evaluating your skills, find answers to your career questions on *Science* Careers

To view the complete collection, visit
ScienceCareers.org/booklets

ScienceCareers
FROM THE JOURNAL SCIENCE AAAS

ScienceCareers online @sciencecareers.org

By **Halley Mastro**

What no one told me

As an undergraduate, I was enthralled by a visiting professor's lecture on the treasure troves of information found in remote frozen environments. As soon as I left the talk, I called my sister and told her I had decided to become a polar paleoclimate scientist—to which she replied, "A what?" No one in my family is a scientist, and no one has a graduate degree. Thus began my journey through the unwritten expectations and presumed knowledge about applying to grad school.

My first misunderstanding centered on funding. I sent that professor an email, asking whether he had time to talk to me about the work he had discussed. He agreed to meet virtually, explained his graduate research, and shared stories of fieldwork—but made no mention of how students were supported. I didn't think to ask. I assumed that pursuing a graduate degree would mean paying tuition and going without income. That was not an option for me. I was finishing my undergraduate degree a semester early to avoid taking out any more loans, and I couldn't imagine supporting myself through school for the next 6 years. So, feeling defeated, I tried to let go of the idea of continuing my education.

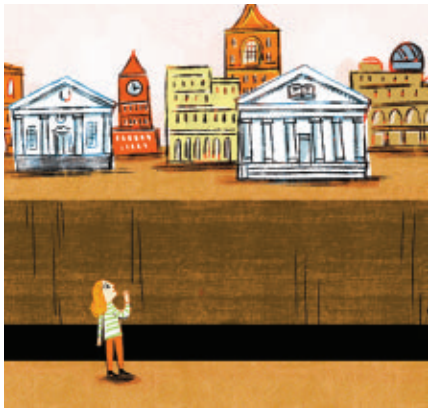

"Thus began my journey through the unwritten expectations [of] applying to grad school."

Then, during my last semester of college, my adviser asked whether I had considered grad school. I said I had but I couldn't possibly afford it. She kindly explained that many programs not only cover tuition, but also offer stipends. With that conversation, my dream became a possibility again.

Then came the next hurdle: figuring out how to apply. Applying to college had been relatively straightforward: Fill out an online application describing my qualifications and interests and wait for a response. But getting into grad school seemed to require sending personalized inquiries and building relationships with faculty before ever opening the formal application page. The expectations and available information varied substantially, even between similar programs.

I fell into a rabbit hole of internet advice from self-appointed experts, each with a different opinion on email etiquette, interview scheduling, and how to express interest in a project. The suggested timelines overlapped and contradicted one another. I felt hopeless again, terrified I would break an unspoken rule.

But I gathered all the advice I could, including some nuggets from my adviser, and plowed forward. I felt I was only pretending to understand the process, and I hoped no one would notice. I spent hours crafting emails to faculty, and I was thrilled when about half of them invited me to interview. Ultimately, I was accepted to work on a master's project in a city where I had always wanted to live. I couldn't believe I had somehow said and done the right things to make it to that point.

Being accepted didn't end my sense that I was out of my depth. Several months before I was scheduled to begin my master's program, I was invited to visit campus to start working on my project. As I made the 8-hour drive, I couldn't shake the nagging feeling that I wouldn't be good enough.

But when I arrived in town and met my host—a recent graduate from the program I was about to begin—and we exchanged stories over Thai food, my panic subsided. The next morning, my new adviser and I got to work, picking tiny fossils out of half-million-year-old sediment dug from beneath the Greenland Ice Sheet and photographing each specimen under the microscope. The first few days, we mainly found plant fragments—until I looked in the lens to see a complete beetle larva staring back at me, with all six legs and a tiny face.

Standing over the microscope that day, finding my first scientific treasure, I realized that—despite my uncertainty—I had made it exactly where I had hoped to be. I had started down this path without personal connections to people with advanced degrees. There was so much I didn't know, and didn't even realize I was missing. To those further along in academia, remember that prospective students may not know many of the unwritten norms—or that they even exist in the first place. ■

Halley Mastro is a master's student at the University of Vermont. Send your career story to SciCareerEditor@aaas.org.

ILLUSTRATION: ROBERT NEUBECKER

CALL FOR PAPERS

SPJ
SCIENCE PARTNER JOURNALS

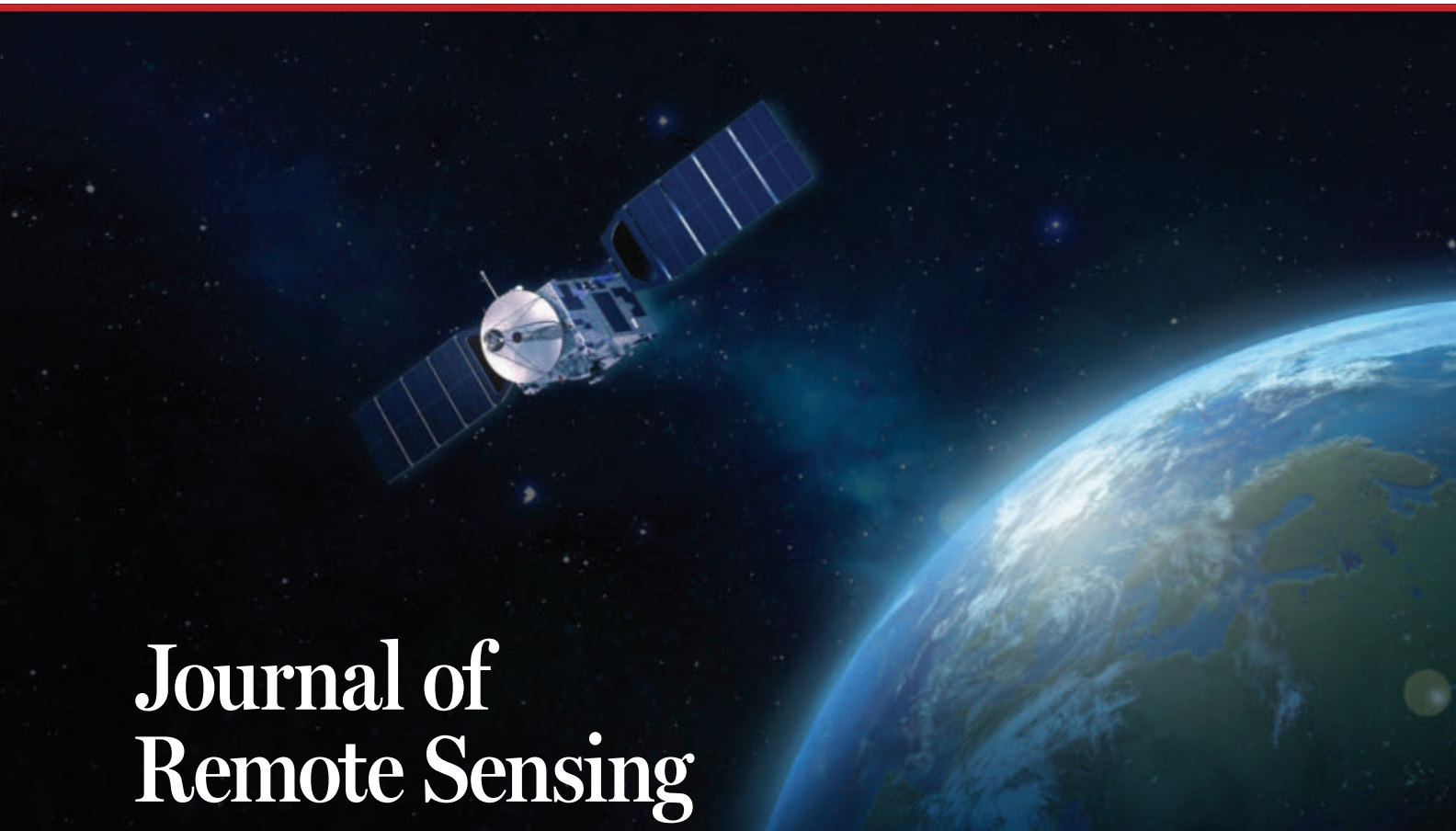

Journal of Remote Sensing

The *Journal of Remote Sensing* is an online-only Open Access Science Partner Journal published in affiliation with **Aerospace Information Research Institute, Chinese Academy of Sciences (AIR-CAS)** and distributed by the **American Association for the Advancement of Science (AAAS)**. Like all partners participating in the Science Partner Journal program, the *Journal of Remote Sensing* is editorially independent from the *Science* family of journals and AIR-CAS is responsible for all content published in the journal. This journal covers multiple research areas that include theory, science, technology of remote sensing, and interdisciplinary research with earth science and information science. Particular topics of interest within the journal include radiative transfer modeling, biogeosciences remote sensing, remote sensing of energy, and more.

Submit your research to the *Journal of Remote Sensing* today!
Learn more at **spj.sciencemag.org/remotesensing**

The Science Partner Journal (SPJ) program was established by the American Association for the Advancement of Science (AAAS), the nonprofit publisher of the *Science* family of journals. The SPJ program features high-quality, online-only, Open Access publications produced in collaboration with international research institutions, foundations, funders and societies. Through these collaborations, AAAS furthers its mission to communicate science broadly and for the benefit of all people by providing top-tier international research organizations with the technology, visibility, and publishing expertise that AAAS is uniquely positioned to offer as the world's largest general science membership society.
Visit us at **spj.sciencemag.org**

@SPJournals **@SPJournals**

OPEN ACCESS

ARTICLE PROCESSING CHARGES WAIVED UNTIL JULY 2023

YOUR RESEARCH HAS ITS REWARDS.

Submit an essay by 3/15/23 to enter to win $25K.

The prestigious international *Science* & PINS Prize is awarded annually to outstanding early-career researchers in the emerging field of neuromodulation. Findings already show improved outcomes in several neurological disorders. To enter, just write a 1000-word essay about your research performed in the last three years. The Grand Prize winner will be presented a US$25,000 award, as well as have their essay published in *Science* magazine and on *Science* Online. A runner-up will have their essay published online. For additional inquiries, email SciencePINSPrize@aaas.org.

SCIENCE-PINS PRIZE FOR NEUROMODULATION

SCIENCE-PINS

SCIENCE.ORG/PINS